Probabilistic modeling in cellular and molecular biology
Romain Yvinec

Université Claude Bernard Lyon 1
Institut Camille Jordan
Laboratoire des Mathématiques
UMR 5208 CNRS-UCBL

Thèse de doctorat
N° d'ordre : 154 - 2012

Modélisation probabiliste en biologie cellulaire et moléculaire

Thèse de doctorat

Spécialité Mathématiques

présentée par

Romain YVINEC

sous la direction de

Mostafa ADIMY, Michael C. MACKEY & Laurent PUJO-MENJOUET

Soutenue publiquement le 05 octobre 2012

Devant le jury composé de :

Mostafa ADIMY	Directeur de Recherches à l'INRIA	Dir. de thèse
Ionel S. CIUPERCA	Maître de Conférence à l'Université Lyon 1	Examinateur
Michael C. MACKEY	Directeur de Recherche à l'Université Mc GIll	Dir. de thèse
Sylvie MÉLÉARD	Professeur à l'Ecole Polytechnique	Examinatrice
Sophie MERCIER	Professeur à l'Université de Pau et des Pays de l'Adour	Rapportrice
Laurent PUJO-MENJOUET	Maître de Conférence à l'Université Lyon 1	Dir. de thèse
Marta TYRAN-KAMIŃSKA	Professeur à l'University of Silesia	Examinatrice
Bernard YCART	Professeur à l'Université de Grenoble	Rapporteur

Ecole Doctorale Informatique et Mathématiques - EDA 512

Résumé

De nombreux travaux récents ont démontré l'importance de la stochasticité dans l'expression des gènes à différentes échelles. On passera tout d'abord en revue les principaux résultats expérimentaux pour motiver l'étude de modèles mathématiques prenant en compte des effets aléatoires. On étudiera ensuite deux modèles particuliers où les effets aléatoires induisent des comportements intéressants, en lien avec des résultats expérimentaux : une dynamique intermittente dans un modèle d'auto-régulation de l'expression d'un gène ; et l'émergence d'hétérogénéité à partir d'une population homogène de protéines par modification post-traductionnelle.

Dans le Chapitre I, nous avons étudié le modèle standard d'expression des gènes à trois variables : ADN, ARN messager et protéine. L'ADN peut être dans deux états, respectivement "ON" et "OFF". La transcription (production d'ARN messagers) peut avoir lieu uniquement dans l'état "ON". La traduction (production de protéines) est proportionnelle à la quantité d'ARN messager. Enfin la quantité de protéines peut réguler de manière non-linéaire les taux de production précédent. Nous avons utilisé des théorèmes de convergence de processus stochastique pour mettre en évidence différents régimes de ce modèle. Nous avons ainsi prouvé rigoureusement le phénomène de production intermittente d'ARN messagers et/ou de protéines. Les modèles limites obtenues sont alors des modèles hybrides, déterministes par morceaux avec sauts Markoviens. Nous avons étudié le comportement en temps long de ces modèles et prouvé la convergence vers des solutions stationnaires. Enfin, nous avons étudié en détail un modèle réduit, calculé explicitement la solution stationnaire, et étudié le diagramme de bifurcation des densités stationnaires. Ceci a permis 1) de mettre en évidence l'influence de la stochasticité en comparant aux modèles déterministes ; 2) de donner en retour un moyen théorique d'estimer la fonction de régulation par un problème inverse.

Dans le Chapitre II, nous avons étudié une version probabiliste du modèle d'agrégation-fragmentation. Cette version permet une définition de la nucléation en accord avec les modèles biologistes pour les maladies à Prion. Pour étudier la nucléation, nous avons utilisé une version stochastique du modèle de Becker-Döring. Dans ce modèle, l'agrégation est réversible et se fait uniquement par attachement/détachement d'un monomère. Le temps de nucléation est définit comme le premier temps où un noyau (c'est-à-dire un agrégat de taille fixé, cette taille est un paramètre du modèle) est formé. Nous avons alors caractérisé la loi du temps de nucléation dans ce modèle. La distribution de probabilité du temps de nucléation peut prendre différente forme selon les valeurs de paramètres : exponentielle, bimodale, ou de type Weibull. Concernant le temps moyen de nucléation, nous avons mis en évidence deux phénomènes importants. D'une part, le temps moyen de nucléation est une fonction non-monotone du paramètre cinétique d'agrégation. D'autre part, selon la valeur des autres paramètres, le temps moyen de nucléation peut dépendre fortement ou très faiblement de la quantité initiale de monomère . Ces caractérisations sont importantes pour 1) expliquer des dépendances très faible en les conditions initiales, observées expérimentalement ; 2) déduire la valeur de certains paramètres d'observations expérimentales. Cette étude peut donc être appliqué à des données biologiques. Enfin, concernant un modèle de polymérisation-fragmentation, nous avons montré un théorème limite d'un modèle purement discret vers un modèle hybride, qui peut-être plus utile pour des simulations numériques, ainsi que pour une étude théorique.

4

Summary

The importance of stochasticity in gene expression has been widely shown recently. We will first review the most important related work to motivate mathematical models that takes into account stochastic effects. Then, we will study two particular models where stochasticity induce interesting behavior, in accordance with experimental results : a bursting dynamic in a self-regulating gene expression model ; and the emergence of heterogeneity from a homogeneous pool of protein by post-translational modification.

In Chapter I, we studied a standard gene expression model, at three variables : DNA, messenger RNA and protein. DNA can be in two distinct states, "ON" and "OFF". Transcription (production of mRNA) can occur uniquely in the "ON" state. Translation (production of protein) is proportional to the quantity of mRNA. Then, the quantity of protein can regulate in a non-linear fashion these production rates. We used convergence theorem of stochastic processes to highlight different behavior of this model. Hence, we rigorously proved the bursting phenomena of mRNA and/or protein. Limiting models are then hybrid model, piecewise deterministic with Markovian jumps. We studied the long time behavior of these models and proved convergence toward a stationary state. Finally, we studied in detail a reduced model, explicitly calculated the stationary distribution and studied its bifurcation diagram. Our two main results are 1) to highlight stochastic effects by comparison with deterministic model ; 2) To give back a theoretical tool to estimate non-linear regulation function through an inverse problem.

In Chapter II, we studied a probabilistic version of an aggregation-fragmentation model. This version allows a definition of nucleation in agreement with biological model for Prion disease. To study the nucleation, we used a stochastic version of the Becker-Döring model. In this model, aggregation is reversible and through attachment/detachment of a monomer. The nucleation time is defined as a waiting time for a nuclei (aggregate of a fixed size, this size being a parameter of the model) to be formed. In this work, we characterized the law of the nucleation time. The probability distribution of the nucleation time can take various forms according parameter values : exponential, bimodal or Weibull. We also highlight two important phenomena for the mean nucleation time. Firstly, the mean nucleation time is a non-monotone function of the aggregation kinetic parameter. Secondly, depending of parameter values, the mean nucleation time can be strongly or very weakly correlated with the initial quantity of monomer. These characterizations are important for 1) explaining weak dependence in initial condition observed experimentally ; 2) deducing some parameter values from experimental observations. Hence, this study can be directly applied to biological data. Finally, concerning a polymerization-fragmentation model, we proved a convergence theorem of a purely discrete model to hybrid model, which may be useful for numerical simulations as well as a theoretical study.

Remerciements

Mes premiers remerciements vont bien sûr à mes directeurs de thèse. Tout d'abord merci à Michael Mackey, qui m'a initié au domaine de la recherche. Mes 3 séjours à Montréal ont été une réussite, en grande partie grâce à lui. Je remercie ensuite Laurent Pujo-Menjouet, qui a su relever le défi d'un encadrement en co-direction, et qui m'a ouvert de nombreuses directions de recherche. Enfin, merci à Mostafa Adimy pour la confiance qu'il m'a accordé et pour l'encadrement de toute une équipe de recherche. L'occasion pour moi de souligner l'environnement inter-disciplinaire fructueux des équipes Dracula et Beagle, dont je remercie chaleureusement tous les membres.

Je suis reconnaissant envers Bernard Ycart et Sophie Mercier, qui ont la patience de relire ma thèse, et qui m'ont beaucoup apporté par leurs retours. Je souhaite aussi remercier Sylvie Méléard, Marta Tyran-Kaminska et Ionel Sorin Ciuperca pour avoir accepté et pris le temps de faire parti de mon Jury. C'est pour moi un grand honneur. Merci également aux personnes de mon entourage qui ont pris le temps de relire (des bouts !) de ma thèse : Adriane, Julien, Erwan, Marianne et Cécile.

Durant mes 3 années de thèse, j'ai eu la chance de rencontrer et travailler avec de nombreuses personnes, et j'aimerais les remercier ici. A Lyon, je pense notamment à Jean Bérard, Thomas Lepoutre, Olivier Gandrillon, et François Morlé. Si notre travail n'a pas encore porté ses fruits, cette collaboration a été très enrichissante. Je remercie également Vincent Calvez, avec qui il est toujours un plaisir de jouer au foot comme de parler de maths, et Erwan Hingant, dont je garderai un souvenir impérissable des séances de travail. À Montréal, je suis très heureux d'avoir croisé les chemins de Lennart Hilbert, Thomas Quail, Bart Borek, Guillaume Attuel, Shahed Riaz, Vahid Shahrezaei, et Changjing Zhuge. Beaucoup de pistes stimulantes ont émergé de nos nombreuses discussions et leur camaraderie m'a été plus que bénéfique ! Au gré des conférences à travers le monde, j'ai eu le plaisir de rencontrer Alex Ramos (Sao Paulo), Tom Chou et Maria Rita D'Orsogna (Los Angeles), Marta Tyran-Kaminska (Katowice), Mario Pineda-Krch (Edmonton) et de travailler avec Jinzhi Lei (Beijing)...Toutes ces personnes ont grandement contribué à l'avancé de mes travaux, et à me donner l'envie de poursuivre sur cette lancée. C'est avec une grande motivation que je souhaite continuer à collaborer avec ces personnes. Parce que l'organisation de la science est au moins aussi importante que la science elle-même, je suis content d'avoir pu aborder des thèmes politiques et philosophiques avec Pierre Crépel, Nicolas Lechopier, Hervé Philippe et le MQDC...

Ces 3 années de globe-trotter ont également été riche sur le plan personnel, et la fin de la thèse va de pair avec la fin d'une page de ma vie. J'aimerais donc remercier spécialement toutes les personnes que j'ai pu côtoyer ici ou là. En premier lieu, les colocs ! Elles/Ils ont su faire que l'adaptation après chaque voyage se passe en douceur, et ont égayé ces 3 années. La palme pour la coloc de Mermoz, sans qui la 3e année aurait été un calvaire ! Un grand merci et vive la convivialité de la colocation ! Ensuite les amiEs, bien sûr, matheuSESx ou non-matheuSESx gratteux ou footeux, déboulonneuses ou déboulonneurs, cyclistes ou vélorutionnaires, dont faire la liste exhaustive me paraît risqué...Un grand merci à mon ami d'enfance Mathieu pour avoir suivi mon parcours avec beaucoup d'intérêt ; à Simon (courage pour la rédaction !) ; à Pierre, Pierre-Adelin, Michael, Anne, Sandrine, Anne-Sandrine, Aline, Xavier, Vincent, Laetitia que j'ai toujours autant de plaisir à revoir ; à Delphine et Romain, toujours enclin à se faire une petite partie ; à Rémi, Catherine, Antoine, Aude, Laetitia avec qui on se sent si bien ; à Julien, Erwan, Thomas, Adriane, Marianne, Mohammed, JB, Amélie, Mickaël, Alain, pour tous les moments de détente au labo (et en dehors...) ; Kiki, Doudou et Carole pour la poutine ou le meilleur...et à touTEs ceLLESux que j'ai oubliéEs !

Merci la famille, toujours présente à mes côtés. Je vais pouvoir jouer davantage au tonton !

Enfin un petit mot spécial pour Cécile. Merci pour tes sacrifices, merci de m'avoir suivi à travers le monde, maintenant je pars sur les routes avec toi !

Table des matières

Chapitre 0

Introduction Générale

1 Biologie, Rappels Historiques

La découverte de phénomènes aléatoires en biologie est relativement récente, contrairement à d'autres domaines comme la physique ou la chimie. En biologie moléculaire plus particulièrement, une vision déterministe (proche du « déterminisme Laplacien ») prévalait il y a encore quelques années. En témoigne par exemple l'influent livre d'Erwin Schrödinger, *What is Life* ([75], 1944), (voir aussi [80]) pour qui l'ordre macroscopique d'un organisme vivant provient d'un même ordre microscopique de ses constituants. Durant un demi-siècle, ces idées ont été dominantes en biologie. Cette vision déterministe en fait un domaine distinct de la physique, où la notion d'ordre à partir du désordre est connue depuis longtemps (notamment grâce à Ludwig Boltzmann, James Clerk Maxwell, et la théorie cinétique des gaz, dans la deuxième moitié du 19e siècle, et plus généralement par les approches de la physique statistique). Il faut bien voir que les ordres de grandeur sont aussi radicalement différents. Dans un volume de gaz macroscopique —une mole—, il y a de l'ordre de 6.10^{23} molécules (nombre d'Avogadro). Si le nombre de cellules dans l'organisme humain est estimé à environ 10^{14}, certaines entités biochimiques ne sont présentes que par centaines voir dizaines de copies dans une cellule !

Depuis la découverte de l'ADN et de son information génétique par James Watson, Maurice Wilkins et Francis Crick (1962) et depuis les travaux de Jacques Monod, François Jacob et André Lwoff (1965) sur l'ARN messager et la notion d'opérons, la vision dominante en biologie moléculaire est une vision mécaniste (voir par exemple [49]). Toute l'information dans un organisme est contenue dans les gènes, qui la transmettent via une série (complexe) de réactions biochimiques à certaines protéines, qui vont à leur tour donner des fonctions aux cellules. Cette vision est à la base de ce qu'on appelle la « cybernétique », théorie initiée par Norbert Wiener (voir par exemple [46]).

Les récents progrès spectaculaires des méthodes et technologies expérimentales ont accumulé les preuves que la perception mécaniste des phénomènes biologiques ne s'accorde plus aux observations expérimentales. Parmi les récentes technologies disponibles, on peut citer la PCR (réaction en chaîne par polymérase —Polymerase Chain Reaction— qui permet notamment de multiplier des fragments d'ADN pour les étudier), les puces d'ADN (qui permettent de mesurer les niveaux d'expression d'un grand nombre de gènes simultanément), les nombreuses techniques d'observation et de détection de molécules dans une cellule (voir par exemple [70]), ainsi que de leur dynamique et structure spatiales (via notamment la spectroscopie de résonance magnétique nucléaire, voir par exemple [13]). Ces technologies ont, entre autres, permis d'étudier les séquences de gènes (avec par exemple le *Human Genome Project* [1]), les niveaux d'expression des gènes et les interactions entre protéines.

Parmi les expériences marquantes qui donnent de moins en moins d'importance à l'entité « gène » et de plus en plus aux interactions avec l'environnement (intérieur et extérieur à la cellule), on peut citer l'expérience d'Elowitz et al. [28]. Ces auteurs observent l'expression de deux gènes « identiques », situés à des endroits similaires dans le génome d'une bactérie (en fait, l'ADN d'une bactérie étant circulaire, ils ont placé les deux gènes de manière symétrique par rapport à l'origine de réplication). Ces deux gènes codent pour des protéines fluorescentes que l'on peut distinguer. En observant une population de cellules clones, mais avec des mesures sur cellule unique, ils ont mis en évidence que les niveaux d'expression de ces gènes varient considérablement d'une cellule à l'autre et à l'intérieur d'une même cellule (voir figure 1). Cette expérience, et de nombreuses autres, ont démontré les effets stochastiques de l'expression des gènes. Ce phénomène a bouleversé le domaine de la biologie moléculaire. On peut citer notamment Ehrenberg et al. [26] :

---

1. http ://www.ornl.gov/sci/techresources/Human_Genome/home.shtml
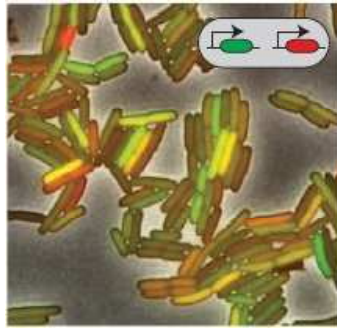
FIGURE 1: Observation expérimentale de population de bactéries. Image tirée de [27]. Le niveau de deux protéines fluorescentes (verte et rouge) est observé en simultané dans chaque cellule. Les deux protéines sont exprimées par des gènes qui possèdent la même séquence d'initiation, et qui sont situés dans des endroits similaires du génome. Cette expérience démontre que les effets de l'environnement sont primordiaux.

> There is a revolution occurring in the biological sciences

ou Paldi [66] :

> Is it possible that in biology also, just as in the physical world, macroscopic order is based on the stochastic disorder of its elementary constituents ?

La précision des expériences permet de quantifier la variabilité dans l'expression des gènes. Une modélisation probabiliste est donc adéquate pour interpréter au mieux les expériences. Notre contribution dans l'étude d'un modèle d'expression des gènes va dans ce sens (Chapitre 1). Au-delà de la quantification de la stochasticité de l'expression des gènes, beaucoup de questions biologiques restent en suspens. En particulier, beaucoup de biologistes se demandent si l'aléatoire dans l'expression des gènes a une fonction propre, ou au contraire est « inutile mais inévitable » (voir par exemple [27]). Il n'est pas sûr que la modélisation mathématique puisse répondre à cette question. En revanche, beaucoup de questions concernent également les phases du développement des organismes et de la différenciation cellulaire. Certains auteurs ont proposé des théories « Darwiniennes » pour le développement (au niveau du *phénotype* (quelles protéines sont exprimées) plutôt que du *génotype* (quels gènes ou allèles sont présents), voir par exemple le travail de Kupiec et al. [47, 48]. Des modèles mathématiques « d'évolution », à l'échelle cellulaire, pourrait probablement apporter une meilleure compréhension des phénomènes de différenciation cellulaire.

Une autre découverte importante en biologie moléculaire a été la mise en évidence d'éléments pathogènes de nature protéique. Les maladies liées à ces éléments sont appelées les maladies à prion. Elles peuvent être transmissibles ou sporadiques, mais ne font pas intervenir de virus, de bactéries ou de mutation de gènes. S'il y a encore de nombreux débats à ce sujet, l'hypothèse la plus répandue actuellement est que les maladies à prion font intervenir uniquement une protéine (appelée prion) qui, lorsqu'elle change de conformation et s'agrège, devient pathogène. Cette hypothèse a d'abord été avancée par Griffith [35] en 1967, puis prouvée par Prusiner [69] en 1982. Depuis, de nombreuses expériences ont été réalisées pour étudier la dynamique d'agrégation de cette protéine, qui est une étape clé pour l'apparition de la maladie. Ces expériences peuvent être réalisées *in vivo* (à l'intérieur de cellules) ou *in vitro* (dans des tubes à essai) (voir par exemple Liautard et al. [54]). Une curiosité de ces expériences est la grande variabilité des résultats obtenus, tant au niveau de la dynamique d'agrégation (temps d'apparition de grands polymères, rapidité de la vitesse d'agrégation, voir figure 2) que de la structure obtenue à la fin de l'expérience (structure spatiale, propriétés physiques des polymères). Là encore, une mo-
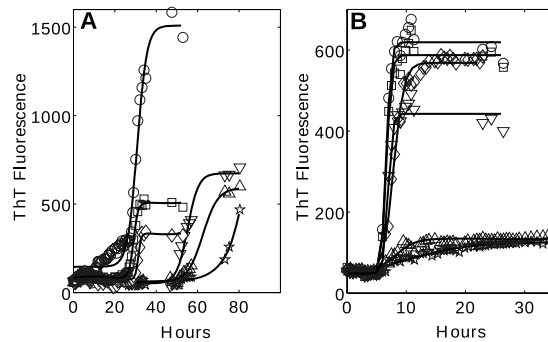
FIGURE 2: Résultats d'expériences d'agrégation de protéines prion, obtenus dans les mêmes conditions expérimentales et avec la même condition initiale. Les données de ces expériences sont tirées de [54].

délisation probabiliste semble donc adéquate pour prendre en compte cette variabilité, et tenter d'expliquer les phénomènes sous-jacents. Notre contribution dans l'étude d'un modèle d'agrégation-fragmentation de protéines va dans ce sens (Chapitre 2).

2   Modélisation Mathématique

C'est dans ce contexte de découverte de mécanismes aléatoires en biologie que s'inscrivent mes travaux de thèse. La modélisation mathématique en biologie est un domaine relativement récent, qui a d'abord concerné surtout la dynamique des populations. Que ce soit en dynamique des populations, ou dans les modèles de réactions biochimiques, la modélisation mathématique apporte une approche qualitative et quantitative. Dans les modèles de réactions biochimiques, la loi d'action de masse permet de représenter la dynamique d'un ensemble d'entités biochimiques, interagissant via des réactions cinétiques, sous forme d'un système d'équations différentielles ordinaires. Une étude qualitative de ces équations (comportement en temps long, états d'équilibre, bifurcations...) permet alors de comprendre le comportement global du système, et de valider ou non le modèle en fonction des observations expérimentales. L'approche quantitative consiste à estimer les valeurs de certains paramètres, ou de variables non observables, soit grâce à une résolution explicite des équations, soit à l'aide de simulations numériques. Dans le contexte des modèles d'expression des gènes, le travail de Goodwin [34], rendu rigoureux mathématiquement peu après [36, 37, 65, 76, 84], est un exemple important. Cette série de travaux a montré que le niveau d'expression d'un gène pouvait présenter un caractère monostable, bistable ou oscillant suivant les hypothèses de régulation. Dans le contexte des modèles d'agrégation de protéines, plus particulièrement le modèle de Becker-Döring [11], les travaux de [4] illustrent également l'approche quantitative, en montrant les propriétés asymptotiques du modèle (convergence vers un état d'équilibre, ou explosion, en fonction de la condition initiale et des paramètres). Pour une revue récente des techniques utilisées pour les modèles déterministes de réactions chimiques, voir Othmer and Lee [64].

Dès 1940, le biophysicien Max Delbrück a démontré que le faible nombre de molécules enzymatiques dans une cellule pouvait donner lieu à de grandes fluctuations d'entités biochimiques à l'intérieur d'une cellule, et avoir des impacts importants sur la physiologie des cellules. Ces idées ont été largement utilisées pour étudier des modèles de réactions chimiques et caractériser les fluctuations possibles [77]. Bartholomay [9] a établi une analogie entre ces modèles et les modèles de naissance et de mort en théorie des probabilités. Mc-

Quarrie [56] a résumé les résultats analytiques connus, pour les réactions uni-moléculaires principalement (voir aussi les récentes contributions de [32],[3]). L'approche classique traduit l'évolution temporelle des entités chimiques en un système d'équations sur la probabilité de trouver tel état du système au temps t (équation maîtresse). Ces équations étant généralement compliquées, on cherche en général uniquement à résoudre les deux premiers moments (moyenne et variance) pour quantifier les fluctuations. Une autre approche concerne les processus stochastiques qui décrivent l'évolution temporelle du nombre de molécules. Dans les modèles biochimiques, les processus stochastiques sont des processus de saut. Les équations stochastiques peuvent ainsi s'écrire à l'aide de processus de Poisson standards. À chaque réaction chimique du type

$$\alpha_1 A_1 + \alpha_2 A_2 + \cdots + \alpha_n A_n \rightleftharpoons \beta_1 A_1 + \beta_2 A_2 + \cdots + \beta_n A_n,$$

on associe un processus de saut d'intensité $\lambda_+(X_{A_1}, X_{A_2}, \cdots, X_{A_n})$ et de saut $X_{A_i} \mapsto X_{A_i} + (\beta_i - \alpha_i)$ pour la réaction directe, et d'intensité $\lambda_-(X_{A_1}, X_{A_2}, \cdots, X_{A_n})$ et de saut $X_{A_i} \mapsto X_{A_i} - (\beta_i - \alpha_i)$ pour la réaction inverse, où X_{A_i} est le nombre de molécules de type A_i. Un choix usuel pour l'intensité des réactions est donné par la loi d'action de masse. L'intensité dépend alors du nombre de rencontres de molécules, donc du nombre de α_i-uplets que l'on peut former avec X_{A_i} molécules. Pour la réaction directe, par exemple, on aurait

$$\lambda_+(X_{A_1}, X_{A_2}, \cdots, X_{A_n}) = k \prod_{i=1}^{n} f(\alpha_i, X_{A_i}),$$

où, pour $\alpha = 0$, $f(\alpha, X) = 1$, et pour tout $\alpha \in \mathbb{N}^*$,

$$f(\alpha, X) = \frac{X(X-1)\cdots(X-\alpha+1)}{\alpha!},$$

et k représente la constante de vitesse de réaction (qui peut dépendre du volume, de la température, *etc.*).

Exemple 1. *Donnons un exemple simple, constitué des réactions*

$$A + A \underset{k_1^-}{\overset{k_1^+}{\rightleftharpoons}} B$$
$$A \underset{k_2}{\longrightarrow} \varnothing.$$

La première réaction est une transformation de deux molécules A pour donner une molécule B. La deuxième réaction est une réaction de dégradation. L'évolution du nombre de molécules (X_A, X_B) est donnée d'après la loi d'action de masse par le système d'équations différentielles stochastiques suivant :

$$\begin{cases} X_A(t) &= X_A(0) - 2Y_1\Big(\int_0^t \frac{k_1^+}{2} X_A(s)(X_A(s)-1)ds\Big) + 2Y_2\Big(\int_0^t k_1^- X_B(s)ds\Big) \\ &\qquad\qquad\qquad\qquad\qquad\qquad\qquad\qquad - Y_3\Big(\int_0^t k_2 X_A(s)ds\Big), \\ X_B(t) &= X_B(0) + 2Y_1\Big(\int_0^t \frac{k_1^+}{2} X_A(s)(X_A(s)-1)ds\Big) - 2Y_2\Big(\int_0^t k_1^- X_B(s)ds\Big), \end{cases}$$

où les Y_i, $i = 1, 2, 3$, sont des processus de Poisson standards indépendants associés à chaque réaction.

Revenons au cas général. Si on note $\mathbf{X}$ le vecteur des quantités de molécules dans le système, $\lambda_i(\mathbf{X})$ l'intensité de la réaction i, et $\boldsymbol{\alpha}_i$, $\boldsymbol{\beta}_i$ les vecteurs de stœchiométrie associés à la réaction i, l'évolution du système se décrit par :

$$\mathbf{X}(t) = \mathbf{X}(0) + \sum_i (\boldsymbol{\beta}_i - \boldsymbol{\alpha}_i) Y_i \left(\int_0^t \lambda_i(\mathbf{X}(s)) ds \right).$$

Remarque 1. *Les hypothèses physiques sous-jacentes d'une telle approche sont :*
  – *une diffusion rapide,*
  – *un système bien mélangé,*
  – *l'absence de corrélation entre les positions des molécules ou entre les réactions.*

Nous utiliserons au cours de cette thèse ce formalisme pour décrire nos modèles (voir section 3). Notre but sera alors d'obtenir une caractérisation qualitative et quantitative des modèles. En particulier, on s'intéressera aux comportements en temps long (convergence vers un état d'équilibre), et à la recherche de solutions analytiques, exactes ou approchées. Cette approche nous permettra en retour de pouvoir exploiter des données expérimentales.

Dans la suite de cette introduction, on présente plus précisément les travaux de cette thèse (section 3), et les perspectives (section 4). Dans la dernière partie, on introduit les différents outils mathématiques sur les processus Markoviens que l'on a utilisés, principalement des résultats de stabilité (section 6) et des théorèmes limites (section 7), utilisant des formalismes de semi-groupes et de martingales.

3 Résultats de Cette Thèse

Au cours de cette thèse, nous étudions deux modèles probabilistes appliqués à la biologie moléculaire. Bien que faisant partie du même domaine d'application, ces deux modèles sont assez distincts, et seront donc présentés séparément. Le premier modèle est un modèle d'expression des gènes, et a été principalement étudié lors de mes séjours (deux fois six mois) à l'Université McGill, à Montréal (Qc, Canada), sous la direction de Michael C. Mackey. Le deuxième modèle est un modèle d'agrégation de protéines, et a été principalement étudié à l'Université Lyon 1, sous la direction de Laurent Pujo-Menjouet. Les deux études font cependant intervenir des outils communs d'analyse mathématique de modèles probabilistes (voir sections 6 et 7).

Dans le Chapitre I, nous étudions le modèle standard d'expression des gènes, à trois étapes : ADN, ARN messager et protéines. L'ADN peut être dans deux états, respectivement « ON » et « OFF ». La transcription (production d'ARN messager) peut avoir lieu uniquement lorsque l'ADN est dans l'état « ON ». La traduction (production de protéine) est proportionnelle à la quantité d'ARN messager. Enfin la quantité de protéines peut réguler de manière non linéaire les taux de production précédent. La version « deterministe », sous forme de système d'équations différentielles ordinaires, modélisant les concentrations des espèces biochimiques, a été étudiée dans les années 60. On connait maintenant précisément les comportements en temps long en fonction des paramètres du modèle. En particulier, on sait que si la régulation est *positive*, et suffisamment non linéaire, il y a une bifurcation fourche. Le système peut avoir deux états d'équilibres stables. Lorsque la régulation est négative, et suffisamment non linéaire, il y a une bifurcation de Hopf. Le système peut avoir des oscillations stables. Nous avons étudié une version « stochastique » de ce modèle, sous forme d'une chaîne de Markov en temps continu. La difficulté de ce modèle est due au fait que certains taux de saut de la chaîne de Markov sont non linéaires, ce qui rend l'analyse mathématique plus délicate. Tout d'abord, nous dérivons les cinétiques de Michaelis-Menten et de Hill, dans le formalisme des processus de saut,

en utilisant des techniques de moyennisation. Ensuite nous donnons des conditions « raisonnables » pour que la chaîne de Markov soit exponentiellement ergodique, en utilisant les critères de stabilité usuels. Pour étudier quantitativement le modèle, nous utilisons une version réduite du modèle, en dimension 1, et avec une production intermittente (*bursting*, ce phénomène a été bien caractérisé expérimentalement). Ce modèle peut-être vu comme un modèle Markovien déterministe par morceaux. Nous donnons ici des conditions précises pour la convergence asymptotique vers un état stationnaire que l'on peut calculer explicitement dans certains cas. Cette résolution explicite nous permet d'abord d'étudier les P-bifurcations (nombre de modes (maxima) de la densité stationnaire) et de comparer ainsi les diagrammes de bifurcations du modèle stochastique avec celui du modèle déterministe. Nous mettons notamment en évidence des phénomènes relativement généraux, de bifurcation avancée et élargie pour l'apparition de deux modes sur la densité stationnaire. Cette étude du comportement en temps long nous permet également de nous intéresser au problème inverse : à partir d'une densité de probabilité mesurée expérimentalement, retrouver la fonction de régulation tout entière (et pas seulement la valeur d'un paramètre). Le traitement de données existantes et adaptées à notre modèle est en cours de réalisation. Enfin, pour compléter l'étude de ce modèle, nous montrons rigoureusement, par des techniques de convergence de processus stochastiques, le passage du modèle initial au modèle réduit. En effectuant une mise à l'échelle, réaliste du point de vue biologique, nous obtenons ainsi une convergence en loi vers le modèle limite, ce qui donne les conditions sur les paramètres pour observer le phénomène de production intermittente d'ARN messagers ou de protéines.

Dans le Chapitre II, nous étudions une version stochastique du modèle d'agrégation-fragmentation de polymères. Dans un premier temps, nous regardons le modèle sans fragmentation, de Becker-Döring, pour modéliser le phénomène de nucléation dans le processus d'agrégation des protéines prion. La nucléation est le passage d'un état défavorable (thermodynamiquement) pour l'agrégation à un état favorable. La caractérisation quantitative de cette étape est donc essentielle pour comprendre la dynamique d'agrégation des protéines. La version stochastique du modèle de Becker-Döring permet une définition de la nucléation en accord avec les modèles biologistes pour les maladies à prion : le temps d'apparition du premier agrégat de taille suffisante. Ces protéines ont une conformation telle que, en-dessous d'une certaine taille, les agrégats ne sont pas stables, alors qu'au-dessus d'une certaine taille, ils deviennent stables. La taille critique correspond à la taille du noyau. Nous caractérisons alors la distribution des temps de nucléation dans les modèles d'agrégation de protéines, en utilisant la théorie des temps de passage pour les chaînes de Markov. La difficulté de ce modèle réside dans la grande taille de l'espace des états de la chaîne de Markov. Nous avons alors mis en évidence plusieurs approximations analytiques, valables dans différentes régions de paramètres. Nous avons validé ces approximations à l'aide de simulations numériques de la chaîne de Markov. Le comportement du temps de nucléation a alors des propriétés à priori contre-intuitives. D'une part, il dépend de manière non-monotone avec les paramètres cinétiques d'agrégation du modèle. D'autre part, dans une certaine région de paramètre, il dépend très faiblement de la quantité initiale de protéines. Le phénomène de nucléation étant un phénomène très répandu en biophysique, ces résultats peuvent avoir un impact important (la dérivation de lois d'échelles permet d'éviter un grand nombre de simulations, et une analyse plus rapide et plus simple de modèles liés). Pour le modèle particulier de l'agrégation des protéines prion, il permet une étude quantitative des observations expérimentales (qui reste à faire).

Dans un deuxième temps, nous étudions un modèle de polymérisation-fragmentation, en présence de grands polymères déjà formés (plus grands que la taille du noyau). Cependant, sous sa forme discrète, au vu du grand nombre de protéines et des différences d'échelles de

temps entre la polymérisation et la fragmentation, il n'est pas très adapté à une approche quantitative. Nous effectuons alors une mise à l'échelle, pour obtenir un modèle limite où la polymérisation est déterministe (donné par une dérive), et la fragmentation est représentée par un processus de saut. Dans ce modèle limite, les protéines non agrégées sont représentées par une variable continue, et le nombre de polymères est discret. Ce modèle permet de prendre en compte la variabilité de la vitesse de polymérisation observée expérimentalement. Sous une forme simple, ce modèle est un processus de branchement. En général, c'est un modèle individu-centré avec une compétition indirecte entre les individus. Enfin, lorsque les deux régimes sont mis bout à bout, la nucléation puis la polymérisation-fragmentation, ce modèle « hybride » peut facilement incorporer un phénomène récemment observé expérimentalement : la possibilité d'apparition de différentes structures de polymères. L'hypothèse biologique sous-jacente est que la protéine prion peut se présenter sous différentes conformations spatiales, et mène ainsi à des agrégats de structure spatiale différente. Ces différents polymères ont des dynamiques de polymérisation et fragmentation propres à leur structure. Notre approche quantitative peut alors aider à l'identification des différents paramètres de polymérisation et fragmentation, et confirmer (ou donner un poids supplémentaire à) l'hypothèse biologique.

4   Perspectives

Du point de vue de la modélisation en biologie, les études des deux modèles que j'ai menées permettent une approche quantitative des données expérimentales. Le traitement des données et l'application de mes résultats par confrontation avec des données expérimentales est encore à finaliser. Pour le modèle d'expression des gènes, la possibilité de trouver la fonction de régulation à partir de la densité stationnaire (et de la mesure d'autres paramètres) devrait intéresser des biologistes expérimentaux. Cela permet en effet d'étudier les interactions précises entre les protéines et les molécules d'activation du gène, qui peuvent notamment être modifiées expérimentalement par des modifications chimiques. Le traitement de données existantes est en cours. Pour le modèle d'agrégation des protéines prion, la possibilité de prendre en compte la variabilité et l'émergence de différentes structures de polymères dans un même modèle permet de réinterpréter un certain nombre de résultats expérimentaux.

Au cours de ce travail, j'ai démontré des théorèmes de convergence pour certains modèles Markoviens, en utilisant les techniques classiques de martingales. Les théorèmes limites obtenus au chapitre I et au chapitre II sont inhabituels dans le sens où le modèle limite est un processus hybride, mêlant un comportement déterministe et un comportement stochastique. Les approximations de second ordre pour ces limites sont intéressantes à regarder. Pour le modèle d'expression des gènes en particulier, la caractérisation des fluctuations autour du modèle limite permettrait une meilleure approximation du modèle initial.

Une première extension, pour le modèle d'expression des gènes, serait d'étudier le modèle avec switch (ON-OFF) *et* avec production intermittente (bursting). Ces phénomènes ont été bien étudiés séparément, mais jamais (à ma connaissance) ensemble. Une étude qualitative et quantitative présenterait un intérêt non négligeable. En particulier, dans ce modèle, les temps entre production ne sont pas exponentiels (lors que le système est dans l'état OFF, il faut au moins deux étapes pour obtenir un événement de production). Ceci peut en faire un modèle plus réaliste, au vu des récentes mesures expérimentales [79] des temps entre événements de production.

Pour le modèle d'expression des gènes toujours, la bifurcation que l'on a obtenue sur le modèle réduit, de dimension un, est analogue à la bifurcation fourche du modèle détermi-

niste. En revanche, le modèle en dimension un ne présente pas de bifurcation de Hopf. Une étude quantitative du modèle en dimension deux, ou à l'aide de simulations numériques, devrait pouvoir caractériser la bifurcation de Hopf dans le modèle stochastique. Ceci reste un problème délicat (voir par exemple dans le cas de modèles Browniens [10, 74, 14, 85])

Concernant le modèle de polymérisation-fragmentation, le modèle limite hybride que l'on a obtenu est intéressant pour plusieurs raisons : d'abord, il peut donner des schémas efficaces de simulation numérique ; ensuite, il peut apporter des résultats quantitatifs sur la vitesse de polymérisation, qui est facilement mesurable expérimentalement. D'un point de vue plus théorique, ce modèle n'a pas (à ma connaissance) été étudié. En particulier, le comportement en temps long, les phénomènes de gélation (perte de masse par création d'une molécule géante) et de poussière (perte de masse par création d'une infinité de particules microscopiques) seraient intéressants à regarder et pourraient être comparés avec les modèles déterministes (type EDO ou EDP) et stochastiques (type chaîne de Markov) [62, 40].

Enfin, dans l'étude que nous avons mené sur le premier temps d'apparition d'un noyau, dans le modèle de Becker-Döring, il reste encore des comportements asymptotiques intéressants à regarder. Nous avons caractérisé le temps de nucléation pour un nombre fini de molécules dans les deux asymptotiques de taux de détachement très faible et très grand. Nous avons aussi montré que le caractère discret de ce problème donne des comportements non monotones en fonction des paramètres d'agrégation. Ces comportements apparaissent surtout lorsque le nombre total de molécules M est comparable avec la taille du noyau N. Une limite naturelle à regarder serait ainsi $M \to \infty$ et $N \to \infty$ avec $M/N < \infty$. Les modèles limites de type champ-moyen pour les modèles d'agrégation-fragmentation sont connus [1], et sont des variantes de l'équation de Smoluchowski. En revanche, à ma connaissance, le problème de la nucléation n'a pas été étudié sur ces modèles. Par ailleurs, pour l'ensemble des approximations du temps de nucléation que nous avons trouvées, et validées numériquement, il reste le problème de la quantification de l'erreur, qui est un problème intéressant tant au point de vue pratique que théorique.

5   Notations

Nous rappelons ici des notations usuelles et des résultats de théorie des semi-groupes. Les semi-groupes que l'on regardera agiront sur les espaces de fonctions bornées (ou des sous-espaces) ou sur les espaces de fonctions intégrables (ou des sous-espaces).

Soit $(L, \| \cdot \|)$ un espace de Banach. On note $\mathcal{D}(A)$ le domaine de l'opérateur linéaire A. On dit que $A \subseteq B$, ou que B est une *extension* de A, si
- $\mathcal{D}(A) \subseteq \mathcal{D}(B)$,
- $Bu = Au$ pour $u \in \mathcal{D}(A)$.

On identifie un opérateur A et son *graphe*

$$\{(f, Af) : f \in \mathcal{D}(A)\}.$$

En particulier, un opérateur A est *fermé* si son graphe est fermé dans $L \times L$. Un opérateur A est dit *fermable* s'il a une extension fermée. Si A est fermable, alors la *fermeture* $\overline{A}$ de A est la plus petite extension fermée de A, c'est-à-dire l'opérateur fermé qui a pour graphe la fermeture dans $L \times L$ du graphe de A. Si A est tel que $\mathcal{D}(A)$ est dense dans L, alors A est fermable.

Si $(A, \mathcal{D}(A))$ est un opérateur linéaire fermé, alors un sous-espace $\mathcal{D}$ de $\mathcal{D}(A)$ est appelé un *core* pour A si la fermeture de la restriction de A à $\mathcal{D}$ est égale à A, c'est-à-dire

$$\overline{A|_{\mathcal{D}}} = A.$$

Un opérateur A est *dissipatif* si

$$\|\lambda u - Au\| \geqslant \lambda \|u\|, \text{ pour tout } u \in \mathcal{D}(A) \text{ et } \lambda > 0.$$

On note l'*image* d'un opérateur $Im(A) := A(\mathcal{D}(A))$. Si A est dissipatif et $Im(A) \subset \overline{A}$, alors A est fermable, et $\overline{A}$ est encore dissipatif.
Pour tout $\sigma > 0$, on définit la résolvante de A par

$$R(\sigma, A) = (\sigma - A)^{-1}.$$

Une famille $\{T(t) : t \geqslant 0\}$ d'opérateurs linéaires bornés sur L est un *semi-groupe* si
- $T(0) = I$,
- $T(t+s) = T(s)T(t)$, pour tout $t, s \geqslant 0$.

Un semi-groupe $\{T(t)\}$ est *fortement continu* si $\lim_{t \to 0} T(t)f = f$ pour tout $f \in L$. Un semi-groupe $\{T(t)\}$ est un semi-groupe de *contraction* si $\|T(t)\| \leqslant 1$ pour tout $t \geqslant 0$. Le *générateur infinitésimal* d'un semi-groupe $\{T(t)\}$ est l'opérateur linéaire A défini par :

$$Af = \lim_{t \to 0} \frac{1}{t}[T(t)f - f].$$

Le domaine $\mathcal{D}(A)$ du générateur infinitésimal A est l'ensemble des $f \in L$ tel que cette limite existe. Pour la théorie des semi-groupes, on se réfère à Engel and Nagel [29].

Dans la suite, $(\Omega, \mathbb{F}, \mathbb{P})$ est un espace de probabilité, et $\mathbb{E}[\cdot]$ est l'intégrale sur Ω suivant $\mathbb{P}$.

6   Étude Théorique de Modèles Stochastiques

Nous allons passer en revue dans cette section les résultats classiques mais fondamentaux sur les modèles Markoviens. Nous regarderons en particulier les problèmes d'existence, d'unicité et de comportement en temps long de ces modèles. Nous nous intéresserons uniquement aux modèles homogènes en temps. Nous voulons présenter dans cette partie les différents types de formalisme utilisés au cours de cette thèse. Nous citerons alors des résultats importants dans l'étude du comportement de ces différents modèles, que nous utiliserons dans les chapitres de cette thèse. Nous mettrons aussi en avant les liens entre les approches probabilistes et analytiques que l'on a utilisées. En aucun cas cette partie ne cherche à être exhaustive concernant l'ensemble des résultats de la littérature !

6.1   Chaîne de Markov à temps discret

Nous suivons dans un premier temps une référence classique pour les chaînes de Markov, le livre de Brémaud [15] ainsi que des notes de cours de Bérard [12]. En temps discret, une chaîne de Markov (homogène) est une généralisation au cas aléatoire d'équations aux différences du type $x_{n+1} = f(x_n)$. Pour une chaîne de Markov à temps discret et à valeurs dans un espace fini ou dénombrable, la définition est plus facile car il n'est pas nécessaire de prendre en compte les questions de mesurabilité. Une chaîne de Markov peut alors être définie simplement par la propriété de Markov et par une matrice (ou plus généralement un noyau) de transition. Dans toute cette partie, E est un espace dénombrable.

Définition 1. *[Chaîne de Markov homogène à temps discret et espace d'états dénombrable] Une suite de variables aléatoires (X_n) définies sur un espace de probabilité $(\Omega, \mathbb{F}, \mathbb{P})$, à valeurs dans E espace d'états dénombrable, est une chaîne de Markov homogène si pour tout entier $n \geqslant 0$ et tous états $i_0, i_1, \cdots, i_{n-1}, i, j$,*

$$\mathbb{P}\{X_{n+1} = j \mid X_n = i, X_{n-1} = i_{n-1}, \cdots, X_0 = i_0\} = \mathbb{P}\{X_{n+1} = j \mid X_n = i\},$$

et si le noyau de transition (indépendant de n) défini par $p_{ij} = \mathbb{P}\{X_{n+1} = j \mid X_n = i\}$ vérifie les propriétés suivantes

$$p_{ij} \geqslant 0, \quad \sum_{k \in E} p_{ik} = 1.$$

Une telle chaîne de Markov est alors entièrement caractérisée par la donnée de sa loi initiale et de son noyau de transition. Soit ν_0 la loi initiale de la chaîne de Markov, c'est à dire $\nu_0(i) = \mathbb{P}\{X_0 = i\}$ pour tout $i \in E$. Il vient directement de la propriété de Markov que la loi ν_n de X_n vérifie la relation de récurrence

$$\nu_{n+1}(j) = \sum_{k \in E} \nu_n(k) p_{kj} = \nu_n^T \mathbf{P}(j), \quad j \in E, n \in \mathbb{N},$$

où $\mathbf{P} = (p_{ij})_{i,j \in E}$, $\nu_n = (\nu_n(i))_{i \in E}$. et ν^T est la transposée de ν. On a alors immédiatement

$$\nu_n^T = \nu_0^T \mathbf{P}^n,$$

et plus généralement que la loi du k-uplet $(X_0, X_1, \cdots X_{k-1})$ vérifie

$$\mathbb{P}\{X_0 = i_0, X_1 = i_1, \cdots, X_{k-1} = i_{k-1}\} = \nu_0(i_0) p_{i_0 i_1} \cdots p_{i_{k-2} i_{k-1}}.$$

Bien qu'élémentaire, la notion de chaîne de Markov est fondamentale dans toute la théorie des processus de Markov. Elle est également largement utilisée dans de nombreux modèles, notamment en biologie, avec le processus de Galton-Watson par exemple dans les modèles de dynamique des populations (voir à ce sujet Kimmel and Axelrod [45])

Pour étudier le comportement en temps long d'une chaîne de Markov, il est naturel de regarder les distributions (ou lois) stationnaires (en temps).

Définition 2. *[Distribution stationnaire] Une loi de probabilité π sur E est dite stationnaire pour la chaîne de Markov de noyau de transition $\mathbf{P}$, si*

$$\pi^T = \pi^T \mathbf{P}. \tag{1}$$

De manière plus générale, une *mesure invariante* est une mesure positive (non nécessairement finie) qui vérifie la relation (1). Si une chaîne de Markov (X_n), de noyau de transition $\mathbf{P}$, est telle que X_0 a pour loi π, stationnaire pour $\mathbf{P}$, alors X_n est de loi π pour tout temps n. Il est alors naturel de se demander ce qu'il en est si la loi initiale est quelconque. Pour cela nous avons besoin de quelques définitions supplémentaires, qui sont utiles pour enlever certaines « pathologies ». Premièrement, la chaîne de Markov peut visiter différents sous-ensembles de l'espace d'états suivant sa condition initiale. Pour cela, on définit la notion d'irréductibilité.

Définition 3. *[Irréductibilité] Une chaîne de Markov est irréductible sur E si tous les états $i, j \in E$ communiquent, c'est à dire s'il existe un chemin fini $i, i_1, \cdots, i_k, j$ tel que*

$$p_{ii_1} p_{i_1 i_2} \cdots p_{i_{k-1} i_k} p_{i_k j} > 0.$$

Deuxièmement, si tous les états de E ont une chance d'être visités, une chaîne de Markov peut avoir un comportement périodique, « trop régulier » pour avoir de la densité. Pour mesurer le comportement périodique, on définit la notion de période.

Définition 4. *[Période] La période d_i d'un état $i \in E$ est par définition*

$$d_i = p.g.c.d\{n \geqslant 1, p_{ii}(n) > 0\},$$

où $p_{ii}(n)$ est la somme des probabilités des chemins de taille n reliant i à i, et $d_i = \infty$ si $p_{ii}(n) \equiv 0$.

Pour une chaîne de Markov irréductible, tous les états sont de même période. Si $d = 1$, on dit alors que la chaîne est *apériodique*.

Avec les notions d'irréductibilité et d'apériodicité, on est assuré que la chaîne visite tout l'espace, de façon « non dégénérée ». De manière informelle, on a alors la dichotomie suivante pour le comportement en temps long. Soit la chaîne « reste » essentiellement dans un compact, soit elle « part » à l'infini. On définit pour cela les notions de récurrence et transience, à l'aide des temps de premier retour

$$T_i = \inf\{n \geqslant 1, X_n = i \mid X_0 = i\}.$$

Définition 5. *[Récurrence et Transience] Un état $i \in E$ est récurrent si*

$$\mathbb{P}\{T_i < \infty\} = 1,$$

et transient sinon. Un état récurrent est positivement récurrent si

$$\mathbb{E}[T_i] < \infty.$$

À nouveau, pour une chaîne de Markov irréductible, si un état $i \in E$ est récurrent (respectivement positivement récurrent), alors tous les états $j \in E$ sont récurrents (respectivement positivement récurrents). On parle alors de chaîne de Markov récurrente (respectivement positivement récurrente). On a une relation forte entre la notion de récurrence et de mesure invariante, donnée par la propriété de régénération suivante :

Proposition 1. *[15, thm 2.1 p101] Soit (X_n) une chaîne de Markov irréductible récurrente, et $j \in E$ un état quelconque. Alors*

$$\nu(i) = \mathbb{E}\Big[\sum_{n \geqslant 1} \mathbf{1}_{\{X_n = i\}} \mathbf{1}_{\{n \leqslant T_j\}} \mid X_0 = j\Big], \quad i \in E,$$

est une mesure invariante pour (X_n).

On peut alors montrer que pour une chaîne de Markov irréductible récurrente, une mesure invariante est toujours unique, à facteur multiplicatif près. L'existence est donnée par le critère suivant, très utile dans la pratique :

Proposition 2. *[15, thm 3.1 p104] Une chaîne de Markov irréductible est positivement récurrente si et seulement s'il existe une distribution stationnaire. De plus, si elle existe, la distribution stationnaire est unique et strictement positive sur E.*

Finalement, le principal théorème de convergence asymptotique pour les chaînes de Markov (homogènes) à temps discret sur un espace d'états dénombrable s'énonce ainsi :

Théorème 2. *[15, thm 2.1 p130] Soit (X_n) une chaîne de Markov irréductible, positivement récurrente et apériodique, de noyau $\mathbf{P}$. Alors, pour tous μ et ν probabilités de distribution sur E, on a*

$$\lim_{n \to \infty} d(\mu^T \mathbf{P^n}, \nu^\mathbf{T} \mathbf{P^n}) = \mathbf{0},$$

où $d(\mu, \nu) = \displaystyle\sum_{i \in E} \mid \mu(i) - \nu(i) \mid.$

Ce théorème donne donc une convergence en *variation totale*. Cette convergence implique bien sûr une convergence en loi. La convergence en variation totale ne fait intervenir que les distributions marginales du processus. L'idée de la preuve est alors la suivante. On

utilise des modifications X'_n et X''_n de X_n pour montrer la convergence ci-dessus. La convergence en temps long revient à trouver deux modifications de X_n tel que $X'_n = X''_n$ après un temps aléatoire τ. On a alors en effet,

$$d(X'_n, X''_n) \leqslant \mathbb{P}\{\tau > n\}. \tag{2}$$

En considérant la chaîne produit (X'_n, X''_n), on montre qu'elle est irréductible (on utilise ici l'apériodicité), et possède une distribution stationnaire (donnée par le produit des deux distributions stationnaires). Par la proposition 2, on a $\mathbb{P}\{\tau < \infty\} = 1$, et on conclut d'après l'éq. (2).
Cette méthode s'appelle la méthode de couplage. Elle peut être étendue pour trouver la vitesse de convergence vers l'état stationnaire [15].

Pour la généralisation à un espace d'états quelconque, nous suivons Durrett [25]. Soit $(S, \mathbb{S})$ un espace mesurable, et un espace de probabilité $(\Omega, \mathbb{F}, \mathbb{P})$ muni d'une suite de filtrations $\mathbb{F}_n$ (que l'on peut penser comme les filtrations générées par $(X_0, X_1, \cdots, X_n)$). On définit maintenant une chaîne de Markov à espace d'états quelconque.

Définition 6. *(X_n) est une chaîne de Markov par rapport à la filtration $\mathbb{F}_n$ si $X_n \in \mathbb{F}_n$ et satisfait la propriété de Markov*

$$\mathbb{P}\{X_{n+1} \in B \mid \mathbb{F}_n\} = p(X_n, B),$$

où $p : S \times \mathbb{S} \to \mathbb{R}$ est tel que :
- *pour tout $x \in S$, $A \mapsto p(x, A)$ est une mesure de probabilité sur $(S, \mathbb{S})$,*
- *pour tout $A \in \mathbb{S}$, $x \mapsto p(x, A)$ est une fonction mesurable.*

Les lois de X_n sont déterminées par la propriété de Markov, comme dans le cas d'un espace dénombrable. L'existence des chaînes de Markov (X_n) est alors donnée par le théorème d'extension de Kolmogorov (voir par exemple [25, thm 7.1 p 474]).

Pour une chaîne de Markov à espace d'états quelconque, la notion d'irréductibilité est remplacée par la notion de chaîne de Harris.

Définition 7. *[Chaîne de Harris] Une chaîne de Markov (X_n) est une chaîne de Harris si on peut trouver deux ensembles $A, B \in \mathbb{S}$, une fonction q et une mesure de probabilité ρ sur B tels que :*
- *$q(x, y) \geqslant \varepsilon > 0$ pour tous $x \in A$, $y \in B$;*
- *si $T_A = \inf\{n \geqslant 0 : X_n \in A\}$, alors $\mathbb{P}\{T_A < \infty \mid X_0 = z\} > 0$ pour tout $z \in \mathbb{S}$;*
- *si $x \in A$ et $C \subset B$, alors $p(x, C) \geqslant \int_C q(x, y)\rho(dy)$.*

L'avantage de cette notion est qu'on peut toujours supposer (quitte à modifier l'espace S et la chaîne X_n) qu'une chaîne de Harris possède un point α qu'elle visite avec probabilité 1. Les notions de périodicité, récurrence et transience peuvent alors s'étendre aux chaînes de Harris en considérant ce point α. Nous donnerons simplement le théorème de convergence analogue au théorème 2 (légèrement moins fort) :

Théorème 3. *[25, thm 6.8 p 332] Soit (X_n) une chaîne de Harris apériodique récurrente. Si (X_n) a une distribution stationnaire π, et si α est tel que*

$$\mathbb{P}\{T_\alpha < \infty \mid X_0 = x\} = 1,$$

alors

$$\lim_{n \to \infty} d_v(\delta_x^T \mathbf{P^n}, \pi) = \mathbf{0}.$$

6.2   Chaîne de Markov à temps continu

Nous allons commencer par rappeler la définition d'un processus ponctuel de Poisson (sur $\mathbb{R}^+$), puis introduire les chaînes de Markov à temps continu, via l'approche des semi-groupes de transition. Cette approche a l'avantage de se généraliser « facilement » aux processus de Markov par morceaux (et à bien d'autres objets), que nous introduirons ensuite. Tout comme les chaînes de Markov en temps discret sont une variante aléatoire des équations aux différences, les chaînes de Markov à temps continu peuvent être vues comme une généralisation des équations différentielles ordinaires. Le « second membre » de l'équation différentielle ordinaire (autonome) $\frac{dx}{dt} = f(x)$ se traduit par le générateur infinitésimal de la chaîne de Markov (homogène). Nous suivons à nouveau le livre de Brémaud [15]. Nous présentons d'abord les chaînes de Markov à espace d'états dénombrables, pour lesquelles une condition naturelle sur le générateur peut être donnée pour que le processus soit de saut pur (voir plus bas). Nous passerons enfin aux chaînes de Markov à espace d'états général (on parle plus généralement de processus de Markov), et présenterons les techniques de martingales et de fonction de Lyapounov pour leur stabilité.

Définition 8. *[Chaîne de Markov homogène à temps continu et espace d'états dénombrable] Une collection de variables aléatoires $(X_t)_{t \geqslant 0}$, indexée par $\mathbb{R}_+$, définie sur un espace de probabilité $(\Omega, \mathbb{F}, \mathbb{P})$, à valeurs dans E espace d'états dénombrable est une chaîne de Markov homogène si pour tout entier $n \geqslant 0$, tous états $i_1, \cdots, i_n, i, j$, et pour tous temps $t, s \geqslant 0$, $0 \leqslant s_1, \cdots, s_n \leqslant s$*

$$\mathbb{P}\big\{X_{t+s} = j \mid X_s = i, X_{s_n} = i_n, \cdots, X_{s_1} = i_1\big\} = \mathbb{P}\big\{X_{t+s} = j \mid X_s = i\big\},$$

dès que les deux membres sont bien définis, et cette quantité ne dépend pas de s.

Soit $\mathbf{P}(t) = \{p_{ij}(t)\}_{i,j \in E}$ où $p_{ij}(t) = \mathbb{P}\big\{X_{t+s} = j \mid X_s = i\big\}$. Alors $\mathbf{P(t)}$ est un semi-groupe de transition, c'est-à-dire :
- $\mathbf{P}(t)$ est une matrice stochastique ($\sum_j p_{ij}(t) = 1$),

- $\mathbf{P}(0) = I$,
- $\mathbf{P}(t+s) = \mathbf{P}(t)\mathbf{P}(s)$.

Pour un semi-groupe continu, tel que $\lim_{h \to 0} \mathbf{P(h)} = \mathbf{P(0)} = \mathbf{I}$ (convergence élément par élément), les quantités suivantes existent toujours :

Définition 9. *[Generateur] Pour tout état $i \in E$, on définit*

$$q_i = \lim_{h \to 0} \frac{1 - p_{ii}(h)}{h} \in [0, \infty],$$

et pour tout $i \neq j \in E$,

$$q_{ij} = \lim_{h \to 0} \frac{p_{ij}(h)}{h} \in [0, \infty].$$

On pose également

$$q_{ii} = -q_i,$$

et la matrice $\boldsymbol{A} = \{q_{ij}\}_{i,j \in E}$ est appelée générateur infinitésimal du semi-groupe (ou de la chaîne de Markov).

Remarque 4. *En notation matricielle, on a*

$$\boldsymbol{A} = \lim_{h \to 0} \frac{\boldsymbol{P}(h) - \boldsymbol{P}(0)}{h}.$$

La notion « équivalente » de chaîne de Markov à temps discret est la notion de processus Markovien de saut pur (régulier), que l'on rencontrera plusieurs fois par la suite :

Définition 10 (Processus de saut pur). *Un processus stochastique $(X_t)_{t \geqslant 0}$ à valeurs dans E (espace d'état général) est un processus de saut pur si, pour presque tout $\omega \in \Omega$, et $t \geqslant 0$, il existe $\varepsilon(t, \omega) > 0$ tel que*

$$X(t + s, \omega) = X(t, \omega), \quad pour\ tout\ s \in [t, t + \varepsilon(t, \omega)).$$

Il est régulier si l'ensemble des discontinuités $D(\omega)$ de $t \mapsto X(t, \omega)$ est σ-discret, c'est-à-dire, pour tout $c \geqslant 0$,

$$card(D(\omega) \cap [0, c]) < \infty.$$

Étant donné une matrice $\mathbf{A}$, on peut donner une construction très simple d'un processus Markovien de saut pur qui admette $\mathbf{A}$ pour générateur, en imposant une condition supplémentaire sur $\mathbf{A}$. Cette construction est à la base des modèles de réactions chimiques, des modèles déterministes par morceaux (utilisés notamment dans le chapitre 1), et des processus ponctuels (utilisés dans le chapitre 2). Nous détaillons donc cette construction ci-dessous. L'ingrédient élémentaire est le processus de Poisson (homogène). Un processus de Poisson est un processus de comptage d'événements sur $\mathbb{R}_+$, qui ont lieu successivement et indépendamment les uns des autres suivant une loi exponentielle. Plus précisément, on peut prendre la définition suivante :

Définition 11. *Un processus $(N_t)_{t \geqslant 0}$ est un processus de Poisson homogène d'intensité $\lambda > 0$ si $N_0 = 0$, et*
- *pour tous temps $0 \leqslant t_1 \leqslant \cdots \leqslant t_k$, les variables aléatoires $N_{t_{k+1}} - N_{t_k}, \cdots, N_{t_2} - N_{t_1}$ sont indépendantes ;*
- *pour tous $0 \leqslant a < b$, $N(b) - N(a)$ est une variable de Poisson de moyenne $\lambda(b - a)$.*

Avec cette définition, on peut montrer qu'un processus de Poisson admet la représentation équivalente,

$$N(t) = \sum_{n \geqslant 1} \mathbf{1}_{\{(0, T]\}}(T_n),$$

où les temps d'événements T_n sont tels que $0 = T_0 < T1 < T_2 < \cdots$ et les variables $S_n = T_n - T_{n-1}$ sont indépendantes et identiquement distribuées suivant une loi exponentielle de paramètre λ. On montre également avec cette définition que deux événements se produisent en même temps avec probabilité nulle (donc le processus de Poisson augmente de 1 en 1) et qu'il n'y a pas d'explosion, c'est-à-dire

$$\lim_{n \to \infty} T_n = \infty, \quad presque\ s\hat{u}rement.$$

Finalement, si on a deux (ou plus généralement une famille dénombrable) processus de Poisson indépendants, on montre aussi que deux événements ne se produisent pas en même temps (avec probabilité un) et que la somme des processus est encore un processus de Poisson, d'intensité donnée par la somme des intensités (si elle est finie dans le cas dénombrable).

Nous pouvons maintenant donner la construction d'un processus Markovien de saut pur qui admette $\mathbf{A}$ pour générateur. On suppose pour cela :

Hypothèse 1. $q_i < \infty, \quad q_i = \sum_{j \neq i} q_{ij}.$

Soit $\{N_{i,j}\}_{i,j\in E, i\neq j}$ une famille de processus de Poisson d'intensités respectives $\{q_{i,j}\}_{i,j\in E, i\neq j}$, et un état initial $X(0)$ indépendant de cette famille de processus. On pose alors

$$X(t) = X_n, \quad \text{pour } t \in [T_n, T_{n+1}),$$

où les couples (T_n, X_n) sont définis récursivement par
- $T_0 = 0$, $X_0 = X(0)$,

et, pour tout $n \geqslant 0$, si $T_n < \infty$, et $X_n = X(T_n) = i \in E$, alors
- si $q_i = 0$, on pose $X_{n+m} = \Delta$ (point cimetière) et $T_{n+m} = \infty$, pour tout $m \geqslant 1$;
- sinon T_{n+1} est le premier événement qui a lieu après T_n des processus $\{N_{i,j}\}_{j\neq i \in E}$, et X_{n+1} est donné par l'index $k \neq i$ pour lequel le processus de Poisson $N_{i,k}$ réalise ce premier événement.

Cette construction est valide (T_n, X_n sont bien définis donc $X(t)$ également) jusqu'au temps d'explosion $T_\infty = \lim_{n\to\infty} T_n$. On a alors la proposition suivante :

Proposition 3. *[15, thm 1.2 p373] Si les conditions données par l'hypothèse 1 sont valables, et si $T_\infty = \infty$ presque sûrement, le processus construit ci-dessus est un processus Markovien de saut pur régulier de générateur infinitésimal* $\mathbf{A}$.

La preuve repose sur le calcul de $\mathbb{P}\{X(t) = j \mid X(0) = i\}$. Si $j \neq i$, alors $T_1 < t$, et, par indépendance, il vient

$$\mathbb{P}\{X(t) = j, T_1 < t \mid X(0) = i\} = (1 - e^{-q_i t})\frac{q_{ij}}{q_i}. \tag{3}$$

Enfin, on montre que $\mathbb{P}\{T_2 \leqslant t \mid X(0) = i\}$ est négligeable devant t, d'où

$$\lim_{t\to 0} \frac{1}{t}\mathbb{P}\{X(t) = j \mid X(0) = i\} = q_{ij}.$$

$\square$

Remarque 5. *Cette approche des processus de saut pur est à la base des équations stochastiques dirigées par des processus de Poisson, et plus généralement des systèmes stochastiques dirigés par des processus ponctuels. Cette approche donne aussi directement une méthode de simulation des trajectoires du processus de saut pur, appelée algorithme de Gillespie [33] dans le contexte des modèles de réactions biochimiques. La méthode de construction décrite ci-dessus correspond à l'algorithme de « la prochaîne réaction ». A chaque événement, on simule uniquement le prochain temps d'événement du processus de Poisson qui correspond à la transition que l'on vient d'effectuer. En gardant en mémoire tous les prochains événements possibles (pour lesquels $q_{ij} \neq 0$, si l'on est dans l'état i), on avance alors le temps au minimum de tous ces prochains événements possibles, on effectue la transition correspondante, et ainsi de suite. Cette version a l'avantage d'être largement généralisable à des processus ponctuels non Markoviens (avec retard, ou distribution de temps d'événement non exponentielle, voir par exemple [2]). Une autre version de cet algorithme, appelée « méthode directe », vient de la formule (3) utilisée dans la preuve ci-dessus. Le prochain temps d'événement est donné par une exponentielle de paramètre $q_i = \sum_{j\neq i} q_{ij}$ et la transition effectuée est déterminée par un autre nombre aléatoire qui vaut j avec probabilité $\frac{q_{ij}}{q_j}$. Cette méthode ne garde pas de valeurs en mémoire (autres que l'état dans lequel on est) mais demande de générer deux nombres aléatoires à chaque pas de temps.*

Avant de passer à la description des processus de Markov plus généraux, citons un critère de convergence en temps long pour les processus Markoviens de saut pur. De la description

trajectorielle que l'on a donnée, on peut voir qu'un processus Markovien de saut pur est lié à une chaîne de Markov discrète, donnée par les valeurs après les sauts X_n. On étend les notions d'irréductibilité, de récurrence et de positive récurrence au processus Markovien de saut pur. La même forme régénératrice (voir proposition 1) est encore valable entre les mesures invariantes (pour le semi-groupe $P(t)$) et les temps de premier retour, et on a alors :

Théorème 6. *Un processus Markovien de saut pur régulier de générateur infinitésimal* **A***, irréductible, est positivement récurrent si et seulement s'il existe une loi de probabilité π sur E telle que*

$$\pi^T \mathbf{A} = \mathbf{0}.$$

Dans ce cas, on a $\lim_{t\to\infty} p_{ij}(t) = \pi(j)$ *pour tous* $i, j \in E$.

Remarque 7. *Notons les différences entre les théorèmes 2 et 6. Dans le cas continu, on n'a pas besoin de supposer la chaîne apériodique. Les temps de passage dans un état sont suffisamment aléatoires pour éviter le comportement périodique. Notons aussi qu'il n'y a pas forcément de relation entre la convergence en temps long du processus Markovien de saut pur et de sa chaîne de Markov en temps discret correspondante. En particulier, on a la relation entre une mesure invariante ν pour le processus Markovien de saut pur et μ pour la chaîne discrète*

$$\mu(i) = q_i \nu(i),$$

qui montre que toutes les possibilités sont ouvertes pour les valeurs respectives de $\sum_{i\in E} \mu(i)$ *et* $\sum_{i\in E} \nu(i)$ *en fonction du comportement de la suite* $(q_i)_{i\in E}$.

Pour une théorie équivalente sur les processus Markoviens de saut pur à valeurs dans un espace quelconque, voir par exemple [22]). Nous passons maintenant au processus de Markov plus généraux.

6.3 Processus de Markov

Dans toute cette partie, E est un espace polonais (*i.e.* métrique séparable complet) muni de sa structure borélienne $\mathbb{B}(E)$. L'ensemble des fonctions mesurables bornées sur E est noté $B(E)$, que l'on munit de la norme « infini » usuelle. L'ensemble des fonctions à valeurs réelles, continues à droite et avec limite finie à gauche (« cad-lag ») sur $[0, \infty)$ est noté $D_E[0, \infty)$. On munit $D_E[0, \infty)$ de la topologie de Skorokhod S_E. Nous suivrons dans un premier temps principalement le livre de Ethier and Kurtz [30]. On utilise la définition suivante :

Définition 12 (Processus de Markov homogène)**.** *Une collection de variables aléatoires $(X_t)_{t\geqslant 0}$, indexées par $\mathbb{R}_+$, définies sur un espace de probabilité $(\Omega, \mathbb{F}, \mathbb{P})$ munie d'une filtration $(\mathbb{F}_t)_{t\geqslant 0}$, à valeurs dans E, un espace polonais, est un processus de Markov homogène par rapport à $(\mathbb{F}_t)_{t\geqslant 0}$ si pour tous $s, t \geqslant 0$ et $B \in \mathbb{B}(B)$,*

$$\mathbb{P}\{X_{t+s} \in B \mid \mathbb{F}_t\} = \mathbb{P}\{X_{t+s} \in B \mid X_t\} =: P(s, X(t), B),$$

La fonction $P(t, x, B)$, définie sur $[0, \infty) \times E \times \mathbb{B}(B)$ est appelée fonction de transition et satisfait :
- *$P(t, x, \cdot)$ est une mesure de probabilité sur E, pour tous (t, x),*
- *$P(0, x, \cdot) = \delta_x$, pour tout x,*
- *$P(\cdot, \cdot, B)$ est mesurable sur $[0, \infty) \times E$, pour tout $B \in \mathbb{B}(B)$,*

- *la relation de Chapman-Kolmogorov, pour tous $s, t \geqslant 0$, $x \in E$ et $B \in \mathbb{B}(B)$*

$$P(t + s, x, B) = \int P(s, y, B) P(t, x, dy). \tag{4}$$

De manière similaire au cas des chaînes de Markov, les lois des n-uplets de X_t sont déterminées par la relation de Chapman-Kolmogorov eq. (4). La topologie sur E (polonais) permet d'assurer que ces lois (dites de *dimensions finies*) déterminent de manière unique un processus de Markov sur E. Comme pour le cas des chaînes de Markov, la relation de Chapman-Kolmogorov définit en un certain sens une structure de semi-groupe sur les fonctions de transition. Cependant, peu de processus stochastiques ont des formules connues pour les fonctions de transition (à l'exception du mouvement Brownien, ou de quelques autres processus comme le Ornstein-Uhlenbeck), et il est plus facile de travailler avec le semi-groupe sur les fonctions bornées de E, donné par

$$T(t)f(x) = \int f(y) P(t, x, dy) = \mathbb{E}\big[f(X(t)) \mid X(0) = x \big].$$

Il est classique que le semi-groupe $\{T(t)\}$ sur $B(E)$ (et même sur un sous-ensemble suffisamment gros), avec une loi initiale, détermine de manière unique les lois de dimensions finies de $X(t)$. Aussi, de par sa définition, $T(t)$ est un semi-groupe de contraction sur $B(E)$ muni de la norme infini sur E. On cherche dans quel cas le générateur infinitésimal de $T(t)$ caractérise le semi-groupe, et donc le processus de Markov $X(t)$. Pour utiliser la théorie classique des semi-groupes, il faut des semi-groupes fortement continus. On va voir que cela définit une sous-classe importante, mais restrictive, de processus de Markov. Ce sont les *processus de Feller*. Il suffit de regarder le semi-groupe $\{T(t)\}$ sur l'espace $C_0(E)$ des fonctions continues sur E et de limite nulle à l'infini, muni de la norme « infini », $\sup_{x \in E} \mid f(x) \mid$. Si $\{T(t)\}$ est un semi-groupe positif de contraction sur $C_0(E)$, fortement continu ($\lim_{t \to 0} T(t)f = f$), le théorème de Hille-Yosida caractérise alors le générateur de $T(t)$ et celui-ci détermine de manière unique un processus de Markov. Le résultat précis, dans le contexte des processus stochastique, est le suivant :

Proposition 4 (Processus de Feller). *[30, thm 2.2 p165] Soit E localement compact et séparable, et $\mathbf{A}$ un opérateur linéaire sur $C_0(E)$, qui vérifie*
- *le domaine de $\mathbf{A}$, $\mathcal{D}(\mathbf{A})$ est dense dans $C_0(E)$,*
- *$\mathbf{A}$ satisfait le principe du maximum positif :*

$$\text{si } f(x_0) = \sup_{x \in E} \mid f(x) \mid \geqslant 0, \text{ alors } \boldsymbol{A}f(x_0) \leqslant 0.$$

- *l'image de $(\lambda I - \boldsymbol{A})$ est dense dans $C_0(E)$ pour un certain $\lambda > 0$.*
Soit alors $T(t)$ le semi-groupe de contraction positif, fortement continu sur $C_0(E)$ généré par la fermeture de $\mathbf{A}$. Alors il existe pour tout $x \in E$ un processus de Markov X_x correspondant à $T(t)$, de loi initiale δ_x et de trajectoires dans $D_E[0, \infty)$ si et seulement si $\mathbf{A}$ est conservatif (c'est-à-dire $(f, g) = (1, 0)$ est dans la fermeture de $\mathbf{A}$). Un tel processus est appelé processus de Feller.

Une autre classe importante de processus pour lesquels le générateur est « facilement » caractérisable sont les processus de saut pur, que l'on a déjà rencontrés dans le cas d'un espace d'états dénombrable. Si $\mu(x, B)$ est une fonction de transition et $\lambda \in B(E)$, alors

$$\mathbf{A}f(x) = \lambda(x) \int (f(y) - f(x)) \mu(x, dy)$$

est un opérateur borné sur $B(E)$, et $\mathbf{A}$ est le générateur d'un processus de saut pur qui peut être construit de manière analogue au cas d'un espace d'états dénombrable (voir proposition 3). En particulier, on peut lui associer une chaîne de Markov Y_n à temps discret sur E, de fonction de transition $\mu(x, B)$ et les temps de saut sont déterminés par des lois exponentielles de paramètres $\lambda(Y_n)$.

Finalement, une approche plus générale, largement reconnue et utilisée actuellement (notamment pour sa commodité avec les théorèmes limites), est celle du problème de martingale, utilisé notamment par Stroock et Varadhan [78] pour caractériser les diffusions sur $\mathbb{R}^d$, et Jacod et Shiryaev [39] pour des processus à accroissements indépendants. Elle repose sur le générateur étendu, défini par :

Définition 13 (Générateur étendu). *Soit $\{T(t)\}$ un semi-groupe de contractions sur $B(E)$. Son générateur étendu est défini comme l'opérateur (possiblement multi-valué)*

$$\hat{A} = \left\{ (f, g) \in B(E) \times B(E) : T(t)f - f = \int_0^t T(s)g\,ds \right\}.$$

On a alors la proposition classique mais fondamentale :

Proposition 5. *[30, thm 1.7 p162] Soit $X(t)$ un processus de Markov à trajectoires dans $D_E[0, \infty)$ de fonction de transition $P(t, x, B)$. Soient $\{T(t)\}$ son semi-groupe sur $B(E)$ associé, et $\hat{A}$ son générateur étendu. Alors, si $(f, g) \in \hat{A}$,*

$$M(t) \equiv f(X(t)) - \int_0^t g(X(s))\,ds,$$

est une martingale par rapport à la filtration $\mathbb{F}_t^X$ canonique associée $X(t)$.

L'hypothèse sur les trajectoires de $X(t)$ est suffisante pour que l'intégrale définissant $M(t)$ ait un sens (mais on peut faire mieux). L'idée de la preuve de cette proposition réside dans un simple calcul :

$$\mathbb{E}\big[M(t + u) \mid \mathbb{F}_t^X\big] = \mathbb{E}\big[f(X(t + u)) \mid \mathbb{F}_t^X\big] - \int_0^{t+u} \mathbb{E}\big[g(X(s)) \mid \mathbb{F}_t^X\big]ds,$$

$$= \mathbb{E}\big[f(X(t + u)) \mid X(t)\big] - \int_t^{t+u} \mathbb{E}\big[g(X(s)) \mid X(t)\big]ds - \int_0^t g(X(s))\,ds,$$

$$= T(u)f(X(t)) - \int_0^u T(s)g(X(t))\,ds - c,$$

$$= f(X(t)) - \mathbb{E}\big[g(X(s)) \mid \mathbb{F}_t^X\big] = M(t).$$

La deuxième ligne est donnée par la propriété de Markov (pour les deux premières intégrales) et la propriété de l'espérance conditionnelle (pour la troisième intégrale). Le reste suit par définition du semi-groupe et de son générateur étendu.

Le problème de martingale consiste, étant donné un générateur A et une loi initiale μ sur E, à trouver une mesure de probabilité $P \in \mathbb{P}\big(D_E[0, \infty)\big)$ telle que le processus défini sur l'espace $(D_E[0, \infty), S_E, P)$ par

$$X(t, \omega) \equiv w(t), \quad \omega \in D_E[0, \infty), \quad t \geqslant 0,$$

vérifie :

$$f(X(t)) - \int_0^t g(X(s))\,ds$$

est une martingale par rapport à la filtration $\mathbb{F}_t^X$ canonique associé $X(t)$, pour tout $(f, g) \in A$, et $X(0)$ a pour loi μ.

Des conditions générales sur le générateur étendu $\hat{A}$ pour avoir existence et unicité de la solution du problème de martingale sont difficiles à obtenir. Ceci est le prix à payer pour une théorie générale. Dans la pratique, par contre, si l'on se donne *a priori* la forme du générateur, il est souvent possible de donner des conditions sur les coefficients du générateur pour que le problème de martingale associé soit bien posé (voir par exemple le cas des diffusions traité par Stroock et Varadhan [78], et des semi-martingales — comprenant les processus ponctuels, les processus à accroissements indépendants, les diffusions avec sauts— traité par Jacod et Shiryaev [39]).

On peut néanmoins dégager plusieurs principes généralement valables pour le problème de l'existence et l'unicité de la solution du problème de martingale. L'existence peut être obtenue par une limite faible de solution d'un problème de martingale approché, donnée par la proposition suivante :

Proposition 6. *[30, prop 5.1 p196] Soit $A \subset C_b(E) \times C_b(E)$ et $A_n \subset B(E) \times B(E)$, $n = 1, 2, \cdots$. On suppose que pour tout couple $(f, g) \in A$, il existe $(f_n, g_n) \in A_n$ tel que*

$$\lim_{n \to \infty} \|f_n - f\| = 0, \quad \lim_{n \to \infty} \|g_n - g\| = 0.$$

Soit alors X_n une solution du problème de martingale pour A_n, avec trajectoires dans $D_E[0, \infty)$, si $X_n \Rightarrow X$ (convergence en loi), alors X est une solution du problème de martingale pour A.

Une autre technique souvent utilisée est la localisation. Elle consiste à se ramener au cas où la solution du problème de martingale est contenue dans un ouvert (que l'on prendra borné en général) de E par un argument de troncature. Une solution du problème de martingale arrêtée en un ouvert U est (formellement) une solution du problème de martingale pour tout temps plus petit que le temps de sortie de U.

Proposition 7. *[30, thm 6.3 p219] Soit $A \subset C_b(E) \times B(E)$. Soit $U_1 \subset U_2 \subset \cdots$ ouvert de E. Soit $\nu \in \mathbb{P}(E)$ une loi initiale, telle que pour tout k il existe une unique solution X_k au problème de martingale (A, ν) arrêtée en U_k, avec trajectoires dans $D_E[0, \infty)$. On pose*

$$\tau_k = \inf\{t : X_k(t) \notin U_k \text{ ou } X_k(t^-) \notin U_k\}.$$

Si pour tout $t > 0$,

$$\lim_{k \to \infty} \mathbb{P}(\tau_k \leqslant t) = 0,$$

alors il existe une unique solution au problème de martingale (A, ν) avec trajectoires dans $D_E[0, \infty)$.

Finalement, donnons un procédé qui sera utilisé dans le chapitre 2 pour obtenir l'unicité de la solution du problème de martingale. Supposons que le générateur A soit le générateur infinitésimal d'un semi-groupe fortement continu. Alors de manière classique l'opérateur A est fermé, et la résolvante $(\lambda - A)^{-1}$ est définie pour tout $\lambda > 0$. Supposons que pour tout $x \in E$, il existe une solution au problème de martingale (A, δ_x) (ce qui sera donné si on sait qu'il existe un processus de Markov associé au semi-groupe fortement continu). Un simple calcul montre que, pour tous $(f, g) \in A$, $\lambda > 0$,

$$e^{-\lambda t} f(X_x(t)) + \int_0^t e^{-\lambda s} (\lambda f(X_x(s)) - g(X_x(s))) ds \tag{5}$$

est une martingale. Il vient alors que

$$f(x) = \mathbb{E}\Big[\int_0^\infty e^{-\lambda s}(\lambda f(X_x(s)) - g(X_x(s)))ds\Big].$$

On en déduit alors $\lambda\|f\| \leqslant \|\lambda f - g\|$. On a donc la proposition :

Proposition 8. *[30, prop 3.5 p178] Soit A opérateur linéaire, $A \subset B(E) \times B(E)$. S'il existe une solution au problème de martingale (A, δ_x) pour tout $x \in E$, alors A est dissipatif (voir section 5).*

Cette proposition permet de montrer de manière simple qu'un opérateur est dissipatif. On peut alors conclure à l'unicité de la solution du problème de martingale en identifiant une classe de fonctions séparatrice, comme dans le théorème suivant :

Théorème 8. *[30, corollaire 4.4 p187] Soit E séparable et $A \subset B(E) \times B(E)$ linéaire et dissipatif. On suppose que pour un (et donc tous) $\lambda > 0$, $\overline{Im(\lambda - A)} \supset \mathcal{D}(A)$, et qu'il existe $M \subset B(E)$ séparatrice, $M \subset \overline{Im(\lambda - A)}$ pour tout $\lambda > 0$. Alors pour toute loi initiale μ, deux solutions du problème de martingale pour (A, μ) à trajectoires dans $D_E[0, \infty)$, ont même loi sur $D_E[0, \infty)$.*

L'ingrédient clé de cette preuve repose toujours sur l'identification de la martingale donnée par l'éq. (5). En particulier, pour tout $h \in M$, si X et Y sont solutions du même problème de martingale,

$$\mathbb{E}\Big[\int_0^\infty e^{-\lambda t}h(X(t))dt\Big] = \int(\lambda - A)^{-1}hd\mu = \mathbb{E}\Big[\int_0^\infty e^{-\lambda t}h(Y(t))dt\Big],$$

ce qui suffit, par propriété de la transformée de Laplace et de l'hypothèse sur M, pour identifier les lois de X et Y.

On termine cette section en discutant de la convergence en temps long pour les processus de Markov. L'approche la plus générale et utile dans la pratique est donnée par les fonctions de Lyapounov pour le générateur étendu. Voir les travaux de Meyn et Tweedie dans une série de trois papiers [58, 59, 60]. Pour des modèles particuliers, les approches par couplage peuvent s'avérer également très puissantes, et donner des taux de convergence explicites très satisfaisants (voir par exemple Bardet et al. [8]). Les idées des méthodes de fonctions de Lyapounov s'appuient sur des conditions de dérive du générateur pour des fonctions bien choisies, qui transmettent des propriétés au processus grâce à la formule de Dynkin. Comme pour les chaînes de Markov à temps discret et à espace d'états quelconque, il faudra supposer une certaine forme de régénération supplémentaire, similaire à la propriété des chaînes de Harris énoncée dans la définition 7. La puissance des théorèmes de Meyn et Tweedie réside dans l'utilisation d'une chaîne discrète obtenue à partir d'un échantillonnage (quelconque) du processus de Markov. Ceci rend leurs résultats largement utilisables dans beaucoup de cas.

Dans tout ce qui suit, on suppose que E est un espace polonais localement compact, muni de sa structure borélienne $\mathbb{B}(E)$. On suppose que $X(t)$ est un processus de Markov à trajectoires dans $D_E[0, \infty)$. On redéfinit les concepts d'explosion, d'irréductibilité, de récurrence, de récurrence de Harris et de récurrence de Harris positive. On note O_n une famille d'ouverts pré-compacts de E tel que $O_n \to E$ quand $n \to \infty$, et τ_n les premiers temps d'entrée de X_t dans O_n^c. On dit alors que $X(t)$ est *non explosif* (ou *régulier*) si

$$\mathbb{P}\Big\{\lim_{n\to\infty} \tau_n = \infty \mid X(0) = x\Big\} = 1, \quad \forall x \in E.$$

On note $\{X_t \to \infty\}$ si $X_t \in C^c$ pour tout compact $C \in \mathbb{B}(E)$ et t suffisamment grand. On dit alors que $X(t)$ est *non évanescent* si

$$\mathbb{P}\big\{\{X_t \to \infty\} \mid X(0) = x\big\} = 0, \quad \forall x \in E.$$

Pour un ensemble mesurable A, on définit

$$T_A = \inf\{t \geqslant 0 : X_t \in A\}, \quad n_A = \int_0^\infty \mathbf{1}_{\{X_t \in A\}}dt.$$

$X(t)$ est ϕ-*irréductible* si pour une mesure σ-finie ϕ,

$$\phi(B) > 0 \Longrightarrow \mathbb{E}\big[T_B \mid X(0) = x\big] < \infty, \forall x \in E.$$

$X(t)$ est *Harris récurrent* si pour une mesure σ-finie ϕ,

$$\phi(B) > 0 \Longrightarrow \mathbb{P}\big\{n_B = \infty \mid X(0) = x\big\} = 1, \forall x \in E.$$

Une mesure invariante μ pour un processus de Markov $X(t)$, de fonction de transition $P(t, x, B)$, est telle que

$$\mu(A) = \mu P(t, \cdot, A) = \int P(t, x, A)\mu(dx).$$

Comme pour les chaînes de Markov récurrentes, un processus de Markov Harris récurrent possède, à un facteur multiplicatif près, une unique mesure invariante. Si elle est finie, on peut alors la normaliser en une distribution de probabilité, et on parle alors de processus de Markov *positivement Harris récurrent*.

Un échantillonnage d'un processus de Markov est donné par les valeurs du processus de Markov à certains temps, déterministes ou aléatoires. L'échantillonnage le plus simple est celui donné par la résolvante, $R : E \times \mathbb{B}(E) \mapsto [0, 1]$,

$$R(x, A) = \int_0^\infty P(t, x, A)e^{-t}dt. \tag{6}$$

Si (t_k) est une suite d'instants générés par des incréments indépendants entre eux (et de X_t) et distribués suivant une loi exponentielle de paramètre 1, alors (X_{t_k}) est une chaîne de Markov à temps discret, de noyau R. Plus généralement, étant donnée une loi de probabilité a sur $\mathbb{R}_+$, on définit

$$K_a(x, A) = \int_0^\infty P(t, x, A)a(dt).$$

Pour (t_k) une suite d'instants d'accroissements indépendants suivant a, X_{t_k} est alors une chaîne de Markov à temps discret, de noyau K_a. Meyn et Tweedie [59, 60, 58] ont prouvé de nombreux liens entre le processus de Markov et les K_a-échantillons.

Une classe importante de processus de Markov pour lesquels des résultats de stabilité existent sont les T-processus :

Définition 14. *Un processus de Markov est un T-processus s'il existe une mesure de probabilité a sur $\mathbb{R}_+$ et une fonction non triviale $T : E \times \mathbb{B}(E) \mapsto \mathbb{R}_+$ ($T(x, E) > 0$) tels que :*
- *pour tout $B \in \mathbb{B}(E)$, $T(\cdot, B)$ est semi-continu inférieurement ;*
- *pour tous $x \in E$, $B \in \mathbb{B}(E)$, $K_a(x, B) \geqslant T(x, B)$.*

En lien avec cette notion, nous avons également la notion d'ensemble *petit* :

Définition 15. *Un ensemble non vide $C \in \mathbb{B}(E)$ est dit ν-petit si ν est une mesure non triviale sur $\mathbb{B}(E)$, et s'il existe a une mesure de probabilité sur $\mathbb{R}_+$ tel que $K_a(x, \cdot) \geqslant \nu(\cdot)$ pour tout $x \in C$. On dit simplement que C est petit si la donnée de ν n'est pas importante.*

La relation entre ces deux notions est donnée par la proposition suivante :

Proposition 9. *[59, prop 4.1] Supposons $\mathbb{P}\big\{\{X_t \to \infty\} \mid X(0) = x\big\} < 1$ pour un $x \in E$. Alors tout ensemble compact est petit si et seulement si X_t est irréductible et est un T-processus.*

Nous donnons maintenant les critères de stabilité pour un processus de Markov basé sur des fonctions de Lyapounov et sur les notions rappelées ci-dessus. On note O_n une famille d'ouverts pré-compacts de E tel que $O_n \to E$ quand $n \to \infty$, et on note X^n le processus stochastique $X(t)$ arrêté en O_n, et A_n son générateur. Dans toute la suite, V est une fonction de Lyapounov $E \to \mathbb{R}_+$, si elle est mesurable, strictement positive et telle que $V(x) \to \infty$ quand $x \to \infty$. Un critère de non explosion s'énonce ainsi :

Proposition 10. *[60, thm 2.1] S'il existe une fonction V de Lyapounov, et $c > 0, d \geqslant 0$ tels que*

$$A_n V(x) \leqslant cV(x) + d, \quad x \in O_n, \quad n \geqslant 1,$$

alors
- *$X(t)$ est non explosif ;*
- *il existe une variable aléatoire D finie presque sûrement tel que $V(X_t) \leqslant De^{ct}$;*
- *la variable aléatoire D satisfait la borne $\mathbb{P}\big\{D \geqslant a \mid X(0) = x\big\} \leqslant \frac{V(x)}{a}$, $a > 0$, $x \in E$;*
- *$\mathbb{E}\big[V(X_t) \mid X(0) = x\big] \leqslant e^{ct}V(x).$*

Un critère de non-évanescence est donné par :

Proposition 11. *[60, thm 3.1] S'il existe une fonction V de Lyapounov, $d > 0$ et C un compact tels que*

$$A_n V(x) \leqslant d\mathbf{1}_{\{C\}}(x), \quad x \in O_n, \quad n \geqslant 1,$$

alors $X(t)$ est non évanescent.

Un critère de récurrence est donnée par :

Proposition 12. *[60, thm 4.1] S'il existe une fonction V de Lyapounov, $d > 0$ et C un compact tels que*

$$A_n V(x) \leqslant d\mathbf{1}_{\{C\}}(x), \quad x \in O_n, \quad n \geqslant 1,$$

et tels que tous les ensembles compacts sont petit, alors $X(t)$ est Harris récurrent.

Un critère de récurrence positive est donnée par :

Proposition 13. *[60, thm 4.2] S'il existe $c, d > 0$, C un ensemble petit fermé, $f \geqslant 1$ et $V \geqslant 0$ borné sur C tels que*

$$A_n V(x) \leqslant -cf(x) + d\mathbf{1}_{\{C\}}(x), \quad x \in O_n, \quad n \geqslant 1,$$

alors, si $X(t)$ est non explosif, $X(t)$ est positivement Harris récurrent et sa mesure invariante est finie.

On termine par un critère d'ergodicité exponentielle :

Proposition 14. *[60, thm 6.1] S'il existe une fonction V de Lyapounov, $c, d > 0$, tels que*

$$A_n V(x) \leqslant -cf(x) + d, \quad x \in O_n, \quad n \geqslant 1,$$

et tels que tous les ensembles compacts sont petit, alors, il existe $\beta < 1$ et $B < \infty$ tels que

$$\|P(t, x, \cdot) - \pi\|_f \leqslant Bf(x)\beta^t, \quad x \in E, \quad t \geqslant 0,$$

avec $f = V + 1$ et où $\|\mu\|_f = \sup_{|g| \leqslant f} |\mu(g)|$.

En revenant aux chaînes de Markov à temps continu et à valeurs dans un espace dénombrable, cette dernière proposition 14 donne immédiatement le critère suivant :

Proposition 15. *[60, thm 7.1] S'il existe une fonction V de Lyapounov, $c, d > 0$, tels que,*

$$\sum_j q_{ij} V(j) \leqslant -cV(i) + d, \quad i \in E,$$

et si $X(t)$ est irréductible alors il existe π une distribution de probabilité invariante pour $X(t)$, $\beta < 1$ et $B < \infty$ tels que

$$\|P(t, i, \cdot) - \pi\|_f \leqslant Bf(i)\beta^t, \quad x \in E, \quad t \geqslant 0,$$

avec $f = V + 1$.

Nous utiliserons les propositions 14 et 15 au Chapitre 1 de cette thèse, pour donner des conditions sur nos modèles Markoviens d'expression des gènes pour qu'ils soient asymptotiquement stables.

6.4   Processus de Markov déterministes par morceaux

Les processus de Markov déterministes par morceaux (PDMP — piecewise deterministic Markov processes) ont été formalisés rigoureusement par Davis [23], qui a notamment montré qu'une construction explicite d'un processus déterministe par morceaux définit une solution d'un certain problème de martingale. Ainsi, Davis a identifié très précisément le générateur étendu d'un PDMP et son domaine. Dans la pratique, comme on a pu le voir dans les propriétés énoncées dans la partie précédente, la connaissance d'un sous-ensemble de fonctions séparatrices inclus dans le domaine est cependant généralement suffisant. Nous donnons la construction d'un PDMP *sans bord*, c'est à dire que le flot déterministe reste toujours inclus dans l'espace d'états. Nous supposerons aussi par la suite que le flot déterministe a toujours la propriété d'existence et d'unicité globale.

Un PDMP (sans bord) est donné en tous temps $t \geqslant 0$ par un couple $(i(t), x(t))$ où $i(t) \in J$ est une variable discrète, $J \subset \mathbb{N}$ et $x(t) \in \mathbb{R}^d$ (on pourrait considérer des espaces plus généraux sans difficulté). Un PDMP est décrit par trois caractéristiques locales :
- un champ de vecteur $H_i(x)$, pour tout $i \in J$;
- une intensité de saut $\lambda_i(x)$, pour tout $i \in J$;
- une mesure de transition Q telle que pour tout (i, x), $Q(\cdot, (i, x))$ est une loi de probabilité sur $J \times \mathbb{R}^d$.

La construction d'un PDMP suit celle d'un processus de saut pur, sauf que la variable x n'est pas constante entre deux sauts, mais suit une équation différentielle déterministe.

On pose alors $(i_n, x_n) = (i(T_n), x(T_n))$ où (T_n, i_n, x_n) sont définis récursivement par :
- $T_0 = 0$, $i_0 = i(0)$, $x_0 = x(0)$ (conditions initiales données) ;

- si $T_n < \infty$, et $(i_n, x_n) = (i(T_n), x(T_n))$, alors pour tous $T_n \leqslant t < T_{n+1}$, $t \mapsto x(t) = g_{i_n}(x_n, t - T_n)$ où $g_{i_n}(x, t)$ est donnée par la solution de l'équation différentielle ordinaire

$$\begin{cases} \dfrac{dy}{dt} &=& H_{i_n}(y), \quad t \geqslant 0, \\ y(0) &=& x. \end{cases}$$

La variable discrète $t \mapsto i(t)$ est constante égale i_n, et $T_{n+1} = T_n + \tau_n$ où τ_n est déterminé par

$$\mathbb{P}\{\tau_n > t\} = \mathbb{E}\Big[exp\Big(-\int_0^t \lambda_{i_n}(g_{i_n}(x_n, s))ds\Big)\Big].$$

Si $\tau_n = \infty$, on pose $x_{n+m} = \Delta$ (point cimetière) et $T_{n+m} = \infty$, pour tout $m \geqslant 1$. Sinon $\tau_n < \infty$, et (i_{n+1}, x_{n+1}) est donné par la probabilité de transition $Q(\cdot, (i_n, x(T_{n+1}^-)))$. Comme dans les processus de saut pur, cette construction est valable jusqu'au temps d'explosion $T_\infty = \lim_{n \to \infty} T_n$. Les conditions générales pour assurer que l'explosion n'a pas lieu en temps fini sont difficiles à obtenir du fait de nombreuses possibilités entre les évolutions déterministes et les transitions possibles. On peut cependant montrer facilement que si :

Hypothèse 2. *Les intensités de saut $\lambda_i(x)$ sont uniformément bornées sur R^d,*

alors $T_\infty = \infty$ presque sûrement. Cette hypothèse est bien trop forte dans la pratique, et par la suite on supposera donc seulement que :

Hypothèse 3.
$$\mathbb{E}\big[N_t\big] < \infty, \quad \forall t \geqslant 0,$$

où $N_t = \displaystyle\sum_n \mathbf{1}_{\{t \geqslant T_n\}}$ *est le nombre de sauts entre $[0, t]$.*

Pour utiliser les résultats suivants, dans la pratique, il faudra donc montrer que cette hypothèse 3 est vérifiée.

Hypothèse 4. *On suppose que*
- *les champs de vecteurs H_i sont C^1 et tels que pour tout $x \in \mathbb{R}^d$, ils définissent un unique flot global $\phi_i(t, x)$;*
- *les intensités de saut sont telles que pour tout couple (i, x), $\lambda_i(\phi_i(t, x))$ est localement intégrable en 0, c'est-à-dire qu'il existe $\varepsilon(i, x) > 0$ tel que*

$$\int_0^{\varepsilon(i,x)} \lambda_i(\phi_i(s, x))ds < \infty.$$

Ces deux conditions impliquent que la construction donnée ci-dessus a un sens. Le flot est toujours défini et on peut choisir un temps de prochain saut strictement positif. Avec les hypothèses 3 et 4, Davis a montré que le processus de Markov (i_t, x_t) sur $J \times \mathbb{R}^d$ ainsi construit est solution du problème de martingale associé au générateur A, qui s'exprime, pour toute fonction bornée de classe C^1 de x (et de dérivée bornée),

$$Af(i, x) = H_i(x)\nabla_x f + \lambda_i(x) \int [f(j, y) - f(i, x)]Q(dj \times dy, (i, x)). \tag{7}$$

L'opérateur adjoint donne (formellement) l'équation d'évolution sur les probabilités de densité $p(i, x, t)$ du processus

$$\frac{\partial p(i, x, t)}{\partial t} = -\nabla(H_i(x)p(i, x, t)) - \lambda_i(x)p(i, x, t) + \int \lambda_j(y)p(j, y, t)Q((i, x), dj \times dy). \tag{8}$$

L'existence de solution au problème de martingale est donc donné par la construction explicite d'un processus stochastique. D'après la proposition 8 et le théorème 8, si l'on montre que le semi-groupe engendré par ce processus stochastique est fortement continu (ce qui est le cas si les intensités λ_i sont bornées par exemple), on peut obtenir l'unicité de la solution du problème de martingale. Les techniques de localisation peuvent aussi être utilisées dans la pratique. Crudu et al. [21] ont montré ainsi, avec des hypothèses fortes (mais qui peuvent être surmontées par des techniques de localisation), le résultat suivant :

Théorème 9. *[21, thm 2.5] Supposons les hypothèses 3 et 4 ainsi que*

Hypothèse 5. *Les fonctions $x \mapsto H_i(x)$, $x \mapsto \lambda_i(x)$ et $x \mapsto \lambda_i(x) \int f(j,y) Q(dj \times dy, (i,x))$ pour $f \in C_b^1$, sont C_b^1 sur $\mathbb{R}^d$.*

Alors, le PDMP déterminé par (H_i, λ_i, Q) est l'unique solution du problème de martingale associé à A défini à l'éq. (7).

Toujours pour le caractère bien posé du problème de martingale, citons un résultat de perturbation qui peut s'appliquer dans la pratique. L'idée est de découper le générateur donné à l'éq. (7) en deux parties. De manière naturelle (par rapport à la construction explicite du processus) on peut séparer la partie dérive, donnée par l'évolution déterministe, de la partie saut. Notons A_1 la partie dérive, et A_2 la partie saut. Supposons que les intensités de saut λ_i sont bornées. Alors l'opérateur A_2 est <u>un opérateur</u> borné. Si l'on s'assure que A_1 est dissipatif, que pour un $\sigma > 0$, $B(E) \subset \overline{Im(\sigma - A_1)}$, alors $B(E) \subset \overline{Im(\sigma - (A_1 + A_2))}$. Le théorème 8 donné ci-dessus permet donc de conclure que l'unicité a lieu pour $A_1 + A_2$. Pour l'existence, on peut utiliser le résultat suivant :

Proposition 16. *[30, prop 10.2 p 256] Supposons que pour toute loi initiale ν sur $J \times \mathbb{R}^d$, il existe une solution au problème de martingale pour (A_1, ν) à trajectoires dans $D_E[0, \infty)$, alors il existe également une solution au problème de martingale pour $(A_1 + A_2, \nu)$ à trajectoires dans $D_E[0, \infty)$ (où A_2 est l'opérateur de saut, avec intensités bornées).*

L'idée de la preuve suit la construction explicite du PDMP. On se ramène d'abord au cas λ constant, puis on construit successivement une solution sur tout $[T_k, T_{k+1})$, avec la loi de $T_{k+1} - T_k$ donnée par une loi exponentielle indépendante du processus, et la condition initiale donnée par la loi du saut Q en la condition finale de l'étape précédente, etc.

6.5 Équation d'évolution d'un PDMP

Nous donnons maintenant une stratégie similaire, mais en regardant le semi-groupe sur L^1, associé à l'équation d'évolution éq. (8). Cette stratégie sera largement utilisée au chapitre 1, sur un modèle PDMP en dimension un, lorsqu'il y a uniquement des sauts dans la variable continue, et un seul champ de vecteurs (il n'y a pas de variable discrète). Supposons donc pour simplifier qu'on est dans un cas où le champ de vecteurs ne change pas et qu'il n'y a pas de dynamique sur la variable discrète. Le générateur donné dans l'éq. (8) est défini par un opérateur de dérive et un opérateur de saut sur la variable continue.

Rappelons quelques notions spécifiques aux semi-groupes sur L^1. Soit $(E, \mathcal{E}, m)$ un espace mesuré σ-fini et $L^1 = L^1(E, \mathcal{E}, m)$ de norme $\|\cdot\|_1$. Un opérateur linéaire P sur L^1 est dit *sous-stochastique* (respectivement *stochastique*) si $Pu \geqslant 0$ et $\|Pu\|_1 \leqslant \|u\|_1$ (respectivement $\|Pu\|_1 = \|u\|_1$) pour tout $u \geqslant 0$, $u \in L^1$. On note D l'ensemble des densités de probabilité sur E :

$$D = \{u \in L^1 : u \geqslant 0, \|u\|_1 = 1\}.$$

Ainsi un opérateur stochastique transforme une densité en une densité. Soit $\mathcal{P}\colon E \times \mathcal{E} \to [0,1]$ un *noyau de transition stochastique*, c'est-à-dire que $\mathcal{P}(x,\cdot)$ est une mesure de probabilité pour tout $x \in E$ et la fonction $x \mapsto \mathcal{P}(x,B)$ est mesurable pour tout $B \in \mathcal{E}$. Soit P un opérateur stochastique sur L^1. Si

$$\int_E \mathcal{P}(x,B)u(x)m(dx) = \int_B Pu(y)m(dy) \quad \text{pour tous } B \in \mathcal{E}, u \in D,$$

alors P est l'opérateur de *transition* associé à $\mathcal{P}$. Un opérateur stochastique P sur L^1 est dit *partiellement intégral* s'il existe une fonction mesurable $p\colon E \times E \to [0,\infty)$ telle que

$$\int_E \int_E p(x,y)\,m(dy)\,m(dx) > 0 \quad \text{et} \quad Pu(y) \geqslant \int_E u(x)p(x,y)\,m(dx),$$

pour toute densité u. De plus, si,

$$\int_E p(x,y)\,m(dy) = 1, \quad x \in E,$$

alors P correspond au noyau stochastique

$$\mathcal{P}(x,B) = \int_B p(x,y)\,m(dy), \quad x \in E, B \in \mathcal{E},$$

et on dit que P est à *noyau p*. Dans le cas particulier d'un ensemble dénombrable E avec $\mathcal{E}$ la famille de tous les sous-ensembles de E et m la mesure de comptage, l'espace L^1 sera noté ℓ^1 et les densités de probabilité sont des suites. Tout opérateur stochastique sur ℓ^1 a un noyau $[p(x,y)]_{x,y \in E}$ qui est donné par une matrice (stochastique).

Un semi-groupe $\{P(t)\}_{t \geqslant 0}$ d'opérateurs linéaires sur L^1 est dit *sous-stochastique* (respectivement *stochastique*) s'il est fortement continu et pour tout $t > 0$ l'opérateur $P(t)$ est sous-stochastique (respectivement stochastique). Une densité u^* est *invariante* ou *stationnaire* pour $\{P(t)\}_{t \geqslant 0}$ si u^* est un point fixe de chaque opérateur $P(t)$, $P(t)u^* = u^*$ pour tout $t \geqslant 0$. Un semi-groupe stochastique $\{P(t)\}_{t \geqslant 0}$ est dit *asymptotiquement stable* s'il existe une densité stationnaire u_* telle que

$$\lim_{t \to \infty} \|P(t)u - u_*\|_1 = 0 \ \text{ pour } \ u \in D,$$

et il est *partiellement intégral* si, pour un $t_0 > 0$, l'opérateur $P(t_0)$ est partiellement intégral.

Théorème 10 ([67, Thm 2]). *Soit $\{P(t)\}_{t \geqslant 0}$ un semi-groupe stochastique partiellement intégral. Si le semi-groupe $\{P(t)\}_{t \geqslant 0}$ a une unique densité invariante u^* et $u^* > 0$ presque partout, alors*

$$\lim_{t \to \infty} \|P(t)u - u^*\|_1 = 0 \ \text{ pour tout } \ u \in D.$$

Dans notre étude sur un modèle donné par un PDMP, il ne sera pas trop difficile de voir que le semi-groupe est partiellement intégral. Les conditions pour obtenir un semi-groupe stochastique (autre que le cas trivial d'intensités de saut bornées) sont plus délicates. Enfin, l'existence d'une densité invariante (c'est-à-dire une fonction mesurable invariante et intégrable, qui peut donc être renormalisée) sera donnée par des calculs sur une résolvante et une chaîne de Markov échantillonnée, que l'on présente plus bas.

Pour s'assurer que le semi-groupe donné par le générateur de l'éq. (8) est stochastique, on utilisera un résultat de perturbation. Ce résultat permet d'abord de construire un semi-groupe sous-stochastique, généré par une extension du générateur associé à l'éq. (8). De

plus, il caractérise la résolvante de ce semi-groupe, ce qui permet de déduire des critères suffisants pour le rendre stochastique.

On note A_0 l'opérateur de transport associé au terme de dérive, et J l'opérateur stochastique sur L^1 associé au noyau Q. L'équation d'évolution sur la densité peut se réécrire

$$\frac{du}{dt} = A_0 u - \lambda u + J(\lambda u).$$

A_0 étant un opérateur de transport, il est raisonnable de penser qu'il est le générateur infinitésimal d'un semi-groupe stochastique fortement continu (du moins on peut trouver dans la pratique des conditions pour qu'il le soit). Alors, même si λ est non bornée, $A_1 u = A_0 u - \lambda u$ est le générateur d'un semi-groupe sous-stochastique. Le domaine $\mathcal{D}(A_1)$ est inclus dans

$$L^1_\lambda = \{u \in L^1 : \int_E \lambda(x) \mid u(x) \mid m(dx) < \infty\}.$$

Soit $A_2 = J(\lambda u)$. L'opérateur J est positif et stochastique, $\|J(\lambda u)\|_1 = \|\lambda u\|_1$, et donc

$$\mathcal{D}(A_1) \subset \mathcal{D}(A_2).$$

De plus, on a clairement

$$\int_E (A_1 u + A_2 u) dm = 0.$$

On peut alors utiliser le résultat de perturbation suivant :

Théorème 11 ([43, 86, 5]). *Supposons que deux opérateurs linéaires $(A_1, \mathcal{D}(A_1))$ et $(A_2, \mathcal{D}(A_2))$ sur L^1 vérifient les hypothèses suivantes :*
- *$(A_1, \mathcal{D}(A_1))$ génère un semi-groupe sous-stochastique $\{S_1(t)\}_{t \geqslant 0}$;*
- *$\mathcal{D}(A_1) \subset \mathcal{D}(A_2)$ et $A_2 u \geqslant 0$ pour tout $u \in \mathcal{D}(A_1)_+$;*
- *pour tout $u \in \mathcal{D}(A_1)_+$,*
$$\int_E (A_1 u + A_2 u) dm = 0.$$

Alors il existe un semi-groupe sous-stochastique $\{P(t)\}_{t \geqslant 0}$ sur L^1 généré par une extension C de $(A_1 + A_2, \mathcal{D}(A_1))$. Le générateur est caractérisé par

$$R(\sigma, C)u = \lim_{N \to \infty} R(\sigma, A_1) \sum_{n=0}^{N} (A_2 R(\sigma, A_1))^n u, \quad u \in L^1, \quad \sigma > 0.$$

De plus, $\{P(t)\}_{t \geqslant 0}$ est le plus petit semi-groupe sous-stochastique dont le générateur est une extension de $(A_1 + A_2, \mathcal{D}(A_1))$. Enfin, les conditions suivantes sont équivalentes :
- *$\{P(t)\}_{t \geqslant 0}$ est un semi-groupe stochastique,*
- *le générateur C est la fermeture de $(A_1 + A_2, \mathcal{D}(A_1))$,*
- *pour un $\sigma > 0$,*
$$\lim_{n \to \infty} \|(A_2 R(\sigma, A_1))^n u\| = 0, \quad \forall u \in L^1.$$

Tyran-Kamińska [83] a montré qu'une condition suffisante pour que $\{P(t)\}_{t \geqslant 0}$ soit stochastique est que l'opérateur K défini par

$$Ku = \lim_{\sigma \to 0} A_2 R(\sigma, A_1)u = \lim_{\sigma \to 0} J(\lambda R(\sigma, A_1)u), \tag{9}$$

soit ergodique en moyenne, c'est-à-dire $\lim_{n \to \infty} \dfrac{1}{n} \sum_{n=0}^{N-1} K^n u$ existe. Cette proposition vient simplement de la monotonie des résolvantes $R(\sigma, A_1)$ d'un opérateur sous-stochastique et

du fait que l'ergodicité en moyenne s'hérite par domination. En pratique, on pourra donc chercher à montrer que K possède une unique densité invariante, transférer cette propriété à l'opérateur $\{P(t)\}_{t \geqslant 0}$ et utiliser le théorème 10 pour conclure. Pour finir, notons les liens entre l'approche probabiliste et analytique sur les PDMP donnés par la proposition suivante

Proposition 17. *Tyran-Kamińska [83, thm 5.2] Soient $X(t)$ le PDMP de caractéristique locale (H, λ, Q), $\{P(t)\}_{t \geqslant 0}$ son semi-groupe sur L^1 associé, J l'opérateur stochastique sur L^1 associé au noyau Q, et $\phi_t(x)$ le flot global associé à H. On note (T_n) la suite de temps de sauts de $X(t)$, avec $T_\infty = \lim_{n \to \infty} T_n$ le temps d'explosion pour $X(t)$. Alors :*
- *pour tous $\sigma > 0$,*

$$\lim_{n \to \infty} (J(\lambda R(\sigma, A_1)u))^{*n} \mathbf{1}_{\{E\}}(x) = \mathbb{E}\big[e^{-\sigma T_\infty} \mid X(0) = x\big] \quad p.p.\ x.$$

- *pour tous $B \in \mathbb{B}(E)$, $u \in \mathcal{D}(A)_+$ et $t > 0$*

$$\int_B P(t)u(x)m(dx) = \int_E \mathbb{P}\big\{X(t) \in B, t < T_\infty \mid X(0) = x\big\}u(x)m(dx),$$

- *l'opérateur K défini à l'éq. (9) est l'opérateur de transition associé à la chaîne de Markov en temps discret $(X(T_n))_{n \geqslant 0}$ de noyau*

$$\mathcal{K}(x, B) = \int_0^\infty Q(B; \phi_t(x))\lambda(\phi_t(x))e^{-\int_0^t \lambda(\phi_r(x))dr}dt, \quad x \in E, B \in \mathbb{B}(E).$$

On conclut avec une série de remarques

Remarque 12. *Cet ensemble de résultats montre que l'on peut ramener l'étude de l'équation d'évolution sur les densités du PDMP (en supposant que la loi initiale a une densité) à l'étude des densités d'un opérateur associé à une chaîne de Markov en temps discret. On verra dans le chapitre 1 que pour un modèle simple, on peut calculer explicitement la résolvante de A_1, l'opérateur K, trouver un unique candidat pour la densité invariante, et ainsi donner des conditions assez fines (sur les caractéristiques locales du PDMP) pour la stabilité asymptotique du semi-groupe associé au PDMP. Les résultats de Tyran-Kamińska [83] contiennent d'autres caractérisations importantes, notamment des conditions pour que le semi-groupe soit fortement stable (perte de masse) qui ont été appliquées à différents modèles de fragmentations (voir aussi [55]).*

Remarque 13. *L'étude d'un processus de Markov par une chaîne de Markov en temps discret est à la base des idées de Meyn et Tweedie présentées dans la sous-section 6.3. Notons également que ces idées ont été appliquées sur les PDMP par Costa and Dufour [20]. L'importance en pratique de ces résultats est de donner des opérateurs explicitement calculables, contrairement aux résolvantes (en général). Comme on l'a vu à la sous-section 6.3, l'échantillonnage donné par des temps aléatoires exponentiels de paramètre 1 correspond exactement à la résolvante (éq. (6)). Cependant, celui-ci est difficilement calculable dans la pratique. L'approche de Marta Tyran-Kamińska donne des conditions équivalentes (voir théorème 11) pour les propriétés du semi-groupe $\{P(t)\}_{t \geqslant 0}$ sur L^1 et l'opérateur $A_2 R(\sigma, A_1)$. Ensuite, l'opérateur $K = \lim_{\sigma \to 0} A_2 R(\sigma, A_1)$, qui correspond à un échantillonnage aux temps de saut du PDMP, donne des conditions suffisantes pour les propriétés de stabilité du semi-groupe $\{P(t)\}_{t \geqslant 0}$. L'échantillonnage utilisé par Costa et Dufour (dans un cadre un peu plus général, avec bord, et avec une approche probabiliste, en regardant le semi-groupe sur les fonctions bornées) correspond à des temps aléatoires donnés par le minimum du temps de prochain saut et d'une exponentielle de paramètre 1. Les auteurs obtiennent alors des conditions d'équivalence entre les propriétés de stabilité de la chaîne échantillonée et du PDMP.*

Remarque 14. *Enfin, ces approches de type « semi-groupe » pour étudier les propriétés de stabilité d'un modèle donnent en général de mauvaises estimations sur les taux de convergence vers l'état d'équilibre. Pour obtenir de « bons » taux de convergence explicites, on utilise généralement des techniques dites de couplage. On renvoie à de récentes études sur des PDMP dans les articles [8],[19] par exemple. On verra au chapitre 1 que cette approche permet de trouver un taux de convergence explicite pour notre modèle.*

7   Théorèmes Limites

Les idées des théorèmes limites en probabilités reposent sur les deux théorèmes fondamentaux que sont la loi des grands nombres (LGN) et le théorème de la limite centrale (TCL). La LGN nous dit que si on somme un grand nombre n de variables indépendantes et identiquement distribuées, intégrables, et que l'on divise par ce nombre n, alors la limite est déterministe, égale à la moyenne de la loi commune des variables aléatoires. Le TCL (pour des variables L^2) caractérise les fluctuations autour de la limite de la LGN, qui sont alors gaussiennes, centrées en la moyenne, de variance qui tend vers 0 en $n^{-1/2}$.

Ces théorèmes ont d'innombrables applications et généralisations, en particulier aux processus stochastiques. Pour le processus stochastique qui nous intéressera le plus, le processus de Poisson, ces théorèmes se traduisent par la proposition suivante :

Proposition 18. *Soit Y un processus de Poisson standard (d'intensité 1). Alors, pour tout $t_0 > 0$,*

$$\lim_{n \to \infty} \sup_{t \leqslant t_0} \big| \frac{Y(nt)}{n} - t \big| = 0, \quad \textit{presque sûrement.}$$

De plus,

$$\lim_{n \to \infty} \mathbb{P}\big\{\frac{Y(nt) - nt}{\sqrt{n}} \leqslant x\big\} = \int_{-\infty}^{x} \frac{1}{\sqrt{2\pi}} e^{-y^2/(2t)} dy = \mathbb{P}\{W(t) \leqslant x\},$$

où W est un mouvement Brownien standard (de moyenne nulle et de variance t).

Pour ce qui nous intéresse, les conséquences et généralisations des ces théorèmes aux processus stochastiques ont principalement pour intérêt de trouver et justifier des modèles réduits et plus abordables analytiquement. On présente ci-après deux approches de réduction de modèles, l'une basée sur la séparation d'échelles de temps, et l'autre basée sur des passages en grandes populations (champ moyen, limite fluide, limite thermodynamique...). Ces deux approches ne sont pas forcément disjointes.

Mais tout d'abord expliquons les outils principaux utilisés. L'approche la plus largement répandue pour prouver des théorèmes limites sur des processus stochastiques, satisfaisant une certaine équation différentielle stochastique, repose sur des arguments topologiques, et notamment de compacité. Si une suite est relativement compacte, et possède une unique valeur d'adhérence, alors cette suite est convergente, vers l'unique valeur d'adhérence. Notons que les convergences obtenues sur les processus stochastiques seront des convergences en loi. Les processus stochastiques (sur $D_E[0, \infty)$ en général) sont vus comme des variables aléatoires d'un plus grand espace, que l'on notera temporairement S, muni d'une certaine topologie. Notons $C_b(S)$ l'ensemble des fonctions continues bornées de S. Notons $\mathbb{P}(S)$ l'ensemble des mesures de probabilités sur S. Une suite $P_n \in \mathbb{P}(S)$ de mesures de probabilités sur S converge faiblement vers P si

$$\lim_{n \to \infty} \int f dP_n = \int f dP, \quad \forall f \in C_b(S).$$

De manière équivalente, une suite de variables aléatoires X_n sur S converge en loi (ou en distribution) vers X si

$$\lim_{n \to \infty} \mathbb{E}\big[f(X_n)\big] = \mathbb{E}\big[f(X)\big], \quad \forall f \in C_b(S).$$

Cette convergence n'est pas spécifique aux processus stochastiques. Un autre type de convergence, beaucoup plus maniable, et spécifique aux processus stochastiques, est la convergence en distribution de dimension finie. Cette convergence est la convergence en loi de tout vecteur fini de variables aléatoires données par les évaluations du processus stochastique en des temps finis. La convergence de dimension finie peut être une manière d'identifier une unique limite via le résultat de Prokhorov :

Proposition 19. *X_n converge en loi vers X si et seulement si X_n converge en distribution de dimension finie et X_n est relativement compact.*

La preuve du sens direct de cette proposition utilise le théorème de représentation de Skorokhod, qui nous dit que si on a convergence en loi, alors on peut toujours trouver (représenter) des variables aléatoires qui ont ces lois et qui convergent presque sûrement. La preuve du sens réciproque utilise le fait que les distributions de dimension finie caractérisent un processus stochastique.

Une deuxième méthode pour caractériser de manière unique la loi du processus limite, largement répandue, est celle du problème de martingale. Si l'on montre que toute limite de la suite de processus stochastiques doit vérifier un certain problème de martingale, et qu'on a unicité (en loi) de la solution du problème de martingale, alors la loi limite est caractérisée de manière unique. On comprend alors que le caractère bien posé (en fait l'unicité) d'un problème de martingale est crucial pour cette approche.

On verra enfin au Chapitre 1 que l'on peut utiliser dans certains cas une généralisation du théorème de Lévy, le théorème de Bochner-Minlos, qui montre que sous de bonnes conditions, la fonctionnelle caractéristique d'un processus stochastique caractérise sa loi.

Après avoir caractérisé la loi limite, la deuxième étape consiste à montrer la relative compacité du processus stochastique (dans l'espace dans lequel il vit). Cette propriété dépend fortement de la topologie que l'on considère. Une notion proche de la compacité pour les lois de probabilité, et très maniable en pratique, est la tension.

Définition 16 (tension). *Une suite de variables aléatoires X_n à valeurs dans S un espace topologique est tendue si pour tout $\varepsilon > 0$, il existe un compact $K \in S$, tel que*

$$\liminf_{n \to \infty} \mathbb{P}\big\{X_n \in K\big\} \geqslant 1 - \varepsilon.$$

Le fameux théorème de Prohorov caractérise la relative compacité par des critères de tension uniformes. En particulier, on peut montrer que si S est un espace métrique complet séparable, une suite est tendue si et seulement si elle est relativement compacte (voir par exemple [30, thm 2.2]). Si X_n est une suite de processus stochastiques à valeurs dans $D_E[0, \infty)$, on cherche donc si cet espace est un métrique complet séparable. Si E est métrique complet séparable, alors on peut munir $D_E[0, \infty)$ d'une métrique (appelé métrique de Skorohod) qui rende $D_E[0, \infty)$ complet séparable. De plus, pour cette topologie, notée S_E, on a le critère de tension suivant trouvé par Aldous (voir par exemple [39, thm 4.5 p 356]) :

Proposition 20. *Une suite X_n est tendue dans $(D_E[0, \infty), S_E)$ si :*

- *pour tous $N \in \mathbb{N}^*$, $\varepsilon > 0$, il existe $n_0 \in \mathbb{N}^*$ et $K > 0$ tels que*

$$(n \geqslant n_0) \Rightarrow \mathbb{P}\big\{ \sup_{t \leqslant N} \mid X_t^n \mid > K \big\} \leqslant \varepsilon.$$

- *pour tous $N \in \mathbb{N}^*$, $\varepsilon > 0$, on a*

$$\lim_{\theta \to 0} \limsup_n \sup_{S \leqslant T \leqslant S+\theta} \mathbb{P}\big\{ \mid X_T^n - X_S^n \mid \geqslant \varepsilon \big\} = 0,$$

où le supremum est parmi tous les temps d'arrêts adaptés à la filtration canonique associée à X_n, bornés par N.

Citons également, toujours pour la topologie de Skorohod, le critère de Rebolledo pour les semi-martingales de dimension finie

Proposition 21. *[41, Cor 2.3.3 p 41] Si X_n est à valeurs dans un espace de dimension finie, et $X_n = A_n + M_n$, avec A_n un processus à variation finie, M_n une martingale locale L^2, et si les suites (A_n) et $(< M_n >)$ (processus de variation quadratique) vérifient le critère d'Aldous, alors X_n est tendue.*

Il arrive que la suite de processus ne puisse être tendue dans $(D_E[0, \infty), S_E)$, notamment lorsque le processus limite « a plus de discontinuités » que la suite de processus. Il faut alors utiliser d'autres topologies, en s'assurant que le théorème de Prohorov reste vrai (ainsi que le théorème de représentation de Skorokhod), pour pouvoir utiliser les mêmes arguments de compacité. C'est le cas pour la topologie de Jakubowski J sur $D_{\mathbb{R}}[0, 1]$, pour laquelle on a le critère de tension suivant :

Proposition 22. *Une suite X_n est tendue dans $(D_{\mathbb{R}}[0, 1], J)$ si*
- *pour tout $\varepsilon > 0$, il existe $n_0 \in \mathbb{N}^*$ et $K > 0$ tels que*

$$(n \geqslant n_0) \Rightarrow \mathbb{P}\big\{ \sup_{t \leqslant 1} \mid X_t^n \mid > K \big\} \leqslant \varepsilon,$$

- *pour tous $a < b$, il existe $C > 0$ tel que*

$$\sup_n N^{a,b}(X_n) \leqslant Cn,$$

où $N^{a,b}$ est le nombre de croisements de niveau $a < b$.

Un critère similaire est valable pour l'espace $L^p[0, 1]$, $1 \leqslant p < \infty$:

Proposition 23. *Une suite X_n est tendue dans $L^p[0, 1]$ si*
- *pour tous $N \in \mathbb{N}^*$, $\varepsilon > 0$, il existe $n_0 \in \mathbb{N}^*$ et $K > 0$ tels que*

$$(n \geqslant n_0) \Rightarrow \mathbb{P}\big\{ \sup_{t \leqslant 1} \mid X_t^n \mid > K \big\} \leqslant \varepsilon,$$

- *pour tout $\varepsilon > 0$, il existe $n_0 \in \mathbb{N}^*$ et $K > 0$ tels que*

$$(n \geqslant n_0) \Rightarrow \mathbb{P}\big\{ \|X_t^n\|_{BV} \geqslant K \big\} \leqslant \varepsilon,$$

où $\|x\|_{BV} = \|x\|_1 + \sup\{\sum_i \mid f(t_{i+1}) - f(t_i) \mid, \quad t_i \quad subdivision \ de \ [0, 1]\}$.

Enfin, si $M[0, \infty)$ est l'espace des fonctions réelles mesurables sur $[0, \infty)$, muni de la métrique

$$d(x, y) = \int_O^\infty e^{-t} \max(1, \mid x(t) - y(t) \mid) dt,$$

alors $(M[0, \infty), d)$ est un espace métrique séparable, et on a le critère de tension suivant :

Proposition 24. *[52, thm 4.1] Une suite X_n est tendue dans $(M[0, \infty), d)$ si :*
- *pour tous $T, \varepsilon > 0$, il existe $K > 0$ tel que*

$$\sup_n \int_0^T \mathbf{1}_{\{|x(t)| > K\}} \leqslant \varepsilon,$$

- *Pour tout $T > 0$*

$$\lim_{h \to 0} \sup_n \int_0^T \max(1, \mid x(t+h) - x(t) \mid) dt = 0.$$

7.1 Réduction de modèles par séparation d'échelles de temps

Les théorèmes limites sont très importants dans le contexte des modèles de réactions biochimiques. En effet, il est courant que dans ces modèles certaines variables ou certaines réactions évoluent à une vitesse beaucoup plus rapide que les autres. Dans ces cas là, on peut soit « simplifier » la réaction (elle peut devenir déterministe, ou provoquer des grands sauts) ou « éliminer » la variable rapide par des techniques de moyennisation. On renvoie à deux récentes publications utilisant ce genre de techniques pour simplifier des processus de saut pur [21],[42], ainsi qu'aux résultats du chapitre 1 sur la simplification du modèle d'expression des gènes. Les techniques de moyennisation remontent à Kash'minski et Kurtz (voir par exemple [50]). De manière heuristique, elles sont basées sur l'hypothèse que la variable rapide est ergodique, et donc converge rapidement vers son état d'équilibre. La variable lente, si elle dépend de la valeur de la variable rapide, ne dépendra alors à la limite que des moments asymptotiques de la variable rapide.

On utilisera ces techniques de réduction dans les deux chapitres de cette thèse, soit pour prouver rigoureusement des liens entre certains modèles, soit pour réduire la dimension d'un modèle et le rendre plus facile à analyser.

Des techniques de réduction similaires peuvent être effectuées directement sur l'équation d'évolution de la densité des variables (Équation maîtresse ou Fokker-Planck) en « intégrant » sur la variable rapide, et par une hypothèse d'ergodicité similaire. Voir pour cette approche [38] ou plus récemment [73].

7.2 Réduction par passage en grande population

Lorsqu'on a un modèle discret, qui évolue par "de petits sauts", si l'on suppose que le nombre d'individus à l'état initial devient grand, alors par une renormalisation appropriée, on peut décrire le nombre d'individus par une variable continue qui vérifiera un modèle limite.

Cette idée remonte à Prokhorov [68] et Kurtz [51]. Pour une chaîne de Markov X_n en temps continu à valeurs dans $\mathbb{N}$, dont l'évolution est décrite par des intensités de saut $\lambda_n(x)$ et une loi de répartition de saut $\mu_n(x, \cdot)$, le résultat classique de Kurtz [51] nous dit que si on accélère les intensités de saut par $\lambda_n(x) = n\lambda(x)$, et que l'on ne change pas la loi de répartition de saut $\mu_n(x, \cdot) = \mu(x, \cdot)$, alors le processus stochastique renormalisé $Y_n = \frac{X_n}{n}$ converge vers la solution de l'équation différentielle ordinaire (sous réserve qu'elle soit bien posée) dirigée par

$$F(x) = \lambda(x) \int_{\mathbb{R}} \mid z - x \mid \mu(x, dz).$$

Ces techniques ont été étendues à de nombreux modèles de population en biologie. La stratégie est de décrire un modèle de population discrète en utilisant des processus ponctuels (la mesure empirique), et de prouver qu'ils convergent, avec une mise à l'échelle

adéquate et de bonnes hypothèses sur les coefficients, vers une mesure qui résout un certain
problème limite. La convergence obtenue est une convergence en loi, et les preuves utilisent
généralement les techniques de martingales (on montre d'abord la compacité, et ensuite
que toute limite est uniquement déterminée, grâce au problème de martingale). Ces idées
remontent à Prokhorov [68], et ont été considérablement améliorées par de nombreux
auteurs [51, 63, 41, 81, 71, 53, 24]. Les intérêts de cette approche sont :

- premièrement, **théorique**. Cette approche peut être utilisée pour prouver l'existence
  d'une solution au problème limite. Si on est capable de trouver un modèle discret
  particulier, qui possède une suite de solutions qui converge, et dont la limite résout
  nécessairement le problème limite, alors on a prouvé l'existence d'une solution du
  modèle limite (voir par exemple [40, 62] dans le contexte de modèle d'agrégation-
  fragmentation) ;
- deuxièmement, **numérique**. Cette approche a été largement utilisée pour obtenir
  des algorithmes rapides et efficaces d'un modèle continu non linéaire, comme les
  nombreuses variantes des équations de Poisson-McKean-Vlasov [82]. Pour une telle
  approche, le taux de convergence du modèle stochastique vers le modèle limite est
  important pour s'assurer de la tolérance de l'approximation réalisée [16, 61] ;
- troisièmement, pour la **modélisation**. Dans un contexte physique ou biologique,
  cette approche permet de justifier rigoureusement les bases et les hypothèses phy-
  siques d'un modèle particulier. En effet, dans les modèles de population discrets,
  on peut spécifier précisément chaque réaction ou les règles d'évolution de la popu-
  lation. Ensuite, avec des hypothèses sur les coefficients décrivant cette évolution, et
  une mise à l'échelle particulière (explicite, en général grande population, ou taux
  de réactions rapides, etc...), on obtient un modèle limite ou un autre. Ainsi, les hy-
  pothèses (parfois) implicites d'un modèle continu sont rendues plus explicites. On
  peut aussi unifier certains modèles en les reliant entre eux avec des mises à l'échelle
  particulières [44] ;
- enfin, du point de vue **pratique**. Cette approche peut être utilisé pour simplifier des
  modèles, en particulier quand les effets discrets rendent l'analyse du modèle délicate.
  On peut obtenir une bonne idée du comportement d'un modèle initial en étudiant
  plusieurs comportements limites.

Récemment, les approches de type « théorèmes limites » appliquées aux modèles de
population en biologie mathématique ont été nombreuses, donnant un changement de
point de vue à la modélisation en biologie, d'une approche macroscopique à une approche
microscopique. On peut donner des exemples concrets :

- **dans les modèles de population cellulaire.** Bansaye et Tran [6] ont considéré
  une population de cellules infectées par des parasites (le nombre de parasites donne
  une variable de structure pour les cellules) et ont regardé la limite quand il y a un
  grand nombre de parasites et une taille finie de population de cellules. On peut faire
  des analogies entre ce modèle et le modèle de polymérisation-fragmentation que l'on
  étudiera au chapitre 2. On peut considérer en effet les polymères comme des cellules,
  et les monomères comme des parasites. On utilisera ainsi les résultats de ce papier,
  et on considérera aussi la limite quand le nombre de petites particules (monomères,
  parasites) devient grand tandis que le nombre de grandes particules (polymères,
  cellules) reste fini, et évolue suivant une fragmentation (ou division) aléatoire. Pour
  d'autres études similaires de modèles hôtes-parasites, voir [7, 57].
- **dans les modèles d'évolution.** Champagnat et Méléard [17] ont étendu les mo-
  dèles d'évolutions (où la population est structurée par un « trait » génotypique, qui
  subit des mutations) avec interaction (voir [31, 18]) en rajoutant une structure d'es-
  pace, typiquement une diffusion réfléchie sur un domaine borné. Les auteurs ont ainsi

obtenu, dans la limite de grandes populations, une équation aux dérivées partielles non- linéaire de type réaction-diffusion, avec condition au bord de Neumann. Leurs hypothèses impliquent que les taux de naissance et mort, et les coefficients de dérive et de diffusion soient bornés et Lipschitziens, pour s'assurer du caractère bien posé du modèle limite. Nous utiliserons aussi cet article dans le chapitre 2, pour modéliser le système d'agrégation-fragmentation de polymères avec mouvement spatial.

Enfin, mentionnons juste que les approches de ce type sur l'équation d'évolution de la densité, très utilisées par les physiciens, portent souvent le nom d'expansion de Van Kampen, ou de Kramers-Moyal (voir par exemple [72]).

Bibliographie

[1] D. J. Aldous. Deterministic and stochastic models for coalescence (aggregation and coagulation) : a review of the mean-field theory for probabilists. *Bernoulli*, 5(1) :3–48, 1999. 17

[2] D. F. Anderson. A modified next reaction method for simulating chemical systems with time dependent propensities and delays. *J. Chem. Phys.*, 127 :1–10, 2007. 24

[3] D. F. Anderson and T. G. Kurtz. *Design and Analysis of Biomolecular Circuits (chapter 1)*. Springer, 2011. 13

[4] J M Ball, J Carr, and O Penrose. The Becker-Döring Cluster Equations : Basic Properties and Asymptotic Behaviour of Solutions. *Commun. Math. Phys.*, 104(4) : 657–692, 1986. 12

[5] J. Banasiak. On an extension of the kato-voigt perturbation theorem for substochastic semigroups and its application. *Taiwanese J. Math.*, 5 :169–191, 2001. 36

[6] V. Bansaye and V. C. Tran. Branching Feller diffusion for cell division with parasite infection. *ALEA-Lat. Am. J. Probab.*, 8 :81–127, 2011. 42

[7] V. Bansaye, J.-F. Delmas, L. Marsalle, and V. C. Tran. Limit theorems for Markov processes indexed by continuous time Galton-Watson trees. *Ann. Appl. Probab.*, 21 (6) :2263–2314, 2011. 42

[8] J.-B. Bardet, A. Christen, A. Guillin, F. Malrieu, and P.-A. Zitt. Total variation estimates for the tcp process. 2011. pre-print arXiv :1112.6298. 29, 38

[9] A. F. Bartholomay. On the linear birth and death processes of biology as markoff chains. *B. Math. Biophys.*, 20 :97–118, 1958. 12

[10] P. H. Baxendale. A stochastic hopf bifurcation. *Probab. Th. Rel. Fields*, 99 :581–616, 1994. 17

[11] R. Becker and W. Döring. Kinetische Behandlung der Keimbildung in übersättigten Dämpfen. *Ann. Phys. (Berlin)*, 416(8) :719–752, 1935. 12

[12] J. Bérard. Chaînes de markov. http ://math.univ-lyon1.fr/ jberard/notes-CM-www.pdf, 2012. 18

[13] N. Blinov, M. Berjanskii, D. S. Wishart, and M. Stepanova. Structural domains and main-chain flexibility in prion proteins. *Biochemistry*, 48(7) :1488–1497, 2009. 10

[14] R. P. Boland, T. Galla, and A. J. Mckane. How limit cycles and quasi-cycles are related in systems with intrinsic noise. *J. Stat. Mech. Theor. Exp.*, P09001 :1–27, 2008. 17

[15] P. Brémaud. *Markov Chains.* Springer, 1999. 18, 20, 21, 22, 24

[16] E. Cepeda and N. Fournier. Smoluchowski's equation : rate of convergence of the Marcus-Lushnikov process. *Stoch. Proc. Appl.*, 121(6) :1–34, 2011. 42

[17] N. Champagnat and S. Méléard. Invasion and adaptive evolution for individual-based spatially structured populations. *J. Math. Biol.*, 55(2) :147–188, 2007. 42

[18] N. Champagnat, R. Ferrière, and S. Méléard. Individual-based probabilistic models of adaptive evolution and various scaling approximations. *Prog. Probab.*, 59 :75–113, 2005. 42

[19] B. Cloez. Wasserstein decay of one dimensional jump-diffusions. 2012. eprint arXiv :1202.1259. 38

[20] O.L.V. Costa and F. Dufour. Stability and ergodicity of piecewise deterministic markov processes. *IEEE Decis. Contr. P.*, 47 :1525–1530, 2008. 37

[21] A. Crudu, A. Debussche, A. Muller, and O. Radulescu. Convergence of stochastic gene networks to hybrid piecewise deterministic processes. *Ann. Appl. Probab. (to appear)*, 2011. 34, 41

[22] D.J. Daley and D. Vere-Jones. *An introduction to the Theory of Point Processes.* Springer series in statistics, 2008. 25

[23] M. H. A. Davis. Piecewise-deterministic markov processes : A general class of non-diffusion stochastic models. *J Roy. Stat. Soc. B Met.*, 46(3) :353–388, 1984. 32

[24] D. Dawson, B. Maisonneuve, and J. Spencer. *Measure-valued markov processes*, volume 1541. Springer Berlin / Heidelberg, 1991. 42

[25] R. Durrett. *Probability : Theory and Examples.* Cambridge U. Press, 2010. 21

[26] M. Ehrenberg, J. Elf, E. Aurell, R. Sandberg, and J. Tegnér. Systems Biology Is Taking Off. *Genome Res.*, 13 :2377–2380, 2003. 10

[27] A. Eldar and M. B. Elowitz. Functional roles for noise in genetic circuits. *Nature*, 467(7312) :167–73, 2010. 11

[28] M.B. Elowitz, A.J. Levine, E.D. Siggia, and P.S. Swain. Stochastic gene expression in a single cell. *Science*, 297 :1183–1186, 2002. 10

[29] K.-J. Engel and R. Nagel. *One-parameter semigroups for linear evolution equations.* Springer-Verlag, 2000. 18

[30] S. N. Ethier and T. G. Kurtz. *Markov Processes : Characterization and Convergence.* Wiley Interscience, 2005. 25, 26, 27, 28, 29, 34, 39

[31] N. Fournier and S. Méléard. A microscopic probabilistic description of a locally regulated population and macroscopic approximations. *Ann. Appl. Probab.*, 14(4) : 1880–1919, 2004. 42

[32] C. Gadgil, C. H. Lee, and H. G. Othmer. A stochastic analysis of first-order reaction networks. *B. Math. Biol.*, 67 :901–946, 2005. 13

[33] D. T. Gillespie. Exact stochastic simulation of coupled chemical reactions. *J. Chem. Phys.*, 81(25) :2340–2361, 1977. 24

[34] B. C. Goodwin. Oscillatory behavior in enzymatic control processes. *Adv. Enzyme. Regul.*, 3 :425–437, 1965. 12

[35] J. S. Griffith. Nature of the scrapie agent : Self-replication and scrapie. *Nature*, 215 (5105) :1043–1044, 1967. 11

[36] J.S. Griffith. Mathematics of cellular control processes. I. Negative feedback to one gene. *J. Theor. Biol.*, 20 :202–208, 1968. 12

[37] J.S. Griffith. Mathematics of cellular control processes. II. Positive feedback to one gene. *J. Theor. Biol.*, 20 :209–216, 1968. 12

[38] H Haken. *Synergetics : An introduction.* Springer-Verlag, 1983. 41

[39] J. Jacod and A. N.Shiryaev. *Limit Theorems for Stochastic Processes.* Springer–Verlag, 1987. 27, 28, 39

[40] I. Jeon. Existence of Gelling Solutions for Coagulation- Fragmentation Equations. *Commun. Math. Phys.*, 567 :541–567, 1998. 17, 42

[41] A. Joffe and M. Metivier. Weak convergence of sequences of semimartingales with applications to multitype branching processes. *Adv. Appl. Probab.*, 18(1) :20–65, 1986. 40, 42

[42] H.-W. Kang and T. G. Kurtz. Separation of time-scales and model reduction for stochastic reaction networks. *Ann. Appl. Probab. (to appear)*, 2012. 41

[43] T. Kato. On the semigroups generated by kolmogoroff's differential equations. *J. Math. Soc. Japan*, 6 :1–15, 1954. 36

[44] M. Kimmel and O. Arino. Comparison of approaches to modeling of cell population dynamics. *SIAM J. Appl. Math.*, 53(5) :1480–1504, 1993. 42

[45] M. Kimmel and D.E. Axelrod. *Branching Processes in Biology.* Springer-Verlag, 2002. 19

[46] H. Kitano. Looking beyond the details : a rise in system-oriented approaches in genetics and molecular biology. *Curr. Genet.*, 41(1) :1–10, 2002. 10

[47] J J Kupiec. A darwinian theory for the origin of cellular differentiation. *Mol. Gen. Genet.*, 255 :201–208, 1997. 11

[48] J.-J. Kupiec, M. Morange, M. Silberstein, and O. Gandrillon. *Le hasard au coeur de la cellule.* Les Éditions Materiologiques, 2009. ISBN 9782849502075. 11

[49] A. Kurakin. Self-organization vs watchmaker : stochastic gene expression and cell differentiation. *Dev. Genes Evol.*, 215 :46–52, 2005. 10

[50] T. G. Kurtz. Averaging for martingale problems and stochastic approximation. *Applied Stochastic Analysis*, 177 :186–209, 1922. 41

[51] T. G. Kurtz. Solutions of Ordinary Differential Equations as Limits of Pure Jump Markov Processes. *J. Appl. Probab.*, 7(1) :49–58, 1970. 41, 42

[52] T. G. Kurtz. Random time changes and convergence in distribution under the meyer-zheng conditions. *Ann. Probab.*, 19(3) :1010–1034, 1991. 41

[53] T G Kurtz. *Approximation of population processes.* CBMS-NSF, 1991. 42

[54] J.-P. Liautard, M.-T. Alvarez-Martinez, C. Feraudet, and J. Torrent. La protéine prion : structure, dynamique et conversion in vitro. *M S-Med. Sci.*, 18(1) :62–69, 2002. 11, 12

[55] M. C. Mackey and M. Tyran-Kamińska. Dynamics and density evolution in piecewise deterministic growth processes. *Ann. Polon. Math.*, 94(2) :111–129, 2008. 37

[56] D. A. McQuarrie. Stochastic approach to chemical kinetics. *J. Appl. Probab.*, 4(3) : 413–478, 1967. 13

[57] S. Méléard and S. Roelly. A host-parasite multilevel interacting process and continuous approximations. pages 1–31, 2011. arXiv :1101.4015. 42

[58] S. P. Meyn and R. L. Tweedie. Stability of markovian processes i : Criteria for discrete-time chains. *Adv. Appl. Probab.*, 24(3) :542–574, September 1992. 29, 30

[59] S. P. Meyn and R. L. Tweedie. Stability of markovian processes ii : Continuous-time processes and sampled chains. *Adv. Appl. Probab.*, 25(3) :487–517, 1993. 29, 30, 31

[60] S. P. Meyn and R. L. Tweedie. Stability of markovian processes iii : Foster-lyapunov criteria for continuous-time processes. *Adv. Appl. Probab.*, 25(3) :518–548, 1993. 29, 30, 31, 32

[61] S Mischler, C Mouhot, and B Wennberg. A new approach to quantitative chaos propagation estimates for drift, diffusion and jump processes. pages 1–45, 2011. arXiv :1101.4727. 42

[62] J R Norris. Smoluchowski's coagulation equation : uniqueness, nonuniqueness, and a hydrodynamic limit for stochastic coalescent. *Ann. Appl. Probab.*, 9(1) :78–109, 1999. 17, 42

[63] K. Oelschlager. A Martingale Approach to the Law of Large Numbers for Weakly Interacting Stochastic processes. *Ann. Appl. Probab.*, 12(2) :458–479, 1984. 42

[64] H. G. Othmer and C. H. Lee. A multi-time-scale analysis of chemical reaction networks : I. deterministic systems. *J. Math. Biol.*, 60(3) :387–450, 2009. 12

[65] H.G. Othmer. The qualitative dynamics of a class of biochemical control circuits. *J. Math. Biol.*, 3 :53–78, 1976. 12

[66] A. Paldi. Stochastic gene expression during cell differentiation : order from disorder ? *Cell. Mol. Life. Sci.*, 60(9) :1775–8, September 2003. 11

[67] K. Pichór and R. Rudnicki. Continuous Markov semigroups and stability of transport equations. *J. Math. Anal. Appl.*, 249(2) :668–685, 2000. 35

[68] Y. V. Prokhorov. Convergence of random processes and limit theorems in probability theory. *Theor. Probab. Appl+*, I(2), 1956. 41, 42

[69] S. B. Prusiner. Prions. *Proc. Natl. Acad. Sci.*, 95(23) :13363–13383, 1998. 11

[70] A. Raj and A. Van Oudenaarden. Single-Molecule Approaches to Stochastic Gene Expression. *Annu. Rev. Biophys.*, 38 :255–270, 2009. 10

[71] S Roelly and A Rouault. Construction et propriétés de martingales des branchements spatiaux interactifs. *Int. Stat. Rev.*, 58(2) :173–189, 1990. 42

[72] F. Sagués, J. Sancho, and J. García-Ojalvo. Spatiotemporal order out of noise. *Rev. Mod. Phys.*, 79(3) :829–882, July 2007. 43

[73] M. Santillán and H. Qian. Irreversible thermodynamics in multiscale stochastic dynamical systems. *Phys Rev E Stat Nonlin Soft Matter Phys.*, 83 :1–8, 2011. 41

[74] K. R. Schenk-Hoppé. Stochastic hopf bifurcation : an example. *Int. J. Non-linear Mechanics*, 31(5) :685–692, 1996. 17

[75] Erwin Schrödinger. *What Is Life ?* Cambridge University Press, 1944. 10

[76] J.F. Selgrade. Mathematical analysis of a cellular control process with positive feedback. *SIAM J. Appl. Math.*, 36 :219–229, 1979. 12

[77] K Singer. Application of the theory of stochastic processes to the study of irreproducible chemical reactions and nucleation processes. *J Roy. Stat. Soc. B Met.*, 15(1) : 192–106, 1953. 12

[78] D. W. Stroock and S. R. S. Varadhan. *Multidimensional diffusion processes.* Springer-Verlag, 1979. 27, 28

[79] D. M. Suter, N. Molina, D. Gatfield, K. Schneider, U. Schibler, and F. Naef. Mammalian genes are transcribed with widely different bursting kinetics. *Science*, 332(6028) : 472–4, 2011. 16

[80] N. Symonds. What is life ? : Schrodinger's influence on biology. *Q. Rev. Biol.*, 61(2) : 221–226, 1986. 10

[81] A.-S. Sznitman. *Topics in Propagation of Chaos*, volume 1464. Springer, 1991. 42

[82] V. C. Tran. *Modèles particulaires stochastiques pour des problèmes d'évolution adaptative et pour l'approximation de solutions statistiques.* PhD thesis, University Paris 10 Nanterre, 2006. 42

[83] M. Tyran-Kamińska. Substochastic semigroups and densities of piecewise deterministic Markov processes. *J. Math. Anal. Appl.*, 357(2) :385–402, 2009. 36, 37

[84] J. J. Tyson. On the existence of oscillatory solutions in negative feedback cellular control processes. *J. Math. Biol.*, 1(4) :311–315, 1975-12-01. 12

[85] M. Vellela and H. Qian. On the poincaré- hill cycle map of rotational random walk : locating the stochastic limit cycle in a reversible schnakenberg model. *P. Roy. Soc. A-Math. Phy.*, pages –, 2009. 17

[86] J. Voigt. On substochastic c_0-semigroups and their generators,. *Transport theory Statist. Phys.*, 16 :453–466, 1987. 36

Chapter 1

The bursting phenomenon as a jump Markov Process

1   Introduction

In neurobiology, when it became clear that some of the fluctuations seen in whole nerve recording, and later in single cell recordings, were not simply measurement noise but actual fluctuations in the system being studied, researchers very quickly started wondering to what extent these fluctuations actually played a role in the operation of the nervous system.

Much the same pattern of development has occurred in cellular and molecular biology as experimental techniques have allowed investigators to probe temporal behavior at ever finer levels, even to the level of individual molecules [110, 147]. Experimentalists and theoreticians alike who are interested in the regulation of gene networks are increasingly focused on trying to access the role of various types of fluctuations on the operation and fidelity of both simple and complex gene regulatory systems. Recent reviews [74, 109] give an interesting perspective on some of the issues confronting both experimentalists and modelers.

Among the increasing number of paper that demonstrate stochasticity in gene expression, at the single cell level, we can quote the work of Elowitz et al. [34], who have used an elegant experimental technique to prove inherent as well as environmental stochasticity. In their work, they measure at a single cell level two different gene reporters that has equal probability to be expressed. They quantify the difference between cells and through time of the total amount of expression of both genes, as well as the difference of proportion of expression of one gene among the two. Their results clearly demonstrate variability coming from the environment as well as coming from intrinsic stochastic event inside cells.

In this chapter, we deal with a model of a single gene, that is able to self-regulate its own expression. We model the dynamics of the level of expression of this gene in a single cell, without taking into account cell division. This model has been extensively used and studied in the last decades with different representations and approximations (see section 7 for a review). The aim of this "minimal model" is to study stochasticity in gene expression together with non-linear effect. Its advantage relies in the ability to obtain analytic results and quantitative prediction (see section 8). Recent improvements in molecular biology allow to identify and to measure precisely the level of gene expression in very small gene network, including single gene network (see the next subsection 2.1). For more complex (in the sense of large) gene network, such approach can be used as a building block to understand nonlinearity and stochasticity in higher network. Even in model of a single gene, the number of steps can vary considerably depending on the level of description chosen. We consider here a model that includes 4 steps, namely the state of the gene, the transcription, the translation and effector production. Again, improvements of molecular biology tend to identify more and more elementary steps and some model intend to take into account a more precise level of description, up to the nucleotide (see subsection 7.9). Finally, the model we consider is a purely dynamical model, and we don't consider any spatial or delay effect (even though, it is clear now that intracellular environment is not well-mixed, and that some processes inside cells take an incompressible time to proceed).

Our choice of level of description allows us to include the pioneer work of Goodwin [48] together with the important recently discovered switching and bursting effect in gene expression (these terms will be made clearer in the following). The Goodwin [48] model focuses on describing the time evolution of the concentration of gene product (mRNA, protein), based on the molecular basics found earlier. For describing the time evolution of a continuous variable, It is usually used an ordinary differential equation approach. When it becomes clear that the evolution of concentration of gene product in single cells could

not be described by deterministic laws, one then starts to consider stochastic description. In order to take into account stochasticity, it can be used a Langevin equation (additive noise) or more generally stochastic differential equation (multiplicative noise) with either Gaussian white noise (no time correlation) or Gaussian colored noise (with positive time correlations, see Shahrezaei et al. [131]). However, in this latter representation, the variable still evolves *continuously*. Whereas it has been well documented experimentally [22, 47, 111, 150] that in some organisms the mRNA and/or protein production is intermittent, and intense during relatively short periods of time. This phenomenon is called *bursting* in molecular biology. The accuracy of experiments permits to characterize the time interval between these production events, and permits to quantify the amount of molecules produced in a single burst event. In particular, in the work referred above, it has been found that in some organisms the bursting production is characterized by an exponential waiting time between production events, and the burst size is exponentially distributed as well. To reproduce such characteristics, it has recently been proposed (Friedman et al. [39], Mackey et al. [91]) to use a stochastic differential equation driven by a compound Poisson white noise, to model explicitly the discontinuous and stochastic production. Such a process can also be viewed as a piecewise-deterministic Markov process.

The mathematical foundation of piecewise-deterministic Markov processes (PDMP) was given by Davis [27]. This class of stochastic process unifies deterministic processes described by ordinary differential equation, and pure jump Markov processes, described by a Markov chain. Such a class of model has found recently an important echo in mathematical biology, since it allows to take into account different dynamics into a single model (Hespanha [60]). The work of Davis [27] shows how we can use the martingale machinery to study such stochastic processes. All the tools available to study convergence of stochastic processes (Ethier and Kurtz [36]) can then be used to study limiting behavior of PDMP. Two recent papers of Crudu et al. [25] and Kang and Kurtz [75] illustrate this approach, and explore various limiting cases using time-scale separation in the context of molecular reaction network. On another approach, PDMP brings new evolution equations on densities, which are typically of integro-differential types (as opposed to second-order partial differential equations associated to diffusion processes). Here, we will make use extensively of the semigroup approach to study long-time behavior of such equation, following the work of Lasota and Mackey [83], Mackey and Tyran-Kamińska [90], and Tyran-Kamińska [145]. In such approach, existence and stability of an invariant density is given by the existence and uniqueness of a solution to a fixed point problem (which presents itself as a system of algebraic equations or differential equations in our examples), associated to a discrete-time Markov chain. We can compare this approach to more traditional results in stochastic process given by Meyn and Tweedie [97], and recent contributions on convergence results of PDMP by Costa and Dufour [23].

On the other hand, the molecular basis for stochasticity in gene expression is also often attributed to low copy numbers of gene products. It is then needed to use discrete variable models rather than continuous one, and to model molecular number rather than concentration. Such ideas are widely used in biochemistry since the work of Gillespie [45]. The recent contribution of Anderson and Kurtz [3] summarizes the foundation and mathematical formulation of such models, as continuous-time Markov processes.

All the different models considered here use different mathematical formulations, namely pure jump Markov process in a discrete state space, continuous state space ordinary differential equation and hybrid models. We will attach an important part to prove these different formulations relate to each other through rigorous limit theorem (see sections 9). In particular, it's quite remarkable that the so-called " central dogma" of molecular biology

(as a chemical reaction network) can explain much of the different experimental observed behaviors, in different parameter space regions.

But first, it is important to emphasize the biochemical reaction network that is behind all these different mathematical formulations, and give some background material in molecular biology (see sections 2, 3 and 4). Once this is set up, we describe our model through a pure jump Markov process in a discrete state space and studie its qualitative behavior (section 5). Then we present its continuous deterministic version, namely the Goodwin model (section 6) and recall how we can precisely study its long time behavior. A review of (many) other linked or intermediate model is provided in section 7.

Then we present an analogous study of the Goodwin model, on a stochastic reduced model (section 8), where we only keep one variable. We consider in detail the probability distribution of the molecular number (with a discrete variable) or concentrations (hence, with a continuous state variable) in generic bacterial operons in the presence of 'bursting' using an analytical approach. As stated above, our work is motivated by the well documented production of mRNA and/or protein in stochastic bursts in both prokaryotes and eukaryotes [22, 47, 111, 150], and follows other contributions by, for example, [104, 77, 39, 13, 129]. All the above mentioned work share common goal, that is to find analytic characterization of a particular stochastic gene expression model, to be able to deduce kinetic parameters from experimental observations and/or to explain qualitatively and quantitatively the amount of variability measured experimentally. It is important to also recognize the pioneering investigation of Berg [9] who first studied the statistical fluctuations of protein numbers in bacterial population (with division) through the master equation approach, and introduced the concept of what is now called bursting. The analytical solution of the steady state density of the molecular distributions in the presence of bursting was first derived by Friedman et al. [39]. Our work extends these results to show the global stability of the limiting densities and examine their bifurcation structure to give a rather complete understanding of the effect of bursting on molecular distributions. The originality of this work is then to give a bifurcation diagram for the stochastic model of gene expression, in complete analogy with the deterministic Goodwin model. As molecular distributions can now be estimated experimentally in single cells, such theoretical framework may also be of importance in practice. We show in section 8.6 how one can estimate the *regulation function* (rather than a single parameter) using an inverse problem approach ([29]). Such estimate may be of importance to understand detail molecular interactions that determines the regulation function (see section 3). It has been the subject of a published work (Mackey et al. [91]). Finally, our framework can be extended to a discrete variable model (see subsection 8.1), and we also investigated the fluid limit (subsection 9.4), which will be the subject of a further publication (Mackey et al. [93]).

The fact that this one-dimensional " bursting" model relies on fundamental molecular basis of previously known mechanism in molecular biology is an important feature of this model, and has been noticed by many authors (see for instance [102] for review). Following recent theoretical contributions on reduction of stochastic hybrid system [25, 75] we rigorously prove that one limiting behavior of the (now) standard model of molecular biology gives a bursting model (see subsection 9.1 and 9.2) In our work, we can prove slight generalization of such reduction, in order to understand the key feature associated with such behavior. We also prove an adiabatic reduction for this bursting model (see subsection 9.3), which will be the subject of a further publication (Mackey et al. [92]). This work justifies the use of a reduce one-dimensional model when some variables are evolving with a fast time scale, in a context of a continuous state hybrid model. The originality of our work is to provide alternative proofs, using either partial differential

equation techniques or probabilistic techniques. Up to our knowledge, adiabatic reduction for stochastic differential equation with jumps hasn't been investigated before.

2 Standard Model

2.1 Background in molecular biology

The so-called "central dogma" of molecular biology, based on the Nobel Prize winning work of Jacob et al. [69] in which they introduced the concept of the operon (see subsection 2.2), is simple to state in principle, but complicated in its detail. Namely through the process of *transcription* of DNA, messenger RNA (mRNA) is produced and, in turn, through the process of *translation* of the mRNA, proteins (or intermediates) are produced. There is often feedback in the sense that molecules (enzymes) whose production is controlled by these proteins can modulate the translation and/or transcription processes. In what follows we will refer to these molecules as *effectors* (see figure 1.1). Rather astonishingly, within a few short years of the publication of the ground breaking work of Jacob et al. [69] the dynamics of this simple feedback system was studied mathematically by [48]. His formulation of the operon concept is now known as the Goodwin model.

We now consider both the transcription and translation processes in detail. We first present these two processes in prokaryotes, and then explain the main differences with eukaryotes. In the transcription process an amino acid sequence in the DNA is copied by an enzyme called RNA polymerase (RNAP) to produce a complementary copy of the DNA segment encoded in the resulting RNA. Thus this is the first step in the transfer of the information encoded in the DNA. The process by which this occurs is as follows.

When the DNA is in a double stranded configuration, the RNAP is able to recognize and bind to the promoter region of the DNA. (The RNAP/double stranded DNA complex is known as the closed complex.) Through the action of the RNAP, the DNA is unwound in the vicinity of the RNAP/DNA promoter site, and becomes single stranded. The RNAP/single stranded DNA is called the open complex. Once in the single stranded configuration, the transcription of the DNA into mRNA commences. A lot of interactions between proteins can promote or block the closed complex formation and its binding to the promoter region of the DNA. These proteins that interact with the RNAP are called transcription factor (TF). There are many different known interactions between TF and DNA and RNAP. Some TF can stabilize or block the binding of RNA polymerase to DNA. They can also recruit coactivator or corepressor proteins to the DNA complex, in order to increase or decrease the rate of gene transcription. In eukaryotes, TF can make the DNA more or less accessible to RNA polymerase by modifying physically its configuration. Obviously, when these TF interact with the DNA that controls its production, then they coincide with the molecules we called above effectors. The interaction between effectors and the DNA and RNAP polymerase then dictates the feedback mechanism (see section 3) and are responsible for what is called the transcriptional regulation or the gene expression regulation. All these interactions are supposedly sequence-specific meaning that specific proteins will be able to bind to specific sequence of DNA, or to specific other proteins. These concepts are however unreliable [80].

In prokaryotes, translation of the newly formed mRNA starts with the binding of a ribosome to the mRNA. The function of the ribosome is to 'read' the mRNA in triplets of nucleotide sequences (codons). Then through a complex sequence of events, initiation and elongation factors bring transfer RNA (tRNA) into contact with the ribosome-mRNA complex to match the codon in the mRNA to the anti-codon in the tRNA. The elongating peptide chain consists of these linked amino acids, and it starts folding into its

final conformation. This folding continues until the process is complete and the polypeptide chain that results is the mature protein. Although there are also many interactions between proteins at the step of translation, there are much less studies reporting for post-transcriptional regulation (see [72] that consider mRNA degradation regulation mechanism and post-transcriptional regulator binding).

The situation in eukaryotes differs from 2 main things.

Firstly, the DNA is found in a structure that is called chromatin. The exact structure of the chromatin is much out of the scope here, and we can keep in mind that the chromatin 'packs' the DNA in a smaller volume. Also, the chromatin prevents the DNA to be easily accessible. Sequence of DNA can be more or less packed, depending on the gene. The state of the chromatin (more or less packed) may also varies during time, leading to a very complex dynamics. This dynamic modification of chromatin (called chromatin remodeling) may be the result of interactions with enzymes and transcription factors (but would not be considered here).

Secondly, mRNA molecules are synthesized inside the nucleus, whereas the ribosomes are located outside the nucleus. Then proteins will be synthesized outside the nucleus, and will have to enter the nucleus to interact with the DNA. These facts usually lead to consider higher delays in the transcription/translation process modeling in eukaryotes than in prokaryotes.

Our framework was conceived for gene expression model in bacteria (prokaryotes). However, a growing number of people argue that similar models can be used for both prokaryotes and eukaryotes, in different parameter space regions (see subsection 2.4).

(a) "Central Dogma"　　　　　　　　(b) "New Central Dogma"
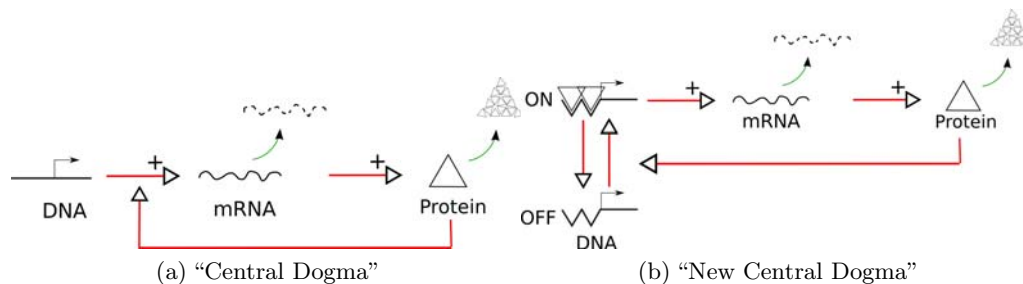
Figure 1.1: Schematic illustration of the so-called "central dogma"of molecular biology. (a) Messenger RNA (mRNA) are produced through the transcription of DNA, and proteins are produced through the translation of mRNA. There is a feedback directly by proteins (or effectors) that can control the transcription of DNA. (b) Similar of the left panel, except that the DNA can enter in an "OFF"state for which transcription is not possible.

2.2　The operon concept

An operon is a piece of DNA containing a cluster of genes under the control of a single promoter. The genes are transcribed together into mRNA. These mRNA are either translated together or separately in the cytoplasm. In most cases, genes contained in the operon are then either expressed together or not at all. Several genes must be both co-transcribed and co-regulated to define an operon. Operons were first discovered in prokaryotes but also exist in eukaryotes. From the experimental and modeling point of view, operons that contain a regulatory gene (repressor or activator) are very key concepts because they provide a very small regulatory gene network. Most famous operon are

　– The lactose (*lac*) operon ([135]) in bacteria is the paradigmatic example of this concept and this much studied system consists of three structural genes named *lacZ*,

lacY, and *lacA*. These three genes contain the code for the ultimate production, through the translation of mRNA, of the intermediates β-galactosidase, *lac* permease, and thiogalactoside transacetylase respectively. The enzyme β-galactosidase is active in the conversion of lactose into allolactose and then the conversion of allolactose into glucose. The *lac* permease is a membrane protein responsible for the transport of extracellular lactose to the interior of the cell. (Only the transacetylase plays no apparent role in the regulation of this system.) The regulatory gene *lacI*, which is part of a different operon, codes for the *lac* repressor. The latter is transformed to an inactive form when it binds with allolactose. Hence, in this system, allolactose acts as the effector molecule. See figure 1.2.

– The tryptophan (*trp*) operon was also extensively studied ([58],[123],[89]). Tryptophan is an amino acid that is incorporated into proteins that are essential to bacterial growth. When tryptophan is present in the growth media, it forms a complex with the tryptophan repressor and the complex binds to the promoter of the trp operon, effectively switching off production of tryptophan biosynthetic enzymes. In the absence of tryptophan, the repressor cannot bind to the promoter and the essential tryptophan biosynthetic enzymes are produced. See figure 1.4.

– The bacteriophage λ system was reviewed recently ([96],[57], [58]). It is a small piece of viral DNA that encode for two proteins (cI and cro) that are mutually antagonist. When a virus infects a bacteria like E. Coli, experiments show that the system exhibits bistability. The system can be in two distinct states. Each state implies a different behavior for the cell. In one state (called lysogenic), the virus lies dormant, and is replicated only with the bacteria. In the other state, the virus expresses proteins that are able to replicate the virus itself, then lyse (kill) the host cell and release its progeny.

2.3   Synthetic network

The ability of design synthetic constructed gene network, reviewed by Hasty et al. [58], provides also an excellent tool for modeling and experimental purposes. Approaches with coupled modeling/experiments were indeed used to design specific small circuits with the desired properties (bistability, oscillations etc...). Amongst the most popular synthetic networks, one can find:

– the genetic toggle switch, such as the λ-switch (Gardner et al. [43]). It consists of two genes that encode for proteins that are co-repressive. It has been experimentally demonstrated that this system displays bistability.

– the Repressilator. It consists of a loop of three genes. Each one inhibits successively the next gene ([33]). It has been experimentally demonstrated that this system can display oscillations.

– Synthetic positive autoregulatory gene (tet-R system, [8], or λ-phage system [67]). It has been experimentally shown that this system displays bistability.

Obviously, it has also some interest on its own (cellular control, biotechnology, genetically engineered microorganisms and so on).

2.4   Prokaryotes vs Eukaryotes models

Although the quite important differences between prokaryotes and eukaryotes, it has been argued several times in the past that the standard stochastic model of gene expression

is *a priori* suitable for both ([95, 115, 46]). The rate constants and the meaning of the stochastic transition can be different though.

In particular, the On/Off switching rate of the gene state (see figure 1.1b) on prokaryotes will usually reflect binding and unbinding events of molecule on the promoter or even pausing of RNA polymerase, while the On/Off switching rate on eukaryotes will reflect opening-closing of chromatin. Indeed, we saw that the presence of nucleosomes and the packing of DNA-nucleosome complexes into chromatin generally make promoters inaccessible to the transcriptional machinery. Transition between open and closed chromatin structures then correspond to active and inactive (repressed) promoter states, and can be fairly slow ([74],[109],[115]) compared to the dynamics of binding and unbinding event of molecules at the promoter region in prokaryotes. We refer to table 1.2 for some parameter values taken from literature.

3   The Rate Functions

From what we presented above, it should be clear now that the transcription rate (and the translation rate) is function of many cellular components, and specially protein numbers/concentrations. Some modeling approaches take into account many details and many variables in order to reflect faithfully the transcription process (see subsection 7.9 for a brief review). However, these approaches increase drastically the number of parameters and the dimension of the model. With some kinetic assumptions, it is possible to reduce the complexity. The justification of it is an important stage of modeling. We detail here some classical derivation of the transcriptional regulation in the deterministic context, and (non-so) classical derivation in the stochastic context. There have been very different mechanisms (for a review in prokaryotes see [154], in yeast [53] and in higher eukaryotes [118]) proposed for the molecular basis of the regulation of the transcription rate by effector molecules. These mechanisms also depends a lot of the system considered. We focus on one particular system (feedback through complex formation) for simplicity. Depending on the model in consideration (eukaryotes or prokaryotes in particular), the feedback mechanism can be involved at different stages (activation/inactivation of the gene, or initiation of the transcription).

During transcription initiation, the reversible binding of an RNAP to the promoter region and subsequent formation of an open complex achieve rapid equilibrium: initiation from the final open complex is the rate-limiting step ([142]). Transcription initiation is therefore assumed to be a pseudo-first-order reaction with rate linearly proportional to the amount of RNAP. In this section we examine the molecular dynamics of both the classical inducible and repressible operon [148] to derive expressions for the dependence of the transcription rate on effector levels. In this view, the effectors first interact with other molecules (repressors) to form a molecular complex. These interactions will modify the binding/unbinding event of repressors on the DNA, and then modify the binding/unbinding event of RNAP to the promoter region of the DNA. The effector molecules can also act by binding directly on to the promoter region and shielding it from RNAP. In all cases, the reactions with effector are considered to be in equilibrium and simply change the fraction of RNAP bound as a closed complex, thereby changing the effective transcriptional rate. See [120] and [148] for experimental evidence that such approach reproduces accurately the rate function.

3.1   Transcriptional rate in inducible regulation

For a typical inducible regulatory situation (such as the *lac* operon), in the *presence* of the effector molecule the repressor is *inactive* (is unable to bind to the operator region preceding the structural genes), and thus DNA transcription can proceed (see figure 1.2). Let R denote the repressor, E the effector molecule, and O the operator. We assume that the effector binds with the active form R of the repressor to form a complex RE_n. This reaction is of the form

$$R + nE \underset{k_c^-}{\overset{k_c^+}{\rightleftharpoons}} RE_n, \tag{3.1}$$

where n is the effective number of molecules of effector required to inactivate the repressor R. Furthermore, the operator O and repressor R are assumed to interact according to

$$O + R \underset{k_b^-}{\overset{k_b^+}{\rightleftharpoons}} OR. \tag{3.2}$$

Finally, the transcription takes place when RNAP binds the free operator O, thereby leading to the reaction

$$O + RNAP \overset{k_M}{\longrightarrow} O + RNAP + M, \tag{3.3}$$
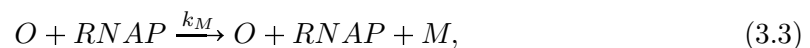
where M denotes the mRNA. The goal of this section is to derive the effective rate of production of M in function of the effector molecules as the binding dynamics between effectors, repressors and operators quickly reach equilibrium. We first present the standard way to derive this rate, using ordinary differential equation, and then using stochastic differential equation. for simplicity, we do not include at his point the fact that effector molecules are constantly degraded and produced. Hence its total level will change over time. However, these variations will occur on a slower time scale than operator fluctuations, so that it won't change the reduction performed here.

Figure 1.2: Figure taken from Wikipedia. Schematic illustration of the lac operon, an inducible operon. Top: Repressed , Bottom: Active. 1: RNA Polymerase, 2: Repressor, 3: Promoter, 4: Operator, 5: Lactose, 6: lacZ, 7: lacY, 8: lacA. In presence of lactose, the repressor is unable to bind to the bind to the operator, and RNA polymerase can proceed.

3.1.1   Deterministic description

The set of chemical reactions (3.1)-(3.2)-(3.3) can be described by the following system of ODE (using standard chemical kinetics argument)

$$
\begin{cases}
\dot{x}_R = -k_c^+ x_R x_E^n + k_c^- x_{RE_n} - k_b^+ x_O x_R + k_b^- x_{OR}, \\
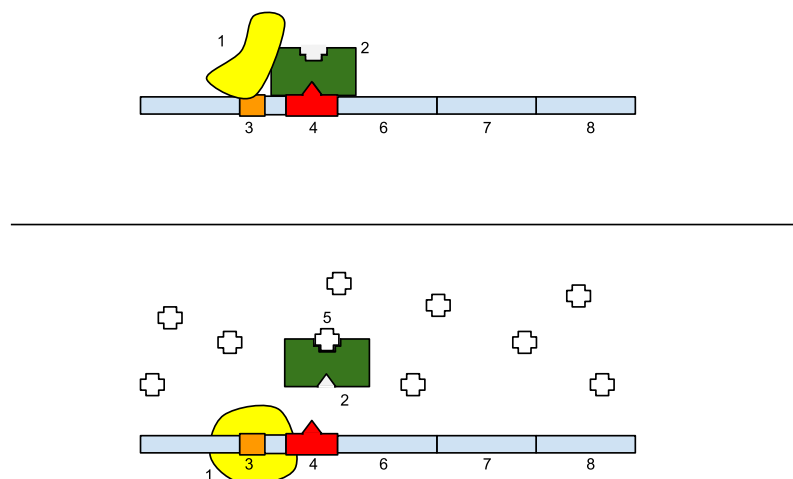\dot{x}_E = -n k_c^+ x_R x_E^n + n k_c^- x_{RE_n}, \\
\dot{x}_{RE_n} = k_c^+ x_R x_E^n - k_c^- x_{RE_n}, \\
\dot{x}_O = -k_b^+ x_O x_R + k_b^- x_{OR}, \\
\dot{x}_{OR} = k_b^+ x_O x_R - k_b^- x_{OR}, \\
\dot{x}_M = k_M x_O x_{RNAP},
\end{cases}
\tag{3.4}
$$

where $x_{entities}$ denotes the concentration of the given biochemical entities. Note that the three following quantities are conserved through time:

– the total amount of operator O_{tot}:

$$
x_{O_{tot}} = x_O + x_{OR}.
$$

– the total amount of repressor R_{tot}:

$$
x_{R_{tot}} = x_R + x_{RE_n} + x_{OR}.
$$

– the total amount of effector E_{tot}:

$$
x_{E_{tot}} = x_E + n x_{RE_n}.
$$

We define the equilibrium rate constants $K_b = \frac{k_b^+}{k_b^-}$ and $K_c = \frac{k_c^+}{k_c^-}$. We now make specific assumptions on reaction rates to prove the following

Proposition 15. *Assume the kinetic reaction rate constants satisfies*

Hypothesis 1. $k_M \ll k_c^+, k_c^-, k_b^+, k_b^-,$

and the total quantity of repressors and effectors are such that

Hypothesis 2. $K_c x_{R_{tot}} x_{E_{tot}}^{n-1} \ll 1.$

Then, the effective mRNA production rate is a function of $x_{E_{tot}}$, given by $k_M k_1(x_{E_{tot}})$, where if $x_{R_{tot}} \gg 1$,

$$
k_1(x_{E_{tot}}) = x_{RNAP} x_{O_{tot}} \frac{1 + K_c x_{E_{tot}}^n}{K_b x_{R_{tot}}},
\tag{3.5}
$$

while if $\frac{x_{R_{tot}}}{x_{O_{tot}}} \gg 1$,

$$
k_1(x_{E_{tot}}) = x_{RNAP} x_{O_{tot}} \frac{1 + K_c x_{E_{tot}}^n}{1 + K_b x_{R_{tot}} + K_c x_{E_{tot}}^n}.
\tag{3.6}
$$

Proof. By hypothesis 1, the reaction (3.3) occurs at a much slower rate than reactions (3.1)-(3.2). We then modify the last equation of eq. (3.4) on x_M by

$$
\dot{x}_M = \varepsilon k_M x_O x_{RNAP},
$$

where $\varepsilon \ll 1$. On the slow time scale $\tau = \varepsilon t$, it is a standard result [143, 38] that the fast dynamics approaches its equilibrium value as $\varepsilon \to 0$. The slow manifold associated is given by the system of algebraic equations

$$\begin{cases} x_R\big(1 + K_c x_E^n + K_b x_O\big) = x_{R_{tot}}, \\ x_O\big(1 + K_b x_R\big) = x_{O_{tot}}, \\ x_E + nK_c x_R x_E^n = x_{E_{tot}}. \end{cases}$$

Now hypothesis 2 makes this system tractable, because the last equation becomes $x_E \approx x_{E_{tot}}$ and the above system reduced to

$$\begin{cases} x_R\big(1 + K_c x_{E_{tot}}^n + K_b x_O\big) = x_{R_{tot}}, \\ x_O\big(1 + K_b x_R\big) = x_{O_{tot}}. \end{cases} \tag{3.7}$$

It is easy to show that this system of equations has a unique strictly positive solution (it can be transformed to a second order polynomial equation), and that this solution is globally stable for the fast dynamics. Although this solution is rather complicated (as a function of the parameters), it has two important asymptotic expressions. When $x_{R_{tot}} \gg 1$, the expression of x_O has the following leading term

$$x_O \approx x_{O_{tot}} \frac{1 + K_c x_{E_{tot}}^n}{K_b x_{R_{tot}}},$$

while when $\frac{x_{R_{tot}}}{x_{O_{tot}}} \gg 1$, the expression of x_O reads

$$x_O \approx x_{O_{tot}} \frac{1 + K_c x_{E_{tot}}^n}{1 + K_b x_{R_{tot}} + K_c x_{E_{tot}}^n}.$$

Considering that x_{RNAP} is constant, the effective mRNA production rate is then, on the slow time scale, $k_M k_1(x_{E_{tot}})$, where in the first case,

$$k_1(x_{E_{tot}}) = x_{RNAP} x_{O_{tot}} \frac{1 + K_c x_{E_{tot}}^n}{K_b x_{R_{tot}}},$$

while in the second case,

$$k_1(x_{E_{tot}}) = x_{RNAP} x_{O_{tot}} \frac{1 + K_c x_{E_{tot}}^n}{1 + K_b x_{R_{tot}} + K_c x_{E_{tot}}^n}.$$

$\square$

In both cases, there will be maximal repression when $E = 0$ but even then there will still be a basal level of mRNA production (which we call the fractional leakage). In the first case, the production rate of mRNA is unbounded with the level of effector, while it is bounded in the second case. For biological motivation, the second expression eq. (3.6) is rather used. However equation 3.5 is sometimes used with $n = 1$ (linear regulation).

3.1.2   Stochastic description

We can also describe the set of chemical reactions (3.1)-(3.2)-(3.3) by the following system of SDE (using standard chemical kinetics argument)

$$
\left\{
\begin{aligned}
X_R(t) &= X_R(0) - Y_1^+\left(\int_0^t k_c^+ X_R(s)\binom{X_E(s)}{n}ds\right) + Y_1^-\left(\int_0^t k_c^- X_{RE_n}(s)ds\right) \\
&\quad - Y_2^+\left(\int_0^t k_b^+ X_O(s)X_R(s)ds\right) + Y_2^-\left(\int_0^t k_b^- X_{OR}(s)ds\right), \\
X_E(t) &= X_E(0) - nY_1^+\left(\int_0^t k_c^+ X_R(s)\binom{X_E(s)}{n}ds\right) + nY_1^-\left(\int_0^t k_c^- X_{RE_n}(s)ds\right), \\
X_{RE_n}(t) &= X_{RE_n}(0) + Y_1^+\left(\int_0^t k_c^+ X_R(s)\binom{X_E(s)}{n}ds\right) - Y_1^-\left(\int_0^t k_c^- X_{RE_n}(s)ds\right), \\
X_O(t) &= X_O(0) - Y_2^+\left(\int_0^t k_b^+ X_O(s)X_R(s)ds\right) + Y_2^-\left(\int_0^t k_b^- X_{OR}(s)ds\right), \\
X_{OR}(t) &= X_{OR}(0) + Y_2^+\left(\int_0^t k_b^+ X_O(s)X_R(s)ds\right) - Y_2^-\left(\int_0^t k_b^- X_{OR}(s)ds\right), \\
X_M(t) &= X_M(0) + Y_3\left(\int_0^t k_M X_O(s)X_{RNAP}(s)ds\right),
\end{aligned}
\right.
\tag{3.8}
$$

where $X_{entities}$ denotes the number of the given biochemical entities, and

$$
\binom{X_E(s)}{n} = \frac{X_E(s)(X_E(s)-1)\cdots(X_E(s)-n+1)}{n!}.
$$

In eq. (3.8), $Y_i^\pm$, $i=1,2,3$ refers to independent unit Poisson processes, that are associated to reactions (3.1)-(3.2)-(3.3). For instance, Y_1^+ (respectively Y_1^-) gives the successive instant the forward (respectively the backward) reaction (3.1) fires. Note that the three following quantities are again conserved through time:

   – the total amount of operator O_{tot}:

$$
X_{O_{tot}} = X_O + X_{OR},
$$

   – the total amount of repressor R_{tot}:

$$
X_{R_{tot}} = X_R + X_{RE_n} + X_{OR},
$$

   – the total amount of effector E_{tot}:

$$
X_{E_{tot}} = X_E + nX_{RE_n}.
$$

We now make specific assumptions on reaction rates to prove the following

Proposition 16. *Assume the kinetic reaction rate constants satisfies hypothesis 1 and that the following scaling holds as $N \to \infty$,*

Hypothesis 3.

$$
\begin{aligned}
X_E^N(0) &\sim N^\alpha, \\
k_c^- &\sim N^{n\alpha},
\end{aligned}
$$

for some $\alpha > 0$. We assume furthermore that $Z_E^N(0) = \frac{X_E^N(0)}{N^\alpha}$ is such that it exists $Z_{E_{tot}} > 0$,

$$
\lim_{N \to \infty} Z_E^N(0) = Z_{E_{tot}}.
$$

Then, as $N \to \infty$, the solution $X_M^N(t)$ of eq. (3.8) converges to the solution of

$$X_M(t) = X_M(0) + Y_3\Big(\int_0^t k_M \mathbb{E}\big[X_O\big](s)X_{RNAP}(s)ds \Big),$$

where $\mathbb{E}\big[X_O\big](s)$ is the asymptotic first moment of X_O on the fast dynamics given by reactions (3.1)-(3.2), and is given by

$$\mathbb{E}\big[X_O\big] = X_{O_{tot}} \frac{1 + K_c Z_{E_{tot}}^n}{1 + K_b X_{R_{tot}} + K_c Z_{E_{tot}}^n}. \tag{3.9}$$

Proof. By hypothesis 1, the reaction (3.3) occurs at a much slower rate than reactions (3.1)-(3.2). We then modify the last equation of eq. (3.4) on X_M by

$$X_M(t) = X_M(0) + Y_3\Big(\int_0^t \varepsilon k_M X_O(s)X_{RNAP}(s)ds \Big),$$

where $\varepsilon \ll 1$. The fast dynamics consist of a closed system on a finite state space (due to mass conservation constraint) and its associated Markov chain is irreducible, so that it has a unique stationary distribution. By the averaging theorem (see [75, thm 5.1]), on the slow time scale, the dynamics can then be reduced to

$$X_M(t) = X_M(0) + Y_3\Big(\int_0^t k_M \mathbb{E}\big[X_O\big](s)X_{RNAP}(s)ds \Big),$$

where $\mathbb{E}\big[X_O\big](s)$ is the asymptotic first moment of X_O on the fast dynamics, and is a function of $K_b, K_c, X_{R_{tot}}(s), X_{E_{tot}}(s)$ and $X_{O_{tot}}(s)$. Its exact expression is out of reach, but we can derive analogous result as in the deterministic case. With hypothesis 3, we define $Z_E^N = \frac{X_E^N}{N^\alpha}$ and rewrite the fast system as (with a slight abuse of notation)

$$
\begin{cases}
\begin{aligned}
X_R^N(t) &= X_R(0) - Y_1^+\Big(\int_0^t N^{n\alpha} k_c^+ X_R^N(s)Z_E^N(1 + O(\tfrac{1}{N^\alpha}))ds \Big) \\
&\quad + Y_1^-\Big(\int_0^t N^{n\alpha} k_c^- X_{RE_n}^N(s)ds \Big) \\
&\quad - Y_2^+\Big(\int_0^t k_b^+ X_O^N(s)X_R^N(s)ds \Big) + Y_2^-\Big(\int_0^t k_b^- X_{OR}^N(s)ds \Big), \\
Z_E^N(t) &= Z_E^N(0) - nN^{-\alpha}Y_1^+\Big(\int_0^t N^{n\alpha} k_c^+ X_R(s)Z_E^N(1 + O(\tfrac{1}{N^\alpha}))ds \Big) \\
&\quad + nN^{-\alpha}Y_1^-\Big(\int_0^t N^{n\alpha} k_c^- X_{RE_n}^N(s)ds \Big), \\
X_{RE_n}^N(t) &= X_{RE_n}(0) + Y_1^+\Big(\int_0^t N^{n\alpha} k_c^+ X_R^N(s)Z_E^N(1 + O(\tfrac{1}{N^\alpha}))ds \Big) \\
&\quad - Y_1^-\Big(\int_0^t N^{n\alpha} k_c^- X_{RE_n}^N(s)ds \Big), \\
X_O^N(t) &= X_O(0) - Y_2^+\Big(\int_0^t k_b^+ X_O^N(s)X_R^N(s)ds \Big) + Y_2^-\Big(\int_0^t k_b^- X_{OR}^N(s)ds \Big), \\
X_{OR}^N(t) &= X_{OR}(0) + Y_2^+\Big(\int_0^t k_b^+ X_O^N(s)X_R^N(s)ds \Big) - Y_2^-\Big(\int_0^t k_b^- X_{OR}^N(s)ds \Big).
\end{aligned}
\end{cases}
$$

With this scaling, the variable X_R^N, Z_E^N and X_{RE_n} then evolve at a faster time scale than X_O^N and X_{OR}^N, so that the averaging theorem again tells us that, at the limit $N \to \infty$,

$$X_O(t) = X_O(0) - Y_2^+\Big(\int_0^t k_b^+ X_O(s)\mathbb{E}[X_R]ds \Big) + Y_2^-\Big(\int_0^t k_b^- (X_{O_{tot}} - X_O(s))ds \Big),$$

so that immediately

$$\mathbb{E}\big[X_O\big](t \to \infty) = \frac{X_{O_{tot}}}{1 + K_b\mathbb{E}\big[X_R\big]}.$$

To find the latter quantity $\mathbb{E}\big[X_R\big]$ we look at the time scale $tN^{-(n-1)\alpha}$. Let then $\gamma = -(n-1)\alpha$. We define $Z_E^{N,\gamma}(t) = Z_E^N(tN^\gamma)$ and similarly $X_R^{N,\gamma}$ and $X_{RE_n}^{N,\gamma}$. The fast system defined by reaction (3.1) becomes

$$\begin{cases} X_R^{N,\gamma}(t) & = & X_R(0) - Y_1^+\Big(\int_0^t N^\alpha k_c^+ X_R^{N,\gamma}(s)Z_E^{N,\gamma}(1 + O(\frac{1}{N^\alpha}))ds\Big) \\[2mm] & & +Y_1^-\Big(\int_0^t N^\alpha k_c^- X_{RE_n}^{N,\gamma}(s)ds\Big), \\[2mm] Z_E^{N,\gamma}(t) & = & Z_E^N(0) - nN^{-\alpha}Y_1^+\Big(\int_0^t N^\alpha k_c^+ X_R^{N,\gamma}(s)Z_E^{N,\gamma}(1 + O(\frac{1}{N^\alpha}))ds\Big) \\[2mm] & & +nN^{-\alpha}Y_1^-\Big(\int_0^t N^\alpha k_c^- X_{RE_n}^{N,\gamma}(s)ds\Big), \\[2mm] X_{RE_n}^{N,\gamma}(t) & = & X_{RE_n}(0) + Y_1^+\Big(\int_0^t N^\alpha k_c^+ X_R^{N,\gamma}(s)Z_E^{N,\gamma}(1 + O(\frac{1}{N^\alpha}))ds\Big) \\[2mm] & & -Y_1^-\Big(\int_0^t N^\alpha k_c^- X_{RE_n}^{N,\gamma}(s)ds\Big). \end{cases}$$

Define now $Z_{RE_n}^{N,\gamma} = N^{-\alpha}X_{RE_n}^{N,\gamma}$ that satisfies the equation

$$Z_{RE_n}^{N,\gamma}(t) = Z_{RE_n}^N(0) + N^{-\alpha}Y_1^+\Big(\int_0^t N^\alpha k_c^+ X_R^{N,\gamma}(s)Z_E^{N,\gamma}(1 + O(\frac{1}{N^\alpha}))ds\Big)$$
$$- N^{-\alpha}Y_1^-\Big(\int_0^t N^{2\alpha} k_c^- Z_{RE_n}^{N,\gamma}(s)ds\Big),$$

so that

$$\begin{aligned} 0 & = \lim_{N \to \infty} Z_{RE_n}^{N,\gamma}(t), \\ & = \lim_{N \to \infty} N^{-\alpha}X_{RE_n}^{N,\gamma}, \\ & = \lim_{N \to \infty} \int_0^t k_c^+ X_R^{N,\gamma}(s)Z_E^{N,\gamma}(s)ds - \int_0^t k_c^- X_{RE_n}^{N,\gamma}(s)ds. \end{aligned}$$

Assuming that $\lim_{N \to \infty} Z_E^N(0) = Z_{E_{tot}}$, we obtain finally

$$\lim_{N \to \infty} Z_E^{N,\gamma}(t) = Z_{E_{tot}}.$$

so that at this time scale, $Z_E^{N,\gamma}$ is constant and contains the whole quantity of effector molecules. Still at this time scale, $X_{RE_n}^{N,\gamma}$ and $X_R^{N,\gamma}$ are fast varying variable, whose behavior is best captured by the occupancy measure

$$V_R^{N,\gamma}(C \times [0,t)) = \int_0^t \mathbf{1}_{\{C\}}(X_R^{N,\gamma}(s))ds.$$

For any bounded function f, the following quantity is a Martingale

$$f(X_R^{N,\gamma}(t)) - f(X_R^{N,\gamma}(0)) - N^\alpha \int_{\mathbb{N}} \int_0^t C_{Z_E^{N,\gamma}} f(x_R)V_R^{N,\gamma}(dx_R \times ds),$$

where

$$C_{Z_E^{N,\gamma}} f(x_R) = k_c^+ x_R Z_E^{N,\gamma}(f(x_R - 1) - f(x_R)) + k_c^-(X_{R_{tot}} - x_r)(f(x_R + 1) - f(x_R)).$$

Dividing by N^{α}, we see that its limiting measure must be solution of

$$0 = \int_{\mathbb{N}} \int_0^t C_{Z_{E_{tot}}} f(x_R) V_R(dx_R \times ds).$$

then V_R has a binomial law of parameter $(X_{R_{tot}}, \frac{1}{1+K_c Z_{E_{tot}}^n})$. Taken all together,

$$\mathbb{E}\big[X_O\big](t \to \infty) = X_{O_{tot}} \frac{1 + K_c Z_{E_{tot}}^n}{1 + K_b X_{R_{tot}} + K_c Z_{E_{tot}}^n},$$

which is then the analog result of the deterministic description. $\square$

Remark 17. *Note that with the scaling we have assumed,*

$$K_c X_{R_{tot}} X_{E_{tot}}^{n-1} \sim N^{-\alpha} \ll 1.$$

The scaling we chose also implies that complex formation reaction occurs at a faster time scale than Repressor-Operator binding reaction. These arguments can then be used to derive operator switching rate function as a function of the effector level. We illustrate our results on figure 1.3, by calculating with a standard stochastic algorithm the statistical asymptotic mean values of X_0 for the subsystem of reaction (3.1)-(3.2). As the scaling parameter N increases, the average values of X_O, as a function of $Z_{E_{tot}}$, become closer and closer of the eq. (3.9). We also show the similar behavior of the deterministic solution of the non-linear system eq. (3.7).

Remark 18. *Other scalings can of course yield similar result, for instance*

$$X_E \sim N^{\alpha},$$
$$k_c^+ \sim N^{-n\alpha},$$

would produce another tractable limiting behavior.

(a) $n = 1$	(b) $n = 2$
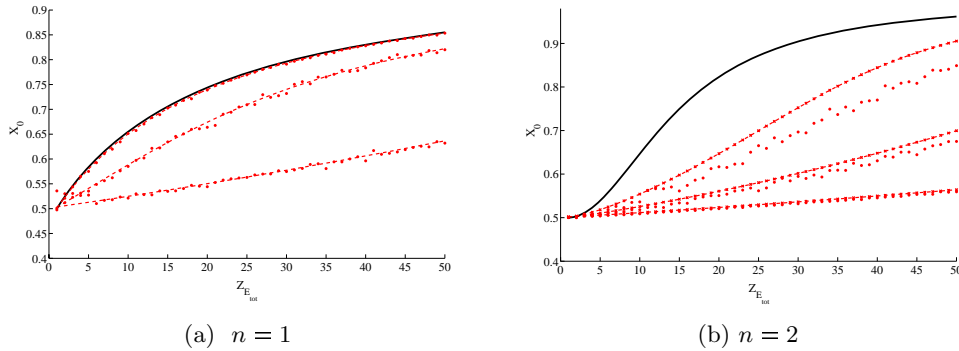
Figure 1.3: Numerical values of the first moment of the free operator variable X_O, as a function of the effector level $Z_{E_{tot}}$. In both figures, the black lines are given by the Hill function, eq. (3.9), the dotted red lines are the numerical solution of the eq. (3.7), and the red points are the numerical mean value of X_0 given by the system of reaction (3.1)-(3.2). Parameters are: (a) $n = \alpha = 1$, $k_c^+ = k_b^+ = 1, k_b^- = 100$, $X_{O_{tot}} = 1$, $X_{R_{tot}} = 100$, $k_c^- = N^{n\alpha}$, $X_{E_{tot}} = N^{\alpha}$, and from down to top, $N = 1, 10, 100$. (b) $n = 2$, $\alpha = 1$, $k_c^+ = k_b^+ = 1, k_b^- = 100$, $X_{O_{tot}} = 1$, $X_{R_{tot}} = 100$, $k_c^- = N^{n\alpha}$, $X_{E_{tot}} = N^{\alpha}$, and from down to top, $N = 1, 5, 10$.

3.2   Transcriptional rate in repressible regulation

In the classic example of a repressible system (such as the *trp* operon), in the *presence* of effector molecules the repressor is *active* (able to bind to the operator region), and thus block DNA transcription (see figure 1.4). We use the same notation as before, but now note that the effector binds with the inactive form R of the repressor so it becomes active. We assume that this reaction is of the same form as in eq. (3.1). The difference now is that the operator O and repressor R are assumed to interact according to
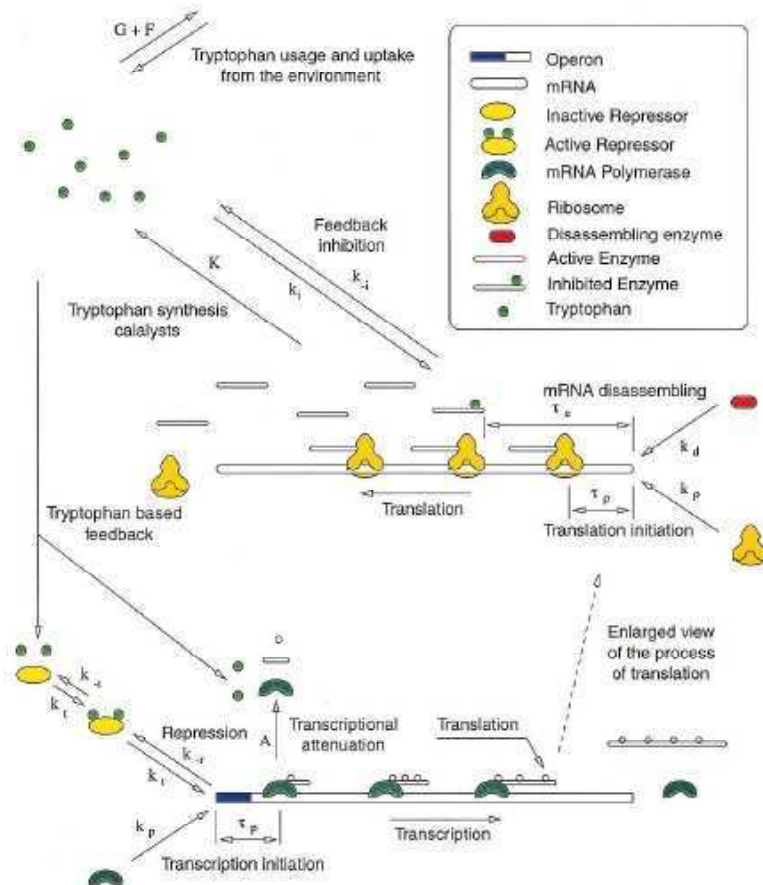
Figure 1.4: Figure taken from [123]. Schematic illustration of the Tryptophan operon, a repressible operon. In presence of Trp, the repressor is active and able to bind to the operator, which prevents RNA polymerase to bind.

$$O + R \cdot E^n \underset{k_b^-}{\overset{k_b^+}{\rightleftharpoons}} ORE_n.$$
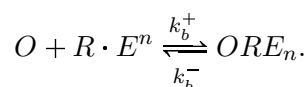
Similar argument as above yields the following transcription rate function. We only state the deterministic result for simplicity.

Proposition 19. *Assume the kinetic reaction rate constants satisfies hypothesis 1 and that*

Hypothesis 4. $K_c x_{R_{tot}} x_{E_{tot}}^{n-1} (1 + K_b x_0) \ll 1.$

Then, the effective mRNA production rate is a function of $x_{E_{tot}}$, given by $k_M k_1(x_{E_{tot}})$,

parameter	inducible	repressible
Λ	$1 + K_b x_{R_{tot}}$	1
Δ	1	$1 + K_b x_{R_{tot}}$
λ_1	$k_M x_{RNAP} x_{O_{tot}}$	

Table 1.1: Definition of the parameters Λ, Δ, used in eq. (3.12), as a general case of eq. (3.6) (see subsection 3.1) and eq. (3.11) (see subsection 3.2).

where if $x_{R_{tot}} \gg 1$,

$$k_1(x_{E_{tot}}) = x_{RNAP} \frac{x_{O_{tot}}}{x_{R_{tot}}} \frac{(1 + K_c x_{E_{tot}}^n)}{K_b K_c x_{E_{tot}}^n}, \tag{3.10}$$

while if $\frac{x_{R_{tot}}}{x_{O_{tot}}} \gg 1$,

$$k_1(x_{E_{tot}}) = x_{RNAP} x_{O_{tot}} \frac{1 + K_c x_{E_{tot}}^n}{1 + (1 + K_b x_{R_{tot}}) K_c x_{E_{tot}}^n}. \tag{3.11}$$

3.3 Summary

The two bounded (above and below) functions given at eq. (3.6) and eq. (3.11) are most commonly used and are special cases (up to a proportional constant) of the function

$$k_1(x_{E_{tot}}) = \frac{1 + K_c x_{E_{tot}}^n}{\Lambda + \Delta K_c x_{E_{tot}}^n} \tag{3.12}$$

where $\Lambda, \Delta \geqslant 0$ are given in table 1.1. We will lump all constants of proportionality that appeared previously in the derivation of the transcriptional rate function into a single parameter, that we name λ_1. The two unbounded functions given at eq. (3.5) and eq. (3.10) lead to ill-posed model, except eq. (3.5) for $n = 1$ which has been used in the past.

It is also important to bear in mind that such rate functions are very model-specific and various different form appeared in the literature, depending on the molecular dynamics considered (for a review in prokaryotes see [154], in yeast [53] and in higher eukaryotes [118]). We provide in table 1.2 some classical parameters found on the literature relevant for such models. This table is not meant to be exhaustive, but to give intuition of the order of magnitude of the relevant process we look at, as well as the variation of the parameters rate one can found on different organism. Hence, the derivation of the Hill kinetics we provide might not always be justified (which explain partially the success of the 'on-off' model which consider fluctuations at the level of the operator). In particular, we can see that for the lac operon [135] or the tryptophan operon [89] the association equilibrium constant is extremely small, making the derivation above safe, while it is not so the case for the phage λ system [67] or the TetR system [30]. Also, in the lac operon or the tryptophan operon, complex constant are scarce, but binds efficaciously the promoter. We also give some examples of number of molecules for the molecule in consideration (binding sites, RNA polymerase, ribosomes, repressor molecules) to show that in some cases, a probabilistic modeling is natural as the number of molecules is relatively small. We also highlight the fact that new experimental techniques are now used to follow individual molecules, and to characterize for example the search time of transcription factor for its binding sites!

Table 1.2: Parameters involved in the determination of the rate function. See subsections 3.1 and 3.2) for details. Note that we give all parameter values in molecule numbers, as they are required for stochastic modeling. For typical cells like E. Coli, 1 molecule per cell corresponds roughly ([142]) to a concentration of 1 nanomolar (nM)

Parameters			References and comments
Complex formation binding constant			Large variation of order of magnitude of these rates relies on the fact that many different complexes can be involved in the interaction with promoter
Association	Dissociation	Equilibrium	
k_c^+	k_c^-	$K_c = \frac{k_c^+}{k_c^-}$	
(min^{-1})	(min^{-1})		
12×10^{-7}	12	10^{-7}	[135] LacI dimer (repressor) binding to Effector molecule in the lac operon. (Fast dimerization of repressors is assumed).
3-9	$1\text{-}5 \times 10^{-3}$	10^3-10^4	[30] aTc binding with TetR to prevent TetR repression
		0.05	[67] Dimer formation (λ repressor protein) in the phage λ system. Value taken from literature.
0.5	2×10^4	2.5×10^{-5}	[89] Tryptophan Operon in E. Coli. Values inferred from literature.
Complex/Promoter binding constant			Again large variation of order of magnitude reflects the diversity of the system considered. Experimentalist may also have the possibility to control affinity rate on promoter.
Association	Dissociation	Equilibrium	
k_b^+	k_b^-	$K_b = \frac{k_b^+}{k_b^-}$	
(min^{-1})	(min^{-1})		
2000	2.4	833	[135] LacI dimer repression by binding to the operator, in the lac operon. Taken from experimental data available on literature.

1-10	6×10^{-4}-10^3	10^5-10^{-3}	[30] Direct repressor protein TetR binding to operator and other complex binding.
		0.03-0.6	[67] Dimer (λ repressor protein) binding to the operator, in the phage λ system. Value taken from Literature.
		$\sqrt[n]{10^{-2}}$-$\sqrt[n]{10^{-3}}$	[142] λ repressor protein binding to the operator, in the phage λ system, for a cooperativity constant of n. Value taken from literature.
		0.03-0.003	[144] tetA protein binding to tetO promoter, in the tet-Off system in S. cerevisiae. The response curve is measured experimentally and fitted to obtain kinetic parameter.
		$\sqrt[n]{10^{-2}}$	[120] phage λ system in E. Coli. The rate of transcription is directly measured with the concentration of effector. The kinetic parameters are deduced by fitting.
1	10^{-2}	10^2	[89] Tryptophan Operon in E. Coli. Values inferred from literature.

Complex affinity (Hill coefficient)	
n	
$1 - 30$	[142] Typical biological values taken from literature.
1	[144] tetA protein binding to tetO promoter, in the tet-Off system in S. cerevisiae. The response curve is measured experimentally and fitted to obtain kinetic parameter.
1.4-2.7	[120] phage λ system in E. Coli. The rate of transcription is directly measured with the concentration of effector. The kinetic parameters are deduced by fitting.
1.2	[89] Tryptophan Operon in E. Coli. Values taken from literature

Number of binding sites	
2-6	[144] tet-Off system in S. cerevisiae

Number of RNA polymerase	
35 ± 3.5	[78] Bacteria
1250	[89] E. Coli
3600	[30] E. Coli
30000	[113] Mammalian macrophage

RNA polymerase binding constant	Note that many authors consider this reaction to be responsible of the switching behavior of the gene state.

Association λ_a (min^{-1})	Dissociation λ_i (min^{-1})	Equilibrium $\frac{\lambda_a}{\lambda_i}$	
60-600	1	60-600	[30] The promoter strength can be varied experimentally, and influence the RNA polymerase association constant
10	600	10^{-2}	[78] LacZ gene in in the Lac Operon. Values taken from literature
10^{-2}			[89] Tryptophan Operon in E. Coli. Values inferred from literature.

Number of ribosomes	
350 ± 35	[78] Bacteria
1400	[89] E.Coli
6×10^6	[113] Mammalian macrophage

Ribosome binding constant			
Association (min^{-1})	Dissociation (min^{-1})	Equilibrium	
10	120	10^{-1}	[78] Association rate given by diffusion-limited aggregation, and dissociation to reproduce translation rate faithfully
10^{-2}			[89] Tryptophan Operon in E. Coli. Values inferred from Literature.

Number of Repressor molecules	
500	[89] Tryptophan Operon in E. Coli.
10	[135] Repressors dimer in Lac Operon in E. Coli.

Effective Diffusion constant (μm^2.min^{-1})	
24	[32] Single Transcription factor detection in single cells, E Coli.

Search time (min)	
$1-6$	[32] Single Transcription factor detection in single cells, E Coli.

Cell Volume (L)	
10^{-15}-10^{-16}	[89],[135] E. Coli
5×10^{-12}	[113] Mammalian macrophage

3.4 Other rate functions

In the standard model, only the steps before (and including) the transcription usually consider nonlinear effect. In prokaryotes, ribosomes can begin binding the newly synthesized ribosome-binding site (on the mRNA) almost immediately as transcription begins (whereas in eukaryotes, a delay between translation and transcription may be relevant). Analogous to transcript initiation, translation initiation of a single mRNA molecule is assumed to proceed with a first-order rate λ_2. We assumed that initiation and elongation rates are such that ribosome queuing does not occur (Thattai and van Oudenaarden [142]). We therefore take each transcription and translation initiation reaction to be independent, and the translation rate would be proportional to the amount of mRNA molecules. Simi-

larly, we assume effector production rate to be proportional to the amount of intermediate protein molecules (with coefficient λ_3). Finally, we assume that all molecules degrade linearly with rates γ_i, $i = 1, 2, 3$ for mRNA, proteins and effector respectively. A decay rate γ gives a half-life of $ln(2)/\gamma$. If growth in cell volume is exponential, the resulting dilution of species concentrations can be incorporated by increasing γ for all species (other than the DNA, which is replicated at a rate exactly matching cell growth). The mRNA decay rate depends on the ribosome-binding rate, because actively translating ribosomes shield the mRNA molecules from the action of nuclease (Thattai and van Oudenaarden [142]).

4   Parameters and Time Scales

We summarize in table 1.3 the parameters used in our model, and the various range of magnitude that have been measured or fitted from experiments. Again, this table does not intend to be exhaustive, but rather to give intuitions. It is also clear that many parameters are not independent within each other, and their values then depend on the model chosen. For instance, an observation of the instantaneous rate of production of an mRNA, as a first step process, or combined with an observation of the gene state kinetics, would not lead to the same transcriptional rate. The mean number of molecules, and burst statistics given at the end of this table, are also obviously function of other parameters. They can however be measured directly. For instance, as individual molecules can be measured, the authors in [20, 47, 150, 111] were able to "count" the number of molecules produced in each burst production event, and to deduce statistics of the burst size event.

As a general trend, it can be noticed that synthesis rate of protein are usually higher than synthesis rate of mRNA, while degradation rate of protein are several order of magnitude lower. Switching rate of the gene state are highly variable, but may be quite slow. Finally, the number of mRNA molecules may be of only dozens, while there may have thousands or more proteins.

Table 1.3: Parameters involved in the standard model of molecular biology. Note that we give all parameter values in molecule numbers, as they are required for stochastic models. For typical cells like E. Coli, 1 molecule per cell corresponds roughly [142] to a concentration of 1 nanomolar (nM)

	Parameters		References and comments
	Gene state		
Activation rate	Inactivation rate		These values depend a lot on modeling choice. As we saw, transcription is a multi-step process. Activation of the gene may mean that an mRNA Polymerase is bound to DNA, and then (almost) ready to start transcription. We may also consider that activation requires a (rare) transcription factor to bound. Or in eukaryotes it may requires chromatin opening.

λ_a (min^{-1})	λ_i (min^{-1})		
60-600	1		[30] TetR system in E. Coli. The promoter strength can be varied experimentally, and influence the RNA polymerase association constant
0.2-1	1-2		[144] tet-Off system in S. cerevisiae.
0.1-1	500		[78] Lac operon in Bacteria
$0.7 - 5 \times 10^{-3}$	2.5×10^{-4}		[94] Interleukin protein in Lymphocytes. These rates represent opening/closing of chromatin, and were derived by fitting a stochastic model to experimental data.
$0.07 - 0.3$	$0.68 - 5.3$		[152]. Parameters inferred from experimental data using single mRNA detection technique in yeast (S. Cerevisiae)
0.02	0.1		[47] Real-time monitoring of lac/ara promoter kinetics in E. Coli
2×10^{-4}	10^{-3}		[111] statistical kinetics inferred from single mRNA counting in mammalian cells.

mRNA			
Synthesis rate λ_1 (min^{-1})	Degradation rate γ_1 (min^{-1})	Transcriptional efficiency $\frac{\lambda_1}{\lambda_i}$	
2.4	0.3	2.4	[30] TetR system in E. Coli.
0.4-1	0.4		[135] Lac operon in E. Coli. Taken from experimental data available on Literature
10	0.61		[89] Tryptophan Operon in E. Coli. Values inferres from literature.
10	0.04	5-10	[144] tet-Off system in S. cerevisiae.
12	$1-6 \times 10^{-3}$		[113] Mammalian Macrophage
50	18	0.1	[78] Lac operon in Bacteria
40	0.01	2×10^5	[94] Interleukin protein in Lymphocytes. Experimentally deduced.
1.3-11		0.2-20	[152]. Parameters inferred from experimental data using single mRNA detection technique in yeast (S. Cerevisiae)
10^{-3}-1	2×10^{-4}-2×10^{-3}		[127] global gene quantification in mammalian cells (mouse fibroblast)
0.23	2×10^{-3}	230	[111] Single mRNA counting in mammalian cells.

Protein			
Synthesis rate	Degradation rate	Transcriptional efficiency	

λ_2 (min^{-1})	γ_2 (min^{-1})	$\frac{\lambda_2}{\gamma_1}$	
6	0.01	18	[30] TetR system in E. Coli. Protein degradation rate equal the dilution rate.
15-30	0.2	30-60	[135] Lac operon in E. Coli.
20	0.01	30	[89] Tryptophan Operon in E. Coli. Protein degradation rate equal the dilution rate.
23.1	0.007	500	[144] tet-Off system in S. cerevisiae.
11.3	4×10^{-4}-1×10^{-2}	10^3-10^4	[113] Mammalian Macrophage
0.5-10	0.003	0.02-0.5	[78] Lac operon in Bacteria
4	0.02	400	[94] Interleukin protein in Lymphocytes. Experimentally deduced.
10^{-2}-10	5×10^{-5}-1×10^{-3}	10-10^5	[127] global gene quantification in mammalian cells (mouse fibroblast)

Effector			
Synthesis rate λ_3 (min^{-1})	Degradation rate γ_3 (min^{-1})		
120	10^{-2}		[89] Tryptophan Operon in E. Coli. Effector degradation rate equal the dilution rate

Mean Number			
mRNA $< X_1 >$	Protein $< X_2 >$		
1-30	100-300		[135] Lac operon in E. Coli
20-100	4×10^5		[113] Mammalian Macrophage
1000	5×10^5		[94] Interleukin protein in Lymphocytes. Experimentally deduced.
2-15			[152]. Parameters inferred from experimental data using single mRNA detection technique in yeast (S. Cerevisiae)
1-1000	100-10^6		[127] global gene quantification in mammalian cells (mouse fibroblast)

Mean Burst size			
mRNA	Protein		
	8-20		[20] Real-time monitoring of β-galactosidase in E. Coli. Their direct measurement also coincide with distribution fitting of a bursting model.

mRNA (min⁻¹)	Protein (min⁻¹)	
4		[47] Real-time monitoring of lac/ara promoter kinetics in E. Coli
	4.2	[150] T_{sT}-Venus protein controlled by the lac promoter in E. Coli.
10-300		[111] Single mRNA counting in mammalian cells.

Mean Burst frequency		
mRNA (min⁻¹)	Protein (min⁻¹)	
	10^{-3}	[20] Real-time monitoring of β-galactosidase in E. Coli. Their direct measurement also coincide with distribution fitting of a bursting model.
	2×10^{-2}	[150] T_{sT}-Venus protein controlled by the lac promoter in E. Coli.
0.2		[22] Real-time monitoring of a developmental gene in a small eukaryotes.

5   Discrete Version

Based on the description above (section 2), we select 4 biochemical species involved in different chemical reactions, namely DNA, mRNA, proteins and effectors. The simplest discrete stochastic description of this system is a continuous time Markov chain, with the state space being the number of each molecules of each species (or the state "ON/OFF" for the DNA — we assume that there is a single DNA molecule), and with state transition given by the biochemical reactions (the stoichiometry of the reaction gives the state space jump, and its reaction rate gives the intensity of the jump). There are several equivalent representations of a continuous time Markov chain with discrete state space (see Introduction, part 0). We present below the transition function of this Markov chain, and its generator. Then we deduce immediate consequences for the long-term behavior of this model.

5.1   Representation of the discrete model

We now write for convenience $X = (X_0, X_1, X_2, X_3)$ for the state of the Markov chain, with X_0 being the state of the DNA, and X_1, X_2, X_3 respectively the numbers of mRNA, proteins and effectors. Then the state space of the chain is $\{0,1\} \times \mathbb{N}^3$. The one-step transitions are summarized in table 1.4.

Note that some reactions are catalytic reactions, that is they do not consume any species. Transition rates (or propensities) associated to first order reactions (degradation and catalytic) are derived according to the Action-Mass law and are then linear with respect to one variable. The other transition rates (k_1, k_i, k_a) were derived in the previous section 3 and can be non-linear functions of the variable X_3. More detailed assumption on these rate functions will be given in the following.

Let us introduce the following notation to simplify the writing.

Notation 1. *For any function $f(x)$ with $x = (x_0, x_1, x_2, x_3)$, we define the following*

Table 1.4:   Transitions and Parameters used for the pure jump Markov process $X = (X_0, X_1, X_2, X_3)$

Biochemical Reaction	State-space change vector	Propensity
Gene activation	$(1, 0, 0, 0)$	$\lambda_a \mathbf{1}_{\{X_0 = 0\}} k_a(X_3)$
Gene inactivation	$(-1, 0, 0, 0)$	$\lambda_i \mathbf{1}_{\{X_0 = 1\}} k_i(X_3)$
Transcription	$(0, 1, 0, 0)$	$\lambda_1 \mathbf{1}_{\{X_0 = 1\}} k_1(X_3)$
mRNA degradation	$(0, -1, 0, 0)$	$\gamma_1 X_1$
Translation	$(0, 0, 1, 0)$	$\lambda_2 X_1$
Protein degradation	$(0, 0, -1, 0)$	$\gamma_2 X_2$
Effector production	$(0, 0, 0, 1)$	$\lambda_3 X_2$
Effector degradation	$(0, 0, 0, -1)$	$\gamma_3 X_3$

operators:

$$E_0^0 f(x) = f(0, x_1, x_2, x_3) \qquad \textit{inactive state,}$$
$$E_0^1 f(x) = f(1, x_1, x_2, x_3) \qquad \textit{active state,}$$
$$E_1^+ f(x) = f(x_0, x_1 + 1, x_2, x_3) \ \textit{mRNA production,}$$
$$E_1^- f(x) = f(x_0, x_1 - 1, x_2, x_3) \ \textit{mRNA degradation,}$$
$$E_2^+ f(x) = f(x_0, x_1, x_2 + 1, x_3) \ \textit{protein production,}$$
$$E_2^- f(x) = f(x_0, x_1, x_2 - 1, x_3) \ \textit{protein degradation,}$$
$$E_3^+ f(x) = f(x_0, x_1, x_2, x_3 + 1) \ \textit{effector production,}$$
$$E_3^- f(x) = f(x_0, x_1, x_2, x_3 - 1) \ \textit{effector degradation.}$$

The generator associated to the Markov chain is then given by

$$
\begin{aligned}
Af(x) \ = \ & \lambda_a k_a(x_3)(E_0^1 f - f)(x) + \lambda_i k_i(x_3)(E_0^0 f - f)(x) \\
& + \lambda_1 \mathbf{1}_{\{x_0 = 1\}} k_1(x_3)(E_1^+ f - f)(x) + \gamma_1 x_1 (E_1^- f - f)(x) \\
& + \lambda_2 x_1 (E_2^+ f - f)(x) + \gamma_2 x_2 (E_2^- f - f)(x) \\
& + \lambda_3 x_2 (E_3^+ f - f)(x) + \gamma_3 x_3 (E_3^- f - f)(x).
\end{aligned}
$$

5.2   Long time behavior

Denote by τ_i the ith jump times of the chain X. Firstly, we are going to show that, under reasonable assumptions, the jump times do not accumulate, that is $\tau_\infty = \infty$. This ensures that the model is well defined for all $t \geqslant 0$.

Hypothesis 5. *The function k_1 is linearly bounded, and specifically, there exists $c > 0$ such that, for any $x_3 \in \mathbb{N}$*

$$k_1(x_3) \leqslant x_3 + c.$$

Now by a simple consequence of the Meyn and Tweedie [97, thm 2.1] criterion (see also part 0 subsection 6.3, proposition 10), we obtain

Proposition 20. *The Markov chain defined in subsection 5.1 is non-explosive.*

Proof. Choose the test function $f(x) = x_1 + x_2 + x_3$, which is a norm-like function, it comes directly that

$$Af(x) \leqslant \max(\lambda_1, \lambda_2, \lambda_3) f(x) + c.$$

$\square$

Secondly, we can show the irreductibility. All states communicate with each other as soon as

Hypothesis 6. *The function k_a, and k_1 are strictly positive for $x_3 = 0$, and all rate constants λ_a, λ_i, λ_k and γ_k, $k = 1, 2, 3$, are positive.*

Then it is classical that the Markov chain is irreductible.

Finally, for discrete state-space Markov process, a simple criterion for exponential ergodicity is provided by [97, Theorem 7.1] (see also part 0 subsection 6.3, proposition 15). Assuming

Hypothesis 7. $\min \gamma_i > \max \lambda_i$,

we then have, with the test function $f(x) = x_1 + x_2 + x_3$, for all x,

$$Af(x) \leqslant (\max \lambda_i - \min \gamma_i) f(x) + \lambda_1 c.$$

So the Markov process is exponentially ergodic. There exists an invariant probability measure p^*, $B < \infty$ and $\beta < 1$ such that the following convergence in distribution holds

$$\| P^t(x, \cdot) - p^* \|_f \leqslant B f(x) \beta^t,$$

where $P^t(x, \cdot)$ denotes the semigroup

$$P^t(x, g) = \mathbb{E}_x \Big[g(X_t) \Big],$$

and

$$\| \mu \|_f = \sup_{|g| \leqslant f} | \mu(g) | .$$

Despite we know the long-term behavior of this Markov chain, it's hard to deduce any quantitative information. To be able to concrete parameters values, one approach is to consider constant or linear reaction rate, thus preventing any non-linearity. Thus, analytic methods through the moment generating function can be used. With such tool, it can be computed moment equations, and stationary probability density function (or at least, its moment generating function). However, this techniques seems strictly limited to constant and linear rate functions. See [104] for a typical example. We sketch some of these results in section 7.

We will see on the next section that for the continuous deterministic version of this model, namely the Goodwin model, the picture is much more complete, and can deal with non-linear rate functions. In particular, bifurcation parameter analysis can provide information on the bistability or oscillatory behavior of the model. To get analog information on the stochastic model, we will have to reduce its dimension. Hence we will study a one-dimensional stochastic model in section 8, and rigorously prove how to perform such reduction in section 9.1.

6   Continuous Version - Deterministic Operon Dynamics

A continuous deterministic version of this model ignores the fluctuation in the DNA state and considers that the three other chemical species (mRNA,proteins and effectors) are present in very large number. We will recall in section 9 standard results to show that the stochastic discrete model converges to the continuous deterministic model, under assumption of fast DNA switching and large molecule number. Note in particular that this model does not represent a statistical mean behavior over a large population of cells,

unless all rates are assumed linear. We refer to [107, 98] for an interesting survey of techniques applicable to this deterministic approach, with in particular models that differs from Ordinary Differential Equation.

We consider in this section the standard Goodwin [48] model. These results are not new but included here for convenience and to illustrate its analogy with our results on the stochastic model. Let (x_1, x_2, x_3) denote mRNA, intermediate protein, and effector concentrations respectively. Then for a generic operon with a maximal level of transcription λ_1 (in concentration over time units), we have dynamics described by the system [48, 51, 52, 100, 128]

$$\begin{cases} \dfrac{dx_1}{dt} = \lambda_1 k_1(x_3) - \gamma_1 x_1, \\[2mm] \dfrac{dx_2}{dt} = \lambda_2 x_1 - \gamma_2 x_2, \\[2mm] \dfrac{dx_3}{dt} = \lambda_3 x_2 - \gamma_3 x_3. \end{cases} \tag{6.1}$$

Here we assume that the rate of mRNA production is proportional to the fraction of time the operator region is active, and that the rates of intermediate and enzyme production are simply proportional to the amount of mRNA and intermediate respectively. All three of the components (x_1, x_2, x_3) are subject to linear degradation. The function k_1 was calculated in the previous section 3 and then taken in this section in the form

$$k_1(x_3) = \frac{1 + K_c x_3^n}{\Lambda + \Delta K_c x_3^n},$$

so that it's a smooth bounded function, positive everywhere. Hence global existence and uniqueness of this system is not a problem, and the solution lies in $(\mathbb{R}_+^*)^3$ for all time.

It will greatly simplify matters to rewrite eq. (6.1) by defining dimensionless concentrations. To this end we define the dimensionless variable

$$y_1 = \frac{\lambda_3 \lambda_2}{\gamma_3 \gamma_2} \sqrt[n]{K_c} x_1,$$

$$y_2 = \frac{\lambda_3}{\gamma_3} \sqrt[n]{K_c} x_2,$$

$$y_3 = \sqrt[n]{K_c} x_3,$$

and the system eq. 6.1 then becomes

$$\begin{cases} \dfrac{dy_1}{dt} = \gamma_1 [\kappa_d f(y_3) - y_1], \\[2mm] \dfrac{dy_2}{dt} = \gamma_2 (y_1 - y_2), \\[2mm] \dfrac{dy_3}{dt} = \gamma_3 (y_2 - y_3). \end{cases} \tag{6.2}$$

where

$$\kappa_d = \frac{\lambda_3 \lambda_2 \lambda_1 \sqrt[n]{K_c}}{\gamma_3 \gamma_2 \gamma_1}.$$

is a dimensionless constant, and the function f is given by

$$f(y_3) = \frac{1 + y_3^n}{\Lambda + \Delta y_3^n}. \tag{6.3}$$

In each equation, γ_i for $i = 1, 2, 3$ denotes a net loss rate (units of inverse time), and thus eq. 6.2 are not in dimensionless form.

The dynamics of this classic operon model can be fully analyzed. Let $Y = (y_1, y_2, y_3)$ and denote by $S_t(Y)$ the flow generated by the system eq. (6.2). For both inducible and repressible operons, for all initial conditions $Y^0 = (y_1^0, y_2^0, y_3^0) \in \mathbb{R}_3^+$ the flow $S_t(Y^0) \in \mathbb{R}_3^+$ for $t > 0$.

Steady states of the system eq. (6.2) are in a one to one correspondence with solutions of the equation

$$\frac{y}{\kappa_d} = f(y), \tag{6.4}$$

and for each solution y^* of eq. (6.4) there is a steady state $Y^* = (y_1^*, y_2^*, y_3^*)$ of eq. (6.2) given by

$$y_1^* = y_2^* = y_3^* = y^*.$$

Whether there is a single steady state y^* or there are multiple steady states will depend on whether we are considering a repressible or inducible operon. The detail derivation of the steady-state and their stability is standard ([48, 146, 51, 52, 100, 133]) and is given for an interesting comparison with the stochastic model discussed in section 8.

6.1   No control (single attractive steady-state)

In this case, $f(y) \equiv 1$, and there is a single steady state $y^* = \kappa_d$ that is globally asymptotically stable.

6.2   Inducible regulation (single versus multiple steady states)

For an inducible operon with f given by eq. (6.3) with $\Delta = 1$ and $\Lambda > 1$, there may be one (Y_1^* or Y_3^*), two ($Y_1^*, Y_2^* = Y_3^*$ or $Y_1^* = Y_2^*, Y_3^*$), or three (Y_1^*, Y_2^*, Y_3^*) steady states, with the ordering $0 < Y_1^* \leqslant Y_2^* \leqslant Y_3^*$, corresponding to the possible solutions of eq. (6.4) (cf. figure 1.5). The smaller steady state (Y_1^*) is typically referred to as an uninduced state, while the largest steady state (Y_3^*) is called the induced state. The steady state values of y are easily obtained from eq. (6.4) for given parameter values, and the dependence on κ_d for $n = 4$ and a variety of values of Λ is shown in figure 1.5. Figure 1.6 shows a graph of the steady states y^* versus κ_d for various values of the leakage parameter Λ.

Analytic conditions for the existence of one or more steady states can be obtained by using eq. (6.4) in conjunction with the observation that the delineation points are marked by the values of κ_d at which y/κ_d is tangent to $f(y)$ (see figure 1.5). Simple differentiation of eq. (6.4) yields the second condition

$$\frac{1}{\kappa_d n (\Lambda - 1)} = \frac{y^{n-1}}{(\Lambda + y^n)^2}. \tag{6.5}$$

From eq. (6.4) and eq. (6.5) we obtain the values of y at which tangency will occur:

$$y_{\pm} = \sqrt[n]{\frac{\Lambda - 1}{2} \left\{ \left[n - \frac{\Lambda + 1}{\Lambda - 1} \right] \pm \sqrt{n^2 - 2n \frac{\Lambda + 1}{\Lambda - 1} + 1} \right\}}. \tag{6.6}$$

The two corresponding values of κ_d at which a tangency occurs are given by

$$\kappa_{d\pm} = y_{\mp} \frac{\Lambda + y_{\mp}^n}{1 + y_{\mp}^n}. \tag{6.7}$$

(Note the deliberate use of $y_{\mp}$ as opposed to $y_{\pm}$.)
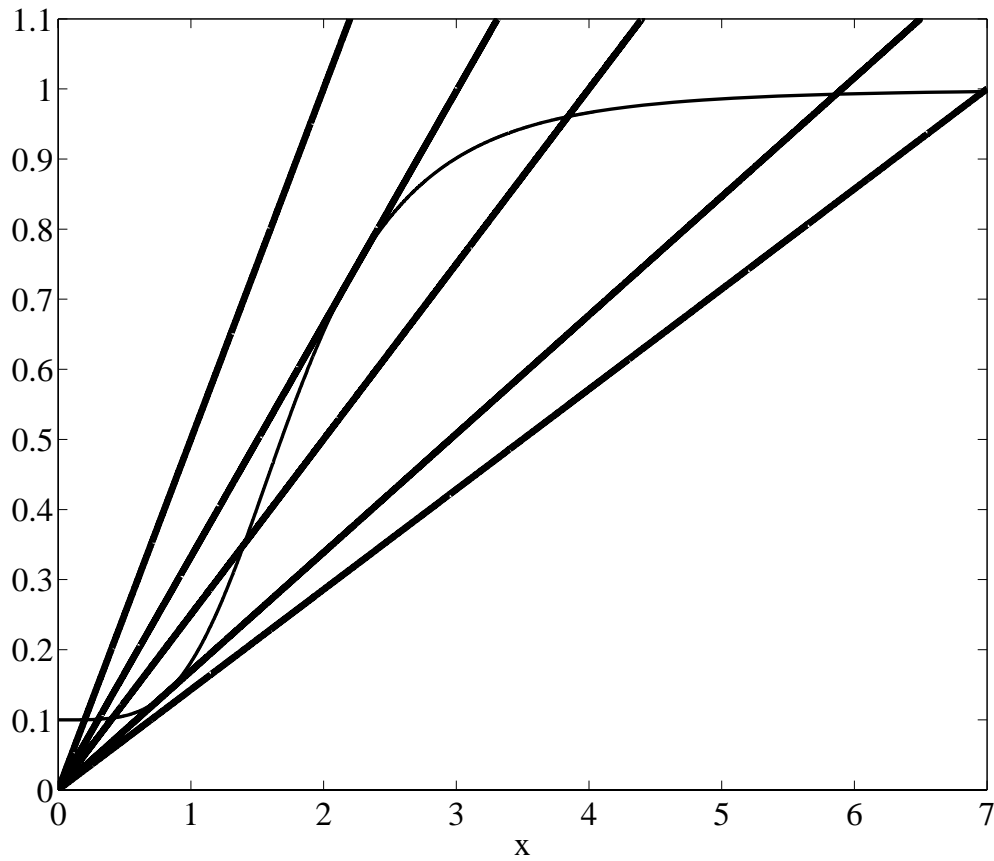
Figure 1.5: Schematic illustration of the possibility of one, two or three solutions of eq. (6.4) for varying values of κ_d with inducible regulation. The monotone increasing graph is the function f of eq. (6.3), and the straight lines correspond to x/κ_d for (in a clockwise direction) $\kappa_d \in [0, \kappa_{d-})$, $\kappa_d = \kappa_{d-}$, $\kappa_d \in (\kappa_{d-}, \kappa_{d+})$, $\kappa_d = \kappa_{d+}$, and $\kappa_{d+} < \kappa_d$. This figure was constructed with $n = 4$ and $\Lambda = 10$ for which $\kappa_{d-} = 3.01$ and $\kappa_{d+} = 5.91$ as computed from eq. (6.7). See the text for further details.
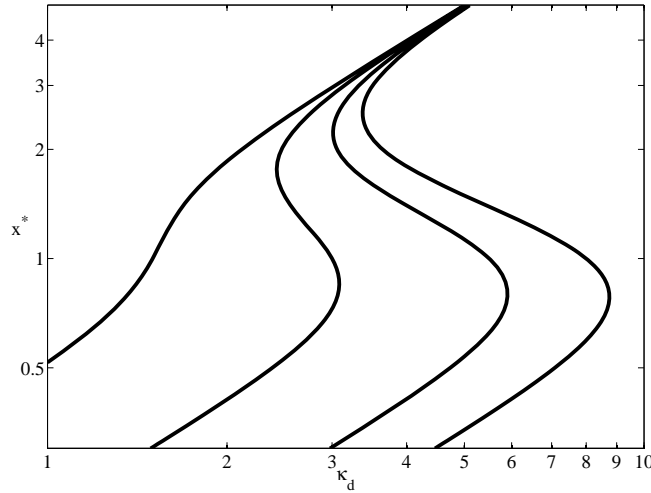
Figure 1.6: Full logarithmic plot of the steady state values of y^* versus κ_d for an inducible system, obtained from eq. (6.4), for $n = 4$ and $\Lambda = 2, 5, 10,$ and 15 (left to right) illustrating the dependence of the occurrence of bistability on Λ. See the text for details.

A necessary condition for the existence of two or more steady states is obtained by requiring that the square root in in eq. (6.6) be non-negative, or

$$\Lambda \geqslant \left(\frac{n+1}{n-1} \right)^2. \tag{6.8}$$

From this a second necessary condition follows, namely

$$\kappa_d \geqslant \frac{n+1}{n-1} \sqrt[n]{\frac{n+1}{n-1}}. \tag{6.9}$$

Further, from eq. (6.4) and (6.5) we can delineate the boundaries in (Λ, κ_d) space in which there are one or three locally stable steady states as shown in figure 1.7. There, we have given a parametric plot (y is the parameter) of κ_d versus Λ, using

$$\Lambda(y) = \frac{y^n[y^n + (n+1)]}{(n-1)y^n - 1} \quad \text{and} \quad \kappa_d(y) = \frac{[\Lambda(y) + y^n]^2}{ny^{n-1}[\Lambda(y) - 1]},$$

for $n = 4$ obtained from eq. (6.4) and (6.5). As is clear from the figure, when leakage is appreciable (small Λ, e.g for $n = 4$, $\Lambda < (5/3)^2$) then the possibility of bistable behavior is lost.

Remark 21. *Some general observations on the influence of n, Λ, and κ_d on the appearance of bistability in the deterministic case are in order.*

1. *The degree of cooperativity (n) in the binding of effector to the repressor plays a significant role. Indeed, $n > 1$ is a necessary condition for bistability.*

2. *If $n > 1$ then a second necessary condition for bistability is that Λ satisfies eq. (6.8) so the fractional leakage (Λ^{-1}) is sufficiently small.*

3. *Furthermore, κ_d must satisfy eq. (6.9) which is quite instructive. Namely for $n \to \infty$ the limiting lower limit is $\kappa_d > 1$ while for $n \to 1$ the minimal value of κ_d becomes fairly large. This simply tells us that the ratio of the product of the production rates to the product of the degradation rates must always be greater than 1 for bistability to occur, and the lower the degree of cooperativity (n) the larger the ratio must be.*
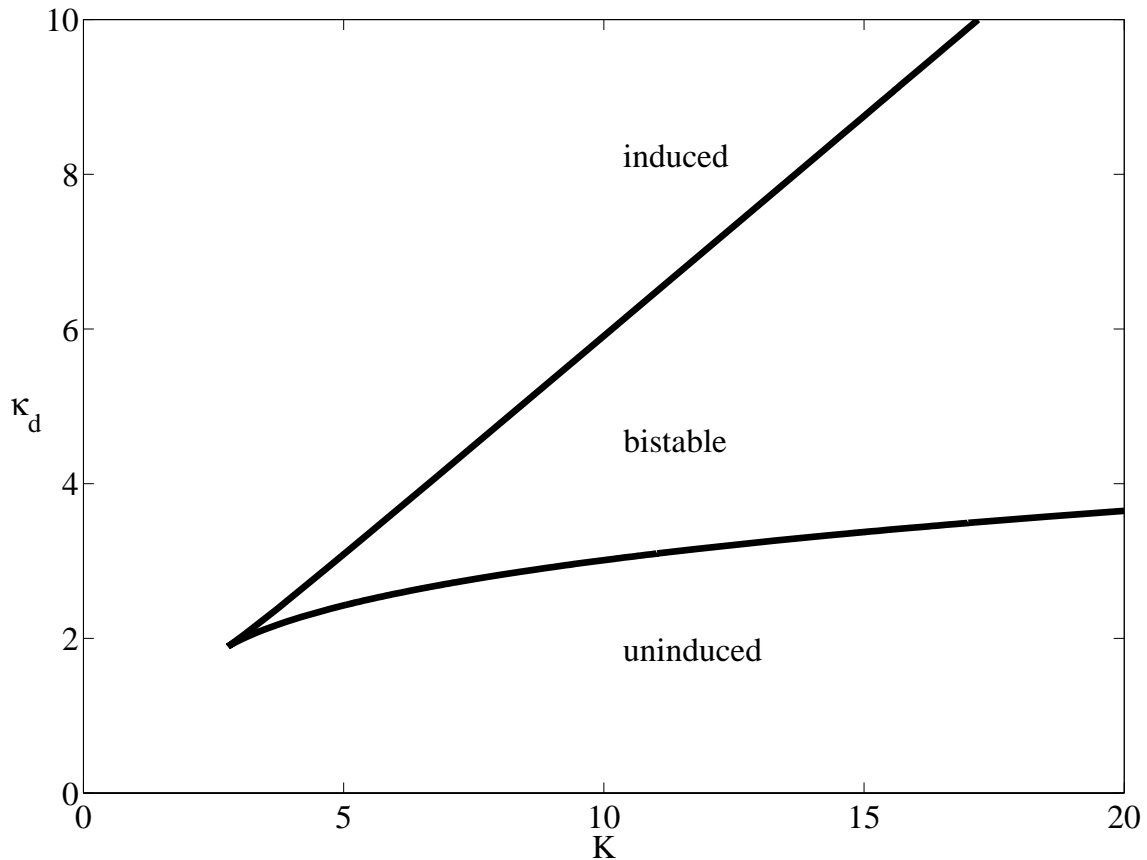
Figure 1.7: In this figure we present a parametric plot (for $n = 4$) of the bifurcation diagram in (Λ, κ_d) parameter space delineating one from three steady states in a deterministic inducible operon as obtained from eq. (6.4) and (6.5). The upper (lower) branch corresponds to κ_{d-} (κ_{d+}), and for all values of (Λ, κ_d) in the interior of the cone there are two locally stable steady states Y_1^*, Y_3^*, while outside there is only one. The tip of the cone occurs at $(\Lambda, \kappa_d) = ((5/3)^2, (5/3)\sqrt[4]{5/3})$ as given by eq. (6.8) and (6.9). For $\Lambda \in [0, (5/3)^2)$ there is but a single steady state.

4. *If n, Λ and κ_d satisfy these necessary conditions then bistability is only possible if $\kappa_d \in \left[\kappa_{d-}, \kappa_{d+}\right]$ (c.f. figure 1.7).*

5. *The locations of the minimal (y_-) and maximal (y_+) values of y bounding the bistable region are independent of κ_d.*

6. *Finally*

   (a) *$(y_+ - y_-)$ is a decreasing function of increasing n for constant κ_d, Λ*

   (b) *$(y_+ - y_-)$ is an increasing function of increasing Λ for constant n, κ_d.*

Local and global stability. The local stability of a steady state y^* is determined by the solutions of the eigenvalue equation [149]

$$(\lambda + \gamma_1)(\lambda + \gamma_2)(\lambda + \gamma_3) - \gamma_1\gamma_2\gamma_3\kappa_d f'_* = 0, \quad f'_* = f'(y^*). \qquad (6.10)$$

Set

$$a_1 = \sum_{i=1}^{3} \gamma_i, \quad a_2 = \sum_{i \neq j = 1}^{3} \gamma_i \gamma_j, \quad a_3 = (1 - \kappa_d f'_*)\prod_{i=1}^{3} \gamma_i,$$

so eq. (6.10) can be written as

$$\lambda^3 + a_1\lambda^2 + a_2\lambda + a_3 = 0. \qquad (6.11)$$

By Descartes's rule of signs, eq. (6.11) will have either no positive roots for $f'_* \in [0, \kappa_d^{-1})$ or one positive root otherwise. With this information and using the notation SN to denote a locally stable node, HS a half or neutrally stable steady state, and US an unstable steady state (saddle point), then there will be:

- A single steady state Y_1^* (SN), for $\kappa_d \in [0, \kappa_{d-})$
- Two coexisting steady states Y_1^* (SN) and $Y_2^* = Y_3^*$ (HS, born through a saddle node bifurcation) for $\kappa_d = \kappa_{d-}$
- Three coexisting steady states $Y_1^*(SN), Y_2^*(US), Y_3^*$ (SN) for $\kappa_d \in (\kappa_{d-}, \kappa_{d+})$
- Two coexisting steady states $Y_1^* = Y_2^*$ (HS at a saddle node bifurcation), and Y_3^* (SN) for $\kappa_d = \kappa_{d+}$
- One steady state Y_3^* (SN) for $\kappa_{d+} < \kappa_d$.

For the inducible operon, other work extends these local stability considerations and we have the following result characterizing the global behavior:

Theorem 22. *Othmer [100], Smith [133, Proposition 2.1, Chapter 4] For an inducible operon with f given by eq. (6.3), define $I_\Lambda = [1/\Lambda, 1]$. There is an attracting box $B_\Lambda \subset \mathbb{R}_3^+$ defined by*

$$B_\Lambda = \{(y_1, y_2, y_3) : x_i \in I_\Lambda, \; i = 1, 2, 3\}$$

such that the flow S_t is directed inward everywhere on the surface of B_Λ. Furthermore, all $y^* \in B_\Lambda$ and

1. *If there is a single steady state, i.e. Y_1^* for $\kappa_d \in [0, \kappa_{d-})$, or Y_3^* for $\kappa_{d+} < \kappa_d$, then it is globally stable.*

2. *If there are two locally stable nodes, i.e. Y_1^* and Y_3^* for $\kappa_d \in (\kappa_{d-}, \kappa_{d+})$, then all flows $S(Y^0)$ are attracted to one of them. (See [128] for a delineation of the basin of attraction of Y_1^* and Y_3^*.)*
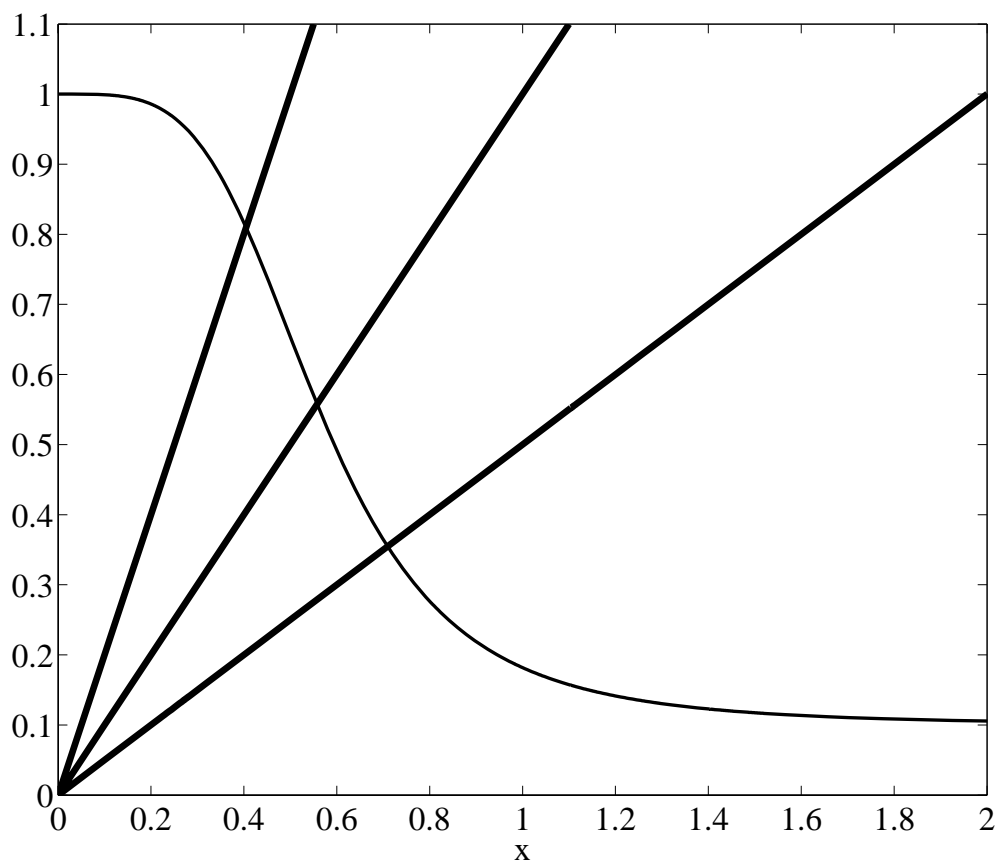
Figure 1.8: Schematic illustration that there is only a single solution of eq. (6.4) for all values of κ_d with repressible regulation. The monotone decreasing graph is f for a repressible operon, while the straight lines are x/κ_d. This figure was constructed with $n = 4$ and $\Delta = 10$. See the text for further details.

6.3   Repressible regulation (single steady-state versus oscillations)

We now consider a repressible operon with f given by eq. (6.3) with $\Delta > 1$ and $\Lambda = 1$. As illustrated in figure 1.8, the repressible operon has a single steady state corresponding to the unique solution y^* of eq. (6.4). To determine its local stability we apply the Routh-Hurwitz criterion to the eigenvalue eq. (6.11). The steady state corresponding to y^* will be locally stable (i.e. have eigenvalues with negative real parts) if and only if $a_1 > 0$ (always the case) and

$$a_1 a_2 - a_3 > 0. \tag{6.12}$$

The well known relation between the arithmetic and geometric means

$$\frac{1}{n} \sum_{i=1}^{n} \gamma_i \geqslant \left(\prod_{i=1}^{n} \gamma_i \right)^{1/n},$$

when applied to both a_1 and a_2 gives, in conjunction with eq. (6.12),

$$a_1 a_2 - a_3 \geqslant (8 + \kappa_d f'_*) \prod_{i=1}^{3} \gamma_i > 0.$$

Thus as long as $f'_* > -8/\kappa_d$, the steady state corresponding to y^* will be locally stable. Once condition eq. (6.12) is violated, stability of y^* is lost via a supercritical Hopf bifurcation and a limit cycle is born. One may even compute the Hopf period of this limit cycle by assuming that $\lambda = j\omega_H$ ($j = \sqrt{-1}$) in eq. (6.11) where ω_H is the Hopf angular frequency. Equating real and imaginary parts of the resultant yields $\omega_H = \sqrt{a_3/a_1}$ or

$$T_H = \frac{2\pi}{\omega_H} = 2\pi \times \sqrt{\frac{\sum_{i=1}^{3} \gamma_i}{(1 - \kappa_d f'_*) \prod_{i=1}^{3} \gamma_i}}.$$

These local stability results tell us nothing about the global behavior when stability is lost, but it is possible to characterize the global behavior of a repressible operon with the following

Theorem 23. *[133, Theorem 4.1 & Theorem 4.2, Chapter 3] For a repressible operon with φ given by eq. (3.11), define $I_\Delta = [1/\Delta, 1]$. There is a globally attracting box $B_\Delta \subset \mathbb{R}_3^+$ defined by*

$$B_\Delta = \{(y_1, y_2, y_3) : x_i \in I_\Delta, \ i = 1, 2, 3\}$$

such that the flow S is directed inward everywhere on the surface of B_Δ. Furthermore there is a single steady state $y^* \in B_\Delta$. If y^* is locally stable it is globally stable, but if y^* is unstable then a generalization of the Poincare-Bendixson theorem [133, Chapter 3] implies the existence of a globally stable limit cycle in B_Δ.

Remark 24. *There is no necessary connection between the Hopf period computed from the local stability analysis and the period of the globally stable limit cycle.*

7   Bursting and Hybrid Models, a Review of Linked Models

We summarize here different models that appeared in the literature and review the analytic results available on these models. For most of these models, these results concern constant or linear reaction rates. All these models are linked with the standard model we present in section 5. We also introduce our labeling for these models, that will be useful

for naming them in section 9. Hence, capital letters D (respectively C) refers for a discrete (respectively continuous) state-space model; capital letters S (respectively B) stands for a model that includes gene switching (respectively bursting). The number $(1, 2, 3)$ refers to the number of variables included in the model among mRNA, protein or effector molecules. All variables and parameters are defined through table 1.4. Below, the stochastic models are stated using a stochastic equation formalism. All Y_i are assumed to be independent unit Poisson processes, and are related to the number of times a given reaction fires (see part 0, subsection 6.2, remark 5). When we refer to the case in the absence of regulation, we mean that the three rate functions k_a, k_i and k_1 are taken constant equal to 1.

7.1   Discrete models with switch

This model is considered in section 5, and takes into account the four steps described in section 2, namely gene state (X_0), mRNA (X_1), protein (X_2) and effector molecules (X_3).

SD3

$$
\begin{cases}
X_0(t) & = & X_0(0) + Y_1\Big(\int_0^t \lambda_a \mathbf{1}_{\{X_0(s)=0\}} k_a(X_3(s)) ds\Big) - Y_2\Big(\int_0^t \lambda_i \mathbf{1}_{\{X_0(s)=1\}} k_i(X_3(s)) ds\Big), \\
X_1(t) & = & X_1(0) + Y_3\Big(\int_0^t \lambda_1 \mathbf{1}_{\{X_0(s)=1\}} k_1(X_3(s)) ds\Big) - Y_4\Big(\int_0^t \gamma_1 X_1(s) ds\Big), \\
X_2(t) & = & X_2(0) + Y_5\Big(\int_0^t \lambda_2 X_1(s) ds\Big) - Y_6\Big(\int_0^t \gamma_2 X_2(s) ds\Big), \\
X_3(t) & = & X_3(0) + Y_7\Big(\int_0^t \lambda_3 X_2(s) ds\Big) - Y_8\Big(\int_0^t \gamma_3 X_3(s) ds\Big).
\end{cases}
$$

Up to our knowledge, no one considered this model!

SD2   This model is more widely used, and consider three steps, namely gene state (X_0), mRNA (X_1), protein (X_2) (which coincide here with effector molecules).

$$
\begin{cases}
X_0(t) & = & X_0(0) + Y_1\Big(\int_0^t \lambda_a \mathbf{1}_{\{X_0(s)=0\}} k_a(X_2(s)) ds\Big) - Y_2\Big(\int_0^t \lambda_i \mathbf{1}_{\{X_0(s)=1\}} k_i(X_2(s)) ds\Big), \\
X_1(t) & = & X_1(0) + Y_3\Big(\int_0^t \lambda_1 \mathbf{1}_{\{X_0(s)=1\}} k_1(X_2(s)) ds\Big) - Y_4\Big(\int_0^t \gamma_1 X_1(s) ds\Big), \\
X_2(t) & = & X_2(0) + Y_5\Big(\int_0^t \lambda_2 X_1(s) ds\Big) - Y_6\Big(\int_0^t \gamma_2 X_2(s) ds\Big).
\end{cases}
$$

For a review of the behavior of this model without regulation, see [74],[130],[110]. In [102] the author derived asymptotic expression of the moments (and of the measure of noise)

and used it to interpret various model behavior in different kinetic parameter range

$$< X_0 > = \mathbb{P}\{X_0 = 1\} = P_{ON} = \frac{\lambda_a}{\lambda_a + \lambda_i}$$

$$< X_1 > = P_{ON} \frac{\lambda_1}{\gamma_1}$$

$$< X_2 > = \frac{\lambda_2}{\gamma_2}$$

$$\frac{\sigma_0^2}{< X_0 >^2} = \frac{1 - P_{ON}}{P_{ON}}$$

$$\frac{\sigma_1^2}{< X_1 >^2} = \frac{1}{< X_1 >} + \frac{\sigma_0^2}{< X_0 >^2} \frac{\gamma_1}{\gamma_1 + \lambda_a + \lambda_i}$$

$$\frac{\sigma_2^2}{< X_2 >^2} = \frac{1}{< X_2 >} + \frac{1}{< X_1 >} \frac{\gamma_2}{\gamma_1 + \gamma_2} + \frac{\sigma_0^2}{< X_0 >^2} \frac{\gamma_2}{\gamma_1 + \gamma_2} \frac{\gamma_2}{\gamma_2 + \lambda_a + \lambda_i} \Big(\frac{\gamma_1}{\gamma_1 + \lambda_a + \lambda_i} + \frac{\gamma_1}{\gamma_2} \Big)$$

In particular, it can be seen from the expressions above, that such model typically present higher fluctuations than a single Poissonian model. Each successive steps brings a contribution in the amount of noise (measured typically as variance over mean squared) of the protein variable for instance.

SD1 This model consider a single variable among the gene products, to be either mRNA or protein. It has the great advantage to be analytically solvable in the absence of non-linearity.

$$\begin{cases} X_0(t) & = & X_0(0) + Y_1 \Big(\int_0^t \lambda_a \mathbf{1}_{\{X_0(s)=0\}} k_a(X_1(s)) ds \Big) - Y_2 \Big(\int_0^t \lambda_i \mathbf{1}_{\{X_0(s)=1\}} k_i(X_1(s)) ds \Big), \\ X_1(t) & = & X_1(0) + Y_3 \Big(\int_0^t \lambda_1 \mathbf{1}_{\{X_0(s)=1\}} k_1(X_1(s)) ds \Big) - Y_4 \Big(\int_0^t \gamma_1 X_1(s) ds \Big). \end{cases}$$

The authors in [104] computed the analytical steady-state distribution in the case without regulation (k_1, k_a, k_i constant) and time-dependent moment dynamics, assuming there's no gene product at time 0;

$$< X_1 > (t) = \frac{\lambda_a}{\lambda_a + \lambda_i} \frac{\lambda_1}{\gamma_1} + \frac{\lambda_a \lambda_1}{(\lambda_a + \lambda_i)(\lambda_a + \lambda_i - \gamma_1)} e^{-(\lambda_a + \lambda_i)t} - \frac{\lambda_a \lambda_1}{\gamma_1(\lambda_a + \lambda_i - \gamma_1)} e^{-\gamma_1 t},$$

$$\lim_{t \to \infty} \sigma_1^2(t) = \frac{\lambda_a}{\lambda_a + \lambda_i} \frac{\lambda_1}{\gamma_1} + \frac{\lambda_a \lambda_1}{(\lambda_a + \lambda_i)^2} \frac{\lambda_1^2}{\gamma_1(\lambda_a + \lambda_i + \gamma_1)},$$

$$g(z) = {}_1F_1(c, a, b(z - 1)),$$

$$p_{x_1}^* = b^{x_1} \frac{e^{-b}}{x_1!} \sum_{i=0}^{x_1} \binom{x_1}{i} (-1)^i \frac{(a - c)_i}{(a)_i} {}_1F_1(a - c + i, a + i, b),$$

$$\mathbb{E}\big[X_1(X_1 - 1) \cdots (X_1 - n + 1) \big] = b^n \frac{c(c + 1) \cdots (c + (n - 1))}{a(a + 1) \cdots (a + n - 1)}.$$

where $g(z)$ denotes the asymptotic moment generating function of X_1, $p_{x_1}^*$ its asymptotic distribution and

$$a = \frac{\lambda_i + \lambda_a}{\gamma_1}$$

$$b = \frac{\lambda_1}{\gamma_1}$$

$$c = \frac{\lambda_a}{\gamma_1}$$

Still in the case without regulation, the authors in [68] derived the time-dependent probability distribution (starting with zero mRNA)

$$g(z,t) = f_1(t) {}_1F_1(c, a, b(z-1)) + f_2(t) {}_1F_1(1 + c - a, 2 - a, b(z-1))$$

where

$$f_1(t) = {}_1F_1(-c, 1 - a, -be^{-\frac{t}{\gamma_1}(z-1)})$$

$$f_2(t) = \frac{bc(1-z)}{a(1-a)} e^{-a\frac{t}{\gamma_1}} {}_1F_1(a - c, 1 + a, -be^{-\frac{t}{\gamma_1}(z-1)})$$

The authors in [63] and [112] extended the result for linear regulation (k_1, k_a constant and $k_i(X_1) = x_1$). All studies put in evidence that this model contains two main time scales, namely the gene switching and the gene product birth-and-death process, and that the distribution of gene product can be seen as a superposition of Poisson distribution. Roughly, when the two time scales are comparable, the probability distribution exhibits a bimodal behavior.

The authors in [126] present numerical simulations of the model with non-linear negative regulation.

7.2 Continuous models with switch

SC3 This model is the continuous analog of SD3.

$$\begin{cases} X_0(t) &= X_0(0) + Y_1\Big(\int_0^t \lambda_a \mathbf{1}_{\{X_0(s)=0\}} k_a(x_3(s)) ds \Big) - Y_2\Big(\int_0^t \lambda_i \mathbf{1}_{\{X_0(s)=1\}} k_i(x_3(s)) ds \Big), \\ \dot{x}_1(t) &= \mathbf{1}_{\{X_0(t)=1\}} \lambda_1 k_1(x_3) - \gamma_1 x_1, \\ \dot{x}_2 &= \lambda_2 x_1 - \gamma_2 x_2, \\ \dot{x}_3 &= \lambda_3 x_2 - \gamma_3 x_3. \end{cases}$$

Here again, up to our knowledge, no-one considered this model!

SC2 This model is the continuous analog of SD2.

$$\begin{cases} X_0(t) &= X_0(0) + Y_1\Big(\int_0^t \lambda_a \mathbf{1}_{\{X_0(s)=0\}} k_a(x_2(s)) ds \Big) - Y_2\Big(\int_0^t \lambda_i \mathbf{1}_{\{X_0(s)=1\}} k_i(x_2(s)) ds \Big), \\ \dot{x}_1(t) &= \mathbf{1}_{\{X_0(t)=1\}} \lambda_1 k_1(x_2) - \gamma_1 x_1, \\ \dot{x}_2 &= \lambda_2 x_1 - \gamma_2 x_2. \end{cases}$$

The authors in [13] considered this model and proved asymptotic stability of the related semi-group on L^1, for continuous function k_a and k_i, and constant function k_1. They used a method based on the "Foguel Alternative". The authors in [87] considered numerical simulation of this model with linear regulation (k_a, k_1 constant and $k_i(x_2) = x_2$)

SC1 This model is the continuous analog of SD1.

$$\begin{cases} X_0(t) &= X_0(0) + Y_1\Big(\int_0^t \lambda_a \mathbf{1}_{\{X_0(s)=0\}} k_a(x_1(s)) ds \Big) - Y_2\Big(\int_0^t \lambda_i \mathbf{1}_{\{X_0(s)=1\}} k_i(x_1(s)) ds \Big), \\ \dot{x}_1(t) &= \mathbf{1}_{\{X_0(t)=1\}} \lambda_1 k_1(x_1) - \gamma_1 x_1. \end{cases}$$

The authors in [87] computed the steady-state distribution of this model with linear regulation (k_a, k_1 constant and $k_i(x_1) = x_1$)

$$p_{x_1} = A e^{\frac{\lambda_i}{\lambda_1} x_1} x_1^{\frac{\lambda_a}{\gamma_1} - 1} (\frac{\lambda_1}{\gamma_1} - x_1)^{\frac{\lambda_i}{\gamma_1} - 1}$$

where A is a normalizing constant. The authors in [144] computed the steady-state distribution of this model with non-linear regulation (k_i, k_1 constant and $k_a(x_1) = \varepsilon + \frac{x_1}{x_1+K}$)

$$p_{x_1} = A x_1^{\frac{\lambda_a}{\gamma_1}\varepsilon - 1}(\frac{\lambda_1}{\gamma_1} - x_1)^{\frac{\lambda_i}{\gamma_1} - 1}(1 + \frac{x_1}{K})^{\frac{\lambda_a}{\gamma_1}}$$

while with (k_a, k_1 constant and $k_i(x_1) = \varepsilon + \frac{K}{x_1+K}$)

$$p_{x_1} = A x_1^{\frac{\lambda_a}{\gamma_1} - 1}(\frac{\lambda_1}{\gamma_1} - x_1)^{\frac{\lambda_i(K(1+\varepsilon)+\varepsilon)}{\gamma_1(1+K)} - 1}(1 + \frac{x_1}{K})^{-\frac{\lambda_i K}{\gamma_1(1+K)}}$$

where A is a normalizing constant. Each expression above can be used to determine which are the conditions for the steady-state distribution to exhibit bimodality.

7.3   Discrete models without switch

In these models, the gene is now assumed to stay active for all times.

D3

$$\begin{cases} X_1(t) & = & X_1(0) + Y_3\Big(\int_0^t \lambda_1 k_1(X_3(s))ds\Big) - Y_4\Big(\int_0^t \gamma_1 X_1(s)ds\Big), \\ X_2(t) & = & X_2(0) + Y_5\Big(\int_0^t \lambda_2 X_1(s)ds\Big) - Y_6\Big(\int_0^t \gamma_2 X_2(s)ds\Big), \\ X_3(t) & = & X_3(0) + Y_7\Big(\int_0^t \lambda_3 X_2(s)ds\Big) - Y_8\Big(\int_0^t \gamma_3 X_3(s)ds\Big). \end{cases}$$

Note that in the absence of regulation, X_1 is independent of X_2, X_3 and follows a one-dimensional Markov-process, known as the immigration and death process. Its asymptotic distribution is Poissonian. For the whole system, up to our knowledge, no study reported its asymptotic distribution (see the case for 2 variables below). However, being an open first-order reaction network, with both conversion and catalytic reaction, the study of Gadgil et al. [40] allows to derive time-dependent first and second moment.

D2

$$\begin{cases} X_1(t) & = & X_1(0) + Y_3\Big(\int_0^t \lambda_1 k_1(X_2(s))ds\Big) - Y_4\Big(\int_0^t \gamma_1 X_1(s)ds\Big), \\ X_2(t) & = & X_2(0) + Y_5\Big(\int_0^t \lambda_2 X_1(s)ds\Big) - Y_6\Big(\int_0^t \gamma_2 X_2(s)ds\Big). \end{cases}$$

In the absence of regulation, asymptotic moments are given by [142].

$$< X_1 > = \frac{\lambda_1}{\gamma_1}$$

$$< X_2 > = \frac{\lambda_1 \lambda_2}{\gamma_1 \gamma_2}$$

$$Var(X_1) = \frac{\lambda_1}{\gamma_1}$$

$$Var(X_2) = \frac{\lambda_1 \lambda_2}{\gamma_1 \gamma_2}\Big(1 + \frac{\lambda_2}{\gamma_1 + \gamma_2}\Big)$$

$$Cov(X_1, X_2 = \frac{\lambda_1 \lambda_2}{\gamma_1(\gamma_1 + \gamma_2)}$$

A complete study of the asymptotic distribution is provided in [14], whose moment generating function is given by

$$\varphi(x, y) = exp\Big(\alpha\beta \int_1^y M(1, 1 + \gamma, \beta(s - 1))ds + \alpha(x - 1)M(1, 1 + \gamma, \beta(y - 1))\Big)$$

where

$$\gamma = \frac{\gamma_1}{\gamma_2}$$
$$\alpha = \frac{\lambda_1}{\gamma_1}$$
$$\beta = \frac{\lambda_2}{\gamma_2}$$

From this expression, the authors in [14] derived asymptotic different behavior of the marginal protein distribution, including Poisson, Neymann, negative Binomial, Gaussian and Gamma distribution.

For the non-linear regulation case, the authors in [142, 139, 140] used the linear noise expansion and simulation to study the asymptotic and transient moment behavior with respect to the regulation function. Their study show that negative regulation can increase or decrease noise strength.

D1

$$X_1(t) = X_1(0) + Y_3\Big(\int_0^t \lambda_1 k_1(X_1(s))ds\Big) - Y_4\Big(\int_0^t \gamma_1 X_1(s)ds\Big)$$

The authors in [132] derived approximation of the time-dependent first moments using moment closure approximation, and successfully compared it with experimental data of the λ-repressor system. As a one-dimensional discrete Markov-chain, its asymptotic distribution can also be derived.

7.4 Continuous models without switch

These models were the first one introduced to model gene self-regulation.

C3

$$\begin{cases} \dot{x}_1 &= \lambda_1 k_1(x_3) - \gamma_1 x_1, \\ \dot{x}_2 &= \lambda_2 x_1 - \gamma_2 x_2, \\ \dot{x}_3 &= \lambda_3 x_2 - \gamma_3 x_3. \end{cases}$$

This model was originally introduced by [48]. See subsection 6 for a complete study of the asymptotic behavior of this model.

C2

$$\begin{cases} \dot{x}_1 &= \lambda_1 k_1(x_2) - \gamma_1 x_1, \\ \dot{x}_2 &= \lambda_2 x_1 - \gamma_2 x_2. \end{cases}$$

In absence of regulation, the above system can be analytically solved

$$x_1(t) = \frac{\lambda_1}{\gamma_1} + \Big(x_1(0) - \frac{\lambda_1}{\gamma_1}\Big)e^{-\gamma_1 t}$$
$$x_2(t) = \frac{\lambda_1\lambda_2}{\gamma_1\gamma_2} + \Big(x_2(0) - \frac{\lambda_1\lambda_2}{\gamma_1\gamma_2}\Big)e^{-\gamma_2 t} + \lambda_2\Big(x_1(0) - \frac{\lambda_1}{\gamma_1}\Big)F(t)$$

where

$$F(t) = \begin{cases} \frac{e^{-\gamma_1 t} - e^{-\gamma_2 t}}{\gamma_2 - \gamma_1} & \text{if } \gamma_1 \neq \gamma_2, \\ te^{-\gamma_2 t} & \text{if } \gamma_1 = \gamma_2. \end{cases}$$

In the presence of positive regulation, this model has essentially similar asymptotic behavior as the previous model C3. In the presence of negative regulation, however, oscillations are not present any more when k_1 is a standard Hill function as in eq. (3.12).

C1

$$\dot{x}_1 = \lambda_1 k_1(x_1) - \gamma_1 x_1.$$

In the presence of positive regulation, this model has essentially similar asymptotic behavior as the previous model C3. In the presence of negative regulation, however, oscillations are not present any more when k_1 is a standard Hill function as in eq. (3.12).

7.5   Discrete models with Bursting

We now turn to Bursting model. Below R_0 is the counting process associated to the number of times a bursting event happens. It is regulated by the effector or protein molecules.

BD2   This model can be obtained from SD2 or D3, upon a particular scaling (see section 9).

$$\begin{cases} R_0(t) &=& Y\Big(\int_0^t \lambda_1 k_1(X_2(s))ds\Big), \\ X_1(t) &=& X_1(0) - Y_0\Big(\int_0^t \gamma_1 X_1(s)ds\Big) + \sum_{i \geqslant 1} iY_i\Big(\int_0^t \mathbf{1}_{\{(q_{i-1},q_i]\}}(\xi_{R_0(s-)})dR_0(s)\Big), \\ X_2(t) &=& X_2(0) + Z_1\Big(\int_0^t \lambda_2 X_1(s)ds\Big) - Z_2\Big(\int_0^t \gamma_2 X_2(s)ds\Big). \end{cases}$$

BD1

$$\begin{cases} R_0(t) &=& Y\Big(\int_0^t \lambda_1 k_1(X_1(s))ds\Big), \\ X_1(t) &=& X_1(0) - Y_0\Big(\int_0^t \gamma_1 X_1(s)ds\Big) + \sum_{i \geqslant 0} iY_i\Big(\int_0^t \mathbf{1}_{\{(q_{i-1},q_i]\}}(\xi_{R_0(s-)})dR_0(s)\Big). \end{cases}$$

The authors in [129] presented stationary and time-dependent probability distribution when k_1 is constant and the jump size a geometric random variable, of mean parameter b.

$$g(z,t) = \Big[\frac{1 + b(1-z)e^{-t/\gamma_1}}{1 + b(1-z)}\Big]^a$$

$$p_{x_1}(t) = \frac{\Gamma(a+n)}{\Gamma(n+1)\Gamma(a)}\Big(\frac{b}{1+b}\Big)^n\Big(\frac{1+be^{-t/\gamma_1}}{1+b}\Big)^a {}_2F_1\Big(-n, -a, 1-a-n, \frac{1+b}{b+e^{-t/\gamma_1}}\Big)$$

$$< X_1 > (t) = ab(1 - e^{-t/\gamma_1})$$

$$\sigma_1^2(t) = < X_1 > (t)(1 + b + be^{-t/\gamma_1})$$

where $a = \frac{\lambda_1}{\gamma_1}$ The authors in [4] computed the analytical stationary distribution for general nonlinear regulation k_1

$$p_{x_1} = \frac{p_0}{x_1}a\prod_{i=1}^{x_1-1}\Big(a\frac{k_1(i)}{i} + \frac{b-1}{b}\Big).$$

7.6   Continuous models with Bursting

In continuous bursting model below, $N(ds, dz, dr)$ stands for a Poisson random measure, of intensity $ds\,h(z)\,dz\,dr$ where h is a probability density that gives the size of the burst.

BC2   This model can be obtained from SC2 or BD2, upon a particular scaling (see section 9). We will consider its adiabatic reduction in subsection 9.3.

$$\begin{cases} x_1(t) &= x_1(0) - \displaystyle\int_0^t \gamma_1 x_1(s-)ds + \int_0^t \int_0^\infty \int_0^\infty z\mathbf{1}_{\{r \leqslant \lambda_1 k_1(x_2(s-))\}} N(ds, dz, dr), \\ x_2(t) &= x_2(0) + \displaystyle\int_0^t \lambda_2 x_1(s-)ds - \int_0^t \gamma_2 x_2(s-)ds. \end{cases}$$

BC1

$$x_1(t) = x_1(0) - \int_0^t \gamma_1 x_1(s-)ds + \int_0^t \int_0^\infty \int_0^\infty z\mathbf{1}_{\{r \leqslant \lambda_1 k_1(x_1(s-))\}} N(ds, dz, dr).$$

The authors in [20] used this model without regulation to successfully fit data from the β-galactosidase protein in E.Coli. The asymptotic distribution is the Gamma distribution

$$p_{x_1} = \frac{1}{b^a \Gamma(a)} x^{a-1} e^{-x/b}$$

where $a = \frac{\lambda_1}{\gamma_1}$ The authors in [39] computed the analytical expression of the steady-state distributions for non-linear regulation rate k_1, and exponential bursting size of mean b.

$$p_{x_1} = A x^{-1} e^{-x/b} e^{a \int \frac{k_1(z)}{z} dz}$$

where A is a normalizing constant.

7.7   Models with both switching and Bursting

These models can be obtained from SD2.

SBD1

$$\begin{cases} X_0(t) &= X_0(0) + Y_1\Big(\displaystyle\int_0^t \lambda_a \mathbf{1}_{\{X_0(s)=0\}} k_a(X_1(s))ds\Big) - Y_2\Big(\int_0^t \lambda_i \mathbf{1}_{\{X_0(s)=1\}} k_i(X_1(s))ds\Big), \\ R_0(t) &= Y\Big(\displaystyle\int_0^t \lambda_1 \mathbf{1}_{\{X_0(s)=1\}} k_1(X_1(s))ds\Big), \\ X_1(t) &= X_1(0) - Y_0\Big(\displaystyle\int_0^t \gamma_1 X_1(s)ds\Big) + \sum_{i \geqslant 1} iY_i\Big(\int_0^t \mathbf{1}_{\{(q_{i-1}, q_i]\}}(\xi_{R_0(s-)})dR_0(s)\Big). \end{cases}$$

The authors in [129] presented stationary probability distribution when k_a, k_i, k_1 are constant, and the burst size is a geometric random variable of mean b.

$$\begin{aligned} p_{x_1} = {} & \frac{\Gamma(\alpha + n)\Gamma(\beta + n)\Gamma(d)}{\Gamma(n+1)\Gamma(\alpha)\Gamma(\beta)\Gamma(d+n)} \\ & \times \Big(\frac{b}{1+b}\Big)^n \Big(1 - \frac{b}{1+b}\Big)^\alpha \\ & \times {}_2F_1\Big(\alpha + n, d - \beta, d + n, \frac{b}{1+b}\Big) \end{aligned}$$

where

$$a = \frac{\lambda_1}{\gamma_1}$$

$$c = \frac{\lambda_a}{\gamma_1}$$

$$d = \frac{\lambda_i + \lambda_a}{\gamma_1}$$

$$\alpha = \frac{1}{2}(a + d + \phi)$$

$$\beta = \frac{1}{2}(a + d - \phi)$$

$$\phi^2 = (a + d)^2 - 4ac$$

SBC1

$$\begin{cases} X_0(t) & = & X_0(0) + Y_1\Big(\int_0^t \lambda_a \mathbf{1}_{\{X_0(s)=0\}} k_a(x_1(s)) ds\Big) - Y_2\Big(\int_0^t \lambda_i \mathbf{1}_{\{X_0(s)=1\}} k_i(x_1(s)) ds\Big), \\ x_1(t) & = & x_1(0) - \int_0^t \gamma_1 x_1(s-) ds + \int_0^t \int_0^\infty \int_0^\infty z \mathbf{1}_{\{r \leqslant \lambda_1 \mathbf{1}_{\{X_0(s)=1\}} k_1(x_1(s-))\}} N(ds, dz, dr). \end{cases}$$

7.8 Hybrid discrete and continuous models

D1C1
$$\begin{cases} X_1(t) & = & X_1(0) + Y_3\Big(\int_0^t \lambda_1 k_1(x_2(s)) ds\Big) - Y_4\Big(\int_0^t \gamma_1 X_1(s) ds\Big), \\ \dot{x}_2 & = & \lambda_2 X_1 - \gamma_2 x_2. \end{cases}$$

In the absence of regulation, the asymptotic characteristic function of the protein variable x_2 has been found to be ([14])

$$\omega(s) = exp\Big(\alpha \int_0^{s\beta} M(1, 1 + \gamma, z) dz\Big)$$

where

$$\gamma = \frac{\gamma_1}{\gamma_2}$$

$$\alpha = \frac{\lambda_1}{\gamma_1}$$

$$\beta = \frac{\lambda_2}{\gamma_2}$$

This asymptotic expression include both the Gamma and Poisson distribution as limiting behavior.

SD1C1

$$\begin{cases} X_0(t) & = & X_0(0) + Y_1\Big(\int_0^t \lambda_a \mathbf{1}_{\{X_0(s)=0\}} k_a(x_1(s)) ds\Big) - Y_2\Big(\int_0^t \lambda_i \mathbf{1}_{\{X_0(s)=1\}} k_i(x_2(s)) ds\Big), \\ X_1(t) & = & X_1(0) + Y_3\Big(\int_0^t \lambda_1 \mathbf{1}_{\{X_0(s)=1\}} k_1(x_2(s)) ds\Big) - Y_4\Big(\int_0^t \gamma_1 X_1(s) ds\Big), \\ \dot{x}_2 & = & \lambda_2 X_1 - \gamma_2 x_2. \end{cases}$$

The author in [101] considered this model as an approximation of the SD2 model, and present moment calculation and numerical simulation of this model.

Obviously, different model can again be built with similar features, and the list above is not exhaustive. Although not directly related to our work, we present in the next paragraph different approach of modeling. Such modeling review is intend to show the variety of possible choices of modeling.

7.9   More detailed models and other approaches

We first review more detailed models of single gene, then models that take into account other source of noise, and finally models with interaction between genes.

In its Ph.D. thesis work, Jia [71] makes the review of the standard model of gene expression and its different limiting behavior, in particular condition for occurrence of bursting. Then he generalizes the model to consider non-exponential waiting time between burst events, as well as non-geometric burst size distributions (see also Pedraza and Paulsson [105]). He gives a specific example of model of post-transcriptional regulation with small mRNA (a different from but related molecule to mRNA) that yields non-geometric burst size distribution. For other models taking into account post-transcriptional regulation by small mRNA, see Bose and Ghosh [15], Gorban et al. [49] and for a review of biological mechanisms of post-transcriptional regulation, see Storz and Waters [136].

For models with more than two states of the promoter, see the pioneering work of Tapaswi et al. [141]. Also, Blake et al. [11] used a model with four promoter states to reproduce faithfully the GAL system in prokaryotes. In agreement with data, the main finding is that the level of noise in gene expression is non-monotonic with respect to the level of transcription efficiency. Coulon et al. [24] also considered a model with more than two states for the promoter, and extensively studied the effect of promoter transition on noise strength on protein level.

For models at a much finer scale, that explicitly take into account dynamics of mRNA polymerase and complex formation, see Dublanche et al. [30], while for mRNA polymerase and ribosome dynamics see Kierzek et al. [78], Gorban et al. [49]. A model that goes up to the single-nucleotide level was proposed by Ribeiro [116]. For spatially extended model, see Sagués et al. [122].

In the standard model we consider here, we implicitly assume that there is only one "intrinsic" source of randomness. Indeed, the stochasticity in the model comes from the random occurrences of the discrete events that constitute the reaction network directly linked to the single gene model (or its product) we study. There are obviously many other sources of randomness that can influence the stochasticity in the gene expression. Firstly, the partitioning event at division is an evident source of randomness when we consider discrete number of molecules. Daughter cells may have different sizes, and each molecule then has to "choose" between the two daughter cells. Common model that include randomness at partition consider a binomial partition law (see pioneering work of Berg [9], and more recently Huh and Paulsson [65]), which has been supported experimentally [120, 47]. Secondly, a lot of experimental and modeling approaches have focused on "extrinsic" sources of noise, in particular since the experimental paper of Elowitz et al. [34]. There, the authors used two reporter genes (one with a red fluorescence, one with a green fluorescence), localized at very similar place in the genome, with the same promoter sequence, and measured the fluorescence level of these two genes in single cells. If there were only extrinsic noise, all cells should have the same proportion of red and green fluorescence, at different global intensities. The observed fluctuations in these proportions from cell to cell is attributed to the intrinsic noise. Lei [86] made a review of the different mathematical formulations of extrinsic noise. Usually, the modeling of extrinsic noise includes fluctuations of kinetic parameter, especially of the gene regulation function (see Rosenfeld et al. [120] for experimental evidence), as a Gaussian colored noise [138, 85] (with a Langevin

formalism). Noise due to randomness in the repressor molecule numbers can also be seen as an extrinsic noise. Ochab-marcinek and Tabaka [99] consider this source of noise and show that it can be responsible for bistability (using similar geometric construction-based proof as in our case, in section 8). See also [30] for an experimental evidence that extrinsic noise can have qualitative impact on the gene expression behavior.

For model with two genes in interaction see for instance the pioneering work of Kepler and Elston [77], followed by instance by [87]. In such study, bifurcation characterization is of importance. Indeed, interaction of two genes has been widely used to explain cell differentiation fate, where each gene codes for a protein that is responsible of a particular cell lineage. In case of bistability, each stable state then represent a stable cell fate. See for example [79, 117, 137] for recent models applied to individuals cell data. For larger network, experiments and modeling has mostly focused on the quantification on the noise strength of the gene expression level (also called variability), as an output of the model, and as a function of the parameters and rate function or functional motif, (see Çagatay et al. [21]). Besides from extensive numerical simulations, the diffusion approximation of the discrete model has been widely used, see for instance [16].

Finally El-Samad and Khammash [31], Karlebach and Shamir [76] review other approaches of modeling of gene regulatory network, including boolean, probabilistic boolean, petri nets, discrete, continuous and hybrid models, See also the review of [1] for piecewise linear ordinary differential equation and delayed differentiation equation approach. For stochastic and delayed models, see Ribeiro [116], Galla [41]

8   Specific Study of the One-Dimensional Bursting Model

We detail here the study of the one-dimensional bursting model, either in a discrete formalism (which is then a pure jump Markov process, subsection 8.1) and in a continuous formalism (which is a piecewise deterministic Markov process, subsection 8.2). For both formalism, we will recall the construction of the stochastic process (and then its existence), and study its long time behavior, using a semigroup formalism (see part 0 subsection 6.5). Once asymptotic convergence has been proved, we study the qualitative property of the invariant probability distribution. The advantage of the one-dimensional model is to possess a probability distribution on the Gibb's form. By analogy to the deterministic modeling, we will speak of a bifurcation when the number of modes of the probability distribution change (called P-bifurcation in the literature). This analogy allows a direct comparison between bifurcation diagrams, and then to deduce the influence of the bursting production on the qualitative dynamics of gene expression. Note that such stochastic bifurcation concept has been applied to empirical measurement data by [134], where the authors obtained an experimental bifurcation diagram by controlling experimentally a parameter and estimating the probability distribution for each parameter value. Up to now, our analytic treatment is restricted to the case of exponential (or geometric in the discrete case) jump distribution. This case is probably the most interesting however, as it is (up to our knowledge) the only case measured experimentally (see [22, 47, 111, 150]).

Finally, we show how can compute an explicit convergence rate towards the steady-state measure in subsection 8.5, and as a corollary of our study of the asymptotic behavior of the bursting model, we present in subsection 8.6 the inverse problem to recover the regulation function from the invariant density. This latter part is an ongoing project, where we try to collect experimental data to apply our theoretical study of the model. The inverse problem may be very interesting in the sense that it permits to deduce molecular interactions that governs the regulation function (see for instance section 3), which are not easily observable experimentally.

Reaction	Propensity	State change vector
Degradation	γ_n	-1
Burst Production r	$h_r \lambda_n$	$+r$

Table 1.5: Definitions of the reactions, propensities and state change vector from the n state in the discrete model. See text for more details.

The first subsection will be the object of a future publication ([93]), and the second one was published in 2011 ([91]).

8.1 Discrete variable model with bursting BD1

In this section we model the number of gene products in a cell as a pure-jump Markov process $X = \{X_t\}_{t \geqslant 0}$ in the state space $E = \{0, 1, 2, \ldots\}$. Thus a Chapman–Kolmogorov governs the probabilities dynamics. A general one-dimensional bursting gene expression model [129] (BD1, see subsection 7.5) may be constructed as follows: let n be the number of gene products and $P_n(t) = \mathrm{Pr}(X_t = n)$ denote the probability for finding n gene products inside the cell at a given time instant t. We shall include a loss ($n \to n-1$) and gain ($n \to n+k$) of functionality processes in terms of the general rates γ_n and λ_n, respectively. The step size assume the values $k = 1, 2, 3, \ldots$ and is a random variable (independent of the actual number of gene product) with probability mass function h, so that $\sum_{k=1}^{+\infty} h_k = 1$. Therefore, the Chapman–Kolmogorov equation (or master equation) describing the time evolution of the probabilities P_n to have n gene products in a cell is an infinite set of differential equations

$$\frac{dP_n}{dt} = \gamma_{n+1} P_{n+1} - \gamma_n P_n + \sum_{k=1}^{n} h_k \lambda_{n-k} P_{n-k} - \lambda_n P_n, \quad n = 0, 1, \ldots, \qquad (8.1)$$

where we use the convention that $\sum_{k=1}^{0} = 0$. We supplement eq. (8.1) with the initial condition $P_n(0) = v_n$, $n = 0, 1, \ldots$, where $v = (v_n)_{n \geqslant 0} \in \ell^1$ is a probability mass function of the initial amount X_0 of the gene product. We give existence and uniqueness of solutions of eq. (8.1) together with convergence to a stationary distribution.

We assume that

$$\lambda_0 > 0, \quad \gamma_0 = 0, \quad \gamma_n > 0, \quad \lambda_n, h_n \geqslant 0, \quad n = 1, 2, \ldots, \quad \sum_{n=1}^{+\infty} h_n = 1. \qquad (8.2)$$

The process X is the minimal pure jump Markov process with the jump rate function $\varphi(n) = \lambda_n + \gamma_n, n \geqslant 0$, and the jump transition kernel $\mathcal{K}$ given by

$$\mathcal{K}(n, \{n+j\}) = \begin{cases} q_n, & \text{if } j = -1, n \geqslant 1, \\ (1 - q_n) h_j, & \text{if } j \geqslant 1, n \geqslant 0, \\ 0, & \text{otherwise.} \end{cases} \qquad q_n = \frac{\gamma_n}{\lambda_n + \gamma_n}, \qquad (8.3)$$

Firstly, we recall the construction of X. Let $\{\xi_k\}_{k \geqslant 0}$, be a discrete time Markov chain in the state space $E = \mathbb{Z}_+ = \{0, 1, \ldots\}$ with transition kernel $\mathcal{K}$ and let $\{\varepsilon_k\}_{k \geqslant 1}$ be a sequence of independent random variables exponentially distributed with mean 1. Set $T_0 = 0$ and define recursively the times of jumps of X as

$$T_k = T_{k-1} + \frac{\varepsilon_k}{\varphi(\xi_{k-1})}, \quad k = 1, 2, \ldots.$$

Starting from $X_0 = \xi_0$ we have

$$X_t = \xi_k, \quad T_k \leqslant t < T_{k+1}, \quad k = 0, 1, 2, \ldots,$$

so that the process is uniquely determined for all $t < T_\infty$, where

$$T_\infty = \lim_{k \to \infty} T_k,$$

is called the explosion time. If the explosion time is finite, we can add the point -1 to the state space and we can set $X_t = -1$ for $t \geqslant T_\infty$. The process X is called *nonexplosive* if $\mathbb{P}_i(T_\infty = \infty) = 1$ for all $i \in E$, where $\mathbb{P}_i$ is the law of the process starting from $X_0 = i$.

We now rewrite eq. (8.1) as an abstract Cauchy problem in the space ℓ^1. We make use of the results from [145]. Let K be the transition operator on ℓ^1 corresponding to $\mathcal{K}$ defined as in eq. (8.3). For $v = (v_n)_{n \geqslant 0} \in \ell^1$ we have $(Kv)_0 = q_1 v_1$ and

$$(Kv)_n = q_{n+1} v_{n+1} + \sum_{k=1}^{n} h_k (1 - q_{n-k}) v_{n-k}, \quad n = 1, 2, \ldots.$$

Let us define the operator

$$Gu = -\varphi u + K(\varphi u) \quad \text{for} \quad u \in \ell_\varphi^1 = \{u \in \ell^1 : \sum_{n=0}^{\infty} \varphi_n |u_n| < \infty\}.$$

There is a substochastic semigroup $\{P(t)\}_{t \geqslant 0}$ on ℓ^1 such that for each initial probability mass function $v \in \ell_\varphi^1$ the equation

$$\frac{du}{dt} = G(u), \quad t > 0, \quad u(0) = v, \tag{8.4}$$

has a nonnegative solution $u(t)$ which is given by $u(t) = P(t)v$ for $t \geqslant 0$ and

$$(P(t)v)_n = \sum_{j=0}^{\infty} \mathbb{P}_j(X_t = n, t < T_\infty) v_j, \quad n = 0, 1, \ldots.$$

The process X is nonexplosive if and only if the semigroup $\{P(t)\}_{t \geqslant 0}$ is stochastic. Equivalently, the generator of the semigroup $\{P(t)\}_{t \geqslant 0}$ is the closure of (G, ℓ_φ^1). In that case the solution $u(t)$ of eq. (8.4) is unique and it is a probability mass function for each t, if v is such. In particular, if the operator K has a strictly positive fixed point, then the semigroup $\{P(t)\}_{t \geqslant 0}$ is stochastic. Thus, we now look for fixed points of K.

The equation for the steady state $p^* = (p_n^*)_{n \geqslant 0}$ of eq. (8.1) is of the form

$$\gamma_{n+1} p_{n+1}^* - \gamma_n p_n^* + \sum_{k=1}^{n} h_k \lambda_{n-k} p_{n-k}^* - \lambda_n p_n^* = 0, \quad n = 0, 1, \ldots. \tag{8.5}$$

Observe that $\gamma_1 p_1^* = \lambda_0 p_0^*$ and we can rewrite eq. (8.5) as

$$\gamma_{n+1} p_{n+1}^* - \gamma_n p_n^* = \lambda_n p_n^* - \sum_{k=0}^{n-1} h_{n-k} \lambda_k p_k^*, \quad n = 1, 2 \ldots.$$

Summing both sides and changing the order of summation, we obtain

$$p_{n+1}^* = \frac{1}{\gamma_{n+1}} \sum_{k=0}^{n} \left(\sum_{j=n-k+1}^{\infty} h_j \right) \lambda_k p_k^*, \quad n = 0, 1, \ldots, \tag{8.6}$$

Thus given p_0^* eq. (8.6) uniquely determines p^*. Consequently, there is one, and up to a multiplicative constant only one, solution of eq. (8.5), and if $p_0^* > 0$ then $p_n^* > 0$ for all $n \geqslant 1$. Now, if

$$\sum_{n=0}^{\infty} p_n^* = 1 \quad \text{and} \quad \sum_{n=0}^{\infty} (\lambda_n + \gamma_n) p_n^* < \infty, \tag{8.7}$$

then $p^* \in \ell_\varphi^1$, $G(p^*) = 0$, and $K(\varphi p^*) = \varphi p^*$, which implies the semigroup $\{p(t)\}_{t \geqslant 0}$ is stochastic. Thus, we have proved the following result.

Theorem 25. *Assume condition eq. (8.2) and suppose that $p^* = (p_n^*)_{n \geqslant 0}$ given by eq. (8.6) satisfies eq. (8.7). Then for each initial probability mass function $v = (v_n)_{n \geqslant 0} \in \ell_\varphi^1$ eq. (8.1) has a unique solution which is a probability mass function for each $t > 0$ and satisfies*

$$\lim_{t \to \infty} \sum_{n=0}^{\infty} |(P(t)v)_n - p_n^*| = 0.$$

Next, we give sufficient conditions for eq. (8.7) in the case when h is geometric

$$h_k = (1 - b)b^{k-1}, \quad k = 1, 2, \ldots, \tag{8.8}$$

with $b \in (0, 1)$. Since

$$\sum_{j=n-k+1}^{\infty} h_j = b^{n-k},$$

we obtain the following equation for $p^* = (p_n^*)_{n \geqslant 0}$

$$\frac{p_{n+1}^*}{p_n^*} = \frac{\lambda_n + b\gamma_n}{\gamma_{n+1}}, \quad n = 0, 1 \ldots. \tag{8.9}$$

Corollary 26. *Suppose that h is geometric as in eq. (8.8). Then $p^* = (p_n^*)_{n \geqslant 0}$ is given by*

$$p_n^* = p_0^* \prod_{k=1}^{n} \frac{\lambda_{k-1} + b\gamma_{k-1}}{\gamma_k}, \quad n = 1, 2, \ldots. \tag{8.10}$$

In particular, if

$$\lim_{n \to \infty} \frac{\lambda_n}{\gamma_n} < 1 - b \quad \text{and} \quad \lim_{n \to \infty*} \frac{\gamma_n}{\gamma_{n+1}} = 1,$$

then the conclusions of theorem 25 hold.

Remark 27. *[Bifurcation] The relation eq. (8.9) can be used to derive bifurcation property in terms of number of modes of the steady-state distribution as a function of parameters. The number of modes are indeed linked to the number of sign change of*

$$n \mapsto \lambda_n + b\gamma_n - \gamma_{n+1}.$$

Remark 28. *Usually one would consider the functionality loss γ_n as a degradation rate with linear dependence on n and the bursting rate λ_n to characterize the regulation the system is submitted to: external for independence on n, positive (or negative) self interaction for monotonically increasing (or decreasing) dependence with n. The functional shape of auto regulation is usually taken as a non-linear Hill function, resulting on a quasi steady state assumption of effectors and/or repressors molecules (see section 3)*

In the following examples we assume that h is geometric with parameter b and $\gamma_n = \gamma n$, $n \geqslant 0$, with $\gamma > 0$. In all examples, the conditions of corollary 26 are satisfied. The following examples are meant to show that analytical formula may be found for a variety of different jump rate function, all restricted to a geometric jump size distribution, however.

Example 1 (Negative binomial)**.** *Suppose that $\lambda_n = \lambda_0 + \lambda n$ with $\lambda_0 > 0, \lambda \geqslant 0$. We have $\lambda_n \geqslant 0$ for each n. Plugging γ_k and λ_k into eq. (8.10) gives*

$$p_n^* = \frac{p_0^*}{n!} \prod_{k=0}^{n-1} \left(\frac{\lambda_0}{b\gamma + \lambda} + k \right) \left(\frac{\lambda + b\gamma}{\gamma} \right)^n, \quad n = 0, 1, \ldots.$$

Thus $p^* \in \ell^1$ if and only if

$$\lambda + b\gamma < \gamma.$$

In that case we obtain the negative binomial distribution

$$p_n^* = \frac{(a)_n}{n!} p^n (1-p)^a, \quad n = 0, 1, \ldots,$$

where

$$p = \frac{\lambda + b\gamma}{\gamma}, \quad a = \frac{\lambda_0}{b\gamma + \lambda},$$

and $(a)_n$ is the Pochhammer symbol defined by

$$(a)_n = \frac{\Gamma(a+n)}{\Gamma(a)} = a(a+1)(a+2)\ldots(a+n-1), \quad (a)_0 = 1.$$

This was previously obtained in [129].

Example 2 (Mixture of logarithmic distribution)**.** *Suppose that $\lambda_0 > 0$ and $\lambda_n = 0$ for $n \geqslant 1$. Then*

$$p_n^* = p_0^* \frac{\lambda_0}{\gamma} \frac{b^{n-1}}{n}, \quad n = 1, 2, \ldots,$$

which can be rewritten as

$$p_n^* = -\frac{b^n}{n \ln(1-b)}(1 - p_0^*), \quad n = 1, 2, \ldots, \quad p_0^* = \frac{b\gamma}{b\gamma - \lambda_0 \ln(1-b)}.$$

The distribution

$$\tilde{p}_0 = 0, \quad \tilde{p}_n = -\frac{b^n}{n \ln(1-b)}, \quad n = 1, 2, \ldots,$$

is called a logarithmic distribution.

    If we assume that $\lambda_n = 0$ for $n > m$, then we obtain the following distribution

$$p_n^* = p_0^* \frac{b^n}{n!} \prod_{k=0}^{n-1} \left(\frac{\lambda_k}{b\gamma} + k \right), \quad n = 0, \ldots, m,$$

and

$$p_n^* = (1 - \sum_{j=0}^{m} p_j^*) \frac{b^n}{cn}, \quad n > m,$$

where c and p_0^* are such that

$$c = \sum_{j=m+1}^{\infty} \frac{b^j}{j} \quad and \quad \sum_{j=0}^{m} p_j^* + p_m^* \frac{mc}{b^m} = 1.$$

In particular, this type of distribution will be obtained if we take $\lambda_0 > 0$, $\lambda < 0$, and

$$\lambda_n = \begin{cases} \lambda_0 + \lambda n, & if\ n \leqslant -\lambda_0/\lambda, \\ 0, & otherwise. \end{cases}$$

Example 3. *We now look at*

$$\lambda_n = \lambda \frac{1 + K_1 n}{K_0 + K_1 n}, \quad n = 0, 1, \dots,$$

where $\lambda > 0, K_1 > 0, K_0 \geqslant 1$. *We find that, for each* n,

$$\frac{\lambda_n + b\gamma n}{\gamma} = \frac{b(n + a_1)(n + a_2)}{n + b_1},$$

where

$$b_1 = \frac{K_0}{K_1}, \quad a_1 = \frac{1}{2}(\alpha - \beta), \quad a_2 = \frac{1}{2}(\alpha + \beta),$$

and

$$\alpha = \frac{K_0}{K_1} + \frac{\lambda}{b\gamma}, \quad \beta^2 = \alpha^2 - \frac{4\lambda}{K_1 b\gamma}.$$

Since $K_0 \geqslant 1$, *we can find a nonnegative* β, *thus* $a_2 \geqslant a_1 > 0$. *Consequently, the stationary distribution is of the form*

$$p_n^* = \frac{1}{{}_2F_1(a_1, a_2; b_1; b)} \frac{(a_1)_n(a_2)_n}{(b_1)_n} \frac{b^n}{n!}, \quad n = 0, 1, \dots,$$

where ${}_2F_1$ *is the Gauss's hypergeometric function*

$${}_2F_1(a_1, a_2; b_1; x) = \sum_{n=0}^{\infty} \frac{(a_1)_n(a_2)_n}{(b_1)_n} \frac{x^n}{n!}.$$

Example 4 (Generalized hypergeometric distributions)**.** *The generalized hypergeometric function* ${}_pF_q$ *is defined to be the real analytical function on* $\mathbb{R}$ *given by the series expansion*

$${}_pF_q(a_1, \dots, a_p; b_1, \dots, b_q; x) = \sum_{n=0}^{\infty} \frac{(a_1)_n \dots (a_p)_n}{(b_1)_n \dots (b_q)_n} \frac{x^n}{n!}.$$

The negative binomial distribution in example 1 for the case of $\lambda = 0$ *has the probability generating function* $s \mapsto {}_1F_0(a_1; bs)/{}_1F_0(a_1; b)$ *with* $a_1 = \lambda_0/b\gamma$. *The distribution obtained in example 3 has the probability generating function* $s \mapsto {}_2F_1(a_1, a_2; b_1; bs)/{}_2F_1(a_1, a_2; b_1; b)$. *Extending both of these examples we suppose that* $\lambda_n \geqslant 0$ *is a rational function of* n *satisfying*

$$\frac{\lambda_n + b\gamma n}{\gamma} = \frac{(n + a_1) \dots (n + a_{q+1})b}{(n + b_1) \dots (n + b_q)}, \quad n = 0, 1, 2, \dots.$$

Then $p^* = (p_n^*)_{n \geqslant 0}$ *has the probability generating function of the form*

$$\frac{{}_{q+1}F_q(a_1, \dots, a_{q+1}; b_1, \dots, b_q; bs)}{{}_{q+1}F_q(a_1, \dots, a_{q+1}; b_1, \dots, b_q; b)}.$$

Example 5. *Consider* λ_n *as a Hill function of the form*

$$\lambda_n = \lambda \frac{1 + K_1 n^N}{K_0 + K_1 n^N},$$

where $K_1, K_0, \lambda > 0$ *and* $N \geqslant 1$. *If* h *is geometric and*

$$\lim_{n \to \infty} \gamma_n = \infty, \quad \lim_{n \to \infty} \frac{\gamma_n}{\gamma_{n+1}} = 1,$$

then irrespective of b *there always exists* $p^* = (p_n^*)_{n \geqslant 0}$ *satisfying eq. (8.6).*

8.2　Continuous variable model with bursting BC1

In this section we consider a continuous state space version of the model presented in section 8.1 (BC1, see subsection 7.6), which is a piecewise deterministic Markov process $Y = \{Y_t\}_{t \geqslant 0}$ with values in $E = (0, \infty)$ where Y_t denotes the amount of the gene product in a cell at time t, $t \geqslant 0$. We assume that protein molecules undergo the process of degradation with rate γ that is interrupted at random times

$$t_1 < t_2 < \ldots$$

occurring with intensity λ and both λ and γ depend on the current amount of molecules. At t_k a random amount of protein molecules is produced, independently of the current number of proteins, so that the process changes from Y_{t_k-} to $Y_{t_k} = Y_{t_k-} + e_k$, $k = 1, 2, \ldots$, where $\{e_k\}_{k \geqslant 1}$ is a sequence of positive independent random variables with probability density function h, which are also independent of Y_0. The time-dependent probability density function $u(t, x)$ is described by the continuous analog of the master equation

$$\frac{\partial u(t,x)}{\partial t} = \frac{\partial(\gamma(x)u(t,x))}{\partial x} - \lambda(x)u(t,x) + \int_0^x \lambda(x-y)u(t,x-y)h(y)dy \qquad (8.11)$$

with the initial probability density $u(0, x) = v(x)$, $x > 0$.

We assume that γ is a continuous function and that λ is a nonnegative measurable function with λ/γ being locally integrable on $(0, \infty)$ and

$$\gamma(x) > 0 \quad \text{for } x > 0, \quad \int_0^\delta \frac{dx}{\gamma(x)} = +\infty, \quad \int_0^\delta \frac{\lambda(x)}{\gamma(x)}dx = +\infty, \qquad (8.12)$$

for some $\delta > 0$. From eq. (8.12) it follows that the differential equation

$$x'(t) = -\gamma(x(t)), \quad x(0) = x > 0,$$

has a unique solution which we denote by $\pi_t x$, $t \geqslant 0$, $x > 0$. For each $x > 0$ we have $\pi_t x \to 0$ as $t \to \infty$ and

$$\int_0^t \lambda(\pi_s x)ds = \int_{\pi_t x}^x \frac{\lambda(y)}{\gamma(y)}dy \to \infty, \quad \text{as } t \to \infty.$$

We now recall the construction of the minimal piecewise deterministic Markov process Y. Let $\{\varepsilon_k\}_{k \geqslant 1}$ be a sequence of independent random variables exponentially distributed with mean 1, which is also independent of $\{e_k\}_{k \geqslant 1}$. Set $t_0 = 0$. For each $k = 1, 2, \ldots$ and given $Y_{t_{k-1}}$ the process evolves as

$$Y_t = \begin{cases} \pi_{t-t_{k-1}} Y_{t_{k-1}}, & t_{k-1} \leqslant t < t_k, \\ Y_{t_k-} + e_k, & t = t_k, \end{cases} \qquad (8.13)$$

where $t_k = t_{k-1} + \Delta t_k$ and Δt_k is a random variable such that

$$\Pr(\Delta t_k \leqslant t | Y_{t_{k-1}} = x) = 1 - e^{-\int_0^t \lambda(\pi_s x)ds}, \quad t, x > 0.$$

The random variable Δt_k can be defined with the help of the exponentially distributed random variable ε_k trough the equality in distribution

$$\varepsilon_k = \int_0^{\Delta t_k} \lambda(\pi_s Y_{t_{k-1}})ds,$$

which can be rewritten as

$$\varepsilon_k = Q(\pi_{\Delta t_k} Y_{t_{k-1}}) - Q(Y_{t_{k-1}}),$$

where the nonincreasing function Q is given by

$$Q(x) = \int_x^{\bar{x}} \frac{\lambda(y)}{\gamma(y)} dy, \tag{8.14}$$

and $\bar{x} = +\infty$, when the integral is finite or any $\bar{x} > 0$ otherwise. Since $Y_{t_k-} = \pi_{\Delta t_k} Y_{t_{k-1}}$, we obtain the following stochastic recurrence equation for $\{Y_{t_k}\}_{k \geqslant 0}$

$$Y_{t_k} = Q^{-1}(Q(Y_{t_{k-1}}) + \varepsilon_k) + e_k, \quad k = 1, 2, \dots,$$

where Q^{-1} is the generalized inverse of Q, $Q^{-1}(r) = \sup\{x : Q(x) \geqslant r\}$. Consequently, Y_t is defined by eq. (8.13) for all $t < t_\infty$, where $t_\infty = \lim_{k \to \infty} t_k$ is the explosion time. As in the discrete state space we can extend the state space E by adding the point -1 and define $Y_t = -1$ for $t \geqslant t_\infty$. Let $\mathbb{P}_x$ be the law of the process Y starting at $Y_0 = x$ and denote by $\mathbb{E}_x$ the expectation with respect to $\mathbb{P}_x$.

Remark 29. *Note that if $Q(0) = \infty$ then the amount of the gene product $\{Y_{t_k}\}_{k \geqslant 0}$ at the jump times is a discrete time Markov process with transition probability function given by*

$$\mathcal{K}(x, B) = \int_B k(x, y) dy, \quad B \in \mathcal{B}((0, \infty)),$$

where

$$k(x, y) = e^{Q(x)} \int_0^x 1_{(0,y)}(z) h(y - z) \frac{\lambda(z)}{\gamma(z)} e^{-Q(z)} dz, \quad x, y > 0. \tag{8.15}$$

We rewrite eq. (8.11) as an abstract Cauchy problem in L^1

$$\frac{du}{dt} = \mathbb{C}u, \quad u(0) = v, \tag{8.16}$$

where the operator

$$\mathbb{C}u(x) = \frac{d(\gamma(x)u(x))}{dx} - \lambda(x)u(x) + \int_0^x \lambda(x - y)u(x - y)h(y) dy$$

is defined on the domain

$$\mathcal{D} = \{u \in L^1 : \gamma u \in \mathrm{AC}, \ (\gamma u)' \in L^1, \ \lim_{x \uparrow \infty}(\gamma(x)u(x)) = 0, \ \lambda u \in L^1\},$$

and $\gamma u \in \mathrm{AC}$ means that the function $x \mapsto \gamma(x)u(x)$ is absolutely continuous. From [90, 145] it follows that there is a substochastic semigroup $\{P(t)\}_{t \geqslant 0}$ on L^1 such that for each initial density $v \in \mathcal{D}$ eq. (8.16) has a nonnegative solution $u(t)$ which is given by $u(t) = P(t)v$ for $t \geqslant 0$ and

$$\int_0^\infty \mathbb{P}_x(Y_t \in B, t < t_\infty)v(x) dx = \int_B P(t)v(x) dx$$

for all Borel subsets B of $(0, \infty)$. The semigroup $\{P(t)\}_{t \geqslant 0}$ is stochastic if the transition operator K on L^1 with kernel k as in eq. (8.15) has a strictly positive fixed point. Let us consider the case of the exponential bursting size

$$h(y) = \frac{1}{b} e^{-y/b}, \quad y > 0, \tag{8.17}$$

where $b > 0$.

Theorem 30. *Assume that condition eq. (8.12) holds and that h is exponential as in eq. (8.17) with $b > 0$. Suppose that*

$$c := \int_0^\infty \frac{1}{\gamma(x)} e^{-x/b - Q(x)} dx < \infty, \quad \int_0^\infty e^{-x/b - Q(x)} dx < \infty. \tag{8.18}$$

Then the semigroup $\{P(t)\}_{t \geqslant 0}$ is stochastic and for each initial density v we have

$$\lim_{t \to \infty} \|P(t)v - u^*\|_1 = 0,$$

where

$$u_*(x) = \frac{1}{c\gamma(x)} e^{-x/b - Q(x)} \tag{8.19}$$

is the unique stationary density of $\{P(t)\}_{t \geqslant 0}$.

Proof. Let k be as in eq. (8.15) and let $v^*(x) = e^{-x/b - Q(x)}$, $x > 0$. The function v^* satisfies

$$v^*(y) = \int_0^\infty v^*(x) k(x, y) dx, \quad y > 0,$$

since for each $y > 0$ we have

$$\int_y^\infty v^*(x) k(x, y) dx = \int_0^y h(y - z) \frac{\lambda(z)}{\gamma(z)} e^{-Q(z)} dz \int_y^\infty e^{-x/b} dx$$

and

$$\int_0^y v^*(x) k(x, y) dx = \int_0^y e^{-x/b} \int_0^x h(y - z) \frac{\lambda(z)}{\gamma(z)} e^{-Q(z)} dz dx,$$

which, by making use of the form of h and changing the order of integration, can be transformed to

$$\int_0^y v^*(x) k(x, y) dx = e^{-y/b} \int_0^y (1 - bh(y - z)) \frac{\lambda(z)}{\gamma(z)} e^{-Q(z)} dz$$

$$= e^{-y/b} e^{-Q(y)} - b e^{-y/b} \int_0^y h(y - z) \frac{\lambda(z)}{\gamma(z)} e^{-Q(z)} dz.$$

By eq. (8.18) the function

$$R_0 v^*(x) := \frac{1}{\gamma(x)} \int_x^\infty e^{Q(y) - Q(x)} v^*(y) dy = b \frac{1}{\gamma(x)} e^{-x/b - Q(x)}$$

is integrable, which implies that $u^* \in \mathcal{D}$ and $\mathbb{C}(u^*) = 0$. The rest of the proof is as in [90]. □

Remark 31. *Note that if $Q(0) = \infty$ and*

$$\lim_{x \to \infty} \frac{\lambda(x)}{\gamma(x)} < \frac{1}{b},$$

then the function $x \mapsto e^{-x/b - Q(x)}$ is integrable on $(0, \infty)$. If, additionally,

$$\limsup_{x \to \infty} \gamma(x) > 0, \quad \lim_{x \to 0} \frac{e^{-Q(x)}}{\gamma(x)^r} < \infty, \quad and \quad \int_0^\delta \gamma(x)^{r-1} dx < \infty$$

for some $\delta, r > 0$, then condition eq. (8.18) holds.

Remark 32. *[Bifurcation] The relation given at eq. (8.19) can be used to derive bifurcation property in terms of number of modes of the steady-state distribution as a function of parameters. The number of extrema are indeed linked to the number of solution of (if this expression has a sense)*

$$\frac{\lambda(x)}{\gamma(x)} = \frac{1}{b} + \frac{\gamma'(x)}{\gamma(x)}$$

The following examples are meant to show that analytical formula may be found for a variety of different jump rate function, all restricted to an exponential jump size distribution, however.

Example 6. *Consider the case of linear regulation with the function λ of the form*

$$\lambda(x) = \lambda_0 + \lambda x,$$

where λ_0, λ are nonnegative constants, and $\gamma(x) = \gamma x$. If

$$\frac{1}{b} > \frac{\lambda}{\gamma} \quad and \quad \lambda_0 > 0,$$

then u_* is integrable and is the gamma distribution

$$u^*(x) = \frac{1}{\Gamma(\lambda_0/\gamma)} \left(\frac{1}{b} - \frac{\lambda}{\gamma}\right)^{\lambda_0/\gamma} x^{\frac{\lambda_0}{\gamma}-1} e^{-(\frac{1}{b}-\frac{\lambda}{\gamma})x},$$

which is a continuous approximation of the negative binomial distribution previously obtained, as in [129].

Example 7. *Let $\gamma(x) = \gamma x^\beta$ with $\gamma > 0$ and $\beta \leqslant 1$. Suppose that $\lambda(x) = \lambda x^\alpha$ with $\lambda > 0$. Then $Q(0) = \infty$ if and only if $\alpha \leqslant \beta - 1$. For $\alpha < \beta - 1$ we have*

$$Q(x) = \frac{\lambda}{\gamma(\beta - 1 - \alpha)} x^{\alpha-\beta+1}.$$

Let $\gamma(x) = \gamma x$ with $\gamma > 0$

Theorem 33. *[90, Theorem 7]. The unique stationary density of eq. (8.11), with λ a measurable bounded function above and under and h an exponential distribution given by eq. (8.17), is*

$$u_*(x) = \frac{\mathcal{C}}{x} e^{-x/b} \exp\left[\frac{1}{\gamma} \int^x \frac{\lambda(y)}{y} dy\right],$$

where $\mathcal{C}$ is a normalizing constant such that $\int_0^\infty u_*(x)dx = 1$. Further, $u(t,x)$ is asymptotically stable.

Remark 34. *Note also that we can also represent u_* as*

$$u_*(x) = \mathcal{C} \exp \int^x \left(\frac{\lambda(y)}{\gamma y} - \frac{1}{b} - \frac{1}{y}\right) dy,$$

where $\mathcal{C}$ is a normalizing constant.

Example 8. *. Consider the function λ of the form*

$$\lambda(x) = \frac{\lambda}{1 + K_1 x^N}$$

where $\lambda, K_1 > 0$. Then

$$Q(x) = \frac{\lambda}{\gamma N} \log(x^{-N} + K_1)$$

and

$$u^*(x) = (c\gamma)^{-1} e^{-x/b} x^{\lambda/\gamma-1} (1 + K_1 x^N)^{-\lambda/(\gamma N)}.$$

Example 9. *Consider the function λ of the form [91]*

$$\lambda(x) = \lambda\frac{1 + x^N}{\Lambda + \Delta x^N} = \frac{\lambda}{\Delta} + \lambda\left(1 - \frac{\Lambda}{\Delta}\right)\frac{1}{\Lambda + \Delta x^N},$$

where λ, Λ, Δ are positive constants and N is a positive integer. Let $\gamma(x) = \gamma x$ with $\gamma > 0$. The stationary density is given by

$$u^*(x) = c^{-1}e^{-x/b}x^{\kappa_b(\Lambda)^{-1}-1}(\Lambda + \Delta x^N)^\theta, \tag{8.20}$$

where c is a normalizing constant and

$$\kappa_b = \frac{\lambda}{\gamma}$$

$$\theta = \frac{\kappa_b}{N\Delta}\left(1 - \frac{\Delta}{\Lambda}\right).$$

    The solution on the last example has been extensively studied in terms of numbers of modes (P-bifurcation) in [91], which we reproduce below. We will constantly make the analogy with the deterministic bifurcation study in section 6.

    The first two terms of eq. (8.20) are simply proportional to the density of the gamma distribution. For $0 < \kappa_b\Lambda^{-1} < 1$ we have $u_*(0) = \infty$ while for $\kappa_b\Lambda^{-1} > 1$, $u_*(0) = 0$ and there is at least one mode at a value of $x > 0$. We have $u_*(x) > 0$ for all $x > 0$ and from remark 34 it follows that

$$u'_*(x) = u_*(x)\left(\frac{\kappa_b\lambda(x)}{x} - \frac{1}{b} - \frac{1}{x}\right), \quad x > 0. \tag{8.21}$$

Observe that if $\kappa_b \leqslant 1$ then u_* is a monotone decreasing function of x, since $\kappa_b f(x) \leqslant 1$ for all $x > 0$. Thus we assume in what follows that $\kappa_b > 1$.

    Since the analysis of the qualitative nature of the stationary density leads to different conclusions for the uncontrolled, inducible or repressible operon cases, we consider each in turn.

8.2.0.1   Protein distribution in the absence of control   When $\Delta = \Lambda = 1$, the density u^* is that of a gamma distribution, as obtained in [39].

$$u_*(x) = \frac{1}{b^{\kappa_b}\Gamma(\kappa_b)}x^{\kappa_b-1}e^{-x/b},$$

where $\Gamma(\cdot)$ denotes the gamma function and $\kappa_b = \frac{\lambda}{\gamma}$. For $\kappa_b \in (0, 1)$, $u_*(0) = \infty$ and u_* is decreasing while for $\kappa_b > 1$, $u_*(0) = 0$ and there is a mode at $x = b(\kappa_b - 1)$.

8.2.0.2   Bursting in the inducible operon   When $\Delta = 1$ and $\Lambda > 1$, we have $\theta > 0$ and the third term of eq. (8.20) is a monotone increasing function of x and, consequently, there is the possibility that u_* may have more than one mode, indicative of the existence of bistable behavior. From eq. (8.21) it follows that we have $u'_*(x) = 0$ for $x > 0$ if and only if

$$\frac{1}{\kappa_b}\left(\frac{x}{b} + 1\right) = \frac{1 + x^n}{\Lambda + x^n}. \tag{8.22}$$

Again, graphical arguments (see figure 1.9) show that there may be up to three roots of eq. (8.22). For illustrative values of n, Λ, and b, figure 1.10 shows the graph of the values of x at which $u'_*(x) = 0$ as a function of κ_b. When there are three roots of eq. 8.22, we label them as $\tilde{x}_1 < \tilde{x}_2 < \tilde{x}_3$.
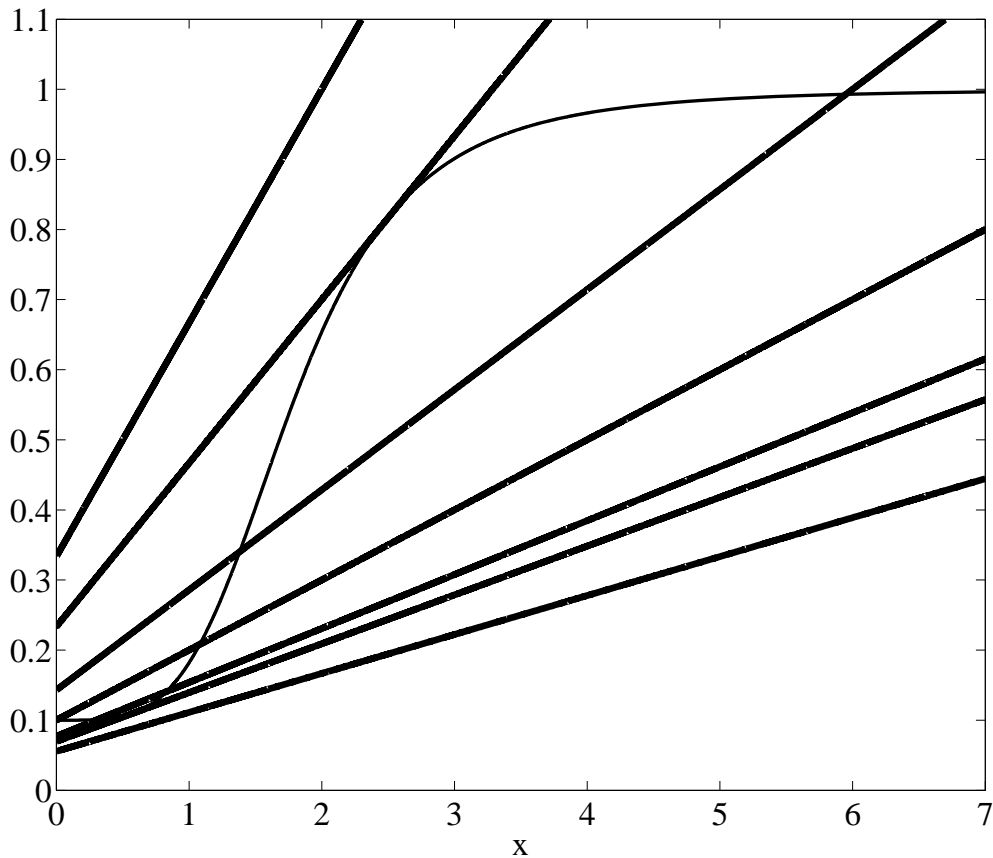
Figure 1.9: Schematic illustration of the possibility of one, two or three solutions of eq. (8.22) for varying values of κ_b with bursting inducible regulation. The straight lines correspond (in a clockwise direction) to $\kappa_b \in (0, \kappa_{b-})$, $\kappa_b = \kappa_{b-}$, $\kappa_b \in (\kappa_{b-}, \kappa_{b+})$ (and respectively $\kappa_b < \Lambda$, $\kappa_b = \Lambda$, $\Lambda < \kappa_b$), $\kappa_b = \kappa_{b+}$, and $\kappa_{b+} < \kappa_b$. This figure was constructed with $n = 4$, $\Lambda = 10$ and $b = 1$ for which $\kappa_{b-} = 4.29$ and $\kappa_{b+} = 14.35$ as computed from eq. (8.25). See the text for further details

Generally we cannot determine when there are three roots. However, we can determine when there are only two roots $\tilde{x}_1 < \tilde{x}_3$ from the argument of subsection 6.2. At $\tilde{x}_1$ and $\tilde{x}_3$ we will not only have eq. (8.22) satisfied but the graph of the right hand side of eq. (8.22) will be tangent to the graph of the left hand side at one of them so the slopes will be equal. Differentiation of eq. (8.22) yields the second condition

$$n\frac{x^{n-1}}{(\Lambda + x^n)^2} = \frac{1}{\kappa_b b(\Lambda - 1)} \tag{8.23}$$

We first show that there is an open set of parameters (b, Λ, κ_b) for which the stationary density u_* is bimodal. From eq. (8.22) and (8.23) it follows that the value of $x_\pm$ at which tangency will occur is given by

$$x_\pm = b(\kappa_b - 1)z_\pm$$

and $z_\pm$ are positive solutions of equation

$$\frac{z}{n} = 1 - z - \beta(1-z)^2, \quad \text{where} \quad \beta = \frac{\Lambda(\kappa_b - 1)}{(\Lambda - 1)\kappa_b}.$$

We explicitly have

$$z_\pm = \frac{1}{2\beta n}\left(2\beta n - (n+1) \pm \sqrt{(n+1)^2 - 4\beta n}\right)$$

provided that

$$\frac{(n+1)^2}{4n} \geqslant \beta = \frac{\Lambda(\kappa_b - 1)}{(\Lambda - 1)\kappa_b}. \tag{8.24}$$

The eq. (8.24) is always satisfied when $\kappa_b < \Lambda$ or when $\kappa_b > \Lambda$ and Λ is as in the deterministic case, eq. (6.8). Observe also that we have $z_+ > 0 > z_-$ for $\kappa_b < \Lambda$ and $z_+ > z_- > 0$ for $\kappa_b > \Lambda$. The two corresponding values of b at which a tangency occurs are given by

$$b_\pm = \frac{1}{(\kappa_b - 1)z_\pm}\sqrt[n]{\frac{\Lambda}{\beta(1 - z_\pm)} - \Lambda} \quad \text{and} \quad z_\pm > 0.$$

If $\kappa_b < \Lambda$ then $u_*(0) = \infty$ and u_* is decreasing for $b \leqslant b_+$, while for $b > b_+$ there is a local maximum at $x > 0$. If $\kappa_b > \Lambda$ then $u_*(0) = 0$ and u_* has one or two local maxima. As a consequence, for $n > 1$ we have a bimodal steady state density u_* if and only if the parameters κ_b and Λ satisfy eq. (8.24), $\kappa_b > \Lambda$, and $b \in (b_+, b_-)$.

We now want to find the analogy between the bistable behavior in the deterministic system and the existence of bimodal stationary density u_*. To this end we fix the parameters $b > 0$ and $\Lambda > 1$ and vary κ_b as in figure 1.9. The eq. (8.22) and (8.23) can also be combined to give an implicit equation for the value of $x_\pm$ at which tangency will occur

$$x^{2n} - (\Lambda - 1)\left[n - \frac{\Lambda + 1}{\Lambda - 1}\right]x^n - nb(\Lambda - 1)x^{n-1} + \Lambda = 0$$

and the corresponding values of $\kappa_{b\pm}$ are given by

$$\kappa_{b\pm} = \left(\frac{x_\mp + b}{b}\right)\left(\frac{\Lambda + x_\mp^n}{1 + x_\mp^n}\right). \tag{8.25}$$

There are two cases to distinguish.
Case 1. $0 < \kappa_b < \Lambda$. In this case, $u_*(0) = \infty$. Further, the same graphical considerations as in the deterministic case show that there can be none, one, or two positive solutions
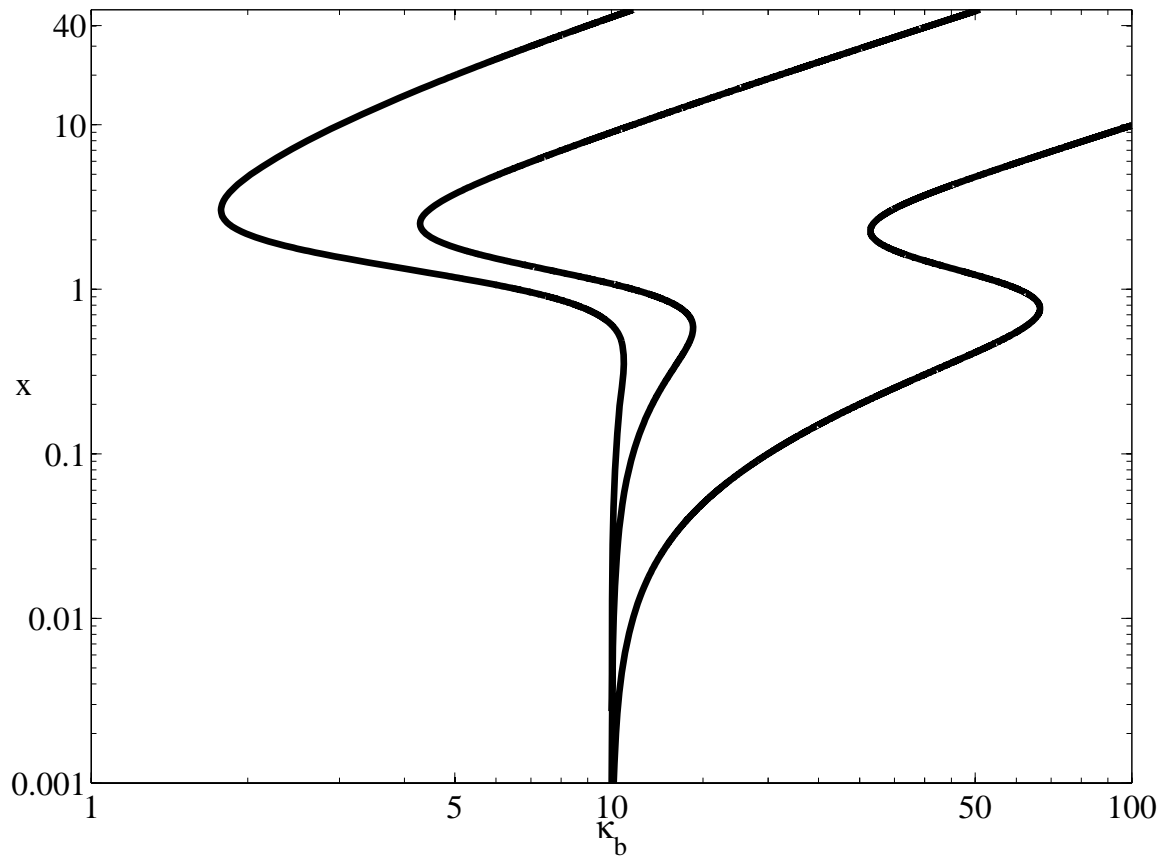
Figure 1.10: Full logarithmic plot of the values of x at which $u'_*(x) = 0$ versus the parameter κ_b, obtained from eq. (8.22), for $n = 4$, $\Lambda = 10$, and (left to right) $b = 5, 1$ and $b = \frac{1}{10}$. Though somewhat obscured by the logarithmic scale for x, the graphs always intersect the κ_b axis at $\kappa_b = \Lambda$. Additionally, it is important to note that $u'_*(0) = 0$ for $\Lambda < \kappa_b$, and that there is always a maximum at 0 for $0 < \kappa_b < \Lambda$. See the text for further details.

to eq. (8.22). If $\kappa_b < \kappa_{b-}$, there are no positive solutions, u_* is a monotone decreasing function of x. If $\kappa_b > \kappa_{b-}$, there are two positive solutions ($\tilde{x}_2$ and $\tilde{x}_3$ in our previous notation, $\tilde{x}_1$ has become negative and not of importance) and there will be a mode in u_* at $\tilde{x}_3$ with a minimum in u_* at $\tilde{x}_2$.

Case 2. $0 < \Lambda < \kappa_b$. Now, $u_*(0) = 0$ and there may be one, two, or three positive roots of eq. (8.22). We are interested in knowing when there are three which we label as $\tilde{x}_1 < \tilde{x}_2 < \tilde{x}_3$ as $\tilde{x}_1, \tilde{x}_3$ will correspond to the location of mode in u_* while $\tilde{x}_2$ will be the location of the minimum between them and the condition for the existence of three roots is $\kappa_{b-} < \kappa_b < \kappa_{b+}$.

   We see then that the different possibilities depend on the respective values of Λ, κ_{b-}, κ_{b+}, and κ_b. To summarize, we may characterize the stationary density u_* for an inducible operon in the following way:

1. **Unimodal type 1**: $u_*(0) = \infty$ and u_* is decreasing for $0 < \kappa_b < \kappa_{b-}$ and $0 < \kappa_b < \Lambda$

2. **Unimodal type 2**: $u_*(0) = 0$ and u_* has a single mode at

   (a) $\tilde{x}_1 > 0$ for $\Lambda < \kappa_b < \kappa_{b-}$ or

   (b) at $\tilde{x}_3 > 0$ for $\kappa_{b+} < \kappa_b$ and $\Lambda < \kappa_b$

3. **Bimodal type 1**: $u_*(0) = \infty$ and u_* has a single mode at $\tilde{x}_3 > 0$ for $\kappa_{b-} < \kappa_b < \Lambda$

4. **Bimodal type 2**: $u_*(0) = 0$ and u_* has two modes at $\tilde{x}_1, \tilde{x}_3$, $0 < \tilde{x}_1 < \tilde{x}_3$ for $\kappa_{b-} < \kappa_b < \kappa_{b+}$ and $\Lambda < \kappa_b$

Remark 35. *Two comments are in order.*

1. *Remember that the case $n = 1$ cannot display bistability in the deterministic case. However, in the case of bursting in the inducible system when $n = 1$, if $\frac{\Lambda}{b} + 1 < \kappa_b < \Lambda$ and $b > \frac{\Lambda}{\Lambda - 1}$, then $u_*(0) = \infty$ and u_* also has a mode at $\tilde{x}_3 > 0$. Thus in this case one can have a bimodal type 1 stationary density.*

2. *Lipshtat et al. [88], in a numerical study of a mutually inhibitory gene arrangement (which is dynamically equivalent to an inducible operon), provided numerical evidence that bistability was possible without cooperative binding (i.e. $n = 1$). The demonstration here of bistability gives analytic support to their conclusion.*

   We now choose to see how the average burst size b affects bistability in the density u_* by looking at the parametric plot of $\kappa_b(x)$ versus $\Lambda(x)$. Define

$$F(x, b) = \frac{x^n + 1}{nx^{n-1}(x + b)}. \tag{8.26}$$

Then

$$\Lambda(x, b) = \frac{1 + x^n F(x, b)}{1 - F(x, b)} \quad \text{and} \quad \kappa_b(x, b) = [\Lambda(x, b) + x^n]\frac{x + b}{b(x^n + 1)}. \tag{8.27}$$

The bifurcation diagram obtained from a parametric plot of Λ versus κ_b (with x as the parameter) is illustrated in figure 1.11 for $n = 4$ and two values of b. Note that it is necessary for $0 < \Lambda < \kappa_b$ in order to obtain Bimodal type 2 behavior.

   For bursting behavior in an inducible situation, there are two different bifurcation patterns that are possible. The two different cases are delineated by the respective values of Λ and κ_b, as shown in figure 1.10 and figure 1.11. Both bifurcation scenarios share the property that while increasing the bifurcation parameter κ_b from 0 to ∞, the stationary density u_* passes from a unimodal density with a peak at a low value (either 0 or $\tilde{x}_1$) to a bimodal density and then back to a unimodal density with a peak at a high value ($\tilde{x}_3$).
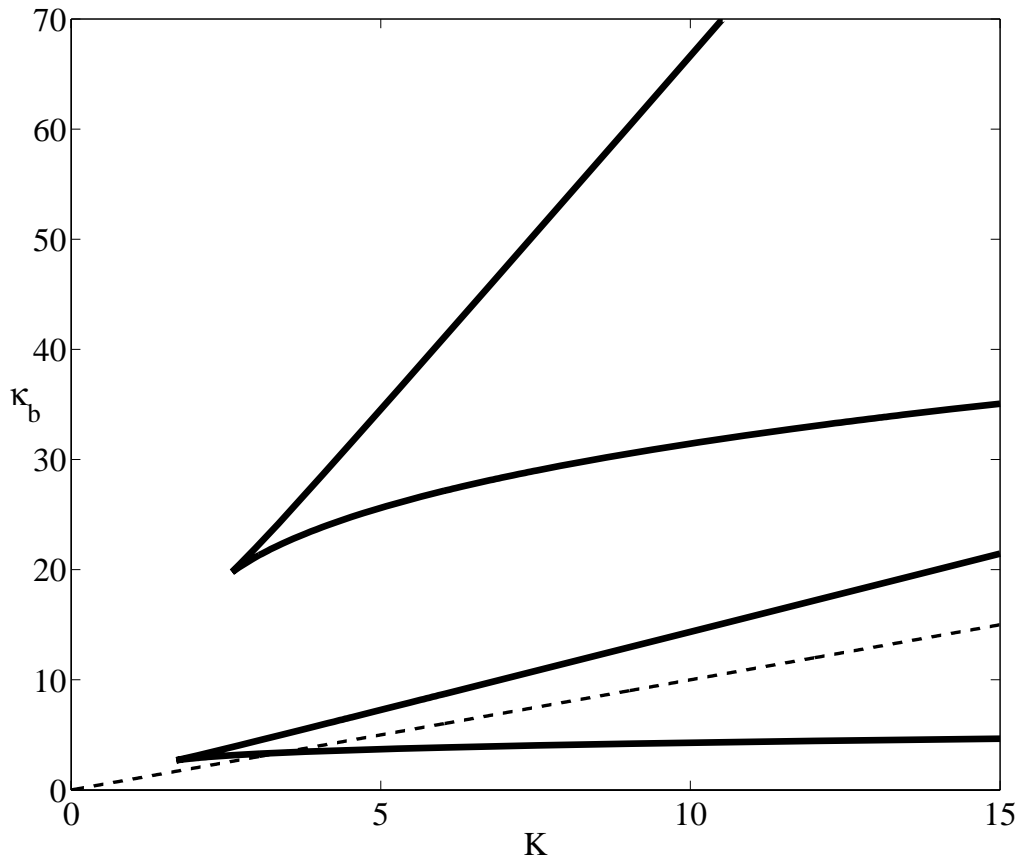
Figure 1.11: In this figure we present two bifurcation diagrams (for $n = 4$) in (Λ, κ_b) parameter space delineating unimodal from bimodal stationary densities u_* in an inducible operon with bursting as obtained from eq. (8.27) and (8.26). The upper cone-shaped plot is for $b = \frac{1}{10}$ while the bottom one is for $b = 1$. In both cone shaped regions, for any situation in which the lower branch is above the line $\kappa_b = \Lambda$ (lower straight line) then bimodal behavior in the stationary solution $u_*(x)$ will be observed with modes in u_* at positive values of x, $\tilde{x}_1$ and $\tilde{x}_3$.
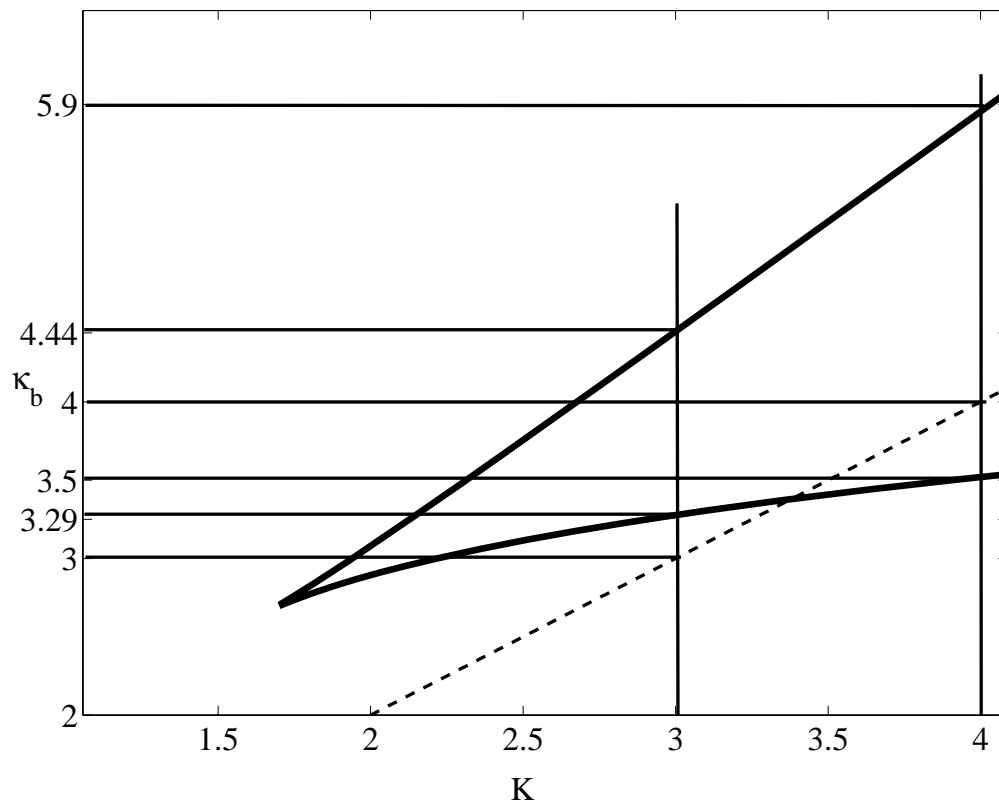
Figure 1.12: This figure presents an enlarged portion of figure 1.11 for $b = 1$. The various horizontal lines mark specific values of κ_b referred to in figures 1.13 and 1.14.
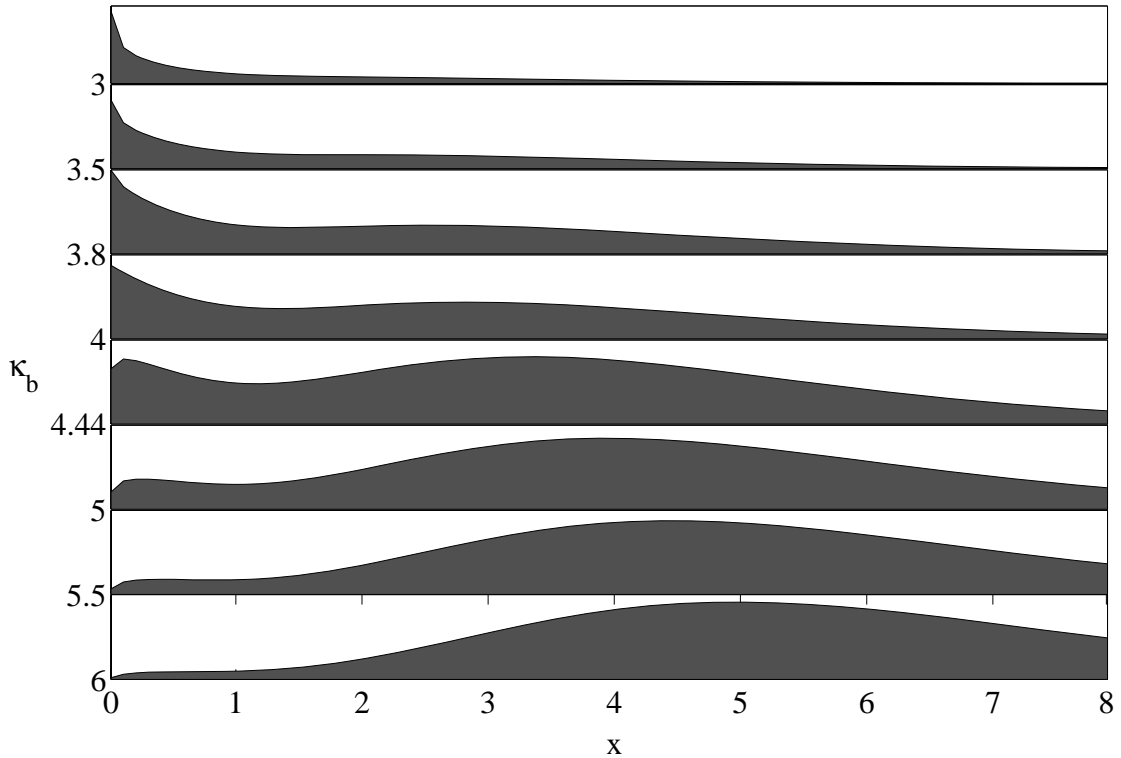
Figure 1.13: In this figure we illustrate **Bifurcation type 1** when intrinsic bursting is present. For a variety of values of the bifurcation parameter κ_b (between 3 and 6 from top to down), the stationary density u_* is plotted versus x between 0 and 8. The values of the parameters used in this figure are $b = 1$, $\Lambda = 4$, and $n = 4$. For $\kappa_b \lesssim 3.5$, u_* has a single mode at $x = 0$. For $3.5 \lesssim \kappa_b < 4$, u_* has two local maxima at $x = 0$ and $\tilde{x}_3 > 1$. For $4 < \kappa_b \lesssim 5.9$, u_* has two local maxima at $0 < \tilde{x}_1 < \tilde{x}_3$. Finally, for $\kappa_b \gtrsim 5.9$, u_* has a single mode at $\tilde{x}_3 > 1$. Note that for each plot of the density, the scale of the ordinate is arbitrary to improve the visualization.

In what will be referred as **Bifurcation type 1**, the maximum at $x = 0$ disappears when there is a second peak at $x = \tilde{x}_3$. The sequence of densities encountered for increasing values of κ_b is then: Unimodal type 1 to a Bimodal type 1 to a Bimodal type 2 and finally to a Unimodal type 2 density.

In the **Bifurcation type 2** situation, the sequence of density types for increasing values of κ_b is: Unimodal type 1 to a Unimodal type 2 and then a Bimodal type 2 ending in a Unimodal type 2 density.

The two different kinds of bifurcation that can occur are easily illustrated for $b = 1$ as the parameter κ_b is increased. An enlarged diagram in the region of interest is shown in figure 1.12. In figure 1.13 we illustrate **Bifurcation type 1**, when $\Lambda = 4$, and κ_b increases from low to high values. As κ_b increases, we pass from a Unimodal type 1 density, to a Bimodal type 1 density. Further increases in κ_b lead to a Bimodal type 2 density and finally to a Unimodal type 2 density. This bifurcation cannot occur, for example, when $b = \frac{1}{10}$ and $\Lambda \leqslant 15$ (see figure 1.11).

In figure 1.14 we show a **Bifurcation type 2**, when $\Lambda = 3$. As κ_b increases, we pass from a Unimodal type 1 density, to a Unimodal type 2 density. Then with further increases in κ_b, we pass to a Bimodal type 2 density and finally back to a Unimodal type 2 density.

Remark 36. *There are several qualitative conclusions to be drawn from the analysis of*
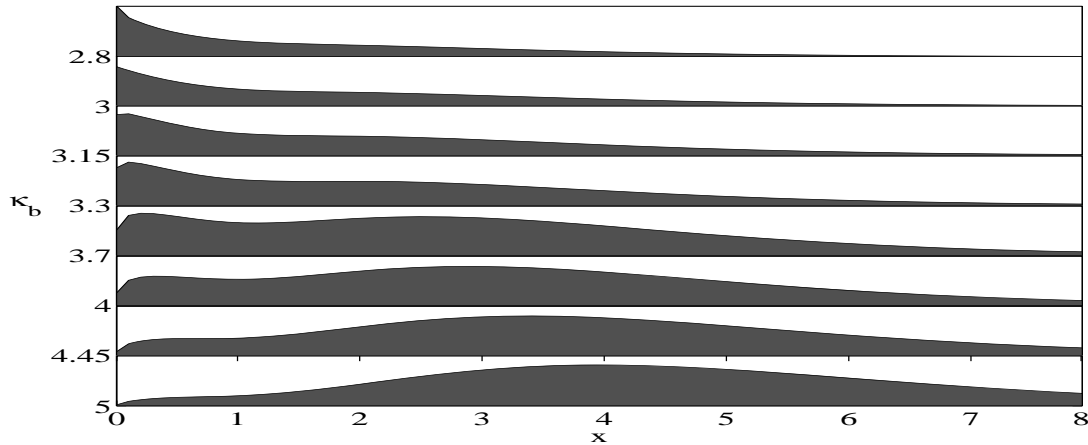
Figure 1.14: An illustration of **Bifurcation type 2** for intrinsic bursting. For several values of the bifurcation parameter κ_b (between 2.8 and 5 from top to down), the stationary density u_* is plotted versus x between 0 and 8. The parameters used are $b = 1$, $\Lambda = 3$, and $n = 4$. For $\kappa_b < 3$, u_* has a single mode at $x = 0$, and for $3 < \kappa_b \lesssim 3.3$, u_* has a single mode at $\tilde{x}_1 > 0$. For $3.3 \lesssim \kappa_b \lesssim 4.45$, u_* has two local maxima at $0 < \tilde{x}_1 < \tilde{x}_3$, and finally for $\kappa_b \gtrsim 4.45$ u_* has a single mode at $\tilde{x}_3 > 0$. Note that for each plot of the density, the scale of the ordinate is arbitrary to improve the visualization.

this section.

1. *The presence of bursting can drastically alter the regions of parameter space in which bistability can occur relative to the deterministic case. In figure 1.15 we present the regions of bistability in the presence of bursting in the $(\Lambda, b \cdot \kappa_b)$ parameter space, which should be compared to the region of bistability in the deterministic case in the (Λ, κ_d) parameter space ($b\kappa_b$ is the mean number of proteins produced per unit of time, as is κ_d).*

2. *When $0 < \kappa_b < \Lambda$, at a fixed value of κ_b, increasing the average burst size b can lead to a bifurcation from Unimodal type 1 to Bimodal type 1.*

3. *When $0 < \Lambda < \kappa_b$, at a fixed value of κ_b, increasing b can lead to a bifurcation from Unimodal type 2 to Bimodal type 2 and then back to Unimodal type 2.*

8.2.0.3   Bursting in the repressible operon   The possible behaviors in the stationary density u_* for the repressible operon are easy to delineate based on the analysis of the previous section, with eq. (8.22) replaced by

$$\frac{1}{\kappa_b}\left(\frac{x}{b} + 1\right) = \frac{1 + x^n}{1 + \Delta x^n}. \tag{8.28}$$

Again graphical arguments (see figure 1.16) show that eq. (8.28) may have either none or one solution. Namely,

1. For $0 < \kappa_b < 1$, $u_*(0) = \infty$ and u_* is decreasing. Eq. 8.28 does not have any solution (Unimodal type 1).

2. For $1 < \kappa_b$, $u_*(0) = 0$ and u_* has a single mode at a value of $x > 0$ determined by the single positive solution of eq. (8.28) (Unimodal type 2).
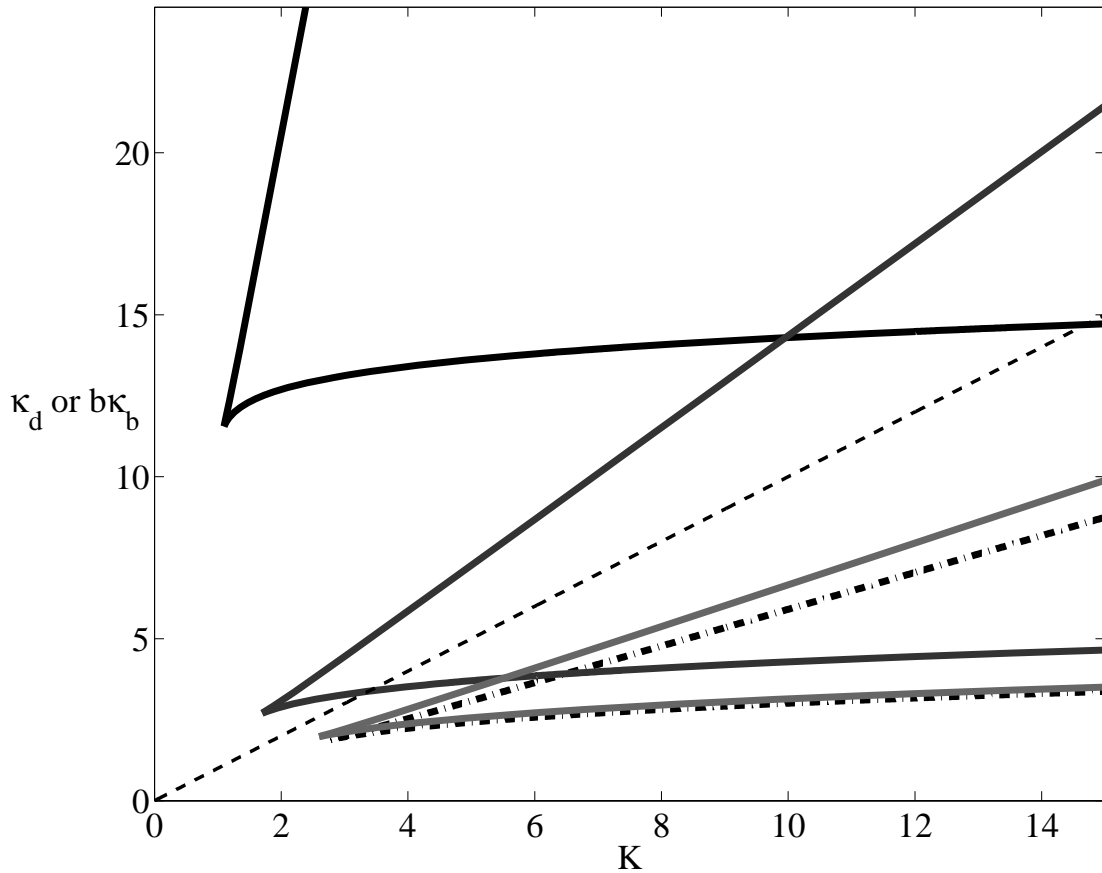
Figure 1.15: The presence of bursting can drastically alter regions of bimodal behavior as shown in this parametric plot (for $n = 4$) of the boundary in $(K, b \cdot \kappa_b)$ parameter space delineating unimodal from bimodal stationary densities u_* in an inducible operon with bursting and in (K, κ_d) parameter space delineating one from three steady states in the deterministic inducible operon. From top to bottom, the regions are for $b = 10$, $b = 1$, $b = 0.1$ and $b = 0.01$. The lowest (heavy dashed line) is for the deterministic case. Note that for $b = 0.01$, the two regions of bistability and bimodality coincide and are indistinguishable from one another.

8.2.0.4 Recovering the deterministic case

We can recover the deterministic behavior from the bursting dynamics with a suitable scaling of the parameters and limiting procedure. With bursting production there are two important parameters (the frequency κ_b and the amplitude b), while with deterministic production there is only κ_d. The natural limit to consider is when

$$b \to 0, \quad \kappa_b \to \infty \quad \text{with} \quad b\kappa_b \equiv \kappa_d.$$

In this limit, the implicit equations which define the maximum points of the steady state density, become the implicit eq. (6.4) and (6.5) which define the stable steady states in the deterministic case.

The bifurcations will also take place at the same points, because we recover eq. (6.7) in the limit. However, Bimodality type 1 as well as the Unimodal type 1 behaviors will no longer be present, as in the deterministic case, because for $\kappa_b \to \infty$ we have $\kappa_b > \Lambda$. Finally, from the analytical expression for the steady-state density, eq. (8.20), u_* will
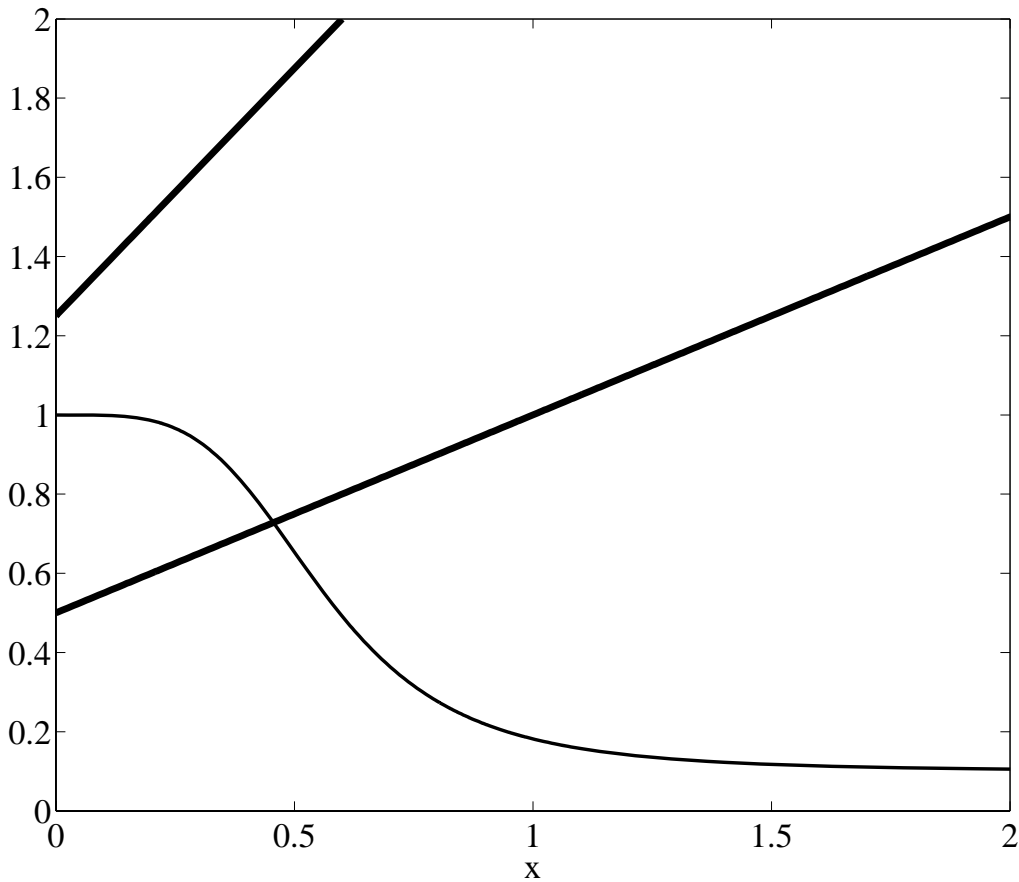
Figure 1.16: Schematic illustration that there can be one or no solution of eq. (8.28),depending on the value of κ_b, with repressible regulation. The straight lines correspond (in a clockwise direction) to $\kappa_b = 2$ and $\kappa_b = 0.8$. This figure was constructed with $n = 4$, $\Delta = 10$ and $b = 1$. See the text for further details.

became more sharply peaked as $b \to 0$. Due to the normalization constant (which depends on b and κ_b), the mass will be more concentrated around the larger maximum of u_*.

8.3 Fluctuations in the degradation rate only

We now look at a model analog to the one studied in section 8.2, but where the noise is included in the degradation rate rather than in the production rate. Such model can be justified in some sense by a limiting procedure. We then look at the stochastic differential equation in the form

$$dx = \gamma[\kappa_d \lambda(x) - x]dt + \sigma\sqrt{x}dw.$$

Within the Ito interpretation of stochastic integration, this equation has a corresponding Fokker Planck equation for the evolution of the ensemble density $u(t,x)$ given by [84]

$$\frac{\partial u}{\partial t} = -\frac{\partial \left[(\gamma\kappa_d \lambda(x) - \gamma x)u\right]}{\partial x} + \frac{\sigma^2}{2}\frac{\partial^2(xu)}{\partial x^2}. \tag{8.29}$$

As by hypothesis $\lambda(0) > 0$, it is natural to consider the boundary at $x = 0$ reflecting and the stationary solution of eq. (8.29) is then given by

$$u_*(x) = \frac{\mathcal{C}}{x}e^{-2\gamma x/\sigma^2}\exp\left[\frac{2\gamma\kappa_d}{\sigma^2}\int^x \frac{\lambda(y)}{y}dy\right].$$

Set $\kappa_e = 2\gamma\kappa_d/\sigma^2$, and take

$$\lambda(x) = \lambda\frac{1 + x^N}{\Lambda + \Delta x^N}$$

Then the steady state solution is given explicitly by

$$u_*(x) = \mathcal{C}e^{-2\gamma x/\sigma^2} x^{\kappa_e \Lambda^{-1} - 1}[\Lambda + \Delta x^n]^\theta, \qquad (8.30)$$

where $\Lambda, \Delta \geqslant 0$ and θ are given in table 1.1. Note that this density has the same expression as eq. (8.20)

Remark 37. *Two comments are in order.*

1. *Because the form of the solutions for the situation with bursting and Gaussian white noise are identical, all of the results of the previous section can be carried over here with the proviso that one replaces the average burst amplitude b with $b \to \sigma^2/2\gamma \equiv b_w$ and $\kappa_b \to \kappa_e = 2\gamma\kappa_d/\sigma^2 \equiv \kappa_d/b_w$.*

2. *We can look for the regions of bimodality in the (K, κ_d)-plane, for a fixed value of b_w. We have the implicit equation for $x_\pm$*

$$x^{2n} - (K - 1)\left[n - \frac{K + 1}{K - 1}\right]x^n - nb_w(K - 1)x^{n-1} + K = 0$$

and the corresponding values of κ_d are given by

$$\kappa_{d\pm} = (x_\mp + b_w)\left(\frac{K + x_\mp^n}{1 + x_\mp^n}\right).$$

Then the bimodality region in the (K, κ_d)-plane with noise in the degradation rate is the same as the bimodality region for bursting in the $(K, b\kappa_b)$-plane.

We have also the following result.

Theorem 38. *[106, Theorem 2]. The unique stationary density of eq. (8.29) is given by eq. (8.30). Further $u(t, x)$ is asymptotically stable.*

8.4 Discussion

In trying to understand experimentally observed distributions of intracellular components from a modeling perspective, the norm in computational and systems biology is often to use algorithms developed initially by Gillespie [45] to solve the chemical master equation for specific situations. See [87] for a typical example. However these investigations demand long computer runs, are computationally expensive, and further offer little insight into the possible diversity of behaviors that different gene regulatory networks are capable of.

There have been notable exceptions in which the problem has been treated from an analytical point of view, c.f. [77], [39], [13], and [129]. The advantage of an analytic development is that one can determine how different elements of the dynamics shape temporal and steady state results for the densities $u(t, x)$ and $u_*(x)$ respectively.

Here we have extended this analytic treatment to simple situations in which there is bursting transcription and/or translation (building on and expanding the original work of [39]), (for the fluctuations in degradation rates case, see subsection 8.3), as an alternative to the Gillespie [45] algorithm approach. The advantage of the analytic approach that we have taken is that it is possible, in some circumstances, to give precise conditions on the statistical stability of various dynamics. Even when analytic solutions are not available

for the partial integro-differential equations governing the density evolution, the numerical solution of these equations may be computationally more tractable than using the Gillespie [45] approach.

The results we have reported here in section 8.2 concern convergence towards a stationary density for a continuous model in the presence of bursting noise. The source noise considered is then in the production term, and was modeled as a compound Poisson process. We have focused on qualitative properties of the stationary density, in particular the number of modes. In subsection 8.3, we have studied a continuous stochastic model where the source noise is in the degradation term, and has been modeled as multiplicative Gaussian white noise. We have focused on convergence towards steady-state, as well as qualitative properties of the stationary density. A surprising result of the work reported here is that the stationary densities in the presence of bursting noise are analytically indistinguishable from those in the presence of degradation noise. We had expected that there would be clear differences that would offer some guidance for the interpretation of experimental data to determine whether one or the other source of noise was of predominant importance. Of course, the next obvious step is to examine the problem in the presence of both noise sources simultaneously.

In terms of the issue of when bistability, or a unimodal versus bimodal stationary density is to be expected, we have pointed out the analogy between the bistable behavior in the deterministic system and the existence of bimodal stationary densities in the stochastic systems. Our analysis makes clear the critical role of the dimensionless parameters n, κ (be it κ_d, κ_b), b, and the fractional leakage Λ^{-1}. The relations between these defining the various possible behaviors are subtle, and we have given these in the relevant sections of our analysis.

The appearance of both unimodal and bimodal distributions of molecular constituents as well as what we have termed Bifurcation Type 1 and Bifurcation Type 2 have been extensively discussed in the applied mathematics literature (c.f. [64], [37] and others) and the bare foundations of a stochastic bifurcation theory have been laid down by [5]. Significantly, these are also well documented in the experimental literature as has been shown by many authors [43, 2, 39, 59, 151, 94, 134] for both prokaryotes and eukaryotes. If the biochemical details of a particular system are sufficiently well characterized from a quantitative point of view so that relevant parameters can be estimated, it may be possible to discriminate between whether these behaviors are due to the presence of bursting transcription/translation or extrinsic noise.

8.5   Ergodicity and explicit convergence rate

In this subsection, we want to obtain an explicit convergent rate towards the asymptotic distribution. Such rate may be used experimentally to determine if the observations are at steady-state or not. We will use here probabilistic arguments. We will first present a result that shows exponential ergodicity using a classical Lyapounov criterion argument. Then, we give an explicit lower bound for the convergent rate using a coupling strategy.

Here we use the semigroup defined on bounded continuous function. The semigroup associated to the BC1 model (see subsection 8.2) has for strong generator

$$\mathcal{A}f(x) = -\gamma x f'(x) + \lambda(x) \int_x^\infty (f(y) - f(x))h(y-x)dy, \tag{8.31}$$

where we have assumed, for simplicity, that $\gamma(x) = \gamma x$ is a linear function. Using Lyapounov criteria for stability of Markov processes (for an introduction of this field, see subsection 6.3), it is easy to see that under reasonable assumption such process is exponentially ergodic. Specifically, we have the

Proposition 39. *Suppose* $x \mapsto \lambda(x)$ *is continuous on* $[0, \infty)$, $\lambda(0) > 0$, $\gamma(x) = \gamma x$, $\int_a^b h(dy) > 0$ *for all* $a < b$ *and that*

$$\lim_{x \to \infty} \frac{\lambda(x)\mathbb{E}[h]}{\gamma x} < 1, \tag{8.32}$$

then it exists $\beta < 1$, $B < \infty$ *and* π *(invariant measure) such that*

$$\|P(t, x, \cdot) - \pi\|_V \leqslant BV(x)\beta^t, \quad x \in E, \quad t > 0,$$

where $\|\mu\|_f = \sup_{|g| \leqslant f} |\mu(g)|$ *and* $V(x) = x + 1$.

$$\|P(t, x, \cdot) - \pi\|_V \leqslant BV(x)\beta^t, \quad x \in E, \quad t > 0,$$

où $\|\mu\|_f = \sup_{|g| \leqslant f} |\mu(g)|$.

Proof. We are going to use the criterion given by [97, thm 6.1] (see part 0, subsection 6.3, proposition 14). We first show that every compacts set are petite, and then exhibits a Lyapounov function that satisfy the drift condition. To show that all compact sets are petite, we show that the stochastic process is a T-process, and use [97, prop 4.1] (see part 0, subsection 6.3, proposition 9).

We first show that the bursting process $(X_t)_{t \geqslant 0}$ is a T-process. Starting at $x > 0$ at time $t = 0$, the transition function satisfies, at time $t = 1$, for any set $B \in \mathbb{B}(\mathbb{R})$,

$$P(1, x, B) \geqslant \mathbb{P}\{X_1 \in B, T_1 > 1\} \tag{8.33}$$

where T_1 is the first instant time. Now, conditioning by the fact that $T_1 > 1$, we have

$$\lambda(X_t) \leqslant \max_{y \in [xe^{-\gamma}, x]} \lambda(y). \tag{8.34}$$

Hence, we deduce

$$P(1, x, B) \geqslant e^{-\overline{\lambda}_x} \delta_{xe^{-\gamma}}(B) =: T(x, B) \tag{8.35}$$

where $\overline{\lambda}_x = \max_{y \in [xe^{-\gamma}, x]} \lambda(y)$. By definition, X is then a T-process (with $a = \delta_1$).

Finally, let us exhibits a Lyapounov function that satisfy the drift condition. Take $V(x) = x + 1$ in (8.31), we have

$$\mathcal{A}V(x) = -\gamma x + \lambda(x)\mathbb{E}[h] \leqslant -\gamma\Big(1 - \frac{\lambda(x)\mathbb{E}[h]}{\gamma V(x)}\Big)V(x) + \gamma,$$

so that due to condition (8.32), V is a Lyapounov function.   □

The above criterion states that the stochastic process generated by eq. (8.31) is exponentially ergodic, with more general condition in h (but with $\gamma(x) = \gamma x$ linear) than in subsection 8.2. However the convergent rate is still not explicit. For that, we are going to use a coupling technique and get an explicit convergence rate in Wasserstein distance. Let us remark that if we take $f(x) = x^p$ in eq. (8.31), we get

$$\mathcal{A}x^p = -\gamma p x^p + \lambda(x)\Big[\int_0^\infty (x + y)^p h(y)dy - x^p\Big]$$

Then if $\lambda(x) \leqslant \lambda_0 + \lambda_1 x$, we have, for $p = 1$,

$$\mathcal{A}x \leqslant \lambda_0 \mathbb{E}[h] - (\gamma - \lambda_1 \mathbb{E}[h])x$$

so that the first moment is exponentially convergent with speed $(\gamma - \lambda_1 \mathbb{E}[h])$ as soon as $\gamma > \lambda_1 \mathbb{E}[h]$. All p-moment are similarly exponentially convergent if h has finite p-moment. Now if $\lambda_0 = 0$, the first moment is exponentially convergent towards 0. This suggest that the difference between two stochastic processes generated by eq. (8.31), with a well-chosen coupling, goes to 0 exponentially fast with an explicit speed. The p-Wasserstein distance is defined by

$$W_p(\mu_1, \mu_2) = \inf_{(X,Y) \in Marg(\mu_1,\mu_2)} \mathbb{E}(\mid X - Y \mid^p)^{1/p},$$

We can then prove the

Theorem 40. *Suppose λ is globally Lipschitz with Lipschitz constant Λ. If $\frac{\Lambda}{\gamma} < \mathbb{E}[h]$, then for any μ, ν, we have*

$$W_1(\mu P_t, \nu P_t) \leqslant e^{-(\gamma - \Lambda \mathbb{E}[h])t} W_1(\mu, \nu).$$

Proof. We follow similar ideas as [7]. For any x,y, we define X_t^x and Y_t^y the stochastic processes that starts at x and y and whose coupling generator is defined by

$$\begin{aligned}
Lf(x,y) = & \ (-\gamma x \partial_x f(x,y) - \gamma y \partial_y f(x,y)) \\
& + \min(\lambda(x), \lambda(y)) \Big(\int_0^\infty (f(x+z, y+z) - f(x,y)) h(z) dz \Big) \\
+ \mid \lambda(x) - \lambda(y) \mid & \ \Big[\int_0^\infty (f(x+z, y) \mathbf{1}_{\{\lambda(x) > \lambda(y)\}} + f(x, y+z) \mathbf{1}_{\{\lambda(y) > \lambda(x)\}}) h(z) dz - f(x,y) \Big],
\end{aligned}$$
$$(8.36)$$

that is, X_t^x and Y_t^y jump together as most as they can, and the one that has a higher jump rate jumps alone occasionally. With $f(x,y) = \mid x - y \mid =: u$, the drift part of the generator gives (first line of eq. 8.36)

$$-\gamma u.$$

The second line vanishes, and, by the triangle inequality and hypothesis on λ, the third one is dominated by

$$\Lambda u \Big[\int_0^\infty g(u+z) h(z) dz - g(u) \Big].$$

Hence,

$$Lu \leqslant -\gamma u + \Lambda u \Big[\int_0^\infty (u+z) h(z) dz - u \Big],$$

and the calculus on moment bounds above show that

$$\mathbb{E}\big[\mid X_t^x - X_t^y \mid \big] \leqslant e^{-(\gamma - \Lambda \mathbb{E}[h])t} \mid x - y \mid$$

which achieves the proof, by the definition of the Wasserstein distance. $\square$

Remark 41. *This coupling strategy can be adapted to get an explicit convergence rate in total variation distance (see [7]).*

Remark 42. *The same demonstration holds for the discrete model as well.*

8.6   Inverse problem

In subsection 8.2, we have shown that for any set of parameters function $\gamma(x), \lambda(x), h$ that satisfies particular assumption, then there exists a unique invariant density for the evolution equation, eq. (8.11). Let us summarize our condition,

Proposition 43. *Assume h is an exponential distribution of mean parameter b, γ is a positive continuous function on $(0, \infty)$, λ a non-negative measurable function on $(0, \infty)$ such that $\frac{\lambda}{\gamma}$ is locally integrable. Denote*

$$Q(x) = \int_x^{\bar{x}} \frac{\lambda(y)}{\gamma(y)} dy,$$

and, suppose that for some $\delta, r > 0$,

$$\int_0^\delta \frac{1}{\gamma(x)} dx = \infty,$$
$$\limsup_{x \to \infty} \gamma(x) > 0,$$
$$\int_0^\delta \gamma(x)^{r-1} dx < \infty,$$
$$\int_0^\delta \frac{\lambda(x)}{\gamma(x)} dx = \infty,$$
$$\lim_{x \to 0} \frac{e^{-Q(x)}}{\gamma(x)^r} < \infty,$$
$$\lim_{x \to \infty} \frac{\lambda(x)}{\gamma(x)} < \frac{1}{b},$$

then there exists a unique globally attractive invariant density for eq. (8.11) given by

$$u_*(x) = \frac{1}{c\gamma(x)} e^{-x/b - Q(x)}$$

We can invert these property to obtain

Proposition 44. *Assume h is an exponential distribution of mean parameter b, γ is a positive continuous function on $(0, \infty)$, and u is an integrable positive function such that for some $\delta, r > 0$,*

$$\int_0^\delta \frac{1}{\gamma(x)} dx = \infty,$$
$$\limsup_{x \to \infty} \gamma(x) > 0,$$
$$\int_0^\delta \gamma(x)^{r-1} dx < \infty,$$
$$\int_0^\delta \frac{u'(x)}{u(x)} + \frac{\gamma'(x)}{\gamma(x)} dx = \infty,$$
$$\lim_{x \to 0} \frac{u(x)}{\gamma(x)^{r-1}} < \infty,$$
$$\lim_{x \to \infty} \frac{u'(x)}{u(x)} + \frac{\gamma'(x)}{\gamma(x)} < 0,$$

then the function λ defined by

$$\lambda(x) = \frac{1}{b} \gamma(x) + \frac{(\gamma(x)u(x))'}{u(x)}, \tag{8.37}$$

is such that the function u is the invariant density for eq. (8.11) associated with h, γ, λ.

Proof. We need to invert the operator given by

$$\frac{d(-\gamma(x)u(x))}{dx} = -\lambda(x)u(x) + \int_0^x \lambda(x-y)u(x-y)h(y)dy.$$

Taking Laplace transform, and noting that by assumption $\lim_{x\to 0} \gamma(x)u(x) = 0$, we obtain

$$\mathcal{L}(\lambda u)(s)\mathcal{L}(h - \delta_0)(s) = -s\mathcal{L}(\gamma u)(s),$$

so that

$$\mathcal{L}(\lambda u)(s) = (s + \frac{1}{b})\mathcal{L}(\gamma u)(s).$$

By inverting the Laplace transform, we get eq. (8.37). That such λ satisfies all the properties of proposition 43 follows then by the assumption and the formula eq. (8.37). □

A series of remark follows.

Remark 45. *The assumption on admissible density u of the last proposition 44 are simply integrability condition in 0 and exponential decay at ∞, that can be seen from the analytical expression eq. (8.19). The result given below could have been more easily obtained by the derivation of $(\gamma(x)u)$ thanks to analytical expression eq. (8.19). However, the demonstration given here show that such inversion of the operator is not restricted to exponential jump distribution, as long as we know its Laplace transform. Hence, to be applicable for more general jump distribution, characterization of the stationary state and convergence condition of the direct problem needs to be investigated for general jump distribution.*

Remark 46. *In practice, the formula eq. (8.37) has been shown to be tractable by using for example statistical kernel estimator of the density. The difficulty relies in estimating properly the derivatives of such function. The authors in [28] have shown statistical estimator bounds in a similar problem (for the aggregation-fragmentation problem). Estimates of the jump rate function will then be accurate in domain where the density is not near 0.*

Remark 47. *Such inverse formula may have a great interest to analyze experimental data. Indeed, from the jump rate function, it is possible to guess the mechanism involved in the regulation (see for instance section 3), which is not necessarily observable experimentally. From the result in proposition 44, it can be deduced the jump rate function $\lambda(x)$ if we have experimental observations in steady-state and if the other parameters $\gamma(x)$ and b are known. As the steady-state is invariant by a time scale change, we cannot deduce all parameters from steady-state observations. The degradation function is however usually well caracterized experimentally using knock-out experiments. In the absence of regulation, the result in paragraph 8.2.0.1 shows that, at steady-state,*

$$b = \frac{Var(X)}{<X>}.$$

Such relation between asymptotic moments were previously used to deduce parameter fitting in different models of gene regulation (see [104, 102]). In the presence of regulation there's no simple formula to find back the mean burst size parameter b. However, if $\lambda(x)$ is assumed to be bounded, the mean burst size parameter can be found using the tail of the asymptotic probability distribution. Indeed, from the analytical expression eq. (8.19), we see that

$$b = -\lim_{x\to\infty} x/\log(u^*(x))$$

9   From One Model to Another

In this section, we are going to prove how all the models presented in section 7 are linked within each other. Briefly, the switching dynamic can lead either to an averaging behavior (if both activation and inactivation rate goes to infinity within the same order, see paragraph 9.1.1) or to a bursting behavior (large jumps appear) (if the inactivation rate and the synthesis rate go to infinity within the same order, see paragraph 9.1.2). However, the switching dynamic is not the only possible scenario to lead to bursting behavior. In the discrete state space model, the adiabatic reduction of mRNA can lead to a bursting production of protein, in a similar manner than the switching model actually (see subsection 9.2). Finally, this bursting behavior can be averaged through the different variables or transmitted (when the degradation rate of a variable go to infinity, see subsection 9.3). We will make extensively use of the notation of section 7 for naming each model and its parameter.

These limiting behavior are well known of modelers and experimentalists. The review paper of Kaern et al. [74] details assumptions for the ODE C2 to be a good approximation of SC2 (macrocscopic limit and fast switching kinetics), and the kinetics assumption that lead from SC2 to transcriptional bursting BD2 and translational bursting SBD1. The authors in [77] show how to take advantage of specific limiting behavior of the SD1 model (fast operator fluctuation, and large quantity of molecules) to rigorously study its qualitative behavior (bifurcation, escape time), and extend their method to the mutual repressor system. The authors in [87] considered similar techniques and validate these approximations by numerical simulations. Importantly, the authors in [115] reported that different genes in eukaryotes can have different kinetics, so that each limiting model can be applicable to different gene kinetics.

On a more theoretical side, the author in [12] used a semi-group theoretical proof to show the averaging reduction of model SC2 to C2, and the adiabatic reduction from SC2 to SC1. The authors in [25, 75] give clues to derive rigorously limiting model in the context of stochastic hybrid model. We recall the available reduction results of the switching model in the first subsection 9.1 and rely on them to extend it to the 2-dimensional variable model, in the discrete state space model in subsection 9.2 and in the continuous state space model in subsection 9.3. In this last case, we derived alternative proofs, based either on partial differential equation and on probabilistic techniques. These have been the subject of a preprint [92]. It is important to mention that the theoretical and rigorous justification of the reduction of a given model towards a bursting limit model actually follows natural ideas that are used by many authors to obtain a simplified model. For instance, the authors in [66] show that different extensions of the standard model of gene expression (without regulation) all leads to bursting model with geometric jump size distribution, basically reasoning by how many proteins can be produced before mRNA is degraded. Firsly, this reasoning suggests that such reduction is a general framework of catalytic reaction, where the reactant is needed for the reaction to occur, but is not consumed by the reaction (so that a new reaction may happen directly). The identification of the limit martingale problem we performed in subsections 9.2 and 9.3 uses a test function that exactly matches with the heuristic above. The idea is to follow the catalytic reaction up to the time the reactant is consumed. See also [129] where the authors used a reduction technique based on the characteristic method associated to the evolution equation of the moment generating equation. Again, in such models, the characteristic method exactly follows the production of the second variable up to the time the first variable vanishes.

Finally, we show in subsection 9.4 how the links between the discrete and the continuous

bursting model, using well known fluid limit techniques ([36]).

9.1 Limiting behavior of the switching model

9.1.1 Averaging results

In the context of model of gene expression, the author in [12] used a result on degenerate convergence of semigroup to show the averaging reduction of model SC2 to C2. The degeneracy means here that the limiting semigroup act on a proper subspace of the starting space. The author considered the special (but biologically natural) case where the transcriptional rate function k_1 is a constant function. In such case, the deterministic part of the model can be solved exactly. But its main advantage is in fact that in such case the dynamics is constrained in a compact subset. Hence, this result could easily be extended to the case where k_1 is a smooth bounded function. With k_i and k_a continuous function, which are then bounded on compact set, the semigroup acting on continuous function of the full model can be constructed by the Philipps perturbation theorem (see [35]) from the deterministic semigroup. The obtained semigroup is a Feller semigroup. We rewrite the limiting theorem with our notation (section 7) below, for the reduction from SC1 (see paragraph. 7.2) to C1 (see paragraph 7.4) (which has obvious extension to 2 and 3 variables).

Theorem 48. *Bobrowski [12, Theorem 2 p. 356] Assume k_1 is a continuous Lipschitz on $\mathbb{R}^+$ and bounded. Then there exists a compact subset $K \subset \mathbb{R}^+$ such that $x_1(t) \in K$ for all $t > 0$ as soon as $x_1(0) \in K$. Assume k_a and k_i are continuous Lipschitz functions, positive such that one of them is strictly positive. Let λ_a^n and λ_i^n sequences of positive numbers such that*

$$\lim_{n \to \infty} \lambda_a^n = \lim_{n \to \infty} \lambda_i^n = \infty$$

$$\lim_{n \to \infty} \frac{\lambda_a^n}{\lambda_i^n} = c > 0.$$

For any continuous function f, g on K, $i \in \{0, 1\}$, $x \in K$, and $t > 0$, let

$$T^n(t)(f, g)(i, x) := \mathbb{E}_{(i,x)}\big[f(x_1(t))\mathbf{1}_{\{X_0(t)=0\}} + g(x_1(t))\mathbf{1}_{\{X_0(t)=1\}}\big]$$

the semigroup acting on continuous function associated to any solution of SC1 (see paragraph. 7.2), starting at (i, x), with parameters λ_a^n and λ_i^n. Similarly, write $T(t)(f)(x)$ the semigroup defined by C1 (see paragraph 7.4), with k_1 being replaced by

$$\lambda_1 \frac{c k_a(x_1)}{c k_a(x_1) + k_i(x_1)} k_1(x_1)$$

Then, using norm of uniform convergence,
– For any continuous function f on K,

$$\lim_{n \to \infty} T^n(t)(f, f) = T(t)(f)$$

uniformly on time on all compact interval of $[0, \infty)$.

– For any continuous function f, g on K,

$$\lim_{n \to \infty} T^n(t)(f, g) = T(t)(Q(f, g))$$

uniformly on time on all compact interval of $[0, \infty)$, where

$$Q(f, g) = \frac{k_i}{c k_a + k_i} f + \frac{c k_a}{c k_a + k_i} g$$

The analog result given in [25] requires only that k_1 is such that C1 defines a global flow, not necessarily restrict to evolve in a compact. However, their result requires that the fast motion given by the switch defines an ergodic semigroup, exponentially mixing, and uniformly with respect to the slow variable x_1. Here, it is easy to see that this semigroup is ergodic, with unique invariant law given by a Bernoulli law of parameter $\frac{\lambda_a k_a(x_1)}{\lambda_a k_a(x_1) + \lambda_i k_i(x_1)}$. Its convergent rate is exponential with rate $\lambda_a k_a(x_1) + \lambda_i k_i(x_1)$. Hence, it is needed to suppose additionally that these rates are bounded with respect to x_1. As before, we rewrite the limiting theorem given in [25] with our notation (section 7) below, for the reduction from SC1 to C1 (which has obvious extension to 2 and 3 variable).

Theorem 49. *Crudu et al. [25, Theorem 5.1 p. 13] Assume $k_1 \in C^1(\mathbb{R}^+)$ and such that the model in paragraph 7.4 defines a global flow. Assume k_a and k_i are C^1 on $\mathbb{R}^+$ and bounded, positive such that one of them is strictly positive. Let $\lambda_a^n = n\lambda_a$ and $\lambda_i^n = n\lambda_i$ with $n \to \infty$. Let $(X_O^n(t), x_1^n(t))_{t \geqslant 0}$ the stochastic process defined by SC1 (see paragraph 7.2), and $(x_1(t))_{t \geqslant 0}$ the solution of C1 (see paragraph 7.4) with k_1 being replaced by*

$$\lambda_1 \frac{\lambda_a k_a(x_1)}{\lambda_a k_a(x_1) + \lambda_i k_i(x_1)} k_1(x_1)$$

Assume $x_1^n(0)$ converges in distribution to $x_1(0)$ in $\mathbb{R}^+$, then $(X_O^n(t), x_1^n(t))_{t \geqslant 0}$ converges in distribution to $(x_1(t))_{t \geqslant 0}$ in $\mathbb{D}(\mathbb{R}^+; \mathbb{R}^+)$.

The restriction of bounded rate k_a and k_i in [25] is essentially to ensure that the fast dynamics stay in a compact in some sense. Here, because the fast dynamics is on a compact state space, this assumption can be released easily. The only remaining restrictions are then that the limiting model posses a unique global solution. These results have very analog counterpart in discrete models SD1 and D1. See also [75] for general results on averaging methods.

9.1.2 Bursting

The limit from a switching (SB1,SC1) model to a continuous bursting model (BC1) was treated explicitly in [25] (together with a fluid limit). Now we let $\lambda_i^n = n\lambda_i$ and $\lambda_1^n = n\lambda_1$. Intuitively, the switching variable X_0^n will then spend most of its time in state 0. However, transition from $X_0^n = 0$ to $X_0^n = 1$ will still be possible (and will not vanish as $n \to \infty$). Convergence of X_0^n to 0 will hold in $L^1(0, t)$ for any finite finite time t. When $X_0^n = 1$, production of x_1 is suddenly very high, but for a brief time. Although x_1 follows a deterministic trajectory, the timing of its trajectory is stochastic. At the limit, this drastic production episode becomes a discontinuous jump, of a random size. All happen as the two successive jumps of X_0 (from 0 to 1 and back to 0) coalesce into a single one, and create a discontinuity in x_1. In such case, convergence cannot hold in the cad-lag space $\mathbb{D}(\mathbb{R}^+; \mathbb{R}^+)$ with the Skorohod topology. The authors in [25] were able to prove tightness in $L^p([0, T], \mathbb{R}^+)$, $1 \leqslant p < \infty$. Their result requires the additional assumption that all rates k_1, k_i and k_a are linearly bounded, and either k_a or k_i is bounded with respect to x_1. This is needed to get a bound on x_1 in $L^\infty([0, T], \mathbb{R}^+)$. The limiting theorem reads

Theorem 50. *Crudu et al. [25, Theorem 6.1 p. 17] Assume $k_1 \in C^1(\mathbb{R}^+)$ and let $\lambda_i^n = n\lambda_i$ and $\lambda_1^n = n\lambda_1$ with $n \to \infty$. Let $(X_O^n(t), x_1^n(t))_{t \geqslant 0}$ the stochastic process defined by SC1 (see paragraph 7.2). Assume $x_1^n(0)$ converges in distribution to $x_1(0)$ in $\mathbb{R}^+$, and $X_O^n(0)$ converges in distribution to 0. The reaction rates k_1, k_i and k_a are such that*
    – there exists $\alpha > 0$ such that $k_i(x_1) \geqslant \alpha$ for all x_1 ;

   – *there exists $M_1 > 0$ such that*

$$k_1(x_1) \leqslant M_1(x_1 + 1),$$
$$k_a(x_1) \leqslant M_1(x_1 + 1),$$
$$k_i(x_1) \leqslant M_1(x_1 + 1);$$

   – *In addition either k_a or k_1 is bounded with respect to x_1 .*
Then $(X_0^n(t))_{t \geqslant 0}$ converges in distribution to 0 in $L^1([0,T], \{0,1\})$ and $(x_1^n(t))_{t \geqslant 0}$ converges in distribution to the stochastic process whose generator is given by

$$
\begin{aligned}
A\varphi(x_1) = -\gamma_1 x_1 \frac{\partial \varphi}{\partial x_1} \\
+ \lambda_a k_a(x_1) \int_0^\infty \Big(\varphi(\phi_1(t,x_1)) - \varphi(x_1)\Big) \lambda_i k_i(\phi_1(t,x_1)) e^{-\int_0^t \lambda_i k_i(\phi_1(s,x_1))ds} dt, \quad (9.1)
\end{aligned}
$$

for every $\varphi \in C_b^1(\mathbb{R}^+)$ and where $\phi_1(t,x_1)$ is the flow associated to

$$\dot{x} = \lambda_1 k_1(x),$$
$$x(0) = x_1.$$

Analogous result on the SD1 model holds as well. The fact that this limiting model is indeed related to BC1 is now detailed in the three following examples.

Example 10. *Consider the special case where both regulation rates k_1 and k_i are constant, with $k_1(x_1) = k_i(x_1) \equiv 1$, for all $x_1 > 0$. Then the flow ϕ_1 is easily calculated and we have*

$$\phi_1(t,x_1) = x_1 + \lambda_1 t, \quad t \geqslant 0,$$
$$\int_0^t \lambda_i k_i(\phi_1(s,x_1))ds = \lambda_i t,$$

and the generator eq. (9.1) becomes

$$A\varphi(x_1) = -\gamma_1 x_1 \frac{\partial \varphi}{\partial x_1} + \lambda_a k_a(x_1) \int_0^\infty \Big(\varphi(x_1 + z) - \varphi(x_1)\Big) \frac{\lambda_i}{\lambda_1} e^{-\frac{\lambda_i}{\lambda_1} z} dz,$$

which is the BC1 model, with an exponential jump size distribution of mean parameter $\frac{\lambda_1}{\lambda_i}$. Such rate has an easy interpretation, being the number of molecules created during an ON period of the gene.

Other choice of regulation rate leads to different model, as illustrated in the next two examples.

Example 11. *Let $k_1 \equiv 1$ and $\lambda_i k_i(x_1) = \lambda_i x_1 + k_0$ (linear negative regulation), so that*

$$\phi_1(t,x_1) = x_1 + \lambda_1 t, \quad t \geqslant 0,$$
$$\int_0^t \lambda_i k_i(\phi_1(s,x_1))ds = (\lambda_i x_1 + k_0)t + \frac{\lambda_1 \lambda_i}{2} t^2,$$

and the generator eq. (9.1) becomes

$$A\varphi(x_1) = -\gamma_1 x_1 \frac{\partial \varphi}{\partial x_1} + \lambda_a k_a(x_1) \int_{x_1}^\infty \Big(\varphi(z) - \varphi(x_1)\Big) \frac{\lambda_i z + k_0}{\lambda_1} e^{-\frac{z-x_1}{\lambda_1}\left[\lambda_i \frac{z+x_1}{2} + k_0\right]} dz.$$

The limiting model is then a bursting model where the jump distribution is a function of the jump position, and has a Gaussian tail.

Example 12. *Let $k_1(x_1) = x_1$ and $k_i(x_1) \equiv 1$ (positive linear regulation), so that*

$$\phi_1(t, x_1) = x_1 e^{\lambda_1 t}, \quad t \geqslant 0,$$

$$\int_0^t \lambda_i k_i(\phi_1(s, x_1))ds = \lambda_i t,$$

and the generator eq. (9.1) becomes

$$A\varphi(x_1) = -\gamma_1 x_1 \frac{\partial \varphi}{\partial x_1} + \lambda_a k_a(x_1) \int_{x_1}^{\infty} \left(\varphi(z) - \varphi(x_1) \right) \frac{\lambda_i}{\lambda_1} x^{\frac{\lambda_i}{\lambda_1}} z^{-1-\frac{\lambda_i}{\lambda_1}} dz.$$

This time, the limiting model is a bursting model where the jump distribution is a function of the jump position with a power-law tail.

9.2   A bursting model from a two-dimensional discrete model

The fact that bursting models arise as a reduction procedure of a higher dimensional model was already observed in [129]-[25]. In [129], the authors show that, within an appropriate scaling, the time-dependent distribution of a 2-dimensional model converge to the time-dependent distribution of a 1-dimensional bursting model. The authors used analytics methods through the transport equation on the generating function. Their result seems to be restricted to first-order kinetics. The first variable is a fast variable that induces infrequent kicks to the second one. In [25], the authors show that, within an appropriate scaling, a fairly general discrete state space model with a binary variable converge to a bursting model with continuous state space. The authors obtained a convergence in law of the solution through martingale techniques. The binary variable is a fast variable that induces kicks to the other variable.

We present below analogous result of [25] when the fast variable is similar to the one of [129]. These results are more precise than the one of [129], and more general (some kinetics rates can be non-linear). We used martingales techniques, with a proof that is similar to [25] and also inspired by results from [75].

We consider the following 2d stochastic kinetic chemical reaction model, that generalizes the D2 model (see paragraph 7.3)

$$\varnothing \xrightarrow{\lambda_1 k_1(X_1, X_2)} X_1, \quad \text{Production of } X_1 \text{ at rate } \lambda_1 k_1(X_1, X_2) \tag{9.2}$$

$$X_1 \xrightarrow{\gamma_1(X_1, X_2)} \varnothing, \quad \text{Destruction of } X_1 \text{ at rate } \gamma_1(X_1, X_2) \tag{9.3}$$

$$\varnothing \xrightarrow{\lambda_2 k_2(X_1, X_2)} X_2, \quad \text{Production of } X_2 \text{ at rate } \lambda_2 k_2(X_1, X_2) \tag{9.4}$$

$$X_2 \xrightarrow{\gamma_2(X_1, X_2)} \varnothing, \quad \text{Destruction of } X_2 \text{ at rate } \gamma_2(X_1, X_2) \tag{9.5}$$
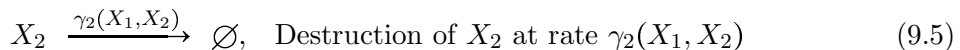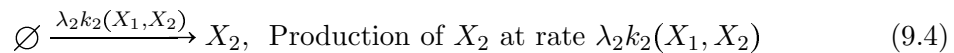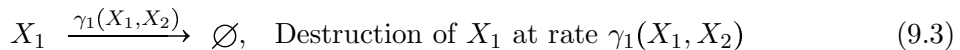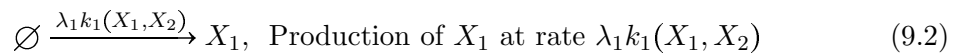
with $\gamma_1(0, X_2) = \gamma_2(X_1, 0) = 0$ to ensure positivity. This model can be represented by a continuous time Markov chain in $\mathbb{N}^2$, and is then a general random walk in $\mathbb{N}^2$. It can be described by the following set of stochastic differential equations

$$X_1(t) = X_1(0) + Y_1\left(\int_0^t \lambda_1 k_1(X_1(s), X_2(s))ds \right) - Y_2\left(\int_0^t \gamma_1(X_1(s), X_2(s))ds \right),$$

$$X_2(t) = X_2(0) + Y_3\left(\int_0^t \lambda_2 k_2(X_1(s), X_2(s))ds \right) - Y_4\left(\int_0^t \gamma_2(X_1(s), X_2(s))ds \right),$$

where Y_i, for $i = 1...4$ are independent standard Poisson processes. The generator of this

process has the form

$$
\begin{aligned}
\mathbb{B}f(X_1, X_2) =& \lambda_1 k_1(X_1, X_2)\Big[f(X_1 + 1, X_2) - f(X_1, X_2)\Big] \\
&+ \gamma_1(X_1, X_2)\Big[f(X_1 - 1, X_2) - f(X_1, X_2)\Big] \\
&+ \lambda_2 k_2(X_1, X_2)\Big[f(X_1, X_2 + 1) - f(X_1, X_2)\Big] \\
&+ \gamma_2(X_1, X_2)\Big[f(X_1, X_2 - 1) - f(X_1, X_2)\Big],
\end{aligned}
\tag{9.6}
$$

for every bounded function f on $\mathbb{N}^2$.

Example 13. *We obviously have in mind the mRNA-Protein system given by the D2 model defined in paragraph 7.3, where $\gamma_i(X_1, X_2) = \gamma_i X_i$, $k_2(X_1, X_2) = X_1$ and $k_1(X_1, X_2) = k_1(X_2)$.*

We suppose the following scaling holds

$$
\begin{aligned}
\gamma_1^N(X_1, X_2) &= N\gamma_1(X_1, X_2), \\
\lambda_2^N &= N\lambda_2,
\end{aligned}
$$

where $N \to \infty$ that is reactions eq. (9.3)- (9.4) occur at a faster time scale than the two other reactions. Then X_1 is degraded very fast, and induces also as a very fast production of X_2. The rescaled model is given by

$$
\begin{aligned}
X_1^N(t) &= X_1^N(0) + Y_1\Big(\int_0^t \lambda_1 k_1(X_1^N(s), X_2^N(s))ds\Big) - Y_2\Big(\int_0^t N\gamma_1(X_1^N(s), X_2^N(s))ds\Big), \\
X_2^N(t) &= X_2^N(0) + Y_3\Big(\int_0^t N\lambda_2 k_2(X_1^N(s), X_2^N(s))ds\Big) - Y_4\Big(\int_0^t \gamma_2(X_1^N(s), X_2^N(s))ds\Big),
\end{aligned}
\tag{9.7}
$$

and the generator of this process has the form

$$
\begin{aligned}
\mathbb{B}_N f(X_1, X_2) =& \lambda_1 k_1(X_1, X_2)\Big[f(X_1 + 1, X_2) - f(X_1, X_2)\Big] \\
&+ N\gamma_1(X_1, X_2)\Big[f(X_1 - 1, X_2) - f(X_1, X_2)\Big] \\
&+ N\lambda_2 k_2(X_1, X_2)\Big[f(X_1, X_2 + 1) - f(X_1, X_2)\Big] \\
&+ \gamma_2(X_1, X_2)\Big[f(X_1, X_2 - 1) - f(X_1, X_2)\Big].
\end{aligned}
\tag{9.8}
$$

We can prove the following reduction holds:

Theorem 51. *We assume that*

    1. The degradation function on X_2 satisfies $\gamma_2(X_1, 0) \equiv 0$.

    2. The degradation function on X_1 satisfies $\gamma_1(0, X_2) \equiv 0$, and

$$
\inf_{X_1 \geqslant 1, X_2 \geqslant 0} \gamma_1(X_1, X_2) = \underline{\gamma} > 0.
$$

    3. The production rate of X_2 satisfies $k_2(0, X_2) = 0$.

    4. The production rate function k_1 and k_2 are linearly bounded by $X_1 + X_2$.

    5. Either k_1 or k_2 is bounded.

et (X_1^N, X_2^N) the stochastic process whose generator is $\mathbb{B}_N$ (defined in eq. (9.8)). Assume that the initial vector $(X_1^N(0), X_2^N(0))$ converge in distribution to $(0, X(0))$, as $N \to \infty$. Then, for all $T > 0$, $(X_1^N(t), X_2^N(t))_{t \geq 0}$ converge in $L^1(0, T)$ (and in L^p, $1 \leq p < \infty$) to $(0, X(t))$ where $X(t)$ is the stochastic process whose generator is given by

$$\mathbb{B}_\infty \varphi(X) = \lambda_1 k_1(0, X) \Big(\int_0^\infty P_t(\gamma_1(1,.)\varphi(.))(X)dt - \varphi(X) \Big) + \gamma_2(0, X) \Big[\varphi(X - 1) - \varphi(X) \Big], \tag{9.9}$$

where

$$P_t g(X) = \mathbb{E} \Big[g(Y(t, X) e^{-\int_0^t \gamma_1(1, Y(s,X))ds} \Big],$$

and $Y(t, X)$ is the stochastic process starting at X at $t = 0$ whose generator is given by

$$Ag(Y) = \lambda_2 k_2(1, Y) \big(g(Y + 1) - g(Y) \big).$$

Remark 52. *The first three hypotheses of theorem 51 are the main characteristics of the mRNA-protein system (see paragraph 7.3). Basically, they impose that quantities remains non-negative, that the first variable has always the possibility to decrease to 0 (no matter the value of the second variable), and that the second variable cannot increase when the first variable is 0. Hence these three hypotheses will guarantee that (with our particular scaling) the first variable converge to 0, and will lead to an intermittent production of the second variable. The last two hypotheses are more technical, and guarantee that the Markov chain is not explosive, and hence well defined for all $t \geq 0$, and that the limiting model is well defined too.*

We divide the proof in several steps.

step 1: moment estimates Because production rates are linearly bounded, it is straightforward that with $f(X_1, X_2) = X_1 + X_2$ in eq. (9.8), there is a constant C_N (that depends on N and other parameters) such that

$$\mathbb{B}_N f(X_1, X_2) \leq C_N(X_1 + X_2).$$

Then $\mathbb{E}\big[X_1^N(t) + X_2^N(t)\big]$ is bounded on any time interval $[0, T]$ and

$$f(X_1^N(t), X_2^N(t)) - f(X_1^N(0), X_2^N(0)) - \int_0^t \mathbb{B}_N f(X_1^N(s), X_2^N(s))ds$$

is a L^1-martingale.

step 2: tightness Clearly, from the stochastic differential equation on X_1^N, we must have $X_1^N(t) \to 0$. We can show in fact that the Lebesgue measure of the set $\{t \leq T : X_1^N(t) > 0\}$ converge to 0. Indeed, taking $f(X_1, X_2) = X_1$ in eq. (9.8), we have

$$X_1^N(t) - X_1^N(0) - \int_0^t (\lambda_1 k_1(X_1^N(s), X_2^N(s)) - N\gamma_1(X_1^N(s), X_2^N(s)))ds \tag{9.10}$$

is a martingale. Thanks to the lower bound assumption on γ_1, we have

$$\underline{\gamma} \mathbb{E}\Big[\int_0^t \mathbf{1}_{\{X_1^N(s) \geq 1\}} ds \Big] \leq \mathbb{E} \int_0^t \gamma_1(X_1^N(s), X_2^N(s))ds.$$

Then, by the martingale property, we deduce

$$\underline{\gamma} N \mathbb{E}\Big[\int_0^t \mathbf{1}_{\{X_1^N(s) \geq 1\}} ds \Big] \leq \mathbb{E}[X_1^N(0)] + \lambda_1 \int_0^t \mathbb{E}\big[k_1(X_1^N(s), X_2^N(s))\big]ds. \tag{9.11}$$

And for X_2^N we obtain from the the eq. (9.7),

$$X_2^N(t) \leqslant X_2^N(0) + Y_3\Big(\int_0^t \lambda_2 N \mathbf{1}_{\{X_1^N(s)\geqslant 1\}} k_2(X_1^N(s), X_2^N(s)) ds\Big).$$

Let us now distinguish between the two cases.

– If k_2 is bounded (say by 1), we have

$$\mathbb{E}\big[X_2^N(t)\big] \leqslant \mathbb{E}\big[X_2^N(0)\big] + \lambda_2 N \mathbb{E}\big[\int_0^t \mathbf{1}_{\{X_1^N(s)\geqslant 1\}} ds\big].$$

As k_1 is linearly bounded (say by 1) by $X_1^N + X_2^N$, the upper bound eq. (9.11) becomes

$$\underline{\gamma} N \mathbb{E}\big[\int_0^t \mathbf{1}_{\{X_1^N(s)\geqslant 1\}} ds\big] \leqslant \mathbb{E}\big[X_1^N(0)\big] + \lambda_1 \int_0^t \Big(\mathbb{E}\big[X_1^N(s)\big] + \mathbb{E}\big[X_2^N(s)\big]\Big) ds.$$

Finally, with eq. (9.10), it is clear that

$$\mathbb{E}\big[X_1^N(t)\big] \leqslant \mathbb{E}\big[X_1^N(0)\big] + \lambda_1 \int_0^t \Big(\mathbb{E}\big[X_1^N(s)\big] + \mathbb{E}\big[X_2^N(s)\big]\Big) ds.$$

Hence, with the three last inequalities, we can conclude by the Grönwall lemma that $\mathbb{E}\big[X_2^N(t)\big]$ is bounded on $[0,T]$, *uniformly* in N. Then

$$N\mathbb{E}\big[\int_0^T \mathbf{1}_{\{X_1^N(s)\geqslant 1\}} ds\big]$$

is bounded and $X_1^N \to 0$ in $L^1([0,T], \mathbb{N})$. By the law of large number, $\frac{1}{N}Y_3(N)$ is almost surely convergent, and hence almost surely bounded. We deduce then there exists a random variable C such that

$$X_2^N(t) \leqslant X_2^N(0) + NC \int_0^t \mathbf{1}_{\{X_1^N(s)\geqslant 1\}} ds,$$

almost everywhere. By Grönwall lemma and Markov inequality

$$\mathbb{P}\big\{\sup_{t\in[0,T]} X_2^N(t) \geqslant K\big\} \to 0$$

as $K \to \infty$, uniformly in N.

– Now if k_1 is bounded (say 1). By the martingale eq. (9.10) (and the same lower bound hypothesis on γ_1, it is clear that

$$N\mathbb{E}\big[\int_0^T \mathbf{1}_{\{X_1^N(s)\geqslant 1\}} ds\big]$$

is bounded and $X_1^N \to 0$ in $L^1([0,T], \mathbb{N})$. Now, let us denote $U^N(t) = \frac{1}{N}X_1^N(t)$, $V^N = \frac{1}{N}X_2^N(t)$ and $W^N = N\mathbf{1}_{\{X_1^N(t)\geqslant 1\}}$ (which is then bounded in $L^1([0,T[))$. From eq. (9.7), and from the linear bound on k_2 (say by 1)

$$V^N(t) \leqslant V^N(0) + \frac{1}{N}Y_3\Big(\int_0^t \lambda_2 N W^N (U^N(s) + V^N(s)) ds\Big).$$

Then, still by the law of the large number there exists a random variable C such that

$$V^N(t) \leqslant V^N(0) + C \int_0^t W^N (U^N(s) + V^N(s)) ds\Big),$$

and hence

$$X_2^N(t) \leqslant X_2^N(0) + C \int_0^t W^N(X_1^N(s) + X_2^N(s))ds\Big).$$

By Grönwall lemma,

$$\sup_{[0,T]} X_2^N(t) \leqslant (X_1^N(0) + X_2^N(0)) \exp\Big(C \int_0^t W^N(s)ds\Big),$$

which is then bounded, uniformly in N.
For any subdivision of $[0,T]$, $0 = t_0 < t_1 < \cdots < t_n = T$,

$$\sum_{i=0}^{n-1} \mid X_2^N(t_{i+1}) - X_2^N(t_i) \mid \;\; \leqslant \;\; \sum_{i=0}^{n-1} Y_3\Big(\int_{t_i}^{t_{i+1}} \lambda_2 N \mathbf{1}_{\{X_1^N(s)\geqslant 1\}} k_2(X_1^N(s), X_2^N(s))ds\Big)$$

$$\leqslant \;\; Y_3\Big(\int_0^T \lambda_2 N \mathbf{1}_{\{X_1^N(s)\geqslant 1\}} k_2(X_1^N(s), X_2^N(s))ds\Big)$$

so by a similar argument as above, we also get the tightness of the BV norm (see proposition 23 part 0)

$$\mathbb{P}\{\|X_2^N\|_{[0,T]} \geqslant K\} \to 0$$

as $K \to 0$, independently in N. Then X_2^N is tight in $L^p([0,T])$, for any $1 \leqslant p < \infty$.

step 3: identification of the limit We choose an adherence value $(0, X_2(t))$ of the sequence $(X_1^N(t), X_2^N(t))$ in $L^1([0,T]) \times L^p([0,T])$. Then a subsequence (again denoted by) $(X_1^N(t), X_2^N(t))$ converge to $(0, X_2(t))$, almost surely and for almost $t \in [0,T]$. We are looking for test-functions such that

$$f(X_1^N(t), X_2^N(t)) - f(X_1^N(0), X_2^N(0)) - \int_0^t \mathbb{B}_N f(0, X_2^N(s)) 1_{X_1^N(s)=0} ds$$

$$- \int_0^t \mathbb{B}_N f(X_1^N(s), X_2^N(s)) 1_{X_1^N(s)\geqslant 1} ds$$

is a martingale and $\mathbb{B}_N f(X_1^N(s), X_2^N(s))$ is bounded independently of N when $X_1 \geqslant 1$. The following choice is inspired by [25]. We introduce the stochastic process $Y_t^{x,y}$, starting at y and whose generator is

$$A^x g(y) = \lambda_2 k_2(x,y)\Big[g(y+1) - g(y)\Big],$$

for any $x \geqslant 1$. and we introduce the semigroup P_t^x defined on $\mathbb{B}_b(\mathbb{R}^+)$, for any $x \geqslant 1$, by

$$P_t^x g(y) = \mathbb{E}\Big[g(Y_t^{x,y}) e^{-\int_0^t \gamma_1(x, Y_s^{x,y})ds}\Big]. \tag{9.12}$$

Then the semigroup P_t^x satisfies the equation

$$\frac{dP_t^x g(y)}{dt} = A^x P_t^x g(y) - \gamma_1(x,y) P_t^x g(y).$$

Now for any bounded function g, define recursively

$$f(0,y) = g(y),$$
$$f(x,y) = \int_0^\infty P_t^x(\gamma_1(x,.)f(x-1,.))(y)dt.$$

Such a test function is well defined by the assumption on γ_1. We then verify that

$$\mathbb{B}_N f(0, y) = \lambda_1 k_1(0, y) \Big(\int_0^\infty P_t^1(\gamma_1(1, .)g(.))(y)dt - g(y) \Big) + \gamma_2(0, y)\Big[g(y - 1) - g(y) \Big],$$

$$\mathbb{B}_N f(x, y) = \lambda_1 k_1(x, y)\Big[f(x + 1, y) - f(x, y) \Big] + \gamma_2(x, y)\Big[f(x, y - 1) - f(x, y) \Big].$$

Indeed, for any $x \geqslant 1$,

$$\begin{aligned}
& A^x f(x, y) - \gamma_1(x, y)f(x, y) \\
& = \int_0^\infty A^x P_t^x(\gamma_1(x, .)f(x - 1, .))(y) - \gamma_1(x, y)P_t^x(\gamma_1(x, .)f(x - 1, .))(y)dt, \\
& = \int_0^\infty \frac{d}{dt} P_t^x(\gamma_1(x, .)f(x - 1, .))(y)dt, \\
& = \lim_{t \to \infty} P_t^x(\gamma_1(x, .)f(x, .))(y) - \gamma_1(x, y)f(x - 1, y), \\
& = -\gamma_1(x, y)f(x - 1, y).
\end{aligned}$$

Then

$$\lambda_2 k_2(x, y)\Big[f(x, y + 1) - f(x, y) \Big] + \gamma_1(x, y)\Big[f(x - 1, y) - f(x, y) \Big] = 0.$$

Hence $\mathbb{B}_N f(x, y)$ is independent of N, and, taking the limit $N \to \infty$ in

$$f(X_1^N(t), X_2^N(t)) - f(X_1^N(0), X_2^N(0)) - \int_0^t \mathbb{B}_N f(X_1^N(s), X_2^N(s))ds,$$

we deduce

$$g(X_2(t)) - g(X_2(0)) - \int_0^t \mathbb{B}_\infty g(X_2)$$

is a martingale where

$$\mathbb{B}_\infty g(y) = \lambda_1 k_1(0, y)\Big(\int_0^\infty P_t(\gamma_1(1, .)g(.))(y)dt - g(y) \Big) + \gamma_2(0, y)\Big[g(y - 1) - g(y) \Big].$$

Uniqueness   Due to assumption on k_1 and k_2, the limiting generator defines a pure-jump Markov process in $\mathbb{N}$ which is not explosive. Uniqueness of the martingale then follows classically.

Remark 53. *The above expression eq. (9.9) is a generator of a bursting model for a "general bursting size distribution". For instance, for constant function γ_1, and $k_2 \equiv 1$, we have*

$$\begin{aligned}
P_t(\gamma_1(.)\varphi(.))(p) &= \gamma_1 P_t(\varphi)(p), \\
&= \gamma_1 \mathbb{E}\Big[\varphi(Y_t^y)e^{-\gamma_1 t} \Big], \\
&= \gamma_1 e^{-\gamma_1 t} \sum_{z \geqslant y} \varphi(z)\mathbb{P}\{Y_t^y = z\}, \\
&= \gamma_1 e^{-\gamma_1 t} \sum_{z \geqslant y} \varphi(z)\frac{(\lambda_2 t)^{z - y}e^{-\lambda_2 t}}{(z - y)!}.
\end{aligned}$$

It follows by integration integration by parts that

$$\int_0^\infty P_t(\gamma_1(.)\varphi(.))(y)dt = \frac{\gamma_1}{\gamma_1 + \lambda_2} \sum_{z \geqslant 0} \varphi(z + y)\Big(\frac{\lambda_2}{\lambda_2 + \gamma_1} \Big)^z,$$

which gives then an additive geometric burst size distribution of parameter $p = \frac{\lambda_2}{\lambda_2 + \gamma_1}$, as expected.

9.3   Adiabatic reduction in a bursting model

In continuous dynamical systems, considerable simplifications and insights into the behavior can be obtained by identifying fast and slow variables. This technique is especially useful when one is initially interested in the approach to a steady state. In this context a fast variable is one that relaxes much more rapidly to a conditional equilibrium than a slow variable [54]. In many systems, including chemical and biochemical ones, this is often a consequence of differences in degradation rates, with the fastest variable the one that has the largest degradation rate. We employ this strategy here to obtain approximations to the two-dimensional bursting model BC2 as a one-dimensional bursting model BC1.

The adiabatic reduction technique gives results that justifies to reduce the dimension of a system and to use an effective set of reduced equations in lieu of dealing with a full, higher dimensional model. This techniques essentially requires that different time scales occur in the system. Adiabatic reduction results for deterministic systems of ordinary differential equations have been available since the very precise results of [143] and [38]. The simplest results, in the hyperbolic case, give an effective construction of an uniformly asymptotically stable slow manifold (and hence a reduced equation) and prove the existence of an invariant manifold near the slow manifold, with (theoretically) any order of approximation of this invariant manifold. Such precise and geometric results have been generalized to random systems of stochastic differential equation with Gaussian white noise ([10], see also [42] for previous work on the Fokker-Planck equation). However, to the best of our knowledge, analogous results for stochastic differential equations with a jump process have not been obtained. We recall how this strategy works in ordinary differential equation, and specially in the model we consider. It is often the case that the degradation rate of mRNA is much greater than the corresponding degradation rates for both the intermediate protein and the effector ($\gamma_1 \gg \gamma_2, \gamma_3$) so in this case the mRNA dynamics are fast and we have from eq. (6.2) the relationship

$$0 = \kappa_d f(y_3) - y_1.$$

It is easy to see that such relation defines a uniformly asymptotically stable slow manifold (with eigenvalue -1). Consequently the three variables system describing the generic operon reduces to a two variables one involving the slower intermediate and effector:

$$\frac{dy_2}{dt} = \gamma_2[\kappa_d f(y_3) - y_2], \tag{9.13}$$

$$\frac{dy_3}{dt} = \gamma_3(y_2 - y_3). \tag{9.14}$$

In our considerations of specific single operon dynamics below we will also have occasion to examine two further sub-cases, namely

Case 1. Intermediate (protein) dominated dynamics. If it should happen that $\gamma_1 \gg \gamma_3 \gg \gamma_2$ (as for the *lac* operon), then the effector also qualifies as a fast variable so

$$0 = y_2 - y_3,$$

and thus from eq.(9.13) and (9.14) we recover the one dimensional equation for the slowest variable, the intermediate:

$$\frac{dy_2}{dt} = \gamma_2[\kappa_d f(y_2) - y_2].$$

Case 2. Effector (enzyme) dominated dynamics. Alternately, if $\gamma_1 \gg \gamma_2 \gg \gamma_3$ then the intermediate is a fast variable relative to the effector and we have

$$0 = \kappa_d f(y_3) - y_2,$$

so our two variable system eq. (9.13) and (9.14)) reduces to a one dimensional system

$$\frac{dy_3}{dt} = \gamma_3[\kappa_d f(y_3) - y_3].$$

for the relatively slow effector dynamic.

The present section gives a theoretical justification of an adiabatic reduction of a particular piecewise deterministic Markov process (and has been the subject of a preprint [92]). The results we obtain do not give a bound on the error of the reduced system, but they do allow us to justify the use of a reduced system in the case of a piecewise deterministic Markov process. In that sense, the results are close to the recent ones by [25] and [75], where general convergence results for discrete models of stochastic reaction networks are given. In particular, these papers give alternative scaling of the traditional ordinary differential equation and the diffusion approximation depending on the different scaling chosen (see [6] for some examples in a reaction network model). After the scaling, the limiting models can be deterministic (ordinary differential equation), stochastic (jump Markov process), or hybrid (piecewise deterministic process). For illustrative and motivating examples given by a simulation algorithm, see [55, 114, 50].

Our particular model is meant to describe stochastic gene expression with explicit bursting [39]. The variables evolve under the action of a continuous deterministic dynamical system interrupted by positive jumps of random sizes that model the burst production. In that sense, the convergence theorems we obtain in this paper can be seen as an example in which there is a reaction with size between 0 and ∞, and give complementary results to those of [25] and [75]. We hope that the results here are generalizable to give insight into adiabatic reduction methods in more general stochastic hybrid systems [60, 18]. We note also that more geometrical approaches have been proposed to reduce the dimension of such systems in [17].

9.3.1 Continuous-state bursting model

The models referred to above have explicitly assumed the production of several molecules *instantaneously*, through a jump Markov process, in agreement with experimental observations. In line with experimental observations, it is standard to assume a Markovian hypothesis (an exponential waiting time between production jumps) and that the jump sizes are exponentially distributed (geometrically in the discrete case) as well. The intensity of the jumps can be a linearly bounded function, to allow for self-regulation.

Let x_1 and x_2 denote the concentrations of mRNA and protein respectively. A simple model of single gene expression with bursting in transcription is given by (SC2 model)

$$\frac{dx_1}{dt} = -\gamma_1 x_1 + \mathring{N}(h, \lambda_1 k_1(x_2)), \tag{9.15}$$

$$\frac{dx_2}{dt} = -\gamma_2 x_2 + \lambda_2 x_1. \tag{9.16}$$

Here γ_1 and γ_2 are the degradation rates for the mRNA and protein respectively, λ_2 is the mRNA translation rate, and $\mathring{N}(h, \lambda_1 k_1(x_2))$ describes the transcription that is assumed to be a compound Poisson *white noise* occurring at a rate $\lambda_1 k_1(x_2)$ with a non-negative jump size Δx_1 distributed with density h.

The eq. (9.15) and (9.16) are a short hand notation for

$$x_1(t) = x_1^0 - \int_0^t \gamma_1 x_1(s^-)ds + \int_0^t \int_0^\infty \int_0^\infty 1_{\{r \leqslant \lambda_1 k_1(x_2(s^-))\}} z N(ds, dz, dr), \tag{9.17}$$

$$x_2(t) = x_2^0 - \int_0^t \gamma_2 x_2(s^-)ds + \int_0^t \lambda_2 x_1(s^-)ds. \tag{9.18}$$

where $X_{s-} = \lim_{t \to s-} X(t)$, and $N(ds, dz, dr)$ is a Poisson random measure on $(0, \infty) \times [0, \infty)^2$ with intensity $ds h(z) dz dr$, where s denotes the times of the jumps, r is the state-dependency in an acceptance/rejection fashion, and z the jump size. Note that $(x_1(t))$ is a stochastic process with almost surely finite variation on any bounded interval $(0, T)$, so that the last integral is well defined as a Stieltjes-integral.

Hypothesis 8. *The following discussion is valid for general rate functions k_1 and density functions $h(\cdot)$ that satisfy*

  – *$k_1 \in C^1$, k_1 is globally Lipschitz and linearly bounded with*

$$0 \leqslant k_1(x) \leqslant c + \overline{k_1} x.$$

  – *$h \in C^0$ and $\int_0^\infty x h(x) dx < \infty$.*

For a general density function h, we denote the average burst size by

$$b = \int_0^\infty x h(x) dx. \tag{9.19}$$

If $k_1 \equiv 1$ is independent of the state x_2, the average transcription rate is $b\lambda_1$, and the asymptotic average mRNA and protein concentrations are

$$
\begin{aligned}
x_1^{\mathrm{eq}} := \mathbb{E}\big[x_1(t \to \infty)\big] &= \frac{b\lambda_1}{\gamma_1}, \\
x_2^{\mathrm{eq}} := \mathbb{E}\big[x_2(t \to \infty)\big] &= \frac{\lambda_2}{\gamma_2} x_1^{\mathrm{eq}} = \frac{b\lambda_1 \lambda_2}{\gamma_1 \gamma_2}.
\end{aligned}
\tag{9.20}
$$

9.3.2   Statement of the results

In the following discussion, we consider the situation when mRNA degradation is a fast process, *i.e.* γ_1 is "large enough", but the average protein concentration x_2^{eq} remains unchanged. In what follows, we denote by γ_1^n, λ_1^n, λ_2^n sequences of parameters, and h^n sequence of density function that will replace γ_1, λ_1, λ_2, h in eq. (9.17)- (9.18). We then denote (x_1^n, x_2^n) its associated solution. We will always assume one of the following three scaling relations:

(S1) Frequent production rate of mRNA, namely $\gamma_1^n = n\gamma_1$, $\lambda_1^n = n\lambda_1$, and $\lambda_2^n = \lambda_2$ $h^n = h$ are independent of n;

(S2) Large burst of mRNA, namely $\gamma_1^n = n\gamma_1$, $h^n(z) = \frac{1}{n} h(\frac{z}{n})$ and $\lambda_1^n = \lambda_1, \lambda_2^n = \lambda_2$ remain unchanged;

(S3) Large production rate of protein, namely $\gamma_1^n = n\gamma_1$, $\lambda_2^n = n\lambda_2$, and $\lambda_1^n = \lambda_1$ $h^n = h$ are independent of n;

In this section we determine an effective reduced equation for eq. (9.16) for each of the three scaling conditions (S1)-(S3). In particular, we show that under assumption (S1), eq. (9.16) can be approximated by the deterministic ordinary differential equation

$$\frac{dx_2}{dt} = -\gamma_2 x_2 + \lambda_2 k(x_2), \tag{9.21}$$

where

$$k(x_2) = b\lambda_1 k_1(x_2)/\gamma_1.$$

We further show that under the scaling relations (S2) or (S3), eq. (9.16) can be reduced to the stochastic differential equation

$$\frac{dx_2}{dt} = -\gamma_2 x_2 + \mathring{N}(\bar{h}, \lambda_1 k_1(x_2)). \tag{9.22}$$

where $\bar{h}$ is a suitable density function in the jump size Δx_2 (to be detailed below).

We first explain, using some heuristic arguments, the differences between the three scaling relations and the associated results. When $n \to \infty$, $\gamma_1^n \to \infty$ and applying a standard quasi-equilibrium assumption we have

$$\frac{dx_1^n}{dt} \approx 0,$$

which yields

$$x_1^n(t) \approx \frac{1}{\gamma_1^n} \mathring{N}(h^n(.), \lambda_1^n k_1(x_2^n)) = \mathring{N}(\gamma_1^n h^n(\gamma_1^n \cdot), \lambda_1^n k_1(x_2^n)),$$

and therefore the second eq. (9.16) becomes

$$\begin{aligned}
\frac{dx_2^n}{dt} &\approx -\gamma_2 x_2^n + \frac{\lambda_2^n}{\gamma_1^n} \mathring{N}(h^n(.), \lambda_1^n k_1(x_2^n)), \\
&\approx -\gamma_2 x_2^n + \mathring{N}\left(\frac{\gamma_1^n}{\lambda_2^n} h^n(\frac{\gamma_1^n}{\lambda_2^n}), \lambda_1^n k_1(x_2^n)\right).
\end{aligned}$$

Hence in eq. (9.22), $\bar{h}(x_2) = (\lambda_2/\gamma_1)^{-1} h((\lambda_2/\gamma_1)^{-1} x_2)$ under the scaling (S2) and (S3). Furthermore, we note that the scaling (S2) also implies $nh^n(n\cdot) = h(\cdot)$, while in (S1), $nh^n(n\cdot) = nh(n\cdot)$ so that the jumps become more frequent and smaller.

We denote $(D[0,\infty), S)$ the cad-lag function space of function defined on $[0,\infty)$ at values in $\mathbb{R}^+$ with the usual Skorohod topology. Similarly $(D[0,T], J)$ is the cad-lag function space on $[0,T]$, with the Jakubowski topology. Also, $L^p[0,T)$ the space of L^p integrable function on $[0,T)$, with $T > 0$, which we endowed with total variation norm, and $M(0,\infty)$ is the space of real measurable function on $[0,\infty)$ with the metric

$$d(x,y) = \int_O^\infty e^{-t} \max 1, |x(t) - y(t)| dt.$$

Our main results can be stated as follows

Theorem 54. *Consider the eq. (9.17)-(9.18) and assume hypothesis 8. If the scaling (S1) is satisfied, i.e., $\lambda_1^n = n\lambda_1$, and if $x_2^n(0) \to x_2^0$, then when $n \to \infty$,*

1. *The stochastic process $x_1^n(t)$ does not converge in any functional sense;*

2. *The stochastic process $x_2^n(t)$ converges in law in $(D[0,\infty), S)$ towards the deterministic solution of the ordinary differential equation*

$$\frac{dx_2}{dt} = -\gamma_2 x_2 + \lambda_2 k(x_2), \quad x_2(0) = x_2^0, \tag{9.23}$$

   where

$$k(x_2) = b\lambda_1 k_1(x_2)/\gamma_1.$$

Theorem 55. *Consider the eq. (9.17)-(9.18) and assume hypothesis 8. If the scaling (S2) is satisfied, i.e., $h^n(z) = \frac{1}{n}h(\frac{z}{n})$, and if $x_2^n(0) \to x_2^0$, then when $n \to \infty$,*

1. *The stochastic process $\frac{x_1^n(t)}{n}$ converges in law in L^p, $1 \leqslant p < \infty$ and in $(D[0,T], J)$ to the (deterministic) fixed value 0;*

2. *The stochastic process $x_2^n(t)$ converges in law in L^p, $1 \leqslant p < \infty$ and in $(D[0,T], J)$ to the stochastic process defined by the solution of the stochastic differential equation*

$$\frac{dx_2}{dt} = -\gamma_2 x_2 + \mathring{N}(\bar{h}, \lambda_1 k_1), \quad x_2(0) = x_2^0 \geqslant 0, \tag{9.24}$$

   where $\bar{h}(x_2) = (\lambda_2/\gamma_1)^{-1} h((\lambda_2/\gamma_1)^{-1} x_2)$.

Moreover, in the constant case $k_1 \equiv 1$, the stochastic process $x_1^n(t)$ converges in law in $M(0, \infty)$ to the compound Poisson white noise $\mathring{N}(h, \lambda_1)$;

Theorem 56. *Consider the eq. (9.17)-(9.18). and assume hypothesis 8. If the scaling (S3) is satisfied, i.e., $\lambda_2^n = n\lambda_2$, and if $x_2^n(0) \to x_2^0$, then when $n \to \infty$,*

1. *The stochastic process $x_1^n(t)$ converges in law in L^p, $1 \leqslant p < \infty$ and in $(D[0,T], J)$ to the (deterministic) fixed value 0;*

2. *The stochastic process $x_2^n(t)$ converges in law in L^p, $1 \leqslant p < \infty$ and in $(D[0,T], J)$ to the stochastic process determined by the solution of the stochastic differential equation*

$$\frac{dx_2}{dt} = -\gamma_2 x_2 + \mathring{N}(\bar{h}, \varphi), \quad x_2(0) = x_2^0 \geqslant 0,$$

where $\bar{h}(x_2) = (\lambda_2/\gamma_1)^{-1} h((\lambda_2/\gamma_1)^{-1} x_2)$.

Remark 57. *Note that scalings (S2) and (S3) give similar results for the equation governing the protein variable $x_2(t)$ but very different results for the asymptotic stochastic process related to the mRNA. In particular, in theorem 55, very large bursts of mRNA are transmitted to the protein, where in theorem 56, very rarely is mRNA present but when present it is efficiently synthesized into a burst of protein.*

In this section, we provide three different proofs of the results mentioned above. In particular, we prove the results using a master equation approach (the Kolmogorov forward equation) as well as starting from the stochastic differential equation. Note that both techniques have been used in the past, in particular within the context of discrete models of stochastic reaction networks. For the master equation approach, see [56, 153, 124] while for the stochastic differential equation approach, we refer to [25, 75].

In paragraph 9.3.4 we first show the tightness result for all three theorems. We then identify the limit using martingale approach in paragraph 9.3.5. In the others section, we provide alternative proof to identify the limit. In paragraph 9.3.6, we consider the situation without auto-regulation so the rate k_1 is independent of protein concentration x_2. In this case the two eq. (9.15)-(9.16) form a set of linear stochastic differential equations. We use then the method of characteristic functionals to identify the limit. Finally in paragraph 9.3.7 we give a similar result on the evolution equation on densities .

9.3.3   General properties and moment estimates

We first summarize the important background results on the stochastic processes used in the next.

9.3.3.1   One dimensional equation   For the one-dimensional stochastic differential equation (9.22) perturbed by a compound Poisson white noise, of (bounded) intensity $k(x_2)$ and jump size distribution $\bar{h}$, the extended generator of the stochastic process $(x_2(t))_{t \geqslant 0}$ is, for any $f \in \mathcal{D}(\mathcal{A})$, (see [27, Theorem 5.5])

$$\mathcal{A}_1 f(x) = -\gamma_2 x \frac{df}{dx} + k(x)\left(\int_x^\infty \overline{h}(z-x) f(z) dz - f(x)\right)$$

$$\begin{aligned}
\mathcal{D}(\mathcal{A}_1) \;=\; & \{f \in \mathcal{M}(0, \infty): \; t \mapsto f(xe^{-\gamma_2 t}) \text{ is absolutely} \\
& \text{continuous for } t \in \mathcal{R}^+ \text{ and} \\
& \mathbb{E} \sum_{T_i \leqslant t} |f(x_2(T_i)) - f(x_2(T_i^-))| < \infty \text{ for all } t \geqslant 0\}
\end{aligned}$$

where $\mathcal{M}(0, \infty)$ denotes a Borel-measurable function of $(0, \infty)$ and the times T_i are the instants of the jump of x_2. It is an extended domain containing all functions that are sufficiently smooth along the deterministic trajectories between the jumps, and with a bounded total variation induced by the jumps.

The operator $\mathcal{A}_1$ is the adjoint of the operator acting on densities $v(t, x)$ given by [90]

$$\frac{\partial v(t, x)}{\partial t} = \frac{\partial}{\partial x}[\gamma_2 x v(t, x)] + \int_0^x k(z) v(t, z) \overline{h}(x - z) dz - k(x) v(t, x).$$

For any $f \in \mathcal{D}(\mathcal{A}_1)$, we have

$$\frac{d}{dt} \mathbb{E} f(x_2(t)) = \mathbb{E} \mathcal{A}_1(f(x_2(t))).$$

9.3.3.2 Two dimensional equation   Consideration of the two-dimensional stochastic differential equation (9.15)-(9.16) perturbed by a compound Poisson white noise, of intensity $\lambda_1 k_1(x_2)$ and jump size distribution h follows along similar lines. Its infinitesimal generator and extended domain are

$$\begin{aligned}
\mathcal{A}_2 g(x_1, x_2) &= -\gamma_1 x_1 \frac{\partial g}{\partial x_1} + (\lambda_2 x_1 - \gamma_2 x_2) \frac{\partial g}{\partial x_2} \\
&\quad + \lambda_1 k_1(x_2) \left(\int_{x_1}^\infty h(z - x_1) g(z, x_2) dz - g(x_1, x_2) \right),
\end{aligned} \quad (9.25)$$

$$\begin{aligned}
\mathcal{D}(\mathcal{A}_2) &= \{ g \in \mathcal{M}((0, \infty)^2) : \; t \mapsto g(\phi_t(x_1, x_2)) \text{ is absolutely} \\
&\qquad \text{continuous for } t \in \mathcal{R}^+ \text{ and} \\
&\qquad \mathbb{E} \sum_{T_i \leqslant t} |g(x_1(T_i), x_2(T_i)) - g(x_1(T_i^-), x_2(T_i^-))| < \infty \text{ for all } t \geqslant 0 \}
\end{aligned} \quad (9.26)$$

where ϕ_t is the deterministic flow given by eq. (9.15) and (9.16).

The evolution equation for densities $u(t, x_1, x_2)$ is

$$\begin{aligned}
\frac{\partial u(t, x_1, x_2)}{\partial t} &= \frac{\partial}{\partial x_1}[\gamma_1 x_1 u(t, x_1, x_2)] - \frac{\partial}{\partial x_2}[(\lambda_2 x_1 - \gamma_2 x_2) u(t, x_1, x_2)] \\
&\quad + \int_0^{x_1} \lambda_1 k_1(x_2) u(t, z, x_2) h(x_1 - z) dz - \lambda_1 k_1(x_2) u(t, x_1, x_2).
\end{aligned}$$

For any $f \in \mathcal{D}(\mathcal{A}_2)$, we have

$$\frac{d}{dt} \mathbb{E} f(x_1(t), x_2(t)) = \mathbb{E} \mathcal{A}_2(f(x_1(t), x_2(t))). \quad (9.27)$$

Using stochastic differential equations (9.17) - (9.18), we can deduce moment estimates, needed to be able to use unbounded test function (namely $f(x_1, x_2) = x_1$ and $f(x_1, x_2) = x_2$) in the martingale formulation. By taking the mean into eq. (9.17) - (9.18) and neglecting negatives values,

$$\begin{aligned}
0 &\leqslant \mathbb{E}[x_1(t)] \leqslant \int_0^t \lambda_1 b \mathbb{E}[k_1(x_2(s))] ds \leqslant \int_0^t \lambda_1 b(c + \overline{k_1} \mathbb{E}[x_2(s)]) ds \\
0 &\leqslant \mathbb{E}[x_2(t)] \leqslant \int_0^t \lambda_2 \mathbb{E}[x_1(s)] ds
\end{aligned}$$

where we note $b = \mathbb{E}[h] = \int_0^\infty z h(z) dz$. By Grönwall inequalities, there exist a constant C such that

$$
\begin{aligned}
\mathbb{E}\big[\sup_{t \in [0,T]} x_1(t)\big] &\leqslant C(\mathbb{E}[x_1(0)] + e^{CT}) \\
\mathbb{E}\big[\sup_{t \in [0,T]} x_2(t)\big] &\leqslant C(\mathbb{E}[x_2(0)] + e^{CT})
\end{aligned}
\tag{9.28}
$$

Then we claim that $f(x_1, x_2) = x_1$ is in the domain of the generator $\mathcal{A}_2$. We only have to verify (see eq. (9.26))

$$
\mathbb{E} \sum_{T_i \leqslant t} |x_1(T_i) - x_1(T_i^-)| < \infty \text{ for all } t \geqslant 0.
$$

By eq. (9.17)

$$
\begin{aligned}
\mathbb{E} \sum_{T_i \leqslant t} |x_1(T_i) - x_1(T_i^-)| &= \mathbb{E} \int_0^t \int_0^\infty \int_0^\infty 1_{\{r \leqslant \lambda_1 k_1(x_2(s^-))\}} z N(ds, dz, dr), \\
&\leqslant b \lambda_1 \mathbb{E}\big[\int_0^t c + \overline{k_1} x_2(s) ds \big].
\end{aligned}
$$

which is finite according to the previous estimates.

9.3.4 Tightness

S1 We first show the tightness property for the scaling (S1) corresponding to theorem 54. In such case x_1^n does no converge in any functional sense because it fluctuates very fast, as more and more jumps appears of size that stay of order 1 (given by h). However, $\mathbb{E}[x_1^n(t)]$ remains bounded, $\frac{x_1^n}{n}$ goes to 0, and by eq. (9.18),

$$
| x_2^n(t) | \leqslant | x_2^n(0) | + \int_0^t \lambda_2 | x_1^n(s) | ds.
$$

For any n, let N_n be a compound Poisson process associated to eq. (9.17), with $\{T_{n,i}\}_{i=1}^\infty$ the jump times which occur at a rate $n\lambda_1 k_1(x_2^n(s))$, and $\{Z_{n,i}\}_{i=1}^\infty$ the jump sizes that are iid random variables with density h (with the convention $T_{n,0} = 0$ and $Z_{n,0} = X_0$). Then

$$
x_1^n(t) = \sum_{T_{n,i} \leqslant t} Z_{n,i} e^{-n\gamma_1 (t - T_{n,i})} \mathbf{1}_{\{t \geqslant T_{n,i}\}}.
$$

By integration,

$$
\int_0^t x_1^n(s) ds = \sum_{T_{n,i} \leqslant t} Z_{n,i} \frac{1}{n\gamma_1} (1 - e^{-\gamma_1 (t - T_{n,i})}) \mathbf{1}_{\{t \geqslant T_{n,i}\}}.
$$

Then,

$$
x_2^n(t) \leqslant x_2^n(0) + \int_0^t \lambda_2 x_1^n(s) ds \leqslant Y_0 + \frac{\lambda_2}{n\gamma_1} \sum_{T_{n,i} \leqslant t} Z_{n,i}.
$$

Finally we deduce, by definition of the compound Poisson process,

$$
x_2^n(t) \leqslant x_2^n(0) + \frac{\lambda_2}{n\gamma_1} N_n(t).
$$

Now, by a time change, there exists a process Y such that $N_n(t) = Y\big(\int_0^t n\lambda_1 k_1(x_2^n(s)) ds\big)$ with Y an unit rate compound Poisson process of jump size iid (with density h). As

$\mathbb{E}[h] < \infty$, by the law of large number, $\frac{1}{n}Y(nt)$ is almost surely convergent (to $\mathbb{E}[h]t$). Then $\frac{1}{n}Y(nt)$ is almost surely bounded, on a compact time interval $[0, T]$. We deduce then that there exists a random variable C such that

$$x_2^n(t) \leqslant x_2^n(0) + \frac{\lambda_2}{\gamma_1}C \int_0^t \lambda_1 k_1(x_2^n(s))ds.$$

By Grönwall lemma and Markov inequality

$$\mathbb{P}\{ \sup_{t \in [0,T]} x_2^N(t) \geqslant K \} \to 0.$$

Similarly, for any $t_1, t_2 \in [0, T]$,

$$\mid x_2^n(t_2) - x_2^n(t_1) \mid \leqslant \frac{\lambda_2}{n\gamma_1} \mid N_n(t_2) - N_n(t_1) \mid .$$

Again, $N_n(t_2) - N_n(t_1) = Y\Big(\int_{t_1}^{t_2} n\lambda_1 k_1(x_2^n(s))ds \Big)$ and, still by the law of large number

$$\mid x_2^n(t_2) - x_2^n(t_1) \mid \leqslant \frac{\lambda_2}{\gamma_1}C \int_{t_1}^{t_2} \lambda_1 k_1(x_2^n(s))ds,$$

so that , for any $\varepsilon > 0$

$$\lim_{\theta \to 0} \limsup_n \sup_{S_1 \leqslant S_2 \leqslant S_1 + \theta} \mathbb{P}\{ \mid x_2^n(S_2) - x_2^n(S_1) \mid \geqslant \varepsilon \} = 0,$$

where the supremum is over stopping times bounded by T. Then by Aldous' tightness criterion ([70, thm 4.5 p 356]), x_2^n is tight in $(D[0, \infty), S)$.

S3   Now we show the tightness property for the scaling (S3) corresponding to theorem 56, with $\lambda_2^n = n\lambda_2$. In such case x_1^n converges to 0 in L^1, and we get a control over $n \int_0^t x_1^n(s)ds$. Indeed using $g(x_1, x_2) = x_1$ in eq. (9.25), we get

$$x_1^n(t) - x_1^n(0) - \int_0^t (-n\gamma_1 x_1^n(s) + \lambda_1 k_1(x_2^n(s))bds),$$

is a martingale so that due to hypothesis 8, there is a constant C such that

$$\gamma_1 \mathbb{E}\Big[n \int_0^t x_1^n(s)ds\Big] \leqslant \mathbb{E}[x_1^n(0)] + \lambda_1(ct + \overline{k_1} \int_0^t \mathbb{E}[x_2^n(s)]ds)$$

By eq. (9.18),

$$x_2^n(t) \quad \leqslant \quad \mathbb{E}[x_2^n(0)] + \lambda_2 n \int_0^t x_1^n(s)ds.$$

then

$$\sup_{t \in [0,T]} x_2^n(t) \quad \leqslant \quad \mathbb{E}[x_2^n(0)] + \lambda_2 n \int_0^T x_1^n(s)ds.$$

Reporting into the estimates for x_1^n yields

$$\gamma_1 \mathbb{E}\Big[n \int_0^t x_1^n(s)ds\Big] \quad \leqslant \quad \mathbb{E}[x_1^n(0)] + \lambda_1(ct + \overline{k_1}(\mathbb{E}[x_2^n(0)] + t\lambda_2 n \int_0^t \mathbb{E}[x_1^n(s)]ds)),$$

$$\leqslant \quad C_T^1 + C_T^2 \mathbb{E}\Big[n \int_0^t x_1^n(s)ds\Big],$$

for two constants C_T^1, C_T^2 that depends solely on T. By Grönwall inequality, $\mathbb{E}\big[n\int_0^t x_1^n(s)ds\big]$ is bounded uniformly in n so that x_1^n converges to 0 in L^1 and

$$\mathbb{P}\big\{ \sup_{t\in[0,T]} x_2^N(t) \geqslant K\big\} \to 0.$$

Now for any subdivision of $[0,T]$, $0 = t_0 < t_1 < \cdots < t_n = T$,

$$\sum_{i=0}^{n-1} \mid x_2^n(t_{i+1}) - x_2^n(t_i) \mid \;\; \leqslant \;\; \mathbb{E}\big[x_2^n(0)\big] + \lambda_2 n \int_0^t x_1^n(s)ds,$$

so that we also get the tightness of the BV norm,

$$\mathbb{P}\big\{\|x_2^n\|_{[0,T]} \geqslant K\big\} \to 0,$$

as $K \to 0$, independently in n. Then x_2^n is tight in $L^p([0,T])$, for any $1 \leqslant p < \infty$.

S2   Now we show the tightness property for the scaling (S2) corresponding to theorem 55, with $h^n = \frac{1}{n}h(\frac{1}{n})$. Remark that on such case, denoting $z^n = \frac{x_1^n}{n}$, the variables (z^n, x_2^n) satisfies eq. (9.17) - (9.18) with the (S3) scaling, so we already know that x_2^n is tight in $L^p([0,T])$, for any $1 \leqslant p < \infty$.

For x_1^n, note that each jumps gives a contribution for $\int x_1^n$ of $\frac{b}{\gamma_1}$ so there's no hope for a convergence to 0 in L^1. However, we still have

$$x_1^n(t) = \sum_{T_{n,i}\leqslant t} Z_{n,i}e^{-n\gamma_1(t-T_{n,i})} 1_{t\geqslant T_{n,i}}.$$

where $T_{n,i}$ appears with rate $\lambda_1 k_1(x_2^n(s))$, and $\{Z_{n,i}\}_{i=1}^{\infty}$ are iid random variables with density h^n. Then

$$x_1^n(t) \;\; \leqslant \;\; \sum_{T_{n,i}\leqslant t} Z_{n,i}\Big(\mathbf{1}_{\{[T_{n,i}, T_{n,i}+\frac{1}{\sqrt{n}}[\}} + e^{-n\gamma_1\frac{1}{\sqrt{n}}} 1_{t\geqslant T_{n,i}}\Big).$$

But for $K > 0$

$$\mathbb{P}\big\{Z_{n,i}e^{-\sqrt{n}\gamma_1} > K\big\} \leqslant \frac{nb}{Ke^{\sqrt{n}\gamma_1}} \leqslant \varepsilon,$$

for any ε and n sufficiently large. Then, conditioning by the jump times,

$$\int_0^t \mathbb{P}\big\{x_1^n(s) > K \mid T_{n,i}\big\} \leqslant \sum_{T_{n,i}\leqslant t} \frac{1}{\sqrt{n}}\mathbf{1}_{\{t\geqslant T_{n,i}\}} + \sum_{T_{n,i}\leqslant t} \varepsilon(t - T_{n,i})\mathbf{1}_{\{t\geqslant T_{n,i}\}} \leqslant \varepsilon.$$

for n large. Because $\int_0^t x_2^n(s)ds$ has been shown to be bounded independently of n, we can drop the conditioning, and $\int_0^t \mathbb{P}\{x_1^n(s) > K\}$ is arbitrary small. We show also similarly that

$$\lim_{h\to 0}\sup_n \int_0^T \max(1, \mid x_1^n(t+h) - x_1^n(t) \mid)dt = 0,$$

so that x_1^n is tight in $M(0,\infty)$ ([82, thm 4.1]).

9.3.5   Identification with the martingale problem

The three theorems below can be proved using martingale techniques, with similar spirit. For each scaling, the generator $\mathcal{A}_2^n$ can be decomposed into a fast component, or order n, and a slow component, of order 1. In each case, one need to find particular condition to ensure that the fast component vanishes. For the scaling $(S1)$, the fast component acts only in the first variable, so ergodicity of this component will ensure that it vanishes. For the other two, the fast component acts on both variables, and we will have to find the particular relation between both variable that ensures this component vanishes.

9.3.5.1   Proof of theorem 54   For any $B \in \mathbb{B}(\mathbb{R}_+)$, $t > 0$, we define the occupation measure

$$V_1^n(B \times [0,t]) = \int_0^t \mathbf{1}_{\{B\}}(x_1^n(s))ds,$$

and we identify V_1^n as a stochastic process with value in the space of finite measure on $\mathbb{R}^+$. Because $\mathbb{E}\big[x_1^n(t)\big]$ remains bounded uniformly in n on any $[0,T]$, it is stochastically bounded and V_1 then satisfies Aldous criterion of tightness. Now take a test function f that depends only on x_1, so that

$$\mathcal{A}_2^n f(x_1) = nC_{x_2}f(x_1),$$

with

$$C_{x_2}f(x_1) = -\gamma_1 x_1 f'(x_1) + \lambda_1 k_1(x_2)\left(\int_{x_1}^{\infty} h(z-x_1)f(z)dz - f(x_1) \right).$$

Then

$$M_t^n = f(x_1^n(t)) - f(x_1^n(0)) - n\int_{\mathbb{R}_+}\int_0^t C_{x_2^n(s)}f(x_1)V_1^n(dx_1 \times ds)$$

is a martingale. Dividing by n, for any limiting point (V_1, x_2), we must have, for any $f \in C_b(\mathbb{R}_+)$,

$$\mathbb{E}\big[\int_{\mathbb{R}_+}\int_0^t C_{x_2(s)}f(x_1)V_1(dx_1 \times ds)\big] = 0.$$

Because for any x_2, the generator C_{x_2} is (exponentially) ergodic (see paragraph 8.5) V_1 is uniquely determined by the invariant measure associated to C_{x_2}. In particular, for any $t > 0$

$$\int_{\mathbb{R}_+}\int_0^t x_1 V_1^n(dx_1 \times ds) \to \int_0^t \frac{b\lambda_1}{\gamma_1}k_1(x_2(s))ds.$$

Then for f that depends only on x_2,

$$f(x_2^n(t)) - f(x_2^n(0)) - \int_{\mathbb{R}_+}\int_0^t (\lambda_2 x_1 - \gamma_2 x_2^n(s))f'(x_2^n(s))V_1^n(dx_1 \times ds)$$

converges to

$$f(x_2(t)) - f(x_2(0)) - \int_0^t (\frac{b\lambda_1\lambda_2}{\gamma_1}k_1(x_2(s)) - \gamma_2 x_2(s))f'(x_2(s))ds$$

Due to the assumption on k_1, there exists a unique solution associated to the (deterministic) eq. (9.21) so x_2 is uniquely determined.

9.3.5.2   Proof of theorem 56   We already seen that x_1^n converge to 0 in $L^1([0,T])$ and x_2^n is tight in $L^p([0,T])$. Doing similarly as in subsection 9.2, we take a subsequence $(x_1^n(t), x_2^n(t))$ that converge to $(0, x_2(t))$, almost surely and for almost $t \in [0,T]$. Then we consider the fast component of the generator $\mathcal{A}_2^n$, given in this case by

$$-\gamma_1 x_1 \frac{\partial f}{\partial x_1} + \lambda_2 x_1 \frac{\partial f}{\partial x_2}.$$

This defines a transport equation. Starting at (x_1, x_2) at time 0, the asymptotic value of the flow associated to the transport equation is $(0, y)$ where

$$y = x_2 + \int_0^\infty \lambda_2 x_1(s) ds = x_2 + \int_0^{x_1} \frac{\lambda_2 z}{\gamma_1 z} dz = x_2 + \frac{\lambda_2}{\gamma_1} x_1$$

We then consider

$$f(x_1, x_2) = g\Big(x_2 + \frac{\lambda_2}{\gamma_1} x_1\Big),$$

that satisfies, for any x_1, x_2,

$$-\gamma_1 x_1 \frac{\partial f}{\partial x_1} + \lambda_2 x_1 \frac{\partial f}{\partial x_2} = 0.$$

Now taking the limit $n \to \infty$ into

$$f(x_1^n(t), x_2^n(t)) - f(x_1^n(0), x_2^n(0)) - \int_0^t \mathcal{A}_2^n f(x_1^n(s), x_2^n(s)) ds,$$

yields

$$g(x_2(t)) - g(x_2(0)) - \int_0^t -\gamma_2 x_2 g'(x_2(s)) + \lambda_1 k_1(x_2(s)) \left(\int_0^\infty \bar{h}(z) g(x_2(s) + z) dz - g(x_2(s)) \right) ds,$$

where $\bar{h}(x_2) = (\lambda_2/\gamma_1)^{-1} h((\lambda_2/\gamma_1)^{-1} x_2)$. Hence the limiting process x_2 must satisfy the martingale problem associated with the generator

$$\mathcal{A}_\infty g(x) = -\gamma_2 x \frac{dg}{dx} + \lambda_1 k_1(x) \Big(\int_x^\infty \bar{h}(z - x) f(z) dz - f(x) \Big),$$

for which uniqueness holds for bounded k_1 (see [25, thm 2.5] or theorem 9 in Chapter 0). A truncation argument allows then to conclude.

9.3.5.3   Proof of theorem 55   As noticed before, (z^n, x_2^n) with $z^n(t) = \frac{x_1^n(t)}{n}$ satisfies the scaling (S3) so similar conclusion holds for x_2^n. The last conclusion on x_1^n is differed to the next subsection.

9.3.6   The case without auto-regulation

In this subsection, we give an alternative proof of the identification of the limit, using the characteristic functional of the stochastic process. This can works when there's no non-linearity, and eq. (9.15) - (9.16) can actually be seen as generalized Langevin equation. We consider the equations

$$\frac{dx_1}{dt} = -\gamma_1 x_1 + \mathring{N}(h, \lambda_1), \quad x_1(0) = x_1^0 \geqslant 0, \tag{9.29}$$

$$\frac{dx_2}{dt} = -\gamma_2 x_2 + \lambda_2 x_1, \quad x_2(0) = x_2^0 \geqslant 0, \tag{9.30}$$

where $\mathring{N}(h, \lambda_1)$ is a compound Poisson *white noise*. The solutions $x_1(t)$ and $x_2(t)$ of eq. (9.29) - (9.30) are stochastic processes uniquely determined by the equation parameters and the stochastic process $\mathring{N}$.

For a stochastic process ξ_t $(t \geqslant 0)$, the characteristic functional $C_\xi : \Sigma \to \mathbb{R}$ is defined as

$$C_\xi[f] = \mathbb{E}\left[e^{\int_0^\infty if(t)\xi_t dt} \right],$$

for any function f in a suitable function space Σ so that the integral $\int_0^\infty if(t)\xi_t dt$ is well defined. Before continuing, we need to introduce some topological background as well as properties of the Fourier transform in nuclear spaces (see [44])

9.3.6.1   Stochastic process as a distribution

We are going to recall here the continuous correspondence between a stochastic process and a distribution. We define $D(\mathcal{R}^+)$, the space of smooth functions with compact support, with the inductive limit topology given by the family of semi-norms $(k = 0, 1, 2...)$ $p_k(f) = \sup|f^{(k)}|$ on every $D([0, n])$, $n \in \mathcal{N}$ (c.f. [125, Example 2, page 57]). Let $f \in D(\mathcal{R}^+)$, and define $\tilde{x}$ in the dual space $D'(\mathcal{R}^+)$ such that

$$\tilde{x}(f) = \int_0^\infty x(t) f(t) dt \tag{9.31}$$

for any x in $D[0, \infty)$, and analogous definition for $x \in L^p[0, T]$ or $M(0, \infty)$.

Lemma 58. *The map*

$$(D[0, \infty), S) \to D'(\mathcal{R}^+)$$
$$(x_t)_{t \geqslant 0} \mapsto \tilde{x},$$

where $\tilde{x}$ is defined by eq. (9.31), is continuous.

Proof. It is a classical result that $x \in \mathcal{D}$ has at most a countable number of discontinuity points so that x is locally integrable, the integral in eq. (9.31) is well defined for all $f \in D(\mathcal{R}^+)$, $\tilde{x} \in D'(\mathcal{R}^+)$ and

$$| \tilde{x}(f) | \leqslant \left(\int_0^T | x(s) | ds \right) \| f \|_\infty,$$

for any f with support in $[0, T]$ [121, Section 6.11, page 142]. We conclude by noticing that

$$| \tilde{x}(f) | \leqslant \sup_{s \leqslant T} | x(s) | \| f \|_\infty T,$$

and $x \mapsto \sup_{s \leqslant T} | x(s) |$ is continuous for the Skorohod topology [70, Proposition 2.4, page 339] for all T such that T is not a discontinuity point. $\square$

Similar continuity property holds respectively in $\mathcal{D}\big((0, \infty), J\big)$, $L^p[0, T]$, $M[0, \infty]$.

9.3.6.2   Bochner-Minlos theorem for a nuclear space

Let E be a nuclear space. We state a key result that will allow us to uniquely identify a measure on the dual E' of E.

Bochner-Minlos Theorem. *[44, Theorem 2, page 146] For a continuous functional C on a nuclear space E that satisfies $C(0) = 1$, and for any complex z_j and elements $x_j \in A$, $j, k = 1, ..., n$,*

$$\sum_{j=1}^n \sum_{k=1}^n z_j \bar{z}_k C(x_j - x_k) \geqslant 0,$$

there is a unique probability measure μ on the dual space E', given by

$$C(y) = \int_{E'} e^{i\langle x, y \rangle} d\mu(x).$$

Note that the space $D(\mathcal{R}^+)$ is a nuclear space [125, Example 2, page 107].

9.3.6.3   The characteristic functional of a Poisson white noise   The use of the characteristic functional allows us to define a generalized stochastic process that does not necessarily have a trajectory in the usual sense (like in $\mathcal{D}$ for instance). Indeed a (compound) Poisson white noise is seen as a random measure on the distribution space D', associated with the characteristic functional (given in [61], here $f \in D(\mathcal{R}^+)$)

$$C_{\mathring{N}}[f] = \exp\left[\varphi \int_0^\infty \int_0^\infty (e^{izf(t)} - 1)h(z)dzdt \right], \tag{9.32}$$

where φ is the Poisson intensity and h the jump size distribution. It is not hard to see that $C_{\mathring{N}}[f - g]$ and $C_{\mathring{N}}[g - f]$ are conjugate to each other, $C_{\mathring{N}}[0] = 1$ and $C_{\mathring{N}}[.]$ is continuous for $h \in L^1(\mathcal{R}^+)$, so the conditions in the Bochner-Minlos theorem 9.3.6.2 are satisfied and therefore $C_{\mathring{N}}$ uniquely defines a measure on $D'(\mathcal{R}^+)$.

Remark 59. *To see that this measure indeed corresponds to the time derivative of the compound Poisson process, consider the following*

$$\mathbb{E}\left[e^{i\langle \mathring{N}, f \rangle} \right] = \lim_{|\Delta_j| \to 0} \mathbb{E}\left[e^{i\sum_j f(t_j) \Delta_j N} \right],$$

where $\Delta_j N = N(t_{j+1}) - N(t_j)$ denotes the increment of a compound Poisson process, and (t_j) is some subdivision of $\mathcal{R}^+$ of maximal step size Δ_j. Due to the independence of the increments of the Poisson process, this limit can be re-written as

$$\mathbb{E}\left[e^{i\langle \mathring{N}, f \rangle} \right] = \lim_{|\Delta_j| \to 0} \prod_j \mathbb{E}\left[e^{if(t_j) \Delta_j N} \right].$$

Now, because of the independence of the jump size and the number of jumps, and the fact that all jumps are independent and identically distributed (with distribution given by h),

$$
\begin{aligned}
\mathbb{E}\left[e^{if(t_j)\Delta_j N} \right] &= \sum_n \mathbb{E}\left[e^{if(t_j)\Delta_j N} \mid \Delta_j N = n \right] \\
&= \sum_n \mathbb{E}\left[e^{if(t_j)(Z_1 + \cdots + Z_n)} \mid \Delta_j N = n \right] \\
&= \sum_n \mathbb{E}\left[e^{if(t_j)(Z_1 + \cdots + Z_n)} \right] \mathbb{P}(\Delta_j N = n) \\
&= \sum_n \left(\mathbb{E}\left[e^{if(t_j)Z} \right] \right)^n \mathbb{P}(\Delta_j N = n) \\
&= e^{-\varphi \Delta_j} \sum_n \left(\int_0^\infty e^{if(t_j)z} h(z)dz \right)^n \frac{(\varphi \Delta_j)^n}{n!} \\
&= exp\left[\varphi \Delta_j \left(\int_0^\infty e^{if(t_j)z} h(z)dz - 1 \right) \right],
\end{aligned}
$$

so

$$
\begin{aligned}
\mathbb{E}\left[e^{i\langle \mathring{N}, f \rangle} \right] &= \lim_{|\Delta_j| \to 0} exp\left[\varphi \sum_j \Delta_j \left(\int_0^\infty e^{if(t_j)z} h(z)dz - 1 \right) \right] \\
&= \exp\left[\varphi \int_0^\infty \int_0^\infty (e^{izf(t)} - 1)h(z)dzdt \right].
\end{aligned}
$$

We refer to [108, 61, 62] for further material on characteristic functionals and generalized stochastic processes.

9.3.6.4   Identification of the limit using characteristic functional   The proofs of theorems 54 to 56 are based on the idea of Levy's continuity theorem. However in the infinite-dimensional case, the convergence of the Fourier transform does not imply convergence in law of the random variable, and one needs to impose more restrictions, namely a compactness condition. We will use the following lemma

Lemma 60. *Let X^n be a sequence of stochastic processes in $(D[0, \infty), S)$. Suppose X^n is tight in $(D[0, \infty), S)$ (respectively in $\mathcal{D}\big((0, \infty), J\big)$, $L^p[0, T]$, $M[0, \infty]$) and that there exists a random variable X such that, for all f in $D(\mathcal{R}^+)$, as $n \to \infty$,*

$$C_{X^n}[f] \to C_X[f].$$

Then X^n converges in law to X in $\mathcal{D}\big((0, \infty), S\big)$ (respectively in $\mathcal{D}\big((0, \infty), J\big)$, $L^p[0, T]$, $M[0, \infty]$).

Proof. The convergence of the characteristic functional, the Bochner-Minlos theorem 9.3.6.2 and the continuity lemma 58 ensure that the sequence X^n has at most one limiting law, which has to be the law of X. The classical Prokhorov Theorem [70, Corollary 3.9, page 348] states that tightness of X^n in $(D[0, \infty), S)$ is equivalent to relative compactness of the law of X^n in $\mathcal{P}(\mathcal{D})$, the space of probability measures on $\mathcal{D}$ (with the topology of the weak convergence). Then X^n converges in law to X in $(D[0, \infty), S)$. The continuity lemma and Prokhorov theorem are also valid in $\mathcal{D}\big((0, \infty), J\big)$, $L^p[0, T]$, $M[0, \infty]$ (see part 0 section 7). $\qquad\square$

Note that the tightness property has already been done in paragraph 9.3.4. Now, we give the identification property of the limit for theorems 54 through 56. The strategy is similar for each, and we only present a detailed proof for theorem 54 and sketch the main differences in the proofs for theorems 55 and 56.

For any $f \in D(\mathcal{R}^+)$, from eq. (9.29) - (9.30) and noting that the initial conditions x_1^0 and x_2^0 are deterministic, it is not difficult to verify that (see also [19])

$$C_{x_1}[f] = e^{ig_1 x_1^0} C_{\mathring{N}}[\tilde{f}_1(t)], \quad C_{x_2}[f] = e^{ig_2 x_2^0} C_{x_1}[\lambda_2 \tilde{f}_2(t)], \tag{9.33}$$

where

$$g_i = \int_0^\infty e^{-\gamma_i s} f(s) ds, \quad \tilde{f}_i(t) = \int_t^\infty e^{-\gamma_i(s-t)} f(s) ds, \quad (i = 1, 2).$$

Note that for any function $f \in D(\mathcal{R}^+)$ the functions $\tilde{f}_i(t)$ also belong to $D(\mathcal{R}^+)$ and therefore the characteristic functionals in eq. (9.33) are well-defined. Furthermore, the characteristic functional of the compound Poisson white noise has been derived in eq. (9.32).
Proof of theorem 54.

Recall that $\lambda_1^n = n\lambda_1$. We omit the dependence in n of function g_i and $\tilde{f}_i$ for simplicity. Now, we are ready to complete the proof by calculating the characteristic functionals $C_{x_1^n}$ and $C_{x_2^n}$ when $n \to \infty$ from eq. (9.33) and (9.32). Firstly, we note that $g_i = \tilde{f}_i(0)$, and when $f \in D(\mathcal{R}^+)$ and $n \to \infty$,

$$\tilde{f}_1(t) = \frac{1}{n\gamma_1} f(t) + O(\frac{1}{n^2}). \tag{9.34}$$

Furthermore, from eq. (9.33) - (9.34), we have

$$
\begin{aligned}
C_{x_1^n}[f] & = e^{ix_1^0(\frac{1}{n\gamma_1}f(0)+O(\frac{1}{n^2}))} C_{\mathring{N}}\left[\frac{1}{n\gamma_1}f(t)+O(\frac{1}{n^2})\right] \\
& = e^{i\frac{1}{n\gamma_1}x_1^0 f(0)} \exp\left[i\int_0^\infty\int_0^\infty \frac{\lambda_1}{\gamma_1}f(t)xh(x)dxdt\right] + O(\frac{1}{n}). \qquad (9.35)
\end{aligned}
$$

Thus, from eq. (9.20), we have

$$
\lim_{n\to\infty} C_{x_1^n}[f] = \exp\left[i\int_0^\infty f(t)x_1^{eq}dt\right], \quad \forall f\in D. \qquad (9.36)
$$

Therefore, eq. (9.33) yields

$$
\begin{aligned}
\lim_{n\to\infty} C_{x_2^n}[f] & = e^{ig_2 x_2^0}\exp\left[i\lambda_2\int_0^\infty \tilde{f}_2(t)x_1^{eq}dt\right] \\
& = e^{ig_2 x_2^0}\exp\left[i\int_0^\infty f(s)(1-e^{-\gamma_2 s})x_2^{eq}ds\right]. \qquad (9.37)
\end{aligned}
$$

Now, it is easy to verify that the right hand sides of eq. (9.36) and (9.37) give, respectively, the characteristic functional of $x_1(t)\equiv x_1^{eq}$ and $x_2(t)$ of the solution of eq. (9.23). Hence we are done.

Proof of theorem 55. Recall that $h^n(x)=\frac{1}{n}h(\frac{x}{n})$. The proof is similar to the proof of theorem 55. Note simply from the scaling (S2) that eq. (9.35) becomes, still from eq. (9.33) - (9.34)

$$
C_{x_1^n}[f] = e^{i\frac{1}{n\gamma_1}x_1^0 f(0)+O(\frac{1}{n^2})}\exp\left[\lambda_1\int_0^\infty\int_0^\infty (e^{i\frac{z}{n\gamma_1}f(t)+O(\frac{1}{n^2})}-1)h^n(z)dzdt\right].
$$

Thus, by a change of variable $x=z/(\gamma_1 n)$, we have

$$
C_{x_1^n}[f] = e^{i\frac{1}{n\gamma_1}x_1^0 f(0)+O(\frac{1}{n^2})}\exp\left[\lambda_1\int_0^\infty\int_0^\infty (e^{ixf(t)+O(\frac{1}{n})}-1)\tilde{h}(x)dxdt\right],
$$

where $\tilde{h}(x)=\gamma_1 h(\gamma_1 x)$. Then

$$
\begin{aligned}
\lim_{n\to\infty} C_{x_1^n}[f] & = \exp\left[i\lambda_1\int_0^\infty\int_0^\infty (e^{if(t)x}-1)\tilde{h}(x)dxdt\right] \\
& = C_{\mathring{N}}[f].
\end{aligned}
$$

where $\mathring{N}$ is a compound Poisson white noise of intensity λ_1 and jump size distributed according to $\tilde{h}$. Furthermore, from eq. (9.33)

$$
\begin{aligned}
\lim_{n\to\infty} C_{x_2^n}[f] & = e^{ig_2 x_2^0}G_{\mathring{N}}[\lambda_2\tilde{f}_2(t)] \\
& = e^{ig_2 x_2^0}\exp\left[i\lambda_1\int_0^\infty\int_0^\infty (e^{i\lambda_2 x\tilde{f}_2(t)}-1)\tilde{h}(x)dxdt\right] \\
& = e^{ig_2 x_2^0}\exp\left[i\lambda_1\int_0^\infty\int_0^\infty (e^{ix\tilde{f}_2(t)}-1)\bar{h}(x)dxdt\right], \qquad (9.38)
\end{aligned}
$$

where $\bar{h}(x_2)=(\lambda_2/\gamma_1)^{-1}h((\lambda_2/\gamma_1)^{-1}x_2)$ It is easy to verify that eq. (9.38) is just the characteristic functional of the stochastic processes given by solutions of eq. (9.24).

Proof of theorem 56 Here, $\lambda_2^n=n\lambda_2$. we have

$$
\lim_{n\to\infty} C_{x_1^n}[f] = \lim_{n\to\infty}\exp\left[\lambda_1\int_0^\infty\int_0^\infty (e^{if(t)x/(n\gamma_1)}-1)h(x)dxdt\right] = 1,
$$

and

$$
\begin{aligned}
\lim_{n \to \infty} C_{x_2^n}[f] &= e^{ig_2 x_2^0} \exp\left[\lambda_1 \int_0^\infty \int_0^\infty (e^{i(\lambda_2/\gamma_1)x\tilde{f}_2(t)} - 1)h(x)\,dx\,dt\right] \\
&= e^{ig_2 x_2^0} \exp\left[\lambda_1 \int_0^\infty \int_0^\infty (e^{ix\tilde{f}_2(t)} - 1)\bar{h}(x)\,dx\,dt\right],
\end{aligned}
$$

where

$$
\bar{h}(x) = \frac{\gamma_1}{\lambda_2} h\left(\frac{\gamma_1}{\lambda_2}x\right).
$$

$\square$

9.3.7   Reduction on the evolution equation

We conclude by a third proof for the reduction, working on the partial differential equation for the evolution equations on densities. Because we work directly on the strong form, results are weaker. In particular,

Hypothesis 9. *In addition of hypothesis 8, we assume that*
    (H1) *The density function $h \in \mathcal{C}^\infty$, and for all $k \geqslant 1$, $\int_0^\infty z^k h(z)\,dz < \infty$.*
    (H2) *The rate function $k_1 \in \mathcal{C}^\infty$, and k_1 is bounded above and under,*

$$
0 < \underline{k_1} \leqslant k_1(x) \leqslant \overline{k_1},
$$

Theses assumption are needed to ensure that evolution equation on densities is well defined (see section 8.2), and allow us to derive scaling laws for arbitrary moments, that are needed for calculus. Regularity will allow us to derive at any order the density functions, which is also needed for the calculus. We start by a scaling property of the moments, which is crucial for the convergence results.

9.3.7.1   Scaling of the marginal moment   Using the generator $\mathcal{A}_2$ for the two-dimensional stochastic process defined by eq. (9.25), we can deduce the scaling laws of the marginal moment of $x_1(t)^n$ as $\gamma_1^n \to \infty$.

Proposition 61. *Let $(x_1^n(t), x_2^n(t))$ be the solutions of eq. (9.15) - (9.16), and $\mu_k^n(t) = \mathbb{E}\big[x_1^n(t)^k\big]$ and $\nu_k^n(t) = \mathbb{E}\big[x_2^n(t)x_1^n(t)^k\big]$. Suppose $\mu_k^n(0) < \infty$ and $\nu_k^n(0) < \infty$ for all $n \geqslant 1$, then $\mu_k^n(t) < \infty$ and $\nu_k^n(t) < \infty$ for all t, $n \geqslant 1$. Moreover, for fixed $t > 0$,*

    1. If the scaling (S1) holds, then both $\mu_k^n(t)$ and $\nu_k^n(t)$ stay uniformly bounded above and below as $n \to \infty$.

    2. For the scaling (S2), then, for $k \geqslant 1$,

$$
\mu_k^n(t) \sim n^{k-1}, \quad \nu_k^n(t) \sim n^{k-1}, \quad (n \to \infty)
$$

      and $\nu_0^n(t)$ is uniformly bounded above and below as $n \to \infty$.

    3. If (S3) holds then, for $k \geqslant 1$,

$$
\mu_k^n(t) \sim n^{-1}, \quad \nu_k^n(t) \sim n^{-1}, \quad (n \to \infty)
$$

      and $\nu_0^n(t)$ is uniformly bounded above and below as $n \to \infty$.

Proof. The proposition is proved using the evolution equation for the marginal moment obtained from the generator $\mathcal{A}_2^n$.

Firstly, we claim that functions x_1^k and $x_1^k x_2$ ($\forall k \in \mathbb{N}^*$) are contained in $\mathcal{D}(\mathcal{A}_2^n)$, for all $n \geqslant 1$. To show this, we only need to verify that

$$\mathbb{E} \sum_{T_i \leqslant t} |x_1^n(T_i)^k x_2^n(T_i^-)^l - x_1^n(T_i^-)^k x_2^n(T_i^-)^l| < \infty, \quad \forall t \geqslant 0, k \in \mathbb{N}^*, l = 0, 1,$$

where the T_i are jump times (that also depends on the scaling n). Since $x_2^n(t)$ is continuous and from estimates eq. (9.28), $\mathbb{E}\big[\sup_{[0,T]} x_2^n(t)\big]$ is bounded. Then we only need to verify the case with $l = 0$. Now by eq. (9.17),

$$\mathbb{E} \sum_{T_i \leqslant t} |x_1^n(T_i)^k - x_1^n(T_i^-)^k| = \mathbb{E} \int_0^t \int_0^\infty \int_0^\infty 1_{\{r \leqslant \lambda_1^n k_1(x_2^n(s-))\}} z^k N^n(ds, dz, dr),$$

$$= b_k^n \lambda_1^n \mathbb{E}\Big[\int_0^t k_1(x_2^n(s))ds\Big],$$

where we note $b_k^n = \int_0^\infty z^k h^n(z) dz$ (so $b_0^n = 1$ and $b_1^n = b^n$). As k_1 is assumed to be linearly bounded, still by estimates eq. (9.28) we conclude that

$$\mathbb{E} \sum_{T_i \leqslant t} |x_1^n(T_i)^k - x_1^n(T_i^-)^k| < \infty, \quad \forall t > 0, \quad \forall n \geqslant 1$$

Now, $\mathcal{A}_2^n x_1^k$ and $\mathcal{A}_2^n x_1^k x_2$ are well defined, for all $k > 0$ and $n \geqslant 1$. A straightforward calculation yields

$$\mathcal{A}_2^n x_1^k = -\gamma_1^n k x_1^k + \lambda_1^n k_1(x_2)\left(\int_{x_1}^\infty h^n(z - x_1)(z - x_1 + x_1)^k dz - x_1^k\right)$$

$$= -\gamma_1^n k x_1^k + \lambda_1^n k_1(x_2) \sum_{i=0}^{k-1} \binom{k}{i} x_1^i \int_{x_1}^\infty h^n(z - x_1)(z - x_1)^{k-i} dz$$

$$= -\gamma_1^n k x_1^k + \lambda_1^n k_1(x_2) \sum_{i=0}^{k-1} \binom{k}{i} x_1^i b_{k-i}^n.$$

Then the kth-marginal moment $\mu_k^n(t)$ of the first variable x_1^n depends only on the lower moment $\mu_i^n(t)$, $i < k$. We then obtain, with hypothesis eq. (9) and eq. (9.27)

$$-\gamma_1^n k \mu_k^n(t) + \lambda_1^n \underline{k_1} \sum_{i=0}^{k-1} \binom{k}{i} \mu_i^n(t) b_{k-i}^n \leqslant \dot{\mu}_k^n(t),$$

$$\dot{\mu}_k^n(t) \leqslant -\gamma_1^n k \mu_k^n(t) + \lambda_1^n \overline{k_1} \sum_{i=0}^{k-1} \binom{k}{i} \mu_i(t) b_{k-i}^n. \tag{9.39}$$

Recall that in all scalings $\gamma_1^n = n\gamma_1$.

Assume scaling (S1), $\lambda_1^n = n\lambda_1$, and h^n, λ_2^n are independent of n. Inequalities eq. (9.39) for $k = 1$ yields, for all $t > 0$,

$$n\lambda_1 \underline{k_1} b \leqslant \dot{\mu}_1^n(t) + n\gamma_1 \mu_1^n(t) \leqslant n\lambda_1 \overline{k_1} b.$$

Multiplying by $e^{n\gamma_1 t}$, a direct integration yields

$$\frac{\lambda_1 \underline{k_1} b}{\gamma_1}(e^{n\gamma_1 t} - 1) \leqslant e^{n\gamma_1 t} \mu_1^n(t) - \mu_1^n(0) \leqslant \frac{\lambda_1 \overline{k_1} b}{\gamma_1}(e^{n\gamma_1 t} - 1),$$

so finally

$$\frac{\lambda_1 \underline{k_1} b}{\gamma_1} + O(\frac{1}{n}) \leqslant \mu_1^n(t) \leqslant \frac{\lambda_1 \overline{k_1} b}{\gamma_1} + O(\frac{1}{n}).$$

Iteratively, for all $t > 0$ and $k > 1$, there is a constant $c_k(t) > 0$ independent of γ_1 (where $c_k(t)$ depends only on the moment of h and lower moments $\mu_j^n(t)$, $j < k$) such that

$$\frac{\lambda_1 \underline{k_1} c_k(t)}{\gamma_1} + O(\frac{1}{n}) \leqslant \mu_k^n(t) \leqslant \frac{\lambda_1 \overline{k_1} c_k(t)}{\gamma_1} + O(\frac{1}{n}).$$

Assume (S2) *i.e.* $b_k^n = n^k b_k$. The case $k = 1$ follows directly from the above calculations, and for all $k > 1$ and $t > 0$,

$$\frac{\lambda_1 \underline{k_1} n^k b_k}{kn\gamma_1} + O(n^{k-2}) \leqslant \mu_k^n(t) \leqslant \frac{\lambda_1 \overline{k_1} n^k b_k}{n\gamma_1} + O(n^{k-2}).$$

Finally, assume (S3). The same method shows that for all $t > 0$ and $k \geqslant 1$, there is a constant c_k independent of γ_1 (c_k depends of the moment of h and of λ_1) such that

$$\frac{c_k}{n\gamma_1} + O(\frac{1}{n^2}) \leqslant \mu_k^n(t) \leqslant \frac{c_k}{n\gamma_1} + O(\frac{1}{n^2}).$$

A similar calculation with $g(x_1, x_2) = x_2 x_1^k$ gives analogous scaling. Namely, we have

$$\mathcal{A}_2^n x_1^k x_2 = (-\gamma_1^n k - \gamma_2) x_1^k x_2 + \lambda_2^n x_1^{k+1} + \lambda_1^n k_1(x_2) \sum_{i=0}^{k-1} \binom{k}{i} x_1^i b_{k-i}^n,$$

so that, for $k \geqslant 1$,

$$(-\gamma_1^n k - \gamma_2) \nu_k^n(t) + \lambda_2^n \mu_{k+1}^n + \lambda_1^n \underline{k_1} \sum_{i=0}^{k-1} \binom{k}{i} \mu_i^n(t) b_{k-i}^n$$

$$\leqslant \dot{\nu}_k^n(t) \leqslant (-\gamma_1^n k - \gamma_2) \nu_k^n(t) + \lambda_2^n \mu_{k+1}^n + \lambda_1^n \overline{k_1} \sum_{i=0}^{k-1} \binom{k}{i} \mu_i^n(t) b_{k-i}^n,$$

while for $k = 0$, we obtain

$$\dot{\nu}_0^n = -\gamma_2 \nu_0 + \lambda_2^n \mu_1^n.$$

Then ν_0^n is uniformly bounded for each scaling (S1),(S2), and (S3). Then, using iteratively the inequalities for $\dot{\nu}_k^n$, the scaling of μ_{k+1}^n and direct integration yields the desired result for each scaling. $\qquad\square$

9.3.7.2 Density evolution equations Let $u^n(t, x_1, x_2)$ be the density function of $(x_1^n(t), x_2^n(t))$ at time t obtained from the solutions of eq. (9.15) - (9.16). The evolution of the density $u^n(t, x_1, x_2)$ is governed by

$$\begin{aligned}
\frac{\partial u^n(t, x_1, x_2)}{\partial t} &= \frac{\partial}{\partial x_1}[\gamma_1^n x_1 u^n(t, x_1, x_2)] - \frac{\partial}{\partial x_2}[(\lambda_2^n x - \gamma_2 x_2) u^n(t, x_1, x_2)] \\
&\quad + \int_0^{x_1} \lambda_1^n k_1(x_2) u^n(t, z, x_2) h^n(x_1 - z) dz - \lambda_1^n k_1(x_2) u^n(t, x_1, x_2)
\end{aligned}$$
$$(9.40)$$

when $(t, x_1, x_2) \in (0, +\infty)^3$. In this subsection, we prove that when $n \to \infty$ the density function $u^n(t, x_1, x_2)$ approaches the density $v(t, x_2)$ for solutions of either the deterministic

eq. (9.21) or the stochastic differential eq. (9.22) depending on the scaling. Evolution of the density function for eq. (9.21) is given by [83]

$$\frac{\partial v(t, x_2)}{\partial t} = -\frac{\partial}{\partial x_2}[-\gamma_2 x_2 u_0 + \lambda_2 k(x_2) u_0]. \tag{9.41}$$

Here we note that

$$k(x_2) = b\lambda_1 k_1(x_2)/\gamma_1.$$

Evolution of the density for eq. (9.22) is given by

$$\frac{\partial v(t, x_2)}{\partial t} = \frac{\partial}{\partial x_2}[\gamma_2 x_2 v(t, x_2)] + \int_0^{x_2} \lambda_1 k_1(z) v(t, z) \bar{h}(x_2 - z) dz - \lambda_1 k_1(x_2) v(t, x_2) \tag{9.42}$$

when $(t, x_2) \in (0, +\infty)^2$. Here $\bar{h}$ is given by

$$\bar{h}(x_2) = \frac{\gamma_1}{\lambda_2} h(\frac{\gamma_1}{\lambda_2} x_2). \tag{9.43}$$

When hypothesis 9 is satisfied, existence of the above densities have been rigorously proved in [90, 145]. In particular, for a given initial density

$$u(0, x_1, x_2) = p(x_1, x_2), \quad 0 < x, y < +\infty \tag{9.44}$$

that satisfies

$$p(x_1, x_2) \geqslant 0, \quad \int_0^\infty \int_0^\infty p(x_1, x_2) dx_1 dx_2 = 1,$$

there is a unique solution $u(t, x_1, x_2)$ (we drop the indices n for now, the following is valid for any $n \geqslant 1$) of eq. (9.40) that satisfies the initial condition eq. (9.44) and

$$u(t, x_1, x_2) \geqslant 0, \quad \int_0^\infty \int_0^\infty u(t, x_1, x_2) dx_1 dx_2 = 1$$

Moreover, if the moments of the initial density satisfy

$$u_k(x_2) = \int_0^\infty x_1^k p(x_1, x_2) dx_1 < +\infty, \quad \forall x_2 > 0, k = 0, 1, \cdots, \tag{9.45}$$

then the marginal moments

$$u_k(t, x_2) = \int_0^\infty x_1^k u(t, x_1, x_2) dx_1,$$

are well defined for $t > 0$ and a.e. $x_2 > 0$, since moments stay finite from the discussion in paragraph 9.3.7.1. Therefore

$$\lim_{x_1 \to \infty} x_1^k u(t, x_1, x_2) = 0, \quad \forall t, a.e\ x_2. \tag{9.46}$$

Here, we will show, using semigroup techniques as in [90, 145], that under the hypothesis 9, the densities are smooth. We will use the following result

Proposition 62. *[103, Corollary 5.6, page 124] Let Y be a subspace of a Banach space X, with $(Y, \| \cdot \|_Y)$ a Banach space as well. Let $T(t)$ be a strongly continuous semigroup on X, with infinitesimal generator C. Then Y is an invariant subspace of $T(t)$ if*
   – For sufficiently large λ, Y is an invariant subspace of $R(\lambda, C)$

– *There exist constants c_1 and c_2 such that, for $\lambda > c_2$,*

$$\parallel R(\lambda, C)^j \parallel_Y \leqslant c_1(\lambda - c_2)^{-j}, \;\; j = 1, 2 ...$$

– *For $\lambda > c_2$, $R(\lambda, C)Y$ is dense in Y.*

Then, we have

Lemma 63. *Assume hypothesis 9. If the initial condition $v(0, x_2) \in \mathcal{C}^\infty \bigcap L^1$ then the unique solution of eq. (9.42) (respectively eq. (9.41)) $v(t, x_2) \in \mathcal{C}^\infty \bigcap L^1$. Similarly if the initial condition $u(0, x_1, x_2) \in (\mathcal{C}^\infty)^2 \bigcap L^1$ then the unique solution of eq. (9.40) $u(t, x_1, x_2) \in (\mathcal{C}^\infty)^2 \bigcap L^1$.*

Proof. Because the dynamical system given by eq. (9.21) is smooth and invertible, the result for eq. (9.41) is standard [83, Remark 7.6.2 page 187]. We will show that the result for eq. (9.42), and the result for eq. (9.40) will follow in a similar fashion. We need to show that the subspace $\mathcal{C}_0^\infty \subseteq L^1$ is invariant under the action of the semigroup defined by eq. (9.42). According to [90] (and references therein), we know that the semigroup defined by eq. (9.42) is a strongly continuous semigroup whose infinitesimal generator C is characterized by the resolvent

$$R(\lambda, C)v = \lim_{N \to \infty} R(\lambda, A) \sum_{j=0}^{N} (P(\lambda_1 k_1 R(\lambda, A)))^j v, \tag{9.47}$$

for all $v \in L^1$, $\lambda > 0$, where the limit holds in L^1 and A and P are the operators given by

$$Av(x_2) = \frac{d(\gamma_2 x_2 v)}{dx_2} - \lambda_1 k_1(x_2)v(x_2),$$
$$Pv(x_2) = \int_0^{x_2} v(z)h(x_2 - z)dz,$$

and the resolvent $R(\lambda, A)$ is given by, for all $v \in L^1$,

$$R(\lambda, A)v(x_2) = \int_{x_2}^{\infty} \frac{1}{\gamma_2 x_2} e^{Q_\lambda(z) - Q_\lambda(x_2)} v(z) dz,$$

with $Q_\lambda(x_2) = -\frac{\lambda ln(x_2)}{\gamma_2} - \int_1^{x_2} \frac{\lambda_1 k_1(z)}{\gamma_2 z} dz$. We also know that for

$$v \in \mathcal{D}(A) = \{v \in L^1 \; : \; (x_2 v) \text{ is absolutely continuous and } \left(\frac{d(x_2 v)}{dx_2}\right) \in L^1\},$$

we have

$$Cv = Av + P(\lambda_1 k_1 v). \tag{9.48}$$

We will now use the result from by proposition 62 above to complete the proof. Note that according to hypothesis 9, Q_λ is a $\mathcal{C}^\infty$ decreasing function, so that for $v \in \mathcal{C}_0^\infty$, $R(\lambda, A)v \in \mathcal{C}_0^\infty$. Moreover, a simple computation yields, for all $\lambda > \gamma$,

$$\mid R(\lambda, A)v(x_2) \mid \;\; \leqslant \;\; \sup_{(x_2, \infty)} \mid v(z) \mid \frac{1}{\lambda - \gamma} \leqslant \parallel v \parallel_\infty \frac{1}{\lambda - \gamma}.$$

Then

$$\parallel (P(\lambda_1 k_1 R(\lambda, A)))v \parallel_\infty \leqslant \parallel v \parallel_\infty \frac{\lambda_1 \overline{k_1}}{\lambda - \gamma},$$

and

$$\| \, (P(\lambda_1 k_1 R(\lambda, A)))^j v \, \|_\infty \leqslant \| \, v \, \|_\infty \left(\frac{\lambda_1 \overline{k_1}}{\lambda - \gamma} \right)^j,$$

so that convergence in eq. (9.47) holds in $\mathcal{C}^\infty$ and $\mathcal{C}_0^\infty$ is invariant for $R(\lambda, C)$. The second condition in proposition 62 follows then by the previous calculations. Finally, because $R(\lambda, C) = (\lambda - C)^{-1}$, to show that $R(\lambda, C)\mathcal{C}_0^\infty$ is dense in $\mathcal{C}_0^\infty$, it is enough to show that

$$(\lambda - C)\mathcal{C}_0^\infty \subseteq \mathcal{C}_0^\infty.$$

According to eq. (9.48) and hypothesis 9, this is true. $\square$

The main result given below shows that when n is large enough,

$$u_0^n(t, x_2) = \int_O^\infty u^n(t, x_1, x_2) dx_1$$

gives an approximate solution of eq. (9.41) or eq. (9.42).

Theorem 64. *Assume hypothesis 9. Let $u^n(0, x_1, x_2) \in (\mathcal{C}^\infty)^2 \bigcap L^1$, for all $n \geqslant 1$. For any $n \geqslant 1$, let $u^n(t, x_1, x_2)$ be the associated solution of eq. (9.40), and define*

$$u_0^n(t, x_2) = \int_0^\infty u^n(t, x_1, x_2) dx_1.$$

(1) Under the scaling (S1), when $n \to \infty$, $u_0^n(t, x_2)$ approaches the solution of eq. (9.41).

(2) Under the scaling (S2) or (S3), when $n \to \infty$, $u_0^n(t, x_2)$ approaches the solution of eq. (9.42) with $\bar{h}$ defined by eq. (9.43).

In all cases, convergence holds in $\mathcal{C}_0^\infty$, uniformly in time on any bounded time interval.

Proof. Throughout the proof, we omit indices n on $u^n(t, x_1, x_2)$ and in the marginal density $u_0^n(t, x_2)$, and keep in mind that they depend on the parameter n through eq. (9.40) and the particular scaling considered. The first calculus is independent of the particular scaling chosen. Let

$$u_k(t, x_2) = \int_0^{+\infty} x_1^k u(t, x_1, x_2) dx_1, \quad k = 0, 1, \cdots$$

which are well defined from the previous discussion. From eq. (9.40) and (9.46), we have

$$
\begin{aligned}
\frac{\partial u_k}{\partial t} \quad = \quad & -k\gamma_1^n u_k - \lambda_2^n \frac{\partial u_{k+1}}{\partial x_2} + \gamma_2 \frac{\partial(x_2 u_k)}{\partial x_2} \\
& + \int_0^\infty \int_0^{x_1} \lambda_1^n k_1(x_2) x_1^k u(t, z, x_2) h^n(x_1 - z) dz dx_1 - \lambda_1^n k_1(x_2) u_k.
\end{aligned}
$$

Since

$$\int_0^\infty \int_0^{x_1} \lambda_1^n k_1(x_2) x_1^k u(t, z, x_2) h^n(x_1 - z) dz dx_1 = \sum_{j=0}^k \binom{k}{j} \lambda_1^n k_1(x_2) u_{k-j} b_j^n,$$

where $b_k^n = \int_0^\infty z^k h^n(z) dz$. We have

$$\frac{\partial u_k}{\partial t} = -k\gamma_1^n u_k - \lambda_2^n \frac{\partial u_{k+1}}{\partial x_2} + \gamma_2 \frac{\partial(x_2 u_k)}{\partial x_2} + \lambda_1^n k_1(x_2) \sum_{j=1}^k \binom{k}{j} u_{k-j} b_j^n.$$

In particular, when $k = 0$,

$$\frac{\partial u_0}{\partial t} = -\lambda_2^n \frac{\partial u_1}{\partial x_2} + \gamma_2 \frac{\partial (x_2 u_0)}{\partial x_2}. \tag{9.49}$$

When $k \geqslant 1$, we have

$$\frac{1}{\gamma_1^n} \frac{\partial u_k}{\partial t} = -k u_k - \frac{\lambda_2^n}{\gamma_1^n} \frac{\partial u_{k+1}}{\partial x_2} + \frac{\gamma_2}{\gamma_1^n} \frac{\partial (x_2 u_k)}{\partial x_2} + \frac{1}{\gamma_1^n} \lambda_1^n k_1(x_2) \sum_{j=1}^{k} \binom{k}{j} u_{k-j} b_j^n. \tag{9.50}$$

Proposition 61 allows us to identify the leading terms of eq. (9.50) as $n \to \infty$ as given below. [1] When $k \geqslant 1$ and $n \to \infty$, note that all the right hand-side terms are bounded, and we apply the quasi-equilibrium assumption to eq. (9.50) by assuming

$$\frac{1}{n} \frac{\partial u_k}{\partial t} \approx 0$$

when $t \geqslant t_0 > 0$, and hence

$$u_k = -\frac{\lambda_2^n}{k \gamma_1^n} \frac{\partial u_{k+1}}{\partial x_2} + \frac{\gamma_2}{k \gamma_1^n} \frac{\partial (x_2 u_k)}{\partial x_2} + \frac{1}{k \gamma_1^n} \lambda_1^n k_1(x_2) \sum_{j=1}^{k} \binom{k}{j} u_{k-j} b_j^n + O(\frac{1}{n}), \quad (\forall k \geqslant 1). \tag{9.52}$$

Now, we are ready to prove the results for the three different scalings.
(S1). For the scaling (S1), $\lambda_1^n = n \lambda_1$ and we have

$$u_k = \frac{1}{k} \frac{\lambda_1 k_1(x_2)}{\gamma_1} \sum_{j=1}^{k} \binom{k}{j} u_{k-j} b_j + O(\frac{1}{n}),$$

so

$$u_1 = \frac{b \lambda_1 k_1(x_2)}{\gamma_1} u_0 + O(\frac{1}{n}), \tag{9.53}$$

Substituting eq. (9.53) into eq. (9.49), we obtain

$$\frac{\partial u_0}{\partial t} = \frac{\partial}{\partial x_2} [\gamma_2 x_2 u_0 - \lambda_2 k(x_2) u_0] + O(\frac{1}{n})$$

with $k(x_2) = b \lambda_1 k_1(x_2) / \gamma_1$. Finally, note that

$$u_0(T, x_2) = \int_0^T \frac{\partial u_0(t, x_2)}{\partial t} dt,$$

so point (1) in theorem 64 follows and convergence holds in $\mathcal{C}_0^\infty$, uniformly in time on any bounded time interval.

---

1. However, to be more exact, one needs to consider the weak form associated with eq. (9.50) to have integrals of u_n, as in proposition 61. The weak form reads, for any smooth function $f \in C_0^\infty$

$$\frac{1}{\gamma_1^n} \frac{d}{dt} \int_0^\infty u_k(x_2) f(x_2) dx_2 = -k \int_0^\infty u_k(x_2) f(x_2) dx_2 - \frac{\lambda_2^n}{\gamma_1^n} \int_0^\infty u_{k+1}(x_2) f'(x_2) dx_2$$
$$+ \frac{\gamma_2}{\gamma_1^n} \int_0^\infty y u_k(x_2) f'(x_2) dx_2 + \frac{1}{\gamma_1^n} k_1(x_2) \sum_{j=1}^{k} \binom{k}{j} b_j^n \int_0^\infty u_{k-j}(x_2) f(x_2) dx_2. \tag{9.51}$$

Since u_k is a smooth function, there is an equivalence between the strong form (9.50) and its weak form (9.51). Here, as f (and all its derivatives) is bounded, similar estimates as in Proposition 61 can be performed, which justifies the identification of leading order terms. To keep the equations simple, we then perform our calculations on the strong form, while keeping in mind that the identification of leading terms is justified by the weak form and Proposition 61.

(S2). We assume the scaling (S2) so $h^n(z) = \frac{1}{n}h(\frac{z}{n})$ and $b_k^n = n^k b_k$ and the re-scaled k^{th} moment

$$b_k = n^{-k}b_k^n$$

is independent of n. Hence, from eq. (9.52) and proposition 61, we have

$$
\begin{aligned}
n^{-(k-1)}u_k &= -\frac{\lambda_2}{k\gamma_1}\frac{\partial(n^{-k}u_{k+1})}{\partial x_2} + \frac{\gamma_2}{kn\gamma_1}\frac{\partial(x_2 n^{-(k-1)}u_k)}{\partial x_2} + \frac{\lambda_1}{k\gamma_1}k_1(x_2)u_0 b_k \\
&\quad + \frac{1}{kn\gamma_1}\lambda_1 k_1(x_2)\sum_{j=1}^{k-1}\binom{k}{j}n^{-(k-j-1)}u_{k-j}b_j \\
&= \frac{\lambda_1 b_k}{k\gamma_1}k_1(x_2)u_0 - \frac{\lambda_2}{k\gamma_1}\frac{\partial(n^{-k}u_{k+1})}{\partial x_2} + O(\frac{1}{n}).
\end{aligned}
$$

Therefore,

$$
\begin{aligned}
u_1 &= \frac{b_1\lambda_1}{\gamma_1}k_1(x_2)u_0 - \frac{\lambda_2}{\gamma_1}\frac{\partial}{\partial x_2}[n^{-1}u_2] + O(\frac{1}{n}) \\
&= \frac{b_1\lambda_1}{\gamma_1}k_1(x_2)u_0 - \frac{\lambda_2}{\gamma_1}\frac{\partial}{\partial x_2}[\frac{\lambda_1 b_2}{2\gamma_1}k_1(x_2)u_0 - \frac{\lambda_2}{2\gamma_1}\frac{\partial(n^{-2}u_3)}{\partial x_2}] + O(\frac{1}{n}) \\
&= \frac{b_1\lambda_1}{\gamma_1}k_1(x_2)u_0 - b_2\frac{\lambda_2}{2!\gamma_1^2}\frac{\partial}{\partial x_2}(\lambda_1 k_1(x_2)u_0) \\
&\quad + \frac{\lambda_2^2}{2!\gamma_1^2}\frac{\partial^2}{\partial x_2^2}[\frac{\lambda_1 b_3}{3\gamma_1}k_1(x_2)u_0 - \frac{\lambda_2}{3\gamma_1}\frac{\partial(n^{-3}u_4)}{\partial x_2}] + O(\frac{1}{n}) \\
&\quad \cdots\cdots\cdots\cdots \\
&= \sum_{k=0}^{\infty}\frac{(-\lambda_2)^k}{(k+1)!\gamma_1^{k+1}}b_{k+1}\frac{\partial^k}{\partial x_2^k}(\lambda_1 k_1(x_2)u_0) + O(\frac{1}{n}).
\end{aligned}
$$

Thus, when $n \to \infty$, we have, using Taylor development series of u_0,

$$
\begin{aligned}
-\lambda_2\frac{\partial u_1}{\partial x_2} &\rightarrow \sum_{k=1}^{\infty}\frac{(-\lambda_2)^k}{k!}(\gamma_1^{-k}b_k)\frac{\partial^k}{\partial x_2^k}(\lambda_1 k_1(x_2)u_0) \\
&= \sum_{k=1}^{\infty}\frac{1}{k!}(-\frac{\lambda_2}{\gamma_1})^k(\int_0^{\infty}x_1^k h(x_1)dx_1)\frac{\partial^k}{\partial x_2^k}(\lambda_1 k_1(x_2)u_0) \\
&= \int_0^{\infty}\bar{h}(x_1)\left[\sum_{k=1}^{\infty}\frac{1}{k!}(-x_1)^k\frac{\partial^k}{\partial x_2^k}(\lambda_1 k_1(x_2)u_0)\right]dx_1 \\
&= \int_0^{\infty}\bar{h}(x_1)(\lambda_1 k_1(x_2 - x_1)u_0(t, x_2 - x_1) - \lambda_1 k_1(x_2)u_0(t, x_2))dx_1 \\
&= \int_0^{\infty}\bar{h}(x_1)\lambda_1 k_1(x_2 - x_1)u_0(t, x_2 - x_1)dx_1 - \lambda_1 k_1(x_2)u_0(t, x_2) \\
&= -\int_{x_2}^{-\infty}\bar{h}(x_2 - z)\lambda_1 k_1(z)u_0(t, z)dz - \lambda_1 k_1(x_2)u_0(t, x_2) \\
&= \int_0^{x_2}\bar{h}(x_2 - z)\lambda_1 k_1(z)u_0(t, z)dz - \lambda_1 k_1(x_2)u_0(t, x_2).
\end{aligned}
$$

(here we note $k_1(z) = 0$ when $z < 0$). Therefore, from eq. (9.49), when $\gamma_1 \to 0$, u_0 approaches to the solution of eq. (9.42), and the desired result follows.

(S3). Now, we consider the case of scaling (S3) so $\lambda_2^n = n\lambda_2$. From eq. (9.52) and proposition 61, we have

$$u_k = -\frac{1}{k}\frac{\lambda_2}{\gamma_1}\frac{\partial u_{k+1}}{\partial x_2} + \frac{\gamma_2}{kn\gamma_1}\frac{\partial(x_2 u_k)}{\partial x_2} + \frac{1}{kn\gamma_1}\lambda_1 k_1(x_2)u_0 b_k$$

$$+ \frac{1}{kn\gamma_1}\lambda_1 k_1(x_2)\sum_{j=1}^{k-1}\binom{k}{j}u_{k-j}b_j$$

$$= \frac{1}{kn\gamma_1}\lambda_1 k_1(x_2)u_0 b_k - \frac{1}{k}\frac{\lambda_2}{\gamma_1}\frac{\partial u_{k+1}}{\partial x_2} + O(\frac{1}{n^2}).$$

Therefore,

$$
\begin{aligned}
u_1 &= \frac{1}{n\gamma_1}\lambda_1 k_1(x_2)u_0 b_1 - \frac{\lambda_2}{\gamma_1}\frac{\partial}{\partial x_2}u_2 + O(\frac{1}{n^2}) \\
&= \frac{1}{n\gamma_1}\lambda_1 k_1(x_2)u_0 b_1 - \frac{\lambda_2}{\gamma_1}\frac{\partial}{\partial x_2}[\frac{1}{2n\gamma_1}\lambda_1 k_1(x_2)u_0 b_2 - \frac{1}{2}\frac{\lambda_2}{\gamma_1}\frac{\partial}{\partial x_2}u_3] + O(\frac{1}{n^2}) \\
&= \frac{1}{n\gamma_1}\lambda_1 k_1(x_2)u_0 b_1 - \frac{1}{2!}\frac{\lambda_2}{n\gamma_1^2}b_2\frac{\partial}{\partial x_2}[\lambda_1 k_1(x_2)u_0] \\
&\quad + \frac{1}{2!}(\frac{\lambda_2}{\gamma_1})^2\frac{\partial}{\partial x_2}[\frac{1}{3n\gamma_1}\lambda_1 k_1(x_2)u_0 b_3 - \frac{1}{3}\frac{\lambda_2}{\gamma_1}\frac{\partial}{\partial x_1}u_4] + O(\frac{1}{n^2}) \\
\cdots &\quad \cdots\cdots \\
&= -\frac{1}{n\lambda_2}\sum_{k=1}^{\infty}\frac{1}{k!}(-\frac{\lambda_2}{\gamma_1})^k b_k\frac{\partial^{k-1}}{\partial x_2^{k-1}}[\lambda_1 k_1(x_2)u_0] + O(\frac{1}{n^2}).
\end{aligned}
$$

Thus, when $n \to \infty$, in a manner similar to the above argument, we have

$$
\begin{aligned}
-n\lambda_2\frac{\partial u_1}{\partial x_2} &\rightarrow \sum_{k=1}^{\infty}\frac{1}{k!}(-\frac{\lambda_2}{\gamma_1})^k b_k\frac{\partial^k}{\partial x_2^k}[\lambda_1 k_1(x_2)u_0] \\
&= \int_0^y \bar{h}(y-z)\lambda_1 k_1(z)u_0(t,z)dz - \lambda_1 k_1(x_2)u_0(t,x_2),
\end{aligned}
$$

and the result follows.   □

9.4   From discrete to continuous bursting model

We show here that the discrete bursting model BD1, converge either to a continuous deterministic model or to a continuous bursting model, when an appropriate scaling is used. The precise result is stated in paragraph 9.4.6.

We are going to state here results of convergence of Pure-Jump Markov processes using standard techniques [36]. We will look from now on the semigroup defined on the space of bounded measurable function, rather than on L^1. While going from the discrete model to the continuous model, one needs to make the *local* jumps smaller and smaller so that they will eventually becomes continuous, whereas the *non-local* jumps will stay discontinuous. Appropriate assumptions on the coefficient needs to be made. We give here a rigorous proof of the validity of the continuous approximation, using a classical generator limit. We obtain a convergence of the stochastic process, that contains more information than solely the asymptotic distribution. As said, these techniques are not knew, but seems to have been rarely used for Piecewise deterministic process with jumps (see for instance the recent reference [25], where various limiting processes are obtained in a general settings for a finite number of reaction).

For the sake of completeness, and to make apparent the specificity on the choices of scaling of coefficient, we first state a mean-field limit where the pure-jump Markov process converges to the solution of an Ordinary Differential Equation (theorem 65) and then state the convergence of the pure-jump Markov process towards the Piecewise deterministic process with jumps (theorem 66).

9.4.1 Discrete model

We look at the continuous-time Markov Chain X_t on the positive integer space, with transition kernel given by

$$K(x, dy) = \gamma(x)\delta_{-1}(dy) + \lambda(x)\sum_{r \geqslant 1} h_r \delta_r(dy)$$

where δ_i denotes the Dirac mass in i. Let F_t be the natural X_t-adapted filtration. Then the following expression holds

$$X_t = X_0 + \int_0^t \Big(-\gamma(X_s) + \lambda(X_s)\mathbb{E}[h] \Big)ds + M_t$$

where M_t is a F_t-Martingale, and

$$M_t = \sum_{J_n \leqslant t} \Delta X_n - \int_0^t \int_{\mathbb{R}+} yK(Xs, dy)ds$$

where J_n are jump times of $(X_t)_{t \geqslant 0}$. Then M_t has for quadratic variation

$$< M >_t = \int_0^t \Big(\gamma(X_s) + \lambda(X_s)\mathbb{E}^2[h] \Big)ds$$

9.4.2 Normalized discrete model

We change the reaction rates γ, λ and jump size probability h_r respectively by $\gamma^N, \lambda^N, h_r^N$. We note the associated solution $\check{X}^N$ and define the process

$$X^N(t) = \frac{1}{N}\tilde{X}^N$$

Then it is easy to see that X^N is a continuous-time Markov chain of transition kernel

$$K^N(x, dy) = \gamma^N(Nx)\delta_{-\frac{1}{N}}(dy) + \lambda^N(Nx)\sum_{r \geqslant 1} h_r^N \delta_{\frac{r}{N}}(dy)$$

and

$$X_t^N = X_0^N + \int_0^t \Big(-\frac{1}{N}\gamma^N(NX_s^N) + \frac{1}{N}\lambda^N(NX_s^N)\mathbb{E}[h^N] \Big)ds + M_t^N \tag{9.54}$$

where M_t^N is an L^2-Martingale

$$M_t^N = \sum_{J_n^N \leqslant t} \Delta X_n^N - \int_0^t \int_{\mathbb{R}+} yK^N(X_s^N, dy)ds$$

and M_t^N has for quadratic variation

$$< M^N >_t = \int_0^t \Big(\frac{1}{N^2}\gamma^N(NX_s^N) + \frac{1}{N^2}\lambda^N(NX_s^N)\mathbb{E}^2[h^N] \Big)ds$$

9.4.3   Limit model 1

We look at the deterministic process defined by

$$x_t^1 = x_0 + \int_0^t \Big(-\gamma(x_s^1) + \lambda(x_s^1)\mathbb{E}[h] \Big) ds$$

9.4.4   Limit model 2

We look at the process defined by

$$x_t = x_0 + \int_0^t \Big(-\gamma(x_s) + \lambda(x_s)\mathbb{E}[h] \Big) ds + M_t \qquad (9.55)$$

where M_t is an L^2-Martingale

$$M_t = \sum_{J_n \leqslant t} \Delta x_{J_n} - \int_0^t \int_{\mathbb{R}^+} yK(x_s, dy)ds$$

and $K(x_s, dy) = \lambda(x_s)1_{y \geqslant x_s}h(y - x_s)$. M_t has for quadratic variation

$$< M >_t = \int_0^t \lambda(x_s)\mathbb{E}^2[h]ds$$

9.4.5   Convergence theorem 1

The first result concern a classical fluid limit (or thermodynamic limit) when the jump intensity is faster and faster and the jump size smaller and smaller, such that the mean velocity stays finite. Because we include unbounded jump rate function, we need to restrict to convergence on compact time interval.

Theorem 65. *Let λ and γ be nonnegative locally Lipschitz functions on $[0, \infty)$, and h be a density function on $(0, \infty)$ with a finite first moment, i.e. $\mathbb{E}[h] = \int_0^\infty xh(x)dx < \infty$. Take any $T > 0$ such that there is a unique solution to the ordinary differential equation on $[0, T]$, starting at $x_0 \geqslant 0$,*

$$\frac{dx}{dt} = \lambda(x)\mathbb{E}[h] - \gamma(x).$$

Now take a closed set D that contains the trajectory up to T, i.e. $(x_t)_{0 \leqslant t \leqslant T} \subset D$. Let S be a relatively open set of D, $S \subset D$. Suppose we have the following scaling laws, for any $N > 0$ and $x \geqslant 0$,

$$\begin{aligned}
\gamma_N(x) &= N\gamma(x) \\
\lambda_N(x) &= N\lambda(x) \\
h_N(x) &= \int_x^{x+1} h(y)dy
\end{aligned}$$

For any sequence $N \to \infty$, let X^N be the associated Pure-Jump Markov Process described above by eq. (9.54). Let τ_N be the exit time of S, i.e. $\tau_N = \inf\{t \geqslant 0, X_t^N \notin S\}$. Then $\lim X^N(0) = x_0$ implies that, for every $\delta > 0$,

$$\lim_{N \to \infty} \mathbb{P}\Big(\sup_{0 \leqslant t \leqslant T} |X_{s \wedge \tau_N}^N - x_{s \wedge \tau_N}| > \delta \Big) = 0$$

Proof. This result is contained in many text books (see for instance [81, thm 2.11], or for the corresponding martingale method [26, thm 2.8]) and is the consequence of the three followings facts (according to [81, thm 2.11]). For any N, let $S_N = S \bigcap (\frac{1}{N} \mathbb{N})$.

– The time-averaged rate of change is always finite,

$$\sup_N \sup_{x \in S_N} \lambda_N(x) \int_{\frac{1}{N} \mathbb{N}} |y - x| K^N(x, dy)$$
$$\leqslant \sup_N \sup_{x \in S_N} \left[\gamma(x) + \lambda(x) \mathbb{E}[h] \right]$$
$$< \infty$$

– There exists a positive sequence $\delta_N \to 0$ such that

$$\lim_{N \to \infty} \sup_{x \in S_N} \lambda_N(x) \int_{|y-x| > \delta_N} |y - x| K^N(x, dy) = 0$$

Indeed, for any $\eta > 0$, consider $\delta_N = \max(M, 1) \frac{1}{N}$ and M is such that

$$\sup_{x \in S} \lambda(x) \int_M^\infty y h(y) dy < \eta$$

– The difference between the deterministic dynamical system and the time-averaged rates of change does to zero

$$\lim_{N \to \infty} \sup_{x \in S_N} \left| (\lambda(x) \mathbb{E}[h] - \gamma(x)) - \lambda_N(x) \int_{\frac{1}{N} \mathbb{N}} (y - x) K^N(x, dy) \right| = 0$$

$\square$

9.4.6 Convergence theorem 2

We are now going to show that the re-scaled discrete model converge to the limiting model 2 as $N \to \infty$ under the specific assumptions

Hypothesis 10.   – $\gamma^N(Nx) = N\gamma(x)$, for all $x \geqslant 0$,
    – $\lambda^N(Nx) = \lambda(x)$, for all $x \geqslant 0$,
    – $\sum_{r \geqslant 1} e^{r \frac{\theta}{N}} h_r^N \xrightarrow{N \to \infty} \int_0^\infty e^{y\theta} h(y) dy$.
    We also suppose that the rates λ and γ are linearly bounded and $\gamma(0) = 0$, namely
    – $0 \leqslant \lambda(x) \leqslant \lambda_0 + \lambda_1 x$
    – $0 \leqslant \gamma(x) \leqslant \gamma_0 + \gamma_1 x$ *and* $\gamma(0) = 0$
The second hypothesis guarantee that the process stay non-negative, and the first one gives non-explosion property. We finally make the additional assumption

$$\int_0^\infty y^2 h(y) dy < \infty,$$

which will allow us to get a control of the second moment.

We prove now that

Theorem 66. *Under hypotheses 10, the process X_t^N solution of eq. 9.54 converges in distribution in $\mathbb{D}([0, T], \mathbb{R}^+)$ towards x_t, solution of eq. 9.55, for any $T > 0$, as $N \to \infty$.*

We will use standard argument and decompose the proof in 3 steps: tightness, identification of the limit and uniqueness of the limit.

Step 1: Tightness We start by proving some moment estimates. Using the expression of the transition kernel K^N, it follows that

$$\mathbb{E}[X_t^N] \leqslant \mathbb{E}[X_0^N] + \int_0^t \mathbb{E}[h^N]\mathbb{E}[\lambda(X_s^N)]ds$$

Then, due to the assumption on λ,

$$\mathbb{E}[X_t^N] \leqslant \mathbb{E}[X_0^N] + \int_0^t \mathbb{E}[h^N](\lambda_0 + \lambda_1\mathbb{E}[X_s^N])ds$$

Note that due to assumption on h^N, $\mathbb{E}[h^N]$ is convergent, hence bounded. Then, by Grönwall inequality, for any $T > 0$, if $\mathbb{E}X_0^N < \infty$, we have

$$\sup_{t\in[0,T]} \mathbb{E}X_t^N < \infty$$

For any $p \geqslant 2$, note that

$$\sum_{r\geqslant 1}(x+\frac{r}{N})^p h_r^N - x^p = \sum_{r\geqslant 1}\Big(\sum_{k=1}^p \binom{p}{k}x^{p-k}\frac{r^k}{N^k}\Big)h_r^N,$$

$$= \sum_{k=1}^p \binom{p}{k}\frac{x^{p-k}}{N^k}\sum_{r\geqslant 1}r^k h_r^N,$$

$$= \sum_{k=1}^p \binom{p}{k}\frac{x^{p-k}}{N^k}\mathbb{E}^k[h^N].$$

Then, we deduce

$$\mathbb{E}[(X_t^N)^p] \quad\leqslant\quad \mathbb{E}[(X_0^N)^p] \;+\; \int_0^t(\lambda_0 \;+\; \lambda_1\mathbb{E}[X_s^N])\sum_{k=1}^p \binom{p}{k}\mathbb{E}[(X_s^N)^{p-k}]\frac{\mathbb{E}^k[h^N]}{N^k}ds.$$

Hence, according to the assumption on h^N and Grönwall inequality, we show by recurrence on p, if $\mathbb{E}[(X_0^N)^p] < \infty$, then

$$\sup_{t\in[0,T]} \mathbb{E}[(X_t^N)^p] < \infty.$$

We prove by similar argument that

$$\sup_n \mathbb{E}[\sup_{t\in[0,T]} X_t^N] \;<\; \infty,$$

$$\sup_n \mathbb{E}[\sup_{t\in[0,T]} (X_t^N)^2] \;<\; \infty.$$

Now note that X_t^N is the semi-Martingale, with finite variation part

$$V_t^N = \int_0^t -\gamma(X_s^N) + \lambda(X_s^N)\frac{\mathbb{E}[h^N]}{N}ds,$$

and Martingale M_t^N of quadratic variation

$$< M^N >_t = \int_0^t \frac{1}{N}\gamma(X_s^N) + \lambda(X_s^N)\frac{\mathbb{E}^2[h^N]}{N^2}ds.$$

Then using moment estimates above and assumptions on rates γ and λ, it comes

$$\sup_N \mathbb{E}[\sup_{t\in[0,T]} |V_t^N|] < \infty,$$

$$\sup_N \mathbb{E}[\sup_{t\in[0,T]} <M^N>_t] < \infty.$$

Similarly, for any $\delta > 0$, for any sequence (S_N, T_N) of couples of stopping times such that $S_n \leqslant T_n \leqslant T$ and $T_n \leqslant S_n + \delta$, we can show that

$$\sup_N \mathbb{E}[|V_{T_N}^N - V_{S_N}^N|] < C\delta,$$

$$\sup_N \mathbb{E}[|<M^N>_{T_N} - <M^N>_{S_N}|] < C\delta,$$

where C is a constant that depends only of $\lambda_0, \lambda_1, \gamma_0, \gamma_1, h$ and T.

Then by Aldous-Rebolledo and Roelly's criteria ([73],[119]), this ensures that X_t^N is tight in $\mathbb{D}(\mathbb{R}^+, \mathbb{R}^+)$ with the standard Skorokhod topology.

step 2: Identification of the limit   Let's consider an adherence value x of the sequence X^N and denote again X^N the subsequence that converges in law to x in $\mathbb{D}([0,T], \mathbb{R}^+)$. For any $k > 0$, let $0 \leqslant t_1 \leqslant \ldots \leqslant t_k < s < t \leqslant T$ and $\phi_1, \ldots, \phi_k \in C_b(\mathbb{R}^+, \mathbb{R})$. For $y \in \mathbb{D}([0,T], \mathbb{R}^+)$, we define, for suitable f

$$\Psi(y) = \phi_1(y_{t_1}) \ldots \phi_k(y_{t_k}) \Big[f(y_t) - f(y_s) - \int_s^t (-\gamma(y_u) f'(y_u)$$
$$+ \lambda(y_u) \int_0^\infty h(y) f(y_u + y) dy - f(y_u)) du \Big].$$

Then $|\mathbb{E}[\Psi(x)]| \leqslant A + B + C$ where

$$A = |\mathbb{E}[\Psi(x)] - \mathbb{E}[\Psi(X^n)]|,$$
$$B = |\mathbb{E}[\Psi(X^n)] - \mathbb{E}[\phi_1(X_{t_1}^N) \ldots \phi_k(X_{t_k}^N)(M_t^{f,N} - M_s^{f,N})]|,$$
$$C = |\mathbb{E}[\phi_1(X_{t_1}^N) \ldots \phi_k(X_{t_k}^N)(M_t^{f,N} - M_s^{f,N})]|.$$

By the Martingale property, $C = 0$. The map $y \in \mathbb{D}([0,T], \mathbb{R}^+) \mapsto \Psi(y)$ is continuous as soon $(t_1, \ldots, t_k, s, t)$ does not intersect a denumerable set of points of $[0,T]$ where y is not continuous. Then the convergence in distribution of X^N to x implies that A converges to 0 when $N \to \infty$. Finally,

$$B \leqslant \mathbb{E}\Bigg[\int_s^t \frac{|\gamma(X_u^N)|}{N} |f''(X_u^N + \frac{\varepsilon_u^n}{n})|$$
$$+ \lambda(X_u^N) | \Big(\sum_{r\geqslant 1} h_r^N f(X_u^N + \frac{r}{N}) - \int_0^\infty h(y) f(X_u^N + y) dy \Big) | du \Bigg],$$

with $\varepsilon_u^n \in [0,1]$. Then $B \to 0$ as $N \to \infty$ according to the assumptions above.

step 3 : Uniqueness   In step 2, we have shown that adherence values of X_n has to be solution of the Martingale problem associated to the generator A,

$$Af(x) = -\gamma(x) \frac{df}{dx} + \lambda(x) \Big(\int_0^\infty f(x+y) h(y) dy - f(x) \Big).$$

It is known ([27]) that under our assumption we have a strong solution of eq. (9.55), so uniqueness of the solution of the martingale problem associated to A holds, using [36, corollaire 4.4 p187] (see part 0 proposition 8).

9.4.7 Interpretation

Lets consider the master equation eq. (8.1) in the specific example 5. We can see this master equation as a biochemical master equation ([45]). Then, the degradation reaction being a first order reaction, the propensity γ_n is independent of the "size" of the cell. But the burst production reaction is a zero-order reaction, and hence is proportional to the size, that is

$$\lambda_n = \lambda V \frac{1 + Kn^N}{\Lambda + \Delta Kn^N}$$

Note that in the last expression, the Hill function occurred as an elimination procedure of the repressors molecule (see for instance [91]). Parameters Λ and Δ are dimensionless parameters, and the parameter K is the reaction rate constant of the binding of N proteins to a single repressor molecule, and then is the reaction rate constant of an $(N+1)$-order reaction. Then

$$K = K_0 V^{-N}$$

Now let define the rescaled variable $X^\varepsilon = K_0^{1/N} \frac{X_t}{V}$, we get, with $\varepsilon = \frac{K_0^{1/N}}{V}$,

$$
\begin{aligned}
\mathcal{P}\left(x \mapsto x - \varepsilon | X_t^\varepsilon = x\right) &= \frac{\gamma}{\varepsilon}x \\
\mathcal{P}\left(x \mapsto x + r\varepsilon | X_t^\varepsilon = x\right) &= \frac{\lambda K_0^{1/N}}{\varepsilon} \frac{1 + x^N}{\Lambda + \Delta x^N}(1 - b)b^{r-1}
\end{aligned}
$$

The mean burst size of this rescaled variable is then $\frac{b}{1-b}\varepsilon$. Hence the jumps become smaller and more frequent as $\varepsilon \to 0$. We recover in the limit a continuous and deterministic process, the situation of the theorem 65.

Now suppose the burst production rate does not increase with the size of the cell, but the burst size does. With the scaling of theorem 66, if h is an exponential distribution of mean parameter b, then h_ε is a geometric distribution of parameter $1 - e^{-b/\varepsilon} \to 1$ as $\varepsilon \to 0$, and then the mean burst size increases inversely proportional to ε.

Remark 67. *In practice, if we don't know a priori the size of the system, we expect the following ε to be appropriate, depending on the case,*

$$
\begin{aligned}
\varepsilon &\sim \frac{\gamma}{\lambda_0} = \frac{Degradation\ rate}{Burst\ frequence} \\
\varepsilon &\sim K^n = (Binding\ Rate\ constant)^n \\
\varepsilon &\sim \frac{1 - b}{b} = \frac{1}{mean\ burst\ size}
\end{aligned}
$$

Much caution must be taken while choosing the ε, because in practice the size of the system doesn't go into infinity, so that a too small ε would lead to misunderstanding. For instance, In [153], one can found the following rates taken from other literatures:

$$
\begin{aligned}
\lambda_{mRNA} &\sim 1,0 min^{-1} \\
\gamma_{mRNA} &\sim 1,0 min^{-1} \\
\gamma_{protein} &\sim 0,01 min^{-1} \\
Number\ of\ protein\ for\ one\ mRNA &\sim 30
\end{aligned}
$$

so that the continuous approximation with $\varepsilon = 0.01$ would give a degradation rate of order $1\,min^{-1}$, a bursting rate of order $1\,min^{-1}$ and a mean burst size of 0.3.

Bibliography

[1] E. Pecou A. Maass, S. Martinez. *Mathematical comments on basic topics in Systems Biology in Mathematical and Computational Methods in Biology.* 2006. 92

[2] M. Acar, A. Becskei, and A. van Oudenaarden. Enhancement of cellular memory by reducing stochastic transitions. *Nature*, 435:228–232, 2005. 114

[3] D. F. Anderson and T. G. Kurtz. *Design and Analysis of Biomolecular Circuits (chapter 1).* Springer, 2011. 51

[4] T. Aquino, E. Abranches, and A. Nunes. Stochastic single-gene auto-regulation. *Phys. Rev. E*, 85:14, 2011. 88

[5] L. Arnold. *Random dynamical systems.* Springer-Verlag, 1998. 114

[6] K. Ball, T. G. Kurtz, L. Popovic, and G. Rempala. Asymptotic analysis of multiscale approximations to reaction networks. *Ann. Appl. Probab.*, 16(4):1925–1961, 2006. 130

[7] J.-B. Bardet, A. Christen, A. Guillin, F. Malrieu, and P.-A. Zitt. Total variation estimates for the tcp process. 2011. arXiv:1112.6298. 116

[8] A. Becskei, B. Seraphin, and L. Serrano. Positive feedback in eukaryotic gene networks: cell differentiation by graded to binary response conversion. *EMBO J.*, 20 (10):2528–2535, 2001. 55

[9] O. G. Berg. A model for the statistical fluctuations of protein numbers in a microbial population. *J. Theor. Biol.*, 71(4):587–603, 1978. 52, 91

[10] N. Berglund and B. Gentz. *Noise-Induced Phenomena in Slow-Fast Dynamical Systems,A Sample-Paths Approach.* Springer, 2006. 129

[11] W.J. Blake, M. Kaern, C.R. Cantor, and J.J. Collins. Noise in eukaryotic gene expression. *Nature*, 422:633–637, 2003. 91

[12] A. Bobrowski. Degenerate convergence of semigroups related to a model of stochastic gene expression. *Semigroup Forum*, 73(3):345–366, 2006-12-14. 119, 120

[13] A. Bobrowski, T. Lipniacki, K. Pichór, and R. Rudnicki. Asymptotic behavior of distributions of mRNA and protein levels in a model of stochastic gene expression. *J. Math. Anal. Appl.*, 333(2):753–769, 2007. 52, 85, 113

[14] P. Bokes, J. R. King, A. T. Wood, and M. Loose. Exact and approximate distributions of protein and mRNA levels in the low-copy regime of gene expression. *J. Math. Biol.*, 64:829–854, 2011. 87, 90

[15] I. Bose and S. Ghosh. Binary response in microrna-mediated regulation of gene expression. pages 1–7, 2012. arXiv:1205.0381v2. 91

[16] F. J. Bruggeman, N. Blüthgen, and H. V. Westerhoff. Noise management by molecular networks. *PLoS Comput Biol*, 5(9):e1000506, 2009. 92

[17] M.L. Bujorianu and J.-P. Katoen. Symmetry reduction for stochastic hybrid systems. *IEEE Decis. Contr. P.*, pages 233–238, 2008. 130

[18] M.L. Bujorianu and J. Lygeros. General stochastic hybrid systems: modelling and optimal control. *IEEE Decis. Contr. P.*, 2, 2004. 130

[19] M. O. Cáceres and A. A. Budini. The generalized ornstein - uhlenbeck process. *J. Phys. A*, 30(24):8427–, 1997. 142

[20] L. Cai, N. Friedman, and X.S. Xie. Stochastic protein expression in individual cells at the single molecule level. *Nature*, 440:358–362, 2006. 69, 71, 72, 89

[21] T. Çagatay, M. Turcotte, M. B. Elowitz, J. Garcia-Ojalvo, and G. M. Süel. Architecture-dependent noise discriminates functionally analogous differentiation circuits. *Cell*, 139(3):512–22, 2009. 92

[22] J.R. Chubb, T. Trcek, S.M. Shenoy, and R.H. Singer. Transcriptional pulsing of a developmental gene. *Curr. Biol.*, 16:1018–1025, 2006. 51, 52, 72, 92

[23] O.L.V. Costa and F. Dufour. Stability and ergodicity of piecewise deterministic markov processes. *IEEE Decis. Contr. P.*, 47(Dec 9-11):1525–1530, 2008. 51

[24] A. Coulon, O. Gandrillon, and G. Beslon. On the spontaneous stochastic dynamics of a single gene: complexity of the molecular interplay at the promoter. *BMC Syst. Biol.*, 4:2, 2010. 91

[25] A. Crudu, A. Debussche, A. Muller, and O. Radulescu. Convergence of stochastic gene networks to hybrid piecewise deterministic processes. *Ann. Appl. Probab.*, 2011. 51, 52, 119, 121, 123, 127, 130, 133, 139, 152

[26] R. W. R. Darling. Fluid limits of pure jump markov processes: a practical guide. 2002. arXiv:math/0210109. 155

[27] M. H. A. Davis. Piecewise-deterministic markov processes: A general class of non-diffusion stochastic models. *J Roy. Stat. Soc. B Met.*, 46(3):353–388, 1984. 51, 133, 157

[28] M. Doumic and L. M. Tine. Estimating the division rate of the growth-fragmentation equation. *J. Math. Biol.*, 2012. 118

[29] M. Doumic Jauffret, M. Hoffmann, P. Reynaud-Bouret, and V. Rivoirard. Non-parametric estimation of the division rate of a size-structured population. *SIAM J. Numer. Anal.*, pages –, 2012. 52

[30] Y. Dublanche, K. Michalodimitrakis, N. Kümmerer, M. Foglierini, and L. Serrano. Noise in transcription negative feedback loops: simulation and experimental analysis. *Mol. Sys. Biol.*, 2:41, 2006. 65, 66, 67, 68, 70, 71, 91, 92

[31] H. El-Samad and M. Khammash. Modelling and analysis of gene regulatory network using feedback control theory. *Int. J. Syst. Sci.*, 41(1):17–33, 2010. 92

[32] J. Elf, G.-W. Li, and X. S. Xie. Probing Transcription Factor Dynamics at the Single-Molecule Level in a Living Cell. *Science*, 316:1191–1194, 2007. 68

[33] M B Elowitz and S Leibler. A synthetic oscillatory network of transcriptional regulators. *Nature*, 403(6767):335–8, 2000. 55

[34] M.B. Elowitz, A.J. Levine, E.D. Siggia, and P.S. Swain. Stochastic gene expression in a single cell. *Science*, 297:1183–1186, 2002. 50, 91

[35] K.-J. Engel and R. Nagel. *One-parameter semigroups for linear evolution equations.* Springer-Verlag, 2000. 120

[36] S. N. Ethier and T. G. Kurtz. *Markov Processes: Characterization and Convergence.* Wiley Interscience, 2005. 51, 120, 152, 157

[37] R. Feistel and W. Ebeling. *Evolution of Complex Systems.* VEB Deutscher Verlag der Wissenschaften, 1989. 114

[38] N. Fenichel. Geometric singular perturbation theory for ordinary differential equations. *J. Differ. Equations*, 31(1):53–98, 1979. 59, 129

[39] N. Friedman, L. Cai, and X.S. Xie. Linking stochastic dynamics to population distribution: An analytical framework of gene expression. *Phys. Rev. Lett.*, 97: 168302–1/4, 2006. 51, 52, 89, 102, 113, 114, 130

[40] C. Gadgil, C. H. Lee, and H. G. Othmer. A stochastic analysis of first-order reaction networks. *B. Math. Biol.*, 67:901–946, 2005. 86

[41] T. Galla. Intrinsic fluctuations in stochastic delay systems: Theoretical description and application to a simple model of gene regulation. *Phys Rev E Stat Nonlin Soft Matter Phys*, 80(2):1–9, 2009. 92

[42] C. W. Gardiner. *Handbook of stochastic methods, for physics, chemistry and the natural sciences.* Springer-Verlag, 1985. 129

[43] T. S. Gardner, C. R. Cantor, and J. J. Collins. Construction of a genetic toggle switch in Escherichia coli. *Nature*, 403(6767):339–42, 2000. 55, 114

[44] I. M. Gel'fand and N. Ya. Vilenkin. *Generalized Functions - vol. 4: Applications of harmonic analysis.* Academic Press, 1964. 140

[45] D. T. Gillespie. Exact stochastic simulation of coupled chemical reactions. *J. Phys. Chem. A*, 81(25):2340–2361, 1977. 51, 113, 114, 158

[46] I. Golding and E. C. Cox. Eukaryotic transcription: What does it mean for a gene to be 'on'? *Curr. Biol.*, 16(10):R371–73, 2006. 56

[47] I. Golding, J. Paulsson, S.M. Zawilski, and E.C. Cox. Real-time kinetics of gene activity in individual bacteria. *Cell*, 123:1025–1036, 2005. 51, 52, 69, 70, 72, 91, 92

[48] B. C. Goodwin. Oscillatory behavior in enzymatic control processes. *Adv. Enzyme. Regul.*, 3:425–437, 1965. 50, 53, 75, 76, 87

[49] A. N. Gorban, A. Zinovyev, N. Morozova, and A. Harel. Modeling coupled transcription, translation and degradation and mirna-based regulation of this process. pages –, 2012. arXiv:1204.5941v1. 91

[50] J. Goutsias. Quasiequilibrium approximation of fast reaction kinetics in stochastic biochemical systems. *J. Chem. Phys.*, 122(18):184102–15, 2005. 130

[51] J.S. Griffith. Mathematics of cellular control processes. I. Negative feedback to one gene. *J. Theor. Biol.*, 20:202–208, 1968. 75, 76

[52] J.S. Griffith. Mathematics of cellular control processes. II. Positive feedback to one gene. *J. Theor. Biol.*, 20:209–216, 1968. 75, 76

[53] S. Hahn and E. T. Young. Transcriptional regulation in saccharomyces cerevisiae: Transcription factor regulation and function, mechanisms of initiation, and roles of activators and coactivators. *Genetics*, 189(3):705–736, 2011. 56, 65

[54] H Haken. *Synergetics: An introduction.* Springer-Verlag, 1983. 129

[55] E. L. Haseltine and J. B. Rawlings. Approximate simulation of coupled fast and slow reactions for stochastic chemical kinetics. *J. Chem. Phys.*, 117(15):6959–6969, 2002. 130

[56] E. L. Haseltine and J. B. Rawlings. On the origins of approximations for stochastic chemical kinetics. *J. Chem. Phys.*, 123(16):164115–16, 2005. 133

[57] J Hasty, J Pradines, M Dolnik, and J J Collins. Noise-based switches and amplifiers for gene expression. *Proc. Natl. Acad. Sci.*, 97(5):2075–80, 2000. 55

[58] J Hasty, D McMillen, F Isaacs, and J J Collins. Computational studies of gene regulatory networks: in numero molecular biology. *Nat. Rev. Genet.*, 2(4):268–279, 2001. 55

[59] K.M. Hawkins and C.D. Smolke. The regulatory roles of the galactose permease and kinase in the induction response of the GAL network in Saccharomyces cerevisiae. *J. Biol. Chem.*, 281:13485–13492, 2006. 114

[60] J. P. Hespanha. Modelling and analysis of stochastic hybrid systems. *IEE P-Contr. Theor. Ap.*, 153(5):520–535, 2006. 51, 130

[61] T. Hida and Si Si. *An Innovation approach to random fields, Application of White Noise Theory.* World Scientific Pub. Co., 2004. 141, 142

[62] T. Hida and Si Si. *Lectures on White Noise Functionals.* World Scientific Pub. Co, 2008. 142

[63] J. E. M. Hornos, D. Schultz, G. C. P. Innocentini, J. Wang, A. M. Walczak, J. N. Onuchic, and P. G. Wolynes. Self-regulating gene: An exact solution. *Phys. Rev. E*, 72(5):051907—-, 2005. 85

[64] W. Horsthemke and R. Lefever. *Noise Induced Transitions: Theory and Applications in Physics, Chemistry, and Biology.* Springer-Verlag, 1984. 114

[65] D. Huh and J. Paulsson. Non-genetic heterogeneity from stochastic partitioning at cell division. *Nat. Genet.*, 43(2):95–100, 2011. 91

[66] P. J. Ingram, M. P. H. Stumpf, and J. Stark. Nonidentifiability of the source of intrinsic noise in gene expression from single-burst data. *PLoS Comput Biol*, 4(10): e1000192, 2008. 119

[67] F. J. Isaacs, J. Hasty, C. R. Cantor, and J. J. Collins. Prediction and measurement of an autoregulatory genetic module. *Proc. Natl. Acad. Sci.*, 100(13):7714–7719, 2003. 55, 65, 66, 67

[68] S. Iyer-Biswas, F. Hayot, and C. Jayaprakash. Stochasticity of gene products from transcriptional pulsing. *Phys Rev E Stat Nonlin Soft Matter PhysE*, 79(3):1–9, 2009. 85

[69] F. Jacob, D. Perrin, C. Sánchez, and J. Monod. L'opéron: groupe de gènes à expression coordonnée par un opérateur. *C. R. Acad. Sci. Paris*, 250:1727–1729, 1960. 53

[70] J. Jacod and A. N. Shiryaev. *Limit theorems for stochastic processes.* Springer-Verlag, 1987. 136, 140, 142

[71] T. Jia. *Stochastic Modeling of Gene Expression and Post-transcriptional Regulation.* PhD thesis, Faculty of the Virginia Polytechnic Institute and State University, 2011. 91

[72] T. Jia and R. Kulkarni. Post-Transcriptional Regulation of Noise in Protein Distributions during Gene Expression. *Phys. Rev. Lett.*, 105(1):1–4, 2010. 54

[73] A. Joffe and M. Metivier. Weak convergence of sequences of semimartingales with applications to multitype branching processes. *Adv. Appl. Probab.*, 18(1):20–65, 1986. 157

[74] M. Kaern, T.C. Elston, W.J. Blake, and J.J. Collins. Stochasticity in gene expression: From theories to phenotypes. *Nat. Rev. Genet.*, 6:451–464, 2005. 50, 56, 83, 119

[75] H.-W. Kang and T. G. Kurtz. Separation of time-scales and model reduction for stochastic reaction networks. *Ann. Appl. Probab. (to appear)*, 2011. 51, 52, 61, 119, 121, 123, 130, 133

[76] G. Karlebach and R. Shamir. Modelling and analysis of gene regulatory networks. *Nat. Rev. Mol. Cell. Biol.*, 9(10):770–780, 2008. 92

[77] T.B. Kepler and T.C. Elston. Stochasticity in transcriptional regulation: Origins, consequences, and mathematical representations. *Biophys. J.*, 81:3116–3136, 2001. 52, 92, 113, 119

[78] A. M. Kierzek, J. Zaim, and P. Zielenkiewicz. The effect of transcription and translation initiation frequencies on the stochastic fluctuations in prokaryotic gene expression. *J. Biol. Chem.*, 276(11):8165–72, 2001. 67, 68, 70, 71, 91

[79] J. J. Kupiec. A Darwinian theory for the origin of cellular differentiation. *Mol. Gen. Genet.*, 255:201–208, 1997. 92

[80] J. J. Kupiec. On the lack of specificity of proteins and its consequences for a theory of biological organization. *Prog. Biophys. Mol. Bio.*, 102(1):45–52, 2010. 53

[81] T. G. Kurtz. Solutions of ordinary differential equations as limits of pure jump markov processes. *J. Appl. Probab.*, 7(1):pp. 49–58, 1970. 155

[82] T. G. Kurtz. Random time changes and convergence in distribution under the meyer-zheng conditions. *Ann. Prob.*, 19(3):1010–1034, 1991. 137

[83] A. Lasota and M. C. Mackey. *Probabilistic properties of deterministic systems.* Cambridge University Press, 1985. 51, 147, 148

[84] A. Lasota and M.C. Mackey. *Chaos, fractals, and noise.* Springer-Verlag, 1994. 112

[85] J. Lei. Stochasticity in single gene expression with both intrinsic noise and fluctuation in kinetic parameters. *J. Theor. Biol.*, 256(4):485–92, 2009. 91

[86] J. Lei. Stochastic Modeling in Systems Biology. *J. Adv. Math. Appl*, in press:1–23, 2010. 91

[87] T. Lipniacki, P. Paszek, A. Marciniak-Czochra, A. R. Brasier, and M. Kimmel. Transcriptional stochasticity in gene expression. *J. Theor. Biol.*, 238(2):348–367, 2006. 85, 92, 113, 119

[88] A. Lipshtat, A. Loinger, N. Balaban, and O. Biham. Genetic Toggle Switch without Cooperative Binding. *Phys. Rev. Lett.*, 96(18):1–4, 2006. 106

[89] M. C. Mackey and M. Santillán. Dynamic regulation of the tryptophan operon : A modeling study and comparison with experimental data. *Proc. Natl. Acad. Sci.*, 98 (4):1364–1369, 2001. 55, 65, 66, 67, 68, 70, 71

[90] M. C. Mackey and M. Tyran-Kamińska. Dynamics and density evolution in piecewise deterministic growth processes. *Ann. Polon. Math.*, 94(2):111–129, 2008. 51, 99, 100, 101, 134, 147, 148

[91] M. C. Mackey, M. Tyran-Kaminska, and R. Yvinec. Molecular distributions in gene regulatory dynamics. *J. Theor. Biol.*, 274(1):84 – 96, 2011. 51, 52, 93, 102, 158

[92] M. C. Mackey, J. Lei, R. Yvinec, and C. Zhuge. Adiabatic reduction of jump processes in a model of stochastic gene expression with bursting transcription. 2012. arXiv:1202.5411. 52, 119, 130

[93] M. C. Mackey, M. Tyran-Kaminska, A. Ramos, and R. Yvinec. Discrete and continuous stochastic gene expression models with bursting. 2012. In preparation. 52, 93

[94] L. Mariani, E. G. Schulz, M. H. Lexberg, C. Helmstetter, A. Radbruch, M. Löhning, and T. Höfer. Short-term memory in gene induction reveals the regulatory principle behind stochastic IL-4 expression. *Mol. Sys. Biol.*, 6:359, 2010. 70, 71, 114

[95] H. H. McAdams and A. Arkin. Stochastic mechanisms in gene expression. *Proc. Natl. Acad. Sci.*, 94(3):814–819, 1997. 56

[96] H. H. McAdams and A. Arkin. It's a noisy business! Genetic regulation at the nanomolar scale. *Trends genet.*, 15(2):65–9, 1999. 55

[97] S. P. Meyn and R. L. Tweedie. Stability of markovian processes iii: Foster-lyapunov criteria for continuous-time processes. *Adv. Appl. Probab.*, 25(3):518–548, 1993. 51, 73, 74, 115

[98] E. L. O'Brien, E. Van Itallie, and M. R. Bennett. Modeling synthetic gene oscillators. *Math. Biosci.*, 236(1):1–15, 2012. 75

[99] A. Ochab-marcinek and M. Tabaka. Bimodal gene expression in noncooperative regulatory systems. *Proc. Natl. Acad. Sci.*, 107(51):22096–22101, 2010. 92

[100] H.G. Othmer. The qualitative dynamics of a class of biochemical control circuits. *J. Math. Biol.*, 3:53–78, 1976. 75, 76, 80

[101] P. Paszek. Modeling stochasticity in gene regulation: characterization in the terms of the underlying distribution function. *B. Math. Biol.*, 69(5):1567–601, 2007. 90

[102] J. Paulsson. Models of stochastic gene expression. *Phys. Life Rev.*, 2(2):157–175, 2005. 52, 83, 118

[103] A. Pazy. *Semigroups of Linear Operators and Applications to Partial Differential Equations*. Springer, 1992. 147

[104] J. Peccoud and B. Ycart. Markovian modelling of Gene Product Synthesis. *Theor. Popul. Biol.*, 48(2):222–234, 1995. 52, 74, 84, 118

[105] J. M. Pedraza and J. Paulsson. Effects of Molecular Memory and Bursting on Fluctuations in Gene Expression. *Science*, 319(5861):339–343, 2008. 91

[106] K. Pichór and R. Rudnicki. Continuous Markov semigroups and stability of transport equations. *J. Math. Anal. Appl.*, 249:668–685, 2000. 113

[107] A. Polynikis, S.J. Hogan, and M. di Bernardo. Comparing differeent ODE modelling approaches for gene regulatory networks. *J. Theor. Biol.*, 261:511–530, 2009. 75

[108] Yu. V. Prokhorov. Convergence of random processes and limit theorems in probability theory. *Theory Probab. Appl.*, 1(2):157–214, 1956. 142

[109] A. Raj and A. van Oudenaarden. Nature, nurture, or chance: Stochastic gene expression and its consequences. *Cell*, 135:216–226, 2008. 50, 56

[110] A. Raj and A. van Oudenaarden. Single-Molecule Approaches to Stochastic Gene Expression. *Annu. Rev. Biophys.*, 38:255–270, 2009. 50, 83

[111] A. Raj, C.S. Peskin, D. Tranchina, D.Y. Vargas, and S. Tyagi. Stochastic mRNA synthesis in mammalian cells. *PLoS Biol.*, 4:1707–1719, 2006. 51, 52, 69, 70, 72, 92

[112] A. Ramos, G. Innocentini, and J. Hornos. Exact time-dependent solutions for a self-regulating gene. *Phys Rev E Stat Nonlin Soft Matter Phys*, 83(6):1–4, 2011. 85

[113] S. Ramsey, A. Ozinsky, A. Clark, K. D. Smith, P. de Atauri, V. Thorsson, D. Orrell, and H. Bolouri. Transcriptional noise and cellular heterogeneity in mammalian macrophages. *Philos. T. Roy. Soc. B*, 361(1467):495–506, 2006. 67, 68, 70, 71

[114] C. V. Rao and A. P. Arkin. Stochastic chemical kinetics and the quasi-steady-state assumption: Application to the gillespie algorithm. *J. Chem. Phys.*, 118(11):4999–5010, 2003. 130

[115] J.M. Raser and E.K. O'Shea. Control of stochasticity in eukaryotic gene expression. *Science*, 304:1811–1814, 2004. 56, 119

[116] A. S. Ribeiro. Stochastic and delayed stochastic models of gene expression and regulation. *Math. Biosci.*, 223(1):1–11, 2010. 91, 92

[117] I. Roeder and I. Glauche. Towards an understanding of lineage specification in hematopoietic stem cells: A mathematical model for the interaction of transcription factors GATA-1 and PU.1. *J. Theor. Biol.*, 241:852–865, 2006. 92

[118] R. G. Roeder. Transcriptional regulation and the role of diverse coactivators in animal cells. *FEBS lett.*, 579(4):909–15, 2005. 56, 65

[119] S. Roelly. A criterion of convergence of measure-valued processes: application to measure branching processes. *Stochastics*, 17(1-2):43–65, 1986. 157

[120] N. Rosenfeld, J. W. Young, U. Alon, P. S. Swain, and M. B. Elowitz. Gene regulation at the single-cell level. *Science*, 307:1962–1965, 2005. 56, 67, 91

[121] W. Rudin. *Functional analysis*. McGraw-Hill Scienc, 1991. 140

[122] F. Sagués, J. Sancho, and J. García-Ojalvo. Spatiotemporal order out of noise. *Rev. Mod. Phys.*, 79(3):829–882, 2007. 91

[123] M. Santillán and M. C. Mackey. Dynamic behavior in mathematical models of the tryptophan operon. *Chaos*, 11(1):261–268, 2001. 55, 64

[124] M. Santillán and H. Qian. Irreversible thermodynamics in multiscale stochastic dynamical systems. *Phys Rev E Stat Nonlin Soft Matter Phys.*, 83:1–8, 2011. 133

[125] H.H. Schaefer. *Topological Vector Spaces*. Springer-Verlag, 1971. 140, 141

[126] D. Schultz, J. N. Onuchic, and P. G. Wolynes. Understanding stochastic simulations of the smallest genetic networks. *J. Chem. Phys.*, 126(24):245102–245102, 2007. 85

[127] B. Schwanhäusser, D.a Busse, N. Li, G. Dittmar, J. Schuchhardt, J. Wolf, W. Chen, and M. Selbach. Global quantification of mammalian gene expression control. *Nature*, 473(7347):337–42, 2011. 70, 71

[128] J.F. Selgrade. Mathematical analysis of a cellular control process with positive feedback. *SIAM J. Appl. Math.*, 36:219–229, 1979. 75, 80

[129] V. Shahrezaei and P.S. Swain. Analytic distributions for stochastic gene expression. *Proc. Natl. Acad. Sci.*, 105:17256–17261, 2008. 52, 88, 89, 93, 96, 101, 113, 119, 123

[130] V. Shahrezaei and P.S. Swain. The stochastic nature of biochemical networks. *Curr. Opin. Biotechnol.*, 19:369–374, 2008. 83

[131] V. Shahrezaei, J.F. Ollivier, and P.S. Swain. Colored extrinsic fluctuations and stochastic gene expression. *Mol. Syst. Biol.*, 4:196–205, 2008. 51

[132] A. Singh and J. P. Hespanha. Noise suppression in auto-regulatory gene networks. *IEEE Decis. Contr. P.*, 2:787–792, 2008. 87

[133] H.L. Smith. *Monotone Dynamical Systems*. American Mathematical Society, 1995. 76, 80, 82

[134] C. Song, H. Phenix, V. Abedi, M. Scott, B. P. Ingalls, and M. Krnand T. J. Perkins. Estimating the Stochastic Bifurcation Structure of Cellular Networks. *PLoS Comput. Biol.*, 6:e1000699/1–11, 2010. 92, 114

[135] M. Stamatakis and N. V. Mantzaris. Comparison of deterministic and stochastic models of the lac operon genetic network. *Biophys. J.*, 96(3):887–906, 2009. 54, 65, 66, 68, 70, 71

[136] G. Storz and L. S. Waters. Regulatory rnas in bacteria. *Cell*, 136(4):615–628, 2009. 91

[137] G. M. Süel, J. Garcia-Ojalvo, L. M. Liberman, and M. B. Elowitz. An excitable gene regulatory circuit induces transient cellular differentiation. *Nature*, 440(7083): 545–550, 2006. 92

[138] P.S. Swain, M.B. Elowitz, and E.D. Siggia. Intrinsic and extrinsic contributions to stochasticity in gene expression. *Proc. Natl. Acad. Sci.*, 99:12795–12800, 2002. 91

[139] Y. Tao, Y. Jia, and T. G. Dewey. Stochastic fluctuations in gene expression far from equilibrium: Omega expansion and linear noise approximation. *J. Chem. Phys.*, 122 (12):124108, 2005. 87

[140] Y. Tao, X. Zheng, and Y. Sun. Effect of feedback regulation on stochastic gene expression. *J. Theor. Biol.*, 247(4):827–36, 2007. 87

[141] P. K. Tapaswi, R. K. Roychoudhury, and T. Prasad. A Stochastic Model of Gene Activation and RNA Synthesis during Embryogenesis. *Sankhya Ser. A*, 49(1):51–67, 1987. 91

[142] M. Thattai and A. van Oudenaarden. Intrinsic noise in gene regulatory networks. *Proc. Natl. Acad. Sci.*, 98(15):8614–8619, 2001. 56, 66, 67, 68, 69, 86, 87

[143] A. N. Tikhonov. Systems of differential equations containing small parameters in the derivatives. *Mat. Sb. (N.S.)*, 31 (73):575–586, 1952. 59, 129

[144] T.-L. To and N. Maheshri. Noise can induce bimodality in positive transcriptional feedback loops without bistability. *Science*, 327(5969):1142–5, 2010. 67, 70, 71, 86

[145] M. Tyran-Kamińska. Substochastic semigroups and densities of piecewise deterministic markov processes. *J. Math. Anal. Appl.*, 357(2):385–402, 2009. 51, 94, 99, 147

[146] J. J. Tyson. On the existence of oscillatory solutions in negative feedback cellular control processes. *J. Math. Biol.*, 1(4):311–315, 1975-12-01. 76

[147] X. S. Xie, P. J. Choi, G.-W. Li, N. K. Lee, and G. Lia. Single-Molecule Approach to Molecular Biology in Living Bacterial Cells. *Annu. Rev. Biophys.*, 37:417–444, 2008. 50

[148] G. Yagil and E. Yagil. On the relation between effector concentration and the rate of induced enzyme synthesis. *Biophys. J.*, 11(1):11–27, 1971. 56

[149] N. Yildirim, M. Santillán, D. Horike, and M. C. Mackey. Dynamics and bistability in a reduced model of the *lac* operon. *Chaos*, 14:279–292, 2004. 80

[150] J. Yu, J. Xiao, X. Ren, K. Lao, and X.S. Xie. Probing gene expression in live cells, one protein molecule at a time. *Science*, 311:1600–1603, 2006. 51, 52, 69, 72, 92

[151] I. Zacharioudakis, T. Gligoris, and D. Tzamarias. A yeast catabolic enzyme controls transcriptional memory. *Curr. Biol.*, 17:2041–2046, 2007. 114

[152] D. Zenklusen, D. R. Larson, and R. H. Singer. Single-RNA counting reveals alternative modes of genes expression in yeast. *Nat. Struct. Mol. Biol*, 15(12):1263–1271, 2008. 70, 71

[153] E. S. Zeron and M. Santillán. Distributions for negative-feedback-regulated stochastic gene expression: Dimension reduction and numerical solution of the chemical master equation. *J. Theor. Biol.*, 264(2):377–385, 2010. 133, 158

[154] D. Zhou and R. Yang. Global analysis of gene transcription regulation in prokaryotes. *Cell. Mol. Life. Sci.*, 63(19-20):2260–90, 2006. 56, 65

Chapter 2

Study of stochastic Nucleation-Polymerization Prion Protein Model

This chapter deals with protein aggregation models. These models are dealing with the dynamics of the formation of polymers (aggregates) formed of proteins, and related to a number of applications in physics and biology.

In section 1, the biological problem associated to prion diseases is presented, along with the experimental observations, obtained by the biologists who work with us, and the interesting questions they raised. We also review the literature on aggregation kinetic models. The application of our theoretical work (to be described below) to the specific model of prion diseases, was done in a collaboration with a team of biologists, directed by Jean-Pierre Liautard (Centre de Recherche sur les Pathogènes et Biologie pour la Santé (CPBS), Université Montpellier-2). *In vitro* nucleation-polymerization experiments has been analyzed quantitatively, and specially their heterogeneity.

In section 2, the formulation of the chosen model is presented, in order to investigate the questions raised by the experimental observations. This model is composed of a discrete size Becker-Döring model with finite maximal size, and a discrete size polymerization-fragmentation model. Then, a time-scale reduction is performed, based on biological hypotheses, to reduce the complexity of the model. This reduction highlights links between a conservative form and a non-conservative form of the Becker-Döring model.

In section 3, the first assembly time of a given fixed size aggregate is studied. Both a conservative and non-conservative form of a Becker-Döring model are used. Our main findings is that the stochastic and finite particle formulation gives different results from the deterministic and infinite particle formulation. In particular, we are able to characterize some discrepancies, to highlight finite system-size effect and to quantify the stochasticity in the first assembly time. In a stochastic formulation, the first assembly time may never be reached (and hence has an infinite mean time), and displays surprising non-monotonicity with respect to aggregation rates. Also, it is found that the mean first assembly time has very different relationship with respect to the initial quantity of particle, depending on the parameter region. Indeed, the mean first assembly time may be strongly correlated with the initial quantity of particle or very weakly. Finally, the distribution of this first assembly time can have various different forms (Exponential, Weibull, bimodal), and may be far from a symmetric Gaussian, as a typical mean-field approach would have predicted. Then, such findings may have significant importance when analyzing aggregation experiments, and help us to understand the experimental observations on prion experiments. This study has been the subject of a preprint, with Maria R D'Orsogna and Tom Chou.

In section 4, the large population limit is investigated. Starting from a purely individual and stochastic polymerization-fragmentation model (sometimes called the direct simulation process), a convergence towards a hybrid infinite monomer population / finite polymer population is shown. This study follows many recent contributions on limit theorem from discrete to continuous model. In particular, standard martingale techniques are used to obtain a convergence in law of the stochastic process. The novelty lies in the fact that the asymptotic model seems to have never been applied in such field. Its hybrid structure may be a good balance between fully discrete and fully continuous model, and may be well adapted to quantify the heterogeneity of the prion proliferation observed experimentally. This work is an ongoing project with Erwan Hingant (Université Lyon 1).

The aim of our analytical study developed in both sections 3 - 4 is to quantify the amount of stochasticity, to validate or invalidate kinetic hypotheses, and to deduce parameter values from experiments. This work is an ongoing project with Teresa Alvarez-Martinez, Samuel Bernard, Jean-Pierre Liautard and Laurent Pujo-Menjouet.

1   Introduction

In this chapter, mathematical models of protein aggregation kinetics are studied. These models are conceived to represent faithfully the aggregation dynamics of a particular protein, the prion protein, and to explain the experimental observations. Thus, we start to introduce the necessary biological concepts and motivations, before going to the mathematical study. Firstly, the diseases linked to the dynamics of aggregation of this prion protein are reviewed in section 1.1. Secondly, the main kinetic hypotheses for this protein aggregation model are introduced in subsections 1.1.0.1 - 1.2. Thirdly, to motivate the mathematical study of such a model, the different experimental techniques used for prion modeling are presented in subsection 1.3. The specific *in vitro* experiments we used on prion aggregation kinetic are described in subsection 1.4, and the main unusual feature associated to it is explained. Finally, we end up this introduction by a mini literature review on coagulation-fragmentation model, in order to give an overall picture of the field.

1.1   Biological background: what is the prion?

Diseases such as Creutzfeldt-Jacob or Kuru for human, and bovine spongiform encephalopathies (BSE), scrapie (in sheep) or chronic-wasting disease for animals are all spongiform encephalopathies and belong to a larger class of neurodegenerative disorders ([103]). The key features of spongiform encephalopathies are the followings:

- they are transmissible, and the agent responsible for such transmission is a protein (rather than a virus, bacteria...), called prion. It is usually referred to the protein-only hypothesis, and to any disease related to it as a "prion disease";
- they are characterized by a long incubation time (up to 50 years in humans). This phase is followed by a rapid and dramatic clinical phase (some months or a few years), leading to brain damage and death. Symptoms are convulsions, dementia, ataxia (balance and coordination dysfunction), and behavioral or personality changes;
- they affect the structure of the brain or other neural tissue, and amyloid plaques, formed of protein aggregates, are observed. Such region are spongiform. No immune response has been detected;
- No treatments are known, and no diagnostic during the incubation time are known.

From an historical point of view, the biologist Tikvah Alper and mathematician John Stanley Griffith ([64]) first developed the hypothesis during the 1960s that some transmissible spongiform encephalopathies are caused by an infectious agent consisting solely of proteins. This hypothesis had lots of impact, in molecular biology, for its potential contradiction with the so-called "central dogma" (see chapter 1). It was in 1982 that Stanley B. Prusiner announced that his team had purified the hypothetical infectious prion, and that the infectious agent consisted only of a specific protein ([123]). Nowadays, prion diseases are still a major public health issue. Such diseases are then transmissible, within a same species or from species to species (including from animals to human), or can also appear spontaneously. The control of occurrences and transmissions of such diseases is related to a better understanding of involved mechanism inside organisms. The difficulty is that the mechanisms involved occur at very different time scale, including large time scale, hardly captured by experimental observations. Then there have been numerous theoretical modeling approaches to help understanding such mechanisms (see subsection 1.5 for a small review).

It has generally been accepted that spongiform encephalopathies result from the aggregation of an ubiquitous protein, the so-called prion protein, into amyloids ([29], [39], [123]). It is also believed that the formation of prion amyloid is due to a change of the

prion protein conformation ([97], [38]). The normal (or non-pathological) conformation of this protein is called PrP^C (standing for cellular Prion Protein). This protein can misfold (change conformation), and the misfolded protein has a tendency to form aggregates. These aggregates are referred as PrP^{Sc} (standing for Scrapie Prion Protein). The aggregation process leads to a decrease of PrP^C level by a conversion mechanism. One difficulty of understanding the cause of the pathology relies on the very different form prion aggregates can take, and the many different possible kinetic pathways that lead to such aggregates (see the next paragraph for aggregation kinetics controversy). In particular, to the best of our knowledge, it is not sure what is the exact cause of the disease. It could be due either to some specific form of aggregates — it is not known actually which of the different aggregate forms of the prion could be toxic, and what are the exact pathogenic mechanisms leading to the disease [74] — or, as said above, it could be due to a PrP^C monomer decay. The protein population decreases is indeed the consequence of protein polymerization to the PrP^{Sc} polymers after a specific conformation change. However, in any case, the overall dynamic of the process is still relevant to understand the main features of the disease.

1.1.0.1 Debates on different aggregation kinetics. In the previous decades, the kinetic of amyloid formations has been the subject to extensive researches and is still currently under investigation. For a good review on protein aggregation kinetics, see [110] for instance. One of the particularity of prion protein aggregation is that the different and many possible pathways leading to the formation of amyloid fibers from single proteins (monomers) or pre-formed seeds (polymers) are not fully understood and still subject to controversy [83], [72].

The early process of transconformation of prion protein is also subject to debate. It is generally accepted that this process does not involve any other molecules although it could be mediated by another misfolded protein ([94], [123], [5]). Recent studies using dynamic models tried to explain possible routes of spontaneous protein folding ([20],[41]).

1.2 The Lansbury's nucleation/polymerization theory

The main stream molecular theory to explain the prion polymer dynamic is the one introduced by Lansbury *et al.* in 1995 [29]. In this paper, the authors investigate the formation of large aggregates of proteins ordered by specific contacts. The model, based on nucleation-dependent protein polymerization, describes various well-characterized processes, including protein crystallization, microtubule assembly, flagellum assembly, sickle-cell hemoglobin fibril formation, bacteriophage procapsid assembly, actin polymerization and amyloid polymerization.
Inspiring different groups of biologists and mathematicians who tried later on to improve this first model, their ideas are based on the following biological assumptions. The normal PrP^C protein does not aggregate by itself. But a misfolded form of it is able to aggregate, and the aggregates are called PrP^{Sc}. Such misfolded form can appear spontaneously from spatial and chemical modification of PrP^C. When PrP^{Sc} are present, they start to aggregate the misfolded protein by addition of one by one protein. Firstly, the early aggregation formation requires a series of association steps that are thermodynamically unfavorable (with an association constant $K \ll 1$). These aggregation steps are unfavorable up to a given size (that is not currently known), which is referred to the nucleus size. Secondly, once a nucleus is formed, further addition of monomer becomes thermodynamically favorable (with an association constant $K \gg 1$) resulting in rapid polymerization/growth ([49], [26], [4], [6]). The model is the named nucleation-dependent polymerization model, be-

cause the overall polymerization dynamic depend strongly on whether a nucleus is present or not. Starting from a homogeneous pool of monomer, the formation of the first nucleus (an event called nucleation), leads to a drastic change in the dynamic. The first step, corresponding to nucleation, is a very unstable process and can be more stochastic than deterministic, while the second and further steps would be quite straightforward and more deterministic.

According to this theory, because of its high stochasticity, nucleus formation would be considered as a kinetic barrier to sporadic prion diseases. But this barrier could be overcome by infection with a large polymer. The disease would not be spontaneous anymore, it could be transmitted (on purpose or not) by a PrP^{Sc} polymer (called seed) which would directly lead to the second deterministic step since no formation of the first nucleus would be required.

Finally, long PrP^{Sc} polymers are also subject to fragmentation. They can break to smaller polymers, which lead to a multiplication of aggregation sites, and then to an exponential growing phase of the total protein mass contained in polymers [29].

1.3 Experimental observations available

There are mainly four levels on which experimental data on prion diseases can be collected.

- A first level is a population level. The number of infected people can be recorded and followed along time. For humans, due to the difficulty of the diagnostic and the long incubation time, few significant and robust data exists. The situation is slightly better for animals, specifically on bovines (mostly in Europe) or deers (North-America) [143].
- A second level is the cellular level. It is possible to follow an *in vivo* cell population in animals, or to make a culture of cells, infected by PrP^{Sc} aggregate. However, for both, the great complexity of cell dynamics (extra cellular interactions, different feedbacks, *etc.*) make it hard to collect pertinent information on the dynamics of the event that lead to cell infection. An open question concerned the interaction between the prion amyloids and the subcellular environment (where the prions are formed? how does it depends on the cell behaviour? and so on...). See [101] for some related questions.
- A third level, which we will be interested in, is the protein level. The progress of physical methods and techniques has made possible to partially study the structure of prion protein, for both the PrP^{C} and the PrP^{Sc}. Then a variety of different structures of prion amyloids have been characterized (see [109, 121] for some review of what is known on the molecular basis). However, due to the highly unstable form of the misfolded prion monomer, and its small size aggregates, the intermediate form (between the monomer to large polymer) are not well characterized. Still at this level, recent techniques allow to perform *in vitro* conversion of prion protein into PrP^{Sc} polymer, and to follow the dynamic of this conversion through fluorescence markers. These techniques requires to use a modified form of the PrP^{C}, called the recombinant PrP^{C}. From a homogeneous pool of recombinant PrP^{C} protein, the formation of polymer and larger amyloids is observable. The amount of mass (or rather the intensity of fluorescence, supposedly linearly correlated) that is present in polymers can be recorded trough time, within a time scale that is conceivable in a laboratory (typically $24h$ or a week). The main drawbacks of such method is that the recombinant PrP^{C} protein has been modified chemically, and may not hence repro-

duce faithfully the feature of the original prion PrP^C protein. It also requires high protein concentration, to a level that exceeds physiological concentration. Whether or not the obtained amyloids are able to generate infectiousity is also still unclear [138]. Finally, let us mention that some techniques also permit to measure the size of the amyloid obtained experimentally.

- A fourth level, even smaller, concern the atomic level of the protein. The idea is to precisely understand the physical and spatial structure of the protein , to characterize its stability and investigate all possible transconformation [20].

In vitro polymerization experiments of prion protein give some interesting insights of what could be the different mechanisms involved in the process. Interestingly, a main dynamical characteristic of the mechanism is used experimentally. Indeed, the PMCA (Protein Misfolding Cyclic Amplification) consists of successive phase of incubation and sonication in order to obtain lot of polymer fragments. During incubation, the polymer are supposed to growth by aggregation, and the sonication breaks large polymers, and hence speed up the next incubation phase, and so on. Agitating during polymerization experiments also speed up the polymerization process. We discern between two kinds of *in vitro* polymerization experiments:

- Those started with a homogeneous pool of protein recombinant are called nucleation experiments. In these experiment, the time required for the polymerization to truly start can be measured. According to Lansbury's theory, such time is related to the waiting time for one nucleus to appear. We refer either to the first assembly time, to the nucleation time, or to the lag time.
- A second kind of experiments is the seeding experiment. In such experiments, a pre-formed seed (a large polymer) is present initially with and a pool of recombinant prion protein.

In both experiments, as well as in nucleation experiments, we can record through time the intensity of fluorescence, which relates to the total mass present in polymers. Such measures allow in particular to look at the speed of the polymerization process. We present more in detail in the next section the qualitative and quantitative behavior of the nucleation-polymerization process.

For *in vitro* polymerization experiments, one of the challenges resides in the low sensitivity to the dynamical properties of the polymerization on initial concentration of prion protein ([13], [54], [115], [120]), as well as to the high heterogeneity of the outcomes. But before precisely defining such concept, the result of polymerization experiments are shown in details.

1.4   Observed Dynamics

We present here the *in vitro* polymerization experiments performed by the biologists who work with us. All experiments were previously published [100], [3]. Firstly, we give details about the experimental set up. Secondly, we present a typical outcome of a polymerization experiments. Thirdly, we show statistics on the nucleation time and polymerization speed deduced from the nucleation experiments. Finally, we explain the qualitative features of the seeding experiments, and the information that can be extracted from it.

Nucleation-Polymerisation experiments were performed with an initial population of recombinant Prion protein ($rPrP$) from Syrian hamster (Misocricetus auratus) and produced as described previously([100]). Protein concentrations were determined by spectrophotometry (Beckman spectrophometer) using an extinction coefficient of 25 327 M-1cm-1 at 278 nm and a molecular mass of 16,227 kDa. Samples containing 0.4 to 1.2

mg/ml of the oxidized form of HaPrP90-231 (recombinant PrP^C, $rPrP$) were incubated for 1-5 days with phosphate-buffered saline (PBS), 1M GdnHCl, 2.44 M urea, 150 mM NaCl (Buffer B). The $rPrP$ spontaneously converted into the fibrillar isoform upon continuous shaking at 250 rpm in conical plastic tubes (Eppendorf). The kinetics of amyloid formation was monitored in SpectraMax Gemini XS (Molecular Devices). Samples containing 0.1 to 1.2 mg/ml of the oxidized form of HaPrP90-231 ($rPrP$) were incubated upon continuous shaking at 1350 rpm in 96-well plates and in the presence of ThT (10 μM). The kinetics was monitored by measuring the fluorescence intensity using 445 nm excitation and 485 and 500 nm emission. Every set of measurements was performed in triplicates, and the results were averaged.

In figure 2.1a are presented results of several nucleation experiments performed as described above. The ThT fluorescence is used as a measurable quantity, correlated (supposedly linearly) to the total mass of polymers during experiments. A population of monomer recombinant Prion protein ($rPrP$) at a given concentration (from 0.1 to 1.2 mg/mL) is present initially, together with ThT fluorescent. The $rPrP$ spontaneously converts into fibrillar isoform (polymer), upon which the ThT binds. Then the polymerization kinetic is monitored by measuring the fluorescence intensity for $1 - 5$ days. From figure 2.1a the diversity and heterogeneity (to be explained further) of the experimental results can be immediately observed. However, experiments were performed in same experimental conditions, with the same recombinant prion protein. The aim of quantitative analysis of polymerization kinetics is to validate or invalidate kinetic hypotheses and to determine parameters values. For this, quantitative information has to be determined from experimental results. For this, the experimental curve is fitted with the general equation of a sigmoid (figure 2.1b).

(a) Time Experimental Series   (b) Fitting Curve
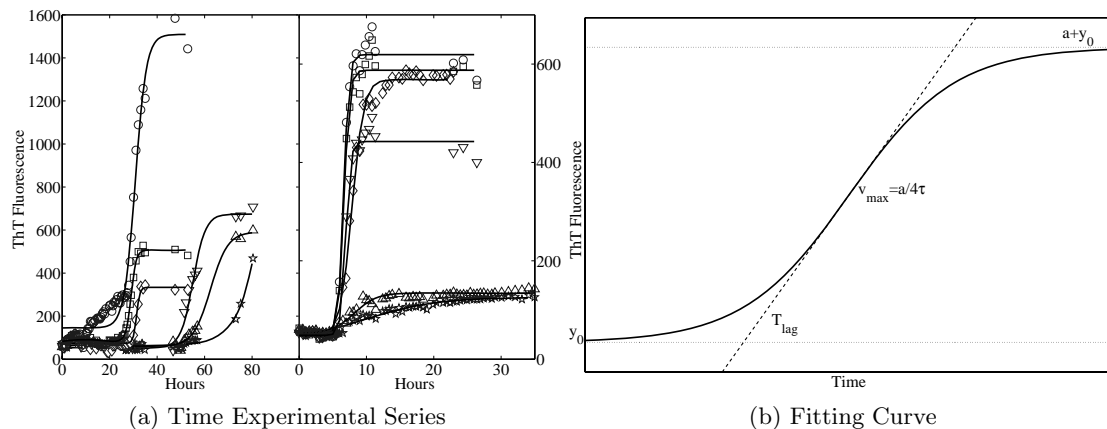
Figure 2.1: (a) Time (in hours) evolution of the ThT fluorescence (arbitraty units) in various spontaneous polymerization. The ThT fluorescence is used as a measurable quantity, correlated to the total mass of polymers. The experiments were performed in two different conditions (left and right panel), with an initial population of recombinant prion protein (PrPc). Each type of symbol corresponds to one experiment, and each symbol corresponds to a time measurement. For each experiment, the experimental set of measurements was fitted according to a sigmoid given by eq. (1.1) and shown in solid lines. (b) The solid line is a sigmoid function given by eq. (1.1). We can see the definition of the key parameters on this curve: v_{max} is the maximal slope of the sigmoid, which is achieved at the inflexion point. The tangent at this point is represented in dotted line. We note $\frac{1}{\tau}$ the maximal speed, normalized by the mass that polymerized, which is named by a on the figure. Then T_{lag} is the waiting time for the polymerization to start. See the text for more details.

We first note that the mass of polymer follows an evolution shaped as a sigmoid (figure 2.1b) given by the general following sigmoid equation,

$$F = y_0 + \frac{a}{1 + e^{\frac{-(t-T_i)}{\tau}}}. \tag{1.1}$$

This equation is phenomenological but gives a rather good estimate of some parameters used to compare the models with the experiments. Four quantities appear to be characteristic of the prion aggregation dynamic. Firstly, $F_{max} = a + y_0$ is the maximal fluorescent value reached asymptotically, at the end of the experiment (while y_0 is the initial level of fluorescence). Secondly, $\frac{1}{\tau}$ is the (normalized) maximal polymerization rate, which is achieved at $t = T_i$, the inflexion point. Finally, the lag time T_{lag} is the waiting time for the true start of polymerization. In our stochastic model, the start of the polymerization is due to a discrete event (the first nucleation). However, this supposedly discrete event is not observable experimentally, and the continuous and smooth sigmoid curve we used to fit experimental results cannot give such information. Then, in agreement with the literature, the lag time is defined as the time required to measure a given fraction of the maximum value, say 10%. This time can only be measured on the sigmoid curve. This time is actually very close [1] to the formula given by Lee et al. ([95]), which linked the lag time to T_i and τ by the equation (see figure 2.1b) as

$$T_{lag} = T_i - 2\tau.$$

All these quantities (F_{max}, y_0, a, τ, T_i, T_{lag}) can be measured on each experimental curve as sampled in figure 2.1a. We can see on figure 2.1a that the dynamic of prion amyloid formation on each experiment is high heterogeneous, even if they were obtained under the same experimental conditions. Namely, each of the three quantities T_{lag}, τ and F_{max}, on which we mainly focus, are highly variable from one experiment to another. Let us first present statistics for each one, how they correlate with the initial concentration of protein, and finally how they correlated within each other. We will see that such analysis suggests a stochastic formulation of a nucleation-polymerization model, which gives rise to a heterogeneity in the dynamics of polymerization, as well as in the obtained structure of polymers. This analysis is partially described in a recent paper [3].

1.4.1   Nucleation Time Statistics

The initial concentration of protein and the lag time are usually inversely correlated in protein nucleation experiments ([54], [40], [13]). This feature is common in different fields of physics and biology (polymer, crystallization). However, in these experiments, these two quantities are very poorly correlated: we found a correlation coefficient of -0.08 and a p-value of 0.49. (figure 2.2 A). These results show that the lag time and the initial concentration are not correlated between each other. Such a phenomenon has been observed previously for prion protein nucleation experiments ([40], [13]).

We look also at the variability of the lag time while repeating experiments in the same conditions. The coefficient of variability (standard deviation over the mean) is respectively 0.77, 0.72 and 0.55 for $m_0 = 0.4$, 0.8, 1.2 mg/L, over 29, 24 and 19 experiments.

The distributions of lag time in experiments are shown in figure 2.2 B. As the initial concentration increase, the main peak is sharper and the tail is fatter (the Kurtosis coefficient varies from -0.07, 4.46 and 0.64). The distribution is very asymmetric for intermediate concentration (the skewness varies from 0.91, 2.1 and 1.03). We note however that the number of experiments is too small to deduce any distribution fitting.

---

1. *note: the ten percent value is actually given by $T_i - ln(9)\tau$
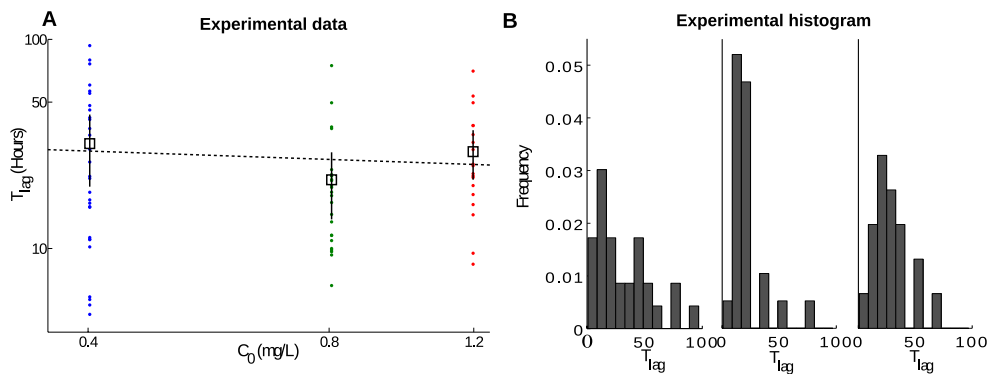
Figure 2.2: **Analysis of the T_{lag} in spontaneous polymerization *in vitro* experiments**. **A** Each triangle represents the T_{lag} (in hours) found by fitting one experimental curve with eq. (1.1), as shown in figure 2.1b. Experiments are performed with the same condition, with respectively initial concentration of 0.4, 0.8 and 1.2 mg/L of $rPrP$ protein. The black squares represent the mean and the dashed line is obtained by a linear fit of these means as a function of the initial concentration. The slope is -0.13 hours^{-1}.mg^{-1}.L. The correlation coefficient between the lag time and the initial concentration is -0.08, with a p-value of 0.49. **B** Histograms of the lag time in spontaneous polymerization experiments. From left to right, the initial concentration of protein is 0.4, 0.8 and 1.2 mg/L. The histograms are constructed based on the points on the left figure, with respectively 29, 24 and 19 experiments.

1.4.2   Polymerization Speed Statistics

The (normalized) maximal polymerization rate is also poorly correlated with the initial concentration of protein (see figure 2.3a). The high heterogeneity of the growth rate (the coefficient of variability are respectively 0.58, 0.23 and 0.55 for 0.4, 0.8 and 1.2 mg/L initial concentration) may explain this weak relationship. We also compute the distributions of polymerization rate in experiments (figure 2.3b).

1.4.3   Maximal Fluorescence Statistics

For a specific set of experiment, the maximal fluorescence get concentrated in two distinct regions, whatever the initial concentration protein is (figure 2.4). Indeed, in independent samples obtained in the same experimental conditions, the histogram of the final fluorescence value was bimodal, with peaks around 520 or 2280 (arbitrary units). We showed that segregating experiments with those giving a low F_{max} value and those giving a high F_{max} value, increased significantly the correlation coefficient (from 0.42 to 0.7 and 0.6, see figure 2.4A) between F_{max} and the initial concentration.

1.4.4   Correlation with each other

The figures and analysis presented here were the subject of a publication [3]. It has been shown that the maximum value F_{max} is not correlated with the remain quantity of monomers at the end of the experiment, neither with the lag time or the maximum growth rate (figure 2.5a - 2.5b).

We also note that the lag time and the maximal growth rate are apparently uncorrelated (figure 2.5c)

(a) Experimental data   (b) Experimental histogram
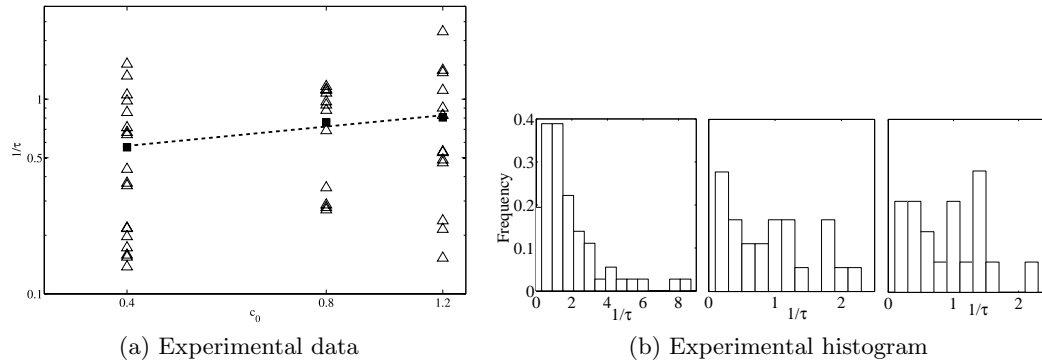
Figure 2.3: Normalized maximal polymerization rate. (a) Normalized maximal polymerization rate with initial quantity of PrP protein (**in log scale**). Each triangle represents the rate $1/\tau$ (in hours^{-1}) found by fitting the experimental curve with eq. (1.1), as explained in the subsection 1.4. Experiments are performed with the same condition, with respectively 0.4, 0.8 and 1.2 mg/L of PrP protein. The black squares represent the mean of the experimental values, for each concentration. The dashed line is obtained by a linear fit of these means as a function of the initial concentration. The slope is 0.33 hours^{-1}.mg^{-1}.L . (b) Histograms of the polymerization rate in spontaneous polymerization experiments. From left to right, the initial concentration of protein is 0.4, 0.8 and 1.2 mg/L. The histograms are constructed based on respectively 29, 24 and 19 experiments.

1.4.5   Seeding experiments and conclusion

1.4.5.1   Heterogeneity of the structure. Such a difference in the F_{max} value, obtained in repeated experiments, cannot be explained by a difference in the polymerized mass, but only by a difference in the final polymer structure, as argued in [3]. The electron microscopy analysis gives a clue to interpret this heterogeneity: we can clearly see that different polymers may appear (figure 2.6a). Actually, it has been shown that different polymers with different structures have a different binding affinity with the ThT-fluorescence. Direct measurements of the size of polymers have indeed confirmed that the relation between the size of polymer with its fluorescence response to ThT highly depends on the structure of the polymer (figure 2.6b). This explains why we observed in paragraph 1.4.3 two distinct peaks for the final fluorescence value F_{max} in polymerization experiments. Intermediate values within this two ranges of values can be explained either by an additional structure or the presence of both structures (figure 2.4B).

1.4.5.2   Seeding experiments. We have seen that there is an heterogeneity in the polymer structure. Further analysis of the experimental results reveals that the different polymer structures are the result of a heterogeneous process before nucleation takes place. For this, we need to look at results of seeding experiments.

It has long been suggested that the seeding experiments explain the infectiousity of the prion disease. Indeed, experiments with increased initial quantity of seed exhibit subsequent reduction of lag time (figure 2.7a). It is also interesting to note how these seeding experiments bring some information into the overall polymerization process.

Firstly, it has to be noticed that this lag time does not disappear, suggesting that it exists a conformational mechanism that could not be suppressed before the polymerization can take place. Secondly, successive seeding experiments (the polymers obtained at the end of an experiment is used as seeds for the next seeding experiment) increase the polymerization growth rate (figure 2.7b). However, it has been shown that successive seedings
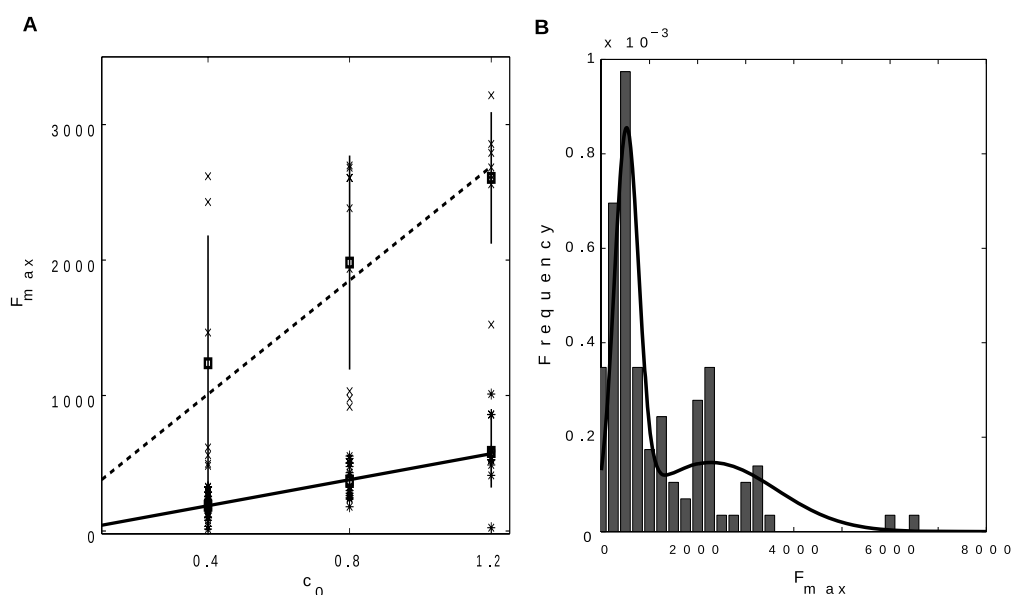
Figure 2.4: **Maximal fluorescent values in spontaneous polymerization**. **A** Each point represent the experimentally measured final value of fluorescence (arbitrary unit), as a function of the initial concentration of proteins. All experiments are performed in the same conditions with initial concentration of proteins respectively 0.4, 0.8 and 1.2 $mg.L^{-1}$. We then segregate arbitrarily the values in two categories: the "highest values"and the "lowest values". The higher dashed line shows a linear fit of the mean among the highest value (as a function of the initial concentration), and the lower solid line shows a linear fit of the mean among the lowest value (as a function of the initial concentration). The slopes are respectively 2.5×10^{-3} and 4.4×10^2 $L.mg^{-1}$. We also calculated the correlation coefficient between the final value of fluorescence F_{max} and the initial concentration. Before separating the values, the correlation value is 0.42 (p-value 2.10^{-2}). After separating the values in two distinct sets, correlation values are 0.72 (p values 5.10^{-9}) for the lowest F_{max} value set, and 0.6 (p value 1.10^{-3}) for the highest F_{max} value set. **B**. Histogram of final value of fluorescence of the same data set as in the left figure. We then fit this histogram with the superposition of two Gaussians, centered in the two peaks, namely 520 and 2280. The fitted variance are respectively 252 and 1362 (arbitrary units).

do not change the structure of the polymers, which suggest that the nucleation formation is predominant in the choice of structure of prion amyloids. The structure of polymers depends on the nucleation process more than on the polymerization process.

1.4.5.3   Conclusion: suggested model   All these observations suggest that an intrinsic conformational change process takes place before the nucleation, and is determinant for the following kinetic. As different polymers structure may appear, it is reasonable that different misfolded monomers may be present. Then a possible mechanism is that each kind of misfolded protein only aggregates with a similar misfolded protein, and lead to possibly different nucleus structures. The first nucleus formed dictates the dynamic and probably the polymers structure (figure 2.8). Because the nucleation process is longer than the polymerization, if there is already a given formed polymer, it grows and leads (by fragmentation) to multiple growing polymers of the same structure, making more and more unlikely the formation of a nucleus of a different structure.

(a) F_{max} and Ti (b) F_{max} and τ (c) T_{lag} and $\frac{1}{\tau}$
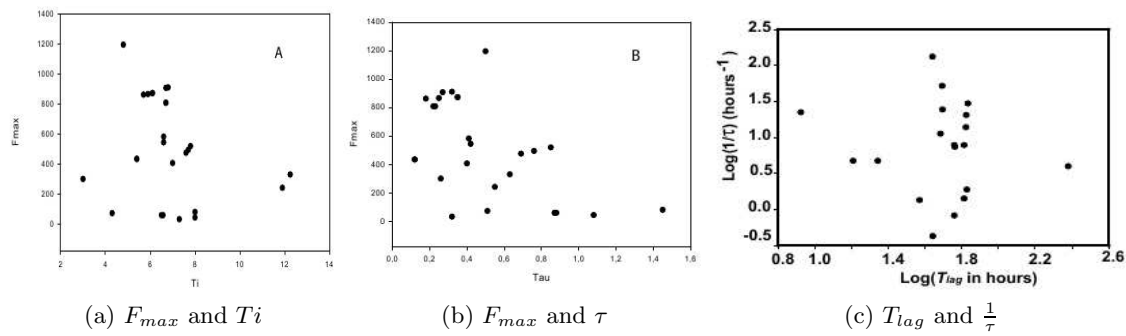
Figure 2.5: **Correlation between F_{max}, T_{lag} and $\frac{1}{\tau}$ in nucleation experiments**. The figures are taken from [3]. For each experiment, the time data series are fitted according to eq. (1.1), and the values of F_{max}, T_{lag} and $\frac{1}{\tau}$ are then deduced as explained in subsection 1.4. The values of these parameters are plotted in : (a))F_{max} (arbitrary unit) as a function of Ti (hours) (b) F_{max} (arbitrary unit) as a function of τ (hours) (c) T_{lag} (hours) as a function of $\frac{1}{\tau}$ (hours^{-1}). See [3] for more details.

(a) Electron microscopy analysis   (b) Relation between Fluorescence and Polymer size
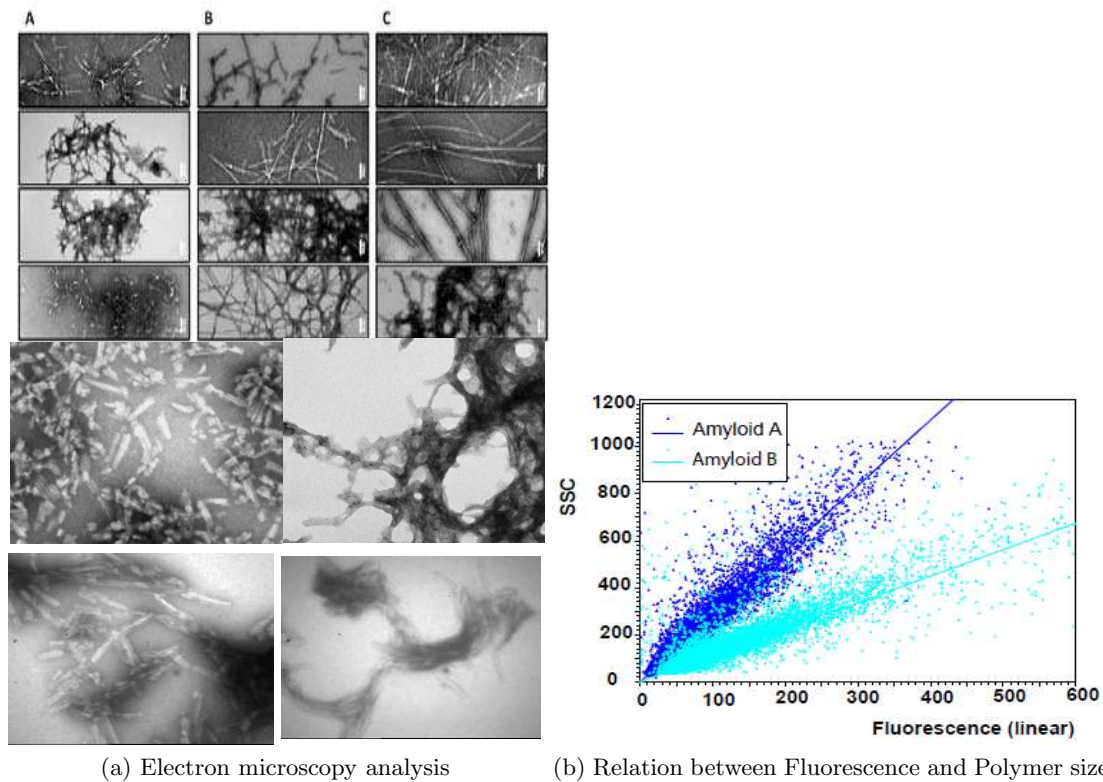
Figure 2.6: **Heterogeneity of the observed structure.** The figures are taken from [3]. (a) Electron microscopy analysis that shows "pictures"of the polymers obtained at the end of nucleation experiments. (b) Each point corresponds to the measurement of the fluorescence versus the size of an individual polymer. See [3] for more details.

Thus, the nucleation experiment would lead to a possible coexistence of different strains in theory while the seeding experiment has small chance to lead to such a phenomenon. A stochastic formulation of the Lansbury's nucleation-polymerization model (subsection 1.2) can easily incorporate the possibility of different structures in competition for the apparition of the first nucleus, and then seems appropriate for the mathematical formulation of

(a) Increased initial quantity of seed   (b) Successive seeding experiment
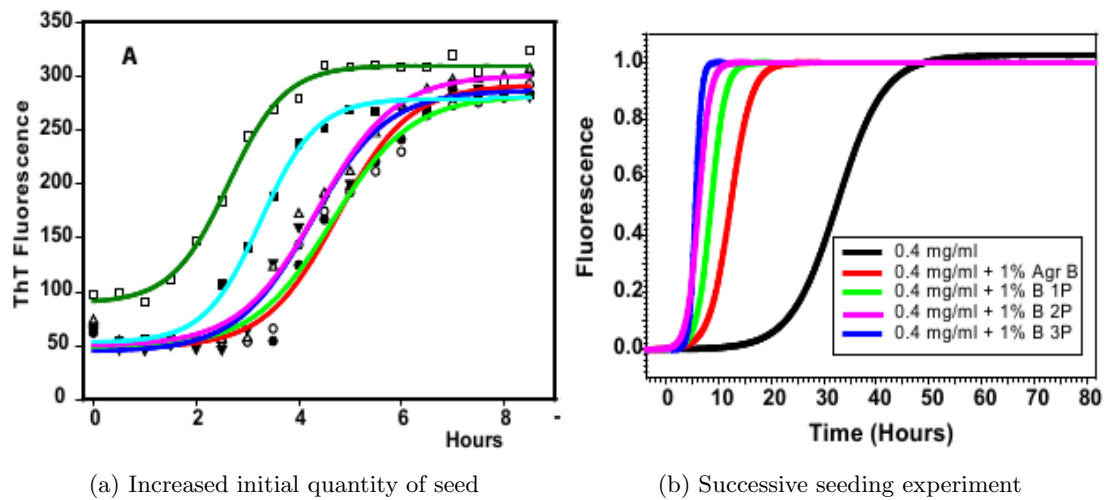
Figure 2.7: Seeding experiments. The figures are taken from [3]. Each type of symbol corresponds to a time data series of a seeding experiment. The time data series was fitted according to eq. (1.1), and the obtained curve is reported here. (a) For down (red line) to up (green line), the initial amount of polymers used as seeds is increased. (b) From right (black line) to left (blue line), the polymers used as a seed come from an increasing number of successive seeding experiments. See [3] for more details.
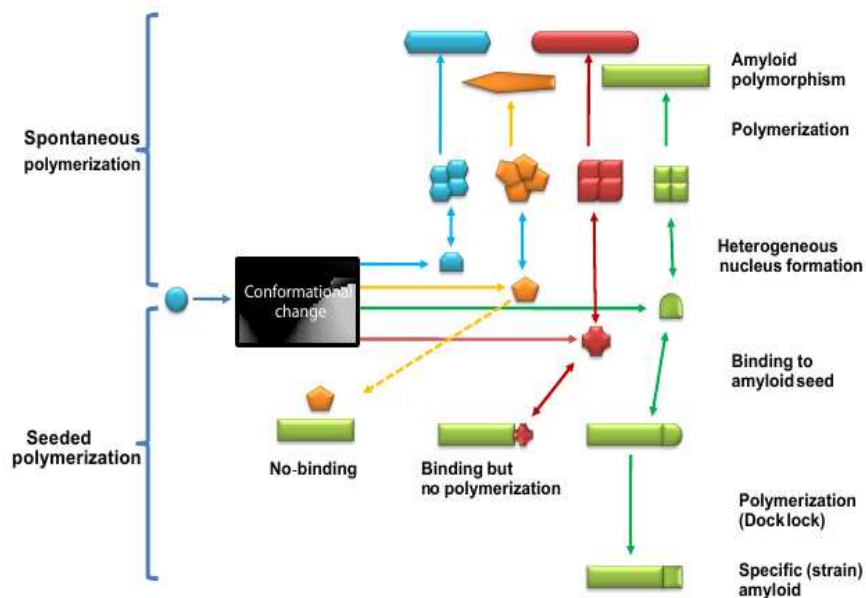
Figure 2.8: Model suggested by [3]. Figure taken from [3]. Each color corresponds to a particular misfolded protein or a polymer structure. This figure illustrates that a conformational change occurs before the polymerization, and during the nucleation process. This conformational change is determinant for the kinetic of the polymerization.

the model shown in figure 2.8 and given by Alvarez-Martinez et al. [3].

What kind of different information a stochastic model gives compare to a deterministic model? Is it more appropriate to describe the dynamic of Prion nucleation? Is it possible to get coexistence of several strains in a same experiment? Is it possible to reproduce this with a mathematical model, starting from an homogeneous population of PrP^C monomer?

Answering these question is the purpose of this work. These questions are fundamental for the next goal: to understand the toxicity of different strains, and to estimate useful parameters.

Indeed different strains would cause different levels of toxicity for the systems, and their dynamics could be totally different from one to another. That is why the overall behavior should be deeply investigated since it may be strongly correlated to the parameters involved in the process, each set of parameters representing a specific strain.
A primary necessary step to the study of a model with multiple strains structure is the study of a stochastic model with one single structure.Thus, we start by studying in section 3 a stochastic formulation of a nucleation model, in order to understand the stochasticity in the nucleation time, as a function of parameters (initial quantity of monomers, aggregation kinetic rates, nucleus size). We continue by studying the polymerization-fragmentation model in section 4.

1.5   Literature review

For each of the four levels of experimental observations mentioned in subsection 1.3, some theoretical mathematical modeling have been used, for which we now briefly give some references. Then, we spend more time on coagulation-fragmentation model, and finally review the specific literature on nucleation modeling that is useful for us.

For the smallest scale, the atomic description of protein configuration, people mostly use molecular dynamic simulations (coarse-grained model, random-coil peptides) for which we can refer to [16, 117, 112, 66]. These techniques allow to combine precise chemical and physical properties of the protein conformation and spatial mechanistic rule of the attachment/detachment of proteins within each other. Hence, in such models, both physical properties and mechanic rule influence the aggregation dynamic.

For the cellular level, models usually take into account the spatial dynamic inside cells, and the cell characteristics (protein synthesis rate, cellular density, cell cycle, cell death ...) together with prion strains characteristics (aggregation dynamic, diffusivity,...). See for instance [116, 131]. If these models usually lead to interesting modeling and mathematical questions, the lack of experimental data, however, is quite problematic (this may change quickly).

For the population level, epidemiologist model can be used to represent the propagation of the disease in an animal population, taking into account possible rules of transmission between animals, within their environment. For an example on a deer population, see [2].

1.5.1   General Coagulation-Fragmentation model

We now review coagulation-fragmentation models, that are mostly adapted to the protein level experimental data. In general, in a coagulation-fragmentation model, each particle is characterized by its size (or mass). It can hence be seen as a structured population model, where the structure variable is the size (or the mass) of the particle. Population model are usually defined in terms of birth and death of particles. In coagulation-fragmentation model, two particles die *simultaneously* when they coagulate (attach) with each other, and a new particle is born also *simultaneously*. If the two old particles are of size respectively x and y, such event appears with rate given by a coagulation kernel $K(x, y)$, and the new particle is of size $x + y$. The fragmentation process is the reverse process. A particle of size x die and gives birth to two new particles of size y and $x - y$, at a rate $F(x, y)$. The mathematical formulation of these mechanistic rule can be deterministic, as a systems of ordinary differential equations or partial differential equations,

or stochastic, as a finite particle model (given by point process) or a superprocess. For every formalism, the typical questions that arise in a mathematical study are the conditions for well-posedness of the model (depending on condition on kernel K, F and initial condition), its long-time behaviour, and particular phenomenon of gelling and dusting solution: while reasonable conditions on the initial condition and on the kernel K, F can be given to ensure that the solution is mass-conservative for all time (the "sum" of mass of all particles of the system stays constant over time), some degeneracy cases have been shown to lead to solutions for which the mass is not conserved during a finite time interval. The gelling phenomena corresponds to the (physical) situation where a single giant particle is created, and a phase transition lead to a gel. The dust phenomena corresponds to the situation where an infinity of particle of mass 0 are created. Apart from deterministic and stochastic models, the size of particles may be of different nature between models. Namely in systems of ordinary differential equations, the size is treated as a discrete variable, and there is one equation for each size of particle. While in partial differential equation model, the size is treated as a continuous variable (the model is usually refer to the Smoluchowski model). The same dichotomy holds as well for stochastic model.

For a review of results on deterministic discrete coagulation-fragmentation model, we refer to Wattis [139]. General results on existence, uniqueness and mass conservation has been first derived by Ball and Carr [8], while Hendriks et al. [70] considered the case of purely coagulation and gave condition for gelation. Since then, results have been improved by Laurençot and Mischler [92], while Cañizo [24], Fournier and Mischler [59] gave conditions for exponential trend to equilibrium.

The study of stochastic pure-coagulation model was first developed by Hendriks et al. [71], Lushnikov [98], Marcus [102]. Such models are usually refer to the "stochastic coalescent" model or the Marcus-Lushnikov model. For an interesting survey of results on pure-coagulation model, see the very popular work of [1], which contains a wide variety of applications, reviews available exact solutions, gelation phenomena, various examples and types of coagulation kernel, and mean-field limit. This author raises a certain number of interesting open problems related to these model. In [113], the author derived the fluid limit of the stochastic coalescent model, namely the Smoluchowski's coagulation equation. The author used such approach to derive a general result of existence of the mean-field Smoluchowski model ($K(x, y) \leqslant \varphi(x)\varphi(y)$, with sub-linear function φ, and $\varphi(x)^{-1}\varphi(y)^{-1}K(x, y) \to 0$ as $(x, y) \to \infty$). The author also provided a review and new result of uniqueness of the mean-field Smoluchowski model for similar aggregation kernel, with an extra assumption on the initial distribution of particle mass. Importantly, he also gave an example of an aggregation kernel for which uniqueness does not hold, by exhibiting two conservative solution of the same equation. Finally, in the special case of discrete mass particle, the author provided a bound of the convergence rate of the stochastic coalescent to the mean-field Smoluchowski model. See also [56] for other results on well-posedness of Smoluchowski's coagulation model, with homogeneous kernel and [30] for a convergence rate of the Marcus-Lushnikov model towards the Smoluchowski's coagulation model, in Wasserstein distance (in $\frac{1}{\sqrt{n}}$).

For pure-fragmentation model we refer to Wagner [136, 137]. The author considers a general pure fragmentation model (with example including binary fragmentation, homogeneous fragmentation). In particular, the author reviews conditions on the fragmentation kernel so that the discrete stochastic model (and its deterministic counterpart) almost surely undergoes an explosion in finite time. As in the pure aggregation model, these conditions involved a lower bound condition, such as the fragmentation kernel explodes sufficiently rapidly in 0. See also [10] for a review on analytical techniques to characterize such phenomenon.

Finally, for the general coagulation-fragmentation model, the first rigorous results seems to have been obtained by Jeon [78]. This author used the stochastic formulation model to study the gelling phenomena of the mean-field Smoluchowski's coagulation-fragmentation equation. In particular, he derived conditions on coagulation kernel $K(x, y)$ and fragmentation kernel $F(x, y)$ to show the tightness of the stochastic coagulation-fragmentation model, and hence existence of solution of Smoluchowski's coagulation-fragmentation equation. His condition on the kernel involved $\lim_{x+y\to\infty} K(x, y)/xy = 0$ and there exists G such that $F(x, y) \leqslant G(x + y) \to 0$ with $\lim_{x\to\infty} G(x) = 0$. Results on gelation phenomena involve a lower bound condition such as the existence of $M, \varepsilon > 0$, and $\varepsilon ij \leqslant K(i, j) \leqslant Mij$. Fluid limit results in the case where gelation occurs were recently obtained in [55, 57] where the authors show that different limiting models are possible, namely the Smoluchowski model and a modified version, named Flory's model.

1.5.2   Becker-Döring Model

A special case of the coagulation-fragmentation model is the Becker-Döring Model, which was originally used by [14]. In such model, aggregation and fragmentation occur only one monomer by one monomer, that is, in a discrete-size description,

$$K(x, y) \neq 0 \Leftrightarrow x = 1, \text{ or } y = 1$$

and similarly for the fragmentation kernel. The theoretical foundations of such models have been laid down by Ball et al. [9], followed by other contributions [7, 28, 127] for the well posedness of the model and its asymptotic behaviour. Convergence rates towards equilibrium have been obtained by Jabin and Niethammer [75].

1.5.3   Prion model

According to the Lansbury's theory, during the nucleation phase, addition of monomer occurs one-by-one but are unfavorable, so that detachment of monomer are also important. Then the Becker-Döring Model seems the most adapted to the nucleation phase. For the polymerization phase, when nuclei are already there, the coagulation still occurs one-by-one, but detachment is negligible. However fragmentation of large polymer does occur. Thus, we use a coagulation-fragmentation model, where coagulation occurs only with single monomer, and fragmentation occurs with a general kernel.

1.5.4   Finite maximal size and Stochastic nucleation models

All the models quoted above do not use any maximal size for the particles, and mostly study the long-time behavior of the system. However, to capture the nucleation phase, it seems more natural to study a model where there is a maximal size, and to study the waiting time for the solution to reach this maximal size. Such approach has been taken in [120] using a maximal size deterministic Becker-Döring Model. In particular, the authors derive general scaling laws for the nucleation, as a function of initial condition and kinetic parameters. Our approach in section 3 can be seen as a generalization of their study to the stochastic version of the Becker-Döring Model.

Previous stochastic models have been used to study the nucleation time, within protein aggregation fields ([132], [53], [73], [87]). In [53], they use a simple autocatalyic conversion kinetic model to get the distribution of incubation time. Under the assumption that the involved constant rate is a stochastic variable, log normally distributed, the incubation time is then also shown to be log normal. In [73],[132], the authors get the distribution

shape of lag time using assumptions on probabilities of nucleus formation event. Hofrichter [73] end up with a delay exponential distribution, while Szabo [132] found a β-distribution, useful to experimentally deduce the rate of single nucleation formation. In [87] the authors used a phenomenological model to get the mean waiting time to reach a certain amount a polymer, from one initial seed and under assumptions on distribution of aggregation and fissioning times. This expression allows them to discuss the influence of initial dose or other parameters on the incubation time. Using a purely stochastic model for sequential aggregation of monomers and dimers, they obtain different waiting time distributions, as a γ-distribution, a β-distribution or a convolution of both.

Our approach is rather different, also close to that last one exposed in [87]. Indeed, for the nucleation phase, we use a purely stochastic Becker-Döring kinetic model, under the assumption that the first polymer is formed by successive additions and disassociations of one misfolded monomer. This discrete stochastic model allows us to define the nucleation time as the waiting time to reach the first nucleus (a polymer of a given size). After the first nucleus is formed, our stochastic kinetic model includes aggregation through monomer additions and fragmentations of polymers (similar to previous prion model).

1.6   Outline

We present in detail the formulation of our model in the next subsection 2. There we give the biochemical reaction steps underlying this model, and its deterministic and stochastic version (both with discrete size). Then, we focus on the misfolding process, and obtain two limiting models by performing a time-scale reduction. These limiting models are easier to handle, in particular to study the nucleation time.

In section 3, we study the nucleation time in a stochastic version of the Becker-Döring Model. We attach importance in finding analytical solutions, either exact or approximate, in order to get general scalings laws as well as quantitative informations on the behavior of the system, with respect to parameters. We show that the stochastic formulation leads to several unexpected features for the nucleation time. Finally, we apply this study to the prion modeling and compare our theoretical results to the experimental data.

In section 4, we focus on the polymerization-fragmentation phase of the model. We consider a slight generalization of the model, including spatial movement, and study the limit when the number of monomer is very large compared to the number of polymer. Using stochastic limit theorem, we show that our purely discrete model converge to a hybrid model, where polymerization is deterministic and fragmentation is a jump process.

2   Formulation of the Model

2.1   Dynamical models of nucleation-polymerization

We use a simplified version of the model introduced by Lansbury *et al.* in 1995 ([29]).

The dynamic is composed of a set of chemical reactions involving only the prion protein. Firstly, it is based on the assumption that the protein is able to spontaneously misfold and unfold again (figure 2.9a). The misfolded form is supposedly very unstable, and this process of folding/unfolding very fast. The misfolded protein is the only form able to actively contribute to the aggregation process, by addition of one monomer at each step [40]. Secondly, the early steps of the aggregation process (figure 2.9b) are thermodynamically unfavorable, meaning that the forward polymerization reaction rate is several orders of magnitude lower than the backward depolymerization reaction rate. These reaction rates, p, q, are supposed to be independent of the size of the aggregates. We called the species formed during this process the oligomers. There are small aggregates of size less than a

(a) Spontaneous Misfoling

(b) Nucleation steps ($n = 5$)

(c) rapid polymerization

(d) polymerization/fragmentation
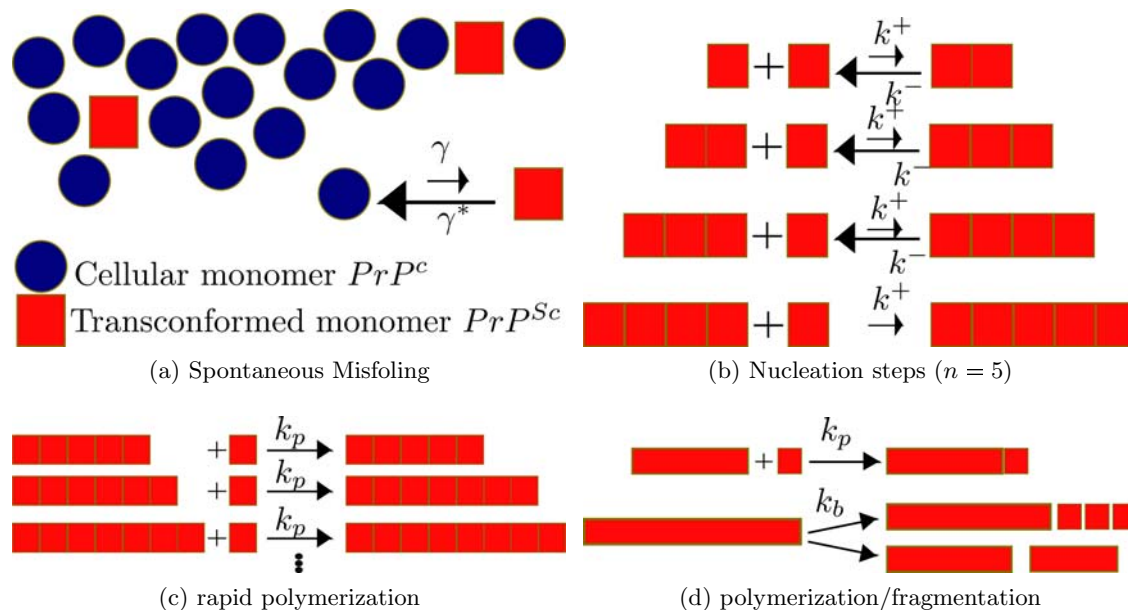
Figure 2.9: In this figure we present the successive reactions steps of the nucleation-polymerization model. (a) Fast equilibrium between normal and transconformed monomer. (b) Nucleation reaction steps . Here $n = 5$. All the steps are composed of unfavorable addition of a single monomer. (c) Polymerization reaction steps. All the steps are composed of irreversible addition of a single monomer. (d) Fragmentation process. The fragmentation rate is proportional to the mass of the polymer. The two parts have equal probability to be of a size between one and the size of the initial polymer minus one. When it gives birth to an oligomer (size less than n) this last one is supposed to break into small monomers immediately due to the instability of the oligomer).

given number, n. At this size, the kinetic steps change, and the aggregation of monomer is irreversible. The particular oligomer size n at which the kinetic steps change is called the nucleus. We emphasize that we use a constant-size nucleus model, which does not necessarily correspond to the most unstable species, as it has been well explained [120]. Finally, the rest of the dynamic (figure 2.9c - 2.9d) is followed by a classical polymerization-fragmentation model [110], resulting in rapid polymerization/growth. The fragmentation process is responsible of the auto-catalytic form of the prion polymerization. We focus on the lag time, so on the early steps of the nucleation-polymerization process. Because we are interested in the time scale of the monomer disappearance (and not of the polymer relaxation), the irreversibility hypothesis on the polymer growth is fairly acceptable [62] (the depolymerization reactions are negligible after the first nucleus is formed because the polymerization reactions are fast). Table 2.1 summarizes the different parameters involved in this model.

According to this theory, because of its high stochasticity, nucleus formation would be considered as a kinetic barrier to sporadic prion diseases. But this barrier could be overcome by infection. The disease would not be spontaneous anymore, it could be transmitted on purpose or not by a PrP^{Sc} polymer seeding which would directly lead to the second step since no formation of the first nucleus would be required. Once again, our main focus here is the sporadic appearance of the first nucleus, rather than its transmission.

Table 2.1: Definitions of variables and parameters. We use small letters for the continuous variables involved in the deterministic model, and capital letters for the discrete variables involved in the stochastic model. We keep the same notation for the parameters in both models, in order to avoid many different notations, although the parameters for second-order reaction has different units.

Name	Definition
m/M	Concentration/Number of Native Monomer
f_1/F_1	Concentration/Number of Misfolded Monomer
f_i/F_i	$i = 2..N-1$, Concentration/Number of aggregates of size i
N	Nucleus size
γ	Folding rate
γ^*	Unfolding rate
$c_0 = \frac{\gamma}{\gamma^*}$	Equilibrium constant between monomers
p	Elongation rate in nucleation steps
q	Dissociation rate in nucleation steps
$\sigma = \frac{q}{p}$	Dissociation equilibrium constant in nucleation steps
k_p	Elongation rate in polymerization steps
k_b	Fragmentation rate in polymerization steps

We look at the following set of chemical reactions defined by (variable and parameter are defined in table 2.1):

$$m \underset{\gamma^*}{\overset{\gamma}{\rightleftharpoons}} f_1 \qquad\qquad \text{(spontaneous conformation)} \quad (2.1)$$

$$f_1 + f_1 \underset{q}{\overset{p}{\rightleftharpoons}} f_2 \qquad\qquad \text{(dimerization)} \quad (2.2)$$

$$\vdots$$

$$f_{k-1} + f_1 \underset{q}{\overset{p}{\rightleftharpoons}} f_k \qquad\qquad \text{((k)-mer formation)} \quad (2.3)$$

$$\vdots$$

$$f_{N-1} + f_1 \overset{p}{\rightarrow} u_N \qquad\qquad \text{(nucleus formation)} \quad (2.4)$$

$$u_i + f_1 \overset{k_p}{\longrightarrow} u_{i+1} \qquad (i \geqslant N) \qquad \text{(elongation)} \quad (2.5)$$

$$u_i \overset{k_b}{\longrightarrow} u_{i-j} + u_j \ (i \geqslant N, 1 \leqslant j \leqslant i-1) \ \text{(polymer break)} \quad (2.6)$$

$$\text{and } u_k \overset{\infty}{\longrightarrow} kf_1 \qquad (\text{ if } k \leqslant N-1) \qquad \text{(oligomer instability)} \quad (2.7)$$
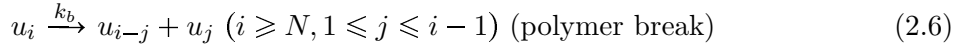
The system of chemical reactions (2.1) - (2.7) defines our full model and consists of four steps: misfolding, nucleation, polymerization, and fragmentation. All reaction rates are assumed to follow the law of Mass-Action, with kinetic constant indicated on each reaction. The reversible reaction (2.1) represents the misfolding process between normal and misfolded protein, occurring at rate γ and γ^*. The reaction (2.2) - (2.3) represent the aggregation process during the nucleation phase, and consist of reversible attachment/detachment of misfolded monomer to aggregate of size k, $k = 1...N-2$, at rate respectively p and q. Such rates are assumed to be independent of the size of the aggregate. The reaction (2.4) is irreversible and represents the formation of a nucleus, by attachment of one misfolded monomer to an aggregate of size $N-1$, at rate p. The irreversibility hypothesis comes from the assumption that all aggregates of size greater than the nucleus size N are stable. These aggregates are called polymers. Then, reaction (2.5)

consists of irreversible polymerization, by addition of one by one misfolded monomer, at rate k_p, also assumed to be independent of the size of the polymer. Reaction (2.6) is the fragmentation process, occurring at rate linearly proportional to the size of the polymer. For a linear polymer of size i, there is $i-1$ connection between monomer, and we take the fragmentation rate to be $k_b(i-1)$. The size repartition kernel of the new-formed polymer is taken uniform along all possible pairs of polymers. Thus, the total fragmentation kernel $F(i,j)$, which gives the probability per unit of time that a polymer of size i breaks into two polymers of size j and $i-j$, is

$$F(i,j) = k_b(i-1)\frac{2}{i-1}\mathbf{1}_{\{j<i\}} = 2k_b\mathbf{1}_{\{j<i\}}. \tag{2.8}$$

The factor 2 comes from the symmetry condition between the pairs $(j, i-j)$ and $(i-j, j)$. Finally, if due to a fragmentation event, a polymer of size less than N appears, we suppose that it breaks *instantaneously* in monomers, which is represented by reaction (2.7).

This model can be seen as a coagulation-fragmentation model, where the coagulation kernel $K(x,y)$ is constant equal to p for $x=1$, $y=1..N$ (and vice-versa), and constant equal to k_p for $x=1$ and $y \geqslant N+1$ (and vice-versa), and zero otherwise. The fragmentation kernel is $F(i,j) = 2k_b\mathbf{1}_{\{j<i\}}$.

2.1.1 Deterministic model of prion polymerization

The above chemical reactions system can be quantitatively studied by law of action-mass and transformed into a set of ordinary differential equations. Although it involves an infinite number of species (one for each size), it is known that this system can be reduced to a finite set of differential equations, as we recall below. It has one equation for each species of size lower than the nucleus size, in addition to two equations for the number of polymers and their mass.

Firstly, a system of an infinite number of differential equations is built based on the reactions (2.1-2.7) with the action-mass law. We get, with the same notations as above:

$$\begin{cases}
\dfrac{dm}{dt} &= -\gamma m + \gamma^* f_1, \\
\dfrac{df_1}{dt} &= \gamma m - \gamma^* f_1 - pf_1\left(f_1 + \sum_{k=2}^{N-1} f_k\right) + q\left(2f_2 + \sum_{k=3}^{N-1} f_k\right) \\
& \quad -k_p f_1\left(\sum_{k=N}^{\infty} u_k\right) + N(N-1)k_b \sum_{k=N}^{\infty} u_k, \\
\dfrac{df_2}{dt} &= pf_1(\frac{f_1}{2} - f_2) - q(f_2 - f_3), \\
\dfrac{df_i}{dt} &= pf_1(f_{i-1} - f_i) - q(f_i - f_{i+1}), \quad 3 \leqslant i \leqslant N-2, \\
\dfrac{df_{N-1}}{dt} &= pf_1(f_{N-2} - f_{N-1}) - qf_{N-1}, \\
\dfrac{du_N}{dt} &= pf_1 f_{N-1} - k_p f_1 u_N - k_b(N-1)u_N + 2k_b \sum_{k=N+1}^{\infty} u_k, \\
\dfrac{du_i}{dt} &= k_p f_1(u_{i-1} - u_i) - k_b(i-1)u_i + 2k_b \sum_{k=i+1}^{\infty} u_k, \quad i \geqslant N+1.
\end{cases}$$

Secondly, with the variables $y = \sum_{i=N}^{\infty} u_i$, $z = \sum_{i=N}^{\infty} iu_i$, it is standard ([104]) to transform this set of infinite number of differential equations into the following finite set of differential

equations

$$
\left\{
\begin{array}{rcl}
\dfrac{dm}{dt} & = & -\gamma m + \gamma^* f_1, \\[2mm]
\dfrac{df_1}{dt} & = & \gamma m - \gamma^* f_1 - p f_1 \left(f_1 + \displaystyle\sum_{k=2}^{N-1} f_k \right) + q \left(2 f_2 + \displaystyle\sum_{k=3}^{N-1} f_k \right) \\[2mm]
& & - k_p f_1 y + N(N-1) k_b y, \\[2mm]
\dfrac{df_2}{dt} & = & p f_1 (\dfrac{f_1}{2} - f_2) - q(f_2 - f_3), \\[2mm]
\dfrac{df_i}{dt} & = & p f_1 (f_{i-1} - f_i) - q(f_i - f_{i+1}), \quad 3 \leqslant i \leqslant N-2, \\[2mm]
\dfrac{df_{N-1}}{dt} & = & p f_1 (f_{N-2} - f_{N-1}) - q f_{N-1}, \\[2mm]
\dfrac{dy}{dt} & = & p f_1 f_{N-1} + k_b z - (2N-1) k_b y, \\[2mm]
\dfrac{dz}{dt} & = & N p f_1 f_{N-1} + k_p f_1 y - N(N-1) k_b z.
\end{array}
\right.
\tag{2.9}
$$

In this model, the lag time T_{lag}^{det} is defined as the waiting time for the mass of polymer to reach ten percent of the total initial mass (cf figure 2.10a). In our simulation, a sigmoid shape is observed for the time evolution of the mass of polymers, which is qualitatively in good agreement with the experiment and previous studies.

Note that this model is a slight modification of the deterministic model studied by Masel ([104]) adapted to the *in vitro* experiments. In this deterministic framework, ordinary differential equations are used to model the evolution of concentrations of the species. Based on biological observations, we introduce a concentration of abnormal monomer (f_1) corresponding to a small proportion of the concentration of normal monomer (m). This low concentration of misfolded protein actively contributes to the aggregation process while the high concentration of normal protein still remains inactive.

2.1.2 Stochastic model of prion polymerization

Let us now give an insight of the stochastic model. To that purpose, we take the same reactions steps as previously explained, but use now a continuous time Markov chain to describe its time evolution. This stochastic model can be treated using the theory of Markov processes. From the reaction (2.1) - (2.7), we can write down a system of stochastic differential equation driven by Poisson processes. However, its complete expression is complicated due to the fragmentation term for small aggregate. We only write down the system for reaction (2.1) - (2.4), that is before nucleation takes places. In that case, the system is described by

$$
\begin{cases}
M(t) = M(0) - Y_1\Big(\int_0^t \gamma M(s)ds\Big) + Y_2\Big(\int_0^t \gamma^* F_1(s)ds\Big), \\[2mm]
F_1(t) = F_1(0) + Y_1\Big(\int_0^t \gamma M(s)ds\Big) - Y_2\Big(\int_0^t \gamma^* F_1(s)ds\Big) \\[2mm]
\qquad\quad -2Y_3\Big(\int_0^t \frac{p}{2}F_1(s)(F_1(s)-1)ds\Big) - \sum_{i=2}^{N-1} Y_{2i+1}\Big(\int_0^t pF_1(s)F_i(s)ds\Big) \\[2mm]
\qquad\quad +2Y_4\Big(\int_0^t qF_2(s)ds\Big) + \sum_{i=3}^{N} Y_{2i}\Big(\int_0^t qF_i(s)ds\Big), \\[2mm]
F_2(t) = N_2(0) + Y_3\Big(\int_0^t \frac{p}{2}F_1(s)(F_1(s)-1)ds\Big) - Y_5\Big(\int_0^t pF_1(s)F_2(s)ds\Big) \\[2mm]
\qquad\quad -Y_4\Big(\int_0^t qF_2(s)ds\Big) + Y_6\Big(\int_0^t qF_3(s)ds\Big), \\[2mm]
F_i(t) = F_i(0) + Y_{2i-1}\Big(\int_0^t pF_1(s)F_{i-1}ds\Big) - Y_{2i+1}\Big(\int_0^t pF_1(s)F_i(s)ds\Big) \\[2mm]
\qquad\quad -Y_{2i}\Big(\int_0^t qF_i(s)ds\Big) + Y_{2i+2}\Big(\int_0^t qF_{i+1}(s)ds\Big), \quad 3\leqslant i \leqslant N-2, \\[2mm]
F_{N-1}(t) = F_i(0) + Y_{2N-4}\Big(\int_0^t pF_1(s)F_{N-2}ds\Big) - Y_{2N-1}\Big(\int_0^t pF_1(s)F_{N-1}(s)ds\Big) \\[2mm]
\qquad\quad -Y_{2N-2}\Big(\int_0^t qF_{N-1}(s)ds\Big), \\[2mm]
U_N(t) = U_N(0) + Y_{2N-1}\Big(\int_0^t pF_1(s)F_{N-1}ds\Big).
\end{cases}
$$

$$(2.10)$$

where Y_i, $1 \leqslant i \leqslant 2N-1$, are independent standard Poisson process. This system may be simulated through a standard stochastic simulation algorithm or Gillespie algorithm ([60]).

The details of the stochastic model allow us to exactly identify the first *discrete* nucleation event (figure 2.10b). Then, in the stochastic model, the lag time is defined as the waiting time to obtain *one* nucleus, that is one aggregate of the critical size at which the dynamic entirely changes, due to the irreversibility of the nucleus and larger polymers. In our simulation, we can observe how the dynamic drastically changes after the first nucleation event (figure 2.10b). This is solely due to the hypothesis of parameters change at that point, and in particular to the irreversible aggregation hypothesis. We notice also that the time evolution of the mass of polymers follows roughly a sigmoid, due to the polymer breaks.

2.2   Misfolding process and time scale reduction

The introduction of the misfolding protein makes the analysis of the nucleation time more delicate. Thus, we use a time scale reduction, based on two different biological hypothesis, to eliminate one of the two variables between the normal and the misfolded protein.
Firstly, if the misfolding process occurs at a very fast time scale, compared to the other time scale of the system, both normal and misfolded protein equilibrate within each other. At the slow time scale, the system only sees the averaged quantity of each protein. In particular, in the deterministic model, the rate of aggregation depends of a fraction of the total quantity of monomers. In the stochastic model, the fast subsystem made up of normal and misfolded monomers converges to a binomial distribution, and the slow system only depends on the first two moments of this binomial distribution. We note that the

(a) Deterministic Simulation   (b) Stochastic Simulation
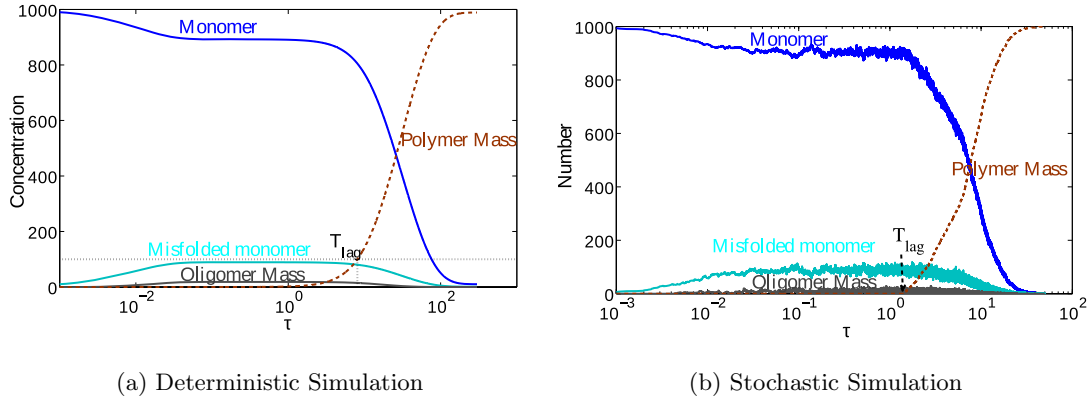
Figure 2.10: (a)**Deterministic Simulation and definition of the lag time in the deterministic model**. One simulation of the deterministic model, with the concentration of normal and folded protein, concentration of oligomers and polymers. The lag time is defined as the waiting time to convert a given fraction of the initial monomers into polymers, here 10%. We used here $m(0) = 1000$, $\gamma^*/\gamma = 10$, $\sigma = 1000$, $n = 7$. The time (in log scale) has been rescaled by $\tau = pt$. (b) **Stochastic Simulation and definition of the lag time in the stochastic model**. One simulation of the stochastic model, with the numbers of normal and misfolded protein, the mass of oligomers and the mass of polymers. The lag time is defined as the waiting time for the formation of the first nucleus . We used $M(0) = 1000$, $\gamma^*/\gamma = 10$, $\sigma = 1000$, $n = 7$. The time (in log scale) has been rescaled by $\tau = pt$.

reduced model can be seen as an original Becker-Döring model where the total mass is conserved.

Secondly, another biological hypothesis is to assume that the misfolded protein is very unstable and hence present in very small quantity compared to the normal protein. Specifically, if we assume that the total quantity of protein is very large, and that the misfolded protein is highly unstable, we obtain a further reduced model where the quantity of misfolded protein is constant over time, and aggregation takes place with constant monomer quantity. Such reduced model can be seen as a Becker-Döring model where the quantity of monomer is conserved (but not the total mass).

For both scaling, we present the derivation of the limiting model in the deterministic and stochastic formulation.

2.2.1   Deterministic equation

2.2.1.1   Fast misfolding process   From the initial system of differential equation (2.9), we first consider the following scaling

$$\begin{aligned} \gamma &\rightarrow \gamma n \\ \gamma^* &\rightarrow \gamma^* n \end{aligned}$$

where $n \to \infty$ and all other parameters remain unchanged. We define the free monomer variable $m_{free}(t) = m(t) + f_1(t)$. Then $m(t)$ and $f_1(t)$ are fast variable, but $m_{free}(t)$ (and all other variables f_i, $i \geqslant 2$, p and u) are slow variables. To see that, consider the fast

time scale $\tau = tn$, so that the previous system writes

$$
\left\{
\begin{array}{rcl}
\dfrac{dm}{d\tau} &=& -\gamma m + \gamma^* f_1, \\[2mm]
\dfrac{df_1}{d\tau} &=& \gamma m - \gamma^* f_1 + \dfrac{1}{n}\left[-pf_1\left(f_1 + \sum_{k=2}^{N-1} f_k\right) + q\left(2f_2 + \sum_{k=3}^{N-1} f_k\right)\right. \\[3mm]
&& \left. -k_p f_1 y + N(N-1)k_b y\right], \\[3mm]
\dfrac{dm_{free}}{d\tau} &=& \dfrac{1}{n}\left[-pf_1\left(f_1 + \sum_{k=2}^{N-1} f_k\right) + q\left(2f_2 + \sum_{k=3}^{N-1} f_k\right)\right. \\[3mm]
&& \left. -k_p f_1\left(\sum_{k=N}^{\infty} u_k\right) + N(N-1)k_b \sum_{k=N}^{\infty} u_k\right], \\[3mm]
\dfrac{df_2}{dt} &=& pf_1(\dfrac{f_1}{2} - f_2) - q(f_2 - f_3), \\[2mm]
\dfrac{df_i}{d\tau} &=& \dfrac{1}{n}\left[pf_1(f_{i-1} - f_i) - q(f_i - f_{i+1})\right], \quad 3 \leqslant i \leqslant N-2, \\[2mm]
\dfrac{df_{N-1}}{d\tau} &=& \dfrac{1}{n}\left[pf_1(f_{N-2} - f_{N-1}) - qf_{N-1}\right], \\[2mm]
\dfrac{dy}{d\tau} &=& \dfrac{1}{n}\left[pf_1 f_{N-1} + k_b z - (2N-1)k_b y\right], \\[2mm]
\dfrac{dz}{d\tau} &=& \dfrac{1}{n}\left[Npf_1 f_{N-1} + k_p f_1 y - N(N-1)k_b z\right].
\end{array}
\right.
$$

Due to the total mass conservation, all concentrations remain bounded as $n \to \infty$, and the fast subsystem becomes

$$
\frac{dm}{d\tau} = -\gamma m + \gamma^* f_1, \tag{2.11}
$$

$$
\frac{df_1}{d\tau} = \gamma m - \gamma^* f_1. \tag{2.12}
$$

This system has a unique asymptotic equilibrium, that depends solely on $m_{free}(0) = m(0) + f_1(0)$ ans is given by

$$
m(\tau \to \infty) = \frac{\gamma^*}{\gamma + \gamma^*} m_{free}(0),
$$

$$
f_1(\tau \to \infty) = \frac{\gamma}{\gamma + \gamma^*} m_{free}(0).
$$

Going back to the original time scale, the slow system becomes now

$$
\left\{
\begin{array}{rcl}
\dfrac{dm_{free}}{dt} &=& -\dfrac{\gamma p}{\gamma + \gamma^*} m_{free}\left(\dfrac{\gamma}{\gamma + \gamma^*} m_{free} + \sum_{k=2}^{N-1} f_k\right) + q\left(2f_2 + \sum_{k=3}^{N-1} f_k\right) \\[3mm]
&& -\dfrac{\gamma k_p}{\gamma + \gamma^*} m_{free} y + N(N-1)k_b y, \\[3mm]
\dfrac{df_2}{dt} &=& \dfrac{\gamma p}{\gamma + \gamma^*} m_{free}(\dfrac{\gamma}{2(\gamma + \gamma^*)} m_{free} - f_2) - q(f_2 - f_3), \\[3mm]
\dfrac{df_i}{dt} &=& \dfrac{\gamma p}{\gamma + \gamma^*} m_{free}(f_{i-1} - f_i) - q(f_i - f_{i+1}), \quad 3 \leqslant i \leqslant N-2, \\[3mm]
\dfrac{df_{N-1}}{dt} &=& \dfrac{\gamma p}{\gamma + \gamma^*} m_{free}(f_{N-2} - f_{N-1}) - qf_{N-1}, \\[3mm]
\dfrac{dy}{dt} &=& \dfrac{\gamma p}{\gamma + \gamma^*} m_{free} f_{N-1} + k_b z - (2N-1)k_b y, \\[3mm]
\dfrac{dz}{dt} &=& N\dfrac{\gamma p}{\gamma + \gamma^*} m_{free} f_{N-1} + \dfrac{\gamma k_p}{\gamma + \gamma^*} m_{free} y - N(N-1)k_b z.
\end{array}
\right.
$$

Remark 68. *In the slow scale system, the variables f_1 and m are instantaneously equilibrated with each other and with m_{free} following relation eq. (2.11) - (2.12). Re-writing the system in terms of the variable f_1, we obtain an original Becker-Döring system where the monomer variable evolves at a slower time scale (given by $\frac{\gamma}{\gamma+\gamma^*}t$) than all other species.*

Finally, with the time change $\tau = \frac{\gamma p}{\gamma+\gamma^*}t$, and with the following notations

$$\sigma = \frac{q}{p},$$

$$c_0 = \frac{\gamma^*}{\gamma},$$

$$\sigma_0 = \sigma(1 + c_0), \tag{2.13}$$

$$K_b = \frac{k_b}{p}(1 + c_0),$$

$$K = \frac{k_p}{p},$$

the system becomes

$$
\begin{cases}
\dfrac{dm_{free}}{d\tau} &=& -m_{free}\left(\dfrac{1}{1+c_0}m_{free} + \displaystyle\sum_{k=2}^{N-1} f_k\right) + \sigma_0\left(2f_2 + \displaystyle\sum_{k=3}^{N-1} f_k\right) \\
 & & -Km_{free}y + N(N-1)K_b y, \\
\dfrac{df_2}{d\tau} &=& m_{free}\left(\dfrac{1}{2(1+c_0)}m_{free} - f_2\right) - \sigma_0(f_2 - f_3), \\
\dfrac{df_i}{d\tau} &=& m_{free}(f_{i-1} - f_i) - \sigma_0(f_i - f_{i+1}), \quad 3 \leqslant i \leqslant N-2, \\
\dfrac{df_{N-1}}{d\tau} &=& m_{free}(f_{N-2} - f_{N-1}) - \sigma_0 f_{N-1}, \\
\dfrac{dy}{d\tau} &=& m_{free}f_{N-1} + K_b z - (2N-1)K_b y, \\
\dfrac{dz}{d\tau} &=& Nm_{free}f_{N-1} + Km_{free}y - N(N-1)K_b z.
\end{cases}
\tag{2.14}
$$

This system can be seen as a Becker-Döring system where the dimerization occurs at as slower rate than all other aggregation rates. This comes from the fact that this reaction is a second-order reaction, and hence depends on the square of the available quantity of active monomers, while other reaction solely depends linearly on the quantity of active monomers.

2.2.1.2 Very large normal monomer and rare transconformed monomer

We continue from the system of eq. (2.14), and assume a further scaling, namely that m_{free} is a large quantity and the rate of de-transconformation γ^* is also very large. We specifically suppose

$$
\begin{aligned}
m_{free}(0) &\rightarrow m_{free}(0)n, \\
\gamma^* &\rightarrow \gamma^* n.
\end{aligned}
$$

and $n \rightarrow \infty$. The system of eq. (2.14) is best described in the time scale $\tau = pt$ and with the variable

$$f_1^n = \frac{\gamma}{\gamma + n\gamma^*}m_{free},$$

so that we get

$$
\left\{
\begin{aligned}
\frac{df_1^n}{d\tau} &= \frac{\gamma}{\gamma + n\gamma^*}\left[-f_1^n\left(f_1^n + \sum_{k=2}^{N-1} f_k\right) + \sigma\left(2f_2 + \sum_{k=3}^{N-1} f_k\right) \right. \\
&\quad \left. -Kf_1^n y + N(N-1)K_b y \right], \\
\frac{df_2}{d\tau} &= f_1^n(\frac{f_1^N}{2} - f_2) - \sigma(f_2 - f_3), \\
\frac{df_i}{d\tau} &= f_1^n(f_{i-1} - f_i) - \sigma(f_i - f_{i+1}), \quad 3 \leqslant i \leqslant N-2, \\
\frac{df_{N-1}}{d\tau} &= f_1^n(f_{N-2} - f_{N-1}) - \sigma f_{N-1}, \\
\frac{dy}{d\tau} &= f_1^n f_{N-1} + K_b z - (2N-1)K_b y, \\
\frac{dz}{d\tau} &= N f_1^n f_{N-1} + K f_1^n y - N(N-1)K_b z.
\end{aligned}
\right.
$$

Then, as $n \to \infty$, $\frac{df_1^n}{d\tau} \to 0$ and so $f_1^n(t) \to \lim f_1^n(0)$ is constant over time. So the system behaves as the quantity of active monomers is constant over time. The resulting equations are

$$
\left\{
\begin{aligned}
f_1(t) &= f_1(0), \\
\frac{df_2}{d\tau} &= f_1(\frac{f_1}{2} - f_2) - \sigma(f_2 - f_3), \\
\frac{df_i}{d\tau} &= f_1(f_{i-1} - f_i) - \sigma(f_i - f_{i+1}), \quad 3 \leqslant i \leqslant N-2 \\
\frac{df_{N-1}}{d\tau} &= f_1(f_{N-2} - f_{N-1}) - \sigma f_{N-1}, \\
\frac{dy}{d\tau} &= f_1 f_{N-1} + K_b z - (2N-1)K_b y, \\
\frac{dz}{d\tau} &= n f_1 f_{N-1} + K f_1 y - N(N-1)K_b z.
\end{aligned}
\right. \tag{2.15}
$$

Note that these equations do not have any more the mass conservation property. We expect them to faithfully reproduce the early step of the nucleation process when $\sigma \gg f_1(0)$, because in such case the mass created during nucleation is negligible. The latter condition is easily verified when there are a small amount of transconformed protein.

The nucleation part of the system of eq. (2.15) is a linear system with a source term. namely

$$
\frac{df}{dt} = Af + B
$$

, with

$$
A = \begin{pmatrix}
-f_1 - \sigma & \sigma & & \\
f_1 & -f_1 - \sigma & \sigma & \\
& \ddots & \ddots & \ddots \\
& & f_1 & -f_1 - \sigma
\end{pmatrix}
$$

and

$$
B = \begin{pmatrix}
\frac{f_1^2}{2} \\
0 \\
\vdots \\
0
\end{pmatrix}
$$

where $f = (f_i)_{i=2,\cdots,N-1}$.

2.2.2   Stochastic equation

The same two scalings can be applied similarly to the stochastic formulation. As the system of equation becomes quite unfriendly, we only sketch the main differences.

2.2.2.1   Fast misfolding process   From the system of eq. (2.10), we now consider the following scaling

$$
\begin{aligned}
\gamma &\rightarrow \gamma n \\
\gamma^* &\rightarrow \gamma^* n
\end{aligned}
$$

where $n \rightarrow \infty$ and all other parameters remain unchanged. We define the free monomer variable $M_{free}(t) = M(t) + F_1(t)$. Then $M(t)$ and $F_1(t)$ are fast variable, but $M_{free}(t)$ (and all other variables F_i, $i \geqslant 2$, U_N) are slow variables. To see that, consider the fast time scale $M^n(t) = M(tn^{-1})$, $F_i^n = F_i(tn^{-1})$. Due to the total mass conservation, all quantities remains bounded as $n \rightarrow \infty$, and, neglecting terms in $O(\frac{1}{n})$, the fast subsystem becomes

$$
M^n(t) = M^n(0) - Y_1\left(\int_0^t \gamma M^n(s)ds \right) + Y_2\left(\int_0^t \gamma^* F_1^n(s)ds \right),
$$

$$
F_1^n(t) = F_1^n(0) + Y_1\left(\int_0^t \gamma M^n s)ds \right) - Y_2\left(\int_0^t \gamma^* F_1^n(s)ds \right).
$$

This system has a unique asymptotic equilibrium distribution, that depends solely on $M_{free}^n(0) = M^n(0) + F_1^n(0)$ ans is given by a Binomial distribution

$$
M^n \sim B(M_{free}^n(0), \frac{\gamma^*}{\gamma + \gamma^*}),
$$

$$
F_1^n = M_{free}^n(0) - M \sim B(M_{free}^n(0), \frac{\gamma}{\gamma + \gamma^*}).
$$

Thus F_1^n is a fast switching variable and the asymptotic first two moments of interest are

$$
< F_1^n > = M_{free}^n(0)\frac{\gamma}{\gamma + \gamma^*},
$$

$$
< F_1^n(F_1^n - 1) > = M_{free}^n(0)(M_{free}^n(0) - 1)\left(\frac{\gamma}{\gamma + \gamma^*} \right)^2.
$$

Going back to the original time scale, with the time change $\tau = \frac{\gamma p}{\gamma + \gamma^*}t$, and with the following notations

$$
\sigma = \frac{q}{p},
$$

$$
c_0 = \frac{\gamma^*}{\gamma},
$$

$$
\sigma_0 = \sigma(1 + c_0),
$$

$$
K_b = \frac{k_b}{p}(1 + c_0),
$$

$$
K = \frac{k_p}{p},
$$

the slow system becomes now (see Theorem 5.1 Kang and Kurtz 2011)

$$
\begin{cases}
M_{free}(\tau) = M_{free}(0) - 2Y_3\Big(\int_0^\tau \frac{1}{2(1+c_0)}M_{free}(s)(M_{free}(s)-1)ds\Big) \\
\qquad\qquad - \sum_{i=2}^{N-1} Y_{2i+1}\Big(\int_0^\tau M_{free}(s)F_i(s)ds\Big) \\
\qquad\qquad + 2Y_4\Big(\int_0^\tau \sigma_0 F_2(s)ds\Big) + \sum_{i=3}^{N} Y_{2i}\Big(\int_0^\tau \sigma_0 F_i(s)ds\Big), \\
F_2(\tau) = N_2(0) + Y_3\Big(\int_0^\tau \frac{1}{2(1+c_0)}M_{free}(s)(M_{free}(s)-1)ds\Big) \\
\qquad\qquad - Y_5\Big(\int_0^\tau M_{free}(s)F_2(s)ds\Big) - Y_4\Big(\int_0^\tau \sigma_0 F_2(s)ds\Big) + Y_6\Big(\int_0^\tau \sigma_0 F_3(s)ds\Big), \\
F_i(\tau) = F_i(0) + Y_{2i-1}\Big(\int_0^\tau M_{free}(s)F_{i-1}ds\Big) - Y_{2i+1}\Big(\int_0^\tau M_{free}(s)F_i(s)ds\Big) \\
\qquad\qquad - Y_{2i}\Big(\int_0^\tau \sigma_0 F_i(s)ds\Big) + Y_{2i+2}\Big(\int_0^\tau \sigma_0 F_{i+1}(s)ds\Big) \quad 3 \leqslant i \leqslant N-2, \\
F_{N-1}(\tau) = F_i(0) + Y_{2N-4}\Big(\int_0^\tau M_{free}(s)F_{N-2}ds\Big) - Y_{2N-1}\Big(\int_0^\tau M_{free}(s)F_{N-1}(s)ds\Big), \\
\qquad\qquad - Y_{2N-2}\Big(\int_0^\tau \sigma_0 F_{N-1}(s)ds\Big), \\
U_N(\tau) = U_N(0) + Y_{2N-1}\Big(\int_0^\tau M_{free}(s)F_{N-1}ds\Big),
\end{cases}
$$

which is, as in the deterministic case, a Becker-Döring model where the dimerization occurs at a slower time scale than other reaction.

2.2.2.2 Very large normal monomer and rare transconformed monomer

As in the deterministic case, we now make the additional assumption that M_{free} is a large quantity and the rate of de-transconformation γ^* is also very large, *i.e.*

$$
\begin{aligned}
M_{free}(0) &\rightarrow M_{free}(0)n, \\
\gamma^* &\rightarrow \gamma^* n.
\end{aligned}
$$

Then, as $n \rightarrow \infty$, The resulting equations are

$$
\begin{cases}
F_1(\tau) = F_1(0), \\
F_2(\tau) = N_2(0) + Y_3\Big(\frac{F_1^2}{2}\tau\Big) - Y_5\Big(\int_0^\tau F_1 F_2(s)ds\Big) \\
\qquad\qquad - Y_4\Big(\int_0^\tau \sigma F_2(s)ds\Big) + Y_6\Big(\int_0^\tau \sigma F_3(s)ds\Big), \\
F_i(\tau) = F_i(0) + Y_{2i-1}\Big(\int_0^\tau F_1 F_{i-1}(s)ds\Big) - Y_{2i+1}\Big(\int_0^\tau F_1 F_i(s)ds\Big) \\
\qquad\qquad - Y_{2i}\Big(\int_0^\tau \sigma F_i(s)ds\Big) + Y_{2i+2}\Big(\int_0^\tau \sigma F_{i+1}(s)ds\Big) \quad 3 \leqslant i \leqslant N-2, \\
F_{N-1}(\tau) = F_i(0) + Y_{2N-4}\Big(\int_0^\tau F_1 F_{N-2}(s)ds\Big) - Y_{2N-1}\Big(\int_0^\tau F_1 F_{N-1}(s)ds\Big), \\
\qquad\qquad - Y_{2N-2}\Big(\int_0^\tau \sigma F_{N-1}(s)ds\Big), \\
U_N(\tau) = U_N(0) + Y_{2N-1}\Big(\int_0^\tau F_1 F_{N-1}(s)ds\Big).
\end{cases}
$$

$$(2.16)$$

The system of eq. (2.16) is a first-order reaction network, namely

$$\varnothing \mathrel{\substack{\frac{F_1^2}{2} \\ \rightleftharpoons \\ \sigma}} F_2 \quad \text{(dimerization)} \tag{2.17}$$

$$\vdots$$

$$F_{k-1} \mathrel{\substack{F_1 \\ \rightleftharpoons \\ \sigma}} F_k \quad \text{((k)-mer formation)} \tag{2.18}$$

$$\vdots$$

$$F_{N-1} \xrightarrow{F_1} U_N \quad \text{(nucleus formation)} \tag{2.19}$$
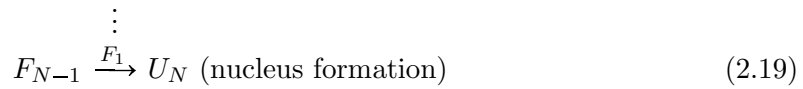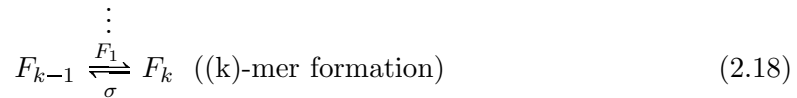
where $\varnothing$ denotes the fact that monomers are not consumed. The time-dependent solution of such a system has been solved by Kingman [85], and is known as a linear Jackson queueing network. We show in the next section 3 that this allows us to deduce the analytical solution of the first assembly time for this model.

3   First Assembly Time in a Discrete Becker-Döring model

This work has been done in collaboration with Maria R. D'Orsogna and Tom Chou, and have been the subject of a preprint.

During this section we deal with the Becker-Döring model (with a fixed maximal size). We deeply study the first assembly time problem, which is defined as a waiting time problem. We use classical tools for such study (scaling laws, dimension reduction methods, time-scale reduction, linear approximation). With the help of analytic approximations and extensive numerical simulations, we end up with a general picture for the different behavior of the first assembly time, as a function of the model parameters. Particularly, we are able to characterize parameter space regions where the first assembly time has distinct properties. Our main findings implies the non-monotonicity of the mean first assembly time as a function of the aggregation rate, and give rise to three different behavior (the following will be made clearer in the next subsections):

- for small quantity of initial particles, the first assembly time follows an exponential distribution, and the mean first assembly time is strongly correlated to the initial quantity of particles;
- for intermediate quantity of initial particles (and large enough nucleus size), the first assembly time has a bimodal distribution, and the mean first assembly time is almost independent of the initial quantity of particles;
- for large quantity of initial particles, the first assembly time has a Weibull distribution, and the mean first assembly time is weakly correlated to the initial quantity of particles

3.1   Introduction

The self-assembly of macromolecules and particles is a fundamental process in physical and chemical systems. Although particle nucleation and assembly have been studied for many decades, interest in this field has recently been intensified due to engineering, biotechnological and imaging advances at the nanoscale level [141, 142, 65]. Aggregating atoms and molecules can lead to the design of new materials useful for surface coatings [35], electronics [145], drug delivery [52] and catalysis [81]. Examples include the self-assembly of DNA structures [34, 107] into polyedric nanocapsules useful for transporting drugs [17] or the self-assembly of semiconducting quantum dots to be used as quantum computing bits [86].

Other important realizations of molecular self-assembly may be found in physiology or virology. One example is the rare self-assembly of fibrous protein aggregates such as $\beta-$amyloid that has long been suspected to play a role in neurodegenerative conditions such as Alzheimer's, Parkinson's, and Huntington's disease [129]. Here, individual PrP^C proteins misfold into PrP^{Sc} prions which subsequently self-assemble into fibrils. The aggregation of misfolded proteins in neurodegenerative diseases is a rare event, usually involving a very low concentration of prions. Fibril nucleation also appears to occur slowly; however once a critical size of about 10-20 proteins is reached, the fibril growth process accelerates dramatically.

$$t = 0 \qquad\qquad 0 < t < t^* \qquad\qquad t = t^*$$
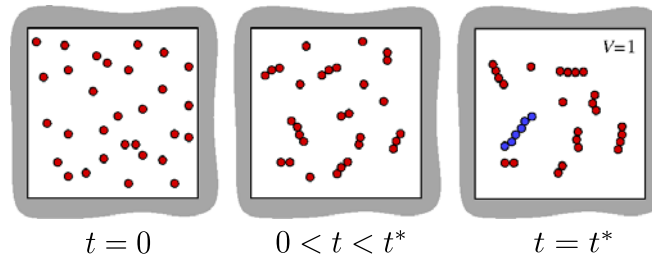
Figure 2.11: Illustration of an homogeneous self-assembly and growth in a closed unit volume initiated with $M = 30$ free monomers. At a specific intermediate time in this depicted realization, there are six free monomers, four dimers, four trimers, and one cluster of size four. For each realization of this process, there is a specific time t^* at which a maximum cluster ($N = 6$ in this example) is first formed (blue cluster).

Viral proteins may also self-assemble to form capsid shells in the form of helices, icosahedra, dodecahedra, depending on virus type. A typical assembly process involves several steps where dozens of dimers aggregate to form more complex subunits which later cooperatively assemble into the capsid shell. Usually, capsid formation requires hundreds of protein subunits that self-assemble over a period of seconds to hours, depending on experimental conditions [147, 148].

Aside from these two illustrative cases, many other biological processes involve a fixed "maximum" cluster size – of tens or hundreds of units – at which the process is completed or beyond which the dynamic change [99]. Developing a stochastic self-assembly model with a fixed "maximum" cluster size is thus important for our understanding of a large class of biological phenomena.

Theoretical models for self-assembly have typically described mean-field concentrations of clusters of all possible sizes using the well-studied mass-action, Becker-Döring equations [119, 140, 128, 36]. While Master equations for the fully stochastic nucleation and growth problem have been derived, and initial analyses and simulations performed [18, 125], there has been relatively less work on the stochastic self-assembly problem. Two collaborators of this present work have recently shown that in finite systems, where the maximum cluster size is capped, results from mean-field mass-action equations are inaccurate and that in this case a stochastic treatment is necessary [47].

In previous work of equilibrium cluster size distributions derived from a discrete, stochastic model, the authors in [47] found that a striking finite-size effect arises when the total mass is not divisible by the maximum cluster size. In particular, they identified the discreteness of the system as the major source of divergence between mean-field, mass action equations and the fully stochastic model. Moreover, discrepancies between the two approaches are most apparent in the strong binding limit where monomer detachment is slow. Before the system reaches equilibrium, or when the detachment is appreciable, the

differences between the mean-field and stochastic results are qualitatively similar, with only modest quantitative disparities.

In this section, we are interested in determining the distribution of the mean first assembly times towards the completion of a full cluster, which can only be done through a fully stochastic treatment. Specifically, we wish to compute the mean time required for a system of M monomers to first assemble into a complete cluster of size N. Statistics of this first passage time [124] may shed light on how frequently fast-growing protein aggregates appear. In principle, one may also construct mean self-assembly times starting from the mean-field, mass action equations, using heuristic arguments. We show however that these mean-field estimates yield mean first assembly times that are quite different from those obtained via exact, stochastic treatments, thus showing their inaccuracy.

In the next subsection 3.2, we review the Becker-Döring mass-action equations for self-assembly and motivate an expression for the first assembly time distribution. We also present the Backward Kolmogorov equations for the fully stochastic self-assembly process and formally develop the associated eigenvalue problem that defines the survival probability and first assembly time distributions. In subsection 3.3, we look at very simple, yet instructive, example were analytical solutions can be found. In subsection 3.4, we study the first assembly time for the constant monomer formulation. Such model is a linear model, and can be solved analytically. In the next four subsections, we explore various limits of the stochastic self-assembly process and obtain analytic expressions for the mean first assembly time in both the strong (see subsections 3.5 and 3.6) and weak (subsections 3.7 and 3.8) binding limits. Then, we adopt a different point of view in subsection 3.9 and look at the limit where initial monomers are present in large quantity. Results from stochastic simulation algorithm (SSA) are presented in subsection 3.10. There, we also discuss the implications of our results and further extensions in the Summary and Conclusions, section 3.10.6. Finally, in the last section 3.11, we comment the implications of these theoretical results for the interpretation of the prion experimental data (shown in previous section 1.4).

3.2 Formulation of the model

We look at a chemical model that is described by the following set of reactions (3.1), where M_1 denotes the monomer specie, and each M_k, $k = 2..n$, denotes the k-mer specie, that is an aggregate composed of k monomers. In this model, N represents the maximal size allowed for such aggregate, called the nucleus size.

$$
\begin{cases}
M_1 + M_1 & \underset{q}{\overset{p}{\rightleftharpoons}} & M_2 & \text{(dimerization)} \\
& \vdots \\
M_{k-1} + M_1 & \underset{q}{\overset{p}{\rightleftharpoons}} & M_k & \text{(k-mer formation)} \\
& \vdots \\
M_{N-1} + M_1 & \underset{q}{\overset{p}{\rightleftharpoons}} & M_N & \text{(nucleus formation)}
\end{cases}
\tag{3.1}
$$
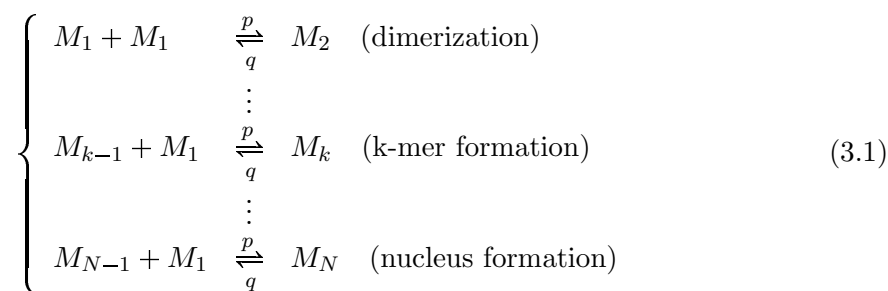
We repeat that such model has been originally used by Becker and Döring [14], and can be seen as a particular case of a general coagulation-fragmentation model, where coagulation and fragmentation only involves monomers (no coagulation of two particles of size larger than 1, and no fragmentation into two particles of size larger than 1 are allowed). In such case, we usually speak of polymerization and depolymerization. It is used to model the spontaneous, homogeneous self-assembly of particles in a closed system of volume V (we take $V = 1$ for simplicity). In particular, no interactions with other particles (solvent,

etc...) are taken into account, neither the spatial structure of the system. There's no loss of particles (through degradation for instance) and no gain neither, so that the total mass is conserved.

Name	symbol
Concentration/Number of Native Monomer	c_1 or C_1
Concentration/Number of aggregate of size $i = 2..n-1$	c_i or C_i
Nucleus size	N
Aggregation rate	p
Dissociation rate	q
Equilibrium constant	$\sigma = \frac{q}{p}$
Total Mass	M

Table 2.2: **Definitions of variables and parameters.** We use small letters for the continuous variables involved in the deterministic model, and capital letters for the discrete variables involved in the stochastic model. We keep the same notation for the parameters in both models, in order to avoid many notation, although the parameters has different units in deterministic or stochastic formulation.

3.2.1 Deterministic Becker-Döring system

Using the law of mass-action, the chemical reaction system (3.1) can be formulated as a system of ordinary differential equation given by

$$
\begin{cases}
\dot{c}_1(t) & = & -pc_1^2 - pc_1 \sum_{i=2}^{N-1} c_i + 2qc_2 + q\sum_{i=3}^{N} c_i, \\
\dot{c}_2(t) & = & -pc_1 c_2 + \frac{p}{2}c_1^2 - qc_2 + qc_3, \\
\dot{c}_i(t) & = & -pc_1 c_i + pc_1 c_{i-1} - qc_i + qc_{i+1}, \quad 3 \leqslant i \leqslant N-1, \\
\dot{c}_N(t) & = & pc_1 c_{N-1} - qc_N.
\end{cases}
\tag{3.2}
$$

where c_i denotes the concentration of chemical entities M_i. This system of differential equation defines a global unique semi-flow in $(\mathbb{R}_+)^N$ and has the important property of conservation of mass

Proposition 69. *For all $t \geqslant 0$, the total mass is conserved,*

$$
\sum_{i=1}^{N} ic_i(t) = \sum_{i=1}^{N} ic_i(0) =: M.
$$

In this section, we will frequently be concerned by the initial condition $c_i(0) = M\delta_{i,1}$, that is starting with only monomers. We can observe that, as soon as $t > 0$, the semi-flow is at values in $]0, M[^N$, or more precisely in the simplex

$$
S_{M,N}^{det} = \{(c_i)_{1 \leqslant iN}, c_i > 0, \sum_{i=1}^{N} c_i = M\}.
$$

For the asymptotic behavior of this system, we have the following

Proposition 70. *For every initial data $(c_i)_{1 \leqslant i \leqslant N} \in \overline{S^c_{M,N}}$, there is a unique global solution to eq. (3.2), which converges at $t \to \infty$ to the unique equilibrium given by*

$$c_i^* = \frac{1}{2}\left(\frac{p}{q}\right)^{i-1}(c_1^*)^i, \tag{3.3}$$

for all $2 \leqslant i \leqslant N$, and c_1^* is the unique solution in $]0, M[$ of

$$c_1^* + \frac{1}{2}\sum_{i=2}^{N} i\left(\frac{p}{q}\right)^{i-1}(c_1^*)^i = c_1(0) = M. \tag{3.4}$$

The proof is based on a Lyapounov function ([9]) given by $V(t) = \sum_{i=1}^{N} c_i(t)\left(\ln(\frac{c_i(t)}{Q_i}) - 1\right)$, where $Q_i = \frac{1}{2}\left(\frac{p}{q}\right)^{i-1}$. For the unicity of the equilibrium, note that eq. (3.4) defines a strictly increasing continuous function.

Remark 71. *The standard results on Becker-Döring equation with infinite maximal size involve similar argument, where an additional difficulty (for general aggregation coefficient) comes from the infinite sum associated to eq. (3.4). The convergence of such infinite sum is critical for the existence and convergence or not towards an equilibrium (see [139] for a review on these results). We refer also to [75] for the rate of convergence to equilibrium, using entropy methods.*

Then, at equilibrium, all concentration c_i^* can be expressed as a function of c_1^*, and the latter is a function of M (and p and q). These considerations allow to have an estimate of the flux of each reaction, given by

$$
\begin{array}{llll}
J_1^+(t) := \dfrac{p}{2}c_1(t)^2 & \approx \dfrac{p}{2}(c_1^*)^2, & \text{(Dimer formation)} \\[2mm]
J_1^-(t) := qc_2(t) & \approx \dfrac{p}{2}(c_1^*)^2, & \text{(Dimer destruction)} \\[2mm]
J_i^+(t) := pc_1(t)c_i(t) \approx \dfrac{p}{2}\left(\dfrac{p}{q}\right)^{i-1}(c_1^*)^{i+1}, & \text{(i-mer formation)} \\[2mm]
J_i^-(t) := qc_{i+1}(t) & \approx \dfrac{p}{2}\left(\dfrac{p}{q}\right)^{i-1}(c_1^*)^{i+1}, & \text{(i-mer destruction)}
\end{array}
\tag{3.5}
$$

for $2 \leqslant i \leqslant N-1$.

3.2.2 Stochastic Becker-Döring system

The chemical reaction system (3.1) can also be formulated as a system of stochastic differential equation, given by

$$
\left\{
\begin{array}{rcl}
C_1(t) & = & C_1(0) - 2Y_1\left(\int_0^t \frac{p}{2}C_1(s)(C_1(s)-1)ds\right) - \sum_{i=2}^{N-1} Y_{2i-1}\left(\int_0^t pC_1(s)C_i(s)ds\right), \\
 & & +2Y_2\left(\int_0^t qC_2(s)ds\right) + \sum_{i=3}^{N} Y_{2i-2}\left(\int_0^t qC_i(s)ds\right), \\
C_2(t) & = & C_2(0) + Y_1\left(\int_0^t \frac{p}{2}C_1(s)(C_1(s)-1)ds\right) - Y_3\left(\int_0^t pC_1(s)C_2(s)ds\right), \\
 & & -Y_2\left(\int_0^t qC_2(s)ds\right) + Y_4\left(\int_0^t qC_3(s)ds\right), \\
C_i(t) & = & C_i(0) + Y_{2i-3}\left(\int_0^t pC_1(s)C_{i-1}ds\right) - Y_{2i-1}\left(\int_0^t pC_1(s)C_i(s)ds\right), \\
 & & -Y_{2i-2}\left(\int_0^t qC_i(s)ds\right) + Y_{2i}\left(\int_0^t qC_{i+1}(s)ds\right), \quad 3 \leqslant i \leqslant N-1, \\
C_N(t) & = & C_N(0) + Y_{2N-3}\left(\int_0^t pC_1(s)C_{N-1}ds\right) - Y_{2N-2}\left(\int_0^t qC_N(s)ds\right),
\end{array}
\right.
$$

$$\tag{3.6}$$

where $(Y_i)_{1 \leqslant 2N-2}$ are independent unit Poisson process. Odd indices i correspond to aggregation event, and even indices i to detachment. Note that contrary to the deterministic formulation for the dimerization process, the propensity of the reaction is given by $\frac{C_1(C_1-1)}{2}$ rather than $\frac{c_1^2}{2}$. The system of eq. (3.6) defines a unique pure-jump Markov process at values in $\mathbb{N}^N$. The mass conservation property still holds

Proposition 72. *For all $t \geqslant 0$, the total mass is conserved,*

$$\sum_{i=1}^{N} iC_i(t) = \sum_{i=1}^{N} iC_i(0) =: M$$

The Markov process takes its value in a finite state space, given by all admissible configurations in $\mathbb{N}^n$,

$$S_{M,N} = \{(n_i)_{1 \leqslant i \leqslant N}, n_i \in \mathbb{N}, \sum_{i=1}^{N} in_i = M\}$$

As soon as p and q are strictly positive, all states in $S_{M,N}$ communicate and the Markov chain is irreducible. We use the notation $\{n\}$ for a typical admissible configuration in $S_{M,N}$. We have

Proposition 73. *For every initial measure on $S_{M,N}$, the Markov process defined by eq. (3.6) is asymptotically convergent to the unique invariant probability measure π, that satisfies the balance condition and is given by (see [82] p 167 Ex 1)*

$$\pi(\{n\}) = B_{M,N} \left(\frac{q}{p}\right)^{\sum_{i=1}^{n} n_i} \prod_{i=1}^{n} \frac{1}{n_i!}, \tag{3.7}$$

for all admissible combination $\{n\} \in S_{M,N}$, and where $B_{M,N}$ is a normalizing constant. This latter constant can be calculated recursively

$$MB_{M,N}^{-1} = \frac{q}{p} \sum_{r=1}^{N} rB_{M-r}^{-1}$$

with $B_0 = 1$ and $B_j = 0$ for $j < 0$.

Analytical expression (for any M, N) of this normalizing constant, and of the asymptotic moments are unfortunately out of reach, even for $N = 2$. However, asymptotic expression when $q \to 0$ for the first moment has been calculated in [47]. We note $\rho = \lfloor \frac{M}{N} \rfloor$ the maximal possible number of largest cluster, so that $M = \rho N + j$, $0 \leqslant j \leqslant N - 1$. In the limit $\sigma = \frac{q}{p} \to 0$, the asymptotic first moments are given by ([47])

$$<C_N>_\infty = \frac{\rho(\rho-1)}{\rho + (j-1)},$$

$$<C_{N-k}>\infty = \frac{\rho(\rho-1)\prod_{l=0}^{k-1}(j-l)}{\prod_{l=j-1-k}^{j-1}(\rho+l)}, \quad 1 \leqslant k \leqslant N-1,$$

for any $0 \leqslant j < N - 1$. While for $j = N - 1$,

$$<C_N>_\infty = (\rho-1)\frac{f(\rho-1,N-1)}{D(\rho,N-1)},$$

$$<C_{N-k}>\infty = \frac{\prod_{l=0}^{k-1}(N-1-l)\prod_{i=1}^{N-1-k}(\rho-2+i)}{f(\rho,N-1)}, \quad 1 \leqslant k < N-1$$

$$<C_1>\infty = \frac{2(N-1)!}{f(\rho,N-1)}$$

with $f(\rho, j) = j! + \prod_{l=1}^{j-1}(\rho + l)$. It has been show that such formulas differ significantly from mean-field formulas eq. (3.3) for M/N finite and relatively small [47]. Other works (see [27] among others) give way to approximate first (and higher) moments in the case $N = 2$, using a moment-closure approximation. For instance, for $N = 2$, $< C_2 >_\infty$ can be approximate by its mean-field deterministic value, and the second moment using a Gaussian truncation. We obtain (see [27])

$$< C2 >_\infty \;\; \approx \;\; \frac{1}{4}\Big((2M + q/p) - \sqrt{(2M + q/p)^2 - 4M^2}\Big)$$

$$< C_1 C_2 >_\infty \;\; \approx \;\; M < C_2 >_\infty - \frac{q < C_2 >_\infty}{-4p < C_2 >_\infty + p(2M + 3) + q} - < C_2 >_\infty^2$$

Such formulas are expected to be valid for large M. the extension for larger N is limited as one need to solve nonlinear equation such as eq. (3.3).

As in the deterministic case, these considerations allow to estimate the flux of each reaction, given by

$$J_1^+(t) = < \frac{p}{2}C_1(t)(C_1(t) - 1) > \approx \frac{p}{2} < C_1(C_1 - 1) >_\infty, \quad \text{Dimer formation} \quad (3.8)$$

$$J_1^-(t) = < qC_2(t) > \qquad\qquad \approx q < C_2 >_\infty, \qquad\qquad \text{Dimer destruction} \quad (3.9)$$

$$J_i^+(t) = < pC_1(t)C_i(t) > \qquad \approx p < C_1 C_i >_\infty, \qquad \text{(i-mer formation)} \quad (3.10)$$

$$J_i^-(t) = < qC_{i+1}(t) > \qquad\quad \approx q < C_{i+1} >_\infty, \qquad \text{(i-mer destruction)} \quad (3.11)$$

for $2 \leqslant i \leqslant n - 1$, where $< X >_\infty$ are the asymptotic mean value of X. Note that all these asymptotic moments are function of M, p, q and N.

Finally, let $\mathbf{A}$ be the matrix of transition rates between the configurations and

$$P(n_1, n_2, \ldots, n_N; t|m_1, m_2, \ldots, m_N; 0)$$

the probability that the system contains n_1 monomers, n_2 dimers, n_3 trimers, etc, at time t, given that the system started in some initial configuration $(m_1, m_2, \ldots m_N)$ at $t = 0$. The Master equation in this representation is given by [47]

$$\dot{P}(\{n\}; t|\{m\}, 0) = \; -\Lambda(\{n\})P(\{n\}; t|\{m\}, 0)$$

$$+\tfrac{p}{2}(n_1 + 2)(n_1 + 1)W_1^+ W_1^+ W_2^- P(\{n\}; t|\{m\}, 0)$$

$$+q(n_2 + 1)W_2^+ W_1^- W_1^- P(\{n\}; t|\{m\}, 0)$$

$$+ \sum_{i=2}^{N-1} p(n_1 + 1)(n_i + 1)W_1^+ W_i^+ W_{i+1}^- P(\{n\}; t|\{m\}, 0) \tag{3.12}$$

$$+ \sum_{i=3}^{N} q(n_i + 1)W_1^- W_{i-1}^- W_i^+ P(\{n\}; t|\{m\}, 0),$$

where $P(\{n\}, t) = 0$ if any $n_i < 0$, where

$$\Lambda(\{n\}) = \frac{p}{2}n_1(n_1 - 1) + \sum_{i=2}^{N-1} pn_1 n_i + \sum_{i=2}^{N} qn_i,$$

is the total rate out of configuration $\{n\}$, and $W_j^\pm$ are the unit raising/lowering operators on the number of clusters of size j. The latter are defined as

$$W_1^+ W_i^+ W_{i+1}^- P(\{n\}; t|\{m\}; 0)$$

$$\equiv P(n_1 + 1, \ldots, n_i + 1, n_{i+1} - 1, \ldots; t|\{m\}; 0).$$

3.2.3 Nucleation time

The nucleation time (or first assembly time) is defined as the waiting time for $C_N(t)$ to reach one, *i.e.*

Definition 1 (Stochastic nucleation time)**.** *Let* $M, N > 0$*, and* $(C_i(\cdot))_{1 \leqslant i \leqslant N}$ *the solution of eq. (3.6). The stochastic nucleation time, starting at a configuration* $\{m\} \in S_{M,N}$ *is*

$$\tau_N(\{m\}) = \inf\{t \geqslant 0; C_N(t) = 1 \mid C_i(0) = \delta_{m_i}, 1 \leqslant i \leqslant N\}.$$

The mean nucleation time is

$$T_N(\{m\}) = \mathbb{E}\big[\tau_N(\{m\})\big]. \tag{3.13}$$

It is a first-passage problem. Note that because the Markov chain is at value in a finite state-space, the first passage time is finite with probability one as soon as $p, q > 0$ (we will see the case $q = 0$ later on) and $M \geqslant N$. When not specified, we speak of the first passage time of $C_N(t) = 1$ for the specific initial condition of all monomers

$$C_i(0) = M\delta_{i,1}.$$

To accurately compute entire assembly time distributions, particularly for small particle numbers M, it is convenient to consider the state-space shown in figure 2.12, where we consider the explicit cases $N = 3$ and $M = 7$ or $M = 8$.

Here, the problem is to evaluate the time it takes for the system to reach an "absorbing" state – a cluster of maximal size N is fully assembled – having started from a given initial configuration. For example, for $N = 3$, absorbing states are those where $n_{N=3} \geqslant 1$. The arrival time from a given initial configuration to any absorbing state depends on the specific trajectory taken by the system. Upon averaging these arrival times over all paths starting from the initial configuration $\{m\}$ and ending at any absorbing state, weighted by their likelihood, we can find the overall probability distribution of the time it takes to first assemble a complete cluster of size N.

The natural way to compute the distribution of first completion times is to consider the "Backward" equation for the probability vector of initial conditions, given a fixed final condition $\{n\}$ at time t. The Backward equation in this representation is simply $\dot{\mathbf{P}} = \mathbf{A}^\dagger \mathbf{P}$, where $\mathbf{A}^\dagger$ is the adjoint of the transition matrix $\mathbf{A}$ defined above, so that

$$
\begin{aligned}
\dot{P}(\{n\}; t|\{m\}, 0) = \ & -\Lambda(\{m\})P(\{n\}; t|\{m\}; 0) \\[6pt]
& + \frac{p_1}{2} m_1(m_1 - 1) W_2^+ W_1^- W_1^- P(\{n\}; t|\{m\}; 0) \\[6pt]
& + q_2 m_2 W_2^- W_1^+ W_1^+ P(\{n\}; t|\{m\}; 0) \\[6pt]
& + \sum_{i=2}^{N-1} p_i m_1 m_i W_1^- W_i^- W_{i+1}^+ P(\{n\}; t|\{m\}; 0) \\
& + \sum_{i=3}^{N} q_i m_i W_1^+ W_{i-1}^+ W_i^- P(\{n\}; t|\{m\}; 0).
\end{aligned}
\tag{3.14}
$$

Here, the operators $W_i^\pm$ operate on the m_i index. It is straightforward to verify that eq. (3.14) is the adjoint of eq. (3.12). The utility of using the Backward equation is that eq. (3.14) can be used to determine the evolution of the "survival" probability defined as

$$S(\{m\};t) \equiv \sum_{\{n\},n_N=0} P(\{n\};t|\{m\};0),$$

where we consider now that states $\{n\}$ with $n_N \geqslant 1$ are absorbing. Thus, the sum is restricted to configurations where the final states $\{n\}$ are set to $n_N = 0$ so as to include all and only "surviving" states that have not yet reached any of the absorbed ones where $n_N \geqslant 1$. $S(\{m\};t)$ thus describes the probability that no maximum cluster has yet been formed at time t, given that the system started in the $\{m\}$ configuration at $t = 0$. By a summation of eq. (3.14) over all final states with $n_N = 0$, it is possible to find an equation for $S(\{m\};t)$. Upon performing this sum, we find that $S(\{m\};t)$ also obeys eq. (3.14) but with $P(\{n\};t|\{m\},0)$ replaced by $S(\{m\};t)$, along with the definition $S(m_1, m_2, \ldots, m_N \geqslant 1;t) = 0$ and the initial condition $S(m_1, m_2, \ldots, m_N = 0;0) = 1$. Thus, the general vector equation for the survival probability is $\dot{\mathbf{S}} = \mathbf{A}^\dagger \mathbf{S}$, where we consider only the subspace of $\mathbf{A}^\dagger$ on non absorbing states. In this representation, each element $S(\{m\};t)$ in the vector $\mathbf{S}(\{m\};t)$ is the survival probability associated with a particular initial condition. The above vector equation may be solved for $\mathbf{S}$, leading to the vector of first assembly time distributions

$$\mathbf{G}(\{m\};t) \equiv -\frac{\partial \mathbf{S}(\{m\};t)}{\partial t}, \tag{3.15}$$

from which all moments of the assembly times can be constructed. To this end, it is often useful to recast eq. (3.15) in Laplace space

$$\tilde{\mathbf{G}}(\{m\};s) = \mathbf{1} - s\tilde{\mathbf{S}}(\{m\};s),$$

where $\tilde{\mathbf{G}}$ is the Laplace transform of $\mathbf{G}$ and similarly for $\mathbf{S}$. The vector $\mathbf{1}$ is the survival probability of any initial, non-absorbing state, and consists of 1's. Its length is given by the dimension of $\mathbf{A}^\dagger$ on the subspace of non-absorbing states. Using this representation we may evaluate the mean assembly time $T_N(\{m\})$ for forming the first cluster of size N starting from the initial configuration $\{m\}$ at $t = 0$

$$
\begin{aligned}
T_N(\{m\}) &\equiv -\int_0^\infty t\frac{\partial S(\{m\};t)}{\partial t}\mathrm{d}t, \\
&= \int_0^\infty S(\{m\};t)\mathrm{d}t, \\
&= \tilde{S}(\{m\};s=0).
\end{aligned} \tag{3.16}
$$

Similarly, the variance $\mathrm{var}_N(\{m\})$ related to the first assembly time can be calculated as

$$
\begin{aligned}
\mathrm{var}_N(\{m\}) &\equiv -\int_0^\infty t^2\frac{\partial S(\{m\};t)}{\partial t}dt - T_N(\{m\})^2, \\
&= 2\int_0^\infty tS(\{m\};t)dt - T_N(\{m\})^2, \\
&= \left[-2\frac{\partial \tilde{S}(\{m\},s)}{ds} - \tilde{S}(\{m\};s)^2\right]_{s=0}.
\end{aligned}
$$

The Laplace-transform of the survival probability can be found via $\dot{\mathbf{S}} = \mathbf{A}^\dagger \mathbf{S}$ which, in Laplace space, is written as

$$\tilde{\mathbf{S}} \;\; = \;\; [s\mathbf{I} - \mathbf{A}^{\dagger}]^{-1}\mathbf{1}, \tag{3.17}$$

so that

$$\tilde{\mathbf{G}} = \mathbf{1} - s[s\mathbf{I} - \mathbf{A}^{\dagger}]^{-1}\mathbf{1}.$$

The mean first assembly time for a specific configuration $\{m\}$ is thus given as

$$T_N(\{m\}) \;\; = \;\; \tilde{S}(\{m\}; s = 0) = - \left[(\mathbf{A}^{\dagger})^{-1}\mathbf{1}\right]_{\{m\}}. \tag{3.18}$$

where the subscript $\{m\}$ refers to the vector element corresponding to the $\{m\}^{\text{th}}$ initial configuration. Similar expressions can be found for the variance and other moments.

In order to invert the matrix $\mathbf{A}^{\dagger}$ on the subspace of non-absorbing states we first note that its dimension $D(M, N)$ rapidly increases with M. In particular, we find that the number of distinguishable configurations with no maximal cluster obeys the induction:

Proposition 74. *for any $M, N > 0$, the dimension of the matrix $\mathbf{A}^{\dagger}$ is given by*

$$D(M, N + 1) = \sum_{j=0}^{\rho} D(M - jN, N), \tag{3.19}$$

with $\rho = \lfloor M/N \rfloor$ the integer part of M/N.

For example, in eq. (3.19), $D(M, 2) = 1$, and the only "surviving" configuration is $(M, 0)$. The next term is $D(M, 3) = 1 + \lfloor M/2 \rfloor$ which, for $M/N \to \infty$ yields $D(M, 3) \simeq M/2$. Similarly $D(M, 4)$ can be written as

$$D(M, 4) = \sum_{j=0}^{\lfloor M/3 \rfloor} D(M - 3j, 3) \simeq \lfloor \frac{M}{3} \rfloor \lfloor \frac{M}{2} \rfloor \simeq \frac{M^2}{6}$$

where the last two approximations are valid in the large M/N limit. By induction, we find

Corollary 75. *In the large M/N limit, the dimension of the matrix $\mathbf{A}^{\dagger}$ is approximated by*

$$D(M, N) \simeq \frac{M^{N-2}}{(N - 1)!}.$$

From these estimates, it is clear that the complexity of the eigenvalue problem in eq. (3.18) increases dramatically for large M and N. Then the theoretical formulation of the first passage problem is of no help to derive quantitative formula and to understand the influence of parameters.

Finally, note that the nucleation time is usually defined in the mean-field context ([120]) as the waiting time for $c_N(t)$ to reach a given fraction of the total mass. However, to allow a direct comparison with the stochastic formulation case, we take the following definition for the deterministic nucleation time. Consider the modified (irreversible) Becker-Döring system

$$\begin{cases} M_1 + M_1 & \overset{p}{\underset{q}{\rightleftharpoons}} & M_2 & \text{(dimerization)} \\ & \vdots & \\ M_{k-1} + M_1 & \overset{p}{\underset{q}{\rightleftharpoons}} & M_k & \text{(k-mer formation)} \\ & \vdots & \\ M_{N-1} + M_1 & \underset{p}{\rightarrow} & M_N & \text{(nucleus formation)} \end{cases} \qquad (3.20)$$

where the last reaction is now considered irreversible. Its deterministic formulation is now

$$\begin{cases} \dot{c}_1(t) & = & -pc_1^2 - pc_1 \sum_{i=2}^{N-1} c_i + 2qc_2 + q\sum_{i=3}^{N} c_i \\ \dot{c}_2(t) & = & -pc_1c_2 + \frac{p}{2}c_1^2 - qc_2 + qc_3 \\ \dot{c}_i(t) & = & -pc_1c_i + pc_1c_{i-1} - qc_i + qc_{i+1}, \quad 3 \leqslant i \leqslant N-2, \\ \dot{c}_{N-1}(t) & = & -pc_1c_{N-1} + pc_1c_{N-2} - qc_{N-1}, \\ \dot{c}_N(t) & = & pc_1c_{N-1}, \end{cases} \qquad (3.21)$$

so that the asymptotic equilibrium is now $c_i^* = \frac{M}{N}\delta_{i,N}$.

Definition 2 (Deterministic nucleation time). *Let $M, N > 0$, and $(c_i(\cdot))_{1 \leqslant i \leqslant N}$ the solution of eq. (3.21). The deterministic nucleation time T^{det}, starting at configuration $\{c\} \in S_{M,N}^{det}$ is*

$$T_N^{det}(\{c\}) = \inf\{t \geqslant 0, c_N(t) = 1 \mid c_i(0) = c_i, 1 \leqslant i \leqslant N\}. \qquad (3.22)$$

Remark 76. $T_N^{det}(\{c\}) < \infty$ *as soon as $M > N$.*

3.3   Example and particular case

3.3.1 $N = 2$

As a first trivial remark, we treat the case $N = 2$. In such case, the "surviving" configuration is $(M, 0)$, and so the nucleation time is given by the following proposition.

Proposition 77. *When $N = 2$ and $M \geqslant 2$, the first assembly time, starting from configuration $\{M, 0\}$ is an exponential random variable of mean parameter*

$$T_2(\{M, 0\}) = \frac{2}{pM(M-1)}.$$

This exponential time is given by the first time the dimerization reaction occurs. Note that a direct integration of eq. (3.21) yields the deterministic nucleation time, for any $M > 2$,

$$T_2^{det}(\{M, 0\}) = \frac{2}{pM(M-2)}.$$

3.3.2 $N = 3$

In the case of $N = 3$, the "surviving" configuration are $\{M - 2i, i, 0\}$, $1 \leqslant i \leqslant \lfloor \frac{M}{2} \rfloor$. These configurations can be well ordered so that the matrix $\mathbf{A}^\dagger$ that defines the first passage problem is tridiagonal, of order $m = \lfloor \frac{M}{2} \rfloor + 1$, whose elements $a_{i,j}^\dagger$ take the form

$$\begin{cases} a_{k,k-1}^\dagger & = & (k-1)q, \quad 2 \leqslant k \leqslant 1 + \lfloor \frac{M}{2} \rfloor, \\ a_{k,k}^\dagger & = & -\frac{(M-2k+2)(M-3k+2)}{2}p - (k-1)q, \quad 1 \leqslant k \leqslant 1 + \lfloor \frac{M}{2} \rfloor, \\ a_{k,k+1}^\dagger & = & \frac{(M-2k+2)(M-2k+1)}{2}p, \quad 2 \leqslant k \leqslant 1 + \lfloor \frac{M}{2} \rfloor. \end{cases}$$

A recurrence relationship can be derived to invert this matrix. However, there's no "simple" close form for the mean assembly time, so we do not write its expression here.

3.3.3 $N = 3$, $M = 7, 8$

As a simple, yet instructive example, we consider the case $N = 3$ and $M = 7$ or 8. The entire dynamic is represented in figure 2.12.
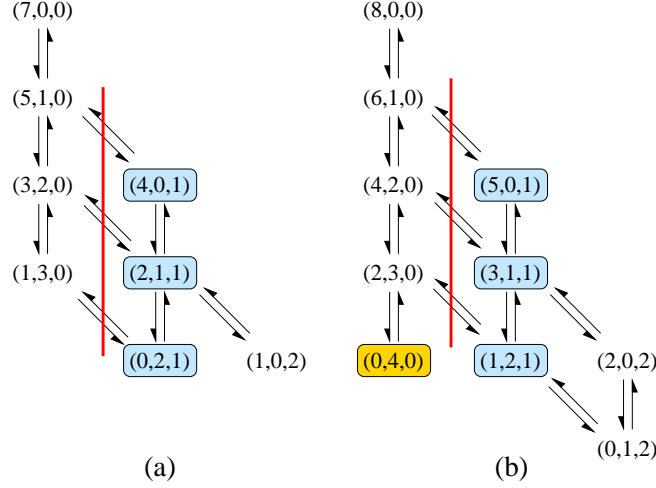
Figure 2.12: Allowed transitions in stochastic self-assembly starting from an all-monomer initial condition. In this simple example, the maximum cluster size is $N = 3$. (a) Allowed transitions for a system with $M = 7$. Since we are interested in the first maximum cluster assembly time, states with $n_3 = 1$ constitute absorbing states. The process is stopped once the system crosses the vertical red line. (b) Allowable transitions when $M = 8$. Note that if monomer detachment is prohibited ($q = 0$), the configuration $(0, 4, 0)$ (yellow) is a trapped state. Since a finite number of trajectories reach this trapped state and never reach a state where $n_3 = 1$ if $q = 0$, the mean first assembly time diverges, $T = \infty$.

For $M = 7$, the equations for the survival probability $S(n_1, n_2, n_3, t)$ can be written in terms of the backward Kolmogorov equations which in this case are

$$
\begin{aligned}
\frac{dS(7,0,0)}{dt} &= \frac{7 \cdot 6}{2}[S(5,1,0) - S(7,0,0)], \\
\frac{dS(5,1,0)}{dt} &= q[S(7,0,0) - S(5,1,0)] + \frac{5 \cdot 4}{2}[S(3,2,0) - S(5,1,0)] + 5[S(4,0,1) - S(5,1,0)], \\
\frac{dS(3,2,0)}{dt} &= 2q[S(5,1,0) - S(3,2,0)] + \frac{3 \cdot 2}{2}[S(1,3,0) - S(3,2,0)] + 3 \cdot 2[S(2,1,1) - S(3,2,0)], \\
\frac{dS(1,3,0)}{dt} &= 3q[S(3,2,0) - S(1,3,0)] + 3[S(0,2,1) - S(1,3,0)],
\end{aligned}
$$

where we have assumed that time is now renormalized so that $p = 1$ and q is unitless. These equations can be numerically solved as a set of coupled (linear) ODEs. The solution to the above ODEs leads to the full survival distributions. If we are only interested in the mean first passage time T, starting from configuration $\{n_1, n_2, n_3\}$, we compute the matrix $\mathbf{A}^\dagger$

$$
\mathbf{A}^\dagger = \begin{pmatrix}
-21 & 21 & 0 & 0 \\
q & -(15 + q) & 10 & 0 \\
0 & 2q & -2q - 9 & 3 \\
0 & 0 & 3q & -3q - 3
\end{pmatrix}
$$

and using eq. (3.18),

$$T_3(\{7,0,0\}) = \frac{1}{105} \frac{744 + 487q + 60q + 2q^3}{27 + 20q + 2q^2} \tag{3.23}$$

$$T_3(\{5,1,0\}) = \frac{1}{105} \frac{609 + 387q + 50q^2 + 2q^3}{27 + 20q + 2q^2}$$

$$T_3(\{3,2,0\}) = \frac{1}{105} \frac{630 + 357q + 44q^2 + 2q^3}{27 + 20q + 2q^2}$$

$$T_3(\{1,3,0\}) = \frac{1}{105} \frac{945 + 385q + 42q^2 + 2q^3}{27 + 20q + 2q^2}$$

Similarly,

$$T_3(\{8,0,0\}) = \frac{105 + 1526q + 488q^2 + 40q^3 + q^4}{168q(49 + 16q + q^2)}$$

$$T_3(\{6,1,0\}) = \frac{105 + 1232q + 392q^2 + 34q^3 + q^4}{168q(49 + 16q + q^2)}$$

$$T_3(\{4,2,0\}) = \frac{147 + 1176q + 350q^2 + 30q^3 + q^4}{168q(49 + 16q + q^2)}$$

$$T_3(\{2,3,0\}) = \frac{343 + 1386q + 350q^2 + 28q^3 + q^4}{168q(49 + 16q + q^2)}$$

$$T_3(\{0,4,0\}) = \frac{2401 + 2058q + 392q^2 + 28q^3 + q^4}{168q(49 + 16q + q^2)}$$

In figure 2.13, we plot the mean first assembly time for $N = 3$, $M = 7$ and $M = 8$ as a function of the relative detachment rate q, starting in initial condition $(M, 0, 0)$. These two examples share a qualitative properties. Firstly, the mean first assembly time is non-monotonic with respect to q. This is a surprising result, that comes from the discrete effect (similar to reported by [47] for asymptotic first moment). This means that for some specific parameters, the system goes faster towards a maximal cluster for higher detachment rate. The cause of such result is the presence of traps, as it will be explain in the following subsections 3.5 and 3.6. For $M = 8$, we even have $T \to \infty$ as $q \to 0$ (whatever the initial configuration). This is due to the fact that the state $\{0, 4, 0\}$ becomes also an absorbing state in the limit $q = 0$. Then, in such case, we need to calculate conditional time assembly (see subsection 3.5). Secondly, both mean first assembly times go to infinity as $q \to \infty$ (as expected), both at an asymptotic linear rate with respect to q. This asymptotic behaviour as $q \to \infty$ will be investigated further in subsection 3.7 and subsection 3.8.
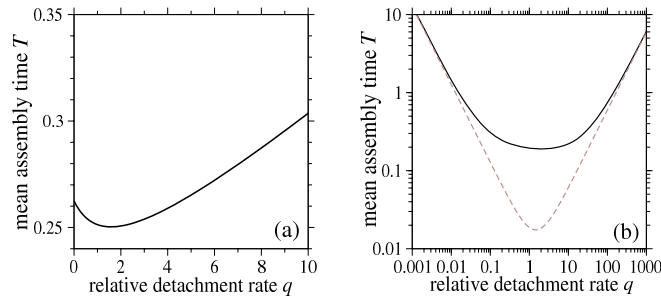
Figure 2.13: (a) Mean first assembly times for $N = 3, M = 7$. (b) Mean first assembly times for $N = 3, M = 8$.

3.4   Constant monomer formulation

In this section, we study the first assembly time for a distinct model, that is the Becker-Döring model with constant monomer. We already encounter such model in subsection 2.2 (see eq. 2.15 for the deterministic model, and eq. 2.16 for the stochastic model). The main advantage of the constant monomer formulation is to be analytically solvable (within our specific choice of parameters, independent of cluster size). The constant monomer formulation can be seen as an open linear Jackson queueing network, where the last queue is absorbing. Entry in the system occurs from the first queue (creation of a dimer, C_2) and every individuals move (an aggregate change of size size) independently of each other between queues according to the transition rates written above. They can leave the system from the first queue or stay in the last absorbing queue (C_N). The propensities of the reaction being linear, it is known that the time-dependent probabilities to have a given number of aggregate of size i are given by a Poisson distribution (see [85]). In particular, the number of individuals in the last queue also follows a Poisson distribution. Because the last queue is absorbing, the survival time of $C_N = 0$ follows

$$S(t) = \mathbb{P}\{C_N(s) = 0, 0 < s \leqslant t\} = \mathbb{P}\{C_N(t) = 0\} = \exp\Big(- \langle C_N \rangle(t) \Big).$$

Such distribution is characterized by a single parameter, its mean for instance. Again, the model being linear, the mean number of aggregates of size i, at time t, is given by the solution of a deterministic ordinary differential equation which can be rewritten as

$$\frac{d\mathbf{c}}{dt} = \mathbf{A}\mathbf{c} + \mathbf{B}, \qquad (3.24)$$
$$\frac{dc_n}{dt} = c_1 c_{n-1},$$

where

$$\mathbf{c} = \begin{pmatrix} c_2 \\ c_3 \\ \vdots \\ c_{n-1} \end{pmatrix}, \quad \mathbf{A} = \begin{pmatrix} -\sigma - c_1 & \sigma & & & \\ c_1 & -\sigma - c_1 & \sigma & & \\ & \ddots & \ddots & \ddots & \\ & & c_1 & -\sigma - c_1 & \sigma \\ & & & c_1 & -\sigma - c_1 \end{pmatrix}, \quad \mathbf{B} = \begin{pmatrix} c_1^2/2 \\ 0 \\ \vdots \\ 0 \end{pmatrix}$$
$$(3.25)$$

In the equations above, c_1 is the constant quantity of monomers, and $c_i(t) = \langle C_i(t) \rangle$ is the mean number of aggregates of size $i \geqslant 2$, and we have rescaled the time by $1/p$ and denoted $\sigma = q/p$ for simplicity. The system of eq. (3.24) above is a linear system and can be solved to find $c_N(t)$, and the first assembly time. A general form for $c_{N-1}(t)$ is given by

$$c_{N-1}(t) = \sum_{k=1}^{N-2} \alpha_k e^{\lambda_k t} V_{N-2}^{(k)} - (A^{-1}B)_{N-2},$$

where $\lambda_k = -(c_1 + \sigma) + 2\sqrt{c_1 \sigma} \cos(\frac{k\pi}{N-2})$ are the eigenvalues of A, $V^{(k)}$ the associated eigenvector (for a general form, see [146]) ($V_{N-2}^{(k)}$ denotes its last components), and α_k are constant given by the initial condition $c_i(t = 0) = 0$, $2 \leqslant i \leqslant N - 1$. By integration,

$$c_N(t) = c_1 \Big[\sum_{k=1}^{N-2} \alpha_k V_{N-2}^{(k)} \frac{e^{\lambda_k t} - 1}{\lambda_k} - (A^{-1}B)_{N-2} t \Big].$$

We detail below two asymptotic expressions, which are of interest for their own, as well for the initial Becker-Döring model. The two limits we look at are $\sigma >> M$ and $M >> \sigma$. In such cases the mean lag time is given by

$$
\begin{aligned}
T_N &\sim_{M \gg \sigma} \frac{(2(N-1)!)^{1/(N-1)}}{M^{N/(N-1)}} \\
T_N &\sim_{M \ll \sigma} \frac{2\sigma^{N-2}}{M^N}
\end{aligned}
\tag{3.26}
$$

Similarly, there is two different asymptotic distributions for the lag time, given respectively by a Weibull and an exponential distribution,

$$
\begin{aligned}
-\frac{dS_N}{dt} &\sim_{t \to 0} \frac{M^N}{2(N-2)!} t^{N-2} \exp\left(-\frac{M^n}{2(N-1)!} t^{N-1}\right) \\
-\frac{dS_N}{dt} &\sim_{t \to \infty} \frac{M^N}{2|\det \mathbf{A}|} \exp\left(-\frac{M^N}{2|\det \mathbf{A}|} t + M(\mathbf{A}^{-2}\mathbf{B})_{N-2}\right)
\end{aligned}
\tag{3.27}
$$

Remark 78. *The large time asymptotic of the linear model eq. 3.24 is of interest to interpret previous formula. At equilibrium, one have indeed, for all $2 \leqslant i \leqslant N-1$, (given by the calculus of $\mathbf{A}^{-1}$)*

$$
c_i^{eq} = \frac{1}{2|\det \mathbf{A}|} \sum_{k=i+1}^{N} c_1^{k-1} \sigma^{N-k}
\tag{3.28}
$$

Hence, for $\sigma >> M$, $c_i^{eq} \sim \frac{M}{2}\left(\frac{M}{\sigma}\right)^{i-1}$, the equilibrium repartition is exponential, and $c_N(t) \sim M c_{N-1}^{eq} t \sim \frac{M^N}{2\sigma^{N-2}} t$. For $M >> \sigma$, however, all quantities at equilibrium become equal, to $c_i^{eq} \sim \frac{M}{2}$. In such case, the lag time is reached before equilibrium takes place, and the asymptotic expression corresponds to an irreversible aggregation (thus independent of σ).

3.5 Irreversible limit ($q = 0$)

We come back to the original formulation of the first assembly time, described for conservative the Becker-Döring model in subsection 3.2. We consider here the irreversible case $q = 0$. We have already seen in one example that the mean first assembly time is not necessarily finite any more. We first explore the case $N = 3$ and then the general N case. This derivation will be extended in a perturbative manner for small $0 < q \ll 1$ in subsection 3.6.

3.5.1 $N = 3$

So let us first restrict ourselves to $N = 3$ and the $q = 0$ case of irreversible self-assembly. Upon setting $q = 0$, the matrix $\mathbf{A}^\dagger$ becomes bi-diagonal and a two-term recursion can be used to solve for the survival probability $\tilde{S}(M - 2n, n, 0; s)$ as follows. If the entries of the bidiagonal matrix $\mathbf{A}^\dagger$ are denoted $a_{ij}^\dagger$, there are all zero except

$$
\begin{aligned}
a_{k,k}^\dagger &= -\frac{(M-2k+2)(M-3k+2)}{2}p, \quad 1 \leqslant k \leqslant 1 + \lfloor\frac{M}{2}\rfloor, \\
a_{k,k+1}^\dagger &= \frac{(M-2k+2)(M-2k+1)}{2}p, \quad 2 \leqslant k \leqslant 1 + \lfloor\frac{M}{2}\rfloor.
\end{aligned}
$$

The elements $b_{i,j}$ of the inverse matrix $\mathbf{B} = \left[s\mathbf{I} - \mathbf{A}^\dagger\right]^{-1}$ are given by

$$
\begin{aligned}
b_{i,i} &= \frac{1}{s - a_{i,i}^\dagger}, \\
b_{i,j} &= 0, \quad \text{if } i > j, \\
b_{i,j} &= \frac{\prod_{k=i}^{j-1} a_{k,k+1}^\dagger}{\prod_{k=i}^{j}(s - a_{k,k}^\dagger)}, \quad \text{if } i < j.
\end{aligned}
\tag{3.29}
$$

The survival probability in Laplace space, according to eq. (3.17) is the sum of entries of each row of $\left[s\mathbf{I} - \mathbf{A}^\dagger\right]^{-1}$ so that

$$
\tilde{S}(M - 2n, n, 0; s) = \frac{1}{s - a_{i,i}^\dagger} + \sum_{j=i+1}^{[M/2]+1} \frac{\prod_{k=i}^{j-1} a_{k,k+1}^\dagger}{\prod_{k=i}^{j}(s - a_{k,k}^\dagger)},
\tag{3.30}
$$

where $i = n + 1$ is the $(n + 1)^{\text{th}}$ row of $\left[s\mathbf{I} - \mathbf{A}^\dagger\right]^{-1}$. Upon taking the Inverse Laplace transform of eq. (3.30) we can write the survival probability $S(M - 2n, n, 0; t)$ as a sum of exponentials, since all poles are of order one. The full first assembly time distribution can be obtained from this quantity, with $-dS(M - 2n, n, 0; t)/dt$. Similarly, the mean first assembly time, according to eq. (3.18) is given by $T_3(M - 2n, n, 0) = \tilde{S}(M - 2n, n, 0; s = 0)$. In particular, from eq. (3.29) we find

$$
\frac{a_{k,k+1}^\dagger}{a_{k+1,k+1}^\dagger} = -\frac{(M - 2k + 2)(M - 2k + 1)}{(M - 2k)(M - 1)}.
\tag{3.31}
$$

so that inserting eq. (3.31) into eq. (3.30) for $s = 0$ we obtain

Proposition 79. *For $N = 3$, the mean assembly time starting from the initial condition $(M - 2n, n, 0)$, $0 \leqslant n \leqslant M/2$ is*

$$
T_3(M - 2n, n, 0) = \frac{2}{(M - 2n)(M - 1)} \left[1 + \sum_{j=1}^{[M/2]} \prod_{k=n+1}^{j} \frac{(M - 2k + 2)(M - 2k + 1)}{(M - 2k)(M - 1)} \right]
\tag{3.32}
$$

Note that the mean first assembly time is finite when M is odd, but is infinite if M is even as in the case of $M = 8$ and $N = 3$, where a trapped state arises. In these case, there is a finite probability that the system arrives in the state $(0, M/2, 0)$, and since the assembly process is irreversible, such realizations remain in $(0, M/2, 0)$ forever: detachment would be the only way out of it. Therefore, averaged over trajectories that include traps, the mean assembly time is infinite.

3.5.2   Traps for $N \geqslant 4$

We now show that when $q = 0$, trapped states exist for any M and $N \geqslant 4$, yielding infinite mean assembly times, starting from any configuration.

Definition 3 (Traps). *For any $M, N > 0$, a trap state is a configuration $\{m\} \in S_{M,N}$ such that*

$$
\tau_N(\{m\}) = \infty, \text{almost surely.}
$$

A trapped state arises whenever a maximum cluster has not been assembled ($n_N = 0$), and all free monomers have been depleted ($n_1 = 0$). In this case the total mass must be distributed according to

$$M = \sum_{j=2}^{N-1} j n_j. \tag{3.33}$$

It is not necessarily the case that this decomposition is possible for all M and N, but if it is, then we have a trapped state and the first assembly time is infinite. To show that the decomposition holds for $N \geqslant 4$ and for all M, we write $M = \rho(N-1) + j$ where ρ is the highest divisor between M and $N-1$, so that $1 \leqslant j \leqslant N-2$. Now, if $j \neq 1$, then the decomposition is achieved with $n_{N-1} = \rho$, $n_j = 1$, and all other $n_k = 0$ for $k \neq j, (N-1)$. We have thus constructed a possible trapped state. If instead $j = 1$, then we can rewrite $M = (\rho - 1)(N-1) + (N-2) + 2$ so that the decomposed state is at $n_{N-1} = \rho - 1$, $n_{N-2} = 1$ and $n_2 = 1$, with all other values of $n_k = 0$. This proves that

Proposition 80. *for all $M \geqslant 4$, $N \geqslant 4$, there are trapped states for $q = 0$.*

The only exception is when $N = 3$, when the last decomposition does not hold, since $N - 2 = 1$ for $N = 3$ and by definition, monomers are not allowed in trapped states. Indeed, for $N = 3$, eq. (3.33) becomes $M = 2n_j$, which is possible only for M even. Such case has been treated in paragraph 3.5.1 above.

According to our stochastic treatment, the possibility of trajectories reaching trapped states for $q = 0$ exists for any value of $M, N \geqslant 4$, giving rise to infinite first assembly times. This is not mirrored in the mean-field approach for $q = 0$, where $c_N(T) = 1$ for finite T (depending on initial conditions), always occur if M is large enough (larger than N) as can be seen in figure 2.14b. For $N = 4$, $M = 9$, indeed T can be evaluated from eq. (3.22) as $c_4(1.7527) = 1$. In the irreversible binding limit, we may thus find examples where the stochastic treatment yields infinite first assembly times due to the presence of traps, while in the mean-field, mass action case, the mean first assembly time is finite.
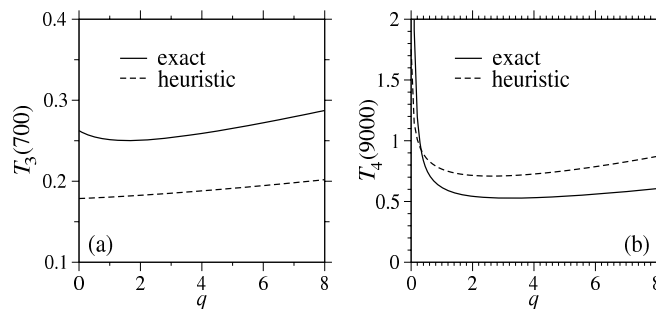
Figure 2.14: Mean first assembly times evaluated via the heuristic definition eq. (3.22) (pink line) and as a function of $q_i = q$ for $M = 7$, $N = 3$ (top) and for $M = 9$, $N = 4$ (bottom). Here $p_i = p = 1$. We also show the exact results (blue line) obtained via the stochastic formulation in eq. (3.16) which we derive in paragraph 3.2.3. Parameters are chosen as above. Qualitative and quantitative differences between the two approaches arise, which become even more evident for $N > 3$ $q \to 0$, as we shall discuss. These discrepancies underline the need for a stochastic approach.

Remark 81. *If we want to count the number of trapped states for general M, N we can do this iteratively. Certainly for $N = 3$ there is only one trapped state, at the configuration $(0, M/2, 0)$ where of course M must be even.*

In the case of $N = 4$, the traps are found by writing the number of ways one can write $M = 2a + 3b$, with a, b integers. We need to distinguish now between M odd or even. If M is even, then the only possible values of b are even ones, so that $b = 2b'$, $b' = 0, 1, 2 \ldots$ up until $b'_{max} = \lfloor M/6 \rfloor$ and $a_{max} = 0$ or $a_{max} = 1$. We thus can explicitly write

$$
\begin{aligned}
M &= 6\lfloor\frac{M}{6}\rfloor + 2a_{max} \\
M &= 6\left(\lfloor\frac{M}{6}\rfloor - 1\right) + 2(a_{max} + 3) \\
M &= 6\left(\lfloor\frac{M}{6}\rfloor - 2\right) + 2(a_{max} + 6) \\
&\cdots \\
M &= 6\left(\lfloor\frac{M}{6}\rfloor - \lfloor\frac{M}{6}\rfloor\right) + 2\left(a_{max} + 3\lfloor\frac{M}{6}\rfloor\right)
\end{aligned}
$$

These are exactly $N_T(M, 4) = \lfloor M/6 \rfloor + 1$ states. For instance, if M=18, we have

$$
\begin{aligned}
18 &= 6 \times 3 + 2 \times 0 \\
18 &= 6 \times 2 + 2 \times 3 \\
18 &= 6 \times 1 + 2 \times 6 \\
18 &= 6 \times 0 + 2 \times 9
\end{aligned}
$$

which is exactly $\lfloor 18/6 \rfloor + 1 = 4$ combinations.

In the case of M odd we note that, by necessity $b = 2b' + 1$ must be odd so that $M = 2a + 3(2b' + 1)$ and so the problem reduces to finding the values of a and b' such that $M - 3 = 2a + 6b'$. This is the same as what we just did, but replacing M with $M - 3$, which is now even, so that there are now exactly $1 + \lfloor \frac{M-3}{6} \rfloor$ states.

So, in summary we can write the number of traps $N_T(M, N)$ for $N = 4$ and general M as follows

$$
N_T(M, 4) = 1 + \lfloor\frac{M}{6}\rfloor, \text{ if } M \text{ even,}
$$
$$
N_T(M, 4) = 1 + \lfloor\frac{M-3}{6}\rfloor, \text{ if } M \text{ odd.}
$$

Now, let us try to iterate for, let's say $N = 5$. In this case, we need to write $M = 2a + 3b + 4c$. We can decide to use $c = 0$, $c = 1$, $c = 2$ up until the largest value of c which is $\lfloor\frac{M}{4}\rfloor$. For every chosen c, thus the problem reduces to arranging $M - 4c$ units into traps of order $N = 4$, that is we need to find a, b such that $M - 4c = 2a + 3b$. The only value of c we cannot accept is when $M - 4c$ is equal to one. In this case, no values of a or b will exist to satisfy the above identity. We thus need to arrest our choice of c values at the point $c = \lfloor\frac{M}{4}\rfloor - 1$ if $M - 4\lfloor\frac{M}{4}\rfloor = 1$.
In general we can thus say that

Proposition 82. *for all $M, N > 0$, the number of traps $N_T(M, N)$ satisfy the induction*

$$
\begin{aligned}
N_T(M, N+1) &= \sum_{j=0}^{\lfloor M/N \rfloor} N_T(M - jN, N), \text{ if } M \neq \lfloor\frac{M}{N}\rfloor N + 1, \\
N_T(M, N+1) &= \sum_{j=0}^{\lfloor M/N \rfloor - 1} N_T(M - jN, N), \text{ if } M = \lfloor\frac{M}{N}\rfloor N + 1.
\end{aligned}
$$

For instance, if $M = 19$, $N = 7$, the above yields

$$N_T(19, 7) = \sum_{j=0}^{2} N_T(19 - 6j, 6) = 36$$

as can be verified by direct substitution.

3.5.3 Conditional first assembly times for $q = 0$

Given the above result – namely that the presence of traps yields infinite first assembly times when $q = 0$ – it is a natural question what is the mean first assembly time *conditioned* on traps not being visited.

Definition 4 (mean *conditioned* nucleation time). *The mean conditioned nucleation time is*

$$T_N(\{m\})^* = \mathbb{E}\big[\tau_N(\{m\}) \mid \tau_N(\{m\}) < \infty\big],$$

which is well defined for any configuration $\{m\}$ that are not traps.

To this end, we explicitly enumerate all paths towards the absorbed states and average the mean first assembly times only over those that avoid such traps (we note that a similar approach was derived by Marcus [102] to compute the time-dependent probability function). To be more concrete, we first consider the case $N = 3$.

3.5.3.1 $N = 3$ Here, in order to reach the absorbing state where $n_3 = 1$, one or more dimers must have been formed. Let us thus consider the specific case $1 \leqslant n_2 \leqslant \left[\frac{M-1}{2}\right]$. Here, the last bound arises from noting that after n_2 dimers are formed, at least one free monomer must exist, so that it can attach to one of the n_2 dimers, thus creating a trimer.

Since at every iteration both the formation of a dimer or of a trimer can occur, the probability of a path that leads to a configuration of exactly n_2 dimers is given by

$$\prod_{k=0}^{n_2-1} \frac{(M - 2k)(M - 2k - 1)}{(M - 2k)(M - 2k - 1) + 2(M - 2k)k}. \tag{3.34}$$

The above quantity must be multiplied by the probability that after these n_2 dimerizations a trimer is formed, which occurs with probability

$$\frac{n_2(M - 2n_2)}{(M - 2n_2)(M - 2n_2 - 1) + 2(M - 2n_2)n_2}. \tag{3.35}$$

Upon multiplying eq. (3.34) and (3.35) and simplifying terms we find that the probability W_{n_2} for a path where n_2 dimers are created before the final trimer is assembled is given by

$$W_{n_2} = \frac{2n_2}{(M - 1)^{n_2+1}} \prod_{k=0}^{n_2-1} (M - 2k - 1). \tag{3.36}$$

Note that if M is even, we must discard paths where $2n_2 = M$, since, as described above, this case represents a trap with no monomers to allow for the creation of a trimer. According to eq. (3.36) the realization $2n_2 = M$ occurs with probability

$$W_{\frac{M}{2}} = \frac{M(M-3)!!}{(M-1)^{\frac{M}{2}}}. \tag{3.37}$$

Thus for M even, $W_{\frac{M}{2}}$ represents the probability the system will end in a trap. Hence the probability that a 3-mer is ever formed is

$$\mathbb{P}\big\{\tau_3(\{M,0,0\}) < \infty\big\} = 1 - \mathbf{1}_{\{M \text{ even}\}} \frac{M(M-3)!!}{(M-1)^{\frac{M}{2}}}.$$

We must now evaluate the time the system spends on each of the paths void of traps. Note that the exit time from a given dimer configuration $(M-2k, k, 0)$ is a random variable taken from an exponential distribution with rate parameter given by the dimerization rate, $\lambda_{d,k} = (M-2k)(M-2k-1)/2$. However, the formation of a trimer is also a possible way out of the dimer configuration, with rate $\lambda_{t,k} = (M-2k)k$. The time to exit the configuration $(M-2k, k, 0)$ is thus a random variable distributed according to the minimum of two exponentially distributed random variables which is still exponentially distributed according to the sum of the two rates

$$\lambda_k = \lambda_{d,k} + \lambda_{t,k} = \frac{(M-2k)(M-1)}{2}.$$

The typical time out of configuration $(M-2k, k, 0)$ is thus given by $\frac{1}{\lambda_k}$. Upon summing over all possible $0 \leqslant k \leqslant n_2$ values we find the mean time for the system to go through n_2 dimerizations

$$T_{n_2} = \sum_{k=0}^{n_2} \frac{1}{\lambda_k} = \sum_{k=0}^{n_2} \frac{2}{(M-2k)(M-1)}.$$

Finally, the mean first assembly time can be calculated as

Proposition 83. *For $N = 3$, The conditioned mean nucleation time is given by*

$$T_3(M, 0, 0)^* = \sum_{n_2=1}^{\left[\frac{M-1}{2}\right]} W_{n_2} T_{n_2}. \tag{3.38}$$

and

$$\mathbb{P}\big\{\tau_3(\{M,0,0\}) < \infty\big\} = 1 - \mathbf{1}_{\{M \text{ even}\}} \frac{M(M-3)!!}{(M-1)^{\frac{M}{2}}}$$

It can be verified that for M odd, eq. (3.38) is the same as eq. (3.32), since the integer part that appears in the sum in eq. (3.38) is the same as its argument, thus including all paths. For M even instead paths with $2n_2 = M$ are discarded, yielding a mean first assembly time averaged over trap-free configurations. These calculations obviously hold as well starting at a configuration $\{M-2n, n, 0\}$.

3.5.3.2 $N \geqslant 4$ Similar calculations can be carried out in the case of larger N; however, keeping track of all possible configurations before any absorbed state can be reached becomes quickly intractable (see [102]). For example, in the case $N = 4$ one would need to consider paths with a specific sequence of $n_{2,k}$ dimers formed between the creation of k and $k+1$ trimers until n_3 trimers are formed. The path would be completed by the

formation of a cluster of size $N = 4$. We would then need to consider all possible choices for $1 \leqslant n_3 \leqslant \left\lceil \frac{M-1}{3} \right\rceil$ such that traps are avoided and evaluate the typical time spent on each viable path. Because of the many branching possibilities, it is clear that the enumeration becomes more and more complicated as N increases. For the sake of completeness, we briefly describe this procedure below.

We choose to start from the initial configuration $(M, 0, 0, 0)$. Choose first n_3 such $1 \leqslant n_3 \leqslant \left\lceil \frac{M-1}{3} \right\rceil$. Then for any $k = 0...n_3$, we create $n_{2,k+1}$ dimers and a trimer (or a 4-mer at the last step $k = n_3$), where we start with an initial condition

$$(n_1, n_2, n_3, n_4) = (M_k, y_{2,k}, k, 0)$$

where $M_k = M - 2y_{2,k} - 3k$ and $y_{2,k} = \sum_{i=0}^{k} n_{2,i} - k$, $n_{2,k}$ being the number of dimers formed between step $k-1$ and k. Note that $n_{2,0} = 0$ and $M_0 = M$. For any $k = 1, \cdots, n_3$, the mean time spent in such path is given by

$$T_{n_{2,k}} = \sum_{i=1}^{n_{2,k}+1} \frac{1}{\lambda_{i,k}},$$

where for $i = 1...n_{2,k} + 1$, the parameter of the waiting exponential time is

$$\begin{aligned}
\lambda_{i,k} &= p(M_{k-1} - 2(i-1))(M_{k-1} - 2i + 1)/2 + p(M_{k-1} - 2(i-1))(y_{2,k-1} + i - 1) \\
&+ p(M_{k-1} - 2(i-1))(k-1), \\
&= p(M_{k-1} - 2(i-1))(M - k)/2.
\end{aligned}$$

The weight of such a path is, for $k = 1...n_3$

$$W_{n_{2,k}} = \frac{2(n_{2,k} + y_{2,k-1})}{(M-k)^{n_{2,k}+1}} \prod_{i=1}^{n_{2,k}} (M_{k-1} - 2i + 1).$$

while for $k = n_3 + 1$, the weight is

$$W_{n_{2,k}} = \frac{2(k-1)}{(M-k)^{n_{2,k}+1}} \prod_{i=1}^{n_{2,k}} (M_{k-1} - 2i + 1),$$

To sum up, for any number $n_3 \in \{1, ... \left\lceil \frac{M-1}{3} \right\rceil\}$ and acceptable numbers $(n_{2,k})_{1 \leqslant k \leqslant n_3+1}$ (such that $\sum_{k=1}^{n_3+1} 2n_{2,k} + n_3 < M$), the time and weight of such path are given by

$$\begin{aligned}
T_{(n_{2,k})_{1 \leqslant k \leqslant n_3+1}} &= \sum_{k=1}^{n_3+1} \sum_{i=1}^{n_{2,k}+1} \frac{1}{\lambda_{i,k}}, \\
W_{(n_{2,k})_{1 \leqslant k \leqslant n_3+1}} &= \prod_{k=1}^{n_3+1} W_{n_{2,k}},
\end{aligned}$$

and the total mean time is given by (given that a 4-mer is ever formed)

$$T_4(M, 0, 0, 0)^* = \sum_{(n_{2,k}), n_3} W_{(n_{2,k})_{1 \leqslant k \leqslant n_3+1}} T_{(n_{2,k})_{1 \leqslant k \leqslant n_3+1}},$$

where the sum ranges over admissible configuration.

3.6 Slow detachment limit ($0 < q \ll 1$)

We are going now to extend our calculation of the mean assembly time for irreversible cases above to $0 < q << 1$ by a perturbative treatment.

Although mean assembly times are infinite in an irreversible process (except when M is odd and $N = 3$), they are finite when $q > 0$. For M even and small $q > 0$, we can find the leading behavior of the mean first assembly time $T(M, 0, 0)$ perturbatively by considering the trajectories from a trapped state into an absorbing state with at least one completed cluster.

Since for $q = 0$ the mean arrival time to an absorbing state is the sum of the probabilities of each pathway, weighted by the time taken along each of them, we expect that the dominant contribution to the mean assembly time in the small q limit can be approximated by the shortest mean time to transition from a trapped state to an absorbing state. This assumption is based on the fact that the largest contribution to the mean assembly time will arise from the waiting time to exit a trap, of the order of $\sim 1/q$, since only detachment is possible from traps. The time to exit any other state instead, when both attachment and detachment are possible, will be much faster, and of order 1. For sufficiently small detachment rates q, we thus expect that the dominant contribution to the mean assembly time comes from the paths that go through traps and that $T_N(M, 0, \dots, 0) \sim 1/q$.

3.6.1 $N = 3$

Again, first consider the tractable case $N = 3$ and M even, where it is clear that the sole trapped state is $(0, M/2, 0)$ and the "nearest" absorbing state is $(1, M/2 - 2, 1)$. Since the largest contribution to the first assembly time occurs along the path out of the trap and into the absorbed state, we pose

$$T_3(M, 0, 0) \simeq P^*(0, \frac{M}{2}, 0) \, T_3(0, \frac{M}{2}, 0),$$

where $P^*(0, M/2, 0)$ is the probability of populating the trap, starting from the $(M, 0, 0)$ initial configuration for $q = 0$. This quantity can be evaluated by considering the different weights of each path leading to the trapped state. An explicit recursion formula has been derived in a previous work [47, Section 4, eq. A.23]. In the $N = 3$ case however, the paths are simple, since only dimers or trimers are formed, leading to

$$P^*(0, \frac{M}{2}, 0) = \frac{M(M-3)!!}{(M-1)^{\frac{M}{2}}}, \tag{3.39}$$

which corresponds to eq. (3.37). The first assembly time $T(0, M/2, 0)$ starting from state $(0, M/2, 0)$ can be evaluated as

$$T_3(0, \frac{M}{2}, 0) = \frac{1}{\frac{M}{2}q} + T_3(2, \frac{M}{2} - 1, 0). \tag{3.40}$$

Here, the first term is the total exit time from the trap, given by the inverse of the detachment rate q multiplied by the number of dimers. The second term is the first assembly time of the nearest and sole state accessible to the trap. This quantity can be evaluated, to leading order in $1/q$, as

$$T_3(2, \frac{M}{2} - 1, 0) \simeq \frac{1}{2(\frac{M}{2} - 1) + 1} T_3(0, \frac{M}{2}, 0), \tag{3.41}$$

where we consider that the trap will be revisited upon exiting the state $(2, M/2-1, 0)$ with probability $1/(2(\frac{M}{2} - 1) + 1)$. Other terms to be included in eq. (3.41) would have been the total time to leave state $(2, M/2 - 1, 0)$ and the possibility of reaching the absorbing state. The contribution of the first term however would be of lower order than $1/q$, since attachment events are of order $\mathcal{O}(1) \ll \mathcal{O}(1/q)$; the contribution of the second term is zero. Upon combining eq. (3.40) and (3.41) we find

$$T_3(0, \frac{M}{2}, 0) \simeq \frac{2(M - 1)}{M(M - 2)} \frac{1}{q}.$$

Finally, $T_3(M, 0, 0)$ can be derived by multiplying the above result by eq. (3.39). We can generalize this procedure to find

Proposition 84. *the dominant term for the mean assembly time starting from any initial state $(M - 2n, n, 0)$ in the limit $q \to 0$, $N = 3$ and for M even is given by*

$$
\begin{aligned}
T_3(M, 0, 0) = T_3(M - 2, 1, 0) &\simeq \frac{2(M - 3)!!}{(M - 2)(M - 1)^{M/2-1}} \frac{1}{q}, \\
T_3(M - 2n, n, 0) &\simeq \frac{2(M - 2n - 1)!!}{(M - 2)(M - 1)^{M/2-n}} \frac{1}{q}, \quad 2 \leqslant n < M/2, \\
T_3(0, M/2, 0) &\simeq \frac{2(M - 1)}{M(M - 2)} \frac{1}{q}.
\end{aligned}
$$

The next order terms do not have an obvious closed-form expression, but are independent of q. Note that when q is small and increasing, the mean first assembly times *decrease*. This is true for M odd cases as well. An increasing q describes a more rapid dissociation process, which may lead one to expect a *longer* assembly time. However due to the multiple pathways to cluster completion in our problem, increasing q actually allows for more mixing among them, so that at times, upon detachment, one can "return" to more favorable paths, where the first assembly time is actually shorter. This effect is clearly understood by considering the case of $q = 0$ when, due to the presence of traps, the first assembly time is infinite. We have already shown that upon raising the detachment rate q to a non-zero value, the first assembly time becomes finite. Here, detachment allows for visiting paths that lead to adsorbed states, which would otherwise not be accessible. This same phenomenon persists for small enough q and for all M, N values. The expectation of assembly times increasing with q is confirmed for large q values, as we shall see in the next section. Taken together, these trends indicate the presence of an optimal q^* value where the mean assembly time attains an optimal, minimum value.

3.6.2 $N \geqslant 4$

We can generalize our estimation of the leading term in $1/q$ for the first assembly time and for larger values of N via

$$T_N(M, 0, \dots, 0) = \sum_{\{\mu\}} P^*(\{\mu\}) T_N(\{\mu\}), \tag{3.42}$$

where μ labels all trapped states. The values of P_μ^* can be calculated as described above using the recursion formula presented in [47]. The mean first assembly times $T_N(\{\mu\})$ instead may be evaluated by considering only the shortest sub-paths that link traps to each other. For instance, in the case of $M = 9$, $N = 4$ the only trapped states are $(0, 3, 1, 0)$ and $(0, 0, 3, 0)$, corresponding to $P^*(0, 0, 3, 0) = 921/5488$ and $P^*(0, 3, 1, 0) = 2873/24696$. The

shortest path linking the two traps is $(0,3,1,0) \to (2,2,1,0) \to (1,1,2,0) \to (0,0,3,0)$, which yields, to first order, $T(0,1,3,0) = T(0,0,3,0) = 1/(2q)$. Finally, from eq. (3.42) we find that $T(9,0,0,0) = 2005/(14112q)$ which can be verified upon constructing the corresponding transition matrix $\mathbf{A}^\dagger$ of dimension $D(9,4) = 12$. The task at hand however becomes increasingly complex as M and N increase since more traps arise, leading to the identification of more entangled sub-paths connecting them.

Remark 85. *We conjecture the leading term to be of order $1/q$. This comes from the fact that leaving a trapped states requires a single step of parameter q. By definition, two trapped states cannot be directly connect to each other, preventing the possibility of having a higher power of q, and so, independently of M, N. We will see that this will be confirm by a different approach in subsection 3.9 and by numerical simulation in subsection 3.10.*

3.7   Fast detachement limit ($q \to \infty$) - Cycle approximation

We turn now to approximation of assembly times in the limit of large detachment rate q. We expect here the mean assembly time to increase monotonically with q. We consider here a similar approach to the previous subsection 3.6 and try to identify the leading path that contribute to the first assembly time. In the limit $q \to \infty$, we expect trajectories involving small numbers of monomers to be rarely sampled so that the full assembly of a cluster is a rare event. Looking at the general form of the invariant distribution eq. (3.7), we see that the most probable states, *in the stationary regimes*, are those for which $\sum_{i=1}^{N} n_i$ is maximal. This tells us that the most likely states, in the stationary regime, is, without surprise, $(M, 0, \cdots, 0)$. The next likely one is $(M-2, 1, 0, \cdots, 0)$. We assume the leading path that contributes to the first assembly time is the path that contain the most likely states. Let us first consider the case of $N = 3$, as usual.

3.7.1 $N = 3$

For $N = 3$, the overwhelmingly dominant path (leading to a maximal cluster size) is then:
$$(M,0,0) \rightleftharpoons (M-2,1,0) \rightleftharpoons (M-3,0,1)$$
These states yield a reduced 2×2 transition matrix $\mathbf{A}^\dagger$ that can be easily inverted to yield (see definition 5 below)

$$
\begin{aligned}
T_3^c(M,0,0) &= \frac{2q}{M(M-1)(M-2)}, \\
T_3^c(M-2,1,0) &= \frac{2q}{M(M-1)(M-2)},
\end{aligned}
$$

where the equality refers to the reduced configuration space, valid only for $q \gg pM$.

3.7.2 $N \geqslant 4$

This dominant direct path can be generalized to any N for $q \gg M$ as follows

$$(M,0,0,...,0) \;\; \rightleftharpoons \;\; (M-2,1,0...,0) \;\; \rightleftharpoons \;\; \cdots \;\; \rightleftharpoons \;\; (M-N,0,...0,1). \tag{3.43}$$

The state space of such system, called the cycle system, is now

$$S_{M,N}^c = \{(n_i)_{1 \leqslant i \leqslant N} \in S_{M,N} \text{ such that there is at most one } i \geqslant 2, n_i = 1\}$$

We extend the definition of nucleation time and mean nucleation time for the path given by eq. (3.43).

Definition 5. *Let $M, N > 0$, and $(C_i(\cdot))_{1 \leqslant i \leqslant N}$ the solution given by the chemical reaction steps eq. (3.43). The cycle stochastic nucleation time, starting at configuration $\{m\} \in S_{M,N}^c$ is*

$$\tau_N^c(\{m\}) = \inf\{t \geqslant 0; C_N(t) = 1 \mid C_i(0) = \delta_{m_i}, 1 \leqslant i \leqslant N\}.$$

The mean nucleation time is

$$T_N^c(\{m\}) = \mathbb{E}\big[\tau_N^c(\{m\})\big].$$

For $N > 3$, the corresponding matrix $\mathbf{A}^\dagger$ is of dimension $(N - 1)$ and tridiagonal. Its $a_{i,j}^\dagger$ elements are given as $r_{1,1}^\dagger = -r_{1,2}^\dagger = -M(M-1)/2$, and for $2 \leqslant k \leqslant (N-1)$

$$\begin{aligned}
a_{k,k-1}^\dagger &= q, \\
a_{k,k}^\dagger &= -q - (M - k), \\
a_{k,k+1}^\dagger &= (M - k).
\end{aligned}$$

The inverse of $\mathbf{A}^\dagger$ can be computed by a three-terms induction formula [135]. While we could consider all initial configurations $\{m\}$, we focus only on the case $\{m\} = (M, 0, \ldots, 0)$, in order to simplify the notation. Results for other choices of $\{m\}$ can be obtained by following the same reasoning here illustrated. After some algebraic manipulations on the recurrence formula [135], we have

Proposition 86. *For any $M \geqslant N$, the mean cycle nucleation time is given by*

$$T_N^c(M, 0, \ldots, 0) = \frac{2}{\prod_{i=0}^{N-1}(M-i)}\left[\sum_{k=0}^{N-2}\prod_{l=1}^{k}(M-(N-l))q^{N-2-k}\right. \tag{3.44}$$

$$\left. + \frac{M(M-1)}{2}\sum_{j=2}^{N-2}\prod_{l=2}^{j-1}(M-l)\sum_{k=0}^{N-j-1}\prod_{l=1}^{k}(M-(N-l))q^{N-j-1-k}\right],$$

Hence we expect the expression $T_N^c(M, 0, \ldots, 0)$ to be an approximation of $T_N(M, 0, \ldots, 0)$ for $q \gg M$. We will see in subsection 3.10 with numerical simulation that this is indeed the case. The highest term in q the above is given by

$$T_N^c(M, 0, \ldots, 0) \approx \frac{2q^{N-2}}{\prod_{i=0}^{N-1}(M-i)}. \tag{3.45}$$

For $M \gg N$ on the other hand, one can approximate $M - i \approx M$ so that eq. (3.44) becomes

$$T_N^c(M, 0, \ldots, 0) \approx \frac{q^{N-1}}{M^N}\left[\sum_{k=2}^{N-1}\frac{kM^k}{q^k} + \frac{2}{q}\sum_{k=0}^{N-2}\frac{M^k}{q^k}\right].$$

Finally, using the symmetry properties of the associated matrix $\mathbf{A}^\dagger$ we can find the Laplace transform of the first assembly time distribution $\tilde{G}^c((M, 0, \ldots, 0); s)$ [33] in the limit $q \gg M$

$$\tilde{G}^c((M, 0, \ldots, 0); s) = \frac{\frac{1}{2}\prod_{i=0}^{N-1}(M-i)}{d_{N-1}(s)}, \tag{3.46}$$

where $d_{N-1}(s)$ is a unitary polynomial of degree $N - 1$, given by the following recurrence

$$
\begin{aligned}
d_1 &= s + \frac{M(M-1)}{2}, \\
d_2 &= (s + (M-2) + q)d_1 - q\frac{M(M-1)}{2}, \\
d_i &= (s + (M-i) + q)d_{i-1} - q(M - (i-1))d_{i-2}, \quad \text{for } i > 2
\end{aligned}
\tag{3.47}
$$

Thus $d_{N-1}(s) = s^{N-1} + \ldots + \beta s^2 + \alpha s + \frac{1}{2}\prod_{i=0}^{N-1}(M-i)$. Note that the first assembly time is given by

$$
T_N(M, 0, \ldots, 0) = \lim_{s \to 0} \frac{1 - \tilde{G}((M, 0, \ldots, 0); s)}{s}.
$$

By comparing eq. (3.46) with eq. (3.44) we note that the term α in the above expansion for $d_{N-1}(s)$, corresponds to the quantity in the square brackets in eq. (3.44) so that

$$
T_N^c(M, 0, \ldots, 0) = \frac{2\alpha}{\prod_{i=0}^{N-1}(M-i)}.
$$

One can also calculate the variance of the first assembly time distribution to obtain

$$
\mathrm{var}_N^c(M, 0, \ldots, 0) = \frac{\alpha^2}{\prod_{i=0}^{N-1}(M-i)^2} - \frac{2\beta}{\prod_{i=0}^{N-1}(M-i)},
$$

and similarly all other moments of the distribution. Finally, we can also estimate the first assembly time distribution $G^c((M, 0 \ldots, 0), t)$ by considering the Inverse Laplace transform of eq. (3.46), specifically by evaluating the dominant poles associated to $d_{N-1}(s)$. In the large q limit, $d_{N-1}(s)$ as evaluated via the recursion relations eq. (3.47) can be approximated as

$$
d_{N-1}(s) \approx q^{N-2}s + \frac{1}{2}\prod_{i=0}^{N-1}(M-i),
$$

yielding the slowest decaying root λ_N

$$
\lambda_N = -\frac{1}{2q^{N-2}}\prod_{i=0}^{N-1}(M-i).
\tag{3.48}
$$

Then

Proposition 87. *As $q \to \infty$, the cycle nucleation time $\tau_N^c(\{m\})$ converge to an exponential random variable of parameter $-\lambda_N$ defined in eq. (3.48),*

$$
G^c((M, 0, \ldots, 0); t) \approx \frac{1}{2}\prod_{i=0}^{N-1}(M-i)e^{\lambda_N t}.
$$

Remark 88. *Note that with the recurrence formula for the d_i, eq. (3.47), we can show that all roots of d_i are simple, real and that, if $\mu_1, ..., \mu_i$ and $\lambda_1, ..., \lambda_{i-1}$ are respectively the roots of d_i and d_{i-1}, the following holds (see [126][p.119])*

$$\mu_1 < \lambda_1 < \mu_2 < \cdots < \lambda_{i-1} < \mu_i$$

Because G is a distribution one must get additionally $\mu_i < 0$. Moreover, d_{N-1} has the asymptotic representation

$$d_{N-1} \quad \approx \quad [(q^{N-2} + 0(q^{N-3}))s + \frac{1}{2}\prod_{i=0}^{N-1}(M-i)][1 + \sum_{j=0}^{N-1}0(\frac{1}{q})s^{i-j-1}]$$

the last relation shows that the highest root of d_{N-1} has the asymptotic, as $q \to \infty$,

$$\lambda_N = -\frac{1}{2q^{N-2}}\prod_{i=0}^{N-1}(M-i)$$

and that all other roots diverge to $-\infty$ as $q \to \infty$. So we conclude that there is one leading exponential, so that G is asymptotically an exponential distribution of parameter $-\lambda_N$.

3.8   Fast detachment limit ($q \to \infty$) - Queueing approximations

In this section we consider a different approach to the fast detachment, $q \to \infty$ limit by using the well-known "pre-equilibrium" or "quasi steady-state" approximation (which has been used in the deterministic context in [120], see also [62]) essentially a separation of time scales between fast and slow varying quantities. We will use the pre-equilibrium approximation on the stochastic formulation of eq. (3.6), however, to illustrate the method, we will first apply it to the Becker-Döring system in eq. (3.21). To illustrate the qualitative differences between a system that satisfies the pre-equilibrium assumption and one that doesn't, we refer to figure 2.15.

3.8.1   Deterministic Pre-equilibrium

To understand the time scale of each reaction, we recall the stationary flux values calculated in eq. (3.5), for $1 \leqslant i \leqslant N-1$,

$$J_i^{\pm}(t) \approx \frac{p^i}{2q^{i-1}}(c_1^{\text{eq}})^{i+1},$$

Note that as $q \to \infty$ all fluxes decrease and that $J_i^{\pm}(t)$ is one order of magnitude larger in q than $J_{i-1}^{\pm}(t)$: this is the condition for the quasi-steady state approximation to hold.

3.8.1.1   Complete pre-equilibrium   We may thus consider the first $N-1$ reactions to be at equilibrium so that eq. (3.21) can be rewritten as a function of the mass contained in all clusters except the largest one. For this, let us define

$$x(t) = \sum_{i=1}^{N-1} ic_i(t),$$

that is the mass of species $(c_1, \cdots, c_{N-1})$. By the mass conservation property,

$$x(t) = M - Nc_N(t),$$
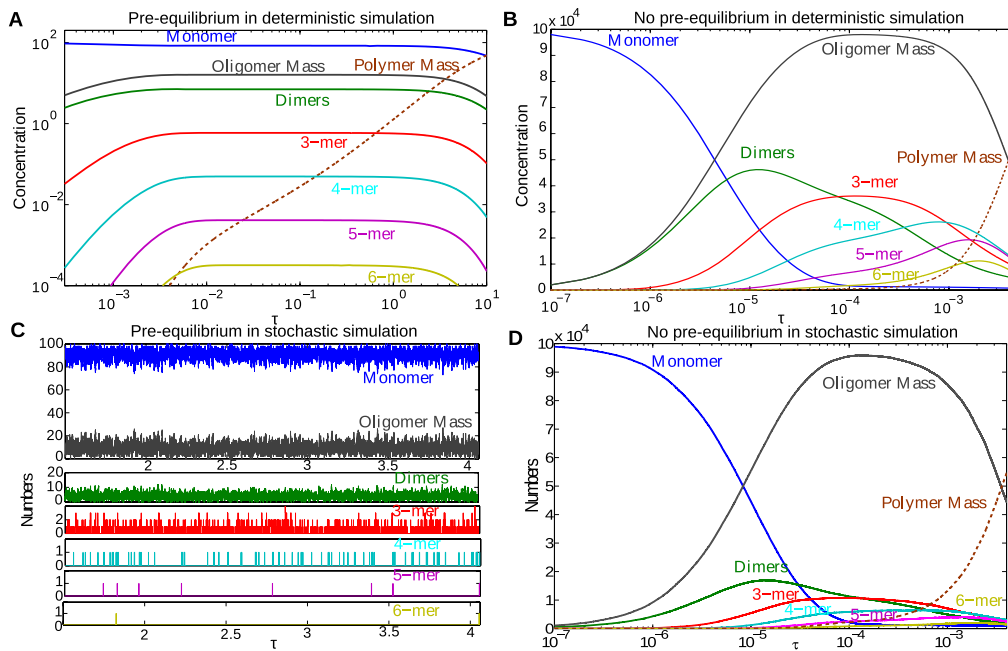
Figure 2.15: **Pre-equilibrium hypothesis in deterministic and stochastic model**.
A Pre-equilibrium in deterministic simulations. $M = 100$, $\sigma = 1000$, $N = 7$. Each
oligomer species quickly reaches a threshold, and then stays in equilibrium with the con-
centration of monomers during the nucleation process. Axis are in log scale. **B** No pre-
equilibrium in deterministic simulations. $M = 10^5$, $\sigma = 1000$, $N = 7$. The dynamic
is much more rapid, there is a large excess of production of oligomers, and the nucle-
ation starts before each oligomer concentration reach their maximal values. Oligomers
and monomers are not in equilibrium during nucleation. **C** Pre-equilibrium in stochastic
simulations. $M = 100$, $\sigma = 1000$, $N = 7$. The number of oligomers fluctuates widely, al-
though it quickly reaches its mean value. **D** No pre-equilibrium in stochastic simulations.
$M = 10^5$, $\sigma = 1000$, $N = 7$. With a large initial number of monomers, the time evolution
of each species becomes regular. Nucleation starts before each oligomer numbers reach
their maximal values.

where M is the total initial mass ($c_1(0) = M$). It comes from the system of differential equations eq. (3.21) (remember that we consider the last reaction to be irreversible, to allow a direct comparison with the stochastic definition)

$$\begin{cases} \dot{x}(t) & = & -pNc_1c_{N-1}, \\ \dot{c}_N(t) & = & pc_1c_{N-1}. \end{cases}$$

The system composed of $(c_1, \cdots, c_{N-1})$, as an isolated Becker-Döring system (of maximal size $N-1$), has a unique and asymptotically stable equilibrium value (see subsection 3.2.1), that depends smoothly on the total mass x. Indeed, we saw that all concentrations of oligomer and monomer concentration can be expressed as a function of the total mass x (eq. (3.3) - (3.4)). Assuming that the subsystem reaches instantaneously its equilibrium, the previous system becomes

$$\begin{cases} \dot{x}(t) & = & -N\frac{p}{2}\left(\frac{p}{q}\right)^{N-2}(c_1(x))^N, \\ \dot{c}_N(t) & = & \frac{p}{2}\left(\frac{p}{q}\right)^{N-2}(c_1(x))^N, \end{cases} \tag{3.49}$$

where $c_1(x)$ is the solution of

$$c_1 + \frac{1}{2}\sum_{i=2}^{N-1} i\left(\frac{p}{q}\right)^{i-1}(c_1)^i = x. \tag{3.50}$$

By analogy to definition 2, we have the

Definition 6. *Let* $(x(t), c_N(t))$ *the solution of eq. (3.49). Then we define*

$$T_N^{det,q}(\{c\}) = \inf\{t \geqslant 0, c_N(t) = 1 \mid c_i(0) = c_i, 1 \leqslant i \leqslant N\}.$$

Upon solving eq. (3.50) we can obtain $c_1(x)$, which can then be used in eq. (3.49) to determine $c_N(t)$. A crude approximation for $q \to \infty$ is $c_1(x) = x$, however, a more accurate result can be found by allowing the sum in eq. (3.50) to go to infinity so that

$$\sum_{i=1}^{N-1} i\left(\frac{p}{q}\right)^{i-1}(c_1)^i \approx \sum_{i=1}^{\infty} i\left(\frac{p}{q}\right)^{i-1}(c_1)^i$$

$$\approx \frac{c_1\sigma^2}{(c_1 - \sigma)^2},$$

where $\sigma = \frac{q}{p}$. Thus, we have

$$\frac{c_1}{2}\left(1 + \frac{c_1\sigma^2}{(c_1 - \sigma)^2}\right) = x.$$

For large σ, we can approximate this last equation by

$$c_1\left(1 + \frac{c_1}{\sigma}\right) = x.$$

The relevant root is given by

$$c_1 = \frac{-\sigma + \sqrt{4\sigma x + \sigma^2}}{2}, \tag{3.51}$$

which, as can be verified easily, goes to x as $q \to \infty$.

For practical use and to find a tractable approximation of the first assembly time, we solve eq. (3.49) with $c_1(x) = x$, which gives

$$x(t) = \frac{M}{\sqrt[N-1]{1 + N\frac{p}{2}\left(\frac{p}{q}\right)^{N-2}M^{N-1}t}}$$

and by conservation of mass $Nc_N(t) = M - x(t)$. The time for which $c_N(t) = 1$ is then found to be

$$T_N^{det,q} \approx \frac{2}{pN}\frac{\sigma^{N-2}}{(M-N)^{N-1}}$$

While taking $c_1(x) \equiv M$ as a constant function, a direct integration gives

$$T_N^{det,q} \approx \frac{2}{p}\frac{\sigma^{N-2}}{M^N}$$

Both expression are found to be substantially improved by replacing M by c_1 given by eq. (3.51) (see [120]).

3.8.1.2 Pre-equilibrium between $r < N$ oligomer species

We can also consider that only the r first species $c_1, c_2, ... c_r$ quickly equilibrates between each other, because the reaction flux between these first r species are of higher magnitude than the reaction flux between the $N - r$ other species. We can separate the time scale of the first r species from the remaining ones. For this, we define the quantity

$$x(t) = \sum_{i=1}^{r} ic_i(t),$$

and the system of differential equations eq. (3.21) reduce to

$$\begin{cases} \dot{x} &= -p(r+1)c_1(x)c_r(x) - pc_1\left(\sum_{k=r+1}^{N-1} c_k\right) + q(r+1)c_{r+1} + \left(\sum_{k=r+2}^{N-1} c_k\right), \\ \dot{c}_i &= pc_1(x)(c_{i-1} - c_i) - q(c_i - c_{i+1}), \quad r+1 \leqslant i \leqslant N-2, \\ \dot{c}_{N-1} &= -pc_1(x)c_{N-1} + pc_1(x)c_{N-2} - qc_{N-1}, \\ \dot{c}_N &= pc_1(x)c_{N-1}, \end{cases} \tag{3.52}$$

where c_1 is a function of x determined by the relevant roots of

$$c_1 + \frac{1}{2}\sum_{i=2}^{r} i\left(\frac{p}{q}\right)^{i-1}(c_1)^i = x, \tag{3.53}$$

and

$$c_r = \frac{1}{2}\left(\frac{p}{q}\right)^{r-1}(c_1)^r.$$

To get a rough, nevertheless tractable approximation with this approach, we consider that

Hypothesis 11. $c_1(x)$ *is a constant over time,*

given by the solution of eq. (3.53) at $t = 0$. The system of eq. (3.52) above is a linear system, namely

$$\dot{Y} = AY + B$$

with

$$A = \begin{pmatrix} -q-pc_1 & q & & & \\ pc_1 & -q-pc_1 & q & & \\ & \ddots & \ddots & \ddots & \\ & & pc_1 & -q-pc_1 & 0 \\ & & & 0 & pc_1 & 0 \end{pmatrix}, \quad B = \begin{pmatrix} pc_1c_r \\ 0 \\ \vdots \\ 0 \\ 0 \end{pmatrix}.$$

As in subsection 3.4, this system can be solved to find $c_N(t)$, and then the nucleation time.

3.8.2 Stochastic Pre-equilibrium

A separation of time scales can also be performed in stochastic systems, where the basic assumptions for pre-equilibration are the same as for the deterministic case. In particular, we require the "fast" subsystem to be ergodic and to possess a unique equilibrium distribution. The dynamic of the "slow" subsystem is obtained by averaging the fast variables over their equilibrium distribution; the basic assumption is that while slow variables evolve, the fast ones equilibrate instantaneously to their average values [80].

Equivalently, due to the equilibrium hypothesis, integrating eq. (3.12) over the variables that constitute the fast subsystem, will lead to the vanishing of all terms that do not modify the slow variable, and all remaining terms will involve averages of the fast variable [68].

3.8.2.1 Complete Pre-equilibrium We thus take the same approach as in the deterministic system, by allowing the first $N-1$ cluster sizes to equilibrate among each other. We define for this the quantity

$$X(t) = \sum_{i=1}^{N-1} iC_i(t) = M - NC_N(t),$$

which is the total mass contained in the cluster of size less than $N-1$. It then comes from the system of stochastic differential equations (3.6)

$$\begin{cases} X(t) & = & X(0) - NY_{2N-3}\Big(\int_0^t pC_1(s)C_{N-1}ds\Big) + NY_{2N-2}\Big(\int_0^t qC_N(s)ds\Big), \\ C_N(t) & = & C_N(0) + Y_{2N-3}\Big(\int_0^t pC_1(s)C_{N-1}ds\Big) - Y_{2N-2}\Big(\int_0^t qC_N(s)ds\Big), \end{cases}$$

and the pre-equilibrium assumption lead to the asymptotic system

$$\begin{cases} X(t) & = & X(0) - NY_{2N-3}\Big(\int_0^t p\langle C_1C_{N-1}\rangle_\infty(X(s))ds\Big) + NY_{2N-2}\Big(\int_0^t qC_N(s)ds\Big), \\ C_N(t) & = & C_N(0) + Y_{2N-3}\Big(\int_0^t p\langle C_1C_{N-1}\rangle_\infty(X(s))ds\Big) - Y_{2N-2}\Big(\int_0^t qC_N(s)ds\Big), \end{cases}$$
$$(3.54)$$

where $\langle C_1C_{N-1}\rangle_\infty(X)$ denotes the asymptotic moment value of C_1C_{N-1}, given that the mass of the subsystem is X.

Remark 89. *A direct integration of eq. (3.12) over all configurations with n_N fixed, yields*

$$\dot{P}(n_N; t|\{m\}, 0) = -\big(p\langle n_1n_{N-1}\rangle(M - Nn_N) + qn_N\big)P(n_N; t|\{m\}, 0)$$

$$+ p\langle n_1n_{N-1}\rangle(M - N(n_N - 1))P(n_N - 1; t|\{m\}, 0)$$

$$+ q(n_N + 1)P(n_N + 1; t|\{m\}, 0),$$

where

$$P(n_N; t|\{m\}, 0) = \int P(\{n\}; t|\{m\}, 0) dn_1 \cdots dn_{N-1},$$

and the pre-equilibrium hypothesis reads

$$P(\{n\}; t|\{m\}, 0) = P(\{n\}; t \to \infty|n_N) P(n_N; t|\{m\}, 0),$$

$$\langle n_1 n_{N-1}\rangle (M - Nn_N) = \int n_1 n_{N-1} P(\{n\}; t \to \infty|n_N) dn_1 \cdots dn_{N-1}.$$

We extend similarly the definition of the stochastic nucleation time for the solution of eq. (3.54).

Definition 7 (Stochastic nucleation time). *Let $M, N > 0$, and $(X(\cdot), C_N(\cdot))$ the solution of eq. (3.54). The queueing stochastic nucleation time is*

$$\tau_N^q = \inf\{t \geqslant 0; C_N(t) = 1 \mid X(0) = M, C_N(0) = 0\}.$$

The mean queueing nucleation time is

$$T_N^q = \mathbb{E}[\tau_N^q].$$

Note that the calculus of the queueing stochastic nucleation time does not require more approximation at this point, as the nucleation time is defined as the first instant the Poisson process Y_{2n-3} fires. And it is clear that $X(s) = X(0) = M$ before that point. Then the survival time is,

$$S_N^q(t) = \mathbb{P}\{\tau_N^q > t\} = \exp\left(-\int_0^t p < C_1 C_{n-1} >_\infty (M)\right),$$

and, we have the

Proposition 90. *For any $M, N > 0$, the queueing nucleation time τ_N^q is an exponential random variable of parameter $p < C_1 C_{N-1} >_\infty (M)$,*

$$G((M, 0, \ldots, 0); t) \approx p < C_1 C_{N-1} >_\infty (M) e^{-p<C_1 C_{N-1}>_\infty(M)t}.$$

The remaining difficulty lays in determining the quantity $\langle n_1 n_{N-1}\rangle(M)$, a second moment value, at equilibrium, of a stochastic Becker-Döring system of maximal size $N - 1$, and total mass M. We may resort to a (very) crude approximation, by using a mean field assumption and Becker-Döring results as follows

$$\langle C_1 C_{N-1}\rangle \approx \langle C_1 \rangle \langle C_{N-1}\rangle$$
$$\approx \frac{1}{2}\left(\frac{p}{q}\right)^{N-2}\langle C_1\rangle^N$$
$$\approx \frac{1}{2}\left(\frac{p}{q}\right)^{N-2}(c_1^*)^N$$

Other approximation involve moment closure approximation ([27]), or one require the use of numerical simulation to calculate such moment.

3.8.2.2   Pre-equilibrium between $r < N - 1$ oligomer species   Upon performing numerical simulations (see next subsection 3.10), it is clear that first assembly time distributions may not necessarily be exponentially distributed, even in the case of large q. We thus perform a less drastic approximation by allowing only the first r species, $1 \leqslant r < N$, to equilibrate instantaneously. Define for this $X(t) = \sum_{i=1}^{r} iC_i(t)$, with the pre-equilibrium assumption, the system of stochastic differential equations (3.6) reduces to

$$
\left\{
\begin{aligned}
X(t) \quad &= \quad X_1(0) - (r+1)Y_{2r-1}\Big(\int_0^t p\langle C_1 C_r \rangle_\infty X_s)ds \Big) \\
&\quad - \sum_{i=r+1}^{N-1} Y_{2i-1}\Big(\int_0^t p\langle C_1 \rangle_\infty (X_s)C_i(s)ds \Big) \\
&\quad + (r+1)Y_{2r}\Big(\int_0^t qC_{r+1}(s)ds \Big) \\
&\quad + \sum_{i=r+2}^{N} Y_{2i-2}\Big(\int_0^t qC_i(s)ds \Big), \\
C_{r+1}(t) \quad &= \quad C_{r+1}(0) + Y_{2r-1}\Big(\int_0^t p\langle C_1 C_r \rangle_\infty (X_s)ds \Big) \\
&\quad - Y_{2r+1}\Big(\int_0^t p\langle C_1 \rangle_\infty (X_s)C_{r+1}(s)ds \Big) \\
&\quad - Y_{2r}\Big(\int_0^t qC_{r+1}(s)ds \Big) + Y_{2r+2}\Big(\int_0^t qC_{r+2}(s)ds \Big), \\
C_i(t) \quad &= \quad C_i(0) + Y_{2i-3}\Big(\int_0^t p\langle C_1 \rangle_\infty (X_s)C_{i-1}ds \Big) - Y_{2i-1}\Big(\int_0^t p\langle C_1 \rangle_\infty (X_s)C_i(s)ds \Big) \\
&\quad - Y_{2i-2}\Big(\int_0^t qC_i(s)ds \Big) + Y_{2i}\Big(\int_0^t qC_{i+1}(s)ds \Big), \quad r+2 \leqslant i \leqslant N-1, \\
C_N(t) \quad &= \quad C_N(0) + Y_{2N-3}\Big(\int_0^t p\langle C_1 \rangle_\infty (X_s)C_{N-1}ds \Big) - Y_{2N-2}\Big(\int_0^t qC_N(s)ds \Big).
\end{aligned}
\right.
$$

Now if we assume

Hypothesis 12. $X(t) \equiv M$ *to be constant over time,*

the nucleation problem can be treated as a first order reaction network, with the transition rate being:

$$
\xrightarrow[q]{p\langle C_1 C_r \rangle_\infty(M)} \quad C_{r+1} \quad \xrightarrow[q]{p\langle C_1 \rangle_\infty(M)} \quad C_{r+2} \quad \cdots \quad \xrightarrow{p\langle C_1 \rangle_\infty(M)} \quad C_N \tag{3.55}
$$
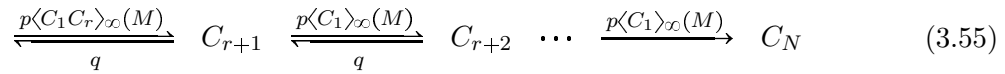
Indeed, if X is constant over time, all reactions are first-order reaction. We define

Definition 8 (Stochastic nucleation time). *Let $M, N > 0$, $1 \leqslant r \leqslant N-1$, and $(C_i(\cdot))_{r+1 \leqslant i \leqslant N}$ the solution of the first-order reaction network eq. (3.55). The r-queueing stochastic nucleation time is*

$$
\tau_N^{q,r} = \inf\{t \geqslant 0; C_N(t) = 1 \mid C_i(0) = 0, \, r+1 \leqslant i \leqslant N\}.
$$

The mean r-queueing nucleation time is

$$
T_N^{q,r} = \mathbb{E}\big[\tau_N^{q,r}\big].
$$

Again, as in subsection 3.4, we can solve this system to get

Proposition 91. *For any $M, N > 0$, $1 \leqslant r \leqslant N - 1$, the survival time $S_N^{q,r}(t) = \mathbb{P}\{\tau_N^{q,r} > t\}$ is given by*

$$S_N^{q,r}(t) = \exp\left[- p^2 \langle C_1 \rangle_\infty(M) \langle C_1 C_r \rangle_\infty(M) \sum_{k=1}^{N-1-r} \beta_k V_{N-1-r}^{(k)} \left(\frac{-t}{\lambda_k} + \frac{e^{\lambda_k t} - 1}{\lambda_k^2} \right) \right] \quad (3.56)$$

where $\lambda_k = -(p\langle C_1 \rangle_\infty(M) + q) + 2\sqrt{p\langle C_1 \rangle_\infty(M)q} \cos(\frac{k\pi}{N-r})$ are the eigenvalues of the $N - 1 - r$-upper block of A, $V^{(k)}$ the associated eigenvector ([146]) ($V_{N-1-r}^{(k)}$ denotes its last components), and β_k are constant given by the initial condition.

3.8.3 Example

We illustrate the result of this section with the case $N = 3$. Note that the above formula eq. (3.56) is valid for any M, N. There is analytical formulas for eigenvalues and eigenvectors, so that the formula can be used in practice if we determine the asymptotic moment values. For this last point, however, there's no other choice than performing a moment closure approximation or numerical simulation. We will consider the numerical results in the next section

3.8.3.1 N=3, r=2 Deterministic The complete pre-equilibrium assumption ($r = 2$) reads in the deterministic context

$$\dot{x}(t) = -3\frac{p}{2}\left(\frac{p}{q}\right)c_1(x)^3,$$
$$\dot{c}_3(t) = \frac{p}{2}\left(\frac{p}{q}\right)c_1(x)^3,$$

with $x(t) = c_1(t) + 2c_2(t)$, and the pre-equilibrium quantity $c_1(x)$ satisfies $c_1 + \frac{c_1^2}{\sigma} = x$ and is given by

$$c_1(x) = \frac{-\sigma + \sqrt{4\sigma x + \sigma^2}}{2}.$$

The above system can not be exactly solved. Taking $c_1(x) = x$, we get

$$c_3(t) = \frac{M}{3}\left(1 - \frac{1}{\sqrt{1 + 3M^2 p^2 t/q}}\right),$$

so that

$$T_3^{det,q} \approx \frac{2}{3p}\frac{\sigma}{(M-3)^2}.$$

Taking $c_1(x) \equiv M$,

$$c_3(t) = \frac{p}{2}\left(\frac{p}{q}\right)M^3 t,$$

and

$$T_3^{det,q} \approx \frac{2}{p}\frac{\sigma}{M^3}.$$

Stochastic In the stochastic context, we have

$$X(t) = M - 2Y_3\left(\int_0^t p < C_1 C_2 >_\infty (X(s))ds\right) + 3Y_4\left(\int_0^t qC_3(s)ds\right), \quad (3.57)$$

$$C_3(t) = Y_3\left(\int_0^t p < C_1 C_2 >_\infty (X(s))ds\right) - Y_4\left(\int_0^t qC_3(s)ds\right), \quad (3.58)$$

and the nucleation time (first time for which $C_3(t) = 1$) is an exponential random variable of parameter $p < C_1 C_2 >_\infty (M)$. This last quantity can not be evaluated exactly, We have, by the mass conservation property, $< C_1 C_2 >_\infty (M) = M < C_2 >_\infty -2 < C_2^2 >_\infty$. The mean value $< C_2 >_\infty$ can be approximate by the deterministic value, and the second moment using a Gaussian truncation (see [27]). We then obtain

$$
\begin{aligned}
< C2 > &= \frac{1}{4}\Big((2M + q/p) - \sqrt{(2M + q/p)^2 - 4M^2}\Big), \\
< C_1 C_2 > &= M < C_2 > - \frac{q < C_2 >}{-4p < C_2 > + p(2M + 3) + q} - < C_2 >^2 .
\end{aligned}
$$

3.8.3.2   N=3, r=1   This case consists in taking c_1 (or C_1) as constant over time.
Deterministic   We obtain

$$
\begin{aligned}
\dot{c}_2(t) &= pM^2 - (q + pM)c_2, \\
\dot{c}_3(t) &= pMc_2.
\end{aligned}
$$

The solution is given by

$$
\begin{aligned}
c_2(t) &= \frac{pM^2}{q + pM}(1 - e^{-(q+pM)t}), \\
c_3(t) &= \frac{p^2 M^3}{q + pM}(t + \frac{1}{pM + q}(e^{-(q+pM)t} - 1)),
\end{aligned}
$$

and $c_3(t) \approx \frac{p^2 M^3}{2}t^2$ as $t \to 0$. Then an approximated expression for the assembly time reads

$$
T_3^{det,q,1} \approx \frac{\sqrt{2}}{pM^{3/2}}.
$$

Stochastic   In the stochastic context, we look at the queueing network

$$
\underset{q}{\overset{pM(M-1)/2}{\rightleftharpoons}} \quad C_2 \quad \overset{pM}{\longrightarrow} \quad C_3
$$
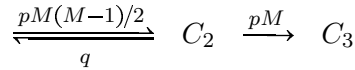
and the forward Kolmogorov equation

$$
\dot{P} = \mathbf{A}P,
$$

with $P(0, i) = \delta_1(i)$, and

$$
\mathbf{A} = \begin{pmatrix} -q - pM & 0 \\ pM & 0 \end{pmatrix}
$$

so that $P(2, t) = \frac{pM}{q+pM}\Big(1 - e^{-(q+pM)t}\Big)$, and the surviving probability is

$$
\mathbb{P}\{\tau_3^{q,1} > t\} = \exp\Big(-\frac{p^2 M^2 (M - 1)}{2(q + pM)}\big(t - \frac{1}{q + pM}(1 - e^{-(q+pM)t})\big)\Big).
$$

3.9   Large initial monomer quantity

We end up our analysis using the correspondence between the stochastic formulation and its deterministic version as M is large. It is known that for the deterministic Becker-Döring model, time trajectories present a metastable property [118, 139]. Indeed, the system has different characteristic time scales. In the first time scale, of order $1/M$, the

system behaves as a pure-aggregation system, up to the time where c_1 becomes of order q, and small aggregates are present in a very large quantity. Then, in a second time scale, the quantity of monomer c_1 stays roughly constant, as well as larger cluster. Such period have been named a metastable state. In the third time scale (of order $1/q$), quantity of monomer stays roughly constant but the cluster distribution evolves following a diffusion with a fixed left boundary, making larger and larger cluster appear. In the infinite maximal size Becker-Döring model, the fourth and final time scale corresponds to the relaxation towards an exponential equilibrium cluster size distribution. In a Becker-Döring with an absorbing maximal size state, the system tends toward a Dirac mass located at the largest cluster size. The lag time depends on whether appreciable quantity of maximal cluster size is reached before, during or after the metastable state. If N is small (to become clearer latter) we expect $c_N(t)$ to reach one in the pure-aggregation period. In such case, the Lag time is close to the constant monomer formulation

$$T_N \sim_{M \gg q, N \text{ small}} \frac{(2(N-1)!)^{1/(N-1)}}{M^{N/(N-1)}} \tag{3.59}$$

Such approximation can be improved using the exact solution of the pure-aggregation model (see remark below).

If N is larger, however, we expect the nucleus to be reached in the diffusion period. During this period, c_1 is almost constant, of same order as q. To obtain an expression of the value of the metastable value of c_1, we can let $\dot{c}_1 = 0$ in the system 3.2, to obtain (we took $p = 1$ for simplicity)

$$c_1^* = q \frac{c_2 + \sum_{i=2}^{N-1} c_i^*}{\sum_{i=2}^{N-1} c_i^*}, \tag{3.60}$$

where all c_i^* are given by the asymptotic value of the irreversible aggregation period (see remark 92 below). Now the problem reduces to a linear one, as in subsection 3.4. Specifically, the same equations as eq. (3.25) can be used, with c_1 replaced by c_1^*, and the initial condition given by $c_i(0) = c_i^*$, $i \geqslant 2$. As a consequence, the lag time depends on M only by the initial condition c_i^*, $i \geqslant 2$, and is found to be (see the numerical subsection 3.10) almost independent of M.

Now criteria to know whether C_N will reach one or not before the metastable period can be easily obtained, by comparing with the deterministic value c_N^*. (see remark 92 below). To precisely know what should be a large N or not, one have to calculate the intermediate cluster distribution at the end of irreversible stage. Such value are linearly proportional to the total quantity of monomers, leading thus to a threshold for M, and are decreasing with N. Note that as $q \to 0$, depending on the relative values of M and N, the deterministic lag time then diverges to $+\infty$ (if $c_N^* < 1$) or remains finite (if $c_N^* > 1$).

Finally, arguing as in the linear model (subsection 3.4), we can calculate the distribution of the lag time in the condition $M \gg q$ and $c_N^* < 1$, for which the survival probabilities is given by

$$S(t) = e^{-c_N(t)} \tag{3.61}$$

where $c_N(t)$ follows the deterministic linear system described above (with $c_1 = c_1^*$). As $c_N^*(0) > 0$, such formula gives in some sense a bimodal distribution. The first peak is given by Dirac mass at 0 (which should be actually of order $1/M$), with a weight given by c_N^*, and the second peak is given by the linear deterministic system.

In the limit $M \to \infty$, for fixed N, we have eventually $c_N^* > 1$, and a maximal cluster will be reached during the pure-aggregation period. Then the mean lag time is close to the deterministic lag time, and the distribution may be approximated by the Weibull distribution found in the monomer-conservative subsection 3.4.

Remark 92. *Using $\tau = \int_0^t c_1(s)ds$, the system of eq. 3.2 (with $p = 1, q = 0$) becomes*

$$
\begin{cases}
\dot{c}_1(\tau) &=& -\sum_{i=1}^{N-1} c_i, \\
\dot{c}_2(\tau) &=& -c_2 + \frac{1}{2}c_1, \\
\dot{c}_i(\tau) &=& -c_i + c_{i-1}, \quad 3 \leqslant i \leqslant N - 1, \\
\dot{c}_N(\tau) &=& c_{N-1}.
\end{cases}
\tag{3.62}
$$

Upon taking Laplace transform, $z_i(s) = \int_0^\infty e^{-s\tau} c_i(\tau)d\tau$, letting N large and using the mass conservation property, we obtain the exact formula

$$
\begin{cases}
z_1(s) &=& \frac{2Ms}{s^2+(1+s)^2}, \\
z_i(s) &=& \frac{Ms}{(s^2+(1+s)^2)(1+s)^{i-1}} \quad 2 \leqslant i,
\end{cases}
\tag{3.63}
$$

Taking Laplace inverse transform, we have

$$
c_1(\tau) = Me^{-\tau/2}\Big(\cos(\tau/2) - \sin(\tau/2)\Big),
\tag{3.64}
$$

which goes to 0 as $\tau \to \pi/2$. The exact expression of $c_1(t)$ in the original time scale can now be obtained (at least, numerically) by the inversion of the nonlinear transformation that defines τ. We can proceed similarly for each c_i to obtain an expression for the lag time in the irreversible aggregation period. Also, we can use the inverse Laplace transform of eq. (3.63) and letting $\tau \to \pi/2$ to obtain asymptotic values c_i^* during the irreversible aggregation period. If $c_N(\tau \to \pi/2) \gg 1$, then a sufficient quantity of nucleus will be reached during the irreversible aggregation period.

3.10 Numerical results and analysis

In this section we present the numerical results obtained by simulating our stochastic assembly system for various values of $\{M, N, q\}$ and compare and contrast these results with the analytical expressions evaluated in the previous sections. We use an exact stochastic simulation algorithm (SSA or Gillespie algorithm) to calculate the first assembly times [60, 22]. For each set of $\{M, N, q\}$ we sample at least 10^4 replicas and follow the time evolution of the cluster populations (given by eq. (3.6)) until $C_N = 1$, when the simulation is stopped and the first assembly time recorded. Each run starts with the same initial cluster population $\{m\} = (M, 0, \cdots, 0)$, which we won't mention any more as a consequence. Quantities such as histograms, means and variances are determined via standard statistics methods.

We start by presenting the good agreement between the exact solution calculated in subsection 3.3 and the numerical solutions, in paragraph 3.10.1. To make our analysis easier to follow, we present the behavior of the mean first passage time T_N as a functions of each parameter separately. Firstly, we look at T_N as a function of the detachment rate q in paragraph 3.10.2. In particular we verify that the two asymptotics we gave in previous section, for small q values and large q values, are in good agreement with the simulations, and confirm that T_N is non-monotonic with respect to q. Secondly, we look T_N as a function of M in paragraph 3.10.3. Such dependence is important in practice, because the initial mass M is a parameter that can be controlled experimentally. T_N is decreasing with M, with very different relationship however depending on other parameters. For large q values, T_N behaves as M^{-N}, as predicted by our approximation. For very large value of M, T_N decreases as M^{-1} approximately, as in the linear model (3.4). For intermediate value of M, and if N is sufficiently large, T_N decreases only as M^{-a}, with $a < 1$. Thirdly, we present T_N as a function of N in paragraph 3.10.4. We find that T_N increases exponentially with N. Finally, we present the distribution of the first passage time and its qualitative change with respect to parameters in paragraph 3.10.5.

3.10.1   Agreement between simulation and theory

As an example, to show the good agreement between our numerical solution and the exact solution, we consider the case $M = 7$, $N = 3$. We recall that we already noticed the discrepancies between the deterministic formulation given by eq. (3.22) and the stochastic formulation given by eq. (3.13). Indeed, we showed in figure 2.14 the differences between both formulation. What clearly arises from figure 2.14 is that while the mean first assembly times obtained stochastically and via the mean-field equations are of the same order of magnitude, they are also quite different and show even qualitative discrepancies. For example, the stochastic mean first assembly time is non-monotonic in q, while the simple mean-field estimate is an increasing function of q for $M = 7$, $N = 3$.

We show in figure 2.16 the mean first assembly time $T_3(7, 0, 0)$ as a function of q obtained via our exact results eq. (3.23) and by runs of 10^5 numerical simulations. Numerics and analytical results are in very good agreement. In the same figure 2.16 we also plot the probability distributions derived from our numerical results for the same case of $M = 7$, $N = 3$. Note that as q increases, the distribution approaches a single parameter exponential with decay rate λ_3 as estimated by eq. (3.48).
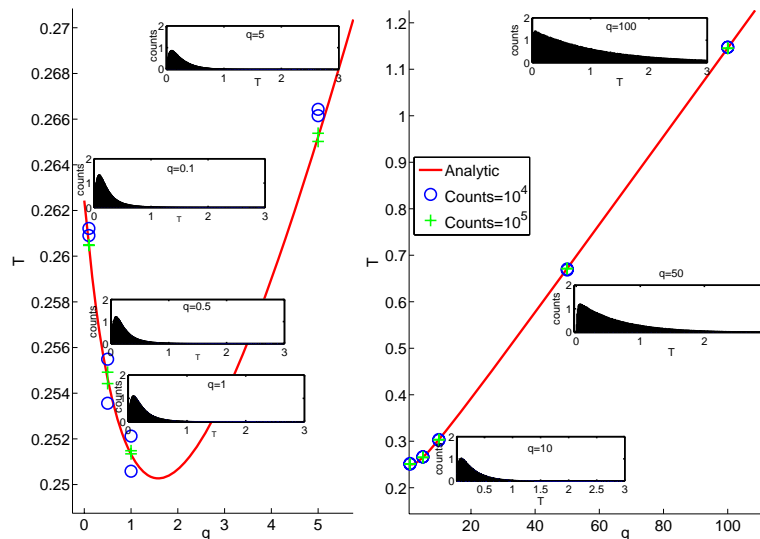
Figure 2.16: Comparison of theory with simultions, $M = 7$, $N = 3$. The red line is obtained from eq. (3.23), blue circle are average time obtained from 10^4 simulations, and green cruces from 10^5 simulations. The left figure show a range of q-value from 0 to 5, the right from 0 to 100. Inset are histograms of the waiting time for different value of q, as indicated of the figures.

3.10.2   Mean assembly time as a function of q

We generalize this analysis by plotting numerical estimates of $T_N(M, \cdots, 0)$ as a function of q for various values of M, and with $N = 10$ in figure 2.17. As expected, for small q, the mean first assembly time will scale as $1/q$. For $M = 200$, the expression given in eq. (3.61) (subsection 3.9) is found to be in good agreement with numerical simulation as soon as $q < 10$. The first assembly time presents a minimum, for all values of M, due to the previously described "opening" of quicker pathways upon increasing q for small values of q. For large q instead we expect the most relevant pathways towards assembly to be

the ones constructed along the linear chain described in eq. (3.43). Indeed, we find that in accordance with eq. (3.45), $T_N(M, 0, \cdots, 0) \simeq 2q^{N-2}/M^N$ as $q \to \infty$. For $M = 200$, the pre-equilibrium expression (with $r = 2$) given in eq. (3.56) (subsection 3.8) is found to be in good agreement with numerical simulation as soon as $q > 10$.

Figure 2.17: Mean first passage time as a function of q, for various values of M and with $N = 10$. The crosses are the result of numerical simulation. (a) $M = 200$ The dashed line is given by the pre-equilibrium expression (with $r = 2$) given in eq. (3.56), and the solid line is given by the metastable expression given in eq. (3.61) (b) Here $M = 50$ to 1000, as indicated by the legend. We only plot the numerical results, to show the overall similar qualitative behavior.

3.10.3 Mean assembly time as a function of M

We now present the numerical estimates of $T_N(M, \cdots, 0)$ as a function of M for various values of N, and with $q = 100$ in figure 2.18. For $N = 10$, we also plot the analytical approximation eq. (3.44) given by the linear chain eq. (3.43). As expected, such approximation is a very good approximation for small M, for which $q >> M$. The approximation breaks down for M of order q. For $M > q$ but $c_N^* < 1$, the expression given in eq. (3.61) (subsection 3.9) is found to be in good agreement with numerical simulation. Finally, for larger M, $c_N^* > 1$ and the linear approximation as $M \to \infty$, given by eq. (3.26), becomes more accurate.

We also notice that the slope of $T_N(M, \cdots, 0)$ with respect to M, in log scale, is of order $-N$ for $q >> M$, while it is close to -0.5 for intermediate M, and finally close to -1 for large M. Hence, such the slope is not monotonic with respect to M.

3.10.4 Mean assembly time as a function of N

Finally, we present the numerical estimates of $T_N(M, \cdots, 0)$ as a function of N for various values of q, and with $M = 1000$ in figure 2.19. All cases calculated here present a power law increase of the mean first passage time with respect to N. The asymptotic exponent, for large N, increases with q.

3.10.5 Probability distribution of the assembly time

As for the distribution of the first assembly time, we present two figures that illustrates the qualitative behaviour of such distribution. In figure 2.20, we show histograms obtained from 10^5 simulations, with $N = 8$ and $M = 200$ and q increasing from 0.01 to 1000. The

(a)   (b)
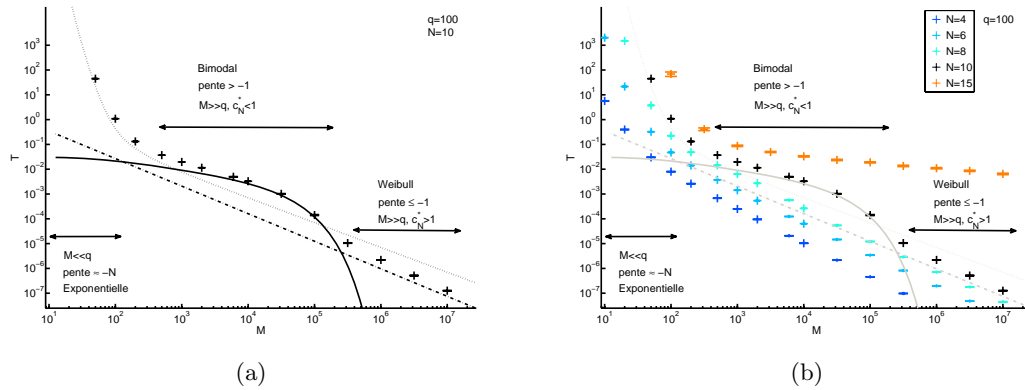
Figure 2.18: Mean first passage time as a function of M, for various values of N and with $q = 100$. The crosses are the result of numerical simulation. (a) $N = 10$. The dotted line is given by the cycle approximation eq. (3.44) (subsection 3.7), the solid line is given by the metastable expression given in eq. (3.61) and the dotted-dashed line is given by the linear approximation as $M \to \infty$, eq. (3.26). (b) $N = 4$ to $N = 15$, as indicated by the legend. We only plot the numerical results, to show the overall similar qualitative behavior.

computed histogram are bimodal for low q values, a phenomenon that we can relate to the analysis of the slow detachment rate in subsection 3.6, and to the analysis of large initial monomer M, in subsection 3.9. In such cases, there are mainly two different path. Those that encountered a "traps", and the others (or those that create a nucleus before the metastable period, and the others). This lead to a separation of time scale, as exit from a trap is penalized by a factor at least 1 over q (the metastable period is also of the same order of time). We can notice that indeed the second peak of the histograms for low q value are of order $\frac{1}{q}$. As q becomes large, one recover the fact that the distribution is exponential, given by the parameter λ_N found in the cycle approximation, subsection 3.7. The distribution given by the queueing approximation (we computed numerically the asymptotic moments by a Gaussian moment closure approximation) becomes also accurate for large q values. We also notice that there is only small differences for all $2 \leqslant r \leqslant N - 2$ between such distribution, and the cases $r = 1$ and $r = N - 1$ are clearly distinct from the others.

In figure 2.21, we show histograms obtained from 10^5 simulations, with $N = 8$ and $q = 100$ and M increasing from 50 to 10000. As expected, the computed histograms are exponential for small M values, and very asymmetric. As M increases, they comes symmetric. The analytical approximation are in good agreement with the simulation for small M values. If it may appear that our various approximation captures somehow the distribution of the first passage time for larger M, it is still unclear exactly how and is very dependent of particular values of M, q, N.

3.10.6   Summary and Conclusions

Let us first recall the discrepancies between the deterministic and stochastic results for the first passage time, by reconsidering the case $M = 9, N = 4$ also shown in figure 2.14. Here, most notably we can point out that for $q = 0$, while the exact mean first assembly time calculated according to our stochastic formulation diverges, it remains finite in the deterministic derivation. This illustrates what we saw in subsection. 3.5 and show the deterministic approach does not yield accurate estimates. A stochastic treatment is thus necessary.
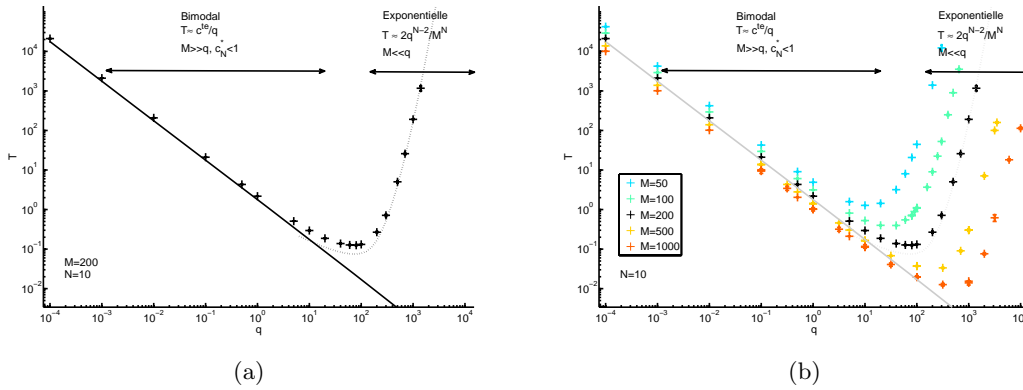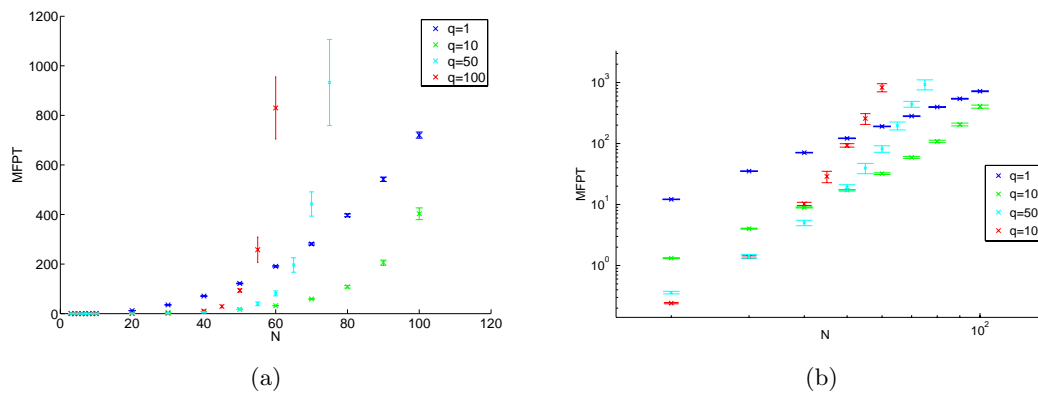
Figure 2.19: Mean first passage time as a function of N, for various values of q and with $M = 1000$. Cruces are the result of numerical simulation, and errorbars given by statistical estimates. (a). in linear scale (b). in log scale.
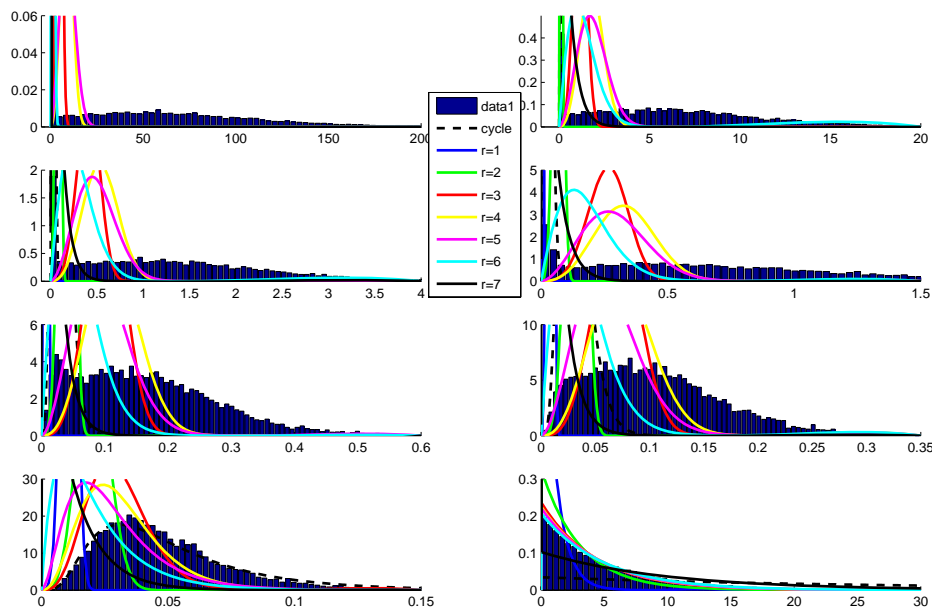
Figure 2.20: Normalized histogram of first assembly time, obtained with 10^5 simulations, and probability density functions computed numerically from the cycle approximation eq. (3.46) (black dashed lines) and from the queueing approximation eq. (3.56) (plain color lines, with r given by the legend). Here $N = 8$ and $M = 200$. The parameter q increases in $[0.01, 0.1, 0.5, 1, 5, 10, 100, 1000]$ from top left to down right. Each analytical distribution computed are indicated by the legend.

Then, we'd like to point out that the various estimates ($q = 0$, $q \ll 1$, $q \gg 1$, $M \gg 1$) we provided for the stochastic first passage time used well known techniques for the study of stochastic models in a large state space. Namely we used several times a reduction of the state space by considering the most likely states. We also used a separation of time scales and an averaging technique to transform our problem into a simpler one. See [91, 111, 80] for further presentation of these techniques. And we finally used the similarity with the
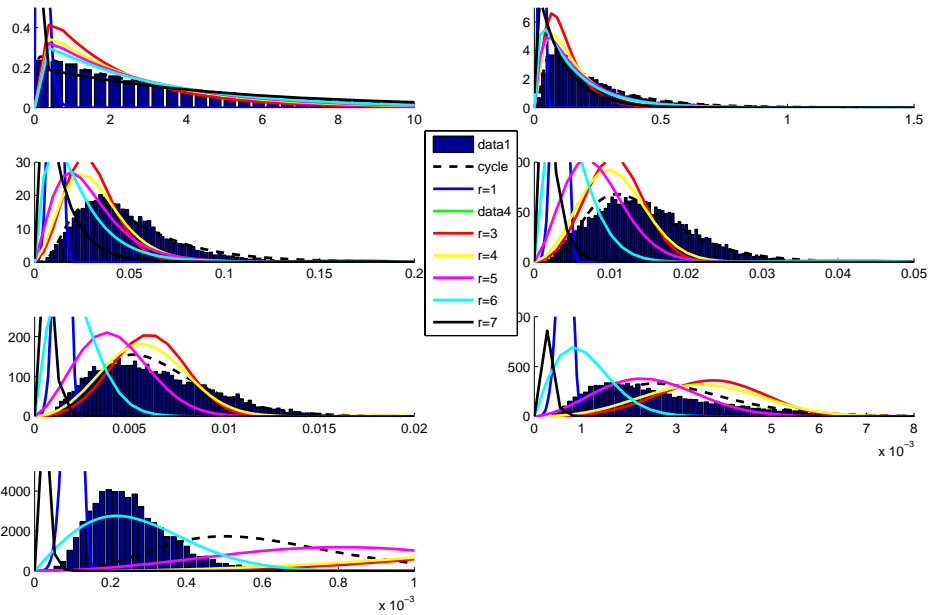
Figure 2.21: Normalized histogram of first assembly time, obtained with 10^5 simulations, nd probability density functions computed numerically from the cycle approximation eq. (3.46) (black dashed lines) and from the queueing approximation, eq. (3.56) (plain color lines, with r given by the legend). Here $N = 8$ and $q = 100$. The parameter M increases in $[50, 100, 200, 500, 1000, 2000, 10000]$ from top left to down right. Each analytical distribution computed are indicated by the legend.

deterministic model, and the constant monomer formulation.

We analyzed the first passage time for the Becker-Döring model with constant aggregation and fragmentation rate. This is a strong limitation, that seems however reasonable when a tractable analytical solution is wanted. We have to mention however that non-constant rates should give also interesting behavior, as meta-stability has been demonstrated by Penrose [118] (see also [139] for a review on the available results for this subject). As the first passage time is a key notion for meta-stability, it will be of interest to develop techniques to quantify first passage time for the Becker-Döring model with non-constant rates.

Our theoretical analyses mainly captures the behavior of the first passage time for small detachment rate and very large detachment rate, confirmed by numerical analysis. We pointed out the presence of traps in the limit $q \to 0$ that makes the mean first passage time to be non-monotonic with respect to q and to diverge to $+\infty$ for $N \geqslant 4$ or $N = 3$ and M even. The presence of traps also lead to bimodal distribution for the first passage time. A different interpretation for this last fact is possible by looking at the limit of M large. As M is large, the stochastic model becomes initially closer to the deterministic system. As metastable period are known for the deterministic model, we have a dichotomy for the first assembly time, when M is large and N too. There are two types of trajectories. The first type of trajectories is such that the first nucleus is formed before the metastable period. The second type of trajectory is such that the first nucleus is formed after (or rather during) the metastable period, where very few monomer are present. Finally, as $q \to \infty$, the first passage time converges to an exponential distribution for which we could

computed exactly the mean parameter.

3.11   Application to prion

As we already pointed out, we have for now too few data of the nucleation time to be able to deduce quantitative parameters from our theoretical analysis. However, even if we dispose of such sufficient data, it may still be hard to deduce all parameters values. If the quantity of total protein is known experimentally, the actual number of misfolded protein, that actively participate to the aggregation process (in the model) is not currently known (no values for misfolding parameters γ or γ^* are known for now). The reduction we performed in subsection 2.2 is due to biological hypothesis and remains to be confirmed experimentally. Apart from the time scale parameter p, we are lead with the parameter q, N and M. Nevertheless, we can already exclude some parameter regions, from the experimental data we have. Indeed, the fact that the total quantity of protein and the experimental nucleation time are weakly correlated suggests that the detachment q rate cannot be very large compared to M (this would imply a nucleus size of less than 1!). This is also confirmed by the fact that the distributions of the nucleation time are clearly not exponentials. Our theoretical analysis suggests rather that $M > q$ and N is not too small. Indeed, the very weak correlation between the total quantity of protein and the experimental nucleation time could be explained by kinetic parameter that satisfies $M > q$, $c_N^* < 1$ for which we found that $T_N = M^{-a}$, with $a > 1$ ($a = 0.5$ with $N = 10$, $a = 0.1$ with $N = 15$ for the example we considered in figure 2.18). Moreover, the nucleation distribution time found experimentally seems asymmetric for small quantity of protein, and becomes slightly more symmetric for larger M. Such qualitative behaviour is in agreement with the model of stochastic first passage time, as M increases. The condition $c_N^* < 1$ also suggests that the ratio M/N is not too large, leading to potential traps and asymmetry or bimodality in the distribution of nucleation time.

4   A lengthening-fragmentation equation for configurational polymer under flow, from discrete to continuous

This section is an ongoing work with Erwan Hingant (Université Lyon 1).

In this section, we construct an hybrid model from a purely discrete model of polymerization-fragmentation, that is adapted to our prion experimental data described in sections 1 and 2, *after nucleation*, that is, when some large polymers are present. In this problem, we study however a slightly more general model, with an additional spatial structure, that is important in other experimental contexts.

In subsection 4.1 we introduce our problem, and recall some results of limit theorem for stochastic processes. In subsections 4.2 - 4.4, we present the mathematical formulation of the model, as an individual and discrete size polymer model. We first derive the evolution equation for a single monomer and a single polymer, based on the laws of physics, and then give the stochastic differential equation on the empirical measure process, together with its properties. Finally, in subsection 4.5, we prove that this model converges to a limiting hybrid model, with continuous and deterministic polymerization and intermittent and stochastic fragmentation.

4.1   Introduction

In this section, we are interested in polymers under flow and particularly, biological polymers composed of proteins. In Ciuperca et al. [37], an *ad hoc* model has been derived to describe polymerization and fragmentation of rod like polymers. This model takes its origin from biological experiments where polymers are studied under flow. The polymers under consideration are formed, for instance, by proteins aggregation. They look like rigid rod polymers thus the model was based on the theory developed in Bird et al. [19], Doi and Edwards [46] for rod-like polymers. This theory involves polymers with a fix length. But, our biological polymers are also subjected to polymerization (addition one by one of proteins) hence the length may increase. Moreover, these polymers can break-up into smaller pieces (fragmentation). A polymerization-fragmentation model has been used in Greer et al. [63] to model prion (protein responsible for several diseases) proliferation. The model in [37] combines both these models: rigid-rod polymers under flow and polymerization-fragmentation, in order to obtain a new brand model to study such polymers.

Here, we present a discrete size and individual model which allows us to write equations for each polymer and monomer and their relative interactions *wrt* to the law of physics. Once the discrete model is established the aim is to justify the mean-field equations of [37]. Another aim is to provide a hybrid model, suitable for quantitative analysis of experimental data of prion aggregation dynamic. For now, only the second goal has been achieved. To clarify the relationship between the models, consider the following diagram in table 2.3

We now discuss the method related to this approach. Our topic here is to prove a limit theorem for a particular stochastic process given by a discrete population model. The strategy is to describe our discrete population model using a point process (the empirical measure), and to prove its convergence under appropriate scaling and coefficient assumptions to a measure that solve a limiting model. The convergence holds in law, and the proof uses martingale techniques (we first show that a certain compacity condition holds, and then prove a unique limit is possible). Such ideas come back to [122, 88, 133] among others. The interest of this approach are multiple.

1. Firstly, for a theoretical interest, this approach can be used to prove existence of solution of the limiting model. If there is a particular discrete model, that has a

Individual and discrete-size $\implies$ Individual and continuous-size (Direct simulation process) (Marcus-Lushnikov process, CTMC [98, 1]. Stochastic coalescent) Jump process, hybrid process, [102, 113, 1].

$\Downarrow$ $\Downarrow$

Mean-field and discrete-size $\implies$ Mean-field and continuous-size (Discrete Smoluchowski model, (Continuous Smoluchowski model) Becker-Döring model) ODE PDE [113, 63]. [14, 78, 104, 139].
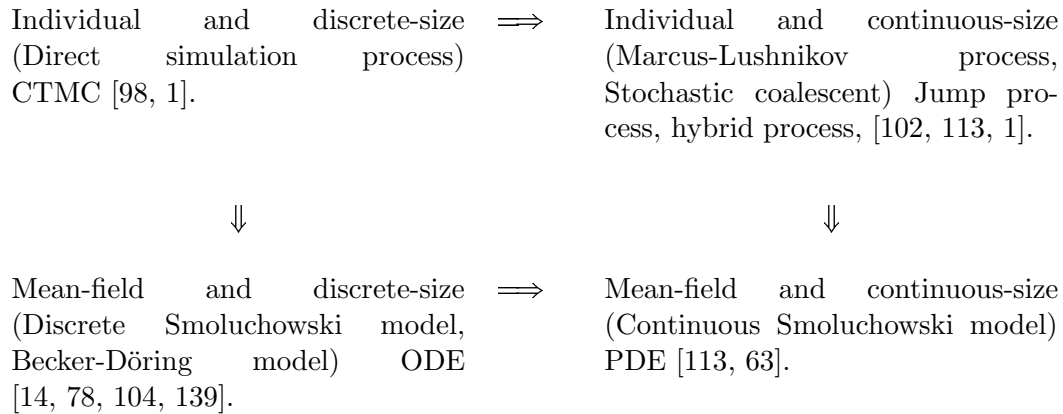
Table 2.3: In polymerization-fragmentation models, there are mainly two types of variables: monomers and polymers. All models referred in this diagram have the mass conservation property. Discrete or continuous refer to the size variable of polymers, and individual or mean-field refers the number of polymers (discrete in individual model, continuous in mean-field model). In individual and discrete-size model, we can use a continuous-time Markov chain (CTMC) formalism, to describe coagulation and fragmentation events. Some particular case of these models reduce to branching process. In individual and continuous-size model, we can use a jump Markov process, or a hybrid process if, as in our case, coagulation is deterministic and fragmentation stochastic. In a mean-field and discrete-size approach, the system is described by an infinite set of ordinary differential equation. In a mean-field and continuous-size approach, the system is described by a partial differential equation for polymers evolution (and an ordinary differential equation for monomers). The arrows mean that we can pass from one formalism to another by a limit theorem. The link between individual and discrete-size model and mean-field and discrete-size can be proved using the approach of Kurtz [88] to show that a Markov chain converges to the solution of an ordinary differential equation using a suitable scaling. The link between a mean-field and discrete-size model and a mean-field and continuous-size model was proved in a context of a prion model by [48]. We are going to show a limit theorem between an individual and discrete-size model and a individual and continuous-size model. Such approach was also taken by Bansaye and Tran [11] in a cell population model. Finally, limit theorem between individual and continuous-size model and mean-field and continuous-size was proved in a coagulation-fragmentation model by [113].

    sequence of solutions that converges, and such that the limit needs to solve the limiting model, then existence is proved (see for instance [78, 113] in the context of aggregation-fragmentation model).

2. Secondly, such approach has been widely used to obtain accurate and fast algorithms of a fully non-linear continuous model, such as many of the variant of Poisson-McKean-Vlasov equations ([134]). For such approach, the convergence rate of the stochastic model is of importance to assess the tolerability of the approximation made ([30, 108]).

3. Thirdly, in physical or biological context, this approach allows to give rigorous basis of a particular model. Indeed, in the discrete population model, one have to specify each reaction or evolution rules very properly. Then, according to the assumption on coefficient describing this evolution, along with a particular scaling (usually large population, or fast reaction rates and so on), one end up with a limiting model

or another. Then the (sometimes) implicit assumptions of a continuous model are made explicit. Different models can be unified by relating each other with particular scalings ([84]).

4. Finally, this approach can be used to simplify models, when the discreteness makes the model intractable analytically. Several limiting behavior of a particular model can be studied to get an overall picture of the behavior of the original model.

Our main goal combines some of these interests. From a particular continuous model [37] (see also [50]), we wanted to give precise and rigorous justification of this model based on physical laws. Also, we are looking to a formulation that could be easier to simulate numerically, as well as to derive analytical results. We ended up with a hybrid model, between the fully discrete population model, which would have a too large population for any realistic values, and a fully continuous model, which does not capture stochastic effect and is hard to simulate.

In the context of coagulation-fragmentation, a limit theorem was proved by Norris [113]. The author derived the fluid limit of the "stochastic coalescent" model (or Marcus-Lushnikov model), towards the mean-field Smoluchowski's coagulation equation. Recently, the authors in [30] provided a bound on the convergence rate of the Marcus-Lushnikov model towards the Smoluchowski's coagulation model, in Wasserstein distance (in $\frac{1}{\sqrt{n}}$). Fluid limit results in the case where gelation occurs were recently derived in [55, 57], where the authors showed that different limiting models are possible, namely the Smoluchowski model and a modified version, named Flory's model. See also [1] for a review of the link between probabilistic and mean-field approaches in these models.

For model with coagulation-fragmentation and spatial structure (with Brownian motion of particles) we can mention the collision-annihilating model (particle are killed as soon as they encounter another particle. The authors in [89] derived the mean-field kinetic equation on the particle number density, assuming that particles are smaller and smaller as they are present in a larger number. Particles undergo Brownian motion in $\mathbb{R}^3$, with constant diffusion (with respect to the scaling parameter). More recently, the author in [114] considered general Brownian-coagulation model, where particles undergo free diffusion and coagulate once they collide. Using specific scaling between radius and diffusivity of the particles, the author derived the mean-field reaction-diffusion equation. Both studies mentioned above made use of results on the waiting time of collision between two particles driven by Brownian motion, and are then strongly dependent on the particular assumption on diffusion. See also [67] for recent spatially inhomogeneous model of coagulation particles system. Let us also mention that deterministic discrete size system of coagulation-fragmentation with diffusion (infinite system of spatially structured PDE) were looked by [144, 93, 92] where the authors derived existence results (for gelation phenomena, see [25, 45]), and for deterministic continuous size analog results, see [44, 37]. Finally, for a physical discussion on the validity of the protein aggregation and diffusion kinetic treated as rigid body, we refer to [19, 46, 77] and for experiments on Brownian coagulation kinetic, see [23].

We also take inspiration of limit theorems proved in a different context, mostly from Bansaye and Tran [11] in a cell population model. The authors considered a cell population with division infected by parasites (which act then as a structure variable for the cell population), and considered a limit model with a large number of parasites within a finite population of cells. It is possible to make an analogy between this model and the polymerization-fragmentation model, considering polymers as cells and parasites as monomer. We will then make extensively used of the results in this paper, as we will also consider a limit where the small particles (monomers, parasites) are present in a large number, while the large particles (polymers, cells) are present in a finite number,

and follows a stochastic fragmentation (or division) model. Other similar studies of host-parasite include [12, 106]. We also mention evolution models and the work of Champagnat and Méléard [31] In this works, the authors extended evolution population models (structured by a "trait" that undergoes mutation) with interaction (see [59, 32]) by including a space structure, namely a reflected diffusion in a bounded domain, and obtained, in the large population limit, a nonlinear reaction-diffusion partial differential equation with Neumann's boundary condition. They prove then a law of large number, with boundedness and Lipschitz assumption on birth and death rates, and on drift and diffusion coefficient to ensure well-posedness of the limiting model. We will make extensively used of this work in the next, as our initial stochastic model could be reformulated as a special case of their model. Note that similar to our case, drift and diffusion coefficient are independent of the scaling.

Some notations used through this paper:

t	time
Space	
Γ	bounded open set in $\mathbb{R}^3$
$\mathbb{S}^2$	Unit sphere in $\mathbb{R}^3$
Function Space	
$\mathcal{D}(\mathbb{R}_+, E)$	*càdlàg* E-valued functions
$\mathcal{C}^{k_1,\ldots,k_n}(E_1$ $\times \cdots \times E_n)$	Continuous functions with k_i continuous derivatives according to the variable belongs to E_i, for all $i = 1, \ldots, n$
$\mathcal{C}_b^{k_1,\ldots,k_n}(E_1$ $\times \cdots \times E_n)$	idem with bounded functions and derivatives
Measure Space	
$\mathcal{M}(E)$	Measure on E
$\mathcal{M}_F(E)$	The space of finite measure
$\mathcal{M}_\delta(E)$	Finite sum of Dirac measures
$\mathcal{M}^+(E)$	The cone of non-negative measure
Monomers	
i	labeled one single monomer
X_t^i	Center of mass in Γ of a single monomer
x	Continuous space variable in Γ
N_t^m	Number of monomer
Polymers	
j	Labeled one single polymer
Y_t^j	Center of mass in Γ of a single polymer
H_t^j	Orientation in $\mathbb{S}^2$ of a single polymer
R_t^j	Length in $\mathbb{N}^*$ of a single polymer
Z_t^j	(R_t^j, H_t^j, Y_t^j)
y	Continuous space variable in Γ
η	Continuous orientation variable in $\mathbb{S}^2$.
r	Continuous length variable in $\mathbb{R}_+$
z	(r, η, y)
N_t^p	Number of polymer
Others	
$u(x,t)$	$\mathbb{R}^3$-valued fluid velocity at $x \in \Gamma$

4.2 An individual and discrete length approach

We are concerned in modeling polymers under flow and particularly dilute solution of rigid rod polymers arising in biology, see [37]. Precisely, we will derive equations standing for polymers formed by protein aggregation and subject to fragmentation. The spatial domain of the problem will be denoted by Γ a bounded open set of $\mathbb{R}^3$, the time by $t \geqslant 0$ and the velocity field of the fluid by $u : \Gamma \times \mathbb{R}_+ \mapsto \mathbb{R}^3$, that is $u(x,t) \in \mathbb{R}^3$ is the velocity at point $x \in \Gamma$ and time $t \geqslant 0$. We assume incompressibility of the given fluid:

$$\nabla_x \cdot u(x,t) = 0, \quad \forall\, (x,t) \in \Gamma \times \mathbb{R}_+\,,$$

and impermeability of the boundary (Neumann type boundary condition):

$$\nabla_x u(x,t) \cdot \vec{n} = 0 \quad \forall\, (x,t) \in \partial\Gamma \times \mathbb{R}_+.$$

The polymer is described by the position of its center of mass $Y_t \in \Gamma$ at time t and a configuration variable $(R_t, H_t) \in \mathbb{R}^+ \times \mathbb{S}^2$, where $R_t > 0$ is the length of the polymer, while $H_t \in \mathbb{S}^2$ is its orientation. The monomers forming the polymer will belong to a certain type of proteins, thus seen as elementary particles. We assume that each polymer is assimilated to perfect rigid-rod with length R_t that can be regarded as the number of monomers (proteins) that compose it. We describe the motion of a free protein in the fluid by its position $X_t \in \Gamma$ at time $t \geqslant 0$. We assume that the free monomers are identical, and assimilated to perfect spheres of radius $a > 0$.

In this section we obtain a model of evolution and motion of the polymers and monomers inside the fluid. However, since it involves several mechanisms, let us first describe the four steps of the method, that will lead to the establishment of the different equations in the model.
- Firstly, we derive in paragraph 4.2.1 the equation of motion of an individual free monomer;
- Secondly, we get in paragraph 4.2.2 equation of motion of an individual polymer. Both these equations are obtained thanks to general laws of physics [19, 46].
- Thirdly, the elongation process of polymers is presented in paragraph 4.2.5. Indeed, to fit with the model introduced in [37] , we have to include in the model that such polymers formed of protein can lengthen: proteins (free monomers) aggregate at both ends of one polymer, successively one by one.
- Finally, another mechanism is involved, a fragmentation process of the polymers, presented in paragraph 4.2.6. Considering a finite population of monomers and polymers, these two last processes will be introduced in term of jump Markov processes.

We want to emphasize here that our model has the advantage of providing explicit equations for a single monomer and a single polymer. These are therefore the starting point, in order to bring a complete justification of future models. We will adopt the point process approach to describe the whole discrete population in subsection 4.4. Then, we will use limit theorem and martingale technique to prove convergence towards a limiting model when there an infinity of monomers, but still a finite number of polymers, in subsection 4.5.

In the following we introduce the equations of the motion and configuration for monomers and polymers. As we use *white noise forces* for particles interactions with the fluid and jump Markov process for the elongation and fragmentation of the polymers, the unknown of the system will be given by in terms of stochastic processes. In order to defined them, we always refer to a stochastic process with respect to a probability space $(\Omega, \mathcal{F}, P)$, sufficiently large, that stands for the realizations.

4.2.1   Individual monomer motion

For this process, we naturally use the Langevin equation [90]. Namely, we consider one single monomer, represented by a microscopic rigid sphere of radius $a > 0$, moving in a fluid domain $\Gamma \subseteq \mathbb{R}^3$, itself moving with velocity $u \in \mathbb{R}^3$. The equation of motion of the monomer reads

$$m\,dV_t = -\xi\left(V_t - u(t, X_t)\right) dt + \sqrt{2k_B T \xi}\ dW_t^{(m)},$$

where m is the mass of the monomer and ξ is the drag constant, while $(V_t)_{t \geqslant 0} \subset \mathbb{R}^3$ and $(X_t)_{t \geqslant 0} \subset \mathbb{R}^3$ are two stochastic processes, corresponding respectively to its velocity and its position. $(W_t^{(m)})_{t \geqslant 0}$ is a standard 3-dimensional Wiener process with independent components and normal reflexive boundary ([130]), representing the interaction of the monomer with the surrounding fluid domain. The constant in front of the increments of the Wiener process follows the Nernst-Einstein relation with k_B the Boltzmann constant and T the temperature, see [46].

Now, assuming that the time scale m/ξ tends to zero (see subsection 4.3), we approach the problem by the following stochastic differential equation (see [69, 21, 15] for more details)

$$dX_t = u(X_t, t)dt + \sqrt{2D}\ dW_t. \tag{4.1}$$

In the case of a spherical particle (the protein), the Einstein-Stokes equation leads to a diffusion coefficient

$$D = \frac{k_B T}{\xi} = \frac{k_B T}{6\pi\nu a},$$

in a fluid of viscosity ν and at small Reynolds number, where a is the radius of the sphere [46]. The generator of this process is denoted by L_m and defined as follow

$$L_m f = u \cdot \nabla f + D\Delta f, \quad \forall f \in D(L_m), \tag{4.2}$$

where $D(L_m)$ is the domain of the operator L_m. Note that function $f \in C^2(\overline{\Gamma})$ with vanishing normal derivatives belongs to $D(L_m)$ and are dense into $C(\overline{\Gamma})$ ([31]). We will then only consider such function on the next.

Now the motion of a single monomer is well described. We treat next the motion of a single polymer.

4.2.2   Individual polymer equations

Here, we establish the equation for the motion of a single polymer, represented as a rigid rod in the fluid domain Γ, with the same velocity field as above $u \in \mathbb{R}^3$. Since there is no more spherical symmetry of the object considered, we need to describe both the rotational motion and the translational motion. Moreover, for now, no lengthening or splitting of the polymer is considered, hence the length of the polymer is fixed equal to $R > 0$. Therefore, its evolution equation reduces simply to

$$dR_t = 0. \tag{4.3}$$

4.2.3   Rotational motion

The configuration of a polymer is given by its length and orientation. Since its length $R_t = R > 0$ is fixed, there is only its orientation, given by a stochastic process $(H_t)_{t \geqslant 0} \subset \mathbb{S}^2$ for which we need to write the evolution equation. The increments of the orientation are given by

$$dH_t = M_t \wedge H_t\, dt, \tag{4.4}$$

where $(M_t)_{t \geqslant 0}$ is the stochastic process giving the angular velocity of the polymer in $\mathbb{R}^3$, which satisfies the Langevin equation,

$$[J]dM_t = T \ dt + \sqrt{2k_B T \xi_r} \ dB_t, \tag{4.5}$$

where $(B_t)_{t \geqslant 0}$ is a standard 3-dimensional Wiener process with independent components, $[J]$ the moment of inertia, T the total torque and ξ_r the rotational friction coefficient [46]. Since we consider the polymer as a rigid rod, in the velocity field u, the torque T (for instance derived in [43, 46]) is given by

$$T = -\xi_r(M_t - H_t \wedge \nabla_x u(t, Y_t)H_t), \tag{4.6}$$

where the stochastic process $(Y_t)_t \subset \Gamma$ represents the position of the center of mass of the polymer, which equation of motion will be derived later. Moreover, the moment of inertia is given by:

$$[J] = j(I - H_t \otimes H_t) \quad \text{with} \quad j = \frac{mR^2}{12},$$

where m is the mass of the rod. Then, as for the motion of one single monomer, we simplify eq. (4.4) when assuming that $\frac{m}{\xi_r}$ tends to zero (see subsection 4.3). Thus, using eq. (4.5) and (4.6), it yields

$$dH_t = -H_t \wedge \left(H_t \wedge \nabla_x u(Y_t, t)H_t \ dt + \sqrt{2D_r} \ dB_t \right), \tag{4.7}$$

where the rotational diffusion coefficient D_r is defined by

$$D_r = \frac{2k_B T}{\xi_r} = \frac{3k_B T(\ln(L/b) - \gamma)}{\pi \nu L^3},$$

where $b = 2a$ the thickness of the polymer (a is the radius of the monomer) and $L = bR$ is the physical length of the polymers. Here, γ is a constant standing for a correction term, see [46].

4.2.4   Translational motion

Due to the nature of the polymer (rod), it feels an anisotropic translational friction, whose coordinates are denoted by $\xi_\perp$ and $\xi_\parallel$, *i.e.* its perpendicular and parallel components respectively, *wrt* to the orientation H_t, see [46]. Let $(V_t)_{t \geqslant 0} \subset \mathbb{R}^3$ be the stochastic process governing the translational velocity of the center of mass of the polymer (and $(W_t^{(p)})_{t \geqslant 0}$ a standard 3-dimensional Wiener process with independent components. Thus, the perpendicular velocity $V_t^\perp = (I_3 - H_t \otimes H_t)V_t$ satisfies again a Langevin equation, namely

$$mdV_t^\perp = (I_3 - H_t \otimes H_t) \left(-\xi_\perp(V_t - u(t, Y_t)) \ dt + \sqrt{2k_B T \xi_\perp} \ dW_t^{(p)} \right),$$

which is the projection of the dynamic onto the perpendicular space to H_t. Also, the parallel velocity $V_t^\parallel = (H_t \otimes H_t)V_t$ satisfies

$$mdV_t^\parallel = (H_t \otimes H_t) \left(-\xi_\parallel(V_t - u(t, Y_t)) \ dt + \sqrt{2k_B T \xi_\parallel} \ dW_t^{(p)} \right).$$

As remarked in [46], drag coefficients satisfy $\xi_\perp = 2\xi_\parallel$, we reduce again these equations by taking $m/\xi_\perp \to 0$ (see subsection 4.3). It leads to

$$
\begin{cases}
(I_3 - H_t \otimes H_t)\, V_t\ dt\ =\ (I_3 - H_t \otimes H_t)\, u(t, Y_t)\ dt \\
\\
\qquad\qquad\qquad\qquad +\sqrt{\frac{2k_B T}{\xi_\perp}}\,(I_3 - H_t \otimes H_t)\ dW_t^{(p)}, \\
\\
(H_t \otimes H_t)\, V_t\ dt\ =\ (H_t \otimes H_t)\, u(t, Y_t)\ dt \\
\\
\qquad\qquad\qquad\qquad +\sqrt{\frac{2k_B T}{\xi_\parallel}}\,(H_t \otimes H_t)\ dW_t^{(p)}.
\end{cases}
$$

Thus, for the position of the center of mass we get:

$$
dY_t = u(Y_t, t)\ dt + \sqrt{2D_\perp}\,(I_3 - H_t \otimes H_t)\ dW_t^{(p)} + \sqrt{2D_\parallel}\,(H_t \otimes H_t)\ dW_t^{(p)}, \qquad (4.8)
$$

with

$$
D_\parallel = \frac{k_B T}{\xi_\parallel} = \frac{k_B T \ln(L/b)}{2\pi\nu L} \text{ and } D_\perp = \frac{1}{2}D_\parallel.
$$

Finally, the generator of the process $(R_t, H_t, Y_t)_{t\geqslant 0}$, denoted by L_p, is

$$
L_p g = u \cdot \nabla_y g + \left[D_\perp \eta \otimes \eta + D_\parallel (I_3 - \eta \otimes \eta) \right] \nabla_y \cdot \nabla_y g
$$

$$
+ \left(P_{\eta^\perp} \nabla_y u\ \eta - 4D_r \eta \right) \cdot \nabla_\eta g + D_r \nabla_\eta \cdot \nabla_\eta g, \qquad (4.9)
$$

$$
\forall g \in D(L_p).
$$

where $D(L_P)$ is the domain of the operator L_P and η denotes the spherical variable. Similarly, note $f \in C^{2,2}(\overline{\Gamma}, \mathbb{S}^2)$ with vanishing normal derivatives belongs to $D(L_p)$ and are dense into $C(\overline{\Gamma}, \mathbb{S}^2)$ ([31]). We will then only consider such function on the next.

Next we treat the polymerization and fragmentation processes, which will be seen as discrete events in time, governed by jump Markov processes. Their descriptions will therefore introduce survivor functions, in order to model when these events happen (see [61, 105] for chemical justifications).

4.2.5 Lengthening process

Let us consider first a single monomer, labeled by i, and a single polymer, labeled by j, in the fluid. As said before, they are characterized by a position $X^i \in \Gamma$ for the monomer (and a given volume constant *wrt* time), while it is a vector $Z^j = (R^j, H^j, Y^j) \in \mathbb{N} \times \mathbb{S}^2 \times \Gamma$ that holds for the polymer j, where R^j is its length, H^j its orientation and Y^j its position. This latter defines actually a given volume occupied by the polymer, and may change by the elongation process.

Then one can define a probability per unit of time that the monomer and the polymer will encounter and polymerize, depending on their relative position and on the size of the polymer:

$$
\tau(X^i, Z^j).
$$

Thus the survivor function associated to this will be

$$
F_{elong}^{ij}(t) = 1 - exp(-\int_0^t \tau(X_s^i, Z_s^j)ds).
$$

Let S_{elong}^{ij} be the stopping time corresponding to F_{elong}^{ij}. For all $t < S_{elong}^{ij}$, the motion of the monomer is governed by eq. (4.1), while for the polymer it holds the three equations for the length, eq. (4.3), the orientation, eq. (4.7) and the translation of its center of mass, eq. (4.8).

At $t = S_{elong}^{ij}(w)$ ($w \in \Omega$ being "the chosen stochastic realization"), the process is stopped. The monomer is killed, and the polymer is changing through a deterministic transition:

$$Z^j(t^+) = Z^j(t^-) + \mathbf{e}_1, \tag{4.10}$$

where $\mathbf{e}_1 = (1, 0, 0)$. In other words, the length of the polymer increases of one monomer.

Remark 93. *The assumption made here is that the polymerization process does not change the position of the center of mass of the polymer, neither its orientation. One can introduce non-local transition for the elongation.*

Consider now a single polymer j in an environment of N_s^m monomers around *wrt* time s. For all $1 \leqslant i \leqslant N_s^m$, this polymer can interact with a monomer i. Because the monomers are present in a finite number, the stopping time for the polymer to elongate will simply be the minimum of all the stopping time of the elongation of the polymer with each monomer. These events are supposed to be independent from each other. The survivor function associated to the minimum of these stopping times is then:

$$F_{elong}^j(t) = 1 - exp\left(-\int_0^t \sum_{i=1}^{N_s^m} \tau(X_s^i, Z_s^j) ds \right).$$

Similarly for a single monomer i with N_s^p polymers

$$F_{elong}^i(t) = 1 - exp\left(-\int_0^t \sum_{j=1}^{N_s^p} \tau(X_s^i, Z_s^j) ds \right).$$

Finally, for the whole population, the stopping time S_{elong} defined as the next elongation event is associate to the survivor function

$$F_{elong}(t) = 1 - exp\left(-\int_0^t \sum_{i=1}^{N_s^m} \sum_{j=1}^{N_s^p} \tau(X_s^i, Z_s^j) ds \right).$$

Hence, as said before, at time $t = S_{elong}(w)$, one monomer i is killed, so the number of monomers satisfies

$$N_{t^+}^m = N_{t^-}^m - 1. \tag{4.11}$$

4.2.6 Fragmentation process

One can use the same reasoning for the fragmentation process. We define a probability per unit of time for a polymer, labeled by j, to break up. This probability depends on its position and configuration given by $Z^j \in \mathbb{N} \times \mathbb{S}^2 \times \Gamma$ and is

$$\beta(Z^j).$$

Then for each polymer j, we can define a stopping time given by the survivor function

$$F_{frag}^j(t) = 1 - exp\left(-\int_0^t \beta(Z_s^j) ds \right).$$

At time $t = S_{frag}^j(w)$ the stopping time corresponding to F_{frag}^j, the polymer j is changing through the transition

$$Z_{t+}^j = ([\theta R_{t-}^j], H_{t-}^j, Y_{t-}^j), \tag{4.12}$$

and a new polymer is created

$$Z_{t+}^{N_{t+}} = ([(1-\theta)R_{t-}^j], H_{t-}^j, Y_{t-}^j), \tag{4.13}$$

with the population of polymers incremented by

$$N_{t+}^p = N_{t-}^p + 1. \tag{4.14}$$

The notation $[r]$ denotes the closest integer from r and $\theta \in (0,1)$ is chosen according to a probability density function k_0 satisfying the symmetry condition, namely

$$k_0(\theta) = k_0(1-\theta), \ \forall \theta \in (0,1),$$

and truncated upon the condition that

$$[\theta R_{t-}^j] \geqslant R_0,$$
$$[(1-\theta)R_{t-}^j] \geqslant R_0.$$

R_0 being a given critical length that ensures no polymers of size 0 is created.

Remark 94. *The assumption made here is that the fragmentation does not change the orientation and the center of mass of the resulting polymers from the original one. Here again, the transition could involve non-local fragmentation. After the fragmentation process, the two resulting polymers will evolve independently of each other according to equations of motion eq. (4.7) - (4.8), with independent Brownian motion.*

The stopping time S_{elong} defined as the next fragmentation event is associated to the survivor function

$$F_{elong}(t) = 1 - exp\left(-\int_0^t \sum_{j=1}^{N_s^p} \beta(Z_s^j)ds\right).$$

Finally, since elongation and fragmentation event are both independents we construct the survivor function of the whole system as

$$F(t) = 1 - exp\left(-\int_0^t \left(\sum_{i=1}^{N_s^m} \sum_{j=1}^{N_s^p} \tau(X_s^i, Z_s^j) + \sum_{j=1}^{N_s^p} \beta(Z_s^j)\right)ds\right).$$

4.3 Some necessary comments on the model

We can give an algorithmic point of view of the model. Let $t_k \geqslant 0$ be a given time with $(X_{t_k}^i)_{i=1,...,N_{t_k}^m}$ the position of the monomers and $(R_{t_k}^j, H_{t_k}^j, Y_{t_k}^i)_{i=1,...,N_{t_k}^p}$ the position-configuration of the polymers. Boundedness assumption on coefficient allows to simulate this stochastic process in an acceptance-reject manner, which we briefly recall below, see [31]. Simulation of Brownian trajectories with reflexion conditions have been discussed in [96]. The algorithm is

 i) Let $t_{k+1} > t_k$ be the next possible stopping time associated to the survivor function F.

ii) For all $t \in (t_k, t_{k+1})$ the motion of the monomers is given by eq. (4.1) and the polymers are governed by eq. (4.3) for the size, eq. (4.7) for the orientation and eq. (4.8) for the center of mass.

iii) If t_{k+1} is associated to an elongation event, the system changes following the transition eq. (4.10) for the corresponding polymer that elongates and eq. (4.11) for the monomers population.

iv) If t_{k+1} is associated to a fragmentation event, the system changes following the transition eq. (4.12-4.13) for the two resulting polymers and eq. (4.14) for the population of polymers.

v) If t_{k+1} is not associated to any event, the system does not change and no transition happens.

vi) We go back to step i).

Because all stochastic differential equations involved in the equation of motion of monomers and polymers have global existence and uniqueness property, this description ensures the existence and unicity of the solutions of this model up to the explosion time, that is the accumulation point of the jump times (see next section).

The model describes above needs some comments:

– Neglecting the inertial effects in the motion of monomers and polymers will be justified later by the fact that the mass will be chosen converging to zero. For a model (without elongation-fragmentation) that take it into account we can refer to [43].

– The modeling of the Brownian intensity is valid under low Reynolds number, thus the fluid model should be a Stokes flow.

– The Brownian motion on the sphere is introduced here as a 3-dimensional Wiener process on the rotational velocity. It is interpreted as all the interaction with surrounding particles, in a different way than [43, 19, 46] where it is derived from a Brownian potential from a given *a priori* density of polymers.

– Due to the difference of order of size between monomers, polymers and the spatial domain, the fact that fragmentation and elongation do not change the center of mass of the polymer could be justified. But one could consider non-local elongation and fragmentation.

– The above choice of the repartition kernel (self-similarity and definition with a reference function k_0) is mainly made to simplify notation on the stochastic differential equations below. More general probability kernel $k(R, R')$ from a polymer of size R providing a polymer of size R' could be taken without any difficulties.

4.4   The measure-valued stochastic process

First of all, let us introduce some technical notations for this section. Consider E a measurable space, we denote by $\mathcal{M}_F(E)$ the set of finite measures on E equipped with the topology of the weak convergence. Moreover, for any $\mu \in \mathcal{M}_F(E)$ and h a measurable bounded function on E, we write

$$\langle \mu, h \rangle_E = \int_E h(x)\mu(dx).$$

Also, we introduce the space

$$\mathcal{M}_\delta(E) := \left\{ \sum_{i=1}^n \delta_{x_i} : n \geqslant 0, \, (x_1, \ldots, x_n) \in E^n \right\},$$

that is the finite sum of Dirac masses which will be useful to describes the configuration of the system.

The last notation is $\mathcal{C}^{k_1,\ldots,k_n}(E_1 \times \cdots \times E_n)$ for the space of continuous functions with k_i continuous derivatives according to the variable belongs to E_i, for all $i = 1, \ldots, n$. Also if $\mathcal{C}$ is replace by $\mathcal{C}_b$, we consider bounded functions as well as all their derivatives.

4.4.1   The empirical measure

Our study focus on describing the evolution of the population of monomers and polymers. To that, we represent the population of monomers and polymers, respectively, with the following measures at time t:

$$\mu_t^m = \sum_{i=1}^{N_t^m} \delta_{X_t^i} \text{ and } \mu_t^p = \sum_{j=1}^{N_t^p} \delta_{Z_t^j}.$$

with $N_t^m = \langle \mu_t^m, 1 \rangle$ the total number of monomers and $N_t^p = \langle \mu_t^p, 1 \rangle$ of polymers. As the dynamic of the two populations is coupled, we introduce what we call the empirical measure of the system:

$$\mu_t = (\mu_t^m, \mu_t^p) \in \mathcal{M}_\delta(\Gamma) \times \mathcal{M}_\delta(\mathbb{N} \times \mathbb{S}^2 \times \Gamma). \tag{4.15}$$

This point of view define $(\mu_t)_{t \geq 0}$ as measure-valued stochastic process that entirely contains the information of the system. The aim of this section is thus to construct the stochastic differential equation of this process, that describes the evolution of our model.

For that, $\mathcal{M}_\delta(\Gamma) \times \mathcal{M}_\delta(\mathbb{N} \times \mathbb{S}^2 \times \Gamma)$ is equipped with the topology product. Until it is mentioned, h stands for a couple of functions

$$h = (f, g) \in \mathcal{C}_b^2(\overline{\Gamma}) \times \mathcal{C}_b^{0,2,2}(\mathbb{N} \times \mathbb{S}^2 \times \overline{\Gamma})$$

with vanishing normal derivatives on $\overline{\Gamma}$ and ϕ a function

$$\phi \in \mathcal{C}_b^2(\mathbb{R}, \mathbb{R}).$$

Also, we denote by

$$\langle \mu, h \rangle = \langle \mu^m, f \rangle_\Gamma + \langle \mu^p, g \rangle_{\mathbb{N} \times \mathbb{S}^2 \times \Gamma}.$$

If no doubt remains, we drop the space on which act $\langle, \rangle$. Finally, for technical reason, the evolution is regarding with respect to *test functions* ϕ_h defines, for all measure $\mu \in \mathcal{M}_F$, by

$$\phi_h(\mu) = \phi(< \mu, h >). \tag{4.16}$$

These functions are know to be convergence determining on the space of finite measure, see [42].

4.4.2   Continuous motion

In order to derive the evolution of $(\mu_t)_{t \geq 0}$ the empirical measure product eq. (4.15), we first focus on the continuous motion between to consecutive stopping time. For sake of clarity let us introduce two operators, first L be

$$Lh = (L_m f, L_p g), \tag{4.17}$$

where L_m and L_p are respectively given in eq. (4.2) and (4.9), and A such that

$$
\begin{aligned}
Ah = \Bigg(& D\nabla_x f^T \nabla_x f \,,\, \tfrac{1}{2}\left(\nabla_\eta g^T \mathcal{R}\right)\left(\mathcal{R}^T \nabla_\eta g\right) \\
& + \tfrac{1}{2}\left(\nabla_y g^T \mathcal{D}_\parallel\right)\left(\mathcal{D}_\parallel^T \nabla_y g\right) + \tfrac{1}{2}\left(\nabla_y g^T \mathcal{D}_\perp\right)\left(\mathcal{D}_\perp^T \nabla_y g\right)\Bigg),
\end{aligned}
\tag{4.18}
$$

where $\mathcal{D}_\perp = \sqrt{2D_\perp}(I_3 - n\otimes n)$, $\mathcal{D}_\parallel = \sqrt{2D_\parallel}n\otimes n$ and $\mathcal{R} = -\sqrt{2D_r}n\wedge\cdot$. Now we are in position to introduce the following lemma which states the evolution of the empirical product measure between jump (stopping) time.

Lemma 95. *Let T_k and T_{k+1} be two consecutive jump time. We assume that μ_t is the empirical product measure defined by eq. (4.15). The evolution of μ_t with respect to the functions ϕ_h defined in eq. (4.16) is given, for any $s, t \in (T_k, T_{k+1})$, by*

$$
\phi_h(\mu_t) = \phi_h(\mu_s) + \int_s^t \mathcal{L}_0\phi_h(\mu_\sigma)d\sigma + M_{t,s},
$$

where $M_{t,s}$ is a process starting in s and $\mathcal{L}_0$ defined by

$$
\mathcal{L}_0\phi_h(\mu) = \phi'(\langle\mu,h\rangle)\langle\mu,Lh\rangle + \phi''(\langle\mu,h\rangle)\langle\mu,Ah\rangle,
$$

with L and A respectively given in eq. (4.17) and eq. (4.18).

This lemma is a straightforward consequence of Itô calculus. Indeed, between two jumping time, the number of monomers N_s^m and polymers N_s^p are constant. Moreover, the size of each polymer is constant thus from the SDE on the motion of the monomers eq. (4.1) and its infinitesimal generator L_m defined in eq. (4.2), together with the SDE on the motion of the polymers eq. (4.8), on their orientation eq. (4.7) and the infinitesimal generator L_p defined in eq. (4.9), so we get by computation of the Itô rules the above lemma. Furthermore, the computation allow us to get the exact expression of the martingale $M_{t,s}$ which is decomposed as

$$
M_{t,s} = M_{t,s}^m + M_{t,s}^p,
\tag{4.19}
$$

with $M_{t,s}^m$ and $M_{t,s}^p$ two processes given by

$$
M_{t,s}^m = \int_s^t \phi'(\langle\mu_\sigma,h\rangle)\sum_{i=1}^{N_\sigma^m}\left(\sqrt{2D}\nabla f(X_\sigma^i)dW_\sigma^{(m)i}\right),
$$

and

$$
\begin{aligned}
M_{t,s}^p = \int_s^t \phi'(\langle\mu_\sigma,h\rangle)\sum_{j=1}^{N_\sigma^p}\Bigg(& \sqrt{2D_r}\nabla_n g(Z_\sigma^j)\cdot dB_\sigma^j \wedge H_\sigma^j \\
& + \nabla_y g(Z_\sigma^j)\cdot\left[\sqrt{2D_\perp}(I_3 - H_\sigma^j\otimes H_\sigma^j) + \sqrt{2D_\parallel}H_\sigma^j\otimes H_\sigma^j\right]dW_\sigma^{(p)j}\Bigg).
\end{aligned}
$$

We notice that $W_s^{(m)i}$, $W_s^{(p)j}$ and B_s^j are a family of 3-dimensional Wiener process with independent components corresponding to each monomers and polymers, respectively labeled by i and j.

4.4.3   The stochastic differential equation

In the previous section we write the evolution of the empirical measure between stopping times. The aim of this section is to describe the whole evolution of this measure with an SDE. To do that, we assume that we have a sequence $0 = T_0 < T_1 < T_2 < \cdots < T_N < T_{N+1}$ of consecutive stopping times and we suppose that the time t belongs to (T_N, T_{N+1}). Consequently, the empirical product measure μ_t satisfies, for any $t \in (T_N, T_{N+1})$

$$\phi_h(\mu_t) = \sum_{k=0}^{N-1} \left(\Delta\phi_h(\mu_{T_k}) + \int_{T_k}^{T_{k+1}^-} d\phi_h(\mu_s) \right) + \Delta\phi_h(\mu_{T_N}) + \int_{T_N}^{t} d\phi_h(\mu_s),$$

where $\Delta\phi_h(\mu_{T_k}) = \phi_h(\mu_{T_k}) - \phi_h(\mu_{T_k^-})$ and the convention $\mu_{0^-} = 0$. Consequently, remarking that the above equality is true for any sequence of stopping time, from lemma 95 we get the evolution of μ_t for any $t \geqslant 0$ given by

$$\phi_h(\mu_t) = \sum_{s \leqslant t} \left(\phi_h(\mu_{s^-} + \Delta\mu_s) - \phi_h(\mu_{s^-}) \right) + \int_0^t \mathcal{L}_0 \phi_h(\mu_s) ds + M_t^0, \qquad (4.20)$$

with $M_t^0 := M_{t,0}$ where $M_{t,0}$ satisfies eq. (4.19) and $\Delta\mu_s = \mu_s - \mu_s^-$. In order to define the transition $\Delta\mu_s$ we introduce the following notation

Notation 2. *We use the purely notional maps S_m^i and S_p^j for all $i, j \in \mathbb{N}$, such that for $\mu = (\mu_m, \mu_p) \in \mathcal{M}_\delta(\Gamma) \times \mathcal{M}_\delta(\mathbb{N} \times \mathbb{S}^2 \times \Gamma)$*

$$S_m^i(\mu) = X^i \ and \ S_p^j(\mu) = (R^j, H^j, Y^i).$$

In order to have a consistent definition of these two maps, we refer to [32].

Let s be a stopping time corresponding to an elongation event, where the monomer i elongate with the polymer j, the transition defines by eq. (4.10) - (4.11) leads to

$$\Delta\mu_s = \Delta_1^{i,j}\mu_s := \left(-\delta_{S_m^i(\mu_{s^-})}, -\delta_{S_p^j(\mu_{s^-})} + \delta_{S_p^j(\mu_{s^-})+\mathbf{e}_1} \right). \qquad (4.21)$$

This formally means that monomer i is killed, polymer j gets a length incremented by one. Now, when s is a stopping time with a fragmentation event, where the polymer j breaks up, the transition defined by eq. (4.14) and eq. (4.12) - (4.13) leads to

$$\Delta\mu_s = \Delta_2^j \mu_s := \left(0, \ \delta_{\Theta(\theta, S_p^j(\mu_{s^-}))} + \delta_{\Theta(1-\theta, S_p^j(\mu_{s^-}))} - \delta_{S_p^j(\mu_{s^-})} \right), \qquad (4.22)$$

where $\Theta(\theta, Z) = ([\theta R], H, Y)$ for all $Z = (R, H, Y) \in \mathbb{N} \times \mathbb{S}^2 \times \Gamma$. This formally means that polymer j of size R breaks up into two new polymers of size $[\theta R]$ and $[(1 - \theta)R]$. Nothing happens to the monomers. Finally, $\Delta\mu_s = (0,0)$ for all non-jump time.

Similarly as in [59, 32], the transition events of elongation and fragmentation will be described in term of Poisson point measures. Let us define them, together with the probabilistic objects of the model.

Definition 9 (Probabilistic objects)**.** *Let $(\Omega, \mathcal{F}, P)$ a sufficiently large probability space. We defined on this space the two independent random Poisson point measures*
i) The elongation point measure $Q^1(ds, di, dj, du)$ on $\mathbb{R}_+ \times \mathbb{N} \times \mathbb{N} \times \mathbb{R}_+$ with intensity

$$E\left[Q_1(ds, di, dj, du)\right] = ds du (\sum_{k \geqslant 1} \delta_k(di))(\sum_{k \geqslant 1} \delta_k(dj)).$$

ii) The fragmentation Poisson measure. $Q_2(ds, dj, d\theta, du)$ *on* $\mathbb{R}_+ \times \mathbb{N} \times (0, 1) \times \mathbb{R}_+$ *with intensity*

$$E\left[Q_2(ds, dj, d\theta, du)\right] = ds\,du\,k_0(\theta)d\theta\Big(\sum_{k \geqslant 1} \delta_k(dj)\Big).$$

where ds and du are Lebesgue measure on $\mathbb{R}^+$, $d\theta$ is the Lebesgue measure on $(0, 1)$ and $\sum_{k\geqslant 1} \delta_k(di)$ is the counting measure on $\mathbb{N}$. Moreover, we define a family of 3-dimensional Wiener process with independent components (and independent of the Poisson measures), indexed by $i \in \mathbb{N}$ and $j \in \mathbb{N}$:

$$(W_t^{(m)i})_{t\geqslant 0}, \ (W_t^{(p)j})_{t\geqslant 0}, \ and \ (B_t^j)_{t\geqslant 0}.$$

Finally, let $\mu_0 \in \mathcal{M}_\delta$ an initial random measure, independent of the above processes and the canonical filtration $(\mathcal{F}_t)_{t\geqslant 0}$ associated to these processes.

From eq. (4.20) together with eq. (4.21) - (4.22) and the probability objects given in definition 9, we are able to state the discrete-individual polymer-flow model that is the SDE on $(\mu_t)_{t\geqslant 0}$ for the function ϕ_h that reads

$$
\begin{aligned}
\phi_h(\mu_t) \ &= \ \phi_h(\mu_0) + \int_0^t \mathcal{L}_0\phi_h(\mu_s)ds \\
&+ \int_0^t \int_{\mathbb{N}\times\mathbb{N}\times\mathbb{R}_+} \Big(\phi_h(\mu_{s-} + \Delta_1^{i,j}\mu_s) - \phi_h(\mu_s^-)\Big) \\
&\qquad\qquad \times \mathbf{1}_{u\leqslant\tau(S_m^i(\mu_{s-}), S_p^j(\mu_{s-}))}\mathbf{1}_{i\leqslant N_{s-}^m, j\leqslant N_{s-}^p} \\
&\qquad\qquad \times Q_1(ds, di, dj, du) \\
&+ \int_0^t \int_{\mathbb{N}\times(0,1)\times\mathbb{R}_+} \Big(\phi_h(\mu_{s-} + \Delta_2^j\mu_s) - \phi_h(\mu_s^-)\Big) \\
&\qquad\qquad \times \mathbf{1}_{\Theta(\theta, S_p^j(\mu_{s-})), \Theta(1-\theta, S_p^j(\mu_{s-}))\geqslant R_0} \\
&\qquad\qquad \times \mathbf{1}_{u\leqslant\beta(S_p^j(\mu_s))}\mathbf{1}_{j\leqslant N_{s-}^p} \\
&\qquad\qquad \times Q_2(ds, dj, d\theta, du) \\
&+ M_t^0,
\end{aligned}
\tag{4.23}
$$

where $\mathcal{L}_0$ is the generator of the piecewise continuous motion defined in lemma 95 and $M_t^0 := M_{t,0}$ is the process given by eq. (4.19). Now, we can compute the infinitesimal of the process that is:

Lemma 96 (Infinitesimal generator). *The infinitesimal generator $\mathcal{L}$ associated to the SDE on $(\mu_t)_t$ for the function ϕ_h given by (4.23) is decomposed as follows*

$$\mathcal{L} = \mathcal{L}_0 + \mathcal{L}_1 + \mathcal{L}_2$$

where $\mathcal{L}_0$ is defined in lemma 95 and

$$
\begin{aligned}
\mathcal{L}_1\phi_h(\mu_t) \ &= \ \int_\Gamma \int_{\mathbb{N}\times\mathbb{S}^2\times\Gamma} \tau(x, z)\left(\phi_h(\mu_{s-} + \Delta_1) - \phi_h(\mu_{s-})\right) \\
&\qquad\qquad \times \mu_{s-}^m(dx)\mu_{s-}^p(dz),
\end{aligned}
$$

with $\Delta_1(x,z) = (-\delta_x, -\delta_z + \delta_{z+\mathbf{e}_1})$ and

$$\mathcal{L}_2\phi_h(\mu_t) \;=\; \int_{\mathbb{N}\times\mathbb{S}^2\times\Gamma}\int_0^1 \beta(z)\left(\phi_h(\mu_{s-}+\Delta_2)-\phi_h(\mu_{s-})\right)$$

$$\times\; \mathbf{1}_{[\theta r],[(1-\theta)r]>R_0}k_0(\theta)d\theta\mu_{s-}^p(dz),$$

with $\Delta_2(z) = (0, \delta_{\Theta(\theta,z)}+\delta_{\Theta(1-\theta,z)}-\delta_z)$.

This lemma is obtained by Markov properties. Indeed, by taking expectation in the eq. (4.23) and the definition of the random Poisson point measure, we identify the generator ([59, 32]). Thus the evolution of the empirical measure μ_t can be re-written as

$$\phi_h(\mu_t) = \phi_h(\mu_0) + \int_0^t \mathcal{L}\phi_h(\mu_s)ds + M_t^{total},$$

where

$$M_t^{total} = M_t^0 + M_t^1 + M_t^2, \tag{4.24}$$

with $M_t^0 := M_{t,0}$ the process given by eq. (4.19) and M_t^1, M_t^2 the compensated random Poisson measure that are for $k = 1,2$:

$$M_t^1 \;=\; \int_0^t\int_{\mathbb{N}\times\mathbb{N}\times\mathbb{R}_+}\cdots\left(Q_1(dsdidjdu)-E[Q_1(dsdidjdu)]\right)$$

$$M_t^2 \;=\; \int_0^t\int_{\mathbb{N}\times(0,1)\times\mathbb{R}_+}\cdots\left(Q_2(dsdjd\theta du)-E[Q_2(dsdjd\theta du)]\right)$$

with dots standing for the terms behind $Q_{k=1,2}$ in the eq. (4.23).

4.4.4   Existence, Uniqueness

In this section we study the well-posedness of the discrete-individual polymer-flow model eq. (4.23). For that we assume the following hypothesis:

(H1) Let τ and β be continuous non-negative function, uniformly bounded respectively by $C > 0$ and $B > 0$, that is

$$\tau(x,z) \leqslant C \text{ and } \beta(z) \leqslant B, \quad \forall x \in \Gamma, \forall z \in \mathbb{N}\times\mathbb{S}^2\times\Gamma.$$

(H2) We recall that $k_0 : (0,1)\mapsto\mathbb{R}_+$ is a symmetrical probability density function, *i.e.*

$$\int_0^1 k_0(\theta)d\theta = 1 \text{ and } k_0(\theta) = k_0(1-\theta), \forall\theta\in(0,1).$$

In order to state well-posedness of the problem we introduce the following definition of admissible solution. Solution are given in terms of a martingale problem. Its advantage relies on the fact that the limiting problem will be identified as a martingale problem.

Definition 10 (Admissible Solution). *Assuming that the probabilistic objects of definition 9 are given. An admissible solution to the discrete-individual polymer-flow model eq. (4.23) is a $(\mathcal{F}_t)_{t\geqslant 0}$-adapted measure-valued Markov process:*

$$\mu = (\mu^m, \mu^p) \in \mathcal{D}\left([0,\infty), \mathcal{M}_\delta(\Gamma)\times\mathcal{M}_\delta(\mathbb{N}\times\mathbb{S}^2\times\Gamma)\right),$$

such that, for all $\phi \in \mathcal{C}_b^2(\mathbb{R}, \mathbb{R})$ and $h \in \mathcal{C}_b^2(\overline{\Gamma}) \times \mathcal{C}_b^{0,2,2}(\mathbb{N} \times \mathbb{S}^2 \times \overline{\Gamma})$,

$$\phi_h(\mu_t) - \phi_h(\mu_0) - \int_0^t \mathcal{L}\phi_h(\mu_s)ds \qquad (4.25)$$

is a $L^1 - (\mathcal{F}_t)_{t \geqslant 0}$ martingale starting in $t = 0$ given by M_t^{total} defined in eq. (4.24) and where $\mathcal{L}$ the infinitesimal generator derived in lemma 96. Moreover, it satisfies

$$\int_\Gamma \mu_t^m(dx) + \int_{\mathbb{N} \times \mathbb{S}^2 \times \Gamma} r\mu_t^p(dz) = \int_\Gamma \mu_0^m(dx) + \int_{\mathbb{N} \times \mathbb{S}^2 \times \Gamma} r\mu_0^p(dz).$$

The last equation in the above definition stands for the mass balance of the system. Indeed, since neither production, nor degradation of monomers and polymers is assumed, together with the impermeability condition at the boundary (Neumann type boundary condition on u), the system preserves the total number of monomers. Now, we are able to state the following proposition:

Proposition 97. *Assuming that the probabilistic objects of definition 9 are given, hypothesis (H1-H2) are fulfilled, and*

$$E\left(\langle \mu_0, 1 \rangle\right) < +\infty,$$

then there exists a unique admissible solution $(\mu_t)_{t \geqslant 0}$ to the discrete-individual polymer-flow model eq. (4.23).

Furthermore, if for some $\alpha \geqslant 1$,

$$E\left(\langle \mu_0, 1 \rangle^\alpha\right) < +\infty,$$

then for any $T < \infty$,

$$E\left(\sup_{t \in [0,T]} \langle \mu_t, 1 \rangle^\alpha\right) < +\infty.$$

Proof. Following [59, 32], we only have to check the last point, and that the mass conservation holds. Indeed, we gave a constructive description of the stochastic process, based on the existence and uniqueness of equation of motion for individuals and on the Poisson measures. That the martingale property holds is a consequence of the generator identification above.

In order to prove the mass conservation, let $\phi = Id$ and $h = (1, \mathbf{r})$ with $\mathbf{r} : (r, \eta, y) \mapsto r$, then

$$\phi_h(\mu_t) = \int_\Gamma \mu_t^m(dx) + \int_{\mathbb{N} \times \mathbb{S}^2 \times \Gamma} r\mu_t^p(dz).$$

In that case we have

$$\phi_h(\mu_{s-} + \Delta_1^{i,j}\mu_s) - \phi_h(\mu_s^-) = \left\langle \Delta_1^{i,j}\mu_s, (1, \mathbf{r}) \right\rangle = 0,$$

and

$$\phi_h(\mu_{s-} + \Delta_2^j \mu_s) - \phi_h(\mu_s^-) = \left\langle \Delta_2^j \mu_s, (1, \mathbf{r}) \right\rangle = 0.$$

Moreover,

$$\mathcal{L}_0 \phi_h(\mu_s) = \langle \mu_{s-}, (L_m 1, L_p \mathbf{r}) \rangle = 0,$$

and $M_t^0 = 0$. Using the SDE eq. (4.23) on the empirical measure, we get the mass conservation.

We now show that jump times do note accumulate, thanks to moment estimates. We note $\tau_n = \inf\{t \geqslant 0, \langle \mu_t, 1 \rangle \geqslant n\}$. With eq. (4.23) and taking $\phi_h(\mu) = (\langle \mu, 1 \rangle)^\alpha$ (and truncating ϕ with $(n+1)^\alpha$ to be more correct) we get, neglecting the negative terms,

$$
\begin{aligned}
\sup_{s \in [0, t \wedge \tau_n]} \langle \mu_s, 1 \rangle^\alpha \;\leqslant\;& \langle \mu_0, 1 \rangle^\alpha \\
& + \int_0^{t \wedge \tau_n} \int_{\mathbb{N} \times (0,1) \times \mathbb{R}_+} [(\langle \mu_{s-}, 1 \rangle + 1)^\alpha - \langle \mu_{s-}, 1 \rangle^\alpha] \\
& \times \mathbf{1}_{u \leqslant \beta(S_p^j(\mu_{s-}))} \mathbf{1}_{j \leqslant N_{s-}^p} Q^2(ds, dj, d\theta, du).
\end{aligned}
$$

Using the standard estimates $(x+1)^\alpha - x^\alpha \leqslant C_\alpha(1 + x^{\alpha-1})$ for all $x \geqslant 0$ for some constant $C_\alpha > 0$, we deduce

$$
\begin{aligned}
\sup_{s \in [0, t \wedge \tau_n]} \langle \mu_s, 1 \rangle^\alpha \;\leqslant\;& \langle \mu_0, 1 \rangle^\alpha \\
& + C_\alpha \int_0^{t \wedge \tau_n} \int_{\mathbb{N} \times (0,1) \times \mathbb{R}_+} \left[1 + \langle \mu_{s-}, 1 \rangle^{\alpha-1} \right] \\
& \times \mathbf{1}_{u \leqslant \beta(S_p^j(\mu_{s-}))} \mathbf{1}_{j \leqslant N_{s-}^p} Q^2(ds, dj, d\theta, du).
\end{aligned}
$$

Taking expectations, since $N_{s-}^p = \langle \mu_{s-}^p, 1 \rangle$, β is bounded by B (*cf.* hypothesis (H1)) and the initial moment is finite, $E[\langle \mu_0, 1 \rangle^\alpha] < \infty$, we have, for some constant $C_\alpha := C_\alpha(\mu_0, B)$ (changing from line to line) depending on α, μ_0 and B

$$
E\left[\sup_{s \in [0, t \wedge \tau_n]} \langle \mu_s, 1 \rangle^p \right] \leqslant C_\alpha \left(1 + \int_0^{t \wedge \tau_n} E\left[\left(1 + \langle \mu_{s-}, 1 \rangle^{\alpha-1} \right) \langle \mu_{s-}^p, 1 \rangle \right] ds \right).
$$

Now remarking that $\langle \mu_{s-}^p, 1 \rangle \leqslant \langle \mu_{s-}, 1 \rangle$ and $\langle \mu_{s-}, 1 \rangle \leqslant \langle \mu_{s-}, 1 \rangle^\alpha$ since $\alpha \geqslant 1$ and $N_s^p \in \mathbb{N}$, we have

$$
E\left[\sup_{s \in [0, t \wedge \tau_n]} \langle \mu_s, 1 \rangle^p \right] \leqslant C_\alpha \left(1 + 2 \int_0^{t \wedge \tau_n} E\left[\langle \mu_{s-}, 1 \rangle^\alpha \right] ds \right).
$$

Using first this inequality with $\alpha = 1$, and then for some $\alpha \geqslant 1$, and using Grönwall's lemma, we can conclude that

$$
E\left[\sup_{s \in [0, t \wedge \tau_n]} \langle \mu_s, 1 \rangle^\alpha \right] < C_\alpha(t). \tag{4.26}
$$

Then the sequence τ_n needs to tends a.s to infinity. If not, we can find $T_0 < \infty$ such that $\epsilon = P(\sup_n \tau_n < T_0) > 0$. This implies $E\left[\sup_{s \in [0, T_0 \wedge \tau_n]} \langle \mu_s, 1 \rangle^\alpha \right] \geqslant \epsilon n^\alpha$, which contradicts eq. (4.26). So τ_n goes to infinity and we conclude by letting n to infinity in eq. (4.26) thanks to Fatou's lemma.

□

We will also need to derive our results to use ϕ unbounded and particularly some ϕ being like $x \mapsto x^\alpha$. For that we introduce the following corollary:

Corollary 98. *Assume (H1-H2) and for some $\alpha \geqslant 2$*

$$
E\left(\langle \mu_0, 1 \rangle^\alpha \right) < +\infty.
$$

1. *If for all measurable functions*

$$\phi \in \mathcal{C}^2(\mathbb{R}, \mathbb{R}) \text{ and } h \in \mathcal{C}_b^2(\overline{\Gamma}) \times \mathcal{C}_b^{0,2,2}(\mathbb{N} \times \mathbb{S}^2 \times \overline{\Gamma}),$$

such that, for all $\mu \in \mathcal{M}_\delta(\Gamma) \times \mathcal{M}_\delta(\mathbb{N} \times \mathbb{S}^2 \times \Gamma)$

$$|\phi_h(\mu)| + |\mathcal{L}\phi_h| \leqslant C(1 + \langle \mu, 1 \rangle^p),$$

2. *Or if*

$$\phi : x \mapsto x^\alpha \text{ with } \alpha \geqslant 1 \text{ and } h \in \mathcal{C}_b^2(\overline{\Gamma}) \times \mathcal{C}_b^{0,2,2}(\mathbb{N} \times \mathbb{S}^2 \times \overline{\Gamma}),$$

then the process

$$\phi_h(\mu_t) - \phi_h(\mu_0) - \int_0^t \mathcal{L}\phi_h(\mu_s)ds$$

is a $L^1 - (\mathcal{F}_t)_{t \geqslant 0}$ martingale starting from 0.

Proof. The first point is immediate thanks to proposition 97. For the second one, we'll use the conservation mass property to get a finner upper bound. The only term that could be a problem is the one given by $\mathcal{L}_1$. Take $\phi(x) = x^\alpha$, so that

$$
\begin{aligned}
| \mathcal{L}_1\phi_h(\mu_t) | &= | \int_\Gamma \int_{\mathbb{N} \times \mathbb{S}^2 \times \Gamma} \tau(x,z) \left(\phi_h(\mu_{s-} + \Delta_1) - \phi_h(\mu_{s-}) \right) \\
&\qquad \times \mu_{s-}^m(dx)\mu_{s-}^p(dz) |, \\
&\leqslant \int_\Gamma \int_{\mathbb{N} \times \mathbb{S}^2 \times \Gamma} \overline{\tau} C(h) \langle \mu_s, h \rangle^{\alpha-1} \mu_{s-}^m(dx)\mu_{s-}^p(dz), \\
&\leqslant \overline{\tau} C(h) t \sup_{[0,t]} \langle \mu_s, 1 \rangle^{\alpha-1} \langle \mu_s^m, 1 \rangle \langle \mu_s^p, 1 \rangle, \\
&\leqslant \overline{\tau} C(h) t \langle \mu_0^m, 1 \rangle \sup_{[0,t]} \langle \mu_s, 1 \rangle^{\alpha-1} \langle \mu_s^p, 1 \rangle, \\
&\leqslant \overline{\tau} C(h) t \langle \mu_0^m, 1 \rangle \sup_{[0,t]} \langle \mu_s, 1 \rangle^\alpha,
\end{aligned}
$$

where used the conservation of mass property in the last but one line. All other term are similarly bounded by $\sup_{[0,t]} \langle \mu_s, 1 \rangle^\alpha$, so that proposition 97 allows to conclude. $\qquad\square$

4.4.5 Coupled weak formulation and Martingale properties

The evolution of the empirical product measure, can be write in term of a system of two equations, one on the monomers measure and another on the polymers measure. We first remind some notations for this problem. The generator $\mathcal{L}$ is decomposed as follows

$$\mathcal{L} = \mathcal{L}^0 + \mathcal{L}^1 + \mathcal{L}^2,$$

with $\mathcal{L}^0$ given in lemma 95 and $\mathcal{L}^{k=1,2}$ in lemma 96. The martingale is given by

$$M_t^{total} = M_t^0 + M_t^1 + M_t^2,$$

with $M_t^0 := M_{t,0}$ given in eq. (4.19) and $M_t^{k=1,2}$ from the compensated Poisson *wrt* $Q_{k=1,2}$.

Now we decompose the martingale in several processes. Firstly, taking $\phi = Id$ and $g = 0$ in the total martingale, we get

$$M_t^m := M_t^{total}(\phi = Id, g = 0) = M_t^{0,m} + M_t^{1,m} + M_t^{2,m}, \tag{4.27}$$

and secondly, with $\phi = Id$ and $f = 0$,

$$M_t^p := M_t^{total}(\phi = Id, f = 0) = M_t^{0,p} + M_t^{1,p} + M_t^{2,p}, \tag{4.28}$$

where $M_t^{i,m} := M_t^i(\phi = Id, g = 0)$ and $M_t^{i,p} := M_t^i(\phi = Id, f = 0)$ for $i = 0, 1, 2$. We also notice that

$$M_t^{total}(\phi = Id) = M_t^m + M_t^p.$$

We are now ready to state our system as a coupled system of two equations. Let us take $\phi = Id$ the identity function in eq. (4.25), then we identify each equation by taking on one hand $h = (f, 0)$ and on the other hand $h = (0, g)$, together with the definition of $\mathcal{L}$ in lemma 96 we get the *weak formulation*:

$$
\begin{cases}
\langle \mu_t^m, f \rangle &= \langle \mu_0^m, f \rangle + \int_0^t \langle \mu_t^m, L_m f \rangle \, ds \\[2mm]
&\quad - \int_0^t \int_\Gamma \langle \mu_{s-}^p, \tau(x, \cdot) \rangle \, f(x) \mu_{s-}^m(dx) ds + M_t^m, \\[4mm]
\langle \mu_t^p, g \rangle &= \langle \mu_0^p, g \rangle + \int_0^t \langle \mu_t^p, L_p g \rangle \, ds \\[2mm]
&\quad + \int_0^t \int_{\mathbb{N} \times \mathbb{S}^2 \times \Gamma} \langle \mu_{s-}^m, \tau(\cdot, z) \rangle \, (g(z + \mathbf{e}_1) - g(z)) \, \mu_{s-}^p(dz) ds \\[2mm]
&\quad - \int_0^t \int_{\mathbb{N} \times \mathbb{S}^2 \times \Gamma} \int_0^1 \beta(z) \mathbf{1}_{[\theta r], [(1-\theta)r] > R_0} k_0(\theta) g(z) d\theta \mu_{s-}^p(dz) ds \\[2mm]
&\quad + 2 \int_0^t \int_{\mathbb{N} \times \mathbb{S}^2 \times \Gamma} \int_0^1 \beta(z) \mathbf{1}_{[\theta r], [(1-\theta)r] > R_0} k_0(\theta) g(\Theta(\theta, z)) d\theta \mu_{s-}^p(dz) ds \\[2mm]
&\quad + M_t^p.
\end{cases}
$$

(4.29)

We note that the integral with the factor 2 in front of it, is obtained by changing of variable and using the symmetry property on k_0 (H2).

The next proposition gives the quadratic variation of all these process.

Proposition 99. *Assume (H1-H2) and that*

$$E\left(\langle \mu_0, 1 \rangle^2 \right) < +\infty.$$

Then the process $M_t^{total}(\phi = Id) = M_t^m + M_t^p$ defined in eq. (4.27) and (4.28) is an $L^2 - (\mathcal{F}_t)_{t \geqslant 0}$ martingale starting from 0 with quadratic variations:

$$\left\langle M^{total} \right\rangle_t = \langle M^m \rangle_t + \langle M^p \rangle_t + \langle M^m, M^p \rangle_t,$$

such that:

The quadratic variation of M^m is

$$\langle M^m \rangle_t = \left\langle M^{0,m} \right\rangle_t + \left\langle M^{1,m} \right\rangle_t,$$

with

$$\left\langle M^{0,m} \right\rangle_t = 2D \int_0^t \int_\Gamma | \nabla f(x) |^2 \, \mu_s^m(dx) ds,$$

$$\left\langle M^{1,m} \right\rangle_t = \int_0^t \int_\Gamma \langle \mu_s^p, \tau(x, \cdot) \rangle \, f^2(x) \mu_s^m(dx) ds.$$

Then for M^p it is

$$\left\langle M^p \right\rangle_t = \left\langle M^{0,p} \right\rangle_t + \left\langle M^{1,p} \right\rangle_t + \left\langle M^{2,p} \right\rangle_t,$$

with

$$\left\langle M^{0,p} \right\rangle_t = \int_0^t \int_{\mathbb{N}\times\mathbb{S}^2\times\Gamma} \Big(\left(\nabla_n g^T \mathcal{R}\right) \left(\mathcal{R}^T \nabla_n g\right)$$
$$+ \left(\nabla_y g^T \mathcal{D}_\parallel\right) \left(\mathcal{D}_\parallel^T \nabla_y g\right) + \left(\nabla_y g^T \mathcal{D}_\perp\right) \left(\mathcal{D}_\perp^T \nabla_y g\right) \Big) \mu_s^p(dz)ds,$$

$$\left\langle M^{1,p} \right\rangle_t = \int_0^t \int_{\mathbb{N}\times\mathbb{S}^2\times\Gamma} \left\langle \mu_s^m, \tau(\cdot,z) \right\rangle \left(g(z+\mathbf{e}_1) - g(z)\right)^2 \mu_s^p(dz)ds,$$

$$\left\langle M^{2,p} \right\rangle_t = \int_0^t \int_{\mathbb{N}\times\mathbb{S}^2\times\Gamma} \int_0^1 \beta(z) \mathbf{1}_{[\theta r],[(1-\theta)r]>R_0} k_0(\theta)$$
$$\times \left(g(\Theta(\theta,z)) + g(\Theta(1-\theta,z)) - g(z)\right)^2 \mu_s^p(dz)d\theta ds.$$

Finally the cross variation is

$$\begin{aligned}
\left\langle M^m, M^p \right\rangle_t &= \left\langle M^{1,m}, M^{1,p} \right\rangle_t, \\
&= -2 \int_0^t \int_\Gamma \int_{\mathbb{N}\times\mathbb{S}^2\times\Gamma} \tau(x,z)f(x) \\
&\qquad \times \left(g(z+\mathbf{e}_1) - g(z)\right) \mu_s^m(dx)\mu_s^p(dz)ds.
\end{aligned}$$

Proof. The proof is standard. Lets take $\phi(x) = x^2$, such that $\phi_h(\mu) = (\langle \mu, 1\rangle)^2$. With corollary 98 we get that

$$(\langle \mu_t, h \rangle)^2 - (\langle \mu_0, h \rangle)^2 - \int_0^t \mathcal{L}(\langle \mu_s, h \rangle)^2 ds$$

is a martingale. Then we use Itô formula to compute $(\langle \mu_t, h \rangle)^2$ from eq. (4.29), which gives

$$(\langle \mu_t, h \rangle)^2 - (\langle \mu_0, h \rangle)^2 - 2 \int_0^t (\langle \mu_s, h \rangle) d(\langle \mu_s, h \rangle) - \left\langle M_t^m + M_t^p \right\rangle_t$$

is a martingale. Now, by unicity of the Doob-Meyer decomposition, comparing these two expressions leads to the quadratic variations given in the proposition. $\qquad\square$

Remark 100. *We notice that all the cross variations which are not given in the proposition are in fact equal to zero.*

4.5 Scaling equations and the limit problem

4.5.1 Infinite monomers approximation with large polymers

Let us introduce a scaling parameter $n \in \mathbb{N}^*$ that will be discussed later. We consider a set of parameter

$$\tau^n \text{ and } \beta^n \text{ satisfying (H1)},$$

$$k_0^n \text{ satisfying (H2) and } R_0^n > 0,$$

that depends on this parameter n, thus $\mathcal{L}_1$ and $\mathcal{L}_2$ are changed in consequences, that leads to a generator denoted by $\tilde{\mathcal{L}}^n$ defined as in lemma 96 but with rescaled parameters.

Remark 101. *We note here that $\mathcal{L}^0$ is unchanged, indeed, we assume that the diffusion coefficients D, $D_\perp$, $D_\parallel$ and D_r are constant. It seems to be a strong hypothesis but the scaling of these coefficients are currently not derived, maybe one could inspired by [46]. We believe that the mathematical analysis is similar when the diffusion is rescaled.*

Now, we rescale the initial condition from this parameter, let $\tilde{\mu}_0^n \in \mathcal{M}_\delta(\Gamma) \times \mathcal{M}_\delta(\mathbb{N} \times \mathbb{S}^2 \times \Gamma)$ from a quantity M_0 of monomers, N_0 of polymers, such that

$$\tilde{\mu}_0^n = \left(\sum_{i=0}^{[nM_0]} \delta_{X_0^i}, \sum_{j=0}^{N_0} \delta_{\tilde{Z}_0^{i,n}} \right).$$

with $\tilde{Z}_0^{i,n} = (\tilde{R}_0^{j,n} = [nR_0^j], H_0^j, Y_0^j)$. This transformation is nothing but considering a large number of monomers and large size of polymers (in terms of numbers of monomers in the polymers). For all $n \in \mathbb{N}^*$, we have a unique solution $\tilde{\mu}_t^n$ given by the eq. (4.23) where the coefficients (τ, β, k_0) and initial condition μ_0 are respectively replaced by (τ^n, β^n, k_0^n) and $\tilde{\mu}_0^n$. The aim of the scaling is now to study the problem when the mass (or the size) of one monomer is given by the parameter $1/n$.

Let us now rescale the solution for a large population of monomers by taking a mass of monomer in $1/n$, thus

$$\mu_t^n = \left(\frac{1}{n} \tilde{\mu}_t^{m,n}, \sum_{j=0}^{\tilde{N}_t^{p,n}} \delta_{Z_t^{i,n}} \right), \tag{4.30}$$

with $\tilde{N}_t^{p,n} = \langle \tilde{\mu}_t^{p,n}, 1 \rangle$ (idem for $\tilde{N}_t^{m,n}$) and

$$Z_t^{i,n} = (R_t^{j,n} = \tilde{R}_t^{j,n}/n, H_t^j, Y_t^j) \in \frac{1}{n}\mathbb{N} \times \mathbb{S}^2 \times \Gamma.$$

Remark 102. *We notice that the size of the polymers (numbers of monomers in the polymers) is rescaled from the size of the monomers, this suggests that the size will describe now a physical length.*

Now, the rescaled empirical measure belongs to a different space that is

$$\mu_t^n \in \mathcal{M}_\delta(\Gamma) \times \mathcal{M}_\delta(\frac{1}{n}\mathbb{N} \times \mathbb{S}^2 \times \Gamma) \hookrightarrow \mathcal{M}_\delta(\Gamma) \times \mathcal{M}_\delta(\mathbb{R}_+ \times \mathbb{S}^2 \times \Gamma).$$

The injection is used to stay in a same state value for the stochastic processes μ_t^n.

From this scaling, we denote several relations that will be used in the next:

$$\begin{aligned}
\langle \tilde{\mu}_t^{m,n}, 1 \rangle &= n \langle \mu_t^{m,n}, 1 \rangle, \\
\langle \tilde{\mu}_t^{p,n}, 1 \rangle &= \langle \mu_t^{p,n}, 1 \rangle, \\
\langle \tilde{\mu}_t^{m,n}, \tau^n(\cdot, z) \rangle &= n \langle \mu_t^{m,n}, \tau^n(\cdot, z)) \rangle, \\
\langle \tilde{\mu}_t^{p,n}, \tau^n(x, \cdot) \rangle &= \langle \mu_t^{p,n}, \tau^n(x, (n, 1, 1)\cdot) \rangle, \\
\langle \tilde{\mu}_t^{p,n}, \beta^n(\cdot) \rangle &= \langle \mu_t^{p,n}, \beta^n((n, 1, 1)\cdot) \rangle,
\end{aligned} \tag{4.31}$$

where $(n, 1, 1) \cdot (r, \eta, y) = (nr, \eta, y)$. The three first ones are the consequences of the fact that the number of monomers increases by a factor n, but not the number of polymers. And the two last ones are the consequences of the fact that the number of monomers in the polymers increases by a factor n. The following proposition is a consequence of these relations eq. (4.31) and proposition 99:

Proposition 103. *Assume that* (τ^n, β^n) *satisfy (H1),* k_0^n *satisfies (H2) and*

$$E\left(\langle \mu_0^n, 1\rangle^2\right) < +\infty.$$

Then the rescaled measure μ_t^n *defined in eq. (4.30) is solution, for all* $f \in C^2(\overline{\Gamma})$ *and* $g \in C_b^{0,2,2}(\mathbb{R}_+ \times \mathbb{S}^2 \times \overline{\Gamma})$ *(still with vanishing normal derivatives), of*

$$
\begin{cases}
\langle \mu_t^{m,n}, f\rangle = \langle \mu_0^{m,n}, f\rangle + \int_0^t \langle \mu_t^{m,n}, L_m f\rangle\,ds \\[2mm]
\qquad - \int_0^t \int_\Gamma \langle \mu_{s-}^{p,n}, \tau^n(x, (n,1,1)\cdot)\rangle\, f(x)\mu_{s-}^{m,n}(dx)ds + M_t^{m,n}, \\[4mm]
\langle \mu_t^{p,n}, g\rangle = \langle \mu_0^{p,n}, g\rangle + \int_0^t \langle \mu_t^{p,n}, L_p g\rangle\,ds \\[2mm]
\qquad + \int_0^t \int_{\mathbb{R}_+ \times \mathbb{S}^2 \times \Gamma} n\langle \mu_{s-}^{m,n}, \tau^n(\cdot, (n,1,1)\cdot z)\rangle \left(g(z + \frac{1}{n}\mathbf{e}_1) - g(z)\right) \\[2mm]
\qquad\qquad\qquad\qquad\qquad\qquad\qquad\qquad\qquad \times\ \mu_{s-}^{p,n}(dz)ds \\[4mm]
\qquad + 2\int_0^t \int_{\mathbb{R}_+ \times \mathbb{S}^2 \times \Gamma} \int_0^1 \beta^n((n,1,1)\cdot z)\mathbf{1}_{[\theta nr],[(1-\theta)nr]>R_0} k_0^n(\theta) \\[2mm]
\qquad\qquad\qquad\qquad\qquad\qquad \times\ (2g(\Theta^n(\theta,z)) - g(z))\,d\theta\mu_{s-}^{p,n}(dz)ds \\[4mm]
\qquad + M_t^{p,n},
\end{cases}
$$

$$(4.32)$$

where $\Theta^n(\theta, Z) = ([\theta n R]/n, H, Y)$ *and* $M_t^{total,n} = M_t^{m,n} + M_t^{p,n}$ *is a square integrable martingale starting at 0 with quadratic variations:*

$$\left\langle M^{total,n}\right\rangle_t = \langle M^{m;n}\rangle_t + \langle M^{p,n}\rangle_t + \langle M^{m,n}, M^{p,n}\rangle_t$$

such that:

The quadratic variation of $M^{m,n}$ *is*

$$\langle M^{m,n}\rangle_t = \left\langle M^{0,m,n}\right\rangle_t + \left\langle M^{1,m,n}\right\rangle_t,$$

with

$$
\begin{aligned}
\left\langle M^{0,m,n}\right\rangle_t &= \frac{2D}{n}\int_0^t |\nabla f(x)|^2\, \mu_s^{m,n}(dx)ds, \\
\left\langle M^{1,m,n}\right\rangle_t &= \frac{1}{n}\int_0^t \int_\Gamma \langle \mu_s^{p,n}, \tau^n(x, (n,1,1)\cdot)\rangle\, f^2(x)\mu_s^{m,n}(dx)ds.
\end{aligned}
$$

Then for $M^{p,n}$ *it is*

$$\langle M^{p,n}\rangle_t = \left\langle M^{0,p,n}\right\rangle_t + \left\langle M^{1,p,n}\right\rangle_t + \left\langle M^{2,p,n}\right\rangle_t,$$

with

$$\left\langle M^{0,p,n}\right\rangle_t = \int_0^t \int_{\mathbb{R}_+\times\mathbb{S}^2\times\Gamma} \Big(\left(\nabla_n g^T \mathcal{R}\right)\left(\mathcal{R}^T \nabla_n g\right)$$
$$+ \left(\nabla_y g^T \mathcal{D}_\|\right)\left(\mathcal{D}_\|^T \nabla_y g\right) + \left(\nabla_y g^T \mathcal{D}_\perp\right)\left(\mathcal{D}_\perp^T \nabla_y g\right)\Big)\mu_s^{p,n}(dz)ds,$$

$$\left\langle M^{1,p,n}\right\rangle_t = \int_0^t \int_{\mathbb{R}_+\times\mathbb{S}^2\times\Gamma} n\left\langle \mu_s^{m,n}, \tau^n(\cdot,(n,1,1)\cdot z)\right\rangle \left(g(z+\frac{1}{n}\mathbf{e}_1) - g(z)\right)^2 \mu_s^{p,n}(dz)ds,$$

$$\left\langle M^{2,p,n}\right\rangle_t = \int_0^t \int_{\mathbb{R}_+\times\mathbb{S}^2\times\Gamma} \int_0^1 \beta^n((n,1,1)\cdot z)\mathbf{1}_{[\theta nr],[(1-\theta)nr]>R_0}k_0^n(\theta)$$
$$\times \left(g(\Theta^n(\theta,z)) + g(\Theta^n(1-\theta,z)) - g(z)\right)^2 \mu_s^{p,n}(dz)d\theta ds.$$

Finally the cross variation is

$$\left\langle M^{m,n}, M^{p,n}\right\rangle_t = \left\langle M^{1,m,n}, M^{1,p,n}\right\rangle_t$$
$$= -2\int_0^t \int_\Gamma \int_{\mathbb{R}_+\times\mathbb{S}^2\times\Gamma} \tau^n(x,(n,1,1)\cdot z)f(x)$$
$$\times \left(g(z+\frac{1}{n}\mathbf{e}_1) - g(z)\right)\mu_s^{m,n}(dx)\mu_s^{p,n}(dz)ds.$$

4.5.2 The limit problem

We now recall our assumptions and make the following mean-field specific scaling

(H1) Let τ and β be continuous non-negative function, uniformly bounded respectively by $\overline{\tau} > 0$ and $\overline{\beta} > 0$, that is

$$\tau(x,z) \leqslant \overline{\tau} \text{ and } \beta(z) \leqslant \overline{\beta}, \quad \forall x \in \Gamma, \forall z \in \mathbb{N}\times\mathbb{S}^2\times\Gamma.$$

Moreover, τ belongs to $C_b^{0,1,0,0}(\Gamma\times\mathbb{R}_+^*\times\mathbb{S}^2\times\Gamma)$.

(H2) Let $k_0 : (0,1) \mapsto \mathbb{R}_+$ is a symmetrical probability density function, *i.e.*

$$\int_0^1 k_0(\theta)d\theta = 1 \text{ and } k_0(\theta) = k_0(1-\theta), \forall\theta \in (0,1).$$

(H3) Let τ^n, β^n, k_0^n and R_0^n defined by $\forall x \in \Gamma$, $\forall z \in \mathbb{N}\times\mathbb{S}^2\times\Gamma$ and $\forall n \in \mathbb{N}$,

$$\begin{aligned}
\tau^n(x,(n,1,1)\cdot z) &= \tau(x,z), \\
\beta^n((n,1,1)\cdot z) &= \beta(z), \\
k_0^n(\theta) &= k_0(\theta), \\
R_0^n &= R_0.
\end{aligned}$$

(H4) The initial measure μ_0^n converge in law and for the weak topology towards a couple (μ_0^m, μ_0^p) of non-negative measure where μ^n is a deterministic finite measure on Γ and μ_0^p a finite random measure in $\mathcal{M}_\delta(\mathbb{R}_+^*\times\mathbb{S}^2\times\Gamma)$, and, for some $\alpha \geqslant 2$,

$$\sup_n E\left(\langle\mu_0^n,1\rangle^\alpha\right) < \infty.$$

Remark 104. *In order to facilitate the following computation, the scaling in (H3) is taken with equalities for all n, but could be easily replaced by strong limit in n.*

Remark 105. *Below we will state the limiting problem, using the same notation as for the **initial** problem of subsection 4.4, in particular for μ^m, μ^p, etc... We hope that no confusion will be made.*

Under these assumptions we formally derive from eq. (4.32) our *candidate* limit problem that is for any $f \in \mathcal{C}_b^2(\overline{\Gamma})$ and $g \in \mathcal{C}_b^{1,2,2}(\mathbb{R}_+ \times \mathbb{S}^2 \times \overline{\Gamma})$,

$$
\begin{cases}
\langle \mu_t^m, f \rangle = \langle \mu_0^m, f \rangle + \int_0^t \langle \mu_t^m, L_m f \rangle \, ds \\
\qquad\qquad - \int_0^t \int_\Gamma \langle \mu_{s-}^p, \tau(x, \cdot) \rangle f(x) \mu_{s-}^m(dx) ds, \\[2mm]
\langle \mu_t^p, g \rangle = \langle \mu_0^p, g \rangle + \int_0^t \langle \mu_t^p, L_p g \rangle \, ds \\
\qquad\qquad + \int_0^t \int_{\mathbb{R}_+ \times \mathbb{S}^2 \times \Gamma} \langle \mu_{s-}^m, \tau(\cdot, z) \rangle \frac{\partial}{\partial r} g(z) \mu_{s-}^p(dz) ds \\
\qquad\qquad - \int_0^t \int_{\mathbb{R}_+ \times \mathbb{S}^2 \times \Gamma} \beta(z) g(z) d\theta \mu_{s-}^p(dz) ds \\
\qquad\qquad + 2 \int_0^t \int_{\mathbb{R}_+ \times \mathbb{S}^2 \times \Gamma} \int_0^1 \beta(z) k_0(\theta) g(\theta r, \eta, y)) d\theta \mu_{s-}^p(dz) ds \\
\qquad\qquad + \overline{M}_t^p.
\end{cases}
\tag{4.33}
$$

where $\overline{M}_t^p = \overline{M}_t^{0,p} + \overline{M}_t^{2,p}$ is a martingale with

$$
\overline{M}_t^{0,p} = \int_0^t \sum_{j=1}^{N_s^p} \left[\sqrt{2D_r} \nabla_n g(Z_s^j) \cdot dB_s^j \wedge H_s^j \right.
$$

$$
\left. + \nabla_y g(Z_s^j) \cdot \left[\sqrt{2D_\perp}(I_3 - H_s^j \otimes H_s^j) + \sqrt{2D_{\|}} H_s^j \otimes H_s^j \right] dW_s^{(p)j} \right],
$$

and

$$
\begin{aligned}
\overline{M}_t^{2,p} &= \int_0^t \int_{\mathbb{N} \times (0,1) \times \mathbb{R}_+} \left(g(\Theta(\theta, Z_s^j)) + g(\Theta(1 - \theta, Z_s^j)) - g(Z_s^j) \right) \\
&\qquad \times \mathbf{1}_{u \leqslant \beta_{s-}^j} \mathbf{1}_{j \leqslant N_{s-}^p} \\
&\qquad \times \left(Q_2(ds, dj, d\theta, du) - E[Q_2(ds, dj, d\theta, du)] \right).
\end{aligned}
$$

Remark 106. *The identification of the limit problem will be through the martingale problem associated to eq. (4.33), which we now state below. As this martingale problem is very much similar to the one studies in paragraph 4.4.4, we omit the justification.*

Before proving a convergence theorem to this limit problem we first need a result on its well-posedness. It is the following lemma:

Lemma 107. *Let us assume (H1-H2) and $\mu_0 \in \mathcal{M}_F^+(\Gamma) \times \mathcal{M}_\delta^+(\mathbb{R}_+^* \times \mathbb{S}^2 \times \Gamma)$. For any $T > 0$, there exists at least one solution $(\mu_t)_{t \geqslant 0}$ to the limit problem eq. (4.33) such that*

$$
\mu \in \mathcal{D}(0, T; \mathcal{M}_F^+(\Gamma) \times \mathcal{M}_F^+(\mathbb{R}_+^* \times \mathbb{S}^2 \times \Gamma)).
$$

Moreover, μ^p remains a point process, that is $\mu^p \in \mathcal{M}_\delta(\mathbb{R}_+^* \times \mathbb{S}^2 \times \Gamma)$ for all $T \leqslant t \geqslant 0$, and we have the following conservation, for any $t \geqslant 0$

$$\langle \mu_t^m, \mathbf{1} \rangle + \langle \mu_t^p, \mathbf{r} \rangle = \langle \mu_0^m, \mathbf{1} \rangle + \langle \mu_0^p, \mathbf{r} \rangle \,,$$

(where $\mathcal{M}^+$ denotes the cone of positive measures)

Proof. Let us consider an auxiliary problem: For any $h = (f, g) \in \mathcal{C}_b^0(\Gamma) \times \mathcal{C}_b^{1,0,0}(\mathbb{R}_+ \times \mathbb{S}^2 \times \Gamma)$ and $t \geqslant 0$

$$
\begin{aligned}
\langle \mu_t^m, f \rangle &= \langle \mu_0^m, f \rangle - \int_0^t \int_\Gamma \langle \mu_s^p, \tau(x, \cdot) \rangle \, f(x) \mu_s^m(dx) ds \\
\langle \mu_t^p, g \rangle &= \langle \mu_0^p, g \rangle + \int_0^t \int_{\mathbb{R}_+ \times \mathbb{S}^2 \times \Gamma} \langle \mu_s^m, \tau(\cdot, z) \rangle \, \partial_r g(z) \mu_s^p(dz) ds
\end{aligned}
\tag{4.34}
$$

This system involves, only, polymerization. We do not consider at this time spacial and rotational motion for sake of simplicity.

We consider through this proof that μ^0 is given such that,

$$\mu_0^m \in \mathcal{M}_F(\Gamma) \text{ a non-negative measure,}$$

and

$$\mu_0^p = \sum_{j=1}^{N^p} \delta_{(R_0^j, H_0^j, Y_0^j)} \in \mathcal{M}_\delta(\mathbb{R}_+^* \times \mathbb{S}^2 \times \Gamma), \text{ with } R_0^j > 0, \ H_0^j \in \mathbb{S}^2, \ Y_0^j \in \Gamma$$

where $N^p = \langle \mu_0^p, \mathbf{1} \rangle$. Hence, a solution to the problem eq. (4.34) is given by a solution to

$$
\begin{aligned}
\langle \mu_t^m, f \rangle &= \langle \mu_0^m, f \rangle - \int_0^t \int_\Gamma \langle \mu_s^p, \tau(x, \cdot) \rangle \, f(x) \mu_s^m(dx) ds \\
R_t^j &= R_0^j + \int_0^t \left\langle \mu_s^m, \tau(\cdot, R_s^j) \right\rangle ds, \ j = 1, \dots, N^p
\end{aligned}
\tag{4.35}
$$

where $\mu_t^p = \sum_{j=1}^{N^p} \delta_{(R_t^j, H_0^j, Y_0^j)}$.

Let us defined S defined on $C(0, T; \mathcal{M}_F(\Gamma) \times \mathbb{R}^{N^p})$ such that $(\tilde{\mu}_t^m, (\tilde{R}_t^i)_i)_{t \geqslant 0}$ is given by

$$
\begin{aligned}
\langle \tilde{\mu}_t^m, f \rangle &= \langle \mu_0^m, f \rangle - \int_0^t \int_\Gamma \langle \mu_s^p, \tau(x, \cdot) \rangle \, f(x) \mu_s^m(dx) ds \\
\tilde{R}_t^j &= R_0^j + \int_0^t \left\langle \mu_s^m, \tau(\cdot, R_s^j) \right\rangle ds, \ j = 1, \dots, N^p
\end{aligned}
$$

We equipped $C(0, T; \mathcal{M}_F(\Gamma) \times \mathbb{R}^{N^p})$ with the metric

$$d_\infty := \sup_{t \in (0, T)} \left(\varrho(\mu_t^m, \mu_t^{m\prime}) + \sup_{1 \leqslant j \leqslant N^p} |R_t^j - R_t^{j\prime}| \right)$$

where

$$\varrho(\mu^m, \mu^{m\prime}) := \sup_{f \in \mathcal{C}_b^0(\Gamma), \|f\|_{L^\infty} \leqslant 1} \int_\Gamma f(x)(\mu^m - \mu^{m\prime})(dx).$$

This metric makes $C(0, T; \mathcal{M}_F(\Gamma) \times \mathbb{R}_+^{*N^p})$ a complete space. We are now in position to state a Banach fixed point on S. We first considered the subset

$$\mathcal{K}_T = \left\{ (\mu^m, (R^j)_j) \in \mathcal{C}^0(0, T; \mathcal{M}_F(\Gamma) \times \mathbb{R}^{N^p}), \right.$$

$$\forall t \geqslant 0, \ \mu_t^m \text{ is a non-negative measure and } R_t^j > 0,$$

$$\forall A \subset \mathcal{B}(\Gamma), \ \forall s \leqslant t, \ \mu_t^m(A) \leqslant \mu_s^m(A),$$

$$\left. \langle \mu_t^m, \mathbf{1} \rangle + \sum_{i=1}^{N^p} R_t^i = \rho_0 \right\}$$

This subset is a non-empty set since the measure 0 together with the sequence $R_t^i = \rho_0/N^p$ belongs to $\mathcal{K}_T$. Moreover, S restricted to $\mathcal{K}_T$ remains into itself whenever T is small enough, that is $S : \mathcal{K}_T \mapsto \mathcal{K}_T$. Indeed, non-negativeness of $\tilde{\mu}^m$ holds true when T is small enough (depending on τ, ρ_0 and N^p) and it is obvious that $\tilde{R}^j$ remains positive, for all j. The mass conservation is also obviously satisfied.

Now, let us take $(\mu^m, (R^j)_j)$ and $(\mu^{m\prime}, (R^{j\prime})_j)$ both in $C(0, T; \mathcal{M}_F(\Gamma) \times \mathbb{R}_+^{*N^p})$, from eq. (4.35), we get

$$\left| R_t^j - R_t^{j\prime} \right| \leqslant \int_0^t \left| \left\langle \mu_s^m - \mu_s^{m\prime}, \tau(\cdot, Z_t^j) \right\rangle \right| ds + \int_0^t \left| \left\langle \mu_s^m, \tau(\cdot, Z_s^j) - \tau(\cdot, Z_s^{j\prime}) \right\rangle \right| ds. \quad (4.36)$$

Moreover, for any $f \in \mathcal{C}_b^0(\Gamma)$

$$\left| \left\langle \mu_t^m - \mu_t^{m\prime}, f \right\rangle \right| \leqslant \int_0^t \int_\Gamma \left| \left\langle \mu_s^p - \mu_s^{p\prime}, \tau(x, \cdot) \right\rangle f(x) \mu_s^m(dx) \right| ds$$

$$+ \int_0^t \left| \int_\Gamma \left\langle \mu_s^{p\prime}, \tau(x, \cdot) \right\rangle f(x)(\mu_s^m - \mu_s^{m\prime})(dx) \right| ds. \quad (4.37)$$

The aim of the following is to bound each terms in eq. (4.36) and (4.37). For that, from (H1) we remark that for any $x \in \mathbb{R}_+^*$,

$$\begin{aligned} \left| \left\langle \mu_t^p - \mu_t^{p\prime}, \tau(x, \cdot) \right\rangle \right| &= \sum_{i=1}^{N^p} \left| \tau(x, Z_t^j) - \tau(x, Z_t^{j\prime}) \right| \\ &\leqslant N^p \|\partial_r \tau\|_{L^\infty} \sup_{1 \leqslant j \leqslant N^p} \left| R_t^j - R_t^{j\prime} \right|. \end{aligned} \quad (4.38)$$

Then, from (H1) for any $f \in \mathcal{C}_b^0(\Gamma)$, $x \mapsto \langle \mu_s^{p\prime}, \tau(x, \cdot) \rangle f(x)$ belongs to $\mathcal{C}_b^0(\Gamma)$ too, thus for any $f \in \mathcal{C}_b^0(\Gamma)$ with $\|f\|_{L^\infty} \leqslant 1$:

$$\int_\Gamma \left\langle \mu_s^{p\prime}, \tau(x, \cdot) \right\rangle f(x)(\mu_s^m - \mu_s^{m\prime})(dx) \leqslant N^p \|\tau\|_{L^\infty} \varrho(\mu_s^m, \mu_s^{m\prime}). \quad (4.39)$$

Hence, combining eq. (4.37), eq. (4.38) and eq. (4.39), there exists M depending on τ, ρ_0 and N^p such that for all $t \geqslant 0$

$$\varrho(\mu_t^m, \mu_t^{m\prime}) \leqslant M \int_0^t \left(\sup_{1 \leqslant j \leqslant N^p} \left| R_s^j - R_s^{j\prime} \right| + \varrho(\mu_s^m, \mu_s^{m\prime}) \right) ds. \quad (4.40)$$

Now, from eq. (4.36) and (H1), there exists a constant still denoted by M (depending on the same parameters) such that for all $t \geqslant 0$

$$\sup_{1 \leqslant j \leqslant N^p} \left| R_t^j - R_t^{j'} \right| \leqslant M \int_0^t \left(\sup_{1 \leqslant j \leqslant N^p} \left| R_s^j - R_s^{j'} \right| + \varrho(\mu_s^m, \nu_s^m) \right) ds, \qquad (4.41)$$

and thus combining eq. (4.40) and eq. (4.41), we get

$$\sup_{1 \leqslant j \leqslant N^p} \left| R_t^j - R_t^{j'} \right| + \varrho(\mu_t^m, \mu_t^{m\prime}) \leqslant 2M \int_0^t \left(\sup_{1 \leqslant j \leqslant N^p} \left| R_s^j - R_s^{j'} \right| + \varrho(\mu_s^m, \mu_s^{m\prime}) \right) ds. \quad (4.42)$$

Finally, when taking the $\sup_{(0,T)}$ in eq. (4.42), it follows that S is a contraction with T small enough. Hence, there exists a unique solution to eq. (4.35). Since the choice of T depends only on τ, ρ_0 and N^p, we are able to extend the solution on any interval $[0, T]$ with $T > 0$. It follows that there exists at least one solution to the weak formulation eq. (4.34). $\qquad\square$

The extension of this proof (for the existence) with space motion does not pose any difficulties as long as each individual stochastic differential equation for polymers' displacement is well defined, and stay in a compact (which is ensured by boundary condition). The existence of the whole stochastic process defined by eq. (4.33) follows then by similar calculation of the paragraph 4.4.4 and moment estimates (see also [31, Prop 3.2] and [134, Prop 2.2.5]). For strong unicity, we refer as well to [134, Prop 2.2.6].

Let us define the following generator, for any $\phi_h(\mu) = \phi(\langle \mu, h \rangle)$ with $h \in \mathcal{C}_b^2(\overline{\Gamma}) \times \mathcal{C}_b^{1,2,2}(\mathbb{R}_+ \times \mathbb{S}^2 \times \overline{\Gamma})$ and $\phi \in \mathcal{C}_b^2(\mathbb{R})$,

$$\mathcal{L}^\infty \phi_h = \mathcal{L}_0 \phi_h + \mathcal{L}_1^\infty \phi_h + \mathcal{L}_2^\infty \phi_h \qquad (4.43)$$

where $\mathcal{L}_0$ defined in lemma 95, and $\mathcal{L}_1^\infty$ is associated to the deterministic elongation process, and reads

$$\mathcal{L}_1^\infty \phi_h = \phi'(\langle \mu, h \rangle) \left\langle \mu, \left(- \langle \tau(x, .), \mu^p \rangle f(x), \langle \tau(., z), \mu^m \rangle \frac{\partial g(z)}{\partial r} \right) \right\rangle$$

and finally $\mathcal{L}_2^\infty$ is associated to the (random) fragmentation process on continuous-size polymer, and reads

$$\mathcal{L}_2^\infty \phi_h = \int_{\mathbb{R}_+ \times \mathbb{S}^2 \times \Gamma} \int_0^1 \beta(z) \Big[\phi\big(\langle \mu, h \rangle + g(\Theta(\theta, z)) + g(\Theta(1 - \theta), z) - g(z) \big) - \phi\big(\langle \mu, h \rangle \big) \Big]$$
$$\times k(\theta) d\theta \mu^p(dz)$$

We have the analogous property of corollary 98 and proposition 99:

Proposition 108. *Assume (H1-H2). Suppose* $\mu_0 \in \mathcal{M}_F^+(\Gamma) \times \mathcal{M}_\delta(\mathbb{R}^* \times \mathbb{S}^2 \times \Gamma)$, *such that the second moment satisfies* $E\Big(\langle \mu_0, 1 \rangle^2 \Big) < \infty$. *Then*

    1. for any
$$\phi \in \mathcal{C}^2(\mathbb{R}, \mathbb{R}) \ and \ h \in \mathcal{C}_b^2(\overline{\Gamma}) \times \mathcal{C}_b^{1,2,2}(\mathbb{R}_+ \times \mathbb{S}^2 \times \overline{\Gamma}),$$
    such that, for all $\mu \in \mathcal{M}_F^+(\Gamma) \times \mathcal{M}_\delta(\mathbb{R}^* \times \mathbb{S}^2 \times \Gamma)$

$$|\phi_h(\mu)| + |\mathcal{L}^\infty \phi_h| \leqslant C(1 + \langle \mu, 1 \rangle^p),$$

    2. Or if
$$\phi : x \mapsto x^2 \ and \ h \in \mathcal{C}_b^2(\overline{\Gamma}) \times \mathcal{C}_b^{1,2,2}(\mathbb{R}_+ \times \mathbb{S}^2 \times \overline{\Gamma}),$$

then the process

$$\phi_h(\mu_t) - \phi_h(\mu_0) - \int_0^t \mathcal{L}^\infty \phi_h(\mu_s) ds$$

is a $L^1 - (\mathcal{F}_t)_{t \geqslant 0}$ *martingale starting from* 0*. Moreover, with* $\phi = Id$*, this martingale is* $\overline{M}_t^p = \overline{M}_t^{0,p} + \overline{M}_t^{2,p}$ *defined in eq. (4.33) and is an* $L^2 - (\mathcal{F}_t)_{t \geqslant 0}$ *martingale starting from* 0 *with quadratic variations:*

$$\left\langle \overline{M}^p \right\rangle_t = \left\langle \overline{M}^{0,p} \right\rangle_t + \left\langle \overline{M}^{2,p} \right\rangle_t$$

where

$$
\begin{aligned}
\left\langle \overline{M}^{0,p} \right\rangle_t &= \int_0^t \int_{\mathbb{R}_+ \times \mathbb{S}^2 \times \Gamma} \Big(\left(\nabla_n g^T \mathcal{R} \right) \left(\mathcal{R}^T \nabla_n g \right) \\
&\quad + \left(\nabla_y g^T \mathcal{D}_{\parallel} \right) \left(\mathcal{D}_{\parallel}^T \nabla_y g \right) + \left(\nabla_y g^T \mathcal{D}_{\perp} \right) \left(\mathcal{D}_{\perp}^T \nabla_y g \right) \Big) \mu_s^p(dz) ds, \\
\left\langle \overline{M}^{2,p} \right\rangle_t &= \int_0^t \int_{\mathbb{R}^+ \times \mathbb{S}^2 \times \Gamma} \int_0^1 \beta(z) \left(g(\Theta(\theta, z)) + g(\Theta(1 - \theta, z)) - g(z) \right)^2 \mu_s^p(dz) d\theta ds.
\end{aligned}
$$

4.6   Convergence theorem

Now we are in position to state our main result, the convergence of the rescaled solutions to the limit problem:

Theorem 109. *Under assumptions (H1-H4), let the sequence of process* $(\mu^n)_{n \geqslant 1}$ *given by eq. (4.32) and the process* μ *given by eq. (4.33). Then*

$$\mu^n \xrightarrow[n \to +\infty]{Law} \mu \ in \ \mathbb{D}\big([0, \infty), w - \mathcal{M}_F(\Gamma) \times \mathcal{M}_F(\mathbb{R}_+^* \times \mathbb{S}^2 \times \Gamma)\big),$$

(convergence in law, where the measure space is equipped with the topology of weak convergence)

Proof. The proof of the scaling result is similar as [58, 11]. We start with moment estimates, that comes directly from the study of the discrete process below. Then we prove that μ^n is tight in $\mathcal{M}_F(\Gamma) \times \mathcal{M}_F(\mathbb{R}_+^* \times \mathbb{S}^2 \times \Gamma)$ endowed with the topology of weak convergence. We finally consider uniqueness of the limiting values of μ^n.

Step 1: Moment estimates   Under our assumption,

$$\sup_n E \left(\sup_{t \in [0,T]} \langle \mu_t^n, 1 \rangle^2 \right) < +\infty,$$

because similar estimates as in proposition 97 holds for μ_t^n with a constant that does not depends on n other than by $E \left(\langle \mu_0^n, 1 \rangle^2 \right)$.

Step 2: Tightness   We first show that μ^n is tight in $\mathcal{M}_F(\Gamma) \times \mathcal{M}_F(\mathbb{R}_+ \times \mathbb{S}^2 \times \Gamma)$ endowed with the vague topology. For this, we need two things [51, Thm 9.1]:
  – prove that for all function h in a dense subset of $\mathcal{C}_b^0(\Gamma) \times \mathcal{C}_b^0(\mathbb{R}_+ \times \mathbb{S}^2 \times \Gamma)$, the sequences $\langle \mu^n, h \rangle$ are tight in $\mathbb{D}\big([0, T], \mathbb{R}\big)$, for any $T > 0$;

– prove that the following compact containment condition holds: $\forall T > 0, \forall \varepsilon > 0, \exists K_{\varepsilon,T}$ compact subset of $\mathcal{M}_F(\Gamma) \times \mathcal{M}_F(\mathbb{R}_+^* \times \mathbb{S}^2 \times \Gamma)$,

$$\inf_n \mathcal{P}\Big(\mu_n \in K_{\varepsilon,T}, \text{ for } t \in [0,T]\Big) \geqslant 1 - \varepsilon.$$

For the tightness of $\langle \mu^n, h \rangle$, note that eq. (4.32) gives us $\langle \mu^n, h \rangle$ as the sum of process with finite variation and a martingale. The advantage to prove tightness for $\langle \mu^n, h \rangle$ rather than μ^n directly is to have a stochastic process at values in a finite-dimensional space. We will then use Rebolledo criterion [79, Cor 2.3.3 p 41], together with Aldous criterion [76, Theorem 4.5, page 356].

Let $h = (f, g) \in \mathcal{C}^2(\overline{\Gamma}) \times \mathcal{C}_b^2(\mathbb{R}_+^* \times \mathbb{S}^2 \times \overline{\Gamma})$. We have

$$\lim_{n \to \infty} \left(g(z + \frac{1}{n}\mathbf{e}_1) - g(z) \right) n = \frac{\partial g}{\partial r}(z),$$

and the limit is controlled, uniformly in n, by the second derivatives of g. Let us denotes $V_t^{i,m,n}$, $i = 0, 1$, $V_t^{i,p,n}$, $i = 0, 1, 2$ the finite variation part of $\langle \mu^n, h \rangle$, with analogy to our martingale notation. Our assumption leads to the following estimates (note that all constant are different and depend on bound of coefficients and test functions as mentioned)

$$
\begin{aligned}
|V_t^{0,m,n}| &\leqslant C(f,u)t \sup_{[0,t]} \langle \mu_s^{m,n}, 1 \rangle, \\
|V_t^{1,m,n}| &\leqslant C(f,\overline{\tau})t \sup_{[0,t]} \langle \mu_s^{m,n}, 1 \rangle \langle \mu_s^{p,n}, 1 \rangle, \\
|V_t^{0,p,n}| &\leqslant C(g,u)t \sup_{[0,t]} \langle \mu_s^{p,n}, 1 \rangle, \\
|V_t^{1,p,n}| &\leqslant C(g,\overline{\tau})t \sup_{[0,t]} \langle \mu_s^{m,n}, 1 \rangle \langle \mu_s^{p,n}, 1 \rangle, \\
|V_t^{2,p,n}| &\leqslant C(g,\overline{\beta})t \sup_{[0,t]} \langle \mu_s^{p,n}, 1 \rangle,
\end{aligned}
$$

which provides immediately, thanks to step 1,

$$\sup_n E\big(\sup_t | V_t^n | \big) < \infty.$$

Using that

$$\lim_{n \to \infty} n \left(g(z + \frac{1}{n}\mathbf{e}_1) - g(z) \right)^2 = 0,$$

$$\lim_{n \to \infty} \left(g(z + \frac{1}{n}\mathbf{e}_1) - g(z) \right) = 0,$$

we obtain similarly

$$\left\langle M^{0,m,n}\right\rangle_t \;\leqslant\; \frac{C(f)}{n}t\sup_{[0,t]}\left\langle\mu_s^{m,n},1\right\rangle,$$

$$\left\langle M^{1,m,n}\right\rangle_t \;\leqslant\; \frac{C(f,\overline{\tau})}{n}t\sup_{[0,t]}\left\langle\mu_s^{m,n},1\right\rangle\left\langle\mu_s^{p,n},1\right\rangle,$$

$$\left\langle M^{0,p,n}\right\rangle_t \;\leqslant\; C(g)\sup_{[0,t]}\left\langle\mu_s^{p,n},1\right\rangle,$$

$$\left\langle M^{1,p,n}\right\rangle_t \;\leqslant\; \frac{C(g,\overline{\tau})}{n}t\sup_{[0,t]}\left\langle\mu_s^{m,n},1\right\rangle\left\langle\mu_s^{p,n},1\right\rangle,$$

$$\left\langle M^{2,p,n}\right\rangle_t \;\leqslant\; C(g,\overline{\beta})t\sup_{[0,t]}\left\langle\mu_s^{p,n},1\right\rangle,$$

$$\left|\left\langle M^{1,m,n},M^{2,m,n}\right\rangle_t\right| \;\leqslant\; \frac{C(f,g,\overline{\tau})}{n}t\sup_{[0,t]}\left\langle\mu_s^{m,n},1\right\rangle\left\langle\mu_s^{p,n},1\right\rangle,$$

and so

$$\sup_n E\big(\sup_t\big|\left\langle M^{total,n}\right\rangle_t\big|\big)<\infty.$$

Let $\delta>0$ and let $((S_n,T_n):n\in\mathbb{N})$ be a sequence of couples of stopping times such that $S_n\leqslant T_n\leqslant T$ and $T_n\leqslant S_n+\delta$. We prove in the same way

$$E\big(\,|\,V_{T_n}^n-V_{S_n}^n\,|\,\big)\leqslant C(h,T)\delta,$$

and

$$E\big(\,|\,\left\langle M^{total,n}\right\rangle_{T_n}-\left\langle M^{total,n}\right\rangle_{S_n}\,|\,\big)\leqslant C(h,T)\delta.$$

We proceed now to show that the compact containment condition holds. Recall that the sets $\mathcal{M}_N(K)$ of measures with mass bounded by N and support included in a compact K are compact. Taking $K=\overline{\Gamma}\times\mathbb{S}^2\times[0,R]$, then μ^n is not in such compact either if

$$\{\exists t,\langle\mu_t^n,1\rangle\geqslant N\},$$

or

$$\{\exists t,\langle\mu_t^{p,n},r\rangle\geqslant R\}.$$

The conservation of mass property shows that this last possibility does not occur for sufficiently large R (given by the initial mass), while for the first possibility,

$$P\{\exists t,\langle\mu_t^n,1\rangle\geqslant N\}\leqslant\frac{1}{N}E\big(\sup_t|\langle\mu_t^n,1\rangle|\big)$$

which is arbitrary small for large N.

Step 3: Identification of the limit   Let us consider an adherence value μ and the subsequence (denoted again by) μ^n, such that μ^n converges in law towards μ in $\mathbb{D}\big([0,T],w-\mathcal{M}_F(\Gamma)\times\mathcal{M}_F(\mathbb{R}_+^*\times\mathbb{S}^2\times\Gamma)\big)$. Let $h\in\mathcal{C}_b^2(\overline{\Gamma})\times\mathcal{C}_b^{1,2,2}(\mathbb{R}_+\times\mathbb{S}^2\times\overline{\Gamma})$. For $k\in\mathbb{N}^*$, let $0\leqslant t_1<\cdots<t_k<s<t\leqslant T$ and $\varphi_1,\cdots,\varphi_k\in\mathcal{C}_b(\mathcal{M}_F(\Gamma)\times\mathcal{M}_F(\mathbb{R}_+^*\times\mathbb{S}^2\times\Gamma),\mathbb{R})$. For $z\in\mathbb{D}\big([0,T],\mathcal{M}_F(\Gamma)\times\mathcal{M}_F(\mathbb{R}_+^*\times\mathbb{S}^2\times\Gamma)\big)$, we define

$$\Psi(z)=\varphi_1(z_{t_1})\cdots\varphi_k(z_{t_k})\Big[\,\langle z_t,h\rangle-\langle z_s,h\rangle-\int_s^t\mathcal{L}^\infty(\langle z_u,h\rangle)\Big],$$

where $\mathcal{L}^\infty$ is the generator defined in eq. (4.43). Then $\mid E(\Psi(\mu)) \mid \leqslant A + B + C$, where

$$A = \mid E(\Psi(\mu)) - E(\Psi(\mu_n)) \mid,$$

$$B = \mid E(\Psi(\mu_n)) - E\big(\varphi_1(\mu^n_{t_1}) \cdots \varphi_k(\mu^n_{t_k}) \big[M^{total,n}_t - M^{total,n}_s \big] \big) \mid,$$

$$C = \mid E\big(\varphi_1(\mu^n_{t_1}) \cdots \varphi_k(\mu^n_{t_k}) \big[M^{total,n}_t - M^{total,n}_s \big] \big) \mid.$$

Since $M^{total,n}$ is a martingale, $C = 0$. By convergence in distribution, A converges to 0 when $n \to \infty$. And

$$B \leqslant C(\varphi) \mid \int_s^t \mathcal{L}^n(\langle \mu^n_\sigma, h \rangle) - \mathcal{L}^\infty(\langle \mu^n_\sigma, h \rangle) d\sigma \mid,$$

which, from Taylor-Young formula, and moment estimates, goes to 0 as $n \to \infty$.

This proves that $E(\Psi(\mu)) = 0$ and hence $\langle \mu_t, h \rangle - \langle \mu_0, h \rangle - \int_0^t \mathcal{L}^\infty(\langle \mu_\sigma, h \rangle)$ is a martingale.

Step 4: Conclusion   In the step 3, we have identified the adherence values of the sequence of processes μ^n as the solutions μ of the martingale problem associated with the limit generator $\mathcal{L}^\infty$. We refer to similar argument as in [11, Prop 2.2] to show that two processes of $\mathbb{D}\big([0,\infty), \mathcal{M}_F(\Gamma) \times \mathcal{M}_F(\mathbb{R}^*_+ \times \mathbb{S}^2 \times \Gamma)\big)$ satisfying the martingale problem associated with $\mathcal{L}^\infty$ have the same distribution (see proposition 8).

$\square$

Bibliography

[1] D. J. Aldous. Deterministic and stochastic models for coalescence (aggregation and coagulation): a review of the mean-field theory for probabilists. *Bernoulli*, 5(1): 3–48, 1999. 183, 241, 242

[2] E. S. Almberg, P. C. Cross, C. J. Johnson, D. M. Heisey, and B. J. Richards. Modeling routes of chronic wasting disease transmission: environmental prion persistence promotes deer population decline and extinction. *PloS one*, 6(5):e19896–e19896, 2011. 182

[3] M.-T. Alvarez-Martinez, P. Fontes, V. Zomosa-Signoret, J.-D. Arnaud, E. Hingant, L. Pujo-Menjouet, and J.-P. Liautard. Dynamics of polymerization shed light on the mechanisms that lead to multiple amyloid structures of the prion protein. *Biochim. Biophys. Acta*, 1814(10):1305–1317, 2011. 174, 176, 177, 178, 180, 181

[4] J.M. Andreu and S.N. Timasheff. The measurement of cooperative protein self-assembly by turbidity and other techniques. *Methods Enzymol.*, 130:47–59, 1986. 172

[5] J. M. Andrews and C. J. Roberts. A lumry-eyring nucleated polymerization model of protein aggregation kinetics: 1. aggregation with pre-equilibrated unfolding. *J. Phys. Chem. B.*, 111(27):7897–913, 2007. 172

[6] S. Asakura. Polymerization of flagellin and polymorphism of flagella. *Adv. Biophys.*, 1:99–155, 1970. 172

[7] J. M. Ball and J. Carr. Asymptotic behaviour of solutions to the Becker-Döring equations for arbitrary initial data. *Proc. Edinburgh Math. Soc.*, 108(1-2):109–116, 1988. 184

[8] J. M. Ball and J. Carr. The discrete coagulation-fragmentation equations: Existence, uniqueness, and density conservation. *J. Stat. Phys.*, 61(1-2):203–234, 1990. 183

[9] J. M. Ball, J. Carr, and O. Penrose. The Becker-Döring Cluster Equations: Basic Properties and Asymptotic Behaviour of Solutions. *Commun. Math. Phys.*, 104(4): 657–692, 1986. 184, 201

[10] J. Banasiak. Shattering and non-uniqueness in fragmentation models: an analytic approach. *Physica D*, 222:63–72, 2006. 183

[11] V. Bansaye and V. C. Tran. Branching Feller diffusion for cell division with parasite infection. *ALEA-Lat. Am. J. Probab.*, 8:81–127, 2011. 241, 242, 269, 272

[12] V. Bansaye, J.-F. Delmas, L. Marsalle, and V. C. Tran. Limit theorems for Markov processes indexed by continuous time Galton-Watson trees. *Ann. Appl. Probab.*, 21 (6):2263–2314, 2011. 243

[13] I. V. Baskakov and O. V. Bocharova. In vitro conversion of mammalian prion protein into amyloid fibrils displays unusual features. *Biochemistry*, 44:2339–2348, 2005. 174, 176

[14] R. Becker and W. Döring. Kinetische Behandlung der Keimbildung in übersättigten Dämpfen. *Ann. Phys. (Berlin)*, 416(8):719–752, 1935. 184, 199, 241

[15] N. Berglund and B. Gentz. *Noise-Induced Phenomena in Slow-Fast Dynamical Systems,A Sample-Paths Approach.* Springer, 2006. 246

[16] M. V. Berjanskii and D. S. Wishart. A simple method to predict protein flexibility using secondary chemical shifts. *J. Am. Chem. Soc.*, 127:14970–14971, 2005. 182

[17] D. Bhatia, S. Mehtab, R. Krishnan, S. S. Indi, A. Basu, and Y. Krishnan. Icosahedral dna nanocapsules by modular assembly. *Angew. Chem. Int. Ed.*, 48:4134–4137, 2009. 197

[18] J. S. Bhatt and I. J. Ford. Kinetics of heterogeneous nucleation for low mean cluster populations. *J. Chem. Phys.*, 118:3166–3176, 2003. 198

[19] R. B. Bird, C. F. Curtiss, R. C. Armstrong, and O. Hassager. *Dynamics of Polymeric Liquids, vol. 2: Kinetic theory.* Wiley, 1987. 240, 242, 245, 251

[20] N. Blinov, M. Berjanskii, D. S. Wishart, and M. Stepanova. Structural domains and main-chain flexibility in prion proteins. *Biochemistry*, 48:1488–1497, 2009. 172, 174

[21] N. N. Borodin. A limit theorem for solutions of differential equations with random right-hand side. *Theor. Popul. Biol.*, 22(3):482–482, 1978. 246

[22] A. B. Bortz, M. H. Kalos, and J. L. Lebowitz. A new algorithm for monte carlo simulation of ising spin systems. *J. Comp. Phys.*, 17:10–18, 1975. 233

[23] M. Bowen. Temporal evolution of the cluster size distribution during brownian coagulation. *J. Colloid Interface Sci.*, 105(2):617–627, 1985. 242

[24] J. A. Cañizo. Convergence to Equilibrium for the Discrete Coagulation-Fragmentation Equations with Detailed Balance. *J. Stat. Phys.*, 129(1):1–26, 2007. 183

[25] J. A. Canizo, L. Desvillettes, and K. Fellner. Absence of Gelation for Models of Coagulation-Fragmentation with Degenerate Diffusion. *Nuovo Cimento C*, 33:79–86, 2010. 242

[26] F. Gaskin C.R. Cantor and M. L. Shelanski. Turbidimetric studies of the in vitro assembly and disassembly of porcine neurotubules. *J. Mol. Biol.*, 84(4):737–740, 1974. 172

[27] Y. Cao, D.T. Gillespie, and L.R. Petzold. The slow-scale stochastic simulation algorithm. *J. Chem. Phys*, 122:1–18, 2005. 203, 228, 231

[28] J. Carr and R. M. Dunwell. Asymptotic behaviour of solutions to the Becker-Döring equations. *Proc. Edinburgh Math. Soc.*, 42(02):415–424, 1999. 184

[29] B. Caughey, D. A. Kocisko, G. J. Raymond, and P. T. Lansbury. Aggregates of scrapie associated prion protein induce the cell-free conversion of protease-sensitive prion protein to the protease-resistant state. *Chem. Biol.*, 2(12):807–817, 1995. 171, 172, 173, 185

[30] E. Cepeda and N. Fournier. Smoluchowski's equation: rate of convergence of the Marcus-Lushnikov process. *Stoch. Proc. Appl.*, 121(6):1–34, 2011. 183, 241, 242

[31] N. Champagnat and S. Méléard. Invasion and adaptive evolution for individual-based spatially structured populations. *J. Math. Biol.*, 55(2):147–188, 2007. 243, 246, 248, 250, 268

[32] N. Champagnat, R. Ferrière, and S. Méléard. Individual-based probabilistic models of adaptive evolution and various scaling approximations. *Prog. Probab.*, 59:75–113, 2005. 243, 254, 256, 257

[33] Y. R. Chemla, J. R. Moffitt, and C. Bustamante. Exact solutions for kinetic models of macromolecular dynamics. *J. Phys. Chem. B*, 112(19):6025–6044, 2008. 221

[34] J. Chen and N. C. Seeman. Synthesis from dna of a molecule with the connectivity of a cube. *Nature*, 350:631–633, 1991. 197

[35] W. K. Cho, S. Park, S. Jon, and I. S. Choi. Water-repellent coating: formation of polymeric self-assembled monolayers on nanostructured surfaces. *Nanotechnology*, 18:395602, 2007. 197

[36] T. Chou and M. R. D'Orsogna. Coarsening and accelerated equilibration in mass-conserving heterogeneous nucleation. *Phys. Rev. E*, 84:011608, 2011. 198

[37] I. S. Ciuperca, E. Hingant, L. I. Palade, and L. Pujo-Menjouet. Fragmentation and monomer lengthening of rod-like polymers, a relevant model for prion proliferation. *Discrete Contin. Dyn. Syst. Ser. B*, 17(3):775–799, 2012. 240, 242, 245

[38] F. E. Cohen and S. B. Prusiner. Pathologic conformations of prion proteins. *Annu. Rev. Biochem.*, 67:793–819, 1998. 172

[39] F. E. Cohen, Z. Huang K. M. Pan, M. Baldwin, R. J. Fletterick, and S. B. Prusiner. Structural clues to prion replication. *Science*, 264(5158):530–1, 1994. 171

[40] S. R. Collins, A. Douglass, R. D. Vale, and J. S. Weissman. Mechanism of prion propagation: Amyloid growth occurs by monomer addition. *PLoS Biol.*, 2:e321, 2004. 176, 185

[41] U. H. Danielsson, M. Lundgren, and A. J. Niemi. A gauge field theory of chirally folded homopolymers with applications to folded proteins. *Phys. Rev.*, E82(021910): 2 Pt 1, 2010. 172

[42] D. Dawson, B. Maisonneuve, and J. Spencer. *Measure-valued markov processes*, volume 1541. Springer Berlin / Heidelberg, 1993. 252

[43] P. Degond and H. Liu. Kinetic models for polymers with inertial effects. *Netw. Heterog. Media*, 4(4):625–647, 2009. 247, 251

[44] L. Desvillettes and K. Fellner. Large time asymptotics for a continuous coagulation-fragmentation model with degenerate size-dependent diffusion. *SIAM J. Math Anal.*, 41(6):2315–2334, 2010. 242

[45] L. Desvillettes, K. Fellner, and J. A. Canizo. Regularity and mass conservation for discrete coagulation-fragmentation equations with diffusion. *Ann. Inst. H. Poincaré Anal. Non Linéaire*, 27(2):639–654, 2010. 242

[46] M. Doi and S. F. Edwards. *The Theory of Polymer Dynamics.* Oxford University Press, Oxford, 1986. 240, 242, 245, 246, 247, 248, 251, 262

[47] M. R. D'Orsogna, G. Lakatos, and T. Chou. Stochastic self-assembly of incommensurate clusters. *J. Chem. Phys.*, 136:084110, 2012. 198, 202, 203, 209, 218, 219

[48] M. Doumic, T. Goudon, and T. Lepoutre. Scaling limit of a discrete prion dynamics model. *Comm. math. sci.*, 7(4):839–865, 2009. 241

[49] W.A. Eaton and J. Hofrichter. Sickle cell hemoglobin polymerization. *Adv. Protein Chem.*, 40:63–279, 1990. 172

[50] L. Edelstein-keshet and G. B. Ermentrout. Models for spatial polymerization dynamics of rod-like polymers. *J. Math. Biol.*, 40:64–96, 2000. 242

[51] S. N. Ethier and T. G. Kurtz. *Markov Processes: Characterization and Convergence.* Wiley Interscience, 2005. 269

[52] O. C. Farokhzad and R. Langer. Impact of nanotechnology on drug delivery. *ACS Nano*, 3:16–20, 2009. 197

[53] A. S. Ferreira, M. A. A. da Silva, and J. C. Cressoni1. Stochastic modeling approach to the incubation time of prionic diseases. *Phys. Rev. Lett.*, 90(19):198101–1 198101–4, 2003. 184

[54] F. A. Ferrone. Nucleation: The connections between equilibrium and kinetic behavior. *Methods Enzymol.*, 412:285–99, 2006. 174, 176

[55] N. Fournier and J.-S. Giet. Convergence of the Marcus-Lushnikov process. *Methodol. Comput. Appl.*, 6(2):219–231, 2004. 184, 242

[56] N. Fournier and P. Laurençot. Well-posedness of Smoluchowski's coagulation equation for a class of homogeneous kernels. *J. Funct. Anal.*, 233(2):351–379, 2006. 183

[57] N. Fournier and P. Laurençot. Marcus-Lushnikov processes, Smoluchowski's and Flory's models. *Stoch. Proc. Appl.*, 119(1):167–189, 2009. 184, 242

[58] N. Fournier and S. Méléard. A microscopic probabilistic description of a locally regulated population and macroscopic approximations. *Ann. Appl. Probab.*, 14(4): 1880–1919, 2004. 269

[59] N. Fournier and S. Mischler. Exponential trend to equilibrium for discrete coagulation equations with strong fragmentation and without a balance condition. *P. Roy. Soc. A-Math. Phy.*, 460(2049):2477–2486, 2004. 183, 243, 254, 256, 257

[60] D. T. Gillespie. Exact stochastic simulation of coupled chemical reactions. *J. Phys. Chem.*, 81:2340–2361, 1977. 190, 233

[61] D. T. Gillespie. Concerning the validity of the stochastic approach to chemical kinetics. *J. Stat. Phys.*, 16 (3):311–318., 1977. 248

[62] R. F. Goldstein and L. Stryer. Cooperative polymerization reactions: Analytical approximations, numerical examples, and experimental strategy. *Biophys. J.*, 50: 583–599, 1986. 186, 223

[63] M. L. Greer, L. Pujo-Menjouet, and G. F. Webb. A mathematical analysis of the dynamics of prion proliferation. *J. Theor. Biol.*, 242(3):598–606, 2006. 240, 241

[64] J. S. Griffith. Nature of the scrapie agent: Self-replication and scrapie. *Nature*, 215 (5105):1043–1044, 1967. 171

[65] R. Großand M. Dorigo. Self-assembly at the macroscopic scale. *Proc. IEEE*, 96: 1490–1508, 2008. 197

[66] J. Gsponer, U. Haberthür, and A. Caflisch. The role of side-chain interactions in the early steps of aggregation: Molecular dynamics simulations of an amyloid-forming peptide from the yeast prion sup35. *Proc. Natl. Acad. Sci.*, 100(9):5154–5159, 2003. 182

[67] A. Hammond and F. Rezakhanlou. Kinetic Limit for a System of Coagulating Planar Brownian Particles. *J. Stat. Phys.*, 124:1–45, 2006. 242

[68] E. L. Haseltine and J. B. Rawlings. On the origins of approximations for stochastic chemical kinetics. *J. Chem. Phys.*, 122:164115–16, 2005. 227

[69] R. Z. Has'minskii. On Stochastic Processes Defined by Differential Equations with a Small Parameter. *Theor. Popul. Biol.*, 11(2):211?228, 1966. 246

[70] E. M. Hendriks, M. H. Ernst, and R. M. Ziff. Coagulation equations with gelation. *J. Stat. Phys.*, 31(3):519–563, 1983. 183

[71] E. M. Hendriks, J. L. Spouge, M. Eibl, and M. Schreckenberg. Exact Solutions for Random Coagulation Processe. *Z. Phys. B*, V:219–227, 1985. 183

[72] S. Hess, S. L. Lindquist, and T. Scheibel. Alternative assembly pathways of the amyloidogenic yeast prion determinant sup35. *EMBO reports*, 8:1196–201, 2007. 172

[73] J. Hofrichter. Kinetics of sickle hemoglobin polymerization. iii. nucleation rates determined from stochastic fluctuations in polymerization progress curves. *J. Mol. Biol.*, 189(3):553–571, 1986. 184, 185

[74] K. Hur, J.-I. Kim, S.-I. Choi, E.-K. Choi, R. I. Carp, and Y.-S. Kim. The pathogenic mechanisms of prion diseases. *Mech. Ageing Dev.*, 123:1637–1647, 2002. 172

[75] P.-E. Jabin and B. Niethammer. On the rate of convergence to equilibrium in the Becker-Döring equations. *J. Differ. Equations*, 191(2):518–543, 2003. 184, 201

[76] J. Jacod and A. N. Shiryaev. *Limit theorems for stochastic processes.* Springer-Verlag Berlin Heidelberg, 1987. 270

[77] J. Janin. The Kinetics of Protein-Protein Recognition. *Proteins*, 161:153–161, 1997. 242

[78] I. Jeon. Existence of gelling solutions for coagulation- fragmentation equations. *Commun. Math. Phys.*, 567:541–567, 1998. 184, 241

[79] A. Joffe and M. Metivier. Weak convergence of sequences of semimartingales with applications to multitype branching processes. *Adv. Appl. Probab.*, 18(1):20–65, 1986. 270

[80] H.-W. Kang and T. G. Kurtz. Separation of time-scales and model reduction for stochastic reaction networks. *Ann. Appl. Probab. (to appear)*, 2012. To appear in Annals of Applied Prob. 227, 237

[81] J. Kang, Santamaria J, G. Hilmersson, and J. Rebek Jr. Self-assembled molecular capsule catalyzes a diels-alder reaction. *J. Am. Chem. Soc.*, 120:7389–7390, 1998. 197

[82] F. P. Kelly. *Reversibility and Stochastic Networks.* Cambridge University Press, 2011. 202

[83] J. W. Kelly. Mechanisms of amyloidogenesis. *Nat. Struct. Biol*, 7(10):824 – 826, 2000. 172

[84] M. Kimmel and O. Arino. Comparison of approaches to modeling of cell population dynamics. *SIAM J. Appl. Math*, 53:1480–1504, 1993. 242

[85] J. F. C. Kingman. Markov population processes. *J. Appl. Probab.*, 6:1–18, 1969. 197, 210

[86] M. Kroutvar, Y. Ducommun, D. Heiss, M. Bichler, D. Schuh, G. Abstreiter, and J. J. Finley. Optically programmable electron spin memory using semiconductor quantum dots. *Nature*, 432:81–84, 2004. 197

[87] R. V. Kulkarni, A. Slepoy, R. R. Singh, D. L. Cox, and F. Pázmándi. Theoretical modeling of prion disease incubation. *Biophys. J.*, 85(2):707–18, 2003. 184, 185

[88] T. G. Kurtz. Solutions of Ordinary Differential Equations as Limits of Pure Jump Markov Processes. *J. Appl. Probab.*, 7(1):49–58, 1970. 240, 241

[89] R. Lang and N. X. Xanh. Smoluchowski's Theory of Coagulation in Colloids Holds Rigorously in the Boltzmann-Grad-Limit. *Z. Wahrscheinlichkeitstheorie verw. Gebiete*, 54:227–280, 1980. 242

[90] P. Langevin. On the Theory of Brownian Motion. *C. R. Acad. Sci.*, 146:530–533, 1908. 246

[91] P. Lastedt and L. Ferm. Dimensional reduction of the fokker?planck equation for stochastic chemical reactions. *Multiscale Model. Simul.*, 5:593?614, 2006. 237

[92] P. Laurençot and S. Mischler. Global existence for the discrete diffusive coagulation-fragmentation equations in l^1. *Rev. Mat. Iberoamericana*, 18:731–745, 2002. 183, 242

[93] P. Laurençot and D. Wrzosek. The Becker Doring Model with Diffusion II. Long Time Behavior. *J. Differ. Equations*, 148:268–291, 1998. 242

[94] M. Laurent. Autocatalytic processes in cooperative mechanisms of prion diseases. *FEBS lett.*, 407(1):1–6, 1997. 172

[95] C.-C. Lee, A. Nayak, A. Sethuraman, G. Belfort, and G. J. McRae. A three-stage kinetic model of amyloid fibrillation. *Biophys. J.*, 92(10):3448?3458, 2007. 176

[96] D. Lépingle. Euler scheme for reflected stochastic differential equations. *Math. Comput. Simulat.*, 38(1-3):119–126, 1995. 250

[97] J.-P. Liautard. Are prions misfolded molecular chaperones? *FEBS lett.*, 294(3): 155–157, 1991. 172

[98] A. A. Lushnikov. Coagulation in Finite Systems. *J. Colloid Interface Sci.*, 65(2), 1978. 183, 241

[99] M. R. D'Orsogna M. Gibbons, T. Chou. Diffusion-dependent mechanisms of receptor engagement and viral entry. *J. Phys. Chem. B*, 114:15403–15412, 2010. 198

[100] J. Torrent et al. M. T. Alvarez-Martinez. Optimized overproduction, purification, characterization and high-pressure sensitivity of the prion protein in the native (prp(c)-like) or amyloid (prp(sc)-like) conformation. *Biochim. Biophys. Acta*, 1645 (2):228–40, 2003. 174

[101] J. Ma and S. Lindquist. Conversion of prp to a self-perpetuating prpsc-like conformation in the cytosol. *Science*, 298(5599):1785–8, 2002. 173

[102] A. H. Marcus. Stochastic Coalescence. *Technometrics*, 10(1):133–143, 1968. 183, 215, 216, 241

[103] J. B. Martin. Molecular basis of the neurodegenative disorders. *New Engl. J. Med.*, 340(25):1970–1981, 1999. 171

[104] J. Masel, V.A. Jansen, and M.A. Nowak. Quantifying the kinetic parameters of prion replication. *Biophys. Chem.*, 77(2-3):139–52, 1999. 188, 189, 241

[105] D. A. McQuarrie. Stochastic Approach to Chemical Kinetics. *J. Appl. Probab.*, 4 (3):413–478, 1967. 248

[106] S. Méléard and S. Roelly. A host-parasite multilevel interacting process and continuous approximations. pages 1–31, 2011. arXiv:1101.4015. 243

[107] C. A. Mirkin, R. L. Letsinger, R. C. Mucic, and J. J. Storhoff. A dna-based method for rationally assembling nanoparticles into macroscopic materials. *Nature*, 382: 607–609, 1996. 197

[108] S Mischler, C Mouhot, and B Wennberg. A new approach to quantitative chaos propagation estimates for drift, diffusion and jump processes. pages 1–45, 2011. arXiv:1101.4727. 241

[109] R. A. Moore, L. M. Taubner, and S. A. Priola. Prion protein misfolding and disease. *Curr. Opin. Struc Biol.*, 19(1):14–22, 2009. 173

[110] A. M. Morris, M. A. Watzki, and R. G. Finke. Protein aggregation kinetics, mechanism, and curve-fitting: A review of the literature. *Biochim. Biophys. Acta*, 1794: 375–397, 2009. 172, 186

[111] B. Munsky and M. Khammash. Reduction and solution of the chemical master equation using time scale separation and finite state projection. *J. Chem. Phys.*, 125:1–13, 2006. 237

[112] H. D. Nguyen and C. K. Hall. Molecular dynamics simulations of spontaneous fibril formation by random-coil peptides. *Proc. Natl. Acad. Sci.*, 101(46):16180–16185, 2004. 182

[113] J. R. Norris. Smoluchowski's coagulation equation: uniqueness, nonuniqueness, and a hydrodynamic limit for stochastic coalescent. *Ann. Appl. Probab.*, 9(1):78–109, 1999. 183, 241, 242

[114] J. R. Norris. Brownian coagulation. *Comm. math. sci.*, Suppl. iss(1):93–101, 2004. 242

[115] S. B. Padrick and A. D. Miranker. Islet amyloid: Phase partitioning and secondary nucleation are central to the mechanism of fibrillogenesis. *Biochemistry*, 41:4694–4703, 2002. 174

[116] R. J. Payne and D. C. Krakauer. The spatial dynamics of prion disease. *Proc. R. Soc. B*, 265(1412):2341–6, 1998. 182

[117] R. Pellarin and A. Caflisch. Interpreting the aggregation kinetics of amyloid peptides. *J. Mol. Biol.*, 360(4):882–92, 2006. 182

[118] O. Penrose. Metastables states for the becker-döring cluster equations. *Commun. Math. Phys.*, 541:515–541, 1989. 231, 238

[119] O. Penrose. The becker-döring equations at large times and their connection with the lsw theory of coarsening. *J. Stat. Phys.*, 89:305–320, 1997. 198

[120] E. T. Powers and D. L. Powers. The kinetics of nucleated polymerizations at high concentrations: Amyloid fibril formation near and above the supercritical concentration. *Biophys. J.*, 91:122–132, 2006. 174, 184, 186, 206, 223, 226

[121] S. A. Priola and I. Vorberg. Molecular aspects of disease pathogenesis in the transmissible spongiform encephalopathies. *Mo. biotechnol.*, 33(1):71–88, 2006. 173

[122] Y. V. Prokhorov. Convergence of random processes and limit theorems in probability theory. *Theor. Popul. Biol.*, I(2):157?214, 1956. 240

[123] S. B. Prusiner. Prions. *Proc. Natl. Acad. Sci.*, 95(23):13363–13383, 1998. 171, 172

[124] S. Redner. *A guide to first passage processes.* Cambridge University Press, 2001. 199

[125] F. Schweitzer, L. Schimansky-Geier, W. Ebeling, and H. Ulbricht. A stochastic approach to nucleation in finite systems: theory and computer simulations. *Physica A*, 150:261–279, 1988. 198

[126] D. Serre. *Matrices : Theory and Applications*. Springer-Verlag, 2002. 223

[127] M. Slemrod. Trend to equilibrium in the Becker-Doring cluster equations. *Nonlinearity*, 2(3):429–443, 1989. 184

[128] P. Smereka. Long time behavior of a modified becker-döring system. *J. Stat. Phys.*, 132:519–533, 2008. 198

[129] C. Soto. Unfolding the role of protein misfolding in neurodegenerative diseases. *Nat. Rev. Neurosci.*, 4:49–60, 2003. 198

[130] D. W. Stroock and S. R. S. Varadhan. Diffusion processes with boundary conditions. *Commun. Pure and Appl.Math.*, 24(2):147–225, 1971. 246

[131] M. P. Stumpf and D. C. Krakauer. Mapping the parameters of prion-induced neuropathology. *Proc. Natl. Acad. Sci.*, 97(19):10573–7, 2000. 182

[132] A. Szabo. Fluctuations in the polymerization of sickle hemoglobin a simple analytic model. *J. Mol. Biol*, 539-542:539–542, 1998. 184, 185

[133] A.-S. Sznitman. *Topics in Propagation of Chaos*. Springer, 1991. 240

[134] V. C. Tran. *Modèles particulaires stochastiques pour des problèmes d'évolution adaptative et pour l'approximation de solutions statistiques*. PhD thesis, University Paris 10 Nanterre, 2006. 241, 268

[135] R.A. Usmani. Inversion of a tridiagonal jacobi matrix. *Lin. Alg. Appl.*, 212:413–414, 1994. 221

[136] W. Wagner. Explosion phenomena in stochastic coagulation-fragmentation models. *Ann. Appl. Probab.*, 15(3):2081–2112, 2005. 183

[137] W. Wagner. Random and deterministic fragmentation models. *Monte Carlo Methods Appl.*, 16(3-4):399–420, 2010. 183

[138] F. Wang, X. Wang, C.-G. Yuan, and J. Ma. Generating a prion with bacterially expressed recombinant prion protein. *Science*, 327(5969):1132–5, 2010. 174

[139] J. A. D. Wattis. An introduction to mathematical models of coagulation-fragmentation processes: a discrete deterministic mean-field approach. *Physica D*, 222(1-2):1–20, 2006. 183, 201, 231, 238, 241

[140] J. A. D. Wattis and J. R. King. Asymptotic solutions of the becker-döring equations. *J. Phys. A: Math. Gen.*, 31:7169–7189, 1998. 198

[141] G. M. Whitesides and M. Boncheva. Beyond molecules: self-assembly of mesoscopic and macroscopic components. *Proc. Natl. Acad. Sci.*, 99:4769–4774, 2002. 197

[142] G. M. Whitesides and B. Grzybowski. Self-assembly at all scales. *Science*, 295: 2418–2421, 2002. 197

[143] E. S. Williams and M. W. Miller. Chronic wasting disease in deer and elk in north america. *Rev. Sci. Tech. Oie*, 21(2):305–16, 2002. 173

[144] D. Wrzosek. Existence of solutions for the discrete coagulation-fragmentation model with diffusion. *Topol. Method Nonl. An.*, 9(558):279–296, 1997. 242

[145] H. Yan, S. H. Park, G. Finkelstein, J. H. Reif, and T. H. Labean. Dna-templated self-assembly of protein arrays and highly conductive nanowires. *Science*, 301:1882–1884, 2003. 197

[146] W.-C. Yueh. Eigenvalues of several tridiagonal matrices. *Applied Mathematics E-Notes*, 5:66–74, 2005. 210, 230

[147] A. Zlotnick. To build a virus capsid: an equilibrium model of the self assembly of polyhedral protein complexes. *J. Mol. Biol.*, 241:59–67, 1994. 198

[148] A. Zlotnick. Theoretical aspects of virus capsid assembly. *J. Mol. Recogn.*, 18: 479–490, 2005. 198